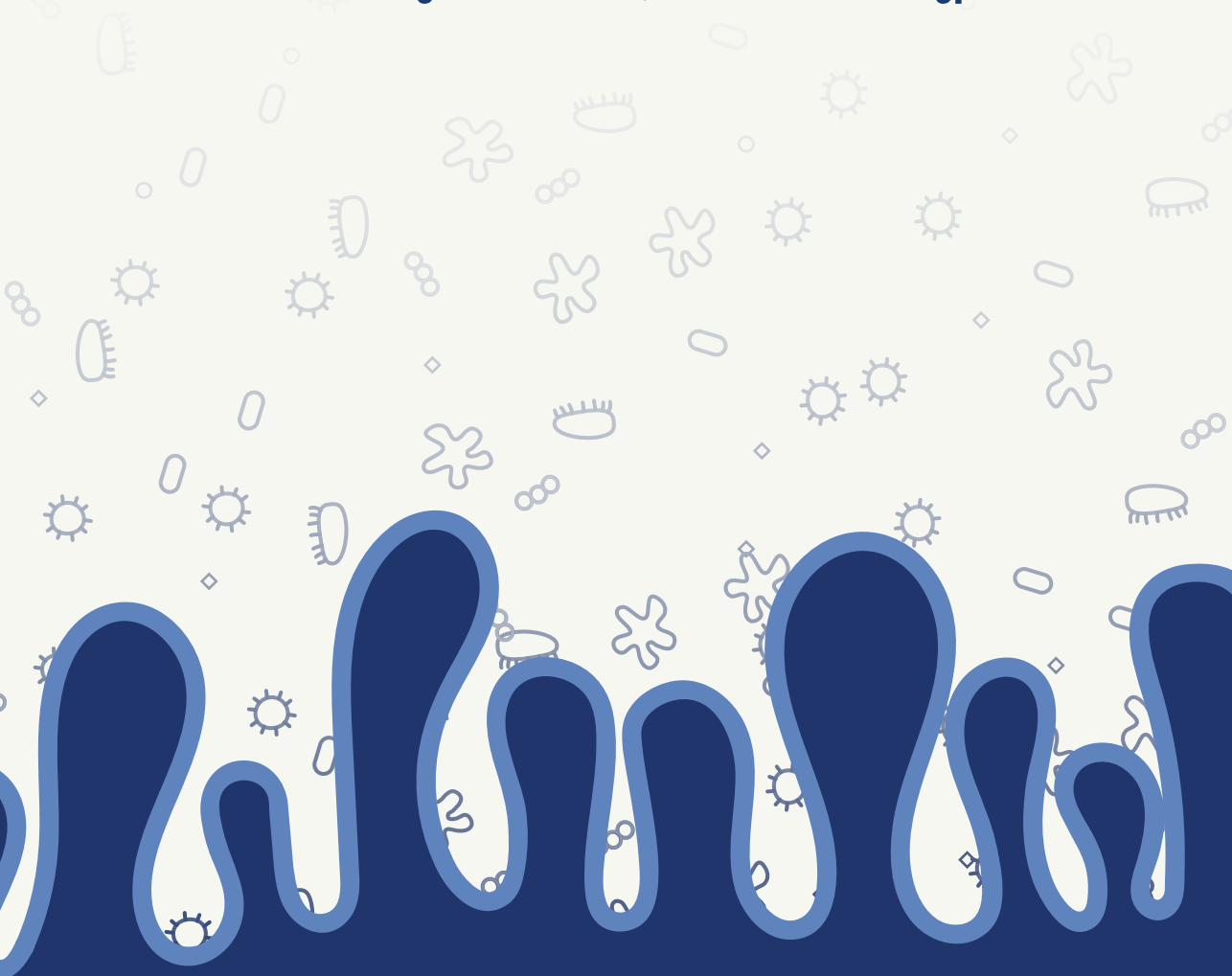


INVESTIGATION INTO MEDIATORS OF METABOLIC HEALTH

a role for the **gut microbiota**, **bile acids** and **Angptl4**



AAFKE W.F. JANSSEN

INVESTIGATION INTO MEDIATORS OF METABOLIC HEALTH

a role for the gut microbiota, bile acids and Angptl4

Aafke W.F. Janssen

Thesis committee

Promotor

Prof. Dr A.H. Kersten
Professor of Nutrition, Metabolism and Genomics
Wageningen University & Research

Other members

Dr E.G. Zoetendal, Wageningen University & Research
Prof. Dr J.M. Wells, Wageningen University & Research
Prof. Dr M. Nieuwdorp, Academic Medical Center Amsterdam
Dr J.W. Jonker, University of Groningen

This research was conducted under the auspices of the Graduate School VLAG (Advanced studies in Food Technology, Agrobiotechnology, Nutrition and Health Sciences).

INVESTIGATION INTO MEDIATORS OF METABOLIC HEALTH

a role for the gut microbiota, bile acids and Angptl4

Aafke W.F. Janssen

Thesis

submitted in fulfilment of the requirements for the degree of doctor
at Wageningen University

by the authority of the Rector Magnificus

Prof. Dr A.P.J. Mol,

in the presence of the

Thesis Committee appointed by the Academic Board

to be defended in public

on Friday 1 December 2017

at 1.30 p.m. in the Aula.

Aafke W.F. Janssen

Investigation into mediators of metabolic health
A role for the gut microbiota, bile acids and Angptl4,
306 pages.

PhD thesis, Wageningen University, Wageningen, the Netherlands (2017)
With references, with summary in English

ISBN: 978-94-6343-689-2

DOI: 10.18174/422846

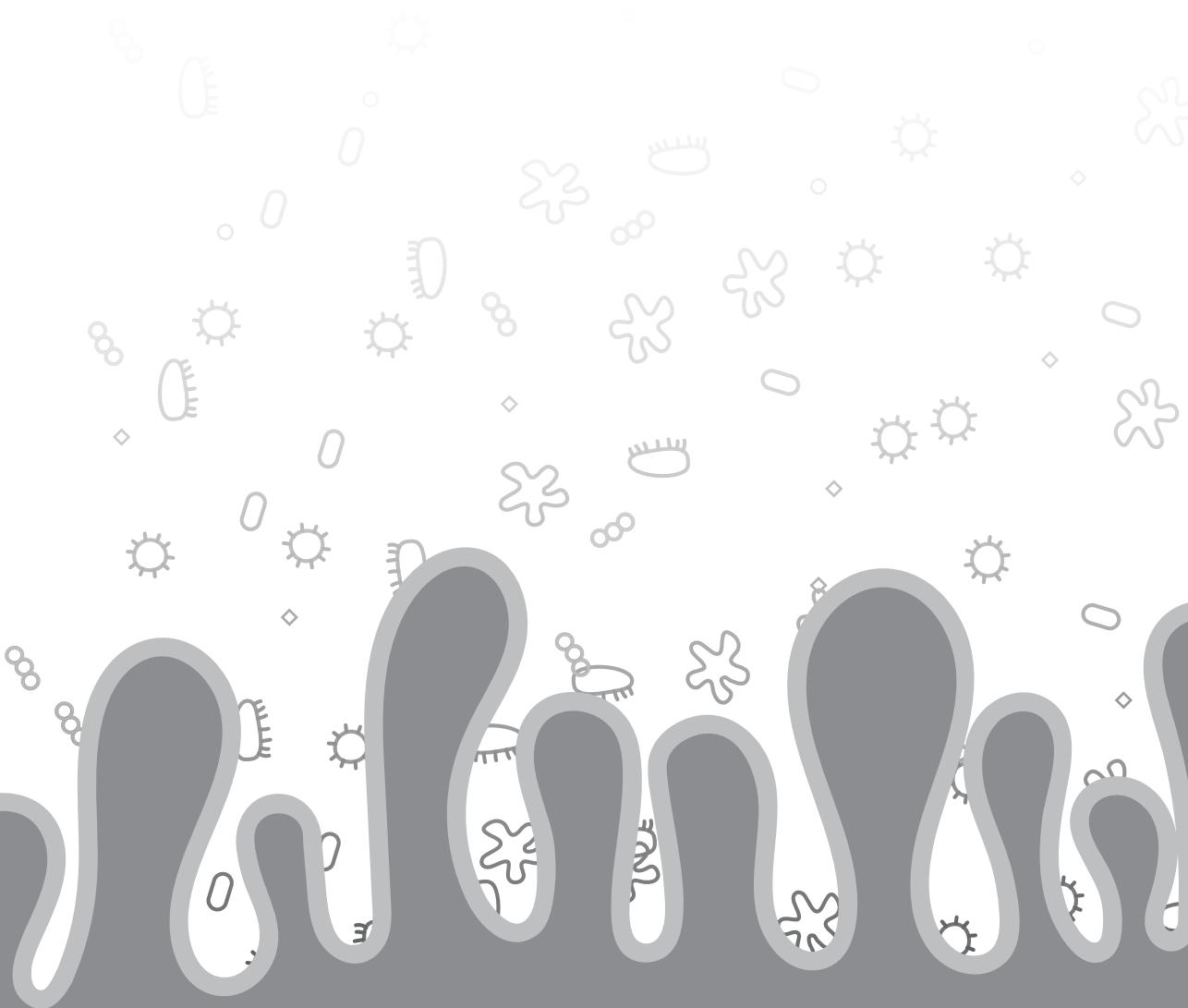
Contents

Chapter 1	General introduction	6
Chapter 2	The role of the gut microbiota in metabolic health	28
Chapter 3	Potential mediators linking the gut bacteria to metabolic health: a critical view	56
Chapter 4	Modulation of the gut microbiota impacts non-alcoholic fatty liver disease: a potential role for bile acids	74
Chapter 5	The mucin-degrading bacteria <i>A. muciniphila</i> and <i>B. thetaiotaomicron</i> have no effect in an obese mouse model of non-alcoholic fatty liver disease	114
Chapter 6	The impact of PPAR α activation on whole genome gene expression in human precision cut liver slices	136
Chapter 7	Gene expression profiling in human precision cut liver slices in response to the FXR agonist obeticholic acid	178
Chapter 8	ANGPTL4 promotes bile acid absorption during taurocholic acid supplementation via a mechanism dependent on the gut microbiota	204
Chapter 9	Loss of ANGPTL4 in diet-induced obese mice uncouples visceral obesity from glucose intolerance partly via a mechanism dependent on the gut microbiota	236
Chapter 10	General discussion	264
	Summary	288
	Acknowledgements	294
	About the author	300

1



General introduction



Metabolic health

Metabolism is a term that describes all the physical and chemical processes occurring within a living cell or organism that are necessary for the maintenance of life. To stay metabolically healthy, the body needs to adapt its metabolism in response to continuously changing external factors such as diet, fasting, exercise and temperature (1, 2). The liver is one of the largest organs of the human body and has a crucial role in metabolism. By producing bile acids, the liver facilitates the digestion and absorption of dietary lipids. Depending on the metabolic state, the liver can also convert carbohydrates, lipids and proteins into substrates to be used by other organs. For example, in the postprandial state glucose is converted into glycogen or into fatty acids when glycogen stores are replenished. These fatty acids are subsequently esterified with glycerol to form triglycerides and stored in the liver as such, or packaged and secreted into the circulation as very low-density lipoproteins. In the fasted state, glycogen will be converted back into glucose and released into the circulation to provide energy for extrahepatic tissues and to maintain blood glucose levels. Upon prolonged fasting when the glycogen stores are depleted, the liver will convert adipose tissue-derived fatty acids into ketone bodies to provide an alternative energy source for the brain (3). In addition to its role in energy metabolism, the liver also has a major role in the detoxification of toxic substances and the production of plasma proteins.

Considering the various functions of the liver, dysfunction of the liver may cause or predispose to disease, including non-alcoholic fatty liver disease (NAFLD). NAFLD describes a spectrum of liver diseases ranging from simple steatosis to non-alcoholic steatohepatitis, liver fibrosis and cirrhosis, and is often associated with impaired metabolic health.

Non-alcoholic fatty liver disease

The prevalence of non-alcoholic fatty liver disease (NAFLD) is closely aligned with the increasing prevalence of obesity and related insulin resistance and has become one of the most common liver diseases worldwide (4). While the estimated prevalence of NAFLD is around 20-30% in the western population, the prevalence rises up to 70% in patients with type 2 diabetes (5) and up to 90% in morbidly obese individuals (6, 7).

The earliest stage of NAFLD is hepatic steatosis and is characterized by intracytoplasmic lipid accumulation in the hepatocytes. The majority of these lipids derive from fatty acids released by the adipose tissue or from dietary fatty acids and sugars which will be turned into triglycerides in the liver (8). NAFLD is in general a benign condition, but about 25% of the patients with NAFLD progress to non-alcoholic steatohepatitis (NASH). NASH is characterized by inflammation, hepatocellular ballooning and often fibrosis, and may lead to cirrhosis. In this advanced form of liver fibrosis, healthy liver tissue is replaced by collagen

and may eventually result in liver failure, portal hypertension and hepatocellular carcinoma (9).

Patients with NAFLD not only exhibit liver-related complications but also have an increased risk of developing cardiovascular disease (10). Importantly, cardiovascular disease is the most common cause of death in patients with NAFLD (11). As the exact pathogenesis of NAFLD is unknown and since NAFLD and cardiovascular disease have shared metabolic risk factors, it is difficult to dissect how NAFLD contributes to cardiovascular disease (10). Therefore, getting a better understanding of the underlying mechanisms of NAFLD may not only provide targets for treatment of NAFLD but also of cardiovascular disease.

In the past two decades several models have been proposed for the progression of steatosis to non-alcoholic steatohepatitis (12, 13). The current ‘multiple parallel hits’ hypothesis considers multiple factors acting together and thereby contributing to the progression of NAFLD, including genetic predisposition, lipid overload and inflammatory insults. Recently, factors deriving from the gastrointestinal tract are increasingly being recognized to play a role in the progression of steatosis to non-alcoholic steatohepatitis (13, 14) (see **Figure 1** for further details).

Gastrointestinal tract

The major functions of gastrointestinal tract are to digest food, to extract and absorb energy and nutrients, and to excrete the remaining waste as feces and urine. These functions are achieved by the different physiological roles of the different organs along the gastrointestinal tract. While the digestive process starts in the mouth and stomach, the majority of the food components will be digested and absorbed in the small intestine. Part of the food components that cannot be digested in the small intestine will reach the large intestine for further microbial fermentation. After the extraction of water and salts, the undigested food material will be excreted as feces (16).

Intestinal barrier

In addition to the primary function of the intestine to digest and absorb nutrients and fluids, the intestine also needs to protect the underlying tissues against harmful substances and pathogens from the external environment. The intestinal barrier is composed of several layers (**Figure 2**). The first line of defence is a layer of mucus that covers the intestinal epithelial cells. The mucus layer is a hydrated gel which is formed by mucins produced by the goblet cells located in the epithelium. The importance of the mucus layer has been shown in mice lacking the main constituent of the mucus layer, Muc2 mucin. These mice spontaneously develop colitis (17). In the intestine, the thickness of the mucus layer gradually increases from ~150-300µm in the small intestine to ~700µm in the large intestine, reflecting the increase

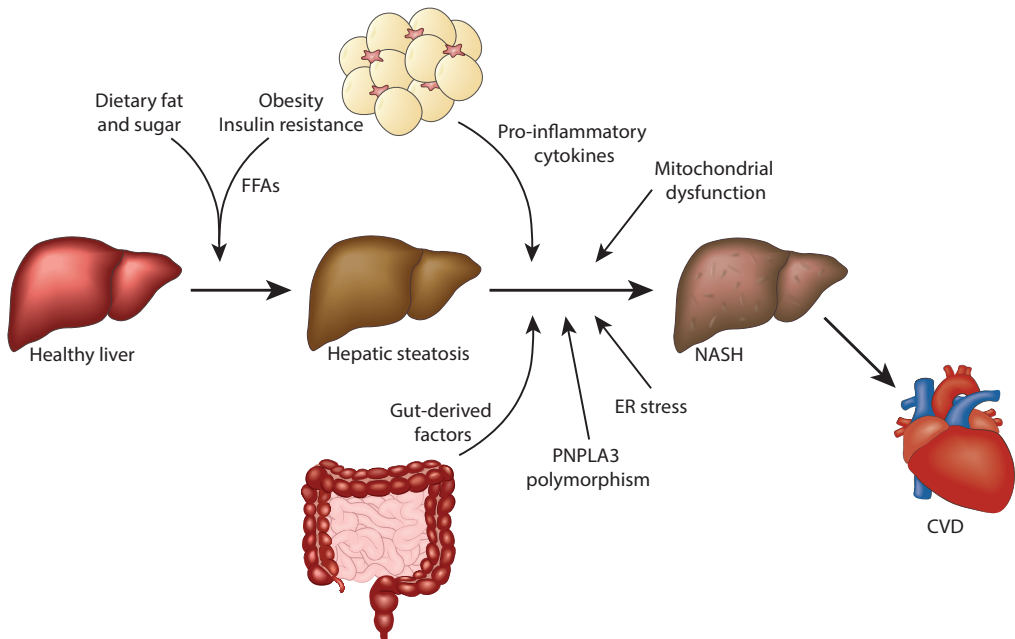


Figure 1. Multiple parallel hits hypothesis in NAFLD

The ‘first hit’ of NAFLD consists of the accumulation of triglycerides in the liver and is thought to be primarily caused by insulin resistance, which is closely related to obesity. Consequently, hyperinsulinemia results in increased lipolysis in the adipose tissue concomitant with increased hepatic *de novo* lipogenesis which, together with increased dietary fat and sugar intake, will lead to triglyceride accumulation in the liver. Hepatic steatosis in turn is considered to enhance the susceptibility of the liver to multiple concurrent hits which may lead to hepatic injury and the progression from simple steatosis to nonalcoholic steatohepatitis (NASH). Such multiple factors may include pro-inflammatory cytokines from the adipose tissue, factors from the gut (e.g. endotoxins), mitochondrial dysfunction and ER stress (13). Moreover, also genetic factors, including a polymorphism in the patatin-like phospholipase domain-containing 3 gene (PNPLA3), have increasingly been recognized as a risk factor for NAFLD progression (15). NASH may eventually lead to cardiovascular disease (CVD), which is the most common cause of death in patients with NAFLD (11).

in microbial numbers along the intestinal tract (18). Based on histological observations, the mucus layer can be divided into two layers, an outer loose layer and a more dense inner layer (19). The outer mucus layer, also known as the non-adherent layer, is constantly degraded by the luminal microbiota and replenished by mucus from the inner layer (20). Whereas the outer mucus layer provides a habitat for commensal microbiota, the inner layer is nearly sterile (21). The inner dense mucus layer prevents penetration of the intestinal microbiota due to its dense polymeric network which is reinforced by a range of antimicrobial peptides produced by Paneth cells (for example α -defensins, RegIII γ and lysozymes) or by enterocytes (RegIII γ) (22) (**Figure 2**). Indeed, mice lacking RegIII γ have increased numbers of bacteria penetrating the mucus layer resulting in low-grade inflammation (23, 24).

The second physical barrier of defence is the epithelial layer and is composed of enterocytes, goblet cells, Paneth cells (located only in the small intestine) and enteroendocrine cells (**Figure 2**). To allow the uptake of nutrients and fluids while preventing the uptake of harmful substances, the passage of these molecules across the intestinal wall needs to be carefully regulated. The absorption of amino acids, sugars and fatty acids occurs via transcellular transport and is regulated by specific transporters at the apical and basolateral membrane of the enterocyte (25–27). To prevent leakage, the epithelial cells are sealed by a number of protein complexes, including tight junctions, adherens junctions and desmosomes. Whereas the desmosomes and adherens junctions are mainly involved in cell-cell adhesion and intracellular signaling respectively, tight junctions have a central role in regulating the permeability of the intestinal barrier (28). Tight junctions are located at the apical site of the endothelium and prevent passage of pathogens, bacteria and toxins, while providing a dynamic barrier for ions, water and other molecules in a size- and charge-dependent manner (29–31). The tight junctional complex is composed of various transmembrane proteins, including occludins and claudins, that are connected to the actin cytoskeleton of adjacent cells via intracellular scaffold proteins such as zonula occludens (28, 32). The structure of the tight junction is constantly remodelled in response to external stimuli and is closely associated with health and susceptibility to disease (31, 33). Disruption of the tight junction affects intestinal barrier function and may lead to increased translocation of pro-inflammatory molecules resulting in inflammation and tissue damage. For example, an increased intestinal permeability is thought to contribute to the pathogenesis of several gastrointestinal diseases, including inflammatory bowel disease and celiac disease (34, 35). Interestingly, disruption of the tight junction complexes have more recently also been linked to obesity and related metabolic disorders (36). Compared to lean mice, obese mice were shown to have reduced expression of occludin and claudin-1 in association with elevated levels of circulating endotoxins and pro-inflammatory cytokines, and increased adipose tissue inflammation (37). In addition to obesity, tight junction proteins have also been found to be reduced in a mouse model of NAFLD (38). Similar results have been observed in humans as patients with NAFLD displayed lower expression of the tight junctional protein zonula occludens 1 than healthy individuals, suggesting that patients with NAFLD have increased intestinal permeability. Intriguingly, it was also found that the degree of intestinal permeability in human subjects positively correlated with the degree of steatosis (39). However, whether aberrant expression of tight junction proteins is causally involved in obesity and related disorders or is a consequence of the disturbed metabolism remains unknown.

The third layer of intestinal defence is composed of the immune cells located in the connective tissue below the epithelial layer called lamina propria and is referred to as the

gut-associated lymphoid tissue (GALT) (**Figure 2**). GALT is comprised of diffusely scattered lymphocytes in the lamina propria and in the epithelial layer, and organized lymphoid structures, including Peyer's patches and isolated lymphoid follicles (40). These organized lymphoid structures are covered by a particular epithelium, called follicular-associated epithelium, which forms the interface between the GALT and intestinal lumen. Specialized microfold (M) cells, located in the follicular-associated epithelium, sample the intestinal lumen and are able to transport antigens to the underlying immune cells (40, 41). In addition to M cells, epithelial cells and dendritic cells also have a key role in initiating an immune response.

Such an immune response can be immunogenic to pathogenic bacteria or tolerogenic to commensal microbes. A subset of dendritic cells is directly connected with the intestinal lumen via extensions through epithelial tight junctions (**Figure 2**). Epithelial cells and immune cells, such as dendritic cells, recognize microbes in the intestinal lumen through pattern recognition receptors. These receptors recognize common structures on microbial surfaces via so-called pathogen- or microbe-associated molecular patterns (42). The Toll-like receptor (TLR) family is the best characterized family of pattern recognition receptors. In humans, ten different toll-like receptors have been identified, thereby enabling the immune system to detect different microbial structures. For example, TLR4 recognizes the gram-negative cell wall component lipopolysaccharide, whereas TLR3 recognizes viral double-stranded RNA (43). Stimulation of these pattern recognition receptors result in activation of immune cells, which in turn regulate the adaptive immune response and enhance the production and secretion of cytokines, chemokines and antimicrobial peptides such as Immunoglobulin A (43–45).

Taken together, the three layers of the intestinal barrier serve as a gatekeeper for harmful substances and pathogens from the external environment and control host defences to maintain intestinal homeostasis.

Factors influencing metabolic health

As mentioned above, the liver and the intestine have an important role in mediating metabolic health but are also affected by changes in metabolic health. Over the last two decades three factors have increasingly been linked to metabolic health, which include the gut microbiota, bile acids and the glycoprotein ANGPTL4.

Gut microbiota

The gastrointestinal tract harbours a large and complex community of microorganisms, collectively known as the gut microbiota. This community consist of approximately 10^{14} microorganisms and includes fungi, archaea, viruses and protozoa but is by far dominated

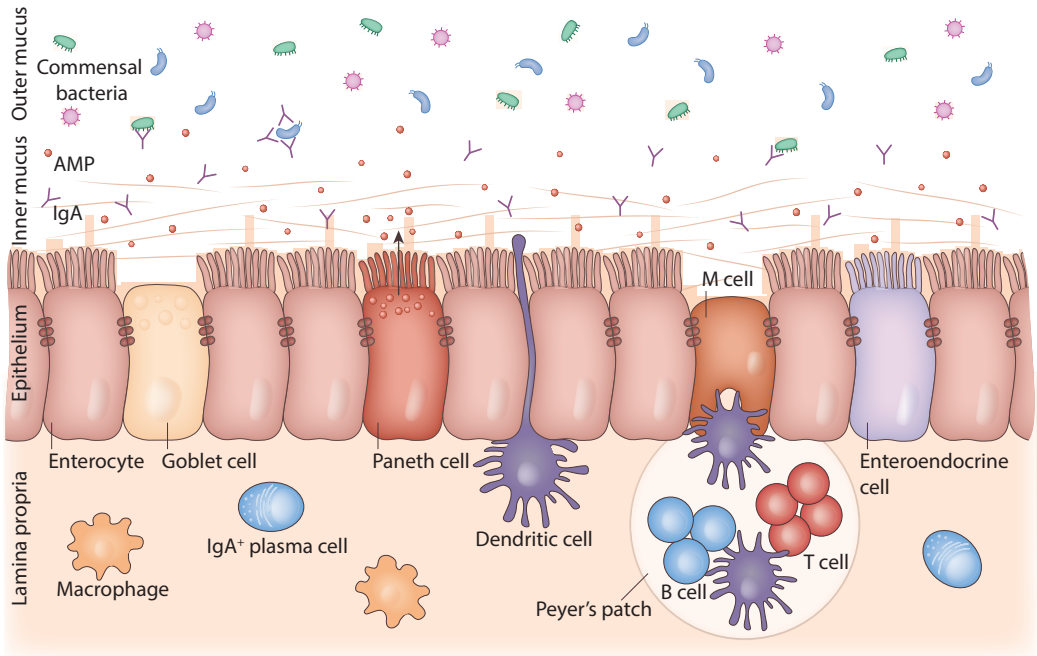


Figure 2. Schematic figure of the intestinal barrier

The three layers of the intestinal barrier consist of the mucus layer, the epithelial layer and the underlying immune cells located in the lamina propria. The mucus layer is composed of mucins produced by goblet cells and consists of an inner dense layer and an outer loose layer. The outer mucus layer is constantly degraded by the luminal microbiota and replenished by mucus from the inner layer. The inner dense mucus layer is devoid of intestinal microbiota due to its dense polymeric network which is reinforced by a range of antimicrobial peptides (AMP) and immunoglobulin A (IgA) (18). The epithelial layer consists of a single layer of epithelial cells which physically separates the intestinal lumen from the underlying tissues of the body. The tight junctions located at the apical site of the endothelium seal adjacent cells and prevent passage of pathogens, bacteria and toxins (28). The gut-associated lymphoid tissue in the lamina propria contains various immune cells, including macrophages, dendritic cells, T cells, B cells and IgA producing plasma cells. These immune cells are diffusely scattered in the lamina propria or are located in organized lymphoid structures, such as Peyer's patches. Microfold (M) cells located in the follicular-associated epithelium of Peyer's patch sample together with dendritic cells and epithelial cells luminal antigens. The resulting immune response can be either immunogenic to pathogenic bacteria or tolerogenic to commensal bacteria (40).

by the presence of ~500-1000 different species of bacteria (46, 47). The gut microbiota lives in close relationship with the host and have an essential role in several aspects of host physiology. For example, the microbiota confers protection against invading pathogens (48), produce essential vitamins (49), maintain tissue homeostasis and are required for the full development of the immune system (50). Indeed, germ-free mice have an undeveloped mucosal immune system displaying smaller and fewer Peyer's patches, mesenteric lymph nodes, goblet cells and IgA-secreting plasma cells than conventionally-raised mice (50–52).

Intestinal microbes also benefit from the mutualistic relationship with the host, as the

host provides a relatively stable habitat that is rich in energy. Whereas some bacterial species (e.g. *Akkermansia muciniphila*) can use mucins in the mucus layer as a source of energy (53), other bacteria (e.g. *Bifidobacterium spp*) obtain their energy from the degradation and fermentation of indigestible complex carbohydrates, such as dietary fibers (54). The fermentation of these carbohydrates liberate short-chain fatty acids (SCFAs), including acetate, propionate and butyrate, which can in turn be utilized by other bacterial species, a phenomenon called cross-feeding (55, 56), or absorbed by the host. Approximately 95% of the produced SCFAs is rapidly absorbed in the colon resulting in limited fecal SCFA loss (57). In the host, butyrate is mainly used as a fuel by the colonic epithelial cells and the remainder of the SCFAs is largely taken up by the liver, where butyrate and acetate can be used as precursors for lipogenesis and propionate can be used for gluconeogenesis (56, 58, 59).

The gut microbiota of a healthy individual is dominated by two phyla, namely Firmicutes and Bacteroidetes, which are complemented with many other minor phyla, including Actinobacteria, Proteobacteria and Verrucomicrobia (60, 61). Although the intraindividual microbiota composition has been reported to be relatively stable over time (62–64), the microbiota composition varies greatly between individuals (61, 65). The interindividual differences in gut microbiota composition are caused by both genetic and environmental factors, such as diet, exercise, medication use and hygiene but may also be influenced by specific diseases (66–68). Alterations in gut microbiota composition may be unfavourable and may in turn also predispose an individual to disease. Indeed, dysbiosis has been implicated in several gastrointestinal diseases, including inflammatory bowel disease and colorectal cancer (69, 70), but is also thought to contribute to metabolic disorders such as obesity, diabetes type 2, cardiovascular disease and NAFLD (71–75). For example, it has been demonstrated that germ-free mice are resistant to diet-induced obesity, hepatic steatosis and insulin resistance (71, 72, 76) and that transplantation of intestinal microbiota from conventionally-raised mice to germ-free mice induced obesity, hepatic steatosis and insulin resistance (71). Several mechanisms have been proposed to mediate the effects of the gut microbiota on metabolic health, including lipopolysaccharides, short-chain fatty acids, bile acids and angiopoietin-like protein 4 (75). In **Chapter 2** and **Chapter 3** of this thesis, the evidence related to the role of the gut microbiota in metabolic health, including potential underlying mechanisms, is more extensively described.

Bile acids

In addition to the gut microbiota, bile acids have also been suggested to impact metabolic health. Bile acids are amphipathic steroids and are best known for their role in lipid absorption. Bile acids are synthesized in the liver from cholesterol via two pathways.

The main pathway, also known as the classical pathway, is initiated by the rate limiting enzyme CYP7A1 and results in the production of cholic acid (CA) and chenodeoxycholic acid (CDCA), whereas the alternative pathway is initiated by CYP27A1 and predominantly generates CDCA (77) (**Figure 3**). In the classical pathway, CYP8B1 is required for the

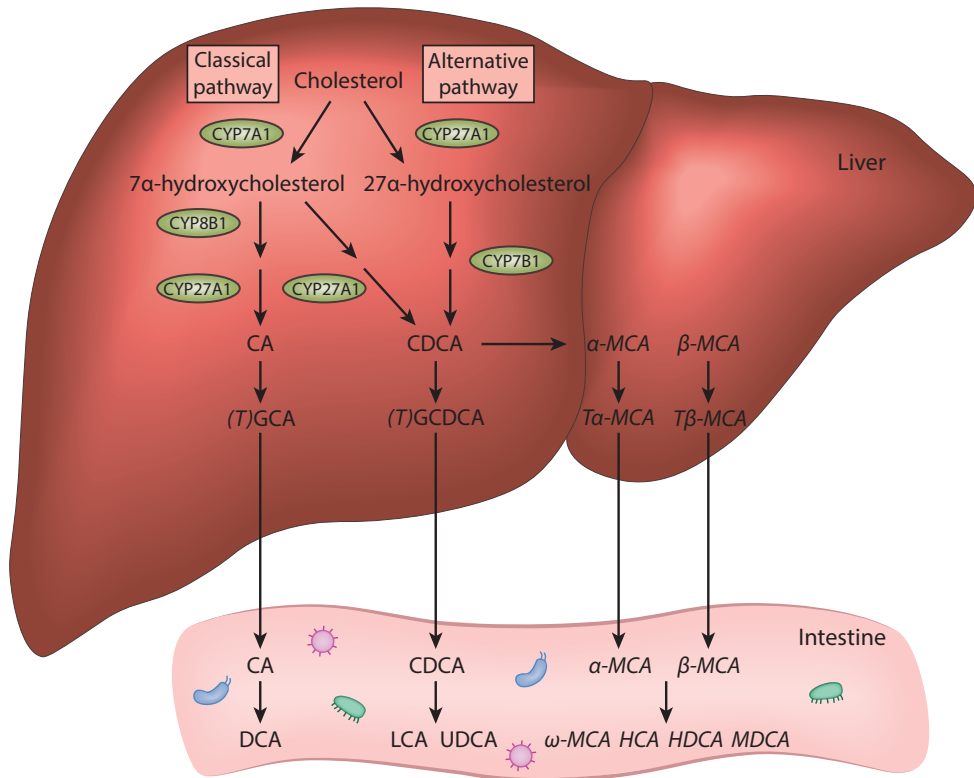


Figure 3. Bile acid synthesis pathways

Bile acids are synthesized in the liver from cholesterol via two pathways: the classical and the alternative pathway. The classical pathway is initiated by the rate-limiting enzyme CYP7A1 which converts cholesterol into 7 α -hydroxycholesterol leading to the formation of cholic acid (CA) and chenodeoxycholic acid (CDCA) (77). The synthesis of CA is regulated by CYP8B1 (78). In the alternative pathway, cholesterol is first converted into 27 α -hydroxycholesterol by the action of CYP27A1, eventually also leading to the formation of CDCA (77). In mouse liver, most of the CDCA is converted to α -muricholic acid (α -MCA) and β -muricholic acid (β -MCA) (79, 80). After the formation, these primary bile acids are predominantly conjugated to either glycine, in humans, or to taurine, in rodents, by the enzymes bile acid-CoA synthetase (BACS) and bile acid-CoA: amino acid N-acetyltransferase (BAT) and subsequently secreted into bile (77, 81). In the intestine, the bacteria deconjugate the bile acids to their respective unconjugated free bile acids by bile salt hydrolases and then form secondary bile acids through 7 α /7 β -dehydroxylation, oxidation and epimerization (82). Bile acids are reabsorbed in the ileum and returned to the liver via the portal vein where the secondary bile acids can also be conjugated to taurine or glycine (83, 84). Bile acids formed in mouse liver and intestine are indicated in italics.

production of CA and therefore determines the relative production of CA and CDCA (78). In contrast to humans, rodents also produce muricholic acid (MCA) as primary bile acid, though the enzyme responsible for the conversion of CDCA into MCAs remains unknown (79, 80). After their formation, bile acids are conjugated predominantly to glycine, in humans, or to taurine, in rodents, which increases the hydrophilicity and thus the solubility of the bile acids (**Figure 3**). These bile acids are subsequently transported into the gall bladder via the bile salt exporter protein (BSEP; ABCB11) where they will be concentrated into bile together with phospholipids and cholesterol (85). Upon the ingestion of a meal, bile is released into the duodenum to facilitate the digestion and absorption of dietary lipids by pancreatic lipase (86). Approximately 95% of the bile acids are actively reabsorbed by the apical sodium-dependent bile acid transporter (ASBT; SLC10A2) in the distal ileum and returned to the liver via a process referred to as the enterohepatic cycle (83) (see **Figure 4** for further details). However, intestinal microbiota possessing active bile salt hydrolase activity can deconjugate the primary bile acids and thereby limit the reabsorption of bile acids from the small intestine (82, 87). These deconjugated primary bile acids are subsequently further converted into more hydrophobic secondary bile acids through $7\alpha/7\beta$ -dehydroxylation, epimerization and oxidation by the intestinal microbiota, of which only a minor part reaches the liver through passive reabsorption (82, 84, 87) (**Figure 3**). Taken together, the microbial metabolism of bile acids increases bile acid diversity but also contributes to a more hydrophobic and thus toxic bile acid pool (87).

To prevent accumulation of potentially cytotoxic bile acids, bile acid transport and metabolism are tightly regulated within the liver and intestine. When the bile acid pool increases, a negative feedback mechanism is activated to suppress bile acid synthesis. In the liver, bile acids can directly inhibit the expression of *CYP7A1* via the activation of farnesoid X receptor (FXR) or indirect via the induction of FGF19 (or FGF15 in rodents) through intestinal FXR activation (77) (see **Figure 4** for further details). FXR can thus be seen as a bile acid sensor controlling the bile acid pool. However, it is now increasingly recognized that beyond the role of regulating bile acid metabolism, FXR also influences lipid, glucose and energy metabolism. Consequently, bile acids have emerged as signaling molecules regulating metabolic homeostasis (91, 92). Indeed, activation of FXR by bile acids has been shown to lower plasma triglyceride levels (93–95), and to suppress gluconeogenesis and lower plasma glucose levels (96, 97). The effects of bile acids on glucose metabolism seem to occur not solely via FXR but may also be mediated via the G protein-coupled bile acid receptor TGR5. Activation of TGR5 by bile acids has been shown to stimulate GLP-1 secretion and enhance glucose tolerance (98, 99). In addition to the effects on glucose homeostasis, bile acid-mediated TGR5 activation is also suggested to affect energy expenditure (100) and inflammation (101). Although it is widely accepted that bile acids are important regulators

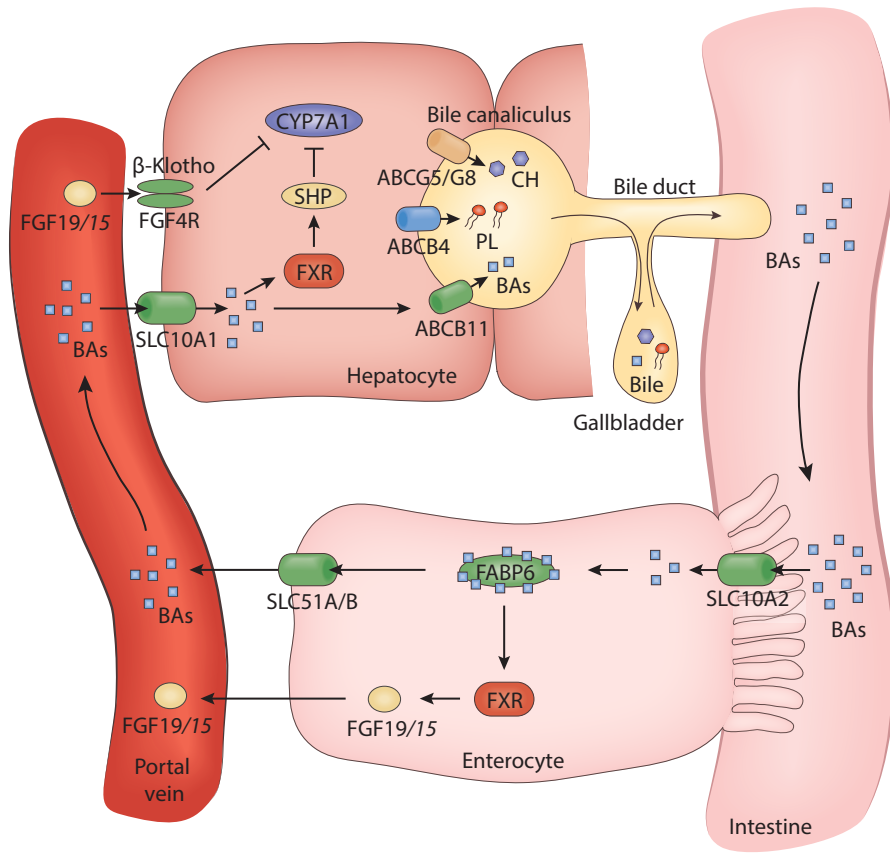


Figure 4. Enterohepatic circulation of bile acids

Bile acids are synthesized in the liver and transported across the bile canalicular membrane into the gall bladder via ABCB11 (BSEP) where they will be concentrated into bile together with phospholipids (PL) and cholesterol (CH) (83, 85). Upon the ingestion of a fatty meal, the gall bladder contracts and bile acids are released into the duodenum to facilitate the digestion and absorption of dietary lipids. Roughly 95% of the bile acids are reabsorbed in the ileum via SLC10A2 (ASBT) present on the enterocyte brush border (83, 84). Within the enterocytes, bile acids activate FXR to induce the expression of *FABP6* (I-BABP) and the transporters *SLC51A* (OST α) and *SLC51B* (OST β) that facilitate the excretion of the bile acids into the portal blood (88, 89). Activation of FXR also induces the expression and secretion of *FGF19* (FGF15 in rodents) which signals via the FGF receptor 4 (FGF4R) – β -Klotho receptor on the hepatocytes to limit bile acid synthesis through inhibition of *CYP7A1* (88, 90). Bile acids are taken up in the hepatocytes via SLC10A1 (NTCP). Binding of bile acids to FXR results in the expression of *SHP*, also leading to downregulation of *CYP7A1* expression (83, 89).

of metabolic homeostasis, the exact relationship between bile acids and metabolism remains unknown. So far it is well-established that the amount and type of reabsorbed bile acids varies as a result of diet, drugs, disease and microbiota. Furthermore, it is known that different bile acid species have a different potency to activate FXR and TGR5 and that the

expression and activity of FXR may be modulated depending on metabolic status e.g. during diabetes type 2 (91).

Angiopoietin-like protein 4

Another important mediator of metabolic health is angiopoietin-like protein 4 (ANGPTL4). ANGPTL4 is a 50kDa glycosylated protein belonging to the angiopoietin-like protein family and is best known for regulating lipid metabolism via the inhibition of LPL activity. Indeed, ANGPTL4 knock-out mice display reduced plasma triglyceride levels (102). As all members of the ANGPTL family, the ANGPTL4 protein consists of a N-terminal coiled-coil domain, a linker region and a C-terminal fibrinogen-like domain. Only ANGPTL8 is an exception as it lacks the fibrinogen-like domain (103, 104). ANGPTL4 is subjected to posttranscriptional modifications including the cleavage of ANGPTL4 into a N-terminal and C-terminal fragment exerted by proprotein convertases (105). Of these two fragments, the N-terminal ANPGTL4 has been shown to inhibit LPL activity by converting active LPL dimers into inactive LPL monomers (106). However a mechanism by which ANGPTL4 noncompetitively inhibits LPL has also been suggested (107). The inactivation of LPL by ANGPTL4 has been suggested to occur in the interstitial space and on the endothelial surface (108) but has more recently also been shown to also occur inside the cell just after posttranslational processing of LPL in the ER (109).

Angptl4 is ubiquitously expressed with the highest expression in the adipose tissue and liver followed by the intestine, heart and skeletal muscle (103, 110–112). The induction of *Angptl4* is under transcriptional control by the peroxisome proliferator-activated receptors (PPARs) family of nuclear receptors that includes PPAR α , PPAR δ and PPAR γ (110, 113–115). As fatty acids are potent inducers of PPARs, the elevation of free fatty acids during various physiological conditions stimulates the expression of *Angptl4*, subsequently leading to the inhibition of LPL. For example, during fasting, the lipolysis-mediated free fatty acid release induces the expression *Angptl4* to inhibit LPL activity specifically in the white adipose tissue (116). Consequently, the hydrolysis of triglycerides by the white adipose tissue is prevented and triglyceride-rich lipoproteins are redirected to other tissues that are in demand of energy (110, 116). Similarly, the induction of *Angptl4* in white adipose tissue upon cold exposure inhibits the activity of LPL to ensure the provision of energy to brown adipose tissue for the generation of heat (117). Also, during exercise, elevated circulating free fatty acid levels induce *Angptl4* specifically in the non-exercising muscle to inhibit the activity of LPL and to direct VLDL-rich lipoproteins to the exercising muscle (111).

As mentioned previously, the liver has a pivotal role in lipid metabolism and also abundantly expresses *Angptl4* (110). However the expression of LPL in the liver is very low. Consequently, as opposed to the local inhibitory effect of ANGPTL4 on LPL in the adipose

tissue, muscle and heart, it has been suggested that ANPGTL4 in the liver may have an endocrine function. Indeed, mice with liver-specific overexpression of *Angptl4* displayed reduced post-heparin plasma LPL activity and increased plasma triglyceride levels (102).

Similar to the liver, *Angptl4* is also well expressed in the intestine while LPL is not. Although it has been suggested that intestinal *Angptl4* also functions in an endocrine fashion by inhibiting LPL activity in peripheral tissues (71), direct evidence is lacking. Recently, however it has been suggested that ANGPTL4 may act locally in the intestine by inhibiting pancreatic lipase, a structural homolog of LPL. Consequently, mice lacking *Angptl4* have enhanced dietary lipid absorption, resulting in higher fat mass and bodyweight (112). The expression of intestinal *Angptl4* has been found to be under transcriptional control of gut microbiota as mice devoid of any microbiota have relatively higher levels of intestinal *Angptl4* mRNA than conventionally-raised mice (118). In apparent contrast, bacterial-derived metabolites, such as short-chain fatty acids, were shown to induce *Angptl4* (119, 120). The exact mechanism by which the gut microbiota regulate the expression of intestinal *Angptl4* is not fully understood.

Outline of this thesis

As discussed above, there are many factors that may influence our metabolism. Since obesity and related metabolic disturbances such as NAFLD have become an immense global health problem, it is of utmost importance to understand the causes of these metabolic disorders. The main aim of this thesis was therefore **to increase our understanding regarding the role of various mediators in metabolic health with a special focus on the gut microbiota, bile acids and ANGPTL4**. This thesis is divided in three parts. In the first part, we focus on the role of the gut microbiota in metabolic health. Therefore, in **Chapter 2**, we provide an overview of the knowledge regarding the role of the gut microbiota in metabolic health. Subsequently, in **Chapter 3**, we more critically evaluate the evidence related to the causal role of the gut microbiota in metabolic diseases. In **Chapter 4**, the objective was to investigate the influence of changes in gut microbiota composition in NAFLD. We therefore first verified a diet-induced mouse model to study NAFLD and subsequently performed a study in which we modulated the gut microbiota using dietary fibers and antibiotics. We demonstrated that the gut microbiota have a marked impact on the development of NAFLD, which is likely mediated via changes in the portal delivery of bile acids. Accordingly, in **Chapter 5** we investigated the therapeutic effect of the administration of the bacteria, *A. muciniphila* and *B. thetaiotaomicron*, on NAFLD. We found that in this experimental setup neither of the two bacterial species influences NAFLD.

In the second part, the focus lies on the establishment of an *ex vivo* system to study the effects of microbial metabolites on human liver. In **Chapter 6**, we demonstrate the suitability

of precision-cut liver slices (PCLS) as a model to study human liver using the PPAR α agonist Wy14643. Subsequently, in **Chapter 7**, we study the effect of the novel drug, obeticholic acid, a semi-synthetic bile acid that is now in phase 3 clinical trial for non-alcoholic steatohepatitis, on whole genome gene expression using human PCLS.

In the third part, we focus on the role of ANGPTL4 in metabolic health and reveal two novel functions of ANGPTL4. Using *Anpgtl4*^{-/-} mice we show in **Chapter 8** that ANGPTL4 influences intestinal bile acid absorption while **Chapter 9** describes an important new role of ANGPTL4 in the regulation of glucose metabolism in diet-induced obese mice. Finally, an overall evaluation and interpretation of the data is provided in **Chapter 10**.

References

1. Galgani, J., and Ravussin, E. (2008) Energy metabolism, fuel selection and body weight regulation. *Int. J. Obes.* **32**, S109–19
2. Jeukendrup, A. E. (2003) Modulation of carbohydrate and fat utilization by diet, exercise and environment. *Biochem. Soc. Trans.* **31**, 1270–1273
3. Rui, L. (2014) Energy Metabolism in the Liver. *Compr Physiol.* **4**, 177–197
4. Dietrich, P., and Hellerbrand, C. (2014) Non-alcoholic fatty liver disease, obesity and the metabolic syndrome. *Best Pract. Res. Clin. Gastroenterol.* **28**, 637–653
5. Targher, G., Bertolini, L., Padovani, R., Rodella, S., Tessari, R., Zenari, L., Day, C., and Arcaro, G. (2007) Prevalence of Nonalcoholic Fatty Liver Disease and Its Association With Cardiovascular Disease Among Type 2. *Diabetes Care.* **30**, 1212–8
6. Morita, S., Neto, D. D. S., Morita, F. H. A., Morita, N. K., and Lobo, S. M. A. (2015) Prevalence of Non-alcoholic Fatty Liver Disease and Steatohepatitis Risk Factors in Patients Undergoing Bariatric Surgery. *Obes. Surg.* **25**, 2335–2343
7. Machado, M., Marques-Vidal, P., and Cortez-Pinto, H. (2006) Hepatic histology in obese patients undergoing bariatric surgery. *J. Hepatol.* **45**, 600–606
8. Neuschwander-Tetri, B. A. (2017) Non-alcoholic fatty liver disease. *BMC Med.* **15**, 45
9. Rinella, M. E. (2015) Nonalcoholic Fatty Liver Disease: a systemic review. *Jama.* **313**, 2263–2273
10. Francque, S. M., van der Graaff, D., and Kwanten, W. J. (2016) Non-alcoholic fatty liver disease and cardiovascular risk: Pathophysiological mechanisms and implications. *J. Hepatol.* **65**, 425–443
11. Angulo, P., Kleiner, D. E., Dam-Larsen, S., Adams, L. A., Bjornsson, E. S., Charatcharoenwithaya, P., Mills, P. R., Keach, J. C., Lafferty, H. D., Stahler, A., Haflidadottir, S., and Bendtsen, F. (2015) Liver fibrosis, but no other histologic features, is associated with long-term outcomes of patients with nonalcoholic fatty liver disease. *Gastroenterology.* **149**, 389–397
12. Day, C. P., James, O. F. W., Macdonald, G., Cowley, L., Walker, N., Ward, P., Jazwinska, E., Powell, L., Fromenty, B., and Pessayre, D. (1998) Steatohepatitis: A tale of two “hits”? *Gastroenterology.* **114**, 842–845
13. Tilg, H., and Moschen, A. R. (2010) Evolution of inflammation in nonalcoholic fatty liver disease: The multiple parallel hits hypothesis. *Hepatology.* **52**, 1836–1846
14. Bashiardes, S., Shapiro, H., Rozin, S., Shibolet, O., and Elinav, E. (2016) Non-alcoholic fatty liver and the gut microbiota. *Mol. Metab.* **5**, 782–794
15. Chen, L. Z., Xin, Y. N., Geng, N., Jiang, M., Zhang, D. D., and Xuan, S. Y. (2015) PNPLA3 I148M variant in nonalcoholic fatty liver disease: Demographic and ethnic characteristics and the role of the variant in nonalcoholic fatty liver fibrosis. *World J. Gastroenterol.* **21**, 794–802
16. Goodman, B. E. (2010) Insights into digestion and absorption of major nutrients in humans. *AJP Adv. Physiol. Educ.* **34**, 44–53
17. Van der Sluis, M., De Koning, B. A. E., De Bruijn, A. C. J. M., Velcich, A., Meijerink, J. P. P., Van Goudoever, J. B., Büller, H. A., Dekker, J., Van Seuningen, I., Renes, I. B., and Einerhand, A. W. C. (2006) Muc2-Deficient Mice Spontaneously Develop Colitis, Indicating That MUC2 Is Critical for Colonic Protection. *Gastroenterology.* **131**, 117–129
18. McGuckin, M. A., Lindén, S. K., Sutton, P., and Florin, T. H. (2011) Mucin dynamics and enteric pathogens. *Nat. Rev. Microbiol.* **9**, 265–278
19. Matsuo, K., Akamatsu, T., and Katsuyama, T. (1997) Histochemistry of the surface mucous gel layer of the human colon. *Gut.* **40**, 782–789
20. Johansson, M. E. V., Larsson, J. M. H., and Hansson, G. C. (2011) The two mucus layers of colon are organized by the MUC2 mucin, whereas the outer layer is a legislator of host-microbial interactions. *Proc. Natl. Acad. Sci.* **108**, 4659–4665
21. Johansson, M. E. V., Phillipson, M., Petersson, J., Velcich, A., Holm, L., and Hansson, G. C. (2008) The inner of the two Muc2 mucin-dependent mucus layers in colon is devoid of bacteria. *Proc Natl Acad Sci U S A.* **105**, 15064–15069
22. Bevins, C. L., and Salzman, N. H. (2011) Paneth cells, antimicrobial peptides and maintenance of intestinal homeostasis. *Nat. Rev. Microbiol.* **9**, 356–368
23. Loonen, L. M., Stolte, E. H., Jaklofsky, M. T., Meijerink, M., Dekker, J., van Baarlen, P., and Wells, J. M. (2013) REG3γ-deficient mice have altered mucus distribution and increased mucosal inflammatory responses to the microbiota and enteric pathogens in the ileum. *Mucosal Immunol.* **7**, 939–947
24. Vaishnava, S., Yamamoto, M., Severson, K. M., Ruhn, K. a, Yu, X., Koren, O., Ley, R., Wakeland, E. K., and Hooper, L. V. (2011) The Antibacterial Lectin RegIII γ Promotes the Spatial Segregation of Microbiota and Host in the Intestine. *Science.* **334**, 255–258
25. Drozdowski, L., and Thomson, A. B. R. (2006) Intestinal sugar transport. *World J. Gastroenterol.* **12**, 1657–1670

26. Hussain, M. M. (2014) Intestinal lipid absorption and lipoprotein formation. *Curr. Opin. Lipidol.* **25**, 200–206
27. Bro, S. (2008) Amino Acid Transport Across Mammalian Intestinal and Renal Epithelia. *Physiol. Rev.* **88**, 249–286
28. Groschwitz, K. R., and Hogan, S. P. (2009) Intestinal barrier function: molecular regulation and disease pathogenesis. *J. Allergy Clin. Immunol.* **124**, 3–22
29. Van Itallie, C. M., Holmes, J., Bridges, A., Gookin, J. L., Coccaro, M. R., Proctor, W., Colegio, O. R., and Anderson, J. M. (2008) The density of small tight junction pores varies among cell types and is increased by expression of claudin-2. *J. Cell Sci.* **121**, 298–305
30. Weber, C. R. (2012) Dynamic properties of the tight junction barrier. *Ann. N. Y. Acad. Sci.* **1257**, 77–84
31. Ulluwishewa, D., Anderson, R. C., McNabb, W. C., Moughan, P. J., Wells, J. M., and Roy, N. C. (2011) Regulation of Tight Junction Permeability by Intestinal Bacteria and Dietary Components. *J. Nutr.* **141**, 769–776
32. Chiba, H., Osanai, M., Murata, M., Kojima, T., and Sawada, N. (2008) Transmembrane proteins of tight junctions. *Biochim. Biophys. Acta - Biomembr.* **1778**, 588–600
33. Bischoff, S. C., Barbara, G., Buurman, W., Ockhuizen, T., Schulzke, J.-D., Serino, M., Tilg, H., Watson, A., and Wells, J. M. (2014) Intestinal permeability – a new target for disease prevention and therapy. *BMC Gastroenterol.* **14**, 189
34. Michielan, A., and D'Inca, R. (2015) Intestinal Permeability in Inflammatory Bowel Disease: Pathogenesis, Clinical Evaluation, and Therapy of Leaky Gut. *Mediators Inflamm.* **2015**, 628157
35. Su, L., Shen, L., Clayburgh, D. R., Nalle, S. C., Sullivan, E. A., Meddings, J. B., Abraham, C., and Turner, J. R. (2009) Targeted Epithelial Tight Junction Dysfunction Causes Immune Activation and Contributes to Development of Experimental Colitis. *Gastroenterology.* **136**, 551–563
36. Teixeira, T. F. S., Collado, M. C., Ferreira, C. L. L. F., Bressan, J., and Peluzio, M. do C. G. (2012) Potential mechanisms for the emerging link between obesity and increased intestinal permeability. *Nutr. Res.* **32**, 637–647
37. Kim, K. A., Gu, W., Lee, I. A., Joh, E. H., and Kim, D. H. (2012) High Fat Diet-Induced Gut Microbiota Exacerbates Inflammation and Obesity in Mice via the TLR4 Signaling Pathway. *PLoS One.* **7**, e47713
38. Brun, P., Castagliuolo, I., Leo, V. Di, Buda, A., Pinzani, M., Palu, G., and Martinez, D. (2007) Increased intestinal permeability in obese mice: new evidence in the pathogenesis of nonalcoholic steatohepatitis. *Am. J. Physiol. - Gastrointest. Liver Physiol.* **292**, 518–525
39. Miele, L., Valenza, V., La Torre, G., Montalto, M., Cammarota, G., Ricci, R., Mascianà, R., Forgione, A., Gabrieli, M. L., Perotti, G., Vecchio, F. M., Rapaccini, G., Gasbarrini, G., Day, C. P., and Grieco, A. (2009) Increased intestinal permeability and tight junction alterations in nonalcoholic fatty liver disease. *Hepatology.* **49**, 1877–1887
40. Mowat, A. M., and Agace, W. W. (2014) Regional specialization within the intestinal immune system. *Nat. Rev. Immunol.* **14**, 667–685
41. Mabbott, N. A., Donaldson, D. S., Ohno, H., Williams, I. R., and Mahajan, A. (2013) Microfold (M) cells: important immunosurveillance posts in the intestinal epithelium. *Mucosal Immunol.* **6**, 666–677
42. Wells, J. M., Rossi, O., Meijerink, M., and van Baarlen, P. (2011) Epithelial crosstalk at the microbiota-mucosal interface. *Proc. Natl. Acad. Sci.* **108**, 4607–4614
43. McClure, R., and Massari, P. (2014) TLR-dependent human mucosal epithelial cell responses to microbial pathogens. *Front. Immunol.* **5**, 1–13
44. Sasai, M., and Yamamoto, M. (2013) Pathogen Recognition Receptors: Ligands and Signaling Pathways by Toll-Like Receptors. *Int. Rev. Immunol.* **32**, 116–133
45. Gutzeit, C., Magri, G., and Cerutti, A. (2014) Intestinal IgA production and its role in host-microbe interaction. *Immunol. Rev.* **260**, 76–85
46. Xu, J., and Gordon, J. I. (2003) Honor thy symbionts. *Proc. Natl. Acad. Sci.* **100**, 10452–10459
47. Savage, D. C. (1977) Microbial Ecology Of The Gastrointestinal Tract. *Annu. Rev. Microbiol.* **31**, 107–133
48. Ubeda, C., Djukovic, A., and Isaac, S. (2017) Roles of the intestinal microbiota in pathogen protection. *Clin. Transl. Immunol.* **6**, e128
49. LeBlanc, J. G., Milani, C., de Giori, G. S., Sesma, F., van Sinderen, D., and Ventura, M. (2013) Bacteria as vitamin suppliers to their host: A gut microbiota perspective. *Curr. Opin. Biotechnol.* **24**, 160–168
50. Macpherson, A. J., and Harris, N. L. (2004) Interactions between commensal intestinal bacteria and the immune system. *Nat. Rev. Immunol.* **4**, 478–485
51. Yi, P., and Li, L. (2012) The germfree murine animal: An important animal model for research on the relationship between gut microbiota and the host. *Vet. Microbiol.* **157**, 1–7
52. Smith, K., McCoy, K. D., and Macpherson, A. J. (2007) Use of axenic animals in studying the adaptation of mammals to their commensal intestinal microbiota. *Semin. Immunol.* **19**, 59–69
53. Derrien, M., van Passel, M. W., van de Bovenkamp, J. H., Schipper, R. G., de Vos, W. M., and Dekker, J. (2010) Mucin-bacterial interactions in the human oral cavity and digestive tract. *Gut Microbes.* **1**,

- 254–268
54. Macfarlane, G. T., and Macfarlane, S. (2011) Fermentation in the human large intestine: its physiologic consequences and the potential contribution of prebiotics. *J. Clin. Gastroenterol.* **45**, S120–S127
 55. Ríos-Covián, D., Ruas-Madiedo, P., Margolles, A., Gueimonde, M., De los Reyes-Gavilán, C. G., and Salazar, N. (2016) Intestinal short chain fatty acids and their link with diet and human health. *Front. Microbiol.* **7**, 1–9
 56. den Besten, G., Lange, K., Havinga, R., van Dijk, T. H., Gerding, A., van Eunen, K., Müller, M., Groen, A. K., Hooiveld, G. J., Bakker, B. M., and Reijngoud, D.-J. (2013) Gut-derived short-chain fatty acids are vividly assimilated into host carbohydrates and lipids. *Am. J. Physiol. Gastrointest. Liver Physiol.* **305**, G900–G910
 57. Ruppin, H., Bar-Meir, S., Soergel, K., Wood, C., and Schmitt MG (1980) Absorption of short-chain fatty acids by the colon. *Gastroenterology.* **78**, 1500–1507
 58. Roediger, W. E. (1982) Utilization of nutrients by isolated epithelial cells of the rat colon. *Gastroenterology.* **83**, 424–429
 59. Canfora, E. E., Jocken, J. W., and Blaak, E. E. (2015) Short-chain fatty acids in control of body weight and insulin sensitivity. *Nat. Rev. Endocrinol.* **11**, 577–591
 60. Qin, J., Li, R., Raes, J., Arumugam, M., Burgdorf, K. S., Manichanh, C., Nielsen, T., Pons, N., Levenez, F., Yamada, T., Mende, D. R., Li, J., Xu, J., Li, S., Li, D., Cao, J., Wang, B., Liang, H., Zheng, H., Xie, Y., Tap, J., Lepage, P., Bertalan, M., Batto, J.-M., Hansen, T., Le Paslier, D., Linneberg, A., Nielsen, H. B., Pelletier, E., Renault, P., Sicheritz-Ponten, T., Turner, K., Zhu, H., Yu, C., Li, S., Jian, M., Zhou, Y., Li, Y., Zhang, X., Li, S., Qin, N., Yang, H., Wang, J., Brunak, S., Doré, J., Guarner, F., Kristiansen, K., Pedersen, O., Parkhill, J., Weissenbach, J., Bork, P., Ehrlich, S. D., and Wang, J. (2010) A human gut microbial gene catalogue established by metagenomic sequencing. *Nature.* **464**, 59–65
 61. Eckburg, P. B., Bik, E. M., Bernstein, C. N., Purdom, E., Dethlefsen, L., Sargent, M., Gill, S. R., Nelson, K. E., and Relman, D. a (2005) Diversity of the human intestinal microbial flora. *Science.* **308**, 1635–8
 62. Faith, J. J., Guruge, J. L., Charbonneau, M., Subramanian, S., Seedorf, H., Goodman, A. L., Clemente, J. C., Knight, R., Heath, A. C., Leibel, R. L., Rosenbaum, M., and Gordon, J. I. (2013) The Long-Term Stability of the Human Gut Microbiota. *Science.* **341**, 1237439
 63. Zoetendal, E. G., Akkermans, A. D. L., Vos, M. De, and Vos, W. M. D. E. (1998) Temperature Gradient Gel Electrophoresis Analysis of 16S rRNA from Human Fecal Samples Reveals Stable and Host-Specific Communities of Active Bacteria Temperature Gradient Gel Electrophoresis Analysis of 16S rRNA from Human Fecal Samples Reveals Stable an. *Appl. Environ. Microbiol.* **64**, 3854–3859
 64. Lozupone, C. A., Stombaugh, J. I., Gordon, J. I., Jansson, J. K., and Knight, R. (2012) Diversity, stability and resilience of the human gut microbiota. *Nature.* **489**, 220–230
 65. Turnbaugh, P. J., Hamady, M., Yatsunenko, T., Cantarel, B. L., Duncan, A., Ley, R. E., Sogin, M. L., Jones, W. J., Roe, B. a, Affourtit, J. P., Egholm, M., Henrissat, B., Heath, A. C., Knight, R., and Gordon, J. I. (2009) A core gut microbiome in obese and lean twins. *Nature.* **457**, 480–4
 66. Sommer, F., and Bäckhed, F. (2013) The gut microbiota--masters of host development and physiology. *Nat. Rev. Microbiol.* **11**, 227–38
 67. Wen, L., and Duffy, A. (2017) Factors Influencing the Gut Microbiota, Inflammation, and Type 2 Diabetes. *J. Nutr.* **147**, 1468S–1475S
 68. David, L. a, Maurice, C. F., Carmody, R. N., Gootenberg, D. B., Button, J. E., Wolfe, B. E., Ling, A. V, Devlin, a S, Varma, Y., Fischbach, M. a, Biddinger, S. B., Dutton, R. J., and Turnbaugh, P. J. (2014) Diet rapidly and reproducibly alters the human gut microbiome. *Nature.* **505**, 559–63
 69. Sartor, R. B. (2008) Microbial Influences in Inflammatory Bowel Diseases. *Gastroenterology.* **134**, 577–594
 70. Gao, R., Gao, Z., Huang, L., and Qin, H. (2017) Gut microbiota and colorectal cancer. *Eur. J. Clin. Microbiol. Infect. Dis.* **36**, 757–769
 71. Bäckhed, F., Ding, H., Wang, T., Hooper, L. V, Koh, G. Y., Nagy, A., Semenkovich, C. F., and Gordon, J. I. (2004) The gut microbiota as an environmental factor that regulates fat storage. *Proc. Natl. Acad. Sci. U. S. A.* **101**, 15718–15723
 72. Rabot, S., Membrez, M., Bruneau, A., Gérard, P., Harach, T., Moser, M., Raymond, F., Mansourian, R., and Chou, C. J. (2010) Germ-free C57BL/6J mice are resistant to high-fat-diet-induced insulin resistance and have altered cholesterol metabolism. *FASEB J.* **24**, 4948–59
 73. Koeth, R. A., Wang, Z., Levison, B. S., Buffa, J. a, Org, E., Sheehy, B. T., Britt, E. B., Fu, X., Wu, Y., Li, L., Smith, J. D., DiDonato, J. a, Chen, J., Li, H., Wu, G. D., Lewis, J. D., Warriar, M., Brown, J. M., Krauss, R. M., Tang, W. H. W., Bushman, F. D., Lusis, A. J., and Hazen, S. L. (2013) Intestinal microbiota metabolism of L-carnitine, a nutrient in red meat, promotes atherosclerosis. *Nat. Med.* **19**, 576–85
 74. De Minicis, S., Rychlicki, C., Agostinelli, L., Saccomanno, S., Candelaresi, C., Trozzi, L., Mingarelli, E., Facinelli, B., Magi, G., Palmieri, C., Marzoni, M., Benedetti, A., and Svegliati-Baroni, G. (2014) Dysbiosis contributes to fibrogenesis in the course of chronic liver injury in mice. *Hepatology.* **59**, 1738–

- 1749
75. Boulangé, C. L., Neves, A. L., Chilloux, J., Nicholson, J. K., and Dumas, M.-E. (2016) Impact of the gut microbiota on inflammation, obesity, and metabolic disease. *Genome Med.* **8**, 42
 76. Caesar, R., Reigstad, C. S., Bäckhed, H. K., Reinhardt, C., Ketonen, M., Lundén, G. Ö., Cani, P. D., and Bäckhed, F. (2012) Gut-derived lipopolysaccharide augments adipose macrophage accumulation but is not essential for impaired glucose or insulin tolerance in mice. *Gut.* **61**, 1701–7
 77. Chiang, J. Y. L. (2009) Bile acids: regulation of synthesis. *J. Lipid Res.* **50**, 1955–1966
 78. Li-hawkins, J., Gåfvels, M., Olin, M., Lund, E. G., Andersson, U., Schuster, G., Björkhem, I., Russell, D. W., and Eggertsen, G. (2002) Cholic acid mediates negative feedback regulation. *J. Clin. Invest.* **110**, 1191–1200
 79. Russell, D. W. (2003) The enzymes, regulation, and genetics of bile acid synthesis. *Annu. Rev. Biochem.* **72**, 137–174
 80. Botham, K. M., and Boyd, G. S. (1983) The metabolism of chenodeoxycholic acid to beta-muricholic acid in rat liver. *Eur. J. Biochem.* **134**, 191–6
 81. Pircher, P. C., Kitto, J. L., Petrowski, M. L., Tangirala, R. K., Bischoff, E. D., Schulman, I. G., and Westin, S. K. (2003) Farnesoid X receptor regulates bile acid-amino acid conjugation. *J. Biol. Chem.* **278**, 27703–27711
 82. Ridlon, J. M., Kang, D. J., and Hylemon, P. B. (2006) Bile salt biotransformations by human intestinal bacteria. *J. Lipid Res.* **47**, 241–259
 83. Dawson, P. A., Lan, T., and Rao, A. (2009) Bile acid transporters. *J. Lipid Res.* **50**, 2340–57
 84. Dawson, P. A., and Karpen, S. J. (2015) Intestinal transport and metabolism of bile acids. *J. Lipid Res.* **56**, 1085–1099
 85. Boyer, and James (2013) Bile Formation and Secretion. *Compr Physiol.* **3**, 1035–1078
 86. Maldonado-Valderrama, J., Wilde, P., MacIerzanka, A., and MacKie, A. (2011) The role of bile salts in digestion. *Adv. Colloid Interface Sci.* **165**, 36–46
 87. Wahlström, A., Sayin, S. I., Marschall, H.-U., and Bäckhed, F. (2016) Intestinal Crosstalk between Bile Acids and Microbiota and Its Impact on Host Metabolism. *Cell Metab.* **24**, 41–50
 88. Stroeve, J. H. M., Brufau, G., Stellaard, F., Gonzalez, F. J., Staels, B., and Kuipers, F. (2010) Intestinal FXR-mediated FGF15 production contributes to diurnal control of hepatic bile acid synthesis in mice. *Lab. Invest.* **90**, 1457–1467
 89. Kim, I., Ahn, S.-H., Inagaki, T., Choi, M., Ito, S., Guo, G. L., Kliewer, S. a, and Gonzalez, F. J. (2007) Differential regulation of bile acid homeostasis by the farnesoid X receptor in liver and intestine. *J. Lipid Res.* **48**, 2664–2672
 90. Inagaki, T., Choi, M., Moschetta, A., Peng, L., Cummins, C. L., McDonald, J. G., Luo, G., Jones, S. A., Goodwin, B., Richardson, J. A., Gerard, R. D., Repa, J. J., Mangelsdorf, D. J., and Kliewer, S. A. (2005) Fibroblast growth factor 15 functions as an enterohepatic signal to regulate bile acid homeostasis. *Cell Metab.* **2**, 217–225
 91. Kuipers, F., Bloks, V. W., and Groen, A. K. (2014) Beyond intestinal soap--bile acids in metabolic control. *Nat. Rev. Endocrinol.* **10**, 488–498
 92. de Aguiar Vallim, T. Q., Tarling, E. J., and Edwards, P. A. (2013) Pleiotropic roles of bile acids in metabolism. *Cell Metab.* **17**, 657–669
 93. Li, P., Ruan, X., Yang, L., Kiesewetter, K., Zhao, Y., Luo, H., Chen, Y., Gucek, M., Zhu, J., and Cao, H. (2015) A liver-enriched long non-coding RNA, lncLSTR, regulates systemic lipid metabolism in mice. *Cell Metab.* **21**, 455–67
 94. Claudel, T., Inoue, Y., Barbier, O., Duran-Sandoval, D., Kosykh, V., Fruchart, J., Fruchart, J.-C., Gonzalez, F. J., and Staels, B. (2003) Farnesoid X receptor agonists suppress hepatic apolipoprotein CIII expression. *Gastroenterology.* **125**, 544–555
 95. Watanabe, M., Houten, S. M., Wang, L., Moschetta, A., Mangelsdorf, D. J., Heyman, R. A., Moore, D. D., and Auwerx, J. (2004) Bile acids lower triglyceride levels via a pathway involving FXR, SHP, and SREBP-1c. *J. Clin. Invest.* **113**, 1408–18
 96. Yamagata, K., Daitoku, H., Shimamoto, Y., Matsuzaki, H., Hirota, K., Ishida, J., and Fukamizu, A. (2004) Bile acids regulate gluconeogenic gene expression via small heterodimer partner-mediated repression of hepatocyte nuclear factor 4 and Foxo1. *J. Biol. Chem.* **279**, 23158–23165
 97. Ma, K., Saha, P. K., Chan, L., and Moore, D. D. (2006) Farnesoid X receptor is essential for normal glucose homeostasis. *J. Clin. Invest.* **116**, 1102–1109
 98. Harach, T., Pols, T. W. H., Nomura, M., Maida, A., Watanabe, M., Auwerx, J., and Schoonjans, K. (2012) TGR5 potentiates GLP-1 secretion in response to anionic exchange resins. *Sci. Rep.* **2**, 430
 99. Thomas, C., Gioiello, A., Noriega, L., Strehle, A., Oury, J., Rizzo, G., Macchiarulo, A., Yamamoto, H., Matak, C., Pruzanski, M., Pellicciari, R., Auwerx, J., and Schoonjans, K. (2009) TGR5-Mediated Bile Acid Sensing Controls Glucose Homeostasis. *Cell Metab.* **10**, 167–177
 100. Watanabe, M., Houten, S. M., Matak, C., Christoffolete, M. A., Kim, B. W., Sato, H., Messaddeq, N.,

- Harney, J. W., Ezaki, O., Kodama, T., Schoonjans, K., Bianco, A. C., and Auwerx, J. (2006) Bile acids induce energy expenditure by promoting intracellular thyroid hormone activation. *Nature*. **439**, 484–489
101. Guo, C., Xie, S., Chi, Z., Zhang, J., Liu, Y., Zhang, L., Zheng, M., Zhang, X., Xia, D., Ke, Y., Lu, L., and Wang, D. (2016) Bile Acids Control Inflammation and Metabolic Disorder through Inhibition of NLRP3 Inflammasome. *Immunity*. **45**, 802–816
 102. Köster, A., Chao, Y. B., Mosior, M., Ford, A., Gonzalez-DeWhitt, P. a, Hale, J. E., Li, D., Qiu, Y., Fraser, C. C., Yang, D. D., Heuer, J. G., Jaskunas, S. R., and Eacho, P. (2005) Transgenic angiotensin-like (angptl)4 overexpression and targeted disruption of angptl4 and angptl3: regulation of triglyceride metabolism. *Endocrinology*. **146**, 4943–50
 103. Santulli, G. (2014) Angiotensin-like proteins: A comprehensive look. *Front. Endocrinol. (Lausanne)*. **5**, 5–10
 104. Mattijssen, F., and Kersten, S. (2012) Regulation of triglyceride metabolism by Angiotensin-like proteins. *Biochim. Biophys. Acta*. **1821**, 782–9
 105. Lei, X., Shi, F., Basu, D., Huq, A., Routhier, S., Day, R., and Jin, W. (2011) Proteolytic processing of angiotensin-like protein 4 by proprotein convertases modulates its inhibitory effects on lipoprotein lipase activity. *J. Biol. Chem.* **286**, 15747–15756
 106. Sukonina, V., Lookene, A., Olivecrona, T., and Olivecrona, G. (2006) Angiotensin-like protein 4 converts lipoprotein lipase to inactive monomers and modulates lipase activity in adipose tissue. *Proc. Natl. Acad. Sci. U. S. A.* **103**, 17450–5
 107. Lafferty, M. J., Bradford, K. C., Erie, D. A., and Neher, S. B. (2013) Angiotensin-like protein 4 inhibition of lipoprotein lipase: Evidence for reversible complex formation. *J. Biol. Chem.* **288**, 28524–28534
 108. Nilsson, S. K., Anderson, F., Ericsson, M., Larsson, M., Makoveichuk, E., Lookene, A., Heeren, J., and Olivecrona, G. (2012) Triacylglycerol-rich lipoproteins protect lipoprotein lipase from inactivation by ANGPTL3 and ANGPTL4. *Biochim. Biophys. Acta - Mol. Cell Biol. Lipids*. **1821**, 1370–1378
 109. Dijk, W., Beigneux, A. P., Larsson, M., Bensadoun, A., Young, S. G., and Kersten, S. (2016) Angiotensin-like 4 (ANGPTL4) promotes intracellular degradation of lipoprotein lipase in adipocytes. *J. Lipid Res.* **58**, 7250–7
 110. Kersten, S., Mandard, S., Tan, N. S., Escher, P., Metzger, D., Chambon, P., Gonzalez, F. J., Desvergne, B., and Wahli, W. (2000) Characterization of the fasting-induced adipose factor FIAF, a novel peroxisome proliferator-activated receptor target gene. *J. Biol. Chem.* **275**, 28488–28493
 111. Catoire, M., Alex, S., Parakevopoulos, N., Mattijssen, F., Evers-van Gogh, I., Schaart, G., Jeppesen, J., Kneppers, A., Mensink, M., Voshol, P. J., Olivecrona, G., Tan, N. S., Hesselink, M. K. C., Berbée, J. F., Rensen, P. C. N., Kalkhoven, E., Schrauwen, P., and Kersten, S. (2014) Fatty acid-inducible ANGPTL4 governs lipid metabolic response to exercise. *Proc. Natl. Acad. Sci. U. S. A.* **111**, E1043-52
 112. Mattijssen, F., Alex, S., Swarts, H. J., Groen, A. K., van Schothorst, E. M., and Kersten, S. (2014) Angptl4 serves as an endogenous inhibitor of intestinal lipid digestion. *Mol. Metab.* **3**, 135–144
 113. Yoon, J. C., Chickering, T. W., Rosen, E. D., Dussault, B., Qin, Y., Soukas, A., Friedman, J. M., Holmes, W. E., and Spiegelman, B. M. (2000) Peroxisome Proliferator-Activated Receptor gamma Target Gene Encoding a Novel Angiotensin-Related Protein Associated with Adipose Differentiation. *Mol. Cell Biol.* **20**, 5343–5349
 114. Georgiadi, A., Lichtenstein, L., Degenhardt, T., Boekschoten, M. V., Van Bilsen, M., Desvergne, B., Müller, M., and Kersten, S. (2010) Induction of cardiac angptl4 by dietary fatty acids is mediated by peroxisome proliferator-activated receptor β/δ and protects against fatty acid-induced oxidative stress. *Circ. Res.* **106**, 1712–1721
 115. Bünger, M., Bosch, H. M. Van Den, Meijde, J. Van Der, Kersten, S., Hooiveld, G. J. E. J., and Mu, M. (2007) Genome-wide analysis of PPAR α activation in murine small intestine. *Physiol. Genomics*. **30**, 192–204
 116. Kroupa, O., Vorrsjö, E., Stienstra, R., Mattijssen, F., Nilsson, S. K., Sukonina, V., Kersten, S., Olivecrona, G., and Olivecrona, T. (2012) Linking nutritional regulation of Angptl4, Gpihbp1, and Lmf1 to lipoprotein lipase activity in rodent adipose tissue. *BMC Physiol.* **12**, 13
 117. Dijk, W., Heine, M., Vergnes, L., Boon, M. R., Schaart, G., Hesselink, M. K., Reue, K., van Marken Lichtenbelt, W. D., Olivecrona, G., Rensen, P. C., Heeren, J., and Kersten, S. (2015) ANGPTL4 mediates shuttling of lipid fuel to brown adipose tissue during sustained cold exposure. *Elife*. **4**, e08428
 118. Bäckhed, F., Manchester, J. K., Semenovich, C. F., and Gordon, J. I. (2007) Mechanisms underlying the resistance to diet-induced obesity in germ-free mice. *Proc. Natl. Acad. Sci. U. S. A.* **104**, 979–84
 119. Alex, S., Lange, K., Amolo, T., Grinstead, J. S., Haakonsson, A. K., Szalowska, E., Koppen, A., Mudde, K., Haenen, D., Al-Lahham, S., Roelofs, H., Houtman, R., van der Burg, B., Mandrup, S., Bonvin, A. M. J. J., Kalkhoven, E., Müller, M., Hooiveld, G. J., and Kersten, S. (2013) Short-chain fatty acids stimulate angiotensin-like 4 synthesis in human colon adenocarcinoma cells by activating peroxisome proliferator-activated receptor γ . *Mol. Cell Biol.* **33**, 1303–16

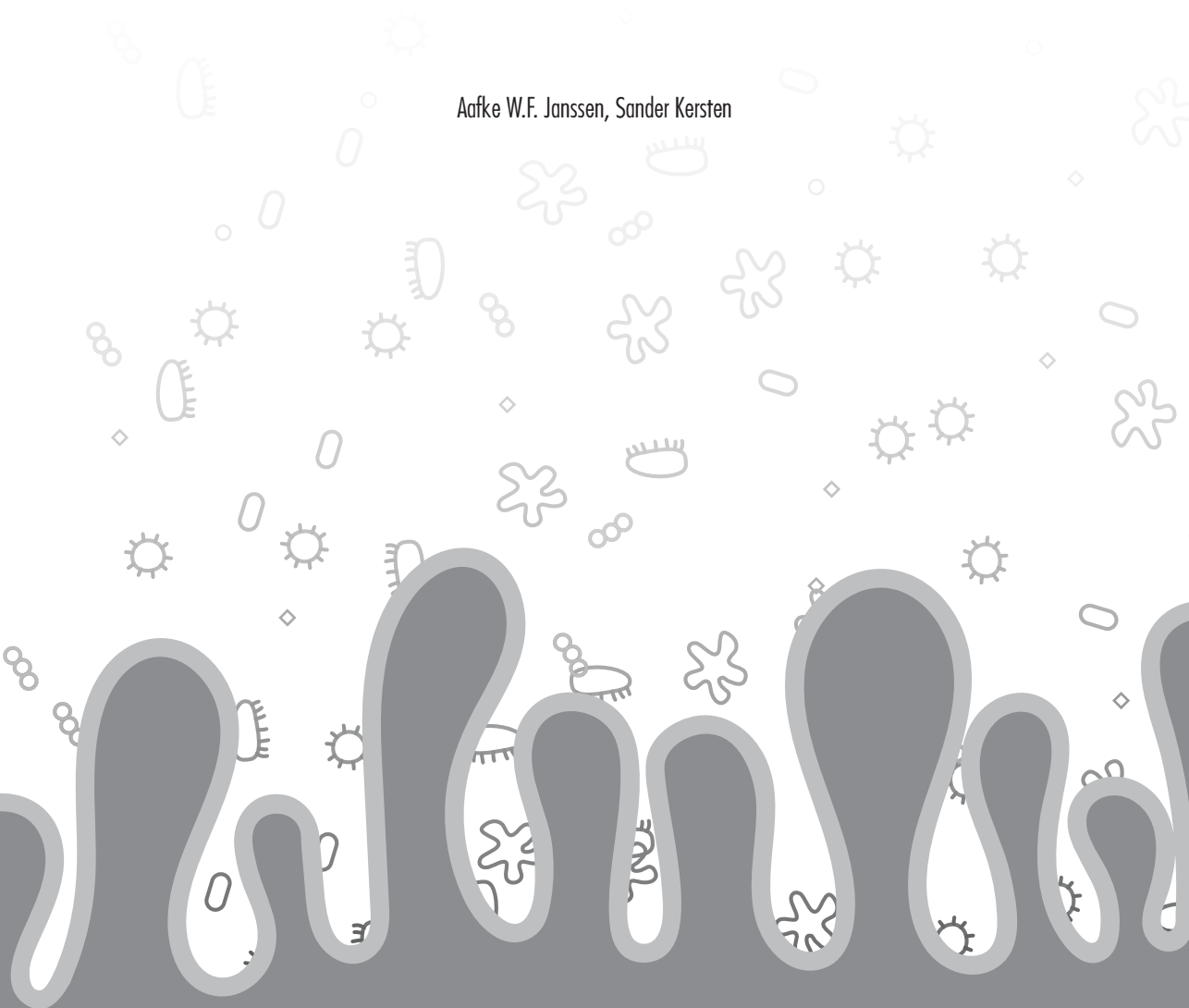
120. Korecka, A., de Wouters, T., Cultrone, A., Lapaque, N., Pettersson, S., Doré, J., Blottière, H. M., and Arulampalam, V. (2013) ANGPTL4 expression induced by butyrate and rosiglitazone in human intestinal epithelial cells utilizes independent pathways. *Am. J. Physiol. Gastrointest. Liver Physiol.* **304**, G1025-37

2



The role of the gut microbiota in metabolic health

Aafke W.F. Janssen, Sander Kersten



FASEB J. 2015;29(8): 3111-3123

Abstract

The global prevalence of obesity and related comorbidities has increased considerably over the last decades. In addition to an increase in food consumption and a reduction in physical activity, growing evidence implicates the microorganisms in our gastrointestinal tract, referred to as the gut microbiota, in obesity and related metabolic disturbances.

The composition of the gut microbiota can fluctuate markedly within an individual and between individuals. Changes in gut microbial composition may be unfavorable and predispose an individual to disease. Studies in mice that are germfree, mice that are cohoused, and mice that are treated with antibiotics have provided some evidence that changes in gut microbiota may causally contribute to metabolic disorders. Several mechanisms have been proposed and explored that may mediate the effects of the gut microbiota on metabolic disorders.-

In this review, we carefully analyse the literature on the connection between the gut microbiota and metabolic health with a focus on studies demonstrating a causal relation and clarifying potential underlying mechanisms. Despite a growing appreciation for a role of the gut microbiota in metabolic health, more experimental evidence is needed to substantiate a cause and effect relationship. If a clear causal relationship between the gut microbiota and metabolic health can be established, dietary interventions may be targeted towards improving gut microbial composition in the prevention and possibly even treatment of metabolic diseases.

Introduction

The global prevalence of obesity has increased substantially over the last decades (1). As a consequence, there has been a rise in obesity-related comorbidities such as diabetes mellitus, dyslipidemia, and hypertension, each of which serve as an independent risk factor for cardiovascular diseases (2-4).

The increase in obesity rates is believed to be the result of increased consumption of calorie- dense foods in combination with reduced levels of physical activity. Interestingly, growing evidence implicates the microorganisms residing within the gastrointestinal tract in obesity and its associated metabolic disturbances (5, 6). Initial studies indicated that diet-induced obesity (DIO) in mice is associated with changes in gut microbial composition (7-9). In addition, obese humans were shown to have an altered composition of their gut microbiota, as compared to lean individuals (10, 11). These early findings have fed the notion that the gut microbiota plays a role in obesity. Besides obesity, changes in the gut microbial community also have been found in patients with symptomatic atherosclerosis (12), in individuals with type 2 diabetes (13) and in patients with non-alcoholic fatty liver disease (NAFLD) (14, 15), suggesting that the gut microbiota has a role these diseases as well.

However, these cross-sectional and correlative studies did not discriminate between the possibilities that the observed changes in gut microbiota causally contribute to obesity and associated diseases or occur as a consequence of the disturbed metabolism or immune system. Therefore, in this review, we examine the role of the gut microbiota in mediating the effects of diet on metabolic health, and explore the potential underlying mechanisms. In the first part, we describe the normal function of the gut microbiota in humans, and in the second part, we discuss the effect of diet on the gut microbiota and the potential relationship with metabolic diseases.

Human gut microbiota

All higher organisms live in an intimate relationship with microorganisms. Microorganisms that live in a particular environment such as the intestine are known collectively as a microbiota. A microbiota is composed of bacteria, viruses, fungi, archaea, and protozoa. They reside at every surface that is in contact with the external environment, but in particular at mucosal surfaces of the gastro-intestinal tract (16-18). The advent of new molecular techniques such as 16S rRNA sequencing and dedicated DNA Chips, has made it possible to identify and study the composition of the human gut microbiome (19, 20). It is estimated that the number of bacteria in the human intestine easily reaches 10^{14} and is predominantly composed of Bacteroidetes and Firmicutes (90%), complemented with Actinobacteria, Proteobacteria and Verrucomicrobia (5, 21, 22).

The gut microbiota live in a mutualistic relationship with its host that is beneficial to both organisms, and it is especially important in the development of the immune system. The complete absence of bacteria in the GI tract leads to large defects in the development of gut-associated lymph tissues, low levels of secretory IgA antibodies in the intestine, and less and smaller mesenteric lymph nodes. Furthermore, the gut microbiota has an important role in protecting the host against invasion of intestinal pathogens and in maintaining tissue homeostasis (18, 23, 24). Without the gut microbiota, dietary fibers such as inulin, pectin, xylans, and mannans would leave the body unaffected. Fermentation of dietary fiber by bacteria yields energy, which is important for the growth and maintenance of the microbial community. In addition, fermentation leads to the formation of metabolic end products that are beneficial to the host (25, 26). The principal end products of carbohydrate fermentation are the short chain fatty acids (SCFAs) acetate, propionate and butyrate, as well as gases such as CO_2 , H_2 and CH_4 (26, 27). SCFAs are very effectively absorbed in the colon, giving rise to minimal loss in the feces. The host utilizes SCFAs for a variety of different purposes. Whereas butyrate is an important energy source for colonic epithelial cells, acetate and propionate can be utilized by the liver for lipogenesis and gluconeogenesis, respectively (5, 25, 28).

Changes in gut microbial composition and metabolic health

The composition of the gut microbiota is not constant but differs between individuals and can fluctuate markedly within an individual. Interindividual variation in bacterial diversity is caused by differences in host genomes, but also by environmental factors, such as antibiotics use, lifestyle, hygiene, and diet. An altered gut microbial composition, defined as dysbiosis, may be unfavorable and may predispose an individual to disease (18, 29, 30).

How diet affects gut microbiota

Wong *et al.* (25) proposed that the gut microbiota evolved in conjunction with the consumption of diets containing large amounts of nondigestible fibers and complex carbohydrates, which presumably was the diet of our prehistoric ancestors. They reasoned that modern diets that are low in dietary fibers malnourish the gut microbiota and thereby negatively influence the health of the host. De Filippo (31) examined to what extent consumption of a Western diet differentially affects human gut microbial composition as compared with diets from our ancestors, which was characterized by large amounts of starch, fiber, and plant polysaccharides, and low amounts of fat and animal protein. In this study, the fecal microbiota of 14 healthy children living in Burkina Faso, Africa, were compared with the fecal microbiota of 15 healthy children from Florence, Italy. Compared to the feces of children from Italy, the feces of the African children contained higher amounts

of Bacteroidetes and lower amounts of Firmicutes. However, not all studies that assessed microbial composition found similar associations. Wu *et al.* (32) showed that Bacteroidetes and Actinobacteria are positively associated with fat-rich diets and negatively associated with fiber-rich diets, whereas the opposite applied to Firmicutes and Proteobacteria. David *et al.* (33) found that an animal-based diet has a more pronounced impact on gut microbial clusters than does a plant-based diet. In addition, it has been found that Firmicutes associated negatively and Bacteroidetes associated positively with animal-based diets. In contrast, no effect of diet on any phyla was observed in a 10-week controlled-feeding study in which obese individuals successively received a control diet, a diet rich in resistant starch or nonstarch polysaccharides, and a reduced carbohydrate weight-loss diet. The diets' effects were only observed at lower taxonomic levels (34). One of the possible reasons that changes in gut microbial composition differed in the various studies is the duration of the diet intervention. Gut microbial composition has been shown to be stable, even up to 10 days after switching to a new diet (32). Besides the duration of the dietary intervention, the composition of an individual's gut microbiota prior to the intervention may also influence the effect of diet on gut microbial composition (34, 35). This notion is supported by a recent mouse study that showed that the gut microbial composition is not only determined by the current diet but also partly depends on dietary history (35). Additionally, a study in human subjects concluded that a change in dietary fiber can produce marked changes in the gut microbiota, but these depend on the initial composition of an individual's gut microbiota (34). In general, it can be concluded that diet markedly affects gut microbial composition at the phylum level and especially at lower taxonomic levels (32, 34, 36, 37), although not necessarily in a manner that is consistent between individuals.

In addition to diet, host genetic makeup, and nondietary environmental factors, such as antibiotic use, lifestyle and hygiene, may also affect microbial composition (18). It has been found that the within-twin similarity in fecal microbial composition is comparable between adult monozygotic twin pairs and dizygotic twin pairs, indicating that environmental factors play a dominant role in determining gut microbial composition (38). Some of these environmental exposures may exert their effects early in life, such in the route of childbirth, feeding method (breast or bottle feeding), and weaning. For instance, the gut microbiota of babies delivered *via* caesarian sections more closely resembles the microbiota of the maternal skin, whereas in babies delivered vaginally the gut microbiota is derived primarily from the maternal birth canal and rectum, giving rise to an abundance of *Lactobacillus*, *Prevotella* and *Atopobium* (39). Taken together, diet markedly influences intestinal microbial composition, but to date there is no evidence that particular dietary components have a specific and consistent effect on gut microbial composition, likely because of the major confounding effects of genetic makeup and various environmental factors.

To overcome the inherent limitations of cross-sectional studies and directly investigate the functional impact of the gut microbiota, investigators have performed studies in germfree mice. Germfree mice are bred and born without exposure to any microorganisms and can be colonized with specific microbial communities to create gnotobiotic mice. These gnotobiotic mice are a powerful tool for exploring the interaction between the gut microbiota and the host, because host genotype, diet, microbial composition and other environmental factors can be strictly controlled (40). A proof-of-principle study showed that the gut microbial composition of germfree C57BL/6 mice colonized with adult human fresh or frozen fecal microbiota largely resembled the microbial composition of the donor. Switching to a western diet with high levels of fat and sugar resulted in a significant decrease in Bacteroidetes and an increase in Erysipelotrichi, a class of bacteria from the phylum Firmicutes (41). A similar shift in microbial community was observed in another study in which germfree mice were cultured with human microbiota, followed by feeding a Western diet (42). Thus, studies with germ free mice are instrumental in dissecting the role of the gut microbiota in mediating the effects of diet on metabolic health without interference by potential confounders.

Association between gut microbiota and metabolic health

As described above, diet markedly affects gut microbial composition. Diet also influences obesity, as seen in wild-type mice fed a high-fat diet rich in saturated fat, which is a frequently used model of DIO. An interesting finding is that, concurrent with enhanced weight gain, DIO mice have an altered gut microbial community, as compared with mice fed a low fat diet, suggesting that obesity is linked to the gut microbiota (7, 43). Alterations in microbial composition were also found in genetically obese mice, which exhibited increased levels of Firmicutes and reduced levels of Bacteroidetes in the cecum in comparison with their lean wild-type and heterozygous littermates (8). An increase in the ratio of Firmicutes to Bacteroidetes was also observed in obese rats (44) and pigs (45) when compared with animals in the lean state. The above studies suggest that obesity influences gut microbial composition or *vice versa*. In contrast, Hildebrandt *et al.* (46) reported that the intestinal microbial composition is primarily influenced by diet and not by the obese state. Using Resistin-like molecule β -knockout mice, which are resistant to DIO, they showed that switching from a chow to a high-fat diet changed gut microbial composition independently of the obese state. Furthermore, ob/ob mice, which are genetically altered obese mice characterized by a mutation in the leptin gene, showed no difference over time in the number of fecal Firmicutes, despite progressive obesity (47). It could thus be argued that high fat feeding *per se*, independent of obesity, may be the primary determinant of gut microbial composition in DIO studies.

Causal link between gut microbiota and metabolic health

The major limitation of the studies mentioned above is that they merely correlated microbial composition to obesity. Whether a relationship between the microbiota and obesity is in fact causal can be ascertained by performing studies with gnotobiotic animals, animals treated with antibiotics, or animals that are co-housed, allowing modulation of the gut microbial composition. The use of such approaches makes it possible to determine whether changes in gut microbial composition directly impact metabolic health or *vice versa*. Studies with germfree mice have supported a causal role for the gut microbiota in obesity. Whereas conventionally-raised mice develop DIO, germfree mice were protected against obesity development (48-50). Furthermore, it has been observed that transplantation of the gut microbial community from conventionally-raised obese mice to germfree or antibiotic-treated mice causes more pronounced weight gain than colonization with microbiota from lean, conventionally-raised donors, indicating that the composition of gut microbiota can affect obesity (9, 51).

To examine whether the human gut microbiota may affect weight gain, germfree mice were colonized with fecal microbiota from adult humans and placed on a Western diet, resulting in increased adiposity when compared to mice colonized with human microbiota followed by a low-fat, plant polysaccharide-rich diet. Strikingly, the feces from mice colonized with human microbiota and fed a Western diet caused higher levels of total body fat when introduced into germfree recipient mice by gavage, as compared with feces from mice colonized with human microbiota and fed a low-fat plant polysaccharide-rich diet (41).

As an extension to the above findings, Ridaura *et al.* (52) transplanted fecal microbiota from adult female twin pairs that were discordant for obesity into germfree mice. An increase in adiposity and total body mass was found in the recipients of the gut microbiota transplanted from the obese twin, as compared to mice that received the lean twin's gut microbiota. Of particular note, the obese state was transferable, as observed, by cohousing mice that received transplants of either the obese or lean twin's microbiota. Because mice are coprophagic, cohousing results in transfer of the gut microbiota *via* the ingestion of other animals' feces.

Further suggesting a causal link between gut microbiota and obesity, treatment of mice with the antibiotic vancomycin, which caused a decrease in the relative amounts of Bacteroidetes and Firmicutes combined with an increase in the abundance of Proteobacteria, reduced weight gain in mice fed a high-fat diet (53). In a recent study, it was shown that antibiotic treatment early in life may set metabolic consequences in motion. Giving mice whose mothers were treated with penicillin before birth of their pups a low-dose penicillin during the weaning period increased DIO and visceral fat accumulation, and affected hepatic gene expression and metabolic hormone levels such as peptide YY (PYY). A causal

role for the microbiota was confirmed by transplanting gut microbiota from antibiotic-treated mice to germfree mice. Remarkably, cessation of the antibiotic treatment induced a marked recovery of microbial composition but did not change the metabolic phenotype (54).

Taken together, the evidence from studies in mice suggest a causal link between gut microbiota and obesity. Complementing the animal studies mentioned above, several human studies support such a correlation between the gut microbiota and obesity. Specifically, humans with obesity were shown to have an increased ratio of Firmicutes/Bacteroidetes when compared with lean individuals (10). In addition, the abundance of Bacteroidetes increased upon weight loss, either by fat- or carbohydrate-restricted low-calorie diets (10) or after a gastric bypass (55). Because people who undergo gastric bypass surgery also have to make major adjustments in their diet, the latter study does not provide any information on whether the changes in microbial composition are dictated by the changes in diet or by the reduced adiposity.

Although other studies have found changes in gut microbial composition in obese individuals, the increase in Firmicutes/Bacteroidetes ratio in obesity and the increase in the presence of Bacteroidetes upon weight loss have not been observed consistently (11, 38, 56-58). Confounding factors such as diet, fasting (59), hygiene, lifestyle (18) and the use of antibiotics (60) affect gut microbial composition and might explain the discrepancies between these studies. These confounding factors, as well as species specific factors, may also explain why vancomycin treatment was associated with weight gain in adults subjects (61), whereas vancomycin reduced weight gain in mice (53). In conclusion, some human studies suggest that intestinal microbial composition is altered in obesity, although more studies are necessary to determine the direction and causality of the relationship.

In addition to obesity itself, the gut microbiota may also be associated with perturbations that are coupled to obesity, including systemic inflammation, insulin resistance and NAFLD (14, 62, 63). Cohousing experiments revealed that the gut microbiota may have an important role in NAFLD. Numerous studies have demonstrated that activation of the inflammasome by endogenous danger signals, such as reactive oxygen species, are involved in the progression of NAFLD. Activation of the inflammasome causes cleavage and thereby activation of the pro-inflammatory cytokine IL-18 (64-66). Intriguingly, Henaoui-Mejia *et al.* showed that mice deficient in IL-18 develop hepatic steatosis and inflammation. In order to investigate whether this phenotype is caused by an altered gut microbial composition, IL-18 knockout mice were cohoused with wild-type mice. Cohousing of these mice unexpectedly exacerbated hepatic steatosis and inflammation in the wild-type mice, indicating that the gut microbiota may promote NAFLD development (63). A causal role of the gut microbiota in NAFLD was supported by the finding that antibiotic treatment reduced hepatic triglyceride

accumulation in mice fed a high fat diet (67) or a diet rich in fructose (68), but also reduced hepatic T-cell infiltration in mice with concanavalin A-induced hepatitis (69).

A causal role for the gut microbiota in systemic inflammation and insulin resistance was found in studies with gnotobiotic and antibiotic-treated animals. Whereas ileal TNF α expression did not differ between germfree mice fed a low- or high-fat diet, TNF α expression was elevated in conventionally-raised mice fed a high-fat diet as compared with mice fed a low-fat diet. Since TNF α is a biomarker of pro-inflammatory changes in the intestine, these data suggest that the gut microbiota, in combination with a high-fat diet, promotes intestinal inflammation. High TNF α levels were shown to correlate significantly with the progression of obesity and the development of insulin resistance (50). A causal role of the gut microbiota in insulin resistance is supported by the finding that vancomycin treatment decreased plasma TNF α levels and improved fasting blood glucose levels in mice fed a high-fat diet (53). Compared to conventionalized mice, germfree mice were also found to have improved insulin sensitivity, which was accompanied by lower plasma TNF α and Serum Amyloid A (SAA) levels (70). High SAA levels lower insulin sensitivity in adipocytes (71) and might therefore explain the insulin resistance observed in conventionalization studies (70, 72, 73). In addition, fasting plasma free fatty acid levels were found to be higher in conventionally-raised mice (70), also potentially contributing to insulin resistance (74). Membrez *et al.* (75) reported that, in two different mouse models of insulin resistance, treatment with norfloxacin and ampicillin lowered fasting and post-GTT glucose and insulin plasma levels. Since norfloxacin and ampicillin suppress Enterobacteriaceae and bacteria from the genus *Bacteroides*, *Lactobacillus* and *Bifidobacterium*, it can be hypothesized that these bacteria have detrimental effects on glucose tolerance.

A recent high profile study indicated that the gut microbiota may have anti-diabetic effects in humans. Infusion of gut microbiota from lean subjects into individuals with the metabolic syndrome increased fecal microbial diversity, including an increase in butyrate-producing bacteria. Along with these changes in their microbial community, recipients of 'lean' microbiota also showed increased insulin sensitivity (73). Although this study needs confirmation, it provides the first evidence for a causal link between gut microbiota and insulin resistance in humans.

How microbiota may affect metabolic health

The studies presented above hint at the notion that instead of merely being a consequence of metabolic disorders, changes in intestinal microbial composition may in fact causally contribute to these disorders, although more evidence is needed. The uncertainty regarding the causal link between gut microbiota and metabolic health has not prevented exploration of the potential underlying mechanisms that may connect the two, which include increased

energy harvest, endotoxemia, altered SCFA signaling, and choline and bile acid metabolism.

Energy harvest and Angptl4

The gut microbiota provides the host with energy by extracting calories from otherwise indigestible carbohydrates *via* bacterial fermentation. In the intestine, complex carbohydrates are degraded by the gut microbiota into monosaccharides, which are subsequently fermented. Fermentation products include the gases H₂, CO₂, CH₄, as well as SCFAs, which can be absorbed by the host and used as an energy source (28). The notion that the gut microbiota provides energy to the host is supported by the finding that germfree mice, which are not naturally colonized with microorganisms, gain less weight when fed a high fat diet than do conventionally-raised mice (48-50).

In support of a role of fermentation in excess fat storage during obesity, ob/ob mice exhibit increased fermentation in their cecum, as revealed by an increase in the SCFAs acetate and propionate (76). Metagenomic analysis revealed that the ob/ob gut microbiome is enriched in genes involved in extracting energy from food, which may suggest that the gut microbiota from obese mice more efficiently extract energy from the diet. This notion was supported by two findings. Firstly, ob/ob mice had significantly less energy in their feces as compared with their wild-type littermates. Second, transplantation of the gut microbiota from ob/ob mice to germfree mice caused a significant increase in total body fat as compared to transplantation from lean wild-type mice (76). Therefore, ob/ob mice may not only become obese because of increased food intake but possibly also due to increased energy harvest by altered gut microbiota.

The main products of bacterial degradation and fermentation are monosaccharides and SCFAs. As a result of increased energy harvest, it was shown that conventionally-raised mice have increased monosaccharide uptake from their gut compared to their germfree counterparts. It was postulated that the increase in monosaccharide uptake promotes hepatic triglyceride synthesis, the accumulation of triglycerides in adipocytes, and subsequently an increase in body fat. Conventionally-raised mice had higher liver triglyceride levels and increased expression of the lipogenic transcription factors sterol regulatory element-binding protein (SREBP)-1 and carbohydrate-responsive element binding protein (ChREBP), as well as their targets acetyl-CoA carboxylase and fatty acid synthase (72). These results are in accordance with those of another study that showed that conventionally-raised mice on a high-fat diet gained more body weight compared to germfree mice, because of the more efficient conversion of ingested food to body weight (70). Additionally, it has been suggested that germfree mice and mice treated with antibiotics are better able to oxidize fatty acids in the liver, muscle and adipose tissue due to increased AMP-activated protein kinase (AMPK) activity and consequently a reduction in acetyl-CoA carboxylase activity, which might

protect them from DIO (48, 77).

It is noteworthy that germfree mice lacking the angiopoietin-like protein 4 (*Angptl4*) gene were not protected against body weight gain (48, 72). Intestinal *Angptl4* expression was shown to be significantly lower in conventionally-raised mice compared to germfree mice (48, 72). ANGPTL4 is an inhibitor of the enzyme lipoprotein lipase, which is responsible for clearing triglycerides from the blood into tissues. Accordingly, suppression of *Angptl4* by the gut microbiota may enhance extraction of triglycerides from the blood and promote their storage in adipose tissue (72, 78). Recently it was shown that ANGPTL4 may regulate intestinal lipid uptake by inhibiting intestinal lipase activity. Microbial suppression of *Angptl4* may therefore promote weight gain *via* the loss of the inhibitory effect of *Angptl4* on intestinal lipase activity, leading to increased intestinal triglyceride hydrolysis and lipid uptake (79).

An overview of how microbiota might affect obesity *via* energy harvest and *Angptl4* is displayed in **Figure 1**.

Gut permeability

It has also been postulated that the microbiota may affect metabolic health by modifying gut permeability. Membrez *et al.* (75) observed that the improved glucose tolerance in mice treated with norfloxacin and ampicillin was not due to differences in body weight but may be related to reduced inflammation and protection against endotoxemia, based on decreased plasma levels lipopolysaccharides (LPS) and jejunal TNF α expression in antibiotic-treated mice.

It has been suggested that endotoxemia can be triggered by diet. Fat-enriched diets alter gut microbial composition, as described earlier, but have also been shown to increase plasma

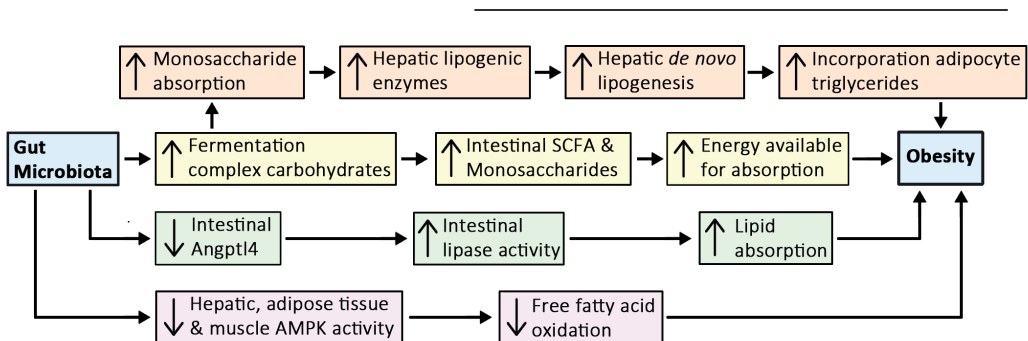


Figure 1. How microbiota may affect obesity *via* energy harvest and *Angptl4*

Gut microbiota may increase energy harvest from the diet by fermenting complex carbohydrates yielding energy in the form of monosaccharides and SCFAs. Increased monosaccharide absorption may lead to increased hepatic lipogenesis and may favor weight gain. The gut microbiota may also contribute to obesity by reducing free fatty oxidation and/or increasing intestinal lipid absorption.

LPS levels in mice (80) and humans (81). LPS is a major constituent of the gram-negative bacterial cell wall. Small amounts of endotoxin in the bloodstream may elicit a low-grade systemic immune response similar to what is observed during obesity (82). A role for the gut microbiota in this process was suggested because mice fed a high-fat diet had increased levels of cecal LPS-containing gram-negative bacteria (80) and also exhibited increased intestinal permeability with reduced expression of the tight junctions zonula occludens (ZO)-1 and occludin (62, 83). Besides reducing the expression of intestinal tight junctions, there is also evidence that the gut microbiota may regulate gut permeability *via* the endocannabinoid system. In a study by Muccioli *et al.* (84), modulation of gut microbial composition, either by colonizing germfree mice or treating mice with antibiotics, reduced colonic and adipose tissue cannabinoid receptor (Cb)-1 expression, whereas feeding the mice a high fat diet increased Cb1 expression. Blocking this receptor in mice through the infusion of a Cb1 receptor antagonist resulted in an improved intestinal integrity, reduced plasma LPS levels, and reduced adiposity and body weight gain compared to the effects observed in saline-infused mice.

Lam *et al.* (62) found that the decrease in relative abundance of *Lactobacillus* and increase in *Oscillibacter* upon high fat feeding significantly correlated with a decreased transepithelial resistance. In turn, Cani *et al.* (83) showed that changing gut microbial composition with antibiotic treatment in mice fed a high fat diet significantly reduced gut permeability and increased tight junction expression, in association with reduced levels of circulating LPS and cecal LPS. Furthermore, it was shown that reduced plasma LPS levels upon antibiotic treatment also improved metabolic health in mice fed a high fat diet. Serum IL-6 and TNF α levels were lowered indicating reduced systemic inflammation. Antibiotic treatment also resulted in less infiltration of macrophages in adipose tissue, less body weight gain and improved insulin and glucose tolerance, all conditions related to systemic inflammation (77). Similar findings have been made in antibiotic treated ob/ob mice. The metabolic and inflammatory effects of antibiotic treatment were mostly mimicked by deletion of the LPS receptor CD14 (83). In addition, LPS also seems to have detrimental effects on the progression of NAFLD (85). Antibiotic treatment in mice with hepatic steatosis reduced hepatic lipid accumulation, which was associated with lower portal vein endotoxin levels(68).

Based on these and other findings, the gut microbiota may thus be involved in modifying intestinal permeability and trigger low grade (metabolic) endotoxemia and related disturbances (49, 75). However, it should be mentioned that several studies have not been able to replicate the elevated plasma LPS levels upon high fat feeding, despite causing obesity (86-88). It has also been suggested that a high fat diet increases the sensitivity of mice to LPS without affecting its plasma level (88).

In addition to LPS, other bacterial cell wall components may be involved in mediating

the effects of gut microbiota on metabolic health. Monocolonization of germfree mice with *Escherichia coli* or a mutant *E. coli* variant has shown that only the wild-type *E. coli* strain raised plasma LPS levels. However, both *E. coli* strains impaired insulin and glucose tolerance and increased adiposity (49). A possible role for the bacterial cell wall component peptidoglycans may be hypothesized based on the finding that activation of the peptidoglycan receptor nucleotide-binding oligomerization domain-containing protein (NOD)-1 induces hepatic and peripheral insulin resistance in mice, whereas loss of NOD1 and NOD2 in mice fed a high-fat diet resulted in higher insulin sensitive and lower adipose tissue inflammation (89).

The possible effects of the gut microbiota on gut permeability, glucose metabolism and inflammation are depicted in **Figure 2**.

Microbial regulation of metabolic processes

SCFAs

SCFAs are the main end products of bacterial fermentation in the intestine. The number of microbiota in the gut, the microbial composition, the gut transit time and the available substrates for microbial fermentation are all factors that influence the production of SCFAs (25, 90), which serve not only as substrates for energy production, lipogenesis, and gluconeogenesis but can also regulate biological processes by serving as signaling molecules.

An important set of molecular target for SCFAs are the G protein-coupled receptors (GPCRs) 41 and 43. These proteins are expressed in numerous tissues, including adipose tissue and enteroendocrine cells, leading to activation of distinct downstream effects (91, 92). GPCR41 and 43 are activated by a similar set of ligands but differ somewhat in their specificity. Whereas GPCR41 is activated more potently by propionate as compared with

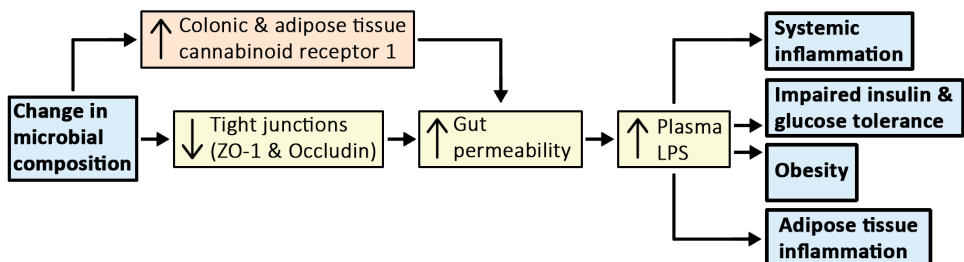


Figure 2. Possible effects of gut microbiota on gut permeability, glucose metabolism and inflammation. High-fat diet-induced changes microbial composition might increase gut permeability *via* cannabinoid receptor 1 and/or the expression of tight junctions. The increase in gut permeability induces endotoxemia and thereby possibly systemic inflammation, obesity, impaired insulin and glucose tolerance and adipose tissue inflammation.

acetate, GPCR43 displays a preference for acetate over propionate (93).

Samuel *et al.* (94) showed that the gut microbiota promotes adiposity and body weight *via* GPCR41-mediated signaling. They demonstrated that conventionally-raised wild-type mice and germfree wild-type mice co-colonized with *Bacteroides thetaiotaomicron* and *Methanobrevibacter smithii* - two prominent bacteria in the distal human gut - had significantly more adiposity and gained more body weight than their conventionally-raised GPCR41 knockout littermates. The increased adiposity and body weight gain may be related to increased serum levels of peptide YY (PYY), leading to a reduced gut transit rate. As a consequence, conventionally-raised wild-type mice may extract calories from their diet more efficiently and absorb more SCFAs, resulting in enhanced hepatic *de novo* lipogenesis, as indicated by increased hepatic triglyceride levels. These features were blunted in germfree wild-type and GPCR41 knockout mice as well as in germfree GPCR41 knockout mice that were co-colonized. In contrast, Lin *et al.* (95) found that bodyweight gain was similar between wild-type and GPCR41 knockout mice, suggesting a lack of effect of GPCR41 on adiposity. However, food intake was higher in GPCR41 knockout mice as compared to wild-type mice, suggesting less efficient energy harvest and thus a decrease in feed efficiency ratio in the GPCR41 knockout mice. Adding to the controversy, oral administration of butyrate and propionate was found to inhibit diet-induced obesity independently of GPCR41. With respect to GPCR43, Kimura *et al.* (96) showed that acetate-mediated signaling *via* GPCR43 may prevent obesity. GPCR43 knockout mice fed a high fat diet and treated with antibiotics and acetate had increased body and white adipose tissue weights, which were reduced in wild-type mice treated with the same regimen. Consistent with an anti-obesity effect of GPCR43, mice with adipose tissue-specific overexpression of GPCR43 had significantly lower body and adipose tissue weight than did their wild-type littermates. These mice also exhibited impaired insulin signaling in white adipose tissue, but not in muscle and liver, and had increased energy expenditure, which seemed to be attributable to a muscle-specific increase in the expression of glycolysis- and β -oxidation genes and reduced expression of gluconeogenesis genes. Taken together, SCFAs, mainly acetate, might activate adipose tissue GPCR43 to reduce uptake of fatty acids and glucose by adipocytes and improve systemic insulin sensitivity, leading to consumption of lipids and glucose by other tissues. It has been speculated that through this mechanism, adipose tissue GPCR43 activation may reduce adiposity and improve systemic insulin sensitivity. Whether circulating SCFA concentrations are sufficiently high to cause substantial activation of GPCR43 in adipose tissue requires further study.

In addition, GPCR43 activation in the intestine may also have an antidiabetic effect. It has been shown that GPCR43 activation by SCFAs promotes the release of glucagon-like peptide-1 by intestinal enteroendocrine L cells, thereby stimulating the release of insulin

and leading to improved glucose tolerance (97).

The above described actions of SCFAs *via* GPCR43 may provide a molecular explanation for the beneficial effects of dietary fiber on metabolic health (98). Diets rich in fiber increase the number of SCFA-producing bacteria and fecal SCFAs, as observed when comparing fecal microbiota from healthy European and African individuals (31). However, SCFA-mediated GPCR41 signaling seems to provoke opposite effects. Therefore, additional studies are necessary to sort out to what extent GPCR43 and -41 mediate the metabolic effects of SCFA in the intestine and other organs. In a recent study, it was shown that, in addition to GPCRs, SCFAs may elicit their effects *via* the peroxisome proliferator-activator receptor γ (PPAR γ). Specifically, it was observed that feeding mice a diet rich in inulin, which leads to enhanced SCFA production, induced PPAR target genes and pathways in the colon. In vitro studies indicated that butyrate and propionate are able to directly activate PPAR γ (99). In another study, SCFA supplementation in mice fed a high fat diet protected against body weight gain, which was accompanied by improved insulin sensitivity and decreased hepatic triglycerides. The reduction in hepatic steatosis by SCFAs was not observed in liver-specific PPAR γ knockout mice, whereas the reduction in bodyweight gain and the improved insulin sensitivity after SCFA supplementation were abolished in adipose tissue-specific PPAR γ knockout mice, indicating that the SCFA-induced effects are mediated *via* a tissue-specific PPAR γ -dependent mechanism (100).

An overview of the possible GPCR and PPAR γ -mediated effects of SCFA on obesity and diabetes is displayed in **Figure 3**.

Choline metabolism

As described in this review, changes in gut microbial composition may be linked to the development of obesity and diabetes. Emerging evidence also links the gut microbiota to cardiovascular diseases (101-103).

Wang *et al.* (101) were the first to report a relationship between microbial choline metabolism and development of atherosclerosis. Choline is an essential nutrient which is present in foods such as eggs and red meat. It is a component of cell membranes and is also involved in lipid metabolism (28). Feeding mice with labeled phosphatidylcholine resulted in increased levels of plasma trimethylamine (TMA) and subsequently trimethylamine N-oxide (TMAO), both metabolites of choline. TMA is formed in the intestine, absorbed and rapidly metabolized in the liver to TMAO by hepatic flavin-containing monooxygenases. It is of interest that plasma TMAO levels were not increased in phosphatidylcholine-fed germfree mice or mice treated with antibiotics, suggesting that the gut microbiota is involved in metabolic processing of dietary choline (101).

Feeding atherosclerosis-prone ApoE knockout mice a diet supplemented with 1% choline

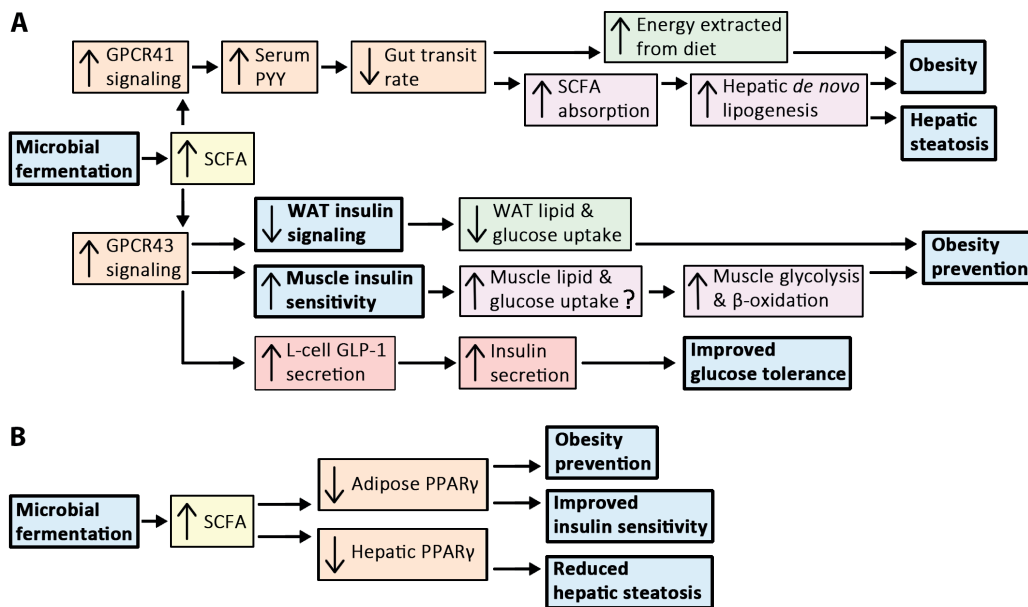


Figure 3. Possible GPCR- and PPAR γ -mediated effects of SCFA on obesity and diabetes

(A) Microbial fermentation induces in the production of SCFAs and subsequent signaling via GPCRs. SCFA-mediated GPCR41 signaling may reduce the gut transit rate, allowing more time to extract energy from the diet and thereby promoting energy uptake and obesity. In contrast, SCFA-mediated GPCR43 signaling in white adipose tissue (WAT) may prevent obesity by reducing insulin-mediated lipid and glucose uptake in WAT and improving muscle and liver insulin sensitivity, thereby promoting fatty acid and glucose consumption. GPCR43 signaling may also have antidiabetic effects by increasing muscle insulin sensitivity and insulin secretion. (B) SCFAs may also act in a PPAR γ -dependent fashion, as observed by SCFA supplementation in mice fed a high fat diet. Whereas SCFA-mediated reduction in adipose PPAR γ may prevent obesity and improve insulin sensitivity, the SCFA-attenuated hepatic PPAR γ may reduce hepatic steatosis.

resulted in increased plasma TMAO levels and a large increase in the number of foam cells, probably due to the increased expression of the cholesterol influx receptors CD36 and SRA. In addition, an increase in atherosclerotic lesion size was observed following addition of choline to the diet. When the gut microbiota was suppressed by antibiotics, foam cell formation and atherosclerotic development were inhibited (101). Similar results were seen in humans. When humans were challenged with phosphatidylcholine, plasma TMAO levels increased. Plasma TMAO levels were almost completely blunted after antibiotic treatment and reappeared when the use of antibiotics was discontinued. In addition, high plasma TMAO levels in humans were found to be associated with a high risk for major adverse cardiovascular events, even when the hazard ratios were adjusted for the traditional risk factors (104).

Expanding on the above findings, Koeth *et al.* (102) found that supplementation with either choline, L-carnitine - a nutrient in red meat that also contains a TMA - or TMAO reduced reverse cholesterol transport, which describes the movement of cholesterol from peripheral tissues back to the liver *via* the plasma. The reduced reverse cholesterol transport was abolished when the gut microbiota was suppressed with antibiotics. Taken together, diets rich in choline or L-carnitine raise plasma TMAO levels, possibly *via* their microbial conversion, which might thereby lead to enhanced development of atherosclerosis. An overview of how the gut microbiota may affect atherosclerotic development *via* the conversion of choline or L-carnitine is displayed in **Figure 4**.

Bile acid metabolism

Bile acids are formed in the liver from cholesterol. The primary bile acids cholic acid and chenodeoxycholic acid are secreted into the small intestine to assist with the emulsification and absorption of dietary lipids and fat-soluble vitamins. The diversity of the primary bile acids is increased through bacterial activity in the gut to form the secondary bile acids deoxycholic acid and lithocholic acid (105). Consequently, the absence of microbiota results in an increased abundance of primary bile acids and a decreased abundance of secondary bile acids, as seen in germfree rats (106) and in humans after oral intake of Vancomycin for 7 days (107). About 95% of the primary and secondary bile acids are reabsorbed in the intestine and returned to the liver *via* a process referred to as the enterohepatic cycle (105).

Bile acids also act as signaling molecules. An important molecular target of bile acids is the farnesoid X receptor (FXR). As the gut microbiota profoundly impacts bile acid metabolism, it can be hypothesized that the microbiota may also have a role in FXR signaling. In fact, it was found that the presence of microbiota downregulates genes involved in bile acid synthesis, such as the rate-limiting enzyme Cyp7a1, while upregulating genes encoding bile acid efflux transporters (106, 108). The effects on bile acid synthesis seems to

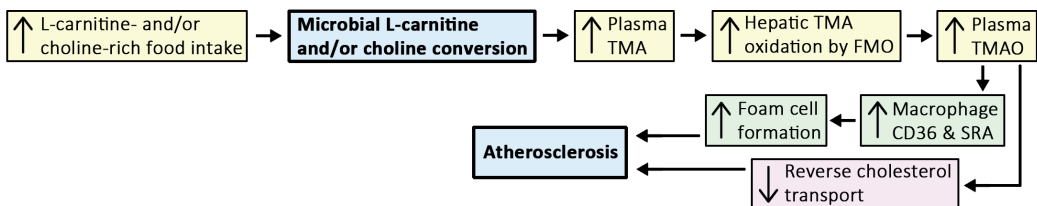


Figure 4. Proposed mechanism by which the gut microbiota may affect atherosclerosis *via* the conversion of choline and/or L-carnitine

The microbiota converts choline and/or L-carnitine to TMA, which is subsequently metabolized to TMAO. TMAO may increase foam cell formation and reduce reverse cholesterol transport, thereby increasing the risk of development of atherosclerosis.

depend on microbial FXR signaling, because the reduced liver Cyp7a1 expression, as seen in conventionally-raised mice as compared to germfree mice, was abolished in FXR knockout mice (108). Besides affecting bile acid metabolism, the gut microbiota has also been shown to alter the expression of genes involved in glucose and lipid metabolism related to the FXR pathway. Indeed, hepatic expression of phosphoenolpyruvate carboxykinase (PEPCK), glucose-6-phosphatase (G6PC), and SREBP-1 was upregulated in germfree and antibiotic-treated rats as compared to conventionally-raised rats (106). In contrast, treatment of mice with antibiotics that had been fed a high fat diet showed downregulation of hepatic SREBP-1c expression, resulting in decreased hepatic *de novo* lipogenesis. The absence of gut microbiota led to a significant increase in intestinal primary tauro- β -muricholic acid, which cannot be converted to secondary bile acids. Tauro- β -muricholic acid in turn inhibited intestinal FXR signaling, leading to inhibition of ceramide synthesis and reduced hepatic SREBP-1 expression and *de novo* lipogenesis (67). In addition to FXR, bile acids also signal *via* the membrane-bound receptor TGR5 to modulate glucose metabolism (28, 106). A recent study found a positive correlation between the abundance of fecal secondary bile acids and peripheral insulin sensitivity after modulation of the gut microbial composition by vancomycin treatment (107). However, a potential role for the FXR or TGR5 pathway was not investigated.

Several studies have shown that dietary fat content influences the gut microbiota, which may be mediated by changes in bile acids. (109-112). High-fat diets elevate bile secretion to enhance lipid emulsification and absorption and thereby also alter bile acid levels in the intestine. It was shown that adding cholic acid to the diet modifies gut microbial composition in favor of the Firmicutes and leads to increased fecal deoxycholic acid concentrations. Consistent with the bactericidal properties of deoxycholic acid, addition of cholic acid to the diet reduced total microbial counts by 51% compared to the control group (110). Accordingly, it can be suggested that the changes in gut microbial composition triggered by a high-fat diet might be the consequence of increased bile acid secretion. Next to its bactericidal property, deoxycholic acid can also induce DNA damage. Deoxycholic acid was found to be significantly increased upon high-fat feeding, promoting hepatocellular carcinoma in mice exposed to a chemical carcinogen. When the gut microbiota was suppressed with antibiotics, serum deoxycholic acid levels were lowered and a significant reduction in hepatocellular carcinomas development was observed, indicating that changes in microbial composition and its metabolites can have detrimental effects in the host (113).

Future perspectives

In this review we carefully analyzed the literature causally linking the gut microbiota to metabolic health with a special interest in potential underlying mechanisms.

Conventionalization studies, studies in germfree mice, and studies using antibiotics have provided evidence that changes in gut microbiota may be causally involved in metabolic disease, rather than merely being a consequence of it. Several different mechanisms have been proposed and explored that may mediate the possible effects of the gut microbiota on metabolic disorders, including increased energy harvest from the diet, increased gut permeability, changes in SCFA-mediated signaling, and altered bile acid metabolism.

Although several studies have provided evidence that the gut microbiota is causally involved in the development of obesity, conflicting reports exist. Indeed, whereas Caesar *et al.* (49) and Backhed *et al.* (48) found that germfree mice are protected against diet-induced obesity, Fleissner *et al.* (114) were unable to reproduce these findings. That the reduced diet-induced weight gain in germfree mice as compared to conventionally raised mice was not observed in rats is intriguing (115). Reports on the metabolic effect of the microbial fermentation products SCFAs in obesity development are also contradictory. SCFAs were suggested to promote obesity *via* GPCR41 signaling (94), whereas they were postulated to be protective against obesity through GPCR43 signaling (96) (**Figure 2**). These apparent contradictions may be explained by differences in how the gut microbiota is modulated. In some studies the composition of gut microbiota was modulated *via* the use of antibiotics, whereas other studies have used germfree mice. Second, diet, age, and the genetic makeup of the host are all confounding factors that vary among studies. Furthermore, differences in the composition of the gut microbiota at the start render it difficult to compare studies and to identify the specific microbes responsible for the observed effects. A problem with the use of antibiotics is that certain bacteria are resistant to antibiotics to them, and other microbes such as yeast may take over, making it difficult to pinpoint to the organisms responsible for the observed effects. Another concern is that nearly all studies characterize the microbiota composition in the feces, which may differ substantially from the microbial composition in the more proximal intestine (22).

A key question is whether studies with germfree and conventionally-raised animals appropriately reflect the role of microbiota in metabolic health in humans. The similarity in gut microbial composition between mice and humans is quite low. Ley *et al.* (8) found that although most of the phyla are present in both humans and mice, 85% of the bacteria genera found in mice are not found in humans. In addition, although studies with germfree animals provide valuable information, these animals are quite ill, perhaps as a result of defects in immune system development, morphological intestinal defects, or poor provision of vitamins to the host (23, 24). As a result, studies of germfree mice may not properly reflect the human physiological situation. Colonization of these mice with microbiota promotes obesity and reduces metabolic health, but it is questionable whether the observed findings are very informative towards the role of microbiota in human metabolic health.

An appropriate alternative approach to germfree mice would be to use mice colonized with human intestinal communities and a proper functioning immune system and intestinal physiology. In this model, the effect of human microbial composition on metabolic health can be studied *via* modulation of the gut microbiota with antibiotics. Furthermore, more emphasis should be placed on assessing changes in microbial gene expression as opposed to only measuring the genomic composition.

Another approach to explore the effects of the gut microbial composition on metabolic health is by performing intervention studies using pre- and probiotics. The term prebiotic describes ‘a selectively fermented ingredient that allows specific changes both in the composition and/or activity in the gastrointestinal microbiota that confers benefits upon host well-being and health’ (116). In principle, all dietary fibers that are fermented are assumed to have prebiotic properties. A large body of evidence suggests that various types of dietary fibers beneficially affect metabolic health. For instance, inulin-type fructans have been shown to counteract high fat diet-induced obesity and insulin resistance (117). Studies using various pre-biotics are an effective way to investigate the direct influence of changes in gut microbial activity on metabolic parameters.

Whereas prebiotics stimulate the growth and activities of gut microbiota, probiotics are orally delivered live bacteria that are assumed to affect health positively. Two reports have suggested that probiotics reduce body weight gain and have antidiabetic effects (118, 119). At the same time, two other studies have not shown any benefits of probiotics for metabolic health (53, 120). A meta-analysis by Million *et al.* (120) demonstrated that the same *Lactobacillus* strain might promote weight gain in undernourished individuals, whereas it may reduce weight gain in obese individuals. Accordingly, the effects of probiotics are not only strain dependent but likely also depend on the characteristics of the host. So far, the European Food Safety Authority has denied any health claims for probiotics. In contrast, numerous claims on prebiotics, including arabinoxylan, beta-glucan, and guar gum, have been approved. Overall, more evidence supporting a positive influence of pre- and probiotics on metabolic health is needed, including data from randomized human intervention trials. Also, additional insight should be gained into their mechanism of action.

In conclusion, there is growing understanding of how changes in intestinal microbial composition may affect the metabolic status of the host. More human trials are needed to substantiate the role of the gut microbiota in metabolic health in humans. Also, targeted studies should be conducted to better identify which bacterial strains positively influence metabolic health. Once the causality between the gut microbiota and metabolic health of the host can be further demonstrated, dietary interventions with, for example, prebiotics, probiotics or a combination of both can be used to modify an individual’s gut microbial composition and activity toward the prevention and possibly even treatment of metabolic

diseases.

Acknowledgements

This work was supported by The Netherlands Cardiovascular Research Committee IN-CONTROL Grant (CVON 2012-03).

References

1. Ng, M., Fleming, T., Robinson, M., Thomson, B., Graetz, N., Margono, C., Mullany, E.C., Biryukov, S., Abbafati, C., Abera, S.F. *et al.* (2014) Global, regional, and national prevalence of overweight and obesity in children and adults during 1980-2013: A systematic analysis for the global burden of disease study 2013. *Lancet* **384**, 766-781
2. Matheus, A.S., Tannus, L.R., Cobas, R.A., Palma, C.C., Negrato, C.A., and Gomes, M.B. (2013) Impact of diabetes on cardiovascular disease: An update. *Int. J. Hypertens.* **2013**, 653789
3. Despres, J.P., Lemieux, I., Bergeron, J., Pibarot, P., Mathieu, P., Larose, E., Rodes-Cabau, J., Bertrand, O.F., and Poirier, P. (2008) Abdominal obesity and the metabolic syndrome: Contribution to global cardiometabolic risk. *Arterioscler. Thromb. Vasc. Biol.* **28**, 1039-1049
4. Pi-Sunyer, X. (2009) The medical risks of obesity. *Postgrad. Med.* **121**, 21-33
5. D'Aversa, F., Tortora, A., Ianiro, G., Ponziani, F.R., Annicchiarico, B.E., and Gasbarrini, A. (2013) Gut microbiota and metabolic syndrome. *Intern. Emerg. Med.* **8** (Suppl 1), S11-5
6. Kau, A.L., Ahern, P.P., Griffin, N.W., Goodman, A.L., and Gordon, J.I. (2011) Human nutrition, the gut microbiome and the immune system. *Nature* **474**, 327-336
7. de Wit, N., Derrien, M., Bosch-Vermeulen, H., Keshtkar, S., Duval, C., de Vogel-van den Bosch, J., Kleerebezem, M., Muller, M., and van der Meer, R. (2012) Saturated fat stimulates obesity and hepatic steatosis and affects gut microbiota composition by an enhanced overflow of dietary fat to the distal intestine. *Am. J. Physiol. Gastrointest. Liver Physiol.* **303**, G589-99
8. Ley, R.E., Backhed, F., Turnbaugh, P., Lozupone, C.A., Knight, R.D., and Gordon, J.I. (2005) Obesity alters gut microbial ecology. *Proc. Natl.Acad.Sci.USA* **102**, 11070-11075
9. Turnbaugh, P.J., Backhed, F., Fulton, L., and Gordon, J.I. (2008) Diet-induced obesity is linked to marked but reversible alterations in the mouse distal gut microbiome. *Cell Host Microbe* **3**, 213-223
10. Ley, R.E., Turnbaugh, P.J., Klein, S., and Gordon, J.I. (2006) Microbial ecology: Human gut microbes associated with obesity. *Nature* **444**, 1022-1023
11. Schwiertz, A., Taras, D., Schafer, K., Beijer, S., Bos, N.A., Donus, C., and Hardt, P.D. (2010) Microbiota and SCFA in lean and overweight healthy subjects. *Obesity (Silver Spring)* **18**, 190-195
12. Karlsson, F.H., Fak, F., Nookaew, I., Tremaroli, V., Fagerberg, B., Petranovic, D., Backhed, F., and Nielsen, J. (2012) Symptomatic atherosclerosis is associated with an altered gut metagenome. *Nat.Commun.* **3**, 1245
13. Qin, J., Li, Y., Cai, Z., Li, S., Zhu, J., Zhang, F., Liang, S., Zhang, W., Guan, Y., Shen, D. *et al.* (2012) A metagenome-wide association study of gut microbiota in type 2 diabetes. *Nature* **490**, 55-60
14. Jiang, W., Wu, N., Wang, X., Chi, Y., Zhang, Y., Qiu, X., Hu, Y., Li, J., and Liu, Y. (2015) Dysbiosis gut microbiota associated with inflammation and impaired mucosal immune function in intestine of humans with non-alcoholic fatty liver disease. *Sci.Rep.* **5**, 8096
15. Zhu, L., Baker, S.S., Gill, C., Liu, W., Alkhourri, R., Baker, R.D., and Gill, S.R. (2013) Characterization of gut microbiomes in nonalcoholic steatohepatitis (NASH) patients: A connection between endogenous alcohol and NASH. *Hepatology* **57**, 601-609
16. Clemente, J.C., Ursell, L.K., Parfrey, L.W., and Knight, R. (2012) The impact of the gut microbiota on human health: An integrative view. *Cell* **148**, 1258-1270
17. Sekirov, I., Russell, S.L., Antunes, L.C., and Finlay, B.B. (2010) Gut microbiota in health and disease. *Physiol. Rev.* **90**, 859-904
18. Sommer, F., and Backhed, F. (2013) The gut microbiota--masters of host development and physiology. *Nat. Rev. Microbiol.* **11**, 227-238
19. Moschen, A.R., Wieser, V., and Tilg, H. (2012) Dietary factors: Major regulators of the gut's microbiota. *Gut Liver* **6**, 411-416
20. Kinross, J.M., von Roon, A.C., Holmes, E., Darzi, A., and Nicholson, J.K. (2008) The human gut microbiome: Implications for future health care. *Curr. Gastroenterol. Rep.* **10**, 396-403
21. Qin, J., Li, R., Raes, J., Arumugam, M., Burgdorf, K.S., Manichanh, C., Nielsen, T., Pons, N., Levenez, F., Yamada, T. *et al.* (2010) A human gut microbial gene catalogue established by metagenomic sequencing. *Nature* **464**, 59-65
22. Eckburg, P.B., Bik, E.M., Bernstein, C.N., Purdom, E., Dethlefsen, L., Sargent, M., Gill, S.R., Nelson, K.E., and Relman, D.A. (2005) Diversity of the human intestinal microbial flora. *Science* **308**, 1635-1638
23. Round, J.L., and Mazmanian, S.K. (2009) The gut microbiota shapes intestinal immune responses during health and disease. *Nat. Rev. Immunol.* **9**, 313-323
24. Smith, K., McCoy, K.D., and Macpherson, A.J. (2007) Use of axenic animals in studying the adaptation of mammals to their commensal intestinal microbiota. *Semin. Immunol.* **19**, 59-69
25. Wong, J.M., Esfahani, A., Singh, N., Villa, C.R., Mirrahimi, A., Jenkins, D.J., and Kendall, C.W. (2012) Gut microbiota, diet, and heart disease. *J.AOAC Int.* **95**, 24-30
26. Chassard, C., and Lacroix, C. (2013) Carbohydrates and the human gut microbiota. *Curr. Opin. Clin.*

- Nutr. Metab. Care* **16**, 453-460
27. Louis, P., Scott, K.P., Duncan, S.H., and Flint, H.J. (2007) Understanding the effects of diet on bacterial metabolism in the large intestine. *J. Appl. Microbiol.* **102**, 1197-1208
 28. Tremaroli, V., and Backhed, F. (2012) Functional interactions between the gut microbiota and host metabolism. *Nature* **489**, 242-249
 29. Benson, A.K., Kelly, S.A., Legge, R., Ma, F., Low, S.J., Kim, J., Zhang, M., Oh, P.L., Nehrenberg, D., Hua, K. *et al.* (2010) Individuality in gut microbiota composition is a complex polygenic trait shaped by multiple environmental and host genetic factors. *Proc. Natl. Acad. Sci. USA* **107**, 18933-18938
 30. Turnbaugh, P.J., Ley, R.E., Hamady, M., Fraser-Liggett, C.M., Knight, R., and Gordon, J.I. (2007) The human microbiome project. *Nature* **449**, 804-810
 31. De Filippo, C., Cavalieri, D., Di Paola, M., Ramazzotti, M., Poullet, J.B., Massart, S., Collini, S., Pieraccini, G., and Lionetti, P. (2010) Impact of diet in shaping gut microbiota revealed by a comparative study in children from europe and rural africa. *Proc. Natl. Acad. Sci. USA* **107**, 14691-14696
 32. Wu, G.D., Chen, J., Hoffmann, C., Bittinger, K., Chen, Y.Y., Keilbaugh, S.A., Bewtra, M., Knights, D., Walters, W.A., Knight, R. *et al.* (2011) Linking long-term dietary patterns with gut microbial enterotypes. *Science* **334**, 105-108
 33. David, L.A., Maurice, C.F., Carmody, R.N., Gootenberg, D.B., Button, J.E., Wolfe, B.E., Ling, A.V., Devlin, A.S., Varma, Y., Fischbach, M.A. *et al.* (2014) Diet rapidly and reproducibly alters the human gut microbiome. *Nature* **505**, 559-563
 34. Walker, A.W., Ince, J., Duncan, S.H., Webster, L.M., Holtrop, G., Ze, X., Brown, D., Stares, M.D., Scott, P., Bergerat, A. *et al.* (2011) Dominant and diet-responsive groups of bacteria within the human colonic microbiota. *ISME J.* **5**, 220-230
 35. Carmody, R.N., Gerber, G.K., Luevano, J.M., Jr, Gatti, D.M., Somes, L., Svenson, K.L., and Turnbaugh, P.J. (2015) Diet dominates host genotype in shaping the murine gut microbiota. *Cell Host Microbe* **17**, 72-84
 36. Zimmer, J., Lange, B., Frick, J.S., Sauer, H., Zimmermann, K., Schwiertz, A., Rusch, K., Klosterhalfen, S., and Enck, P. (2012) A vegan or vegetarian diet substantially alters the human colonic faecal microbiota. *Eur. J. Clin. Nutr.* **66**, 53-60
 37. Yan, H., Potu, R., Lu, H., Vezzoni de Almeida, V., Stewart, T., Ragland, D., Armstrong, A., Adeola, O., Nakatsu, C.H., and Ajuwon, K.M. (2013) Dietary fat content and fiber type modulate hind gut microbial community and metabolic markers in the pig. *PLoS ONE* **8**, e59581
 38. Turnbaugh, P.J., Hamady, M., Yatsunenko, T., Cantarel, B.L., Duncan, A., Ley, R.E., Sogin, M.L., Jones, W.J., Roe, B.A., Affourtit, J.P. *et al.* (2009) A core gut microbiome in obese and lean twins. *Nature* **457**, 480-484
 39. Nicholson, J.K., Holmes, E., Kinross, J., Burcelin, R., Gibson, G., Jia, W., and Pettersson, S. (2012) Host-gut microbiota metabolic interactions. *Science* **336**, 1262-1267
 40. Yi, P., and Li, L. (2012) The germfree murine animal: An important animal model for research on the relationship between gut microbiota and the host. *Vet. Microbiol.* **157**, 1-7
 41. Turnbaugh, P.J., Ridaura, V.K., Faith, J.J., Rey, F.E., Knight, R., and Gordon, J.I. (2009) The effect of diet on the human gut microbiome: A metagenomic analysis in humanized gnotobiotic mice. *Sci. Translat. Med.* **1**, 6ra14
 42. Goodman, A.L., Kallstrom, G., Faith, J.J., Reyes, A., Moore, A., Dantas, G., and Gordon, J.I. (2011) Extensive personal human gut microbiota culture collections characterized and manipulated in gnotobiotic mice. *Proc. Natl. Acad. Sci. USA* **108**, 6252-6257
 43. Benoit, B., Laugerette, F., Plaisancie, P., Geloën, A., Bodennec, J., Estienne, M., Pineau, G., Bernalier-Donadille, A., Vidal, H., and Michalski, M.C. (2015) Increasing fat content from 20 to 45 wt% in a complex diet induces lower endotoxemia in parallel with an increased number of intestinal goblet cells in mice. *Nutr. Res.* **35**, 346-356
 44. Mozes, S., Bujnakova, D., Sefcikova, Z., and Kmet, V. (2008) Intestinal microflora and obesity in rats. *Folia Microbiol. (Praha)* **53**, 225-228
 45. Guo, X., Xia, X., Tang, R., Zhou, J., Zhao, H., and Wang, K. (2008) Development of a real-time PCR method for firmicutes and bacteroidetes in faeces and its application to quantify intestinal population of obese and lean pigs. *Lett. Appl. Microbiol.* **47**, 367-373
 46. Hildebrandt, M.A., Hoffmann, C., Sherrill-Mix, S.A., Keilbaugh, S.A., Hamady, M., Chen, Y.Y., Knight, R., Ahima, R.S., Bushman, F., and Wu, G.D. (2009) High-fat diet determines the composition of the murine gut microbiome independently of obesity. *Gastroenterology* **137**, 1716-24.e1-2
 47. Murphy, E.F., Cotter, P.D., Healy, S., Marques, T.M., O'Sullivan, O., Fouhy, F., Clarke, S.F., O'Toole, P.W., Quigley, E.M., Stanton, C. *et al.* (2010) Composition and energy harvesting capacity of the gut microbiota: Relationship to diet, obesity and time in mouse models. *Gut* **59**, 1635-1642
 48. Backhed, F., Manchester, J.K., Semenkovich, C.F., and Gordon, J.I. (2007) Mechanisms underlying the resistance to diet-induced obesity in germ-free mice. *Proc. Natl. Acad. Sci. USA* **104**, 979-984

49. Caesar, R., Reigstad, C.S., Backhed, H.K., Reinhardt, C., Ketonen, M., Lunden, G.O., Cani, P.D., and Backhed, F. (2012) Gut-derived lipopolysaccharide augments adipose macrophage accumulation but is not essential for impaired glucose or insulin tolerance in mice. *Gut* **61**, 1701-1707
50. Ding, S., Chi, M.M., Scull, B.P., Rigby, R., Schwerbrock, N.M., Magness, S., Jobin, C., and Lund, P.K. (2010) High-fat diet: Bacteria interactions promote intestinal inflammation which precedes and correlates with obesity and insulin resistance in mouse. *PLoS ONE* **5**, e12191
51. Ellekilde, M., Selfjord, E., Larsen, C.S., Jaksevic, M., Rune, I., Tranberg, B., Vogensen, F.K., Nielsen, D.S., Bahl, M.I., Licht, T.R., Hansen, A.K., and Hansen, C.H. (2014) Transfer of gut microbiota from lean and obese mice to antibiotic-treated mice. *Sci. Rep.* **4**, 5922
52. Ridaura, V.K., Faith, J.J., Rey, F.E., Cheng, J., Duncan, A.E., Kau, A.L., Griffin, N.W., Lombard, V., Henrissat, B., Bain, J.R. *et al.* (2013) Gut microbiota from twins discordant for obesity modulate metabolism in mice. *Science* **341**, 1241214
53. Murphy, E.F., Cotter, P.D., Hogan, A., O'Sullivan, O., Joyce, A., Fouhy, F., Clarke, S.F., Marques, T.M., O'Toole, P.W., Stanton, C. *et al.* (2013) Divergent metabolic outcomes arising from targeted manipulation of the gut microbiota in diet-induced obesity. *Gut* **62**, 220-226
54. Cox, L.M., Yamanishi, S., Sohn, J., Alekseyenko, A.V., Leung, J.M., Cho, I., Kim, S.G., Li, H., Gao, Z., Mahana, D. *et al.* (2014) Altering the intestinal microbiota during a critical developmental window has lasting metabolic consequences. *Cell* **158**, 705-721
55. Furet, J.P., Kong, L.C., Tap, J., Poitou, C., Basdevant, A., Bouillot, J.L., Mariat, D., Corthier, G., Dore, J., Henegar, C., Rizkalla, S., and Clement, K. (2010) Differential adaptation of human gut microbiota to bariatric surgery-induced weight loss: Links with metabolic and low-grade inflammation markers. *Diabetes* **59**, 3049-3057
56. Zhang, H., DiBaise, J.K., Zuccolo, A., Kudrna, D., Braidotti, M., Yu, Y., Parameswaran, P., Crowell, M.D., Wing, R., Rittmann, B.E., and Krajmalnik-Brown, R. (2009) Human gut microbiota in obesity and after gastric bypass. *Proc. Natl. Acad. Sci. USA* **106**, 2365-2370
57. Duncan, S.H., Lopley, G.E., Holtrop, G., Ince, J., Johnstone, A.M., Louis, P., and Flint, H.J. (2008) Human colonic microbiota associated with diet, obesity and weight loss. *Int. J. Obes.* **32**, 1720-1724
58. Liou, A.P., Paziuk, M., Luevano, J.M., Jr, Machineni, S., Turnbaugh, P.J., and Kaplan, L.M. (2013) Conserved shifts in the gut microbiota due to gastric bypass reduce host weight and adiposity. *Sci. Translat. Med.* **5**, 178ra41
59. Crawford, P.A., Crowley, J.R., Sambandam, N., Muegge, B.D., Costello, E.K., Hamady, M., Knight, R., and Gordon, J.I. (2009) Regulation of myocardial ketone body metabolism by the gut microbiota during nutrient deprivation. *Proc. Natl. Acad. Sci. USA* **106**, 11276-11281
60. Dethlefsen, L., Huse, S., Sogin, M.L., and Relman, D.A. (2008) The pervasive effects of an antibiotic on the human gut microbiota, as revealed by deep 16S rRNA sequencing. *PLoS Biol.* **6**, e280
61. Thuny, F., Richet, H., Casalta, J.P., Angelakis, E., Habib, G., and Raoult, D. (2010) Vancomycin treatment of infective endocarditis is linked with recently acquired obesity. *PLoS ONE* **5**, e9074
62. Lam, Y.Y., Ha, C.W., Campbell, C.R., Mitchell, A.J., Dinudom, A., Oscarsson, J., Cook, D.I., Hunt, N.H., Caterson, I.D., Holmes, A.J., and Storlien, L.H. (2012) Increased gut permeability and microbiota change associate with mesenteric fat inflammation and metabolic dysfunction in diet-induced obese mice. *PLoS ONE* **7**, e34233
63. Henao-Mejia, J., Elinav, E., Jin, C., Hao, L., Mehal, W.Z., Strowig, T., Thaiss, C.A., Kau, A.L., Eisenbarth, S.C., Jurczak, M.J. *et al.* (2012) Inflammasome-mediated dysbiosis regulates progression of NAFLD and obesity. *Nature* **482**, 179-185
64. Dixon, L.J., Flask, C.A., Papouchado, B.G., Feldstein, A.E., and Nagy, L.E. (2013) Caspase-1 as a central regulator of high fat diet-induced non-alcoholic steatohepatitis. *PLoS ONE* **8**, e56100
65. Peverill, W., Powell, L.W., and Skoien, R. (2014) Evolving concepts in the pathogenesis of NASH: Beyond steatosis and inflammation. *Int. J. Mol. Sci.* **15**, 8591-8638
66. Wree, A., McGeough, M.D., Pena, C.A., Schlattjan, M., Li, H., Inzaugarat, M.E., Messer, K., Canbay, A., Hoffman, H.M., and Feldstein, A.E. (2014) NLRP3 inflammasome activation is required for fibrosis development in NAFLD. *J. Mol. Med.* **92**, 1069-1082
67. Jiang, C., Xie, C., Li, F., Zhang, L., Nichols, R.G., Krausz, K.W., Cai, J., Qi, Y., Fang, Z.Z., Takahashi, S. *et al.* (2015) Intestinal farnesoid X receptor signaling promotes nonalcoholic fatty liver disease. *J. Clin. Invest.* **125**, 386-402
68. Bergheim, I., Weber, S., Vos, M., Kramer, S., Volynets, V., Kaserouni, S., McClain, C.J., and Bischoff, S.C. (2008) Antibiotics protect against fructose-induced hepatic lipid accumulation in mice: Role of endotoxin. *J. Hepatol.* **48**, 983-992
69. Lin, Y., Yu, L.X., Yan, H.X., Yang, W., Tang, L., Zhang, H.L., Liu, Q., Zou, S.S., He, Y.Q., Wang, C., Wu, M.C., and Wang, H.Y. (2012) Gut-derived lipopolysaccharide promotes T-cell-mediated hepatitis in mice through toll-like receptor 4. *Cancer Prev. Res. (Phila.)* **5**, 1090-1102
70. Rabot, S., Membrez, M., Bruneau, A., Gerard, P., Harach, T., Moser, M., Raymond, F., Mansourian, R.,

- and Chou, C.J. (2010) Germ-free C57BL/6J mice are resistant to high-fat-diet-induced insulin resistance and have altered cholesterol metabolism. *FASEB J* **24**, 4948-4959
71. Ye, X.Y., Xue, Y.M., Sha, J.P., Li, C.Z., and Zhen, Z.J. (2009) Serum amyloid A attenuates cellular insulin sensitivity by increasing JNK activity in 3T3-L1 adipocytes. *J. Endocrinol. Invest.* **32**, 568-575
72. Backhed, F., Ding, H., Wang, T., Hooper, L.V., Koh, G.Y., Nagy, A., Semenkovich, C.F., and Gordon, J.I. (2004) The gut microbiota as an environmental factor that regulates fat storage. *Proc. Natl. Acad. Sci. USA* **101**, 15718-15723
73. Vrieze, A., Van Nood, E., Holleman, F., Salojarvi, J., Kootte, R.S., Bartelsman, J.F., Dallinga-Thie, G.M., Ackermans, M.T., Serlie, M.J., Oozeer, R. *et al.* (2012) Transfer of intestinal microbiota from lean donors increases insulin sensitivity in individuals with metabolic syndrome. *Gastroenterology* **143**, 913-6.e7
74. Pankow, J.S., Duncan, B.B., Schmidt, M.I., Ballantyne, C.M., Couper, D.J., Hoogeveen, R.C., Golden, S.H., and Atherosclerosis Risk in Communities Study. (2004) Fasting plasma free fatty acids and risk of type 2 diabetes: The atherosclerosis risk in communities study. *Diabetes Care* **27**, 77-82
75. Membrez, M., Blancher, F., Jaquet, M., Bibiloni, R., Cani, P.D., Burcelin, R.G., Corthesy, I., Mace, K., and Chou, C.J. (2008) Gut microbiota modulation with norfloxacin and ampicillin enhances glucose tolerance in mice. *FASEB J* **22**, 2416-2426
76. Turnbaugh, P.J., Ley, R.E., Mahowald, M.A., Magrini, V., Mardis, E.R., and Gordon, J.I. (2006) An obesity-associated gut microbiome with increased capacity for energy harvest. *Nature* **444**, 1027-1031
77. Carvalho, B.M., Guadagnini, D., Tsukumo, D.M., Schenka, A.A., Latuf-Filho, P., Vassallo, J., Dias, J.C., Kubota, L.T., Carvalheira, J.B., and Saad, M.J. (2012) Modulation of gut microbiota by antibiotics improves insulin signalling in high-fat fed mice. *Diabetologia* **55**, 2823-2834
78. Velagapudi, V.R., Hezaveh, R., Reigstad, C.S., Gopalacharyulu, P., Yetukuri, L., Islam, S., Felin, J., Perkins, R., Boren, J., Oresic, M., and Backhed, F. (2010) The gut microbiota modulates host energy and lipid metabolism in mice. *J. Lipid Res.* **51**, 1101-1112
79. Mattijssen, F., Alex, S., Swarts, H.J., Groen, A.K., van Schothorst, E.M., and Kersten, S. (2013) Angptl4 serves as an endogenous inhibitor of intestinal lipid digestion. *Mol. Metab.* **3**, 135-144
80. Cani, P.D., Amar, J., Iglesias, M.A., Poggi, M., Knauf, C., Bastelica, D., Neyrinck, A.M., Fava, F., Tuohy, K.M., Chabo, C. *et al.* (2007) Metabolic endotoxemia initiates obesity and insulin resistance. *Diabetes* **56**, 1761-1772
81. Pendyala, S., Walker, J.M., and Holt, P.R. (2012) A high-fat diet is associated with endotoxemia that originates from the gut. *Gastroenterology* **142**, 1100-1101.e2
82. Wellen, K.E., and Hotamisligil, G.S. (2005) Inflammation, stress, and diabetes. *J. Clin. Invest.* **115**, 1111-1119
83. Cani, P.D., Bibiloni, R., Knauf, C., Waget, A., Neyrinck, A.M., Delzenne, N.M., and Burcelin, R. (2008) Changes in gut microbiota control metabolic endotoxemia-induced inflammation in high-fat diet-induced obesity and diabetes in mice. *Diabetes* **57**, 1470-1481
84. Muccioli, G.G., Naslain, D., Backhed, F., Reigstad, C.S., Lambert, D.M., Delzenne, N.M., and Cani, P.D. (2010) The endocannabinoid system links gut microbiota to adipogenesis. *Mol. Syst. Biol.* **6**, 392
85. Fukunishi, S., Sujishi, T., Takeshita, A., Ohama, H., Tsuchimoto, Y., Asai, A., Tsuda, Y., and Higuchi, K. (2014) Lipopolysaccharides accelerate hepatic steatosis in the development of nonalcoholic fatty liver disease in Zucker rats. *J. Clin. Biochem. Nutr.* **54**, 39-44
86. Lichtenstein, L., Mattijssen, F., de Wit, N.J., Georgiadi, A., Hooiveld, G.J., van der Meer, R., He, Y., Qi, L., Koster, A., Tamsma, J.T. *et al.* (2010) Angptl4 protects against severe proinflammatory effects of saturated fat by inhibiting fatty acid uptake into mesenteric lymph node macrophages. *Cell Metab.* **12**, 580-592
87. Laugerette, F., Furet, J.P., Debar, C., Daira, P., Loizon, E., Gelo, A., Soulage, C.O., Simonet, C., Lefils-Lacourtablaie, J., Bernoud-Hubac, N. *et al.* (2012) Oil composition of high-fat diet affects metabolic inflammation differently in connection with endotoxin receptors in mice. *Am. J. Physiol. Endocrinol. Metab.* **302**, E374-86
88. Huang, H., Liu, T., Rose, J.L., Stevens, R.L., and Hoyt, D.G. (2007) Sensitivity of mice to lipopolysaccharide is increased by a high saturated fat and cholesterol diet. *J. Inflamm. (Lond.)* **4**, 22
89. Schertzer, J.D., Tamrakar, A.K., Magalhaes, J.G., Pereira, S., Bilan, P.J., Fullerton, M.D., Liu, Z., Steinberg, G.R., Giacca, A., Philpott, D.J., and Klip, A. (2011) NOD1 activators link innate immunity to insulin resistance. *Diabetes* **60**, 2206-2215
90. Bergman, E.N. (1990) Energy contributions of volatile fatty acids from the gastrointestinal tract in various species. *Physiol. Rev.* **70**, 567-590
91. Le Poul, E., Loison, C., Struyf, S., Springael, J.Y., Lannoy, V., Decobecq, M.E., Brezillon, S., Dupriez, V., Vassart, G., Van Damme, J., Parmentier, M., and Detheux, M. (2003) Functional characterization of human receptors for short chain fatty acids and their role in polymorphonuclear cell activation. *J. Biol. Chem.* **278**, 25481-25489
92. Nohr, M.K., Pedersen, M.H., Gille, A., Egerod, K.L., Engelstoft, M.S., Husted, A.S., Sichlau, R.M.,

- Grunddal, K.V., Poulsen, S.S., Han, S. *et al.* (2013) GPR41/FFAR3 and GPR43/FFAR2 as cosensors for short-chain fatty acids in enteroendocrine cells vs FFAR3 in enteric neurons and FFAR2 in enteric leukocytes. *Endocrinology* **154**, 3552-3564
93. Brown, A.J., Goldsworthy, S.M., Barnes, A.A., Eilert, M.M., Tcheang, L., Daniels, D., Muir, A.I., Wigglesworth, M.J., Kinghorn, I., Fraser, N.J. *et al.* (2003) The orphan G protein-coupled receptors GPR41 and GPR43 are activated by propionate and other short chain carboxylic acids. *J. Biol. Chem.* **278**, 11312-11319
94. Samuel, B.S., Shaito, A., Motoike, T., Rey, F.E., Backhed, F., Manchester, J.K., Hammer, R.E., Williams, S.C., Crowley, J., Yanagisawa, M., and Gordon, J.I. (2008) Effects of the gut microbiota on host adiposity are modulated by the short-chain fatty-acid binding G protein-coupled receptor, Gpr41. *Proc. Natl. Acad. Sci. USA* **105**, 16767-16772
95. Lin, H.V., Frassetto, A., Kowalik, E.J., Jr, Nawrocki, A.R., Lu, M.M., Kosinski, J.R., Hubert, J.A., Szeto, D., Yao, X., Forrest, G., and Marsh, D.J. (2012) Butyrate and propionate protect against diet-induced obesity and regulate gut hormones via free fatty acid receptor 3-independent mechanisms. *PLoS ONE* **7**, e35240
96. Kimura, I., Ozawa, K., Inoue, D., Imamura, T., Kimura, K., Maeda, T., Terasawa, K., Kashiwara, D., Hirano, K., Tani, T. *et al.* (2013) The gut microbiota suppresses insulin-mediated fat accumulation via the short-chain fatty acid receptor GPR43. *Nat. Commun.* **4**, 1829
97. Tolhurst, G., Heffron, H., Lam, Y.S., Parker, H.E., Habib, A.M., Diakogiannaki, E., Cameron, J., Grosse, J., Reimann, F., and Gribble, F.M. (2012) Short-chain fatty acids stimulate glucagon-like peptide-1 secretion via the G-protein-coupled receptor FFAR2. *Diabetes* **61**, 364-371
98. Galisteo, M., Duarte, J., and Zarzuelo, A. (2008) Effects of dietary fibers on disturbances clustered in the metabolic syndrome. *J. Nutr. Biochem.* **19**, 71-84
99. Alex, S., Lange, K., Amolo, T., Grinstead, J.S., Haakonsson, A.K., Szalowska, E., Koppen, A., Mudde, K., Haenen, D., Al-Lahham, S. *et al.* (2013) Short-chain fatty acids stimulate angiopoietin-like 4 synthesis in human colon adenocarcinoma cells by activating peroxisome proliferator-activated receptor gamma. *Mol. Cell. Biol.* **33**, 1303-1316
100. den Besten, G., Bleeker, A., Gerding, A., van Eunen, K., Havinga, R., van Dijk, T.H., Oosterveer, M.H., Jonker, J.W., Groen, A.K., Reijngoud, D.J., and Bakker, B.M. (2015) Short-chain fatty acids protect against high-fat diet-induced obesity via a PPAR γ -dependent switch from lipogenesis to fat oxidation. *Diabetes* **64**, 2398-2408
101. Wang, Z., Klipfell, E., Bennett, B.J., Koeth, R., Levison, B.S., Dugar, B., Feldstein, A.E., Britt, E.B., Fu, X., Chung, Y.M. *et al.* (2011) Gut flora metabolism of phosphatidylcholine promotes cardiovascular disease. *Nature* **472**, 57-63
102. Koeth, R.A., Wang, Z., Levison, B.S., Buffa, J.A., Org, E., Sheehy, B.T., Britt, E.B., Fu, X., Wu, Y., Li, L. *et al.* (2013) Intestinal microbiota metabolism of L-carnitine, a nutrient in red meat, promotes atherosclerosis. *Nat. Med.* **19**, 576-585
103. Koeth, R., Levison, B., Culley, M., Buffa, J., Wang, Z., Gregory, J., Org, E., Wu, Y., Li, L., Smith, J. *et al.* (2014) γ -Butyrobetaine is a proatherogenic intermediate in gut microbial metabolism of L-carnitine to TMAO. *Cell Metab.* **20**, 799-812
104. Tang, W.H., Wang, Z., Levison, B.S., Koeth, R.A., Britt, E.B., Fu, X., Wu, Y., and Hazen, S.L. (2013) Intestinal microbial metabolism of phosphatidylcholine and cardiovascular risk. *N. Engl. J. Med.* **368**, 1575-1584
105. Hamer, H.M., De Preter, V., Windey, K., and Verbeke, K. (2012) Functional analysis of colonic bacterial metabolism: Relevant to health? *Am. J. Physiol. Gastrointest. Liver Physiol.* **302**, G1-9
106. Swann, J.R., Want, E.J., Geier, F.M., Spagou, K., Wilson, I.D., Sidaway, J.E., Nicholson, J.K., and Holmes, E. (2011) Systemic gut microbial modulation of bile acid metabolism in host tissue compartments. *Proc. Natl. Acad. Sci. USA* **108** (Suppl 1), 4523-4530
107. Vrieze, A., Out, C., Fuentes, S., Jonker, L., Reuling, I., Kootte, R.S., van Nood, E., Holleman, F., Knaapen, M., Romijn, J.A. *et al.* (2014) Impact of oral vancomycin on gut microbiota, bile acid metabolism, and insulin sensitivity. *J. Hepatol.* **60**, 824-831
108. Sayin, S.I., Wahlstrom, A., Felin, J., Jantti, S., Marschall, H.U., Bamberg, K., Angelin, B., Hyotylainen, T., Oresic, M., and Backhed, F. (2013) Gut microbiota regulates bile acid metabolism by reducing the levels of tauro-beta-muricholic acid, a naturally occurring FXR antagonist. *Cell Metab.* **17**, 225-235
109. Yokota, A., Fukiya, S., Islam, K.B., Ooka, T., Ogura, Y., Hayashi, T., Hagio, M., and Ishizuka, S. (2012) Is bile acid a determinant of the gut microbiota on a high-fat diet? *Gut Microbes* **3**, 455-459
110. Islam, K.B., Fukiya, S., Hagio, M., Fujii, N., Ishizuka, S., Ooka, T., Ogura, Y., Hayashi, T., and Yokota, A. (2011) Bile acid is a host factor that regulates the composition of the cecal microbiota in rats. *Gastroenterology* **141**, 1773-1781
111. Devkota, S., Wang, Y., Musch, M.W., Leone, V., Fehlner-Peach, H., Nadimpalli, A., Antonopoulos, D.A., Jabri, B., and Chang, E.B. (2012) Dietary-fat-induced taurocholic acid promotes pathobiont expansion and colitis in IL10 $^{-/-}$ mice. *Nature* **487**, 104-108

112. Binder, H.J., Filburn, B., and Floch, M. (1975) Bile acid inhibition of intestinal anaerobic organisms. *Am. J. Clin. Nutr.* **28**, 119-125
113. Yoshimoto, S., Loo, T.M., Atarashi, K., Kanda, H., Sato, S., Oyadomari, S., Iwakura, Y., Oshima, K., Morita, H., Hattori, M. *et al.* (2013) Obesity-induced gut microbial metabolite promotes liver cancer through senescence secretome. *Nature* **499**, 97-101
114. Fleissner, C.K., Huebel, N., Abd El-Bary, M.M., Loh, G., Klaus, S., and Blaut, M. (2010) Absence of intestinal microbiota does not protect mice from diet-induced obesity. *Br. J. Nutr.* **104**, 919-929
115. Swartz, T.D., Sakar, Y., Duca, F.A., and Covasa, M. (2013) Preserved adiposity in the fischer 344 rat devoid of gut microbiota. *FASEB J* **27**, 1701-1710
116. Robles Alonso, V., and Guarner, F. (2013) Linking the gut microbiota to human health. *Br. J. Nutr.* **109** (Suppl 2), S21-6
117. Dewulf, E.M., Cani, P.D., Neyrinck, A.M., Possemiers, S., Van Holle, A., Muccioli, G.G., Deldicque, L., Bindels, L.B., Pachikian, B.D., Sohet, F.M. *et al.* (2011) Inulin-type fructans with prebiotic properties counteract GPR43 overexpression and PPARgamma-related adipogenesis in the white adipose tissue of high-fat diet-fed mice. *J. Nutr. Biochem.* **22**, 712-722
118. Arora, T., Singh, S., and Sharma, R.K. (2013) Probiotics: Interaction with gut microbiome and antiobesity potential. *Nutrition* **29**, 591-596
119. Panwar, H., Rashmi, H.M., Batish, V.K., and Grover, S. (2013) Probiotics as potential biotherapeutics in the management of type 2 diabetes - prospects and perspectives. *Diabetes Metab. Res. Rev.* **29**, 103-112
120. Million, M., Lagier, J.C., Yahav, D., and Paul, M. (2013) Gut bacterial microbiota and obesity. *Clin. Microbiol. Infect.* **19**, 305-313

3



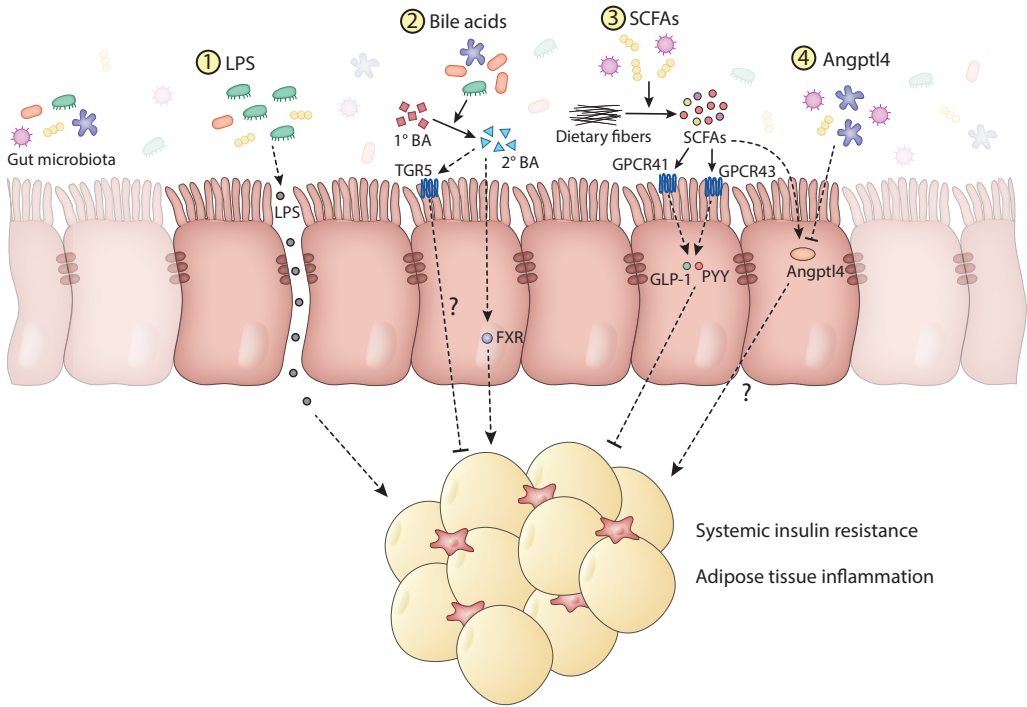
Potential mediators linking the gut bacteria to metabolic health: a critical view

Aafke W.F. Janssen, Sander Kersten



Abstract

Growing evidence suggests that the bacteria present in our gut may play a role in mediating the effect of genetics and lifestyle on obesity and metabolic diseases. Most of the current literature on gut bacteria consists of cross-sectional and correlative studies, rendering it difficult to make any causal inferences as to the influence of gut bacteria on obesity and related metabolic disorders. Interventions with germ-free animals, treatment with antibiotic agents, and microbial transfer experiments have provided some evidence that disturbances in gut bacteria may causally contribute to obesity-related insulin resistance and adipose tissue inflammation. Several potential mediators have been hypothesized to link the activity and composition of gut bacteria to insulin resistance and adipose tissue function, including lipopolysaccharide, Angiopoietin-like protein 4, bile acids, and short-chain fatty acids. In this review we critically evaluate the current evidence related to the direct role of gut bacteria in obesity-related metabolic perturbations, with a focus on insulin resistance and adipose tissue inflammation. It is concluded that the knowledge base in support of a role for the gut microbiota in metabolic regulation and in particular insulin resistance and adipose tissue inflammation needs to be strengthened.



3

Abstract figure. Hypothetical model of gut microbial participation in adipose tissue inflammation and insulin resistance

Several mediators are hypothesized to link changes in gut bacteria composition to adipose tissue inflammation and insulin resistance. (1) Disturbances in gut microbial composition may disrupt gut barrier thereby causing leakage of lipopolysaccharides (LPS) into the bloodstream. Low levels of LPS in the bloodstream can cause adipose tissue inflammation and insulin resistance. (2) Alterations in gut microbiota and subsequent changes in the conversion of primary to secondary bile acids may alter FXR signalling and impact adipose tissue inflammation and insulin resistance. Whether alterations in gut microbiota influence adipose tissue inflammation and insulin resistance *via* bile acid-mediated TGR5 signalling is completely unknown. (3) Microbial fermentation of dietary fibers generates short-chain fatty acids (SCFAs). By activating G protein-coupled receptors (GPCR) 41 and 43, SCFAs induce secretion of GLP-1 and PYY, which may inhibit adipose tissue inflammation and insulin resistance. (4) Inhibition of Angiopoietin-like protein 4 (ANGPTL4) by the gut microbiota may promote adiposity, but whether regulation of (intestinal) ANGPTL4 by the gut microbiota affects adipose tissue inflammation and insulin resistance is completely unknown. Dashed arrows indicate putative pathways for which more research is needed to investigate the direct impact of microbiota on adipose tissue inflammation and insulin resistance.

Introduction

Obesity is associated with a variety of metabolic complications including dyslipidemia and insulin resistance. Evidence is accumulating that development of insulin resistance and other complications of obesity may be driven by a heightened inflammatory state of the adipose tissue. Elevated adipose tissue inflammation is characterized by the influx of various immune cells, including macrophages, and the upregulation of numerous inflammatory cytokines (Boutens & Stienstra, 2016).

Obesity and related metabolic diseases are believed to be the result of an interaction between genetics and lifestyle factors, such as diet and physical activity. In the last decade, there has been growing realization that part of the effect of genetics and lifestyle on obesity and metabolic diseases may be mediated by the microorganisms residing in our gastrointestinal tract, which are referred to as the gut microbiota (Janssen & Kersten, 2015; Wu *et al.*, 2015). Indeed, changes in gut microbiota composition have been observed in people with obesity (Ley RE, Turnbaugh PJ, Klein S, 2006; Schwiertz *et al.*, 2010), and obesity-related diseases such as type 2 diabetes (Qin *et al.*, 2012), non-alcoholic fatty liver disease (Mouzaki *et al.*, 2013; Jiang *et al.*, 2015), and cardiovascular disease (Karlsson *et al.*, 2012).

The gut microbiota predominantly consists of bacteria but also includes viruses, fungi, protozoa, and archaea. The composition of the gut microbiota varies greatly between individuals, reflecting the impact of the host genome and environmental factors, such as lifestyle, hygiene, the use of antibiotics, and especially diet. In addition, the intestinal microbiota composition may be affected by specific disease states (Benson *et al.*, 2010; Sommer & Bäckhed, 2013). Conversely, the intestinal microbiota may impact the host and contribute to certain diseases (Rabot *et al.*, 2010; Ridaura *et al.*, 2013; Gregory *et al.*, 2015; Schaubeck *et al.*, 2016). Most of the contemporary literature on the relation between the composition of the gut microbiota and obesity and related parameters consists of cross-sectional and correlative studies. Because of the complicated interaction between the host, environmental factors, and the gut microbiota, no causal inferences can be drawn from these studies about the influence of gut bacteria on obesity and obesity-related disturbances, which represent a major limitation. In this review we discuss the current evidence related to the direct role of gut bacteria in obesity-related metabolic perturbations, with a focus on insulin resistance and adipose tissue inflammation. In the first part, we describe the results of various interventions that addressed the causal role of gut bacteria in metabolic diseases. In the second part, we describe mechanistic studies on potential mediators that may link changes in gut bacteria to obesity-related insulin resistance and adipose tissue inflammation.

Possible interventions to study the role of gut bacteria in metabolic diseases

To investigate whether the gut bacteria contribute to insulin resistance and adipose tissue inflammation, interventions with germ-free animals, treatment with antibiotic agents, and bacterial transfer experiments are employed. Germ-free animals are maintained free from any microorganisms throughout life and are therefore useful to elucidate the role of the gut microbiota in metabolic disorders. Compared to conventionalized mice, germ-free mice fed a high-fat diet were found to have an improved glucose tolerance, improved insulin sensitivity, and reduced adipose tissue inflammation (Bäckhed *et al.*, 2004; Rabot *et al.*, 2010; Caesar *et al.*, 2012). However, it is unclear whether the elevated insulin resistance and adipose tissue inflammation in conventionalized mice as compared to germ-free mice are directly mediated by the gut microbiota, or indirectly *via* a higher bodyweight gain. To circumvent the effects of body weight and adiposity on adipose tissue inflammation, Caesar *et al.* compared germ-free and bodyweight-matched conventionally raised mice. Interestingly, adipose tissue inflammation was improved in germ-free mice as compared with conventionally raised mice. While this study thus suggests that the gut microbiota promote adipose tissue inflammation (Caesar *et al.*, 2015), it is important to realize that interventions with germ-free mice have certain limitations. Indeed, germ-free mice have large defects in the development of the immune system and antibody production, show morphological defects in the intestine, and may suffer from a vitamin deficiency, which may significantly affect the experimental outcome (Smith *et al.*, 2007; Yi & Li, 2012).

To overcome these limitations, administration of antibiotics and microbial transfer are a popular alternative to modulate gut bacterial composition. Antibiotics suppress the gut bacteria (Cani *et al.*, 2008; Carvalho *et al.*, 2012). Similar to the observations in germ-free mice, treatment with antibiotics improved the glucose tolerance and reduced the infiltration of macrophages in adipose tissue in mice (Cani *et al.*, 2008; Membrez *et al.*, 2008; Carvalho *et al.*, 2012). In contrast, in humans, administration of a cocktail of antibiotics for 4 days had no effect on glucose tolerance (Mikkelsen *et al.*, 2015), while treatment with vancomycin for 1 week decreased the peripheral insulin sensitivity (Vrieze *et al.*, 2014). One disadvantage of antibiotics is that they do not suppress all gut bacteria, which might result in the overgrowth of non-targeted bacteria (Walsh *et al.*, 2014; Morgun *et al.*, 2015), or outgrowth of intestinal fungi (Mulligan *et al.*, 1982; Dollive *et al.*, 2013). Furthermore, it is important to note that antibiotics possess direct anti-inflammatory properties and may cause mitochondrial dysfunction, independent of their bactericidal or bacteriostatic effects (Tauber & Nau, 2008; Steel *et al.*, 2012; Wang *et al.*, 2015).

Microbial transfer can be achieved by oral gavage or intrarectal administration of bacteria,

or by cohousing animals. Transfer of microbiota from obese-prone—but not from obese-resistant—mice to germ-free mice increased weight gain, increased HOMA-IR (homeostasis model assessment of insulin resistance), and stimulated the infiltration of macrophages in adipose tissue (Duca *et al.*, 2014). Another study showed that mice receiving microbiota from obese mice at weaning had an improved glucose tolerance as compared with mice receiving microbiota from lean mice, but not when the microbial transfer was performed at 8 weeks of age (Ellekilde *et al.*, 2014). The role of the gut microbiota in human obesity and insulin resistance has been investigated by transplanting fecal microbiota from female adult twins discordant in obesity to germ-free mice. While an increase in obesity and adiposity was observed in mice receiving the gut microbiota from the obese twin as compared with mice receiving the gut microbiota from the lean twin, only a trend towards impaired glucose tolerance ($p=0.06$) was observed (Ridaura *et al.*, 2013). Interestingly, the transplantation of gut microbiota from lean individuals to patients with metabolic syndrome improved insulin sensitivity (Vrieze *et al.*, 2012). Of importance, the effectiveness of bacterial transfer depends on whether bacteria are able to colonize in the recipients' intestinal microbial niche.

Microbial transfer can also be achieved by co-housing, which is exclusively applied in animals. Importantly, cohousing of mice with different genotypes will equalize intestinal bacterial composition in the cohoused animals. Therefore, only if the gut microbiota have profound effects on the phenotype, differences between the two co-housed groups might yield significant results (Laukens *et al.*, 2016).

The interventions mentioned above are commonly used to investigate the role of the gut bacteria in metabolic health. However, these interventions cannot discriminate between pathogenic and beneficial bacteria. Bacteria also confer health benefits related to—for example—vitamin supplementation, tissue homeostasis, and immune function (Smith *et al.*, 2007; Sommer & Bäckhed, 2013). As a result, the loss of beneficial bacteria can have detrimental effects on the host. A more targeted approach to modulate the intestinal bacteria, for example by administering specific bacterial species, is expected to give more specific insight into which and how bacteria can affect the health of the host. For instance, administration of *Escherichia coli* to germ-free mice has been shown to impair glucose tolerance (Caesar *et al.*, 2012), whereas administration of *Akkermansia muciniphila* to conventional mice was shown to improve glucose tolerance (Everard *et al.*, 2013). To successfully administer bacterial species, bacteria need to remain viable during storage, survive the passage through the gastrointestinal tract, and be able to colonize the intestine. Although the number of bacteria that can be cultured has gone up significantly, still many gastrointestinal bacteria cannot be cultured (Li *et al.*, 2014; Rajilić-Stojanović & de Vos, 2014). Hence, due to this limitation, the more targeted approach is only applicable to a selection of bacterial strains.

Overall, current evidence lends some credence to the notion that changes in the gut bacterial composition contribute to insulin resistance and adipose tissue inflammation. However, additional human and animal studies are needed to bolster the causal link between the gut bacteria and obesity-related metabolic parameters.

Potential mediators

Several potential mediators have been hypothesized to link the activity and composition of the gut microbiota to insulin resistance and adipose tissue function, including lipopolysaccharide (LPS), Angiopoietin-like protein 4 (ANGPTL4), bile acids, and short-chain fatty acids (SCFAs).

Lipopolysaccharides

LPS or so-called endotoxin is a major component of the gram-negative bacterial cell wall. The first indications that LPS may be involved in obesity and related metabolic disorders were reported by Cani *et al.* (Cani *et al.*, 2007). Continuous subcutaneous infusion of LPS for 4 weeks induced weight gain, insulin resistance, and adipose tissue inflammation to a similar extent as high-fat feeding. Importantly, high-fat feeding was found to elevate plasma LPS levels, which was associated with an increased gut permeability and a decreased expression of the tight junction proteins zona occludens-1 and occludin. Treatment of mice fed a high-fat diet with antibiotics did not increase the gut permeability and plasma LPS levels, suggesting a role for the gut bacteria in this process. In addition to reduced LPS levels, antibiotic-treated mice also displayed less macrophage infiltration in adipose tissue and improved glucose and insulin tolerance (Cani *et al.*, 2008). The finding that the suppression of the gut bacteria improves insulin resistance and adipose tissue inflammation concurrent with a reduction in plasma LPS levels has also been found in other studies that used either mice fed a high-fat diet (Membrez *et al.*, 2008; Carvalho *et al.*, 2012), *ob/ob* mice (Cani *et al.*, 2008), or germ-free mice (Caesar *et al.*, 2012). Interestingly, supplementing *A. muciniphila* during high-fat feeding reduced fat mass gain and improved glucose tolerance in association with reduced serum LPS levels. These findings were not observed with heat-killed *A. muciniphila*, suggesting that live *A. muciniphila* has a profound role in gut barrier function (Everard *et al.*, 2013).

It is important to note that not all mouse studies have provided supportive evidence for a role of LPS in insulin resistance (Lichtenstein *et al.*, 2010; Laugerette *et al.*, 2012; Caesar *et al.*, 2012, 2015). Whereas administration of the gram-negative bacteria *E. coli* W3110 to germ-free mice increased plasma LPS, administration of the isogenic mutant MLK1067 did not. However, both strains increased adipose tissue weight and impaired glucose tolerance, suggesting that gut-derived LPS is not essential for adiposity and glucose and insulin

tolerance in mice (Caesar *et al.*, 2012). In another study by the same authors, obesity, adipose tissue inflammation, and insulin resistance in mice fed a lard-based high-fat diet were not accompanied by a significant elevation in plasma LPS levels as compared with mice fed a fish oil-based high-fat diet (Caesar *et al.*, 2015). However, lard-feeding significantly increased toll-like receptor 4 activation (Caesar *et al.*, 2015), which might reflect an increased sensitivity of the mice to LPS, a notion that was also raised in another study (Huang *et al.*, 2007).

Whereas the original publication by Cani and colleagues in mice reported a stimulatory effect of LPS on insulin resistance (Cani *et al.*, 2008), subsequent studies in rats have failed to find an effect of LPS administration on insulin resistance (Liu *et al.*, 2010; Dudele *et al.*, 2015). In humans, LPS injection in healthy subjects was shown to induce insulin resistance and adipose tissue inflammation (Dandona *et al.*, 2010; Mehta *et al.*, 2010). To investigate whether the changes in gut bacteria composition associated with overfeeding and obesity can elevate plasma LPS levels in humans, healthy humans were placed on high-fat/hypercaloric diets in two independent studies. Laugerette *et al.* reported that although overfeeding for 8 weeks caused marked weight gain, it did not influence the fasting plasma LPS levels (Laugerette *et al.*, 2014). By contrast, Pendyala *et al.* observed that 4 weeks of Western diet raised the plasma LPS levels. Interestingly, the increased LPS levels were not accompanied by higher serum pro-inflammatory cytokine levels (Pendyala *et al.*, 2012).

Taken together, the current literature on LPS as a potential causal link between disturbances in the gut microbiota and obesity-related insulin resistance and adipose tissue inflammation is inconsistent. One possible explanation for the inconsistent results might be the difficulty of accurately measuring LPS in blood. Most studies have used the FDA-approved Limulus Amoebocyte Lysate (LAL) assay, which measures LPS activity via an enzymatic reaction. One drawback of the LAL assay is that several factors in plasma—such as bile salts and lipoproteins—can interact and thereby inactivate LPS, rendering LPS undetectable. In addition, anticoagulants, including EDTA and heparin, might interfere with the LAL assay (Hurley, 1995; Boutagy *et al.*, 2015). Another drawback is the risk of contaminations, which may give rise to false-positive results.

Angiopoietin-like protein 4

Angiopoietin-like protein 4 (ANGPTL4) is a ubiquitously expressed glycoprotein that plays an important role in lipid metabolism by inhibiting the activity of the enzyme lipoprotein lipase (Dijk & Kersten, 2014). Lipoprotein lipase catalyzes the hydrolysis of circulating triglycerides along the capillary lumen of muscle and fat tissue. Bäckhed *et al.* first identified ANGPTL4 as a potential link between the gut microbiota and fat storage (Bäckhed *et al.*, 2004, 2007). Whereas germ-free mice were protected against diet-induced obesity, germ-free mice lacking the *Angptl4* gene were not. Conventionalization of germ-free mice

resulted in the suppression of *Angptl4* expression in the intestines but not in adipose tissue. Consequently, it was suggested that downregulation of intestinal *Angptl4* expression by gut microbiota may promote adipose tissue lipoprotein lipase activity and thereby peripheral fat storage (Bäckhed *et al.*, 2004, 2007; El Aidy *et al.*, 2013). In contrast, although Fleissner *et al.* similarly observed increased intestinal *Angptl4* expression in germ-free mice, conventional mice were leaner than their germ-free counterparts (Fleissner *et al.*, 2010).

Currently, it is still unclear to what extent ANGPTL4 produced in the intestine has an endocrine function and is able to lower LPL activity in adipose tissue. Indeed, there is growing evidence suggesting that ANGPTL4 acts more locally instead of systemically (Dijk & Kersten, 2014). In the intestine, ANGPTL4 may primarily target pancreatic lipase and thereby reduce fat absorption (Mattijssen *et al.*, 2014). Consequently, the inhibition of intestinal *Angptl4* upon conventionalization may promote fat storage *via* elevated pancreatic lipase activity. In terms of glucose metabolism, while some studies have found an effect of ANGPTL4 overexpression on glucose metabolism (Xu *et al.*, 2005; Lichtenstein *et al.*, 2007), it remains to be determined whether ANGPTL4 plays an important regulatory role in insulin sensitivity and glucose homeostasis.

In apparent contrast to the finding of reduced intestinal *Angptl4* expression upon conventionalization, specific bacterial species and short-chain fatty acids potentially induce ANGPTL4 in colonic cell lines (Are *et al.*, 2008; Aronsson *et al.*, 2010; Alex *et al.*, 2013; Korecka *et al.*, 2013). To further investigate the role of intestinal ANGPTL4 as a potential link between the gut microbiota and metabolic health, future studies using intestinal-specific *Angptl4* knockout mice should be performed.

Bile acids

Alterations in the gut bacterial composition have profound consequences for bile acid metabolism. For instance, it is known that the conversion of primary bile acids to secondary bile acids is carried out by the gut bacteria. Besides having an important role in the emulsification and absorption of dietary lipids, bile acids also serve as important signalling molecules that act through the farnesoid X receptor (FXR) and G-protein coupled bile acid receptor 1 (TGR5). By activating FXR and TGR5, bile acids can influence a variety of biological processes including bile acid metabolism, intestinal hormone secretion, inflammation, and lipid, glucose and energy metabolism. Accordingly, disturbances in the gut bacteria are suggested to affect metabolic parameters and pathways *via* changes in bile acid metabolism (Fiorucci & Distrutti, 2015).

Experiments in germ-free and antibiotic-treated mice (Swann *et al.*, 2011; Sayin *et al.*, 2013), as well as in humans treated with antibiotics (Vrieze *et al.*, 2014), have indicated that the gut bacteria play an important role in the conversion of primary into secondary bile

acids. In addition, germ-free and antibiotic-treated mice have an increased bile acid pool, increased biliary bile acid secretion and intestinal reabsorption, and decreased fecal bile acid excretion, indicating that the gut microbiota have a major impact on bile acid homeostasis (Sayin *et al.*, 2013; Out *et al.*, 2015). In turn, bile acids may impact the gut bacteria *via* their bactericidal properties, illustrating the complex relationship between the gut bacteria and bile acids (Mikkelsen *et al.*, 2016).

The nuclear bile acid receptor FXR is expressed at high levels in the liver and small intestine, which are both tissues characterized by high concentrations of bile acids. Intestinal FXR signalling has been shown to protect against the development of obesity and to improve insulin resistance (Li *et al.*, 2013). The impact of the microbiota on FXR signalling has been studied using germ-free and conventional-raised wild-type and FXR knockout mice. While the effect of the gut microbiota on insulin tolerance was found to be dependent on FXR, the influence of the gut microbiota on glucose tolerance was not (Pars us *et al.*, 2016). Adipose tissue inflammation was significantly increased upon conventionalization in wild-type mice, but not in FXR-deficient mice, suggesting that the microbiota promote adipose tissue inflammation in a FXR-dependent manner (Pars us *et al.*, 2016). Expression of FXR is relatively low in adipose tissue suggesting that effects of bile acids on adipose tissue inflammation are likely mediated *via* intestinal FXR.

The membrane bile acid receptor TGR5 is also mainly expressed in the intestine and has been implicated in glucose metabolism. Specifically, activation of TGR5 by bile acids was shown to improve insulin sensitivity and glucose tolerance *via* enhanced glucagon-like peptide-1 (GLP-1) secretion, which was blunted in mice lacking TGR5 (Harach *et al.*, 2012; Potthoff *et al.*, 2013).

Different bile acids are known to have a different potency towards FXR and TGR5 (de Aguiar Vallim *et al.*, 2013). Accordingly, it is difficult to predict how changes in the gut bacterial composition and hence fecal bile acid composition affect bile acid signalling and subsequently impact metabolic processes. Moreover, the bile acid composition is substantially different between mice and humans, including differences in the production of the various primary bile acids and their conjugation with glycine in humans versus taurine in mice (Chiang, 2013). For this reason, the results obtained in mice studies cannot easily be extrapolated to humans.

Short-chain fatty acids

SCFAs are the main intestinal bacterial fermentation end products of indigestible dietary components, such as dietary fibers. It has been hypothesized that part of the beneficial health effects of dietary fibers is mediated by SCFAs (Jakobsdottir *et al.*, 2013; den Besten *et al.*, 2014; Chassaing *et al.*, 2015). In line with this notion, supplementation of SCFAs to

a high-fat diet protected against diet-induced obesity and improved insulin sensitivity (Gao *et al.*, 2009; Lin *et al.*, 2012; den Besten *et al.*, 2015a). Although these data support a direct impact of SCFA on metabolic health, absorption of orally ingested SCFAs takes place already in the small intestine and not in the cecum or colon. Different hormones with various physiological functions are produced along the gastrointestinal tract (Murphy & Bloom, 2006) and as a result, SCFAs absorbed in the small intestine may give rise to different metabolic effects as compared to SCFA produced by bacterial fermentation and absorbed in the large intestine (den Besten *et al.*, 2015b).

The effects of SCFAs on glucose homeostasis are thought to be mediated *via* the secretion of GLP-1 and peptide YY (PYY) from enteroendocrine L-cells by activation of the G protein-coupled receptors (GPCR) 41 and 43. *In vitro* primary colonic cells lacking either GPCR41 or -43 were shown to secrete less GLP-1 and PYY after SCFA stimulation (Tolhurst *et al.*, 2012; Psichas *et al.*, 2015). Targeted delivery of the SCFA propionate to the colon increased GLP-1 and PYY in the portal vein in wild-type mice but not in mice lacking GPCR43 (Psichas *et al.*, 2015). Additionally, mice lacking GPCR41 and -43 had impaired glucose tolerance (Tolhurst *et al.*, 2012; Kimura *et al.*, 2013). In humans, rectal propionate infusions have been shown to increase serum glucose levels, consistent with the hypothesis of propionate being a substrate for gluconeogenesis (Wolever *et al.*, 1991). By contrast, while targeted delivery of propionate via an inulin-propionate ester effectively increased propionate in the colon and increased the postprandial plasma PYY and GLP-1 concentrations, no acute effects on plasma glucose levels were found (Chambers *et al.*, 2015). Interestingly, inulin-propionate supplementation for 24 weeks prevented a deterioration in the glycaemic response in overweight adults (Chambers *et al.*, 2015). However, it is unclear whether these effects are directly mediated by propionate impacting gut hormones, or indirectly *via* the reduction in bodyweight gain and adiposity in the inulin-propionate group as compared to the control group.

The direct effects of SCFAs on adipose tissue inflammation have been investigated in only a few studies. Since the effects of SCFAs on metabolic health frequently involve changes in obesity development (Canfora *et al.*, 2015), which can be predicted to lead to changes in adipose tissue inflammation, the direct effects of SCFAs on adipose tissue inflammation are difficult to assess *in vivo*.

In vitro, SCFAs have been shown to exert anti-inflammatory effects by affecting cytokine production and chemotaxis (Cox, 2009; Maa *et al.*, 2010; Liu *et al.*, 2012). The effect of SCFAs on inflammation seems to be dependent on the concentration and the type of SCFA as well as on the type of immune cell (Vinolo *et al.*, 2009; Bailón *et al.*, 2010; Meijer *et al.*, 2010). For example, Al-Lahham *et al.* showed that propionate reduced several inflammatory cytokines and chemokines in human omental adipose tissue explants (Al-Lahham *et al.*, 2012), which could only be achieved using supraphysiological concentrations (3 mmol/L).

Taken together, there is some evidence that SCFAs affect insulin resistance and adipose tissue inflammation but further research is necessary to better study the impact of intestinally-derived SCFAs on insulin resistance and adipose tissue inflammation *in vivo*.

Conclusion

In conclusion, several potential mediators, including LPS, ANGPTL4, bile acids, and SCFAs, have been proposed to link disturbances in the gut bacteria to obesity-related insulin resistance and adipose tissue inflammation. Currently, the literature on LPS as a potential causal link between the gut microbiota and obesity-related insulin resistance and adipose tissue inflammation is inconsistent, which may be related to the difficulty of accurately measuring LPS in blood. Bile acids are also suggested as a possible mediators, but evidence from *in vivo* studies is limited. Since the gut bacteria impact bile acid composition and vice versa, it is difficult to investigate the role of bile acids as causal mediators of the gut microbiota. ANGPTL4 has been proposed as a link between the gut microbiota and obesity, but whether regulation of (intestinal) *Angptl4* by the gut microbiota also affects insulin resistance and adipose tissue inflammation is completely unknown. In contrast to LPS, ANGPTL4, and bile acids, SCFAs have been suggested to improve glucose tolerance and reduce adipose tissue inflammation, although further research is necessary to better study the impact of intestinally-derived SCFAs on insulin resistance and adipose tissue inflammation *in vivo*.

It should be noted that the observed effects of the gut microbiota and its potential mediators on insulin resistance and adipose inflammation are often confounded by changes in obesity development, which automatically impact insulin resistance and adipose tissue inflammation. Therefore, studies should be designed to better tease out the direct effect of the gut microbiota on insulin resistance and adipose tissue inflammation independent of obesity.

Studies on potential mediators linking disturbances in gut bacteria to insulin resistance and adipose tissue inflammation are mostly performed in mice. Although murine models provide a powerful tool to study host-gut microbe interactions, they do not always very well recapitulate the human situation, partly because the composition of the gut bacteria is quite dissimilar between humans and mice (Ley *et al.*, 2005). Pre-clinical studies exploring the role of gut bacteria in obesity and metabolic regulation should therefore ideally be undertaken in a variety of mouse models on different diets. Moreover, as the gut bacteria composition can vary substantially in the same mouse strain depending on the animal facility and background diet, it is worthwhile to try to repeat existing studies in different animal facilities and using different diets. Finally, a more targeted approach involving modification of only one bacterial strain may provide more useful insight into the role of

the gut bacteria in obesity and metabolic regulation, as compared to interventions in which nearly the entire bacterial population is modulated.

Acknowledgements

This work was supported by The Netherlands Cardiovascular Research Committee IN-CONTROL Grant (CVON 2012-03).

References

- de Aguiar Vallim TQ, Tarling EJ & Edwards PA (2013). Pleiotropic roles of bile acids in metabolism. *Cell Metab* **17**, 657–669.
- El Aidy S, Merrifield CA, Derrien M, van Baarlen P, Hooiveld G, Levenez F, Doré J, Dekker J, Holmes E, Claus SP, Reijngoud DJ, Kleerebezem M, Dore J, Dekker J, Holmes E, Claus SP, Reijngoud DJ & Kleerebezem M (2013). The gut microbiota elicits a profound metabolic reorientation in the mouse jejunal mucosa during conventionalisation. *Gut* **62**, 1306–1314.
- Alex S, Lange K, Amolo T, Grinstead JS, Haakonsson AK, Szalowska E, Koppen A, Mudde K, Haenen D, Al-Lahham S, Roelofsen H, Houtman R, van der Burg B, Mandrup S, Bonvin AMJJ, Kalkhoven E, Müller M, Hooiveld GJ & Kersten S (2013). Short-chain fatty acids stimulate angiopoietin-like 4 synthesis in human colon adenocarcinoma cells by activating peroxisome proliferator-activated receptor γ . *Mol Cell Biol* **33**, 1303–1316.
- Al-Lahham S, Roelofsen H, Rezaee F, Weening D, Hoek A, Vonk R & Venema K (2012). Propionic acid affects immune status and metabolism in adipose tissue from overweight subjects. *Eur J Clin Invest* **42**, 357–364.
- Are A, Aronsson L, Wang S, Greicius G, Lee YK, Gustafsson J-A, Pettersson S & Arulampalam V (2008). Enterococcus faecalis from newborn babies regulate endogenous PPAR γ activity and IL-10 levels in colonic epithelial cells. *Proc Natl Acad Sci U S A* **105**, 1943–1948.
- Aronsson L, Huang Y, Parini P, Korach-André M, Håkansson J, Gustafsson JÅ, Pettersson S, Arulampalam V & Rafter J (2010). Decreased fat storage by *Lactobacillus paracasei* is associated with increased levels of angiopoietin-like 4 protein (ANGPTL4). *PLoS One* **5**, e13087.
- Bäckhed F, Ding H, Wang T, Hooper L V, Koh GY, Nagy A, Semenkovich CF & Gordon JI (2004). The gut microbiota as an environmental factor that regulates fat storage. *Proc Natl Acad Sci U S A* **101**, 15718–15723.
- Bäckhed F, Manchester JK, Semenkovich CF & Gordon JI (2007). Mechanisms underlying the resistance to diet-induced obesity in germ-free mice. *Proc Natl Acad Sci U S A* **104**, 979–984.
- Bailón E, Cueto-Sola M, Utrilla P, Rodríguez-Cabezas ME, Garrido-Mesa N, Zarzuelo A, Xaus J, Gálvez J & Comalada M (2010). Butyrate in vitro immune-modulatory effects might be mediated through a proliferation-related induction of apoptosis. *Immunobiology* **215**, 863–873.
- Benson AK, Kelly SA, Legge R, Ma F, Low SJ, Kim J, Zhang M, Oh PL, Nehrenberg D, Hua K, Kachman SD, Moriyama EN, Walter J, Peterson DA & Pomp D (2010). Individuality in gut microbiota composition is a complex polygenic trait shaped by multiple environmental and host genetic factors. *Proc Natl Acad Sci U S A* **107**, 18933–18938.
- den Besten G, Bleeker A, Gerding A, van Eunen K, Havinga R, van Dijk TH, Oosterveer MH, Jonker JW, Groen AK, Reijngoud D-J & Bakker BM (2015a). Short-Chain Fatty Acids Protect Against High-Fat Diet-Induced Obesity via a PPAR γ -Dependent Switch From Lipogenesis to Fat Oxidation. *Diabetes* **64**, 2398–2408.
- den Besten G, Gerding A, van Dijk TH, Ciapaite J, Bleeker A, van Eunen K, Havinga R, Groen AK, Reijngoud D-J & Bakker BM (2015b). Protection against the Metabolic Syndrome by Guar Gum-Derived Short-Chain Fatty Acids Depends on Peroxisome Proliferator-Activated Receptor γ and Glucagon-Like Peptide-1. *PLoS One* **10**, e0136364.
- den Besten G, Havinga R, Bleeker A, Rao S, Gerding A, van Eunen K, Groen AK, Reijngoud D-J & Bakker BM (2014). The short-chain Fatty Acid uptake fluxes by mice on a guar gum supplemented diet associate with amelioration of major biomarkers of the metabolic syndrome. *PLoS One* **9**, e107392.
- Boutagy NE, McMillan RP, Frisard MI & Hulver MW (2015). Metabolic endotoxemia with obesity: Is it real and is it relevant? *Biochimie*; DOI: 10.1016/j.biochi.2015.06.020, in press.
- Boutens L & Stienstra R (2016). Adipose tissue macrophages: going off track during obesity. *Diabetologia*; DOI: 10.1007/s00125-016-3904-9, in press.
- Caesar R, Reigstad CS, Bäckhed HK, Reinhardt C, Ketonen M, Lundén GÖ, Cani PD & Bäckhed F (2012). Gut-derived lipopolysaccharide augments adipose macrophage accumulation but is not essential for impaired glucose or insulin tolerance in mice. *Gut* **61**, 1701–1707.
- Caesar R, Tremaroli V, Kovatcheva-Datchary P, Cani PD & Bäckhed F (2015). Crosstalk between gut microbiota and dietary lipids aggravates WAT inflammation through TLR signaling. *Cell Metab* **22**, 658–668.
- Canfora EE, Jocken JW & Blaak EE (2015). Short-chain fatty acids in control of body weight and insulin sensitivity. *Nat Rev Endocrinol* **11**, 577–591.
- Cani PD, Amar J, Iglesias MA, Poggi M, Knauf C, Bastelica D, Neyrinck AM, Fava F, Tuohy KM, Chabo C, Sulpice T, Chamontin B, Gibson GR, Casteilla L, Delzenne NM & Alessi MC (2007). Metabolic endotoxemia initiates obesity and insulin resistance. *Diabetes* **56**, 1761–1772.
- Cani PD, Bibiloni R, Knauf C, Neyrinck AM & Delzenne NM (2008). Changes in Gut Microbiota Control Metabolic Endotoxemia-Induced Inflammation in High-Fat Diet – Induced Obesity and Diabetes in Mice. *Diabetes* **57**, 1470–1481.

- Carvalho BM, Guadagnini D, Tsukumo DML, Schenka a a, Latuf-Filho P, Vassallo J, Dias JC, Kubota LT, Carnevalheira JBC & Saad MJ a (2012). Modulation of gut microbiota by antibiotics improves insulin signalling in high-fat fed mice. *Diabetologia* **55**, 2823–2834.
- Chambers ES et al. (2015). Effects of targeted delivery of propionate to the human colon on appetite regulation, body weight maintenance and adiposity in overweight adults. *Gut* **64**, 1744–1754.
- Chassaing B, Miles-Brown J, Pellizzon M, Ulman E, Ricci M, Zhang L, Patterson AD, Vijay-Kumar M & Gewirtz AT (2015). Lack of soluble fiber drives diet-induced adiposity in mice. *Am J Physiol - Gastrointest Liver Physiol* **309**, G528–G541.
- Chiang JYL (2013). Bile acid metabolism and signaling. *Compr Physiol* **3**, 1191–1212.
- Cox MA (2009). Short-chain fatty acids act as antiinflammatory mediators by regulating prostaglandin E 2 and cytokines. *World J Gastroenterol* **15**, 5549.
- Dandona P, Ghanim H, Bandyopadhyay A, Korzeniewski K, Lia CL, Dhindsa S & Chaudhuri A (2010). Insulin Suppresses Endotoxin-Induced Oxidative, Nitrosative, and Inflammatory Stress in Humans. *Diabetes Care* **33**, 2416–2423.
- Dijk W & Kersten S (2014). Regulation of lipoprotein lipase by Angptl4. *Trends Endocrinol Metab* **25**, 146–155.
- Dollive S, Chen Y-Y, Grunberg S, Bittiger K, Hoffmann C, Vandivier L, Cuff C, Lewis JD, Wu GD & Bushman FD (2013). Fungi of the Murine Gut: Episodic Variation and Proliferation during Antibiotic Treatment. *PLoS One* **8**, e71806.
- Duca FA, Sakar Y, Lepage P, Devime F, Langelier B, Doré J & Covasa M (2014). Replication of obesity and associated signaling pathways through transfer of microbiota from obese-prone rats. *Diabetes* **63**, 1624–1636.
- Dudele A, Fischer CW, Elfving B, Wegener G, Wang T & Lund S (2015). Chronic exposure to low doses of lipopolysaccharide and high-fat feeding increases body mass without affecting glucose tolerance in female rats. *Physiol Rep* **3**, e12584.
- Ellekilde M, Selfjord E, Larsen CS, Jaksevic M, Rune I, Tranberg B, Vogensen FK, Nielsen DS, Bahl MI, Licht TR, Hansen AK & Hansen CHF (2014). Transfer of gut microbiota from lean and obese mice to antibiotic-treated mice. *Sci Rep* **4**, 5922.
- Everard A, Belzer C, Geurts L, Ouwerkerk JP, Druart C, Bindels LB, Guiot Y, Derrien M, Muccioli GG, Delzenne NM, de Vos WM & Cani PD (2013). Cross-talk between Akkermansia muciniphila and intestinal epithelium controls diet-induced obesity. *Proc Natl Acad Sci U S A* **110**, 9066–9071.
- Fiorucci S & Distrutti E (2015). Bile Acid-Activated Receptors, Intestinal Microbiota, and the Treatment of Metabolic Disorders. *Trends Mol Med* **21**, 702–714.
- Fleissner CK, Huebel N, Abd El-Bary MM, Loh G, Klaus S & Blaut M (2010). Absence of intestinal microbiota does not protect mice from diet-induced obesity. *Br J Nutr* **104**, 919–929.
- Gao Z, Yin J, Zhang J, Ward RE, Martin RJ, Lefevre M, Cefalu WT & Ye J (2009). Butyrate improves insulin sensitivity and increases energy expenditure in mice. *Diabetes* **58**, 1509–1517.
- Gregory JC, Buffa J a, Org E, Wang Z, Levison BS, Zhu W, Wagner M a, Bennett BJ, Li L, Didonato J a, Lusis AJ, Hazen SL, Gregory JC, Buffa J a, Org E, Wang Z, Levison BS & Zhu W (2015). Transmission of Atherosclerosis Susceptibility with Gut Microbial Transplantation. *J Biol Chem* **290**, 5647–5660.
- Harach T, Pols TWH, Nomura M, Maida A, Watanabe M, Auwerx J & Schoonjans K (2012). TGR5 potentiates GLP-1 secretion in response to anionic exchange resins. *Sci Rep* **2**, 2–8.
- Huang H, Liu T, Rose JL, Stevens RL & Hoyt DG (2007). Sensitivity of mice to lipopolysaccharide is increased by a high saturated fat and cholesterol diet. *J Inflamm (Lond)* **4**, 22.
- Hurley JC (1995). Endotoxemia: Methods of detection and clinical correlates. *Clin Microbiol Rev* **8**, 268–292.
- Jakobsdottir G, Xu J, Molin G, Ahrné S & Nyman M (2013). High-Fat Diet Reduces the Formation of Butyrate, but Increases Succinate, Inflammation, Liver Fat and Cholesterol in Rats, while Dietary Fibre Counteracts These Effects. *PLoS One* **8**, e80476.
- Janssen AWF & Kersten S (2015). The role of the gut microbiota in metabolic health. *FASEB J* **29**, 3111–3123.
- Jiang W, Wu N, Wang X, Chi Y, Zhang Y, Qiu X, Hu Y, Li J & Liu Y (2015). Dysbiosis gut microbiota associated with inflammation and impaired mucosal immune function in intestine of humans with non-alcoholic fatty liver disease. *Sci Rep* **5**, 1–7.
- Karlsson FH, Fåk E, Nookaew I, Tremaroli V, Fagerberg B, Petranovic D, Bäckhed F & Nielsen J (2012). Symptomatic atherosclerosis is associated with an altered gut metagenome. *Nat Commun* **3**, 1245.
- Kimura I, Ozawa K, Inoue D, Imamura T, Kimura K, Maeda T, Terasawa K, Kashihara D, Hirano K, Tani T, Takahashi T, Miyauchi S, Shioi G, Inoue H & Tsujimoto G (2013). The gut microbiota suppresses insulin-mediated fat accumulation via the short-chain fatty acid receptor GPR43. *Nat Commun* **4**, 1829.
- Korecka A, de Wouters T, Cultrone A, Lapaque N, Pettersson S, Doré J, Blottière HM & Arulampalam V (2013). ANGPTL4 expression induced by butyrate and rosiglitazone in human intestinal epithelial cells utilizes independent pathways. *Am J Physiol Gastrointest Liver Physiol* **304**, G1025–G1037.
- Laugerette F, Alligier M, Bastard JP, Draï J, Chanséaume E, Lambert-Porcheron S, Laville M, Morio B, Vidal H & Michalski MC (2014). Overfeeding increases postprandial endotoxemia in men: Inflammatory

- outcome may depend on LPS transporters LBP and sCD14. *Mol Nutr Food Res* **58**, 1513–1518.
- Laugerette F, Furet J-P, Debad C, Daira P, Loizon E, Geloën a., Soulage CO, Simonet C, Lefils-Lacourtablaise J, Bernoud-Hubac N, Bodennec J, Peretti N, Vidal H & Michalski M-C (2012). Oil composition of high-fat diet affects metabolic inflammation differently in connection with endotoxin receptors in mice. *AJP Endocrinol Metab* **302**, E374–E386.
- Laukens D, Brinkman BM, Raes J, De Vos M & Vandenabeele P (2016). Heterogeneity of the gut microbiome in mice: guidelines for optimizing experimental design. *FEMS Microbiol Rev* **40**, 117–132.
- Ley RE, Bäckhed F, Turnbaugh P, Lozupone C a, Knight RD & Gordon JI (2005). Obesity alters gut microbial ecology. *Proc Natl Acad Sci U S A* **102**, 11070–11075.
- Ley RE, Turnbaugh PJ, Klein S GJ (2006). Human gut microbes associated with obesity. *Nature* **444**, 1022–1023.
- Li F, Jiang C, Krausz KW, Li Y, Albert I, Hao H, Fabre KM, Mitchell JB, Patterson AD & Gonzalez FJ (2013). Microbiome remodelling leads to inhibition of intestinal farnesoid X receptor signalling and decreased obesity. *Nat Commun* **4**, 2384.
- Li L, Mendis N, Trigui H, Oliver JD & Faucher SP (2014). The importance of the viable but non-culturable state in human bacterial pathogens. *Front Microbiol* **5**, 1–1.
- Lichtenstein L, Berbee JFP, van Dijk SJ, van Dijk KW, Bensadoun A, Kema IP, Voshol PJ, Müller M, Rensen PCN & Kersten S (2007). Angptl4 upregulates cholesterol synthesis in liver via inhibition of LPL- and HL-dependent hepatic cholesterol uptake. *Arterioscler Thromb Vasc Biol* **27**, 2420–2427.
- Lichtenstein L, Mattijssen F, de Wit NJ, Georgiadi A, Hooiveld GJ, van der Meer R, He Y, Qi L, Köster A, Tamsma JT, Tan NS, Müller M & Kersten S (2010). Angptl4 protects against severe proinflammatory effects of saturated fat by inhibiting fatty acid uptake into mesenteric lymph node macrophages. *Cell Metab* **12**, 580–592.
- Lin H V, Frassetto A, Kowalik EJ, Nawrocki AR, Lu MM, Kosinski JR, Hubert J a, Szeto D, Yao X, Forrest G & Marsh DJ (2012). Butyrate and propionate protect against diet-induced obesity and regulate gut hormones via free fatty acid receptor 3-independent mechanisms. *PLoS One* **7**, e35240.
- Liu T, Kao C, Chung C & Hsieh P (2010). Chronic Hepatic Inflammation Induced by Mild Portal Endotoxemia is not Associated with Systemic Insulin Resistance in Rats. *J Med Sci* **30**, 015–020.
- Liu T, Li J, Liu Y, Xiao N, Suo H, Xie K, Yang C & Wu C (2012). Short-chain fatty acids suppress lipopolysaccharide-induced production of nitric oxide and proinflammatory cytokines through inhibition of NF- κ B pathway in RAW264.7 cells. *Inflammation* **35**, 1676–1684.
- Maa MC, Chang MY, Hsieh MY, Chen YJ, Yang CJ, Chen ZC, Li YK, Yen CK, Wu RR & Leu TH (2010). Butyrate reduced lipopolysaccharide-mediated macrophage migration by suppression of Src enhancement and focal adhesion kinase activity. *J Nutr Biochem* **21**, 1186–1192.
- Mattijssen F, Alex S, Swarts HJ, Groen AK, van Schothorst EM & Kersten S (2014). Angptl4 serves as an endogenous inhibitor of intestinal lipid digestion. *Mol Metab* **3**, 135–144.
- Mehta NN, McGillicuddy FC, Anderson PD, Hinkle CC, Shah R, Pruscino L, Tabita-Martinez J, Sellers KE, Rickels MR & Reilly MP (2010). Experimental Endotoxemia Induces Adipose Inflammation and Insulin Resistance in Humans. *Diabetes* **59**, 172–181.
- Meijer K, de Vos P & Priebe MG (2010). Butyrate and other short-chain fatty acids as modulators of immunity: what relevance for health? *Curr Opin Clin Nutr Metab Care* **13**, 715–721.
- Membrez M, Blancher F, Jaquet M, Bibiloni R, Cani PD, Burcelin RG, Corthesy I, Macé K & Chou CJ (2008). Gut microbiota modulation with norfloxacin and ampicillin enhances glucose tolerance in mice. *FASEB J* **22**, 2416–2426.
- Mikkelsen KH, Allin KH & Knop FK (2016). Effect of antibiotics on gut microbiota, glucose metabolism and bodyweight regulation - a review of the literature. *Diabetes Obes Metab*; DOI: 10.1002/dom.12637, in press.
- Mikkelsen KH, Frost M, Bahl MI, Licht TR, Jensen US, Rosenberg J, Pedersen O, Hansen T, Rehfeld JF, Holst JJ, Vilsbøll T & Knop FK (2015). Effect of Antibiotics on Gut Microbiota, Gut Hormones and Glucose Metabolism. *PLoS One* **10**, e0142352.
- Morgun A, Dzutsev A, Dong X, Greer RL, Sexton DJ, Ravel J, Schuster M, Hsiao W, Matzinger P & Shulzhenko N (2015). Uncovering effects of antibiotics on the host and microbiota using transkingdom gene networks. *Gut* **0**, 1–12.
- Mouzaki M, Comelli EM, Arendt BM, Bonengel J, Fung SK, Fischer SE, McGilvray ID & Allard JP (2013). Intestinal microbiota in patients with nonalcoholic fatty liver disease. *Hepatology* **58**, 120–127.
- Mulligan ME, Citron DM, McNamara BT & Finegold SM (1982). Impact of cefoperazone therapy on fecal flora. *Antimicrob Agents Chemother* **22**, 226–230.
- Murphy KG & Bloom SR (2006). Gut hormones and the regulation of energy homeostasis. *Nature* **444**, 854–859.
- Out C, Patankar J V., Doktorova M, Boesjes M, Bos T, de Boer S, Havinga R, Wolters H, Boverhof R, van Dijk TH, Smoczek A, Bleich A, Sachdev V, Kratky D, Kuipers F, Verkade HJ & Groen AK (2015). Gut microbiota inhibit Asbt-dependent intestinal bile acid reabsorption via Gata4. *J Hepatol* **63**, 697–704.

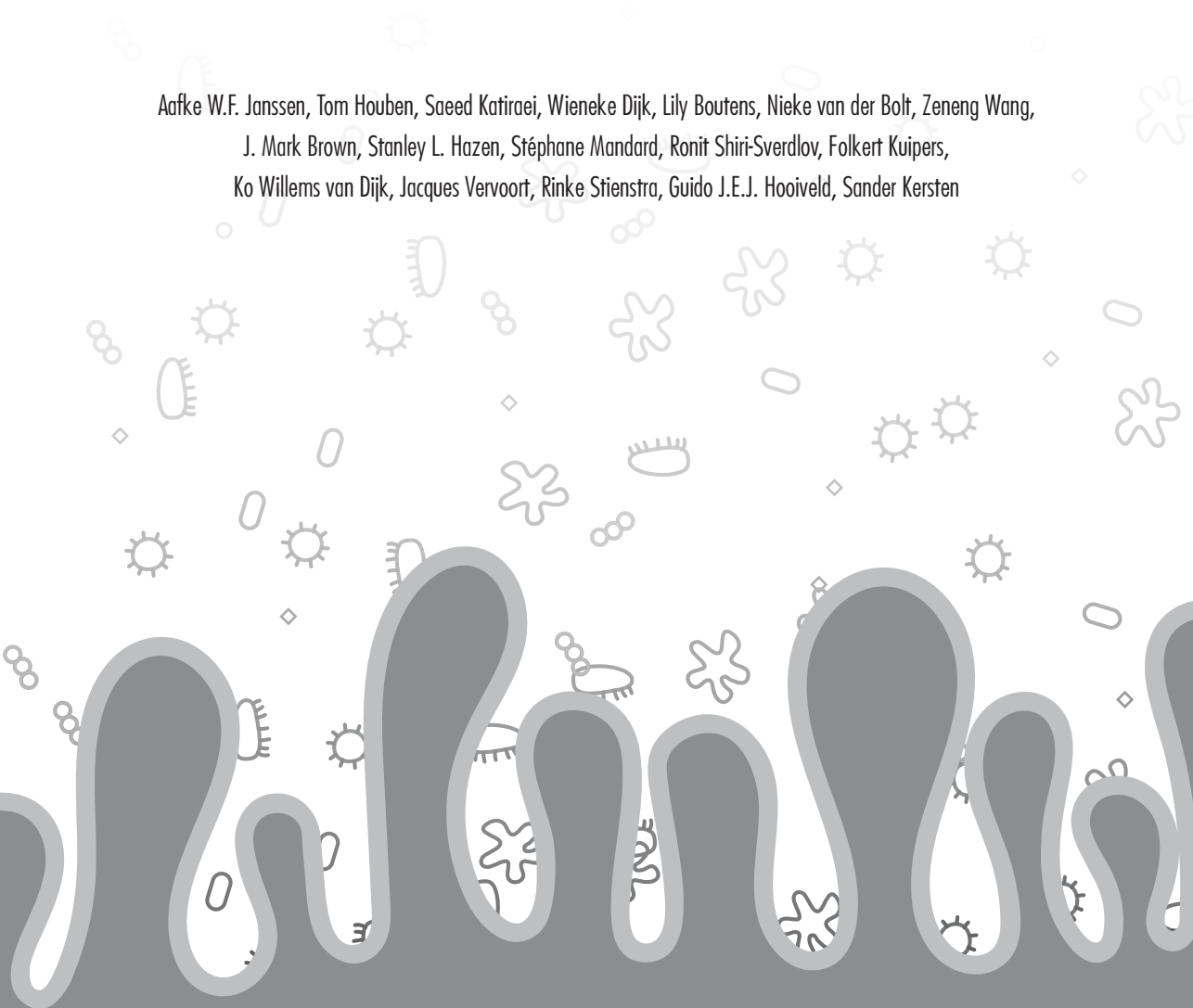
- Pars us A, Sommer N, Sommer F, Caesar R, Molinaro A, St hlman M, Greiner TU, Perkins R & B ckhed F (2016). Microbiota-induced obesity requires farnesoid X receptor. *Gut* **0**, 1–9.
- Pendyala S, Walker JM & Holt PR (2012). A high-fat diet is associated with endotoxemia that originates from the gut. *Gastroenterology* **142**, 1100–1101.e2.
- Potthoff MJ, Potts A, He T, Duarte J a G, Taussig R, Mangelsdorf DJ, Kliewer S a & Burgess SC (2013). Colesevelam suppresses hepatic glycogenolysis by TGR5-mediated induction of GLP-1 action in DIO mice. *Am J Physiol Gastrointest Liver Physiol* **304**, G371–G380.
- Psichas A, Sleeth ML, Murphy KG, Brooks L, Bewick GA, Hanyaloglu AC, Ghatei MA, Bloom SR & Frost G (2015). The short chain fatty acid propionate stimulates GLP-1 and PYY secretion via free fatty acid receptor 2 in rodents. *Int J Obes (Lond)* **39**, 424–429.
- Qin J et al. (2012). A metagenome-wide association study of gut microbiota in type 2 diabetes. *Nature* **490**, 55–60.
- Rabot S, Membrez M, Bruneau A, G rard P, Harach T, Moser M, Raymond F, Mansourian R & Chou CJ (2010). Germ-free C57BL/6J mice are resistant to high-fat-diet-induced insulin resistance and have altered cholesterol metabolism. *FASEB J* **24**, 4948–4959.
- Rajili -Stojanovi  M & de Vos WM (2014). The first 1000 cultured species of the human gastrointestinal microbiota. *FEMS Microbiol Rev* **38**, 996–1047.
- Ridaura VK et al. (2013). Gut microbiota from twins discordant for obesity modulate metabolism in mice. *Science* **341**, 1241214.
- Sayin SI, Wahlstr m A, Felin J, J ntti S, Marschall H-U, Bamberg K, Angelin B, Hy t yl inen T, Ore i  M & B ckhed F (2013). Gut microbiota regulates bile acid metabolism by reducing the levels of tauro-beta-muricholic acid, a naturally occurring FXR antagonist. *Cell Metab* **17**, 225–235.
- Schaubeck M, Clavel T, Calasan J, Lagkouravdos I, Haange SB, Jehmlich N, Basic M, Dupont A, Hornef M, Bergen M Von, Bleich A & Haller D (2016). Dysbiotic gut microbiota causes transmissible Crohn's disease-like ileitis independent of failure in antimicrobial defence. *Gut* **65**, 225–237.
- Schwartz A, Taras D, Sch fer K, Beijer S, Bos N a, Donus C & Hardt PD (2010). Microbiota and SCFA in lean and overweight healthy subjects. *Obesity (Silver Spring)* **18**, 190–195.
- Smith K, McCoy KD & Macpherson AJ (2007). Use of axenic animals in studying the adaptation of mammals to their commensal intestinal microbiota. *Semin Immunol* **19**, 59–69.
- Sommer F & B ckhed F (2013). The gut microbiota--masters of host development and physiology. *Nat Rev Microbiol* **11**, 227–238.
- Steel HC, Theron AJ, Cockeran R, Anderson R & Feldman C (2012). Pathogen- and host-directed anti-inflammatory activities of macrolide antibiotics. *Mediators Inflamm* **2012**, Article ID 584262.
- Swann JR, Want EJ, Geier FM, Spagou K, Wilson ID, Sidaway JE, Nicholson JK & Holmes E (2011). Systemic gut microbial modulation of bile acid metabolism in host tissue compartments. *Proc Natl Acad Sci U S A* **108 Suppl**, 4523–4530.
- Tauber SC & Nau R (2008). Immunomodulatory properties of antibiotics. *Curr Mol Pharmacol* **1**, 68–79.
- Tolhurst G, Heffron H, Lam YS, Parker HE, Habib AM, Diakogiannaki E, Cameron J, Grosse J, Reimann F & Gribble FM (2012). Short-chain fatty acids stimulate glucagon-like peptide-1 secretion via the G-protein-coupled receptor FFAR2. *Diabetes* **61**, 364–371.
- Vinolo MAR, Rodrigues HG, Hatanaka E, Hebeda CB, Farsky SHP & Curi R (2009). Short-chain fatty acids stimulate the migration of neutrophils to inflammatory sites. *Clin Sci (Lond)* **117**, 331–338.
- Vrieze A et al. (2012). Transfer of intestinal microbiota from lean donors increases insulin sensitivity in individuals with metabolic syndrome. *Gastroenterology* **143**, 913–916.
- Vrieze A et al. (2014). Impact of oral vancomycin on gut microbiota, bile acid metabolism, and insulin sensitivity. *J Hepatol* **60**, 824–831.
- Walsh CJ, Guinane CM, O'Toole PW & Cotter PD (2014). Beneficial modulation of the gut microbiota. *FEBS Lett* **588**, 4120–4130.
- Wang X, Ryu D, Houtkooper RH & Auwerx J (2015). Antibiotic use and abuse: A threat to mitochondria and chloroplasts with impact on research, health, and environment. *BioEssays* **37**, 1045–1053.
- Wolever T, Spadafora P & Eshuis H (1991). Interaction between colonic and propionate in humans. *Am J Clin Nutr* **53**, 681–687.
- Wu H, Tremaroli V & B ckhed F (2015). Linking Microbiota to Human Diseases: A Systems Biology Perspective. *Trends Endocrinol Metab* **26**, 758–770.
- Xu A, Lam MC, Chan KW, Wang Y, Zhang J, Hoo RLC, Xu JY, Chen B, Chow W, Tso AWK & Lam KSL (2005). Angiopoietin-like protein 4 decreases blood glucose and improves glucose tolerance but induces hyperlipidemia and hepatic steatosis in mice. **2–7**.
- Yi P & Li L (2012). The germfree murine animal: An important animal model for research on the relationship between gut microbiota and the host. *Vet Microbiol* **157**, 1–7.

4



Modulation of the gut microbiota impacts non-alcoholic fatty liver disease: a potential role for bile acids

Aafke W.F. Janssen, Tom Houben, Saeed Katiraei, Wieneke Dijk, Lily Boutens, Nieke van der Bolt, Zeneng Wang, J. Mark Brown, Stanley L. Hazen, Stéphane Mandard, Ronit Shiri-Sverdlov, Folkert Kuipers, Ko Willems van Dijk, Jacques Vervoort, Rinke Stienstra, Guido J.E.J. Hooiveld, Sander Kersten



Abstract

Non-alcoholic fatty liver disease (NAFLD) is the most common liver disease worldwide, yet the pathogenesis of NAFLD is only partially understood. Here, we investigated the role of the gut bacteria in NAFLD by stimulating the gut bacteria via feeding mice the fermentable dietary fiber guar gum and suppressing the gut bacteria via chronic oral administration of antibiotics.

Guar gum feeding profoundly altered the gut microbiota composition, in parallel with reduced diet-induced obesity and improved glucose tolerance. Strikingly, despite reducing adipose tissue mass and inflammation, guar gum enhanced hepatic inflammation and fibrosis, concurrent with markedly elevated plasma and hepatic bile acid levels. Consistent with a role of elevated bile acids in the liver phenotype, treatment of mice with taurocholic acid stimulated hepatic inflammation and fibrosis. In contrast to guar gum, chronic oral administration of antibiotics effectively suppressed the gut bacteria, decreased portal secondary bile acid levels, and attenuated hepatic inflammation and fibrosis. Neither guar gum or antibiotics influenced plasma lipopolysaccharide levels.

In conclusion, our data indicate a causal link between changes in gut microbiota and hepatic inflammation and fibrosis in a mouse model of NAFLD, possibly via alterations in bile acids.

Introduction

The worldwide epidemic of obesity is the primary driver for the global increase in the prevalence of type 2 diabetes and non-alcoholic fatty liver disease (NAFLD) (1). While caloric overconsumption and the associated positive energy balance are the sine qua non of obesity development, emerging evidence implicates gut microbes in the promotion of obesity and related metabolic disturbances (2–5).

The human intestine contains a variety of microbiota, mainly consisting of bacteria and complemented by other microorganisms such as fungi, protozoa and viruses. The gut microbiota form a mutualistic relationship with the host and have an important role in host health. Besides protecting the host against invading pathogenic microorganisms, intestinal bacteria facilitate the digestion of otherwise indigestible carbohydrates, produce essential vitamins, stimulate the development of the immune system and maintain tissue homeostasis (6, 7). In recent years, the gut microbiota have increasingly been connected with a number of diseases, including irritable bowel syndrome, Crohn's disease, obesity, type 2 diabetes, atherosclerosis and NAFLD (5, 8–10).

NAFLD describes a spectrum of related liver diseases ranging from simple steatosis to non-alcoholic steatohepatitis (NASH), liver fibrosis, and cirrhosis (11). Although the exact pathogenesis of NAFLD is unknown, multiple factors likely contribute to the progression of NAFLD, including genetic predisposition, lipid overload, and inflammatory insults. Indeed, it is believed that inflammatory mediators released locally or derived from tissues such as the intestine and adipose tissue play an important role in the progression of steatosis to NASH (12, 13).

Recent studies have raised the possibility that NAFLD may be related to disturbances in the gut microbial composition. In particular, it was found that the gut microbial composition was different between healthy individuals and patients with NAFLD (14, 15). Furthermore, mouse studies suggest that changes in the gut microbial community may impact the development of hepatic steatosis (16), inflammation (17, 18) and fibrosis (18).

To further elaborate the concept that the gut microbiota may affect the development of NAFLD, we studied the influence of modulation of the gut microbiota on NAFLD. To that end, in a mouse model of NAFLD, we stimulated the gut bacteria by feeding mice the highly fermentable dietary fiber guar gum, using the poorly fermentable dietary fiber resistant starch as control. Inasmuch as guar gum escapes digestion in the small intestine and is thought to act exclusively via bacterial fermentation and concomitant alterations in gut microbiota, feeding guar gum is an attractive strategy to study the role of the gut microbes in NAFLD. Additionally, in the same mouse model of NAFLD, we studied the effect on NAFLD of suppressing the gut bacteria using a mixture of antibiotics.

Overall, our data indicate that the gut microbiota have a marked impact on NAFLD. Specifically, specific modulation of the gut microbiota by feeding guar gum worsened features of NAFLD, whereas suppression of the gut bacteria using oral antibiotics protected against NAFLD, possibly via changes in the portal delivery of bile acids.

Materials and methods

Animals and diet

Animal studies were performed using pure-bred male C57Bl/6 mice. Mice were individually housed in temperature- and humidity-controlled specific pathogen-free conditions. Mice had *ad libitum* access to food and water. In study 1, 11-week-old mice received a low fat diet or a high fat/high cholesterol/high fructose diet (HFCFD) for 18 weeks, providing 10% or 45% energy as triglycerides (formula D12450B or D12451 from Research Diets, Inc., manufactured by Research Diet Services, Wijk bij Duurstede, Netherlands). The fat source of this HFCFD was replaced by safflower oil and supplemented with 1% cholesterol (Dishman, Veenendaal, Netherlands). Mice receiving the HFCFD were provided with 20% fructose water (wt/vol) to promote development of NAFLD (19). The fiber-enriched diets were identical to the HFCFD (CTRL) except that corn starch and part of the maltodextrin 10 were replaced by 10% (wt/wt) resistant starch (RS) or guar gum (GG). The composition of the diets is shown in **Supplemental Table 1**. Resistant starch, a retrograded tapioca starch classified as RS type 3 (brand name C* Actistar 11700) and guar gum (brand name Viscogum) were obtained from Cargill R&D Centre Europe (Vilvoorde, Belgium). Bodyweight and food intake were assessed weekly. One mouse fed the GG-enriched diet died during the study for reasons unrelated to the intervention.

In study 2, 10-week-old mice received a high fat/high cholesterol/high fructose diet (CTRL) for 18 weeks, providing 45% energy as triglycerides (formula 58V8 manufactured by TestDiet, St. Louis, USA). This diet was supplemented with 1% cholesterol (Dishman, Veenendaal, Netherlands). The mice received 20% fructose (wt/vol) in the drinking water. The TMAO-enriched diet was identical to the CTRL diet except that 0.296 % of sucrose (wt/wt) was replaced by 0.296% TMAO-dihydrate (wt/wt) (Sigma, Zwijndrecht, The Netherlands) to obtain a final concentration of 0.2% TMAO (wt/wt). Bodyweight and food intake were assessed weekly. One mouse fed the TMAO-enriched diet died during the study for reasons unrelated to the intervention. One mouse in the CTRL group and one mouse fed the TMAO-enriched diet failed to thrive and were excluded from further analysis.

In study 3, 4 month-old male mice received either chow (CTRL) or chow supplemented with 0.5% (wt/wt) taurocholic acid (TCA) (Calbiochem) for 7 days (20). Bodyweight and food intake were assessed daily.

In study 4, 10-week old mice received a high fat/high cholesterol/high fructose diet (CTRL) for 18 weeks, providing 45% energy as triglycerides (formula 58V8 manufactured by TestDiet, St. Louis, USA). The diet was supplemented with 1% cholesterol (Dishman, Veenendaal, Netherlands). The mice received 20% fructose (wt/vol) in the drinking water. Mice that were given antibiotics received the same CTRL diet with the addition of 1g/l

Ampicillin, 1g/l Neomycin sulphate, 1g/l Metronidazole and 0.5g/l Vancomycin in the drinking water for 22 weeks. This antibiotic cocktail has previously been shown to deplete all detectable commensal bacteria (21). Bodyweight and food intake were assessed weekly. One mouse in the CTRL group and one mouse in the antibiotics group failed to thrive and were excluded from further analysis.

At the end of each study, mice were anesthetized using isoflurane and blood was collected by orbital puncture. Mice were euthanized via cervical dislocation after which tissues were excised and weighed and intestinal content was sampled. The mice were not fasted prior to euthanasia (e.g. ad libitum fed state). The animal experiments were approved by the local animal ethics committee of Wageningen University.

Intraperitoneal glucose tolerance test

In study 1, mice were fasted for 5 hours prior to the intraperitoneal glucose tolerance test. During this period fructose water was replaced by tap water. Blood samples were collected from the tail vein immediately before (t=0 min) and at selected time points after intraperitoneal injection with glucose (0.8 g/kg bodyweight). Glucose was measured using Accu-chek Compact. Plasma concentrations of insulin were quantified after 5 hour fasting according to manufacturer's instructions (Crystal Chem, Downers Grove, USA).

RNA isolation and qPCR

Total RNA was extracted from epididymal white adipose tissue, liver and scrapings of the distal small intestine using TRIzol reagent (Life technologies, Bleiswijk, Netherlands). Subsequently, 500ng RNA was used to synthesize cDNA using iScript cDNA synthesis kit (Bio-Rad Laboratories, Veenendaal, Netherlands). Changes in gene expression were determined by real-time PCR on a CFX384 Real-Time PCR detection system (Bio-Rad Laboratories, Veenendaal, Netherlands) by using SensiMix (Bioline, GC biotech, Alphen aan den Rijn, Netherlands). The housekeeping gene 36b4 or β -actin was used for normalization. Sequences of the used primers are listed in **Supplemental Table 2**.

Histology/Immunohistochemistry

Hematoxylin and Eosin (H&E) staining of sections was performed using standard protocols. Paraffin-embedded liver sections (5 μ m) were stained for collagen using fast green FCF/ Sirius Red F3B. Staining of neutral lipids was performed on frozen liver sections using Oil Red O according to standard protocols.

Visualization of hepatic stellate cells was performed on paraffin-embedded liver sections with an antibody against alpha smooth muscle actin (α SMA)(M0851, Dako, Heverlee, Belgium). To detect macrophages, 5 μ m frozen liver sections were stained for Cd68 Kupffer

cells (Cd68 marker, FA11) as described previously (22).

Plasma/serum measurements

In study 1 and 3, blood was collected in EDTA-coated tubes and centrifuged for 15 minutes at 3000 rpm to obtain plasma. In study 2 and 4, blood was collected, allowed to clot for 45 minutes and centrifuged for 15 minutes at 3000 rpm to obtain serum. The mice were not fasted prior to blood collection. Plasma and serum alanine aminotransferase activity was measured with a kit from Abcam (Cambridge, UK). The commercially available Limulus Amebocyte Lysate assay (Lonza, Walkerville, USA) was used to quantify plasma and portal serum endotoxin levels. Plasma concentration of total bile acids were determined using a colorimetric assay kit (Diazyme Laboratories, Poway, USA). Free and conjugated bile acid subspecies were quantified by liquid chromatography tandem MS (LC-MS/MS) using a SHIMADZU liquid chromatography system (SHIMADZU, Kyoto, Japan) and tandem AB SCIEX API-3200 triple quadrupole mass spectrometry (AB SCIEX, Framingham, USA) as previously described (23). TMA and TMAO plasma levels and TMAO serum levels were quantified by stable isotope dilution liquid chromatography tandem mass spectrometry as previously described (24, 25).

Fecal measurements

In study 1, during the 6th week of dietary intervention feces were collected over a period of 48 hours. Total lipids and free fatty acids were measured in the fecal samples as mentioned by Govers *et al.* (26). Briefly, 100mg of fecal samples were weighed, dried and acidified using HCl. Lipids were then extracted using petroleum and diethyl ether. Ether fraction was collected, evaporated and the total lipids were weighed.

Free and conjugated bile acid subspecies in the feces, collected at the end of the dietary intervention in study 1 and 4, were determined by capillary gas chromatography (Agilent 6890, Amstelveen, the Netherlands) as described previously (27).

Microarray analysis

Microarray analysis was performed on liver samples from 8 mice of the CTRL group and 8 mice of the GG group. RNA was isolated as described above and subsequently purified using the RNeasy Microkit from Qiagen (Venlo, The Netherlands). RNA integrity was verified with RNA 6000 Nanochips on a Agilent 2100 bioanalyzer (Agilent Technologies, Amsterdam, the Netherlands). Purified RNA (100 ng) was labeled with the Ambion WT expression kit (Invitrogen, Carlsbad, USA) and hybridized to an Affymetrix Mouse Gene 1.1 ST array plate (Affymetrix, Santa Clara, USA). Hybridization, washing, and scanning were carried out on an Affymetrix GeneTitan platform according to the instruction by

the manufacturer. Arrays were normalized using the Robust Multiarray Average method (28, 29). Probe sets were defined according to Dai *et al.* (30). In this method, probes are assigned to Entrez IDs as an unique gene identifier. The p-values were calculated using an Intensity-Based Moderated T-statistic (IBMT) (31). The q-value was calculated as measure of significance for false discovery rate (32). To identify the pathways most significantly altered in the livers of the GG group compared to the CTRL group, Ingenuity Pathway Analysis (Ingenuity Systems, Redwood City, USA) was performed. Input criteria were a relative fold change equal to or above 1.3 and a q-value equal to or below 0.01. Array data have been submitted to the Gene Expression Omnibus under accession number GSE76087.

A publicly available dataset (GSE34730) was downloaded from Gene Expression Omnibus and further processed as described above to obtain individual gene expression data. Ingenuity Pathway Analysis was performed on genes induced by deoxycholic acid by at least two-fold.

Western blot

Liver homogenates were prepared by lysing liver tissue in ice-cold Pierce IP lysis buffer (ThermoScientific, Rockford, USA) containing complete protease inhibitor and PhosSTOP phosphatase inhibitor (both from Roche, Mannheim, Germany). Equal amounts of protein were loaded on a Mini Protean TGX gel, 4-15% and subsequently transferred to a PVDF membrane (both from Bio-Rad Laboratories, Veenendaal, The Netherlands). The primary antibodies for TIMP1 (Abcam, Cambridge, UK) and HSP90 (Cell Signalling) were incubated at 4°C overnight followed by incubation with the appropriate secondary peroxidase-conjugated antibody (Sigma, Zwijndrecht, The Netherlands). Protein bands were visualized using an Enhanced Chemiluminescent substrate (Bio-Rad Laboratories, Veenendaal, The Netherlands).

Liver measurements

For liver triglyceride measurement, livers were homogenized in a buffer containing 10mM Tris, 2mMEDTA and 250mM sucrose at pH 7.5 in a Tissue Lyser II (Qiagen, Hilden, Germany) to obtain 2% homogenates. Triglycerides were subsequently quantified using a Triglycerides liquidcolor^{mono} from HUMAN Diagnostics (Wiesbaden, Germany). 4-hydroxyproline content was determined spectrophotometrically in liver hydrolysates as described previously (33).

For hepatic myeloperoxidase activity, liver homogenates were prepared and myeloperoxidase activity was measured according to manufacturer's instructions (Abcam, Cambridge, UK).

For the quantification of liver total bile acid content, livers were homogenized in 75% ethanol, incubated at 50°C and centrifuged. After the collection of the supernatant, the

concentration of total bile acids were determined using a colorimetric assay kit (Diazyme Laboratories, Poway, USA).

FACS analysis

Epididymal white adipose tissue was isolated, minced and digested with 1.5 mg/ml collagenase type 2 (Sigma, Zwijndrecht, The Netherlands) in DMEM containing 0.5% fatty acid free BSA for 45 minutes at 37°C by shaking. Cell suspensions were filtered through a 100µM filter and centrifuged at 200g for 10 minutes. Floating mature adipocytes were discarded and the stromal vascular cell pellet was resuspended in erythrocyte lysis buffer for 5 minutes. Cells were washed twice with FACS buffer (PBS + 1% BSA) and incubated with fluorescently labeled antibodies including CD45-ECD (Beckman Coulter, Fullerton, USA), F4/80-FITC and Cd11b-PE (Biolegend, San Diego, USA). Samples were analyzed using a FC500 Flow Cytometer (Beckman Coulter, Fullerton, USA).

DNA extraction

In study 1, fecal samples derived from the second part of the colon were suspended in 10 mM Tris, 1mM EDTA, 0.5% SDS and 0.2mg/ml Proteinase K (ThermoScientific, Rockford, USA). After addition of 0.1-0.25mm and 4mm glass beads, buffered phenol (Invitrogen, Carlsbad, USA) was added and cells were lysed by mechanical disruption using a bead beater (MP biomedical, Santa Ana, USA) for 3 minutes. DNA was subsequently extracted using phenol:chloroform:isoamylalcohol [25:24:1] (Invitrogen, Carlsbad, USA), precipitated with isopropanol and washed with 70% ethanol.

In study 4, fecal samples (~15-60mg) derived from the second part of the colon were suspended in 500µL S.T.A.R. buffer (Roche). After addition of 0.1mm zirconia and 2.5mm glass beads (BioSpec, Bartlesville, USA), cells were lysed by mechanical disruption using a bead beater (MP biomedical, Santa Ana, USA) for 3x1 minute. DNA was subsequently extracted and purified using Maxwell 16 System (Promega). In brief, homogenates (250 µL) were transferred to a prefilled reagent cartridge (Maxwell® 16 Tissue LEV Total RNA Purification Kit, Custom-made, Promega). Sixteen samples were processed at the same time. After 30 minutes the purification process was completed and DNA was eluted in 50 µL of water (Nuclease free)(Promega).

16S rRNA gene sequencing

For 16S rRNA gene sequencing DNA samples were sent to the Broad Institute of MIT and Harvard (Cambridge, USA). Microbial 16S rRNA gene was amplified targeting the hyper-variable region V4 using forward primer 515F (5'-GTGCCAGCMGCCGCGGTAA-3') and the reverse primer 806R (5'-GGACTACHVGGGTWTCTAAT-3'). The cycling conditions

consisted of an initial denaturation of 94°C for 3 min, followed by 25 cycles of denaturation at 94°C for 45 sec, annealing at 50 °C for 60 sec, extension at 72°C for 5 min, and a final extension at 72°C for 10 min. Sequencing was performed using the Illumina MiSeq platform generating paired-end reads of 175 bp in length in each direction. Overlapping paired-end reads were subsequently aligned. Detailed of this protocol are as previously described (34).

Raw sequence data quality was assessed using FastQC, version: 0.11.2 (<http://www.bioinformatics.babraham.ac.uk/projects/fastqc/>). Reads quality was checked with Sickel, version: 1.33 (<https://github.com/najoshi/sickle>) and low quality reads were removed. For visualising the taxonomic composition of the fecal microbiota and further beta diversity analysis, QIIME, version: 1.9.0 was used (35). In brief, closed reference OTU picking with 97% sequence similarity against GreenGenes 13.8 reference database was done. Jackknifed beta-diversity of unweighted UniFrac distances with 10 jackknife replicates was measured at rarefaction depth of 22000 reads/sample. For statistical significance, biological relevance and visualisation we used linear discriminant analysis (LDA) effect size (LEfSe) method (<https://bitbucket.org/biobakery/biobakery/wiki/lefse>) (36).

Bacterial 16S rRNA gene and fungal ITS1-5.8S-ITS2 region quantification

In study 4, real-time PCR was used to quantify 16S rRNA gene and ITS1-5.8S-ITS2 region in equal amounts of extracted DNA on a CFX384 Real-Time PCR detection system (Bio-Rad Laboratories, Veenendaal, Netherlands) by using SensiMix (Bioline, GC biotech, Alphen aan den Rijn, Netherlands). 16S rRNA gene was amplified using the forward primer 1369F (5'-CGGTGAATACGTTTCYCGG-3') (37) and the reverse primer 1492R (5'-GGWTACCTTGTTACGACTT-3') (38). The cycling conditions consisted of an initial denaturation of 95°C for 5 min, followed by 40 cycles of denaturation at 95°C for 15 sec, annealing at 60 °C for 30 sec and extension at 72°C for 30 sec. The ITS1-5.8S-ITS2 region was amplified using universal fungal primers V9D (5'-TTAAGTCCCTGCCCTTTGTA-3') and LS266 (5'-GCATTCCTCAACAACCTCGACTC-3') encompassing highly conserved regions encoding fungal rDNA (39). The cycling conditions consisted of an initial denaturation of 94°C for 10 min, followed by 30 cycles of denaturation at 94°C for 30 sec, annealing at 58 °C for 30 sec, extension at 72°C for 30 sec and a final extension at 72°C for 10 min.

¹H NMR spectroscopy

Contents of the cecum and first part of the colon were collected, mixed with phosphate buffer (pH 8) containing 10% deuterium oxide (D₂O) and stored at -20°C. For short chain fatty acid (SCFA), ethanol and choline quantification samples were thawed, mixed and centrifuged at 14000 rpm for 5 minutes. Supernatant was collected and diluted in phosphate buffer containing 2mM maleic acid as standard. Subsequently, 200µl sample was transferred

to 3mm NMR tubes (Bruker Match System) and measured at 300K in an Avance III NMR spectrometer operated at 600.13 MHz as described previously (40).

Statistical analysis

Data are presented as mean \pm SEM. Statistical significant differences were determined with one way analysis of variance followed by Tukey's post hoc multiple comparison test. Comparisons between two groups were made using two-tailed Student's t-test. $P < 0.05$ was considered as statistically significant. SPSS software (Version 21, SPSS Inc., Chicago, USA) was used for statistical analysis.

Results

High fat/high cholesterol/high fructose diet as model for NAFLD

Feeding mice a diet rich in fat, cholesterol and/or fructose are commonly used strategies to induce NAFLD (41–43). To verify the suitability of the high fat/high cholesterol/high fructose diet (HFCFD) as model for NAFLD, we tested the effect of HFCFD on various relevant parameters in comparison with a commonly used low fat diet. Weight gain, adipose tissue weight and liver weight were significantly higher in the mice fed HFCFD as compared to mice fed the low fat diet (**Figure 1A–C**). Hepatic lipid storage was markedly higher in mice fed HFCFD, as shown by a five-fold increase in liver triglycerides (**Figure 1D**) and by Oil Red O staining (**Figure 1E**). H&E confirmed the presence of microvesicular and macrovesicular steatosis, and showed mild infiltration of immune cells (**Figure 1F**). Hepatic

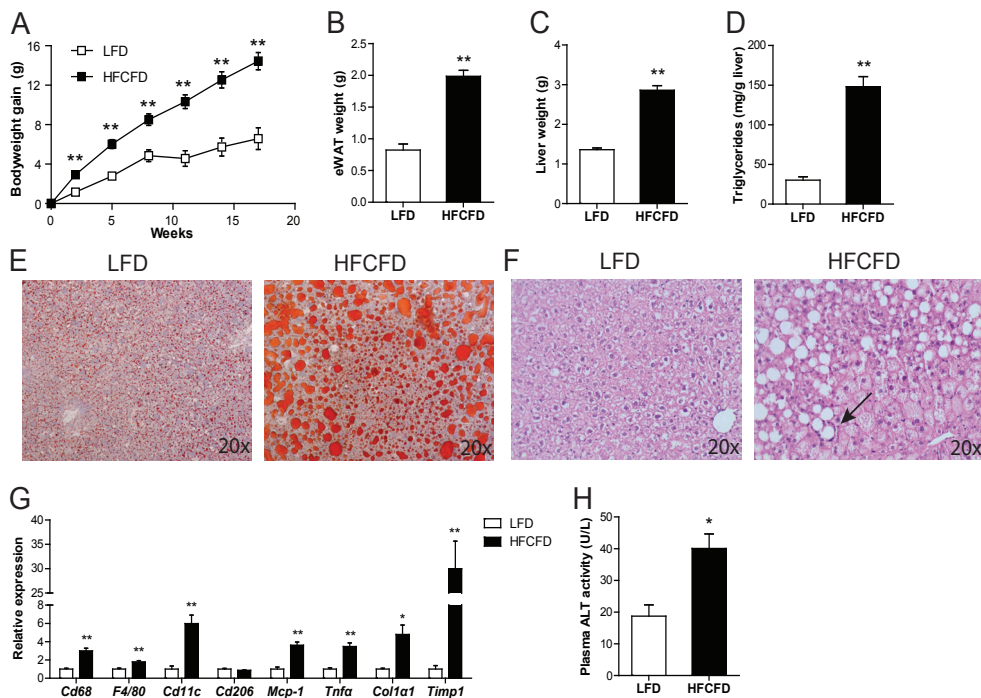


Figure 1. Effect of HFCFD on obesity and features of NAFLD

(A) Bodyweight gain in C57Bl/6 mice fed a low fat diet or a high fat/high cholesterol/high fructose diet (HFCFD). Weight of (B) epididymal white adipose tissue (eWAT) and (C) liver after 18 weeks of dietary intervention. (D) Quantitative analysis of liver triglyceride levels. (E) Oil Red O staining and (F) H&E staining of representative liver sections. Arrow denotes inflammatory infiltrate. (G) Relative expression of inflammation and fibrosis-related genes in the liver. Gene expression levels of mice fed low fat diet were set at 1. (H) Activity of alanine aminotransferase (ALT) in plasma. Data are presented as mean ± SEM. Asterisks indicate significantly different compared with low fat diet. * $p < 0.05$, ** $p \leq 0.001$.

expression of macrophage markers *Cd68*, *F4/80* and *Cd11c* and pro-inflammatory cytokines *Mcp-1* and *Tnfa* were significantly elevated in mice fed HFCFD, as was the expression of fibrosis markers collagen type I alpha 1 and *Timp1* (Figure 1G). Finally, plasma ALT levels were doubled in mice fed HFCFD (Figure 1H). Taken together, these data show that feeding HFCFD represents a suitable model to study NAFLD in mice.

Dietary guar gum alters colonic microbial composition

To evaluate the potential impact of alterations in the gut microbial community on the development of NAFLD, we fed mice the highly fermentable dietary fiber guar gum (GG) on a background of HFCFD for 18 weeks. Mice fed the poorly fermentable dietary fiber resistant starch (RS) and mice that were not fed any dietary fiber (CTRL) served as negative controls. To assess the effect of GG on colonic microbial composition and the relative abundance of specific gut microbiota taxa, 16S rRNA gene sequencing was performed on faecal samples

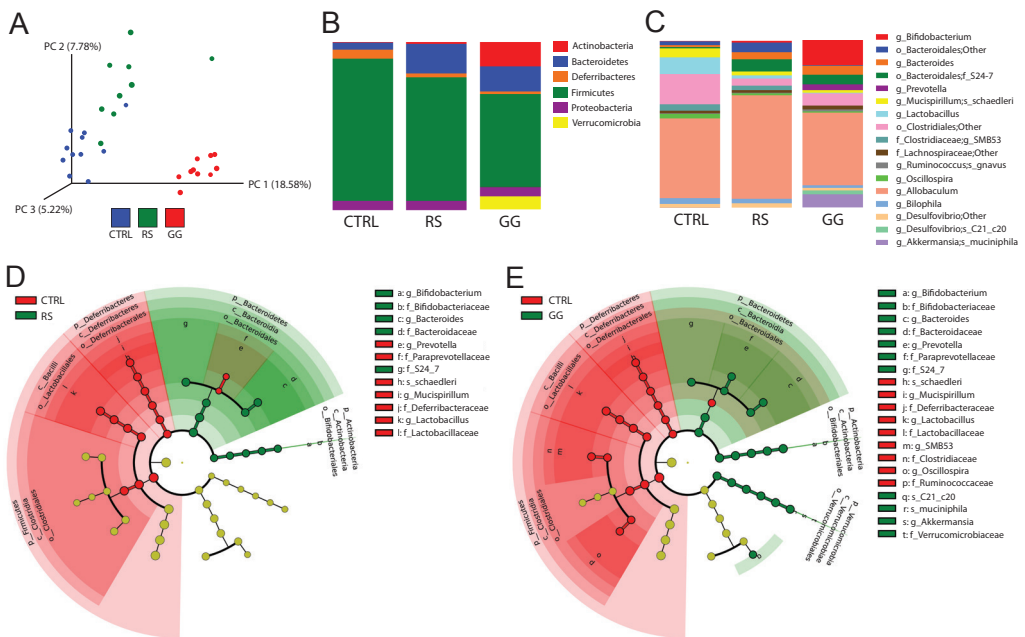


Figure 2. Guar gum alters the colonic microbial composition

(A) Principle coordinates analysis plot of unweighted UniFrac distances indicating clustering 16S rRNA gene sequences. Each circle represents an individual mouse. (B) Mean relative abundance of the predominant phyla (>0.5% in at least one of the three diet groups). (C) Mean relative abundance of bacteria reported to the lowest identifiable level. Taxonomic level is indicated by letter preceding the underscore: o, order; f, family; g, genus; s, species. (D) Cladogram representing significant enrichment of taxa in CTRL (red) or RS (green) colonic microbiota. (E) Cladogram representing significant enrichment of taxa in CTRL (red) or GG (green) colonic microbiota. The central point in the cladogram represents the domain bacteria and each ring represents the next lower taxonomic level (phylum to genus).

collected at the end of the dietary intervention. Clustering of 16S rRNA gene sequences by unweighted UniFrac distances per mouse revealed a sharp clustering of microbiome sequence data of the GG mice, indicating that the colonic microbial community was distinct between CTRL and GG mice. In contrast, the microbiota of the RS mice more closely resembled that of the CTRL mice (**Figure 2A**). Analysis of the microbiota at various taxonomic levels indicated differences in microbial composition depending on fiber type. In comparison with CTRL, both types of dietary fibers significantly reduced the relative abundance of Deferribacteres and Firmicutes, and increased the relative abundance of Bacteroidetes. The abundance of Actinobacteria was particularly increased in the GG mice. With a relative proportion of 8.23% of all phyla, the phylum Verrucomicrobia was overrepresented in the GG mice, whereas it was almost completely absent in CTRL and RS mice (**Figure 2B** and **Supplemental Table 3**).

The differences in microbial community between the RS and GG groups became more apparent at lower taxonomic levels. Whereas GG increased the abundance of the genera *Bifidobacterium* and *Prevotella*, RS had relatively small effects on these genera. The decreased abundance of the phylum Firmicutes for both dietary fibers can be mainly explained by a decrease within the genus *Lactobacillus*. GG also markedly suppressed *SMB53* and *Oscillospira* and increased the abundance of the species *Desulfovibrio C21_c20* (**Figure 2C-E** and **Supplemental Table 3**). Overall, these data indicate that GG feeding markedly altered the bacterial composition in the colon.

Modulation of the gut microbiota by guar gum is associated with protection against diet-induced obesity and improved glucose tolerance

Whereas RS did not influence bodyweight gain, GG markedly attenuated bodyweight gain as compared to control (CTRL) (**Figure 3A**). The lower bodyweight could not be attributed to a reduced food intake (**Figure 3B**) or an increased fecal output (**Figure 3C**). Fecal lipid excretion was significantly higher in the GG mice as compared to the CTRL mice (**Figure 3C**), suggesting that the lower bodyweight in the GG mice may be explained by decreased lipid absorption. Along with the lower bodyweight, weights of epididymal and mesenteric fat pads and liver were significantly lower in the GG group as compared with the CTRL group, while weight of the caecum was higher in both RS and GG groups (**Figure 3D**).

In line with the suppression of bodyweight gain, GG improved whole body glucose tolerance (**Figure 3E**), reduced fasting plasma insulin levels (**Figure 3F**), and attenuated immune cells infiltration in adipose tissue. Specifically, flow cytometry analysis demonstrated that the abundance of leukocytes (CD45+) and macrophages (CD45+F4/80+CD11B+) was significantly lower in the epididymal fat depot of the GG mice as compared to the CTRL mice, while it was not different in the RS mice (**Figure 3G-I**). The decreased macrophage

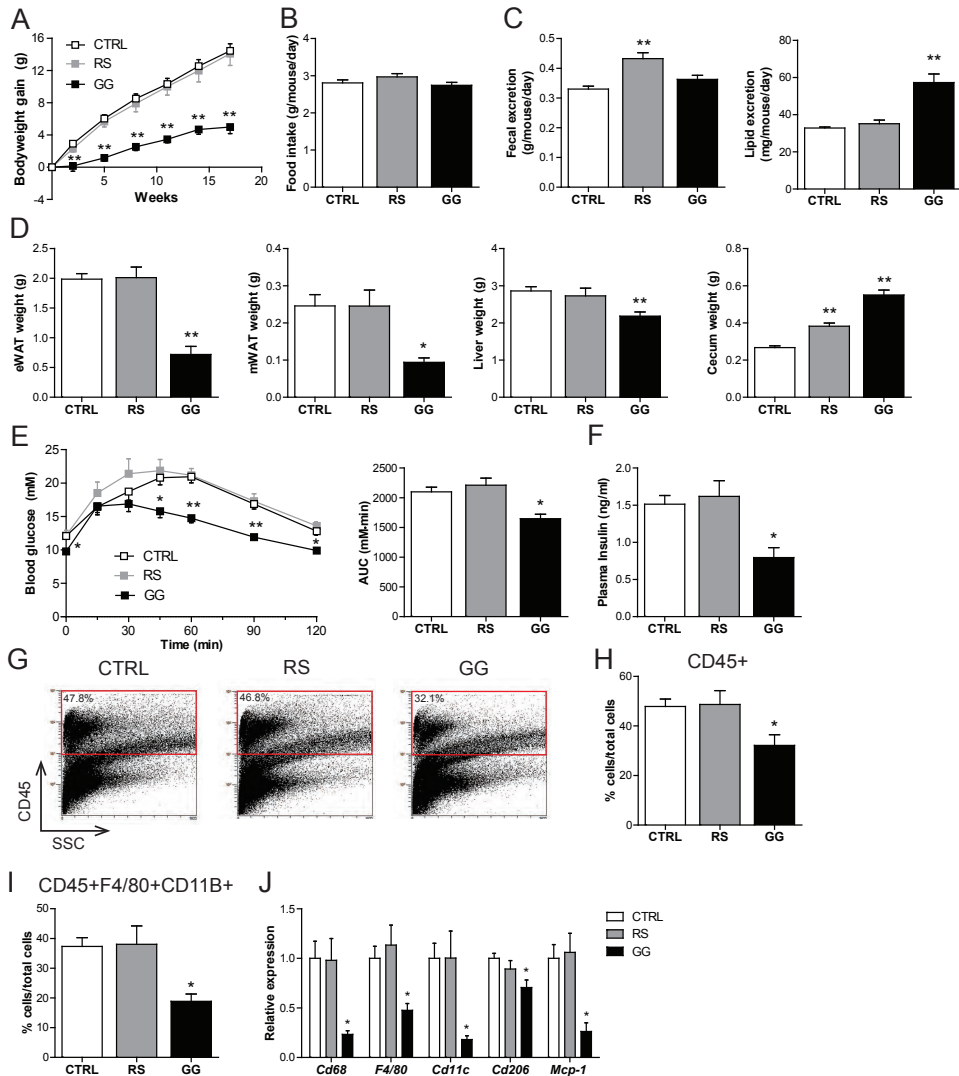


Figure 3. Stimulation of the gut microbiota by guar gum is associated with protection against the development of diet-induced obesity, improved glucose tolerance and decreased adipose tissue inflammation

(A) Changes in bodyweight in C57Bl/6 mice fed a HFCFD (CTRL) or a HFCFD supplemented with RS or GG. (B) Mean food intake per day during the dietary intervention. (C) Mean fecal and lipid excretion per mouse per day in the sixth week of dietary intervention. (D) Weight of epididymal white adipose tissue (eWAT), mesenteric white adipose tissue (mWAT), liver and cecum after 18 weeks of dietary intervention. (E) Plasma glucose levels of CTRL, RS and GG mice following an intraperitoneal glucose tolerance test (GTT) and areas under the curve (AUC) after 17 weeks of dietary intervention. (F) Plasma insulin concentration after 5 hours of fasting. (G) Representative flow cytometry plots and (H) corresponding quantitative analysis of infiltrated leukocytes (CD45+) in epididymal white adipose tissue (eWAT). (I) Quantitative analysis of macrophages (F4/80+CD11b+). (J) Relative expression of inflammatory genes in eWAT. Gene expression levels in CTRL mice were set at 1. Data are presented as mean \pm SEM. Asterisks indicate significantly different compared with CTRL. * $p < 0.05$ ** $p < 0.001$.

abundance was corroborated by decreased expression of chemoattractant protein *Mcp-1* and macrophages markers *F4/80* and *Cd68*. *Cd11c* and *Cd206* mRNA were also decreased in the GG group, suggesting lower presence of pro-inflammatory M1 macrophages and anti-inflammatory M2 macrophages, respectively (**Figure 3J**). Taken together, GG suppressed bodyweight gain, which was accompanied by decreased adipose tissue inflammation and improved glucose tolerance.

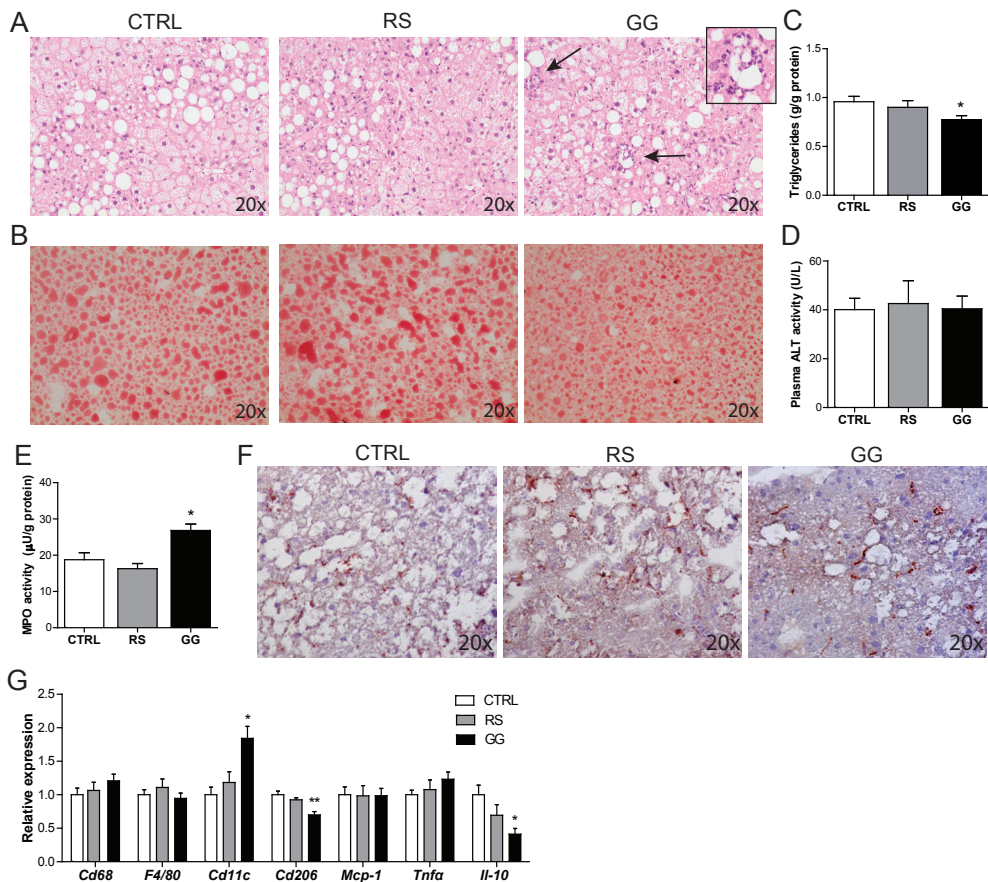


Figure 4. Stimulation of the gut microbiota by guar gum is associated with reduced hepatic steatosis but enhanced hepatic inflammation

(A) H&E staining of representative liver sections. Arrows denote inflammatory infiltrate and inset a higher magnification of the inflammatory infiltrate as observed in the livers of the GG mice. (B) Representative pictures of Oil Red O staining of liver sections. (C) Quantitative analysis of liver triglyceride levels. (D) Activity of alanine aminotransferase (ALT) in plasma. (E) Liver myeloperoxidase (MPO) activity representing hepatic neutrophil content. (F) Representative pictures of liver sections stained for the macrophage marker *Cd68*. (G) Relative expression of inflammatory genes in the liver. Gene expression levels in CTRL mice were set at 1. Data are presented as mean \pm SEM. Asterisks indicate significantly different compared with CTRL. * $p < 0.05$, ** $p < 0.001$.

Modulation of the gut microbiota by guar gum is associated with reduced hepatic steatosis but enhanced hepatic inflammation

In accordance with a lower fat mass in the GG mice, hepatic lipid accumulation was significantly lower in mice fed GG, as revealed by H&E and Oil Red O stainings and quantitation of liver triglycerides (**Figure 4A-C**). Plasma alanine aminotransferase activity, however, was not different between the 3 groups (**Figure 4D**). Interestingly, despite the reduction in liver triglycerides, H&E staining showed more pronounced inflammation in livers of GG mice, as revealed by the presence of inflammatory infiltrates (**Figure 4A**). Consistent with these data, elevated myeloperoxidase activity (**Figure 4E**) indicated a higher number of neutrophils in the livers of the GG mice. In contrast, the total macrophage abundance assessed by Cd68 staining and *Cd68* and *F4/80* expression was not different between the GG and CTRL mice (**Figure 4F-G**). Intriguingly, the higher expression of *Cd11c* and the lower expression of *Cd206* and the anti-inflammatory cytokine *Il-10*, suggested that the macrophages present in the liver of the mice fed GG had a more pro-inflammatory phenotype (**Figure 4G**). To further elucidate the inflammatory status of the liver of the GG mice, whole genome expression profiling was performed. It was found that expression of 3,722 genes was significantly different between the GG mice compared with the CTRL mice ($p < 0.01$) (**Supplemental Figure 1A**). Numerous immune-related pathways, including IL-8 signaling ($p = 1.05 \times 10^{-6}$) and complement system activation ($p = 7.76 \times 10^{-7}$), were altered in the livers of the GG mice, as determined by Ingenuity pathway analysis (**Supplemental Figure 1B**). Together, these data demonstrate that although feeding GG suppressed diet-induced obesity, it stimulated specific inflammatory cells and pathways in the liver, whereas RS had no effect.

Modulation of the gut microbiota by guar gum is associated with enhanced hepatic fibrosis

Strikingly, further study revealed that livers of the mice fed GG exhibited pronounced features of hepatic fibrosis. Sirius Red staining showed enhanced collagen deposition in the GG mice as compared with CTRL and RS mice (**Figure 5A**). Likewise, hepatic stellate cell activation as visualized by α SMA immunostaining and 4-hydroxyproline content were also increased in the GG mice (**Figure 5B-C**). Expression profiling followed by Ingenuity pathway analysis pointed to hepatic fibrosis/hepatic stellate cell activation as the most significantly regulated pathway ($p = 7.94 \times 10^{-11}$), which was illustrated by the differential expression of numerous genes involved hepatic fibrosis and hepatic stellate cell activation (**Figure 5D**). Genes highly induced in livers of GG mice included various collagens and genes involved in regulation of extracellular matrix turnover (*Timp2*) and TGF β signaling (*Tgfb1*). Elevated expression of fibrosis-related genes was corroborated by qPCR (**Figure 5E**). Finally, TIMP1 protein levels

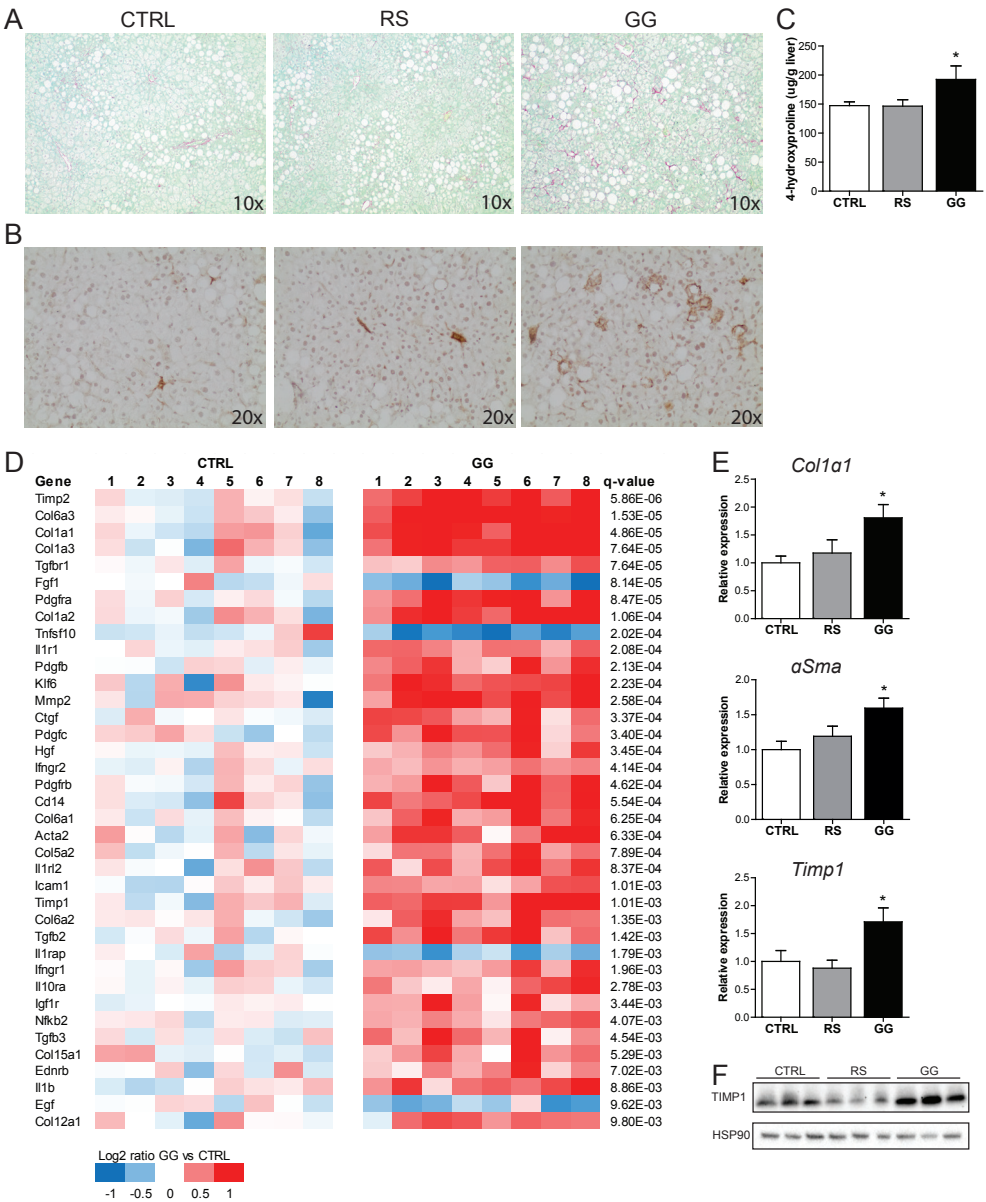


Figure 5. Stimulation of the gut microbiota by guar gum is associated with enhanced hepatic fibrogenesis Representative pictures of liver sections stained for (A) collagen using fast green FCF/Sirius Red F3B and (B) hepatic stellate cell activation using an antibody against alpha smooth muscle actin (α SMA). (C) 4-hydroxyproline content in the liver. (D) Heat map showing significant changes in expression of genes involved in hepatic fibrosis / hepatic stellate cell activation in the livers of CTRL and GG mice. The Log2 expression signals of the CTRL group were arbitrarily set at 0. (E) Relative expression of fibrosis-related genes in the liver. Gene expression levels in CTRL mice were set at 1. Data are presented as mean \pm SEM. Asterisks indicate significantly different compared with CTRL. * $p < 0.05$. (F) TIMP1 protein expression measured by western blotting. HSP90 was used as loading control.

were elevated in livers of the GG mice (**Figure 5F**). These data indicate that feeding GG not only increased hepatic inflammation but also promoted more advanced features of NASH i.e. liver fibrosis.

Modulation of the gut microbiota by guar gum is associated with altered levels of gut-derived metabolites

To explore the possible mechanisms linking changes in gut microbiota composition to the observed liver pathology, we focused our attention on several microbial compounds that

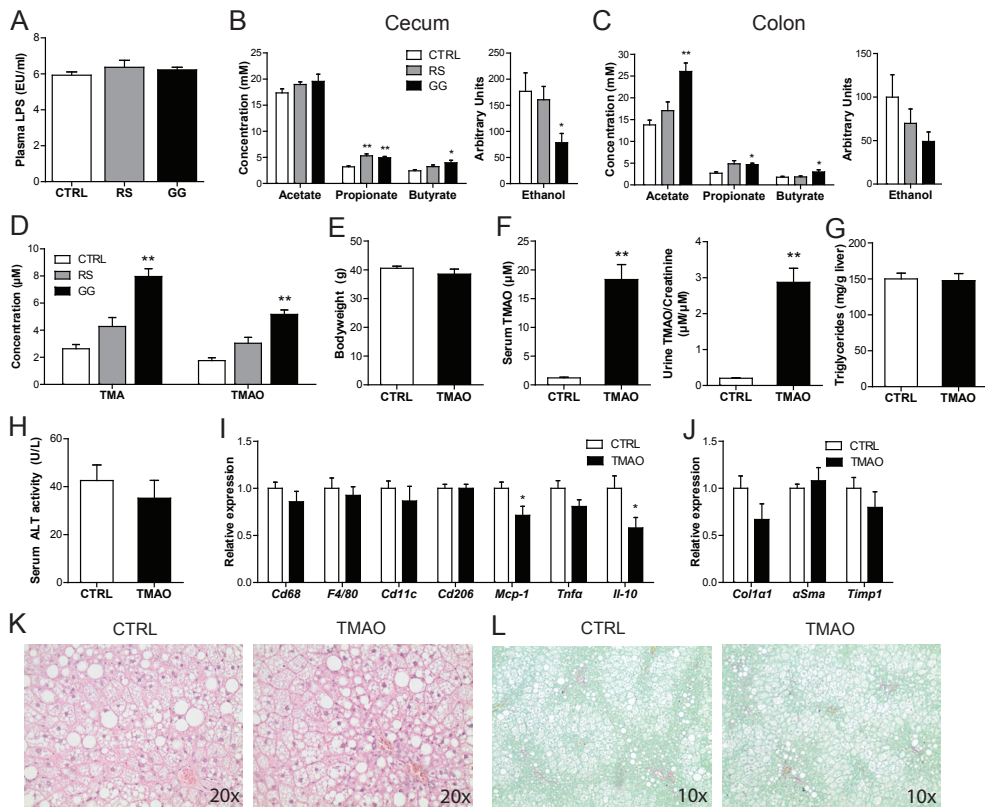


Figure 6. Guar gum-induced elevation of TMAO does not contribute to enhanced NALFD development (A) Plasma LPS levels. (B) Cecal and (C) colonic SCFA concentration and ethanol abundance. (D) Plasma TMA and TMAO levels. Mice were fed the HFCFD for 18 weeks with or without supplementation with TMAO. (E) Final bodyweight of mice fed CTRL or TMAO-enriched diet for 18 weeks. (F) Serum and urinary TMAO levels. Urinary TMAO levels are corrected for creatinine levels to adjust for urinary dilution (G) Quantitative analysis of liver triglyceride levels. (H) Activity of alanine aminotransferase (ALT) in serum. Relative expression of (I) inflammation and (J) fibrosis-related genes in the liver. Gene expression levels in CTRL mice were set at 1. Data are presented as mean \pm SEM. Asterisks indicate significantly different compared with CTRL. * $p < 0.05$, ** $p < 0.001$. (K) H&E staining of representative liver sections. (L) Representative pictures of liver sections stained for collagen using fast green FCF/Sirius Red F3B.

have been proposed to mediate the effects of the gut bacteria on host metabolism, including the pro-inflammatory LPS and ethanol, and the anti-inflammatory short-chain fatty acids (SCFA) (44). Plasma levels of LPS were comparable between the GG mice and CTRL mice (**Figure 6A**), while ethanol levels in cecum and colon were decreased in the GG group (**Figure 6B-C**). With respect to the SCFA, in the cecum, the concentration of propionate was increased in both dietary fiber groups, whereas the butyrate concentration was only elevated in the GG group (**Figure 6B**). In the colon, GG but not RS significantly elevated acetate, propionate and butyrate concentrations as compared to CTRL (**Figure 6C**). In short, the observed changes in NAFLD phenotype in the GG mice are unlikely to be mediated by LPS, ethanol, or SCFAs.

Interestingly, plasma levels of the gut-derived metabolites trimethylamine (TMA)—a product of microbial conversion of choline—and trimethylamine N-oxide (TMAO), which is synthesized from TMA in the liver, were both significantly increased by GG, while RS had no effect (**Figure 6D**). Previously, TMAO was causally implicated in atherosclerosis and kidney fibrosis (9, 45, 46).

Accordingly, to investigate if the elevated plasma TMAO levels may contribute to the NAFLD phenotype, mice were fed the HFCFD diet with or without 0.2% TMAO (w/w) for 18 weeks. 18 weeks of TMAO feeding did not affect final bodyweight (**Figure 6E**). Although serum and urinary TMAO levels were about 15-fold higher in the mice fed the TMAO-enriched diet (**Figure 6F**), provision of TMAO did not affect hepatic steatosis, inflammation, or fibrosis, as indicated by measurement of liver triglycerides (**Figure 6G**), serum alanine aminotransferase activity (**Figure 6H**), the expression of inflammation and fibrosis-related genes (**Figure 6I-J**), H&E staining (**Figure 6K**), and Sirius Red stainings (**Figure 6L**).

Bile acids are also potential candidates for linking changes in gut bacteria to NAFLD. Strikingly, total plasma bile acid levels were nearly 4-fold higher in the GG than the CTRL mice, whereas they were not different in the RS mice (**Figure 7A**). Specifically, plasma levels of various primary bile acids including cholic acid, taurocholic acid, muricholic acids and taumuricholic acids, as well as the secondary bile acids deoxycholic acid, taurodeoxycholic acid, ursodeoxycholic acid, hyodeoxycholic acid and taurohyodeoxycholic acid were significantly higher in the GG mice as compared with CTRL mice (**Figure 7A**). Moreover, total bile acid levels in the liver were also increased in the GG mice as compared with the CTRL mice (**Figure 7B**). The higher plasma and hepatic bile acid levels were accompanied by elevated hepatic expression of the FXR target *Slc51b* and a compensatory downregulation of *Cyp7a1* and *Cyp8b1*, enzymes involved in bile acid synthesis, and *Ntcp* (*Slc10a1*), a bile salt importer (**Figure 7C**). No change was observed in the expression of the bile acid exporter *Bsep* (*Abcb11*) (**Figure 7C**). Interestingly, levels of bile acids in the feces were significantly

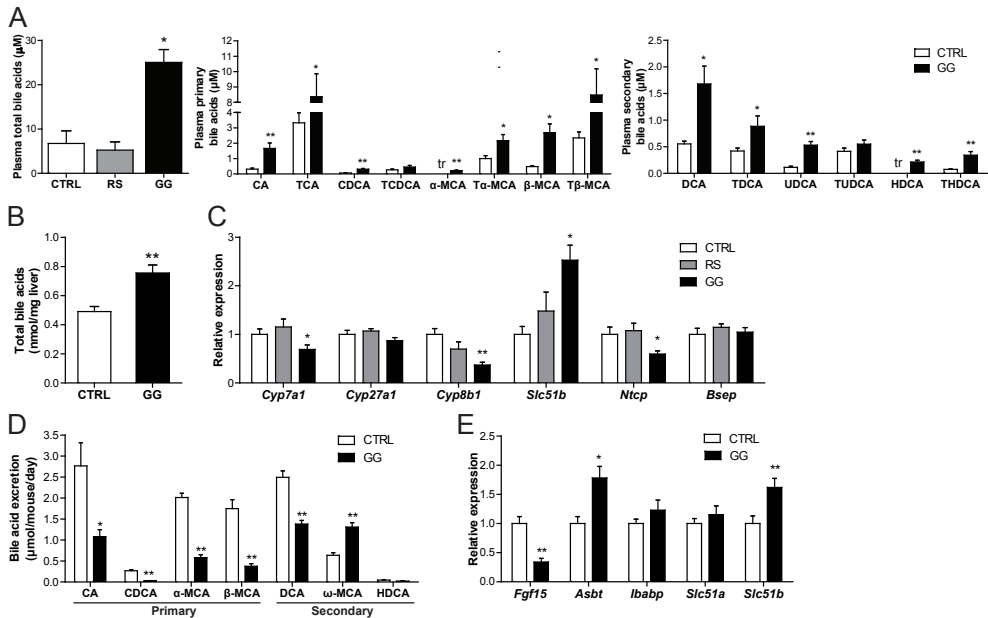


Figure 7. Guar gum elevates plasma bile acid levels likely by promoting bile acid reabsorption

(A) Total bile acid concentration in plasma of CTRL, RS and GG mice and concentration of free and conjugated primary and secondary bile acid subspecies in the plasma of CTRL and GG mice. (B) Total bile acid content in the liver of CTRL and GG mice. (C) Relative expression of genes encoding enzymes of bile acid synthesis and bile acid transporters. Gene expression levels in CTRL mice were set at 1. (D) Mean excretion of free and conjugated bile acid subspecies per mouse per day in the CTRL and GG group at the end of the dietary intervention. (E) Relative expression of *Fgf15* and bile acid transporters in the ileum. Gene expression levels in CTRL mice were set at 1. Data are presented as mean ± SEM. Asterisks indicate significantly different compared with CTRL. * $p < 0.05$, ** $p < 0.001$.

lower in the GG mice (Figure 7D), concomitant with reduced ileal expression of *Fgf15* and elevated expression of the ileal bile acid transporter *Asbt* (*Slc10a2*) and *Slc51b* (Figure 7E). Together, these data suggest that GG enhanced bile acid absorption, leading to higher bile acid levels in the plasma and elevated bile acid content in the liver, which in turn triggered compensatory changes in the expression of genes involved in hepatic bile acid synthesis and uptake.

To examine if the elevated plasma levels of bile acids may contribute to hepatic inflammation and fibrosis, we gave mice the bile acid taurocholic acid for 7 days by mixing it in their feed (0.5% (wt/wt)). Provision of taurocholic acid raised plasma taurocholic acid levels by 40-fold as compared to CTRL (Figure 8A). In addition, taurocholic acid also significantly increased the primary bile acids cholic acid, glycocholic acid, chenodeoxycholic acid, taurochenodeoxycholic acid and unconjugated muricholic acids, as well as the secondary bile acids deoxycholic acid, taurodeoxycholic acid, glycodeoxycholic acid, ursodeoxycholic

acid and ω -muricholic acid (**Figure 8A**). The higher plasma bile acid levels were associated with compensatory downregulation of *Cyp7a1*, *Cyp27a1*, *Cyp8b1* and *Ntcp* and upregulation of *Slc51b* in liver (**Figure 8B**). Importantly, provision of taurocholic acid markedly increased plasma alanine aminotransferase activity (**Figure 8C**), upregulated the expression of inflammatory genes (**Figure 8D**), and stimulated leukocyte infiltration (**Figure 8E**). Moreover, taurocholic acid promoted hepatic fibrosis as revealed by elevated expression of the fibrosis markers collagen type I alpha 1 and *Timp1* (**Figure 8F**), and enhanced collagen

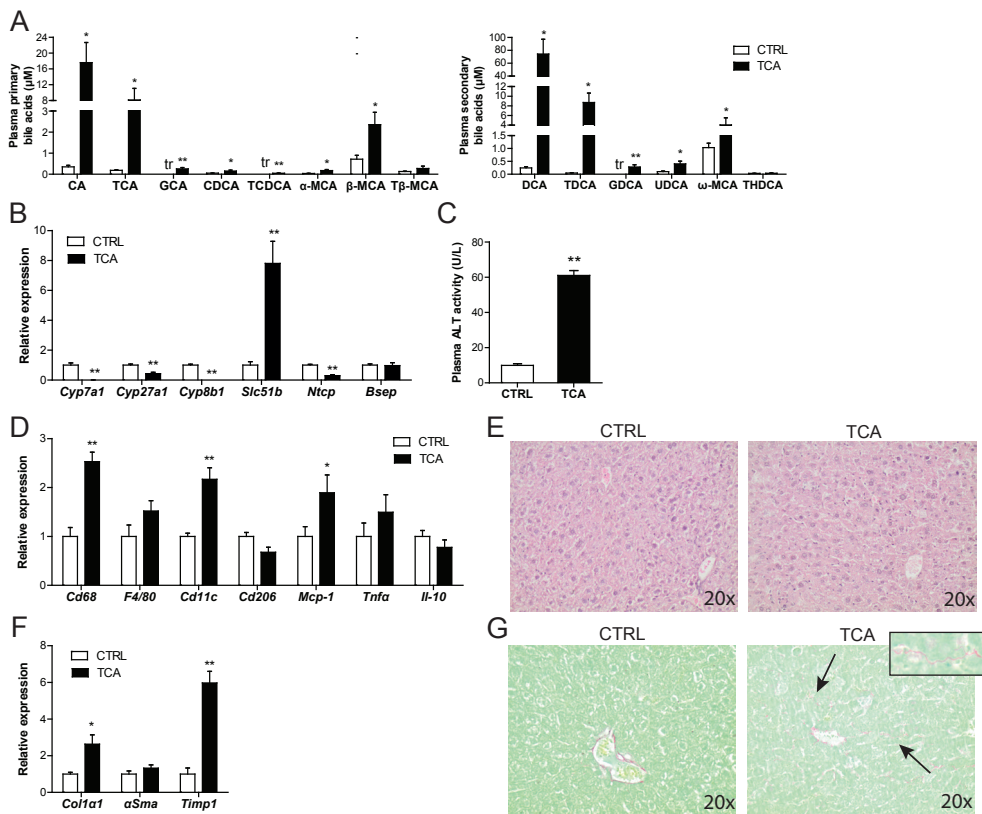


Figure 8. Bile acids promote hepatic injury

(A) Concentration of free and conjugated bile acid subspecies in the plasma of CTRL and taurocholic acid-fed mice. Tr indicates that only trace levels of this bile acid could be measured. (B) Relative expression of genes encoding enzymes of bile acid synthesis and bile acid transporters. Gene expression levels in CTRL mice were set at 1. (C) Activity of alanine aminotransferase (ALT) in plasma. (D) Relative expression of inflammation-related genes in the liver. Gene expression levels in CTRL mice were set at 1. (E) H&E staining of representative liver sections. (F) Relative expression of fibrosis-related genes in the liver. Gene expression levels in CTRL mice were set at 1. (G) Representative pictures of liver sections stained for collagen using fast green FCF/Sirius Red F3B. Inset is a higher magnification of the collagen deposition as observed in the livers of the taurocholic acid-fed mice. Data are presented as mean \pm SEM. Asterisks indicate significantly different compared with CTRL. * $p < 0.05$, ** $p \leq 0.001$.

deposition (**Figure 8G**). Analysis of a publicly available transcriptomics dataset (GSE34730) of livers of mice treated with cholic acid or deoxycholic acid for 2 weeks confirmed the marked stimulatory effect of oral administration of bile acids on genes implicated in hepatic inflammation and fibrosis. Specifically, Ingenuity pathway analysis showed the significant induction of numerous pathways related to immune cells and cytokines signaling, including IL-8 signaling and acute phase response signaling, as well as hepatic fibrosis/hepatic stellate activation. These effects were similarly observed in conventionalized and germ-free mice, indicating that the effects of oral cholic and deoxycholic acid on liver inflammation and fibrosis are not dependent on bacterial conversion (**Supplemental Figure 2**). Together, these data suggest that elevated plasma levels of bile acids can lead to hepatic inflammation and fibrosis in mice fed GG.

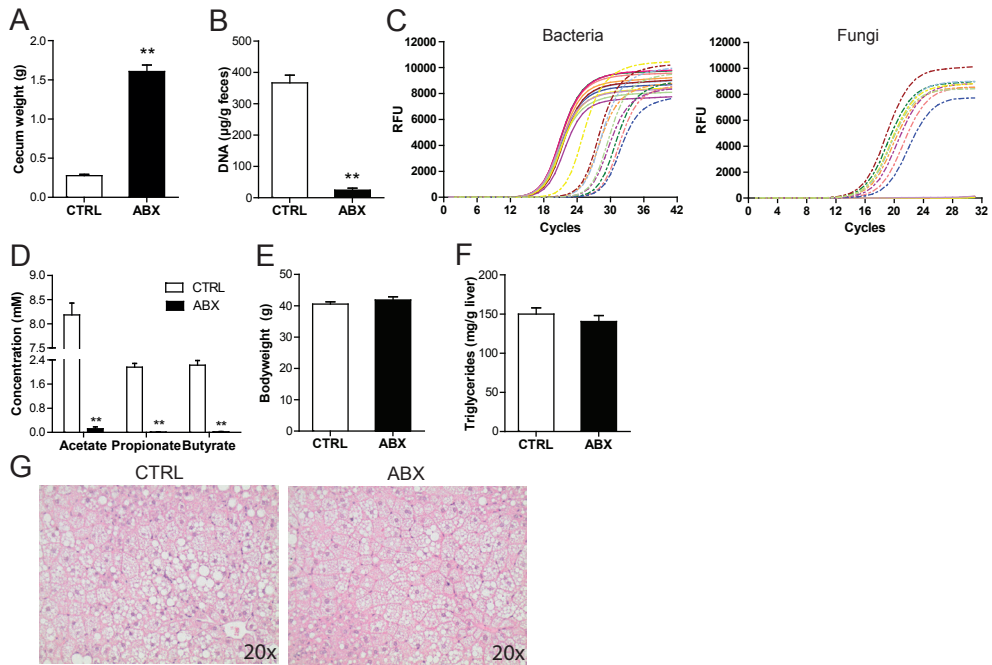


Figure 9. Suppression of the gut bacteria using antibiotics does not affect hepatic steatosis

(A) Weight of the cecum. (B) Quantitative analysis of fecal DNA levels. (C) qPCR amplification plot for 16S rRNA gene and fungal ITS1-5.8S-ITS2 region in equal amounts of fecal DNA. Solid lines indicate CTRL mice and dashed lines indicate ABX mice. (D) Cecal SCFA concentration. (E) Final bodyweight of mice fed CTRL diet with or without antibiotics supplementation. (F) Quantitative analysis of liver triglyceride levels. (G) H&E staining of representative liver sections. Data are presented as mean \pm SEM. Asterisks indicate significantly different compared with CTRL. ** $p \leq 0.001$.

Suppression of the gut bacteria by oral antibiotics attenuates NAFLD development

In order to study the direct impact of the gut microbiota on features of NAFLD, mice fed the HFCFD diet were given antibiotics via the drinking water for the entire duration of the dietary intervention. Oral administration of antibiotics led to a large increase in the weight of the cecum (**Figure 9A**), and caused a massive decrease in fecal DNA levels (**Figure 9B**) and levels of the 16S rRNA gene (**Figure 9C**). In addition, antibiotics dramatically reduced SCFA levels in the cecum (**Figure 9D**), demonstrating the effective suppression of the bacteria in the colon. Interestingly, antibiotics triggered an outgrowth of fungi (**Figure 9C**). At the end of the dietary intervention, final bodyweights were similar between the antibiotic-treated and control mice (**Figure 9E**). Antibiotics treatment did not affect hepatic steatosis development, as indicated by quantitative measurement of liver triglycerides (**Figure 9F**) and H&E staining (**Figure 9G**).

Strikingly, oral antibiotic caused a marked decrease in serum ALT activity (**Figure 10A**), as well as a decrease in the expression of inflammatory markers in the liver (**Figure 10B**). In addition, antibiotics treatment reduced hepatic fibrosis as indicated by markedly lower expression of the fibrosis markers collagen type I alpha 1, α SMA and *Timp1* (**Figure 10C**), and less collagen deposition (**Figure 10D**). While LPS levels in portal blood were not different between control and antibiotic-treated mice (**Figure 10E**), antibiotics treatment led to a non-significant reduction in the portal concentration of primary bile acids and a highly significant 10-fold reduction in the concentration of secondary bile acids (**Figure 10F**), hinting at a potential role of bile acids in the attenuation of features of NAFLD in the livers of the antibiotic-treated mice. Specifically, in the portal blood the primary bile acids cholic acid, chenodeoxycholic acid and muricholic acids and almost all secondary bile acids were reduced upon antibiotics treatment (**Figure 10G**). The reduction in portal delivery of bile acids was accompanied by a significant reduction in hepatic expression of the FXR target *Slc51b* and a compensatory induction of genes involved in bile acids synthesis, including *Cyp7a1*, *Cyp27a1*, and *Cyp8b1*, as well as the bile acid importer *Ntcp* and exporter *Bsep* (**Figure 10H**). Surprisingly, total hepatic bile acid levels were increased in the antibiotic-treated mice (**Figure 10I**). As expected, treatment with antibiotics caused a marked reduction in fecal excretion of secondary bile acid levels, whereas excretion of primary bile acids remained unchanged (**Figure 10J**). Together, these data indicate that suppression of the gut bacteria attenuates features of NAFLD, possibly via reduced portal delivery of bile acids.

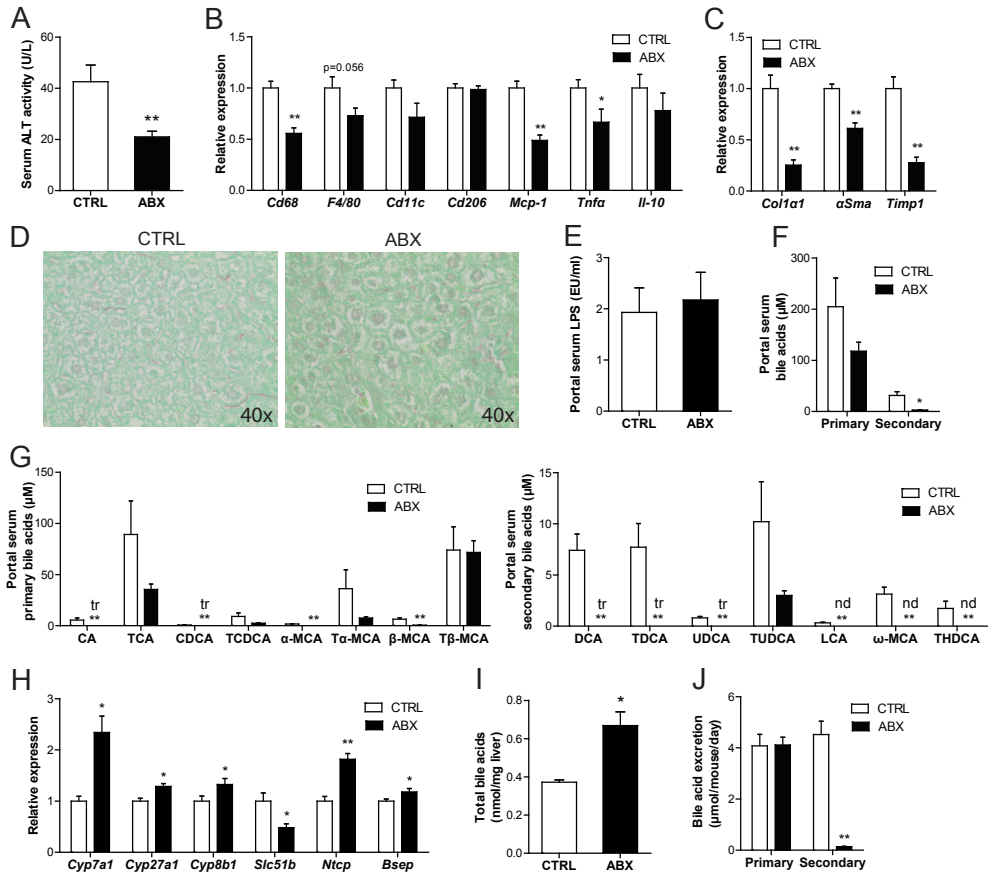


Figure 10. Antibiotics attenuate hepatic inflammation and fibrosis

(A) Activity of alanine aminotransferase (ALT) in serum. Relative expression of (B) inflammatory and (C) fibrosis-related genes in the liver. Gene expression levels in CTRL mice were set at 1. (D) Representative pictures of liver sections stained for collagen using fast green FCF/Sirius Red F3B. (E) Portal serum lipopolysaccharide levels. (F) Concentration of primary and secondary bile acids in portal serum. (G) Concentration of free and conjugated primary and secondary bile acid subspecies in the portal serum of CTRL and GG mice. Tr indicates that only trace levels of this bile acid could be measured. Nd indicates that levels of this bile acid were below detectable limit. (H) Relative expression of genes encoding enzymes of bile acid synthesis, the FXR target gene *Slc51b* and hepatic bile acid transporters. Gene expression levels in CTRL mice were set at 1. (I) Total bile acid content in the liver. (J) Mean excretion of primary and secondary bile acids per mouse per day in the CTRL and ABX group at the end of the dietary intervention. Data are presented as mean ± SEM. Asterisks indicate significantly different compared with CTRL. * $p < 0.05$, ** $p \leq 0.001$.

Discussion

Emerging evidence points to an association between the gut microbiota and NAFLD (47). However, data on an actual causal role of the gut microbiota in NAFLD are very scarce. Here we found that stimulation of the gut microbiota using guar gum promoted liver inflammation and fibrosis. Inasmuch as guar gum is a pre-biotic non-digestible carbohydrate and is thus expected to act exclusively via its fermentation by the gut bacteria, our results suggest a direct impact of the gut microbiota on the pathogenesis of NAFLD. By contrast, suppression of the gut bacteria using oral antibiotics attenuated liver inflammation and fibrosis. The effects of microbial modulation by guar gum could be linked to altered circulating and hepatic levels of bile acids, which were shown to induce features of hepatic inflammation and fibrosis. Our data thus suggest that the gut bacteria may be able to influence NAFLD via bile acids.

It should be noted that the stimulation of hepatic inflammation and fibrosis by guar gum was unrelated to obesity—an important causal factor of NAFLD—as guar gum suppressed diet-induced weight gain and concomitant glucose intolerance and adipose tissue inflammation. In contrast to guar gum, resistant starch did not have any impact on NAFLD, probably due to the minor effect of resistant starch on gut microbial composition and levels of fermentation products (48).

Ideally, feeding guar gum should be combined with the use of antibiotics, thereby allowing direct investigation of the role of the gut microbiota in the effects of guar gum. However, in our experience it is impossible to combine the use of antibiotics with feeding a diet enriched in dietary fiber. Specifically, we found that giving mice antibiotics while on a high fiber diet quickly led to an intestinal blockage and massive weight loss, forcing us to end the experiment prematurely. This observation underscores that dietary fiber cannot be properly processed in the absence of a well-functioning gut microbiota.

Several mechanisms have been proposed to explain the link between the gut microbiota and host metabolism. These mechanisms mainly revolve around specific microbial metabolites or compounds, including lipopolysaccharide, SCFA, TMA, ethanol and bile acids, the latter of which are extensively metabolized by the gut microbiota. TMA has been linked to NAFLD by reflecting the microbial conversion and depletion of choline (49). We found significantly higher plasma TMA levels in mice fed GG. Upon absorption, TMA is rapidly oxidized in the liver to TMAO by flavin monooxygenases. Gao *et al.* showed that dietary TMAO increases adipose tissue mRNA levels and serum levels of MCP-1 in mice (50). In addition, TMAO has also been shown to exacerbate atherosclerosis development in mice and is positively linked to cardiovascular disease risk in humans. Importantly, suppression of the gut microbiota using antibiotics lowered plasma TMAO levels and reduced atherosclerosis (9, 45). Furthermore, TMAO was also recently implicated in kidney fibrosis

(46). In our study, however, elevated plasma TMAO levels did not seem to be responsible for the aggravation of NALFD in mice fed guar gum, as feeding mice TMAO for 18 weeks had no effect on any indicators of NALFD or fibrosis, despite markedly elevating circulating and urinary TMAO levels.

In addition to TMA and TMAO, plasma total bile acids were elevated in the GG but not RS mice. The parallel reduction in fecal bile acids suggests that bile acids are more efficiently absorbed in the mice fed guar gum. The increase in plasma bile acid levels was accompanied by elevated hepatic bile acid content and worsening of NAFLD and fibrosis. To investigate if bile acids could be causally involved in the progression of NAFLD upon guar gum feeding, mice were fed chow supplemented with taurocholic acid. Taurocholic acid feeding increased plasma levels of a range of different bile acids, which was associated with activation of specific features of NAFLD. These data suggest that elevated plasma and hepatic bile acids are a plausible mechanistic link between changes in gut microbial composition in mice fed guar gum and worsening of NAFLD. Consistent with this hypothesis, hepatic bile acid levels were found to be elevated in humans with steatohepatitis (51). Furthermore, NAFLD was found to be associated with intestinal dysbiosis and altered fecal bile acid levels in human subjects (52).

One type of bile acid that may be particularly involved in promoting liver injury and NAFLD is deoxycholic acid, levels of which were increased by 4.2-fold in the plasma of mice fed guar gum. Recently, Yoshimoto *et al.* (53) linked increased deoxycholic acid levels upon high-fat feeding to the development of NAFLD-related hepatocellular carcinomas. Suppression of the microbiota by antibiotics lowered serum deoxycholic acid levels and mitigated hepatocellular carcinoma development, suggesting that microbial production of deoxycholic acid may have detrimental effects on the liver. The mechanism by which bile acids may promote liver injury and hepatic inflammation and fibrosis may involve enhanced leakage of tight junctions of bile duct epithelial cells causing cholangitis, as well as the activation and proliferation of periductal myofibroblasts leading to periductal fibrosis (54). Furthermore, it is well established that elevated intrahepatic bile acid levels trigger hepatocyte apoptosis, possibly leading to NASH (55–57). Future studies should address the cellular mechanism(s) by which microbiota-dependent changes in portal and hepatic bile acids may influence NAFLD.

The increase in liver bile acid content in the mice treated with antibiotics may be taken as evidence that bile acids cannot be responsible for the reduced liver injury, inflammation and fibrosis in these mice. However, it is likely that the increase in liver bile acid content reflects increased bile acid synthesis, as opposed to increased portal delivery of bile acids, which in fact was substantially decreased. It is conceivable that the newly synthesized bile acids are immediately secreted and are primarily located in the bile ducts, where they may

not inflict liver injury. By contrast, the reduction in portal delivery of bile acids may lead to lower uptake of bile acids by hepatocytes, and thereby attenuate liver injury, inflammation and fibrosis.

Our results are consistent with previous studies showing that modulation of the gut microbiota influences bile acid levels and metabolism (58–60). These studies have pointed to intestinal FXR signaling and resultant changes in FGF15 and ceramides as potential intermediate between microbiota-induced changes in bile acids on the one hand, and liver triglycerides and bile acid synthesis on the other hand. Although our data are not inconsistent with a role of intestinal FXR signaling, FGF15, and ceramides, our study highlights the potential role of bile acids as causal factor in linking changes in the gut bacteria to altered liver inflammation and fibrosis.

It should be noted that in contrast to previous data (61–63), we did not find any evidence that the protective effect of antibiotics on the development of NAFLD might be mediated by LPS, as portal LPS levels were not altered upon antibiotic-treatment.

In our study, specific gut microbial taxa could be linked to the transition from simple steatosis to NASH and fibrosis. The higher relative abundance of the genera *Bifidobacterium* and *Prevotella*, and of the species *Desulfovibrio C21_c20* and *Akkermansia muciniphila* as observed in the colonic luminal content of the GG mice, have not been observed in other mouse studies linking specific gut microbial taxa to the progression of NAFLD. However, these studies used either bile duct ligation (18, 64), a methionine choline-deficient diet (65) or carbon-tetrachloride injections (64) to induce liver injury. Bacteria within the genera *Lactobacillus*, *Bifidobacterium* and *Streptococcus* have been demonstrated to suppress hepatic inflammation in mice and humans (66, 67). In addition to dampening hepatic inflammation, *Lactobacillus* and *Bifidobacterium* have also been shown to reduce hepatic fibrosis (68). Furthermore, *Bifidobacteria* are known to be able to ferment guar gum (69, 70) and possess active bile salt hydrolases (71). Since unconjugated bile acids are less efficient in the solubilization and absorption of intestinal lipids (71), one possible scenario is that by increasing bile salt hydrolase activity and unconjugated bile acids, the increase in *Bifidobacterium* may be responsible for the elevated fecal lipid excretion.

Guar gum is composed of galactose and mannose residues and is extracted from the seeds of guar beans. It is mainly used as a thickening agent in several food products including ice creams, sauces and cheese spreads (72). Although we show that dietary guar gum promotes the progression of NAFLD, caution should be exercised in extrapolating these data to the human situation because, 1) the dose of guar gum used substantially exceeds the amounts ingested by humans, 2) the microbiota composition is vastly different between mice and humans. In our study, we used guar gum as a model compound to study the effect of modulating the gut microbiota composition on NAFLD.

In conclusion, we find that stimulation of the gut bacteria by guar gum leads to deleterious effects on hepatic inflammation and fibrosis in a mouse model of NAFLD, whereas suppression of the gut bacteria by antibiotics attenuates NAFLD. Overall, we provide evidence of a causal link between disturbances in gut bacteria, bile acids, and NAFLD.

Acknowledgements

We thank Dr. A.H. Mulder (Rijnstate Hospital, the Netherlands) for excellent advice with histopathological analysis and Martijn Koehorst for the bile acid measurements. This research was supported by The Netherlands Cardiovascular Research Committee IN-CONTROL grant (CVON 2012-03) and the Rembrandt Institute for Cardiovascular Research 2012. TMA and TMAO analyses were supported by grants from the National Institutes of Health and the Office of Dietary Supplements (HL103866, HL122283, and AA024333). LPS measurement was supported by the Institut National de la Santé et de la Recherche Médicale (INSERM, Centre de Recherches U1231), and the French Government Grant managed by the French National Research Agency under the program “Investissements d’Avenir” ANR-11-LABX-0021. We are grateful to Dr Jean-Paul Pais de Barros and Hélène Choubley (Plateforme de Lipidomique, INSERM UMR1231, LabEx LipSTIC/Endoquant, Dijon, France) for their technical expertise in LPS quantification.

References

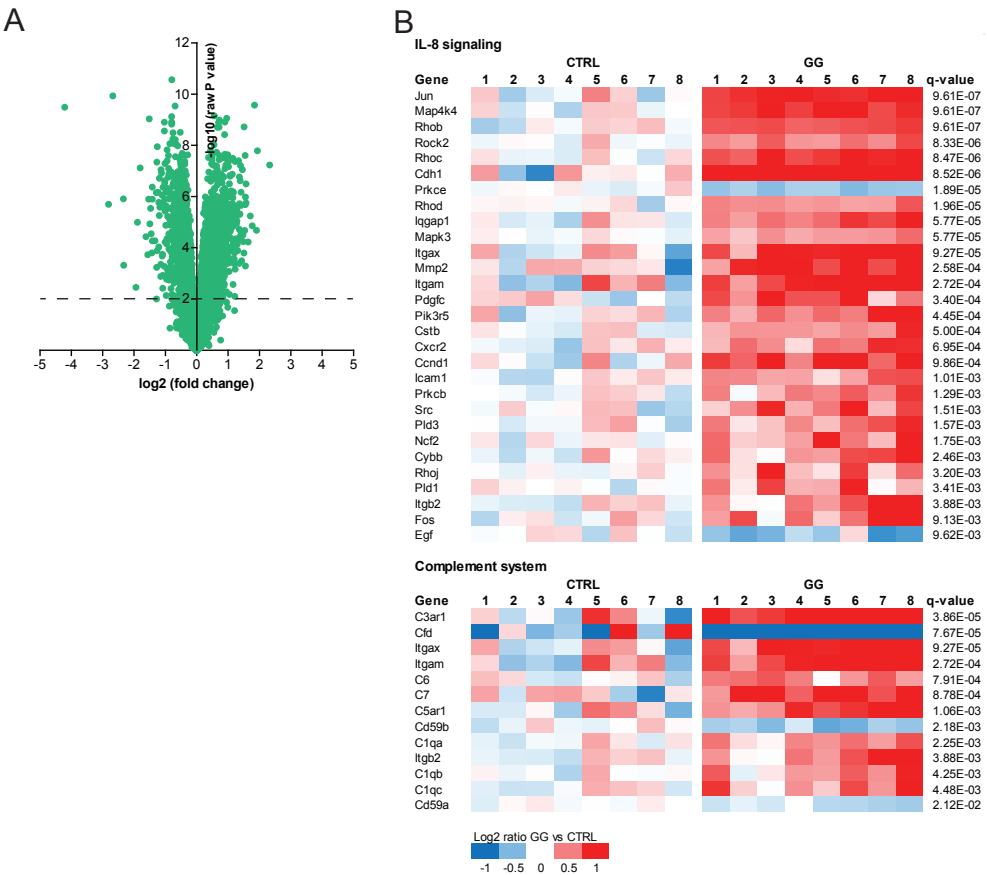
1. Finucane, M. M., G. A. Stevens, M. J. Cowan, G. Danaei, J. K. Lin, C. J. Paciorek, G. M. Singh, H. R. Gutierrez, Y. Lu, A. N. Bahalim, F. Farzadfar, L. M. Riley, and M. Ezzati. 2011. National, regional, and global trends in body-mass index since 1980: Systematic analysis of health examination surveys and epidemiological studies with 960 country-years and 9.1 million participants. *Lancet*. **377**: 557–567.
2. Ridaura, V. K., J. J. Faith, F. E. Rey, J. Cheng, A. E. Duncan, A. L. Kau, N. W. Griffin, V. Lombard, B. Henrissat, J. R. Bain, M. J. Muehlbauer, O. Ilkayeva, C. F. Semenkovich, K. Funai, D. K. Hayashi, B. J. Lyle, M. C. Martini, L. K. Ursell, J. C. Clemente, W. Van Treuren, W. a Walters, R. Knight, C. B. Newgard, A. C. Heath, and J. I. Gordon. 2013. Gut microbiota from twins discordant for obesity modulate metabolism in mice. *Science*. **341**: 1241214.
3. Vrieze, A., E. Van Nood, F. Holleman, J. Salojärvi, R. S. Kootte, J. F. W. M. Bartelsman, G. M. Dallinga-Thie, M. T. Ackermans, M. J. Serlie, R. Oozeer, M. Derrien, A. Druesne, J. E. T. Van Hylckama Vlieg, V. W. Bloks, A. K. Groen, H. G. H. J. Heilig, E. G. Zoetendal, E. S. Stroes, W. M. de Vos, J. B. L. Hoekstra, and M. Nieuwdorp. 2012. Transfer of intestinal microbiota from lean donors increases insulin sensitivity in individuals with metabolic syndrome. *Gastroenterology*. **143**: 913–6.
4. Lam, Y. Y., C. W. Y. Ha, C. R. Campbell, A. J. Mitchell, A. J. Dinudom, J. Oscarsson, D. I. Cook, N. H. Hunt, I. D. Caterson, A. J. Holmes, and L. H. Storlien. 2012. Increased gut permeability and microbiota change associate with mesenteric fat inflammation and metabolic dysfunction in diet-induced obese mice. *PLoS One*. **7**: e34233.
5. Janssen, A. W. F., and S. Kersten. 2015. The role of the gut microbiota in metabolic health. *FASEB J*. **29**: 3111–3123.
6. Sommer, F., and F. Bäckhed. 2013. The gut microbiota--masters of host development and physiology. *Nat. Rev. Microbiol.* **11**: 227–38.
7. Clemente, J. C., L. K. Ursell, L. W. Parfrey, and R. Knight. 2012. The impact of the gut microbiota on human health: An integrative view. *Cell*. **148**: 1258–1270.
8. Biedermann, L., and G. Rogler. 2015. The intestinal microbiota: its role in health and disease. *Eur. J. Pediatr.* **174**: 151–167.
9. Wang, Z., E. Klipfell, B. J. Bennett, R. Koeth, B. S. Levison, B. Dugar, A. E. Feldstein, E. B. Britt, X. Fu, Y.-M. Chung, Y. Wu, P. Schauer, J. D. Smith, H. Allayee, W. H. W. Tang, J. a DiDonato, A. J. Lusis, and S. L. Hazen. 2011. Gut flora metabolism of phosphatidylcholine promotes cardiovascular disease. *Nature*. **472**: 57–63.
10. Janssen, A. W. F., and S. Kersten. 2017. Potential mediators linking gut bacteria to metabolic health: a critical view. *J. Physiol.* **595**: 477–487.
11. Schuppan, D., and J. M. Schattenberg. 2013. Non-alcoholic steatohepatitis: pathogenesis and novel therapeutic approaches. *J. Gastroenterol. Hepatol.* **28 Suppl 1**: 68–76.
12. Tilg, H., and A. R. Moschen. 2010. Evolution of inflammation in nonalcoholic fatty liver disease: The multiple parallel hits hypothesis. *Hepatology*. **52**: 1836–1846.
13. Nassir, F., and J. Ibdah. 2014. Role of mitochondria in nonalcoholic fatty liver disease. *Int. J. Mol. Sci.* **15**: 8713–8742.
14. Jiang, W., N. Wu, X. Wang, Y. Chi, Y. Zhang, X. Qiu, Y. Hu, J. Li, and Y. Liu. 2015. Dysbiosis gut microbiota associated with inflammation and impaired mucosal immune function in intestine of humans with non-alcoholic fatty liver disease. *Sci. Rep.* **5**: 1–7.
15. Mouzaki, M., E. M. Comelli, B. M. Arendt, J. Bonengel, S. K. Fung, S. E. Fischer, I. D. McGilvray, and J. P. Allard. 2013. Intestinal microbiota in patients with nonalcoholic fatty liver disease. *Hepatology*. **58**: 120–127.
16. Jiang, C., C. Xie, F. Li, L. Zhang, R. G. Nichols, K. W. Krausz, J. Cai, Y. Qi, Z. Fang, S. Takahashi, N. Tanaka, D. Desai, S. G. Amin, I. Albert, A. D. Patterson, and F. J. Gonzalez. 2015. Intestinal farnesoid X receptor signaling promotes nonalcoholic fatty liver disease. *J. Clin. Invest.* **125**: 386–402.
17. Henao-Mejia, J., E. Elinav, C. Jin, L. Hao, W. Z. Mehal, T. Strowig, C. a Thaiss, A. L. Kau, S. C. Eisenbarth, M. J. Jurczak, J.-P. Camporez, G. I. Shulman, J. I. Gordon, H. M. Hoffman, and R. a Flavell. 2012. Inflammasome-mediated dysbiosis regulates progression of NAFLD and obesity. *Nature*. **482**: 179–85.
18. De Minicis, S., C. Rychlicki, L. Agostinelli, S. Saccomanno, C. Candelaresi, L. Trozzi, E. Mingarelli, B. Facinelli, G. Magi, C. Palmieri, M. Marziani, A. Benedetti, and G. Svegliati-Baroni. 2014. Dysbiosis contributes to fibrogenesis in the course of chronic liver injury in mice. *Hepatology*. **59**: 1738–1749.
19. Nomura, K., and T. Yamanouchi. 2012. The role of fructose-enriched diets in mechanisms of nonalcoholic fatty liver disease. *J. Nutr. Biochem.* **23**: 203–8.
20. Song, P., Y. Zhang, and C. D. Klaassen. 2011. Dose-response of five bile acids on serum and liver bile acid concentrations and hepatotoxicity in mice. *Toxicol. Sci.* **123**: 359–367.
21. Rakoff-Nahoum, S., J. Paglino, F. Eslami-Varzaneh, S. Edberg, and R. Medzhitov. 2004. Recognition of

- commensal microflora by toll-like receptors is required for intestinal homeostasis. *Cell*. **118**: 229–241.
22. Bieghs, V., K. Wouters, P. J. van Gorp, M. J. J. Gijbels, M. P. J. de Winther, C. J. Binder, D. Lütjohann, M. Febbraio, K. J. Moore, M. van Bilsen, M. H. Hofker, and R. Shiri-Sverdlov. 2010. Role of Scavenger Receptor A and CD36 in Diet-Induced Nonalcoholic Steatohepatitis in Hyperlipidemic Mice. *Gastroenterology*. **138**: 2477–2486.
 23. Nagy, R. A., A. P. A. van Montfoort, A. Dikkers, J. van Echten-Arends, I. Homminga, J. A. Land, A. Hoek, and U. J. F. Tietge. 2015. Presence of bile acids in human follicular fluid and their relation with embryo development in modified natural cycle IVF. *Hum. Reprod.* **30**: 1102–1109.
 24. Wang, Z., B. S. Levison, J. E. Hazen, L. Donahue, X. M. Li, and S. L. Hazen. 2014. Measurement of trimethylamine-N-oxide by stable isotope dilution liquid chromatography tandem mass spectrometry. *Anal. Biochem.* **455**: 35–40.
 25. Koeth, R. A., B. S. Levison, M. K. Culley, J. A. Buffa, Z. Wang, J. C. Gregory, E. Org, Y. Wu, L. Li, J. D. Smith, W. H. W. Tang, J. A. DiDonato, A. J. Lusis, and S. L. Hazen. 2014. γ -Butyrobetaine Is a Proatherogenic Intermediate in Gut Microbial Metabolism of L-Carnitine to TMAO. *Cell Metab.* **20**: 799–812.
 26. Govers, M. J., and R. Van der Meet. 1993. Effects of dietary calcium and phosphate on the intestinal interactions between calcium, phosphate, fatty acids, and bile acids. *Gut*. **34**: 365–370.
 27. van Meer, H., G. Boehm, F. Stellaard, A. Vriesema, J. Knol, R. Havinga, P. J. Sauer, and H. J. Verkade. 2008. Prebiotic oligosaccharides and the enterohepatic circulation of bile salts in rats. *Am. J. Physiol. Gastrointest. Liver Physiol.* **294**: G540–G547.
 28. Bolstad, B. M., R. A. Irizarry, M. Åstrand, and T. P. Speed. 2003. A comparison of normalization methods for high density oligonucleotide array data based on variance and bias. *Bioinformatics*. **19**: 185–193.
 29. Irizarry, R. A., B. M. Bolstad, F. Collin, L. M. Cope, B. Hobbs, and T. P. Speed. 2003. Summaries of Affymetrix GeneChip probe level data. *Nucleic Acids Res.* **31**: e15.
 30. Dai, M., P. Wang, A. D. Boyd, G. Kostov, B. Athey, E. G. Jones, W. E. Bunney, R. M. Myers, T. P. Speed, H. Akil, S. J. Watson, and F. Meng. 2005. Evolving gene/transcript definitions significantly alter the interpretation of GeneChip data. *Nucleic Acids Res.* **33**: 1–9.
 31. Sartor, M. a, C. R. Tomlinson, S. C. Wesselkamper, S. Sivaganesan, G. D. Leikauf, and M. Medvedovic. 2006. Intensity-based hierarchical Bayes method improves testing for differentially expressed genes in microarray experiments. *BMC Bioinformatics*. **7**: 538.
 32. Storey, J. D., and R. Tibshirani. 2003. Statistical significance for genomewide studies. *Proc. Natl. Acad. Sci. U. S. A.* **100**: 9440–9445.
 33. Jamall, I. S., V. N. Finelli, and S. S. Que Hee. 1981. A simple method to determine nanogram levels of 4-hydroxyproline in biological tissues. *Anal. Biochem.* **112**: 70–75.
 34. Gevers, D., S. Kugathasan, L. A. Denson, Y. Vázquez-Baeza, W. Van Treuren, B. Ren, E. Schwager, D. Knights, S. J. Song, M. Yassour, X. C. Morgan, A. D. Kostic, C. Luo, A. González, D. McDonald, Y. Haberman, T. Walters, S. Baker, J. Rosh, M. Stephens, M. Heyman, J. Markowitz, R. Baldassano, A. Griffiths, F. Sylvester, D. Mack, S. Kim, W. Crandall, J. Hyams, C. Huttenhower, R. Knight, and R. J. Xavier. 2014. The treatment-naïve microbiome in new-onset Crohn's disease. *Cell Host Microbe*. **15**: 382–392.
 35. Caporaso, J. G., J. Kuczynski, J. Stombaugh, K. Bittinger, F. D. Bushman, E. K. Costello, N. Fierer, A. G. Peña, J. K. Goodrich, J. I. Gordon, G. a Huttley, S. T. Kelley, D. Knights, J. E. Koenig, R. E. Ley, C. a Lozupone, D. McDonald, B. D. Muegge, M. Pirrung, J. Reeder, J. R. Sevinsky, P. J. Turnbaugh, W. a Walters, J. Widmann, T. Yatsunenko, J. Zaneveld, and R. Knight. 2010. QIIME allows analysis of high-throughput community sequencing data. *Nat. Methods*. **7**: 335–336.
 36. Segata, N., J. Izard, L. Waldron, D. Gevers, L. Miropolsky, W. S. Garrett, and C. Huttenhower. 2011. Metagenomic biomarker discovery and explanation. *Genome Biol.* **12**: R60.
 37. Suzuki, M. T., L. T. Taylor, and E. F. DeLong. 2000. Quantitative analysis of small-subunit rRNA genes in mixed microbial populations via 5'-nuclease assays. *Appl. Environ. Microbiol.* **66**: 4605–4614.
 38. Weisburg, W. G., S. M. Barns, D. A. Pelletier, and D. J. Lane. 1991. 16S ribosomal DNA amplification for phylogenetic study. *J. Bacteriol.* **173**: 697–703.
 39. Pryce, T. M., S. Palladino, I. D. Kay, and G. W. Coombs. 2003. Rapid identification of fungi by sequencing the ITS1 and ITS2 regions using an automated capillary electrophoresis system. *Med. Mycol.* **41**: 369–381.
 40. Haenen, D., C. Souza, J. Zhang, S. J. Koopmans, G. Bosch, J. Vervoort, W. J. J. Gerrits, B. Kemp, H. Smidt, and M. Mu. 2013. Resistant Starch Induces Catabolic but Suppresses Immune and Cell Division Pathways and Changes the Microbiome in the Proximal Colon of Male Pigs. *J. Nutr.* **143**: 1889–1898.
 41. Charlton, M., a. Krishnan, K. Viker, S. Sanderson, S. Cazanave, a. McConico, H. Masuoko, and G. Gores. 2011. Fast food diet mouse: novel small animal model of NASH with ballooning, progressive fibrosis, and high physiological fidelity to the human condition. *AJP Gastrointest. Liver Physiol.* **301**:

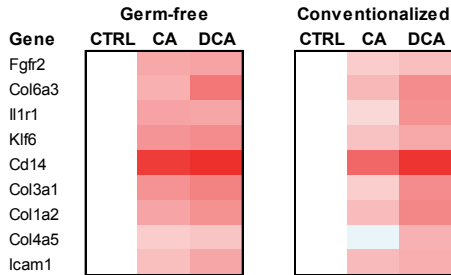
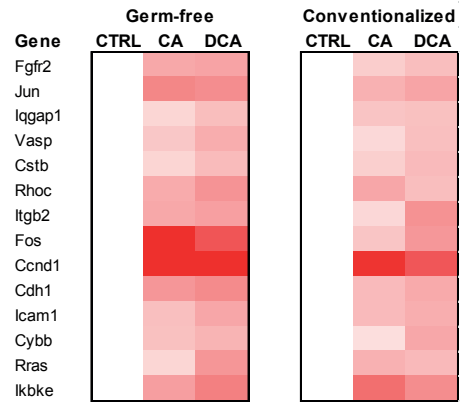
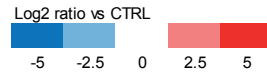
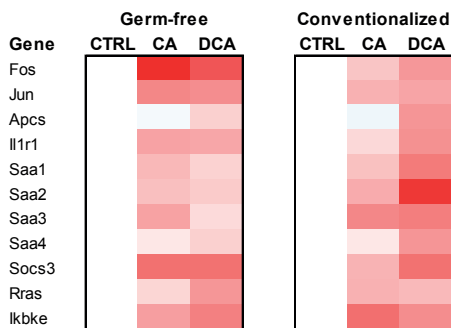
- G825–G834.
42. Kawanishi, N., H. Yano, T. Mizokami, M. Takahashi, E. Oyanagi, and K. Suzuki. 2012. Exercise training attenuates hepatic inflammation, fibrosis and macrophage infiltration during diet induced-obesity in mice. *Brain. Behav. Immun.* **26**: 931–41.
 43. Savard, C., E. V Tartaglione, R. Kuver, W. G. Haigh, G. C. Farrell, S. Subramanian, A. Chait, M. M. Yeh, L. S. Quinn, and G. N. Ioannou. 2013. Synergistic interaction of dietary cholesterol and dietary fat in inducing experimental steatohepatitis. *Hepatology*. **57**: 81–92.
 44. Bashiardes, S., H. Shapiro, S. Rozin, O. Shibolet, and E. Elinav. 2016. Non-alcoholic fatty liver and the gut microbiota. *Mol. Metab.* **5**: 782–794.
 45. Koeth, R. A., Z. Wang, B. S. Levison, J. a Buffa, E. Org, B. T. Sheehy, E. B. Britt, X. Fu, Y. Wu, L. Li, J. D. Smith, J. a DiDonato, J. Chen, H. Li, G. D. Wu, J. D. Lewis, M. Warrier, J. M. Brown, R. M. Krauss, W. H. W. Tang, F. D. Bushman, A. J. Lusis, and S. L. Hazen. 2013. Intestinal microbiota metabolism of L-carnitine, a nutrient in red meat, promotes atherosclerosis. *Nat. Med.* **19**: 576–85.
 46. Tang, W. H. W., Z. Wang, D. J. Kennedy, Y. Wu, J. a. Buffa, B. Agatsuma-Boyle, X. S. Li, B. S. Levison, and S. L. Hazen. 2015. Gut Microbiota-Dependent Trimethylamine N-Oxide (TMAO) Pathway Contributes to Both Development of Renal Insufficiency and Mortality Risk in Chronic Kidney Disease. *Circ. Res.* **116**: 448–455.
 47. Lau, E., D. Carvalho, and P. Freitas. 2015. Gut Microbiota: Association with NAFLD and Metabolic Disturbances. *Biomed Res. Int.* **2015**.
 48. Lange, K., F. Hugenholtz, M. C. Jonathan, H. a Schols, M. Kleerebezem, H. Smidt, M. Müller, and G. J. E. J. Hooiveld. 2015. Comparison of the effects of five dietary fibers on mucosal transcriptional profiles, and luminal microbiota composition and SCFA concentrations in murine colon. *Mol. Nutr. Food Res.* **59**: 1590–1602.
 49. Dumas, M.-E., R. H. Barton, A. Toye, O. Cloarec, C. Blancher, A. Rothwell, J. Fearnside, R. Tatoud, V. Blanc, J. C. Lindon, S. C. Mitchell, E. Holmes, M. I. McCarthy, J. Scott, D. Gauguier, and J. K. Nicholson. 2006. Metabolic profiling reveals a contribution of gut microbiota to fatty liver phenotype in insulin-resistant mice. *Proc. Natl. Acad. Sci. U. S. A.* **103**: 12511–12516.
 50. Gao, X., X. Liu, J. Xu, C. Xue, Y. Xue, and Y. Wang. 2014. Dietary trimethylamine N-oxide exacerbates impaired glucose tolerance in mice fed a high fat diet. *J. Biosci. Bioeng.* **118**: 476–481.
 51. Aranha, M. M., H. Cortez-Pinto, A. Costa, I. B. M. da Silva, M. E. Camilo, M. C. de Moura, and C. M. P. Rodrigues. 2008. Bile acid levels are increased in the liver of patients with steatohepatitis. *Eur. J. Gastroenterol. Hepatol.* **20**: 519–525.
 52. Mouzaki, M., A. Y. Wang, R. Bandsma, E. M. Comelli, B. M. Arendt, L. Zhang, S. Fung, S. E. Fischer, I. G. McGilvray, and J. P. Allard. 2016. Bile Acids and Dysbiosis in Non-Alcoholic Fatty Liver Disease. *PLoS One*. **11**: e0151829.
 53. Yoshimoto, S., T. M. Loo, K. Atarashi, H. Kanda, S. Sato, S. Oyadomari, Y. Iwakura, K. Oshima, H. Morita, M. Hattori, K. Honda, Y. Ishikawa, E. Hara, and N. Ohtani. 2013. Obesity-induced gut microbial metabolite promotes liver cancer through senescence secretome. *Nature*. **499**: 97–101.
 54. Fickert, P., A. Fuchsichler, H.-U. Marschall, M. Wagner, G. Zollner, R. Krause, K. Zatloukal, H. Jaeschke, H. Denk, and M. Trauner. 2006. Lithocholic acid feeding induces segmental bile duct obstruction and destructive cholangitis in mice. *Am. J. Pathol.* **168**: 410–422.
 55. Woudenberg-Vrenken, T. E., L. Conde de la Rosa, M. Buist-Homan, K. N. Faber, and H. Moshage. 2013. Metformin Protects Rat Hepatocytes against Bile Acid-Induced Apoptosis. *PLoS One*. **8**.
 56. Sodeman, T., S. F. Bronk, P. J. Roberts, H. Miyoshi, and G. J. Gores. 2000. Bile salts mediate hepatocyte apoptosis by increasing cell surface trafficking of Fas. *Am. J. Physiol. Gastrointest. Liver Physiol.* **278**: G992–G999.
 57. Higuchi, H., S. F. Bronk, Y. Takikawa, N. Werneburg, R. Takimoto, W. El-deiry, and G. J. Gores. 2001. The Bile Acid Glycochenodeoxycholate Induces TRAIL-Receptor 2 / DR5 Expression and Apoptosis. *J. Biol. Chem.* **276**: 38610–38618.
 58. Swann, J. R., E. J. Want, F. M. Geier, K. Spagou, I. D. Wilson, J. E. Sidaway, J. K. Nicholson, and E. Holmes. 2011. Systemic gut microbial modulation of bile acid metabolism in host tissue compartments. *Proc. Natl. Acad. Sci. U. S. A.* **108**: 4523–30.
 59. Sayin, S. I., A. Wahlström, J. Felin, S. Jäntti, H.-U. Marschall, K. Bamberg, B. Angelin, T. Hyötyläinen, M. Orešič, and F. Bäckhed. 2013. Gut microbiota regulates bile acid metabolism by reducing the levels of tauro-beta-muricholic acid, a naturally occurring FXR antagonist. *Cell Metab.* **17**: 225–235.
 60. Zhang, Y., P. B. Limaye, H. J. Renaud, and C. D. Klaassen. 2014. Effect of various antibiotics on modulation of intestinal microbiota and bile acid profile in mice. *Toxicol. Appl. Pharmacol.* **277**: 138–145.
 61. Rahman, K., C. Desai, S. S. Iyer, N. E. Thorn, P. Kumar, Y. Liu, T. Smith, A. S. Neish, H. Li, S. Tan, P. Wu, X. Liu, Y. Yu, A. B. Farris, A. Nusrat, C. A. Parkos, and F. A. Anania. 2016. Loss of Junctional Adhesion Molecule A Promotes Severe Steatohepatitis in Mice on a Diet High in Saturated Fat, Fructose, and

- Cholesterol. *Gastroenterology*. **151**: 733–746.e12.
62. Carvalho, B. M., D. Guadagnini, D. M. L. Tsukumo, a a Schenka, P. Latuf-Filho, J. Vassallo, J. C. Dias, L. T. Kubota, J. B. C. Carvalheira, and M. J. a Saad. 2012. Modulation of gut microbiota by antibiotics improves insulin signalling in high-fat fed mice. *Diabetologia*. **55**: 2823–34.
 63. Douhara, A., K. Moriya, H. Yoshiji, R. Noguchi, T. Namisaki, M. Kitade, K. Kaji, Y. Aihara, N. Nishimura, K. Takeda, Y. Okura, H. Kawaratani, and H. Fukui. 2015. Reduction of endotoxin attenuates liver fibrosis through suppression of hepatic stellate cell activation and remission of intestinal permeability in a rat non-alcoholic steatohepatitis model. *Mol. Med. Rep.* **11**: 1693–1700.
 64. Fouts, D. E., M. Torralba, K. E. Nelson, D. A. Brenner, and B. Schnabl. 2012. Bacterial translocation and changes in the intestinal microbiome in mouse models of liver disease. *J. Hepatol.* **56**: 1283–1292.
 65. Henao-Mejia, J., E. Elinav, C. A. Thaïss, and R. A. Flavell. 2013. The Intestinal Microbiota in Chronic Liver Disease. *Adv. Immunol.* **117**: 73–97.
 66. Li, Z., S. Yang, H. Lin, J. Huang, P. a. Watkins, A. B. Moser, C. DeSimone, X. Y. Song, and A. M. Diehl. 2003. Probiotics and antibodies to TNF inhibit inflammatory activity and improve nonalcoholic fatty liver disease. *Hepatology*. **37**: 343–350.
 67. Eslamparast, T., H. Poustchi, F. Zamani, M. Sharafkhah, R. Malekzadeh, and A. Hekmatdoost. 2014. Synbiotic supplementation in nonalcoholic fatty liver disease : a randomized, double-blind, placebo-controlled pilot study. *Am J Clin Nutr.* **99**: 535–542.
 68. Okubo, H., H. Sakoda, A. Kushiyama, M. Fujishiro, Y. Nakatsu, T. Fukushima, Y. Matsunaga, H. Kamata, T. Asahara, Y. Yoshida, O. Chonan, M. Iwashita, F. Nishimura, and T. Asano. 2013. *Lactobacillus casei* strain Shirota protects against nonalcoholic steatohepatitis development in a rodent model. *Am. J. Physiol. Gastrointest. Liver Physiol.* **305**: G911–8.
 69. Noack, J., B. Kleessen, J. Proll, G. Dongowski, and M. Blaut. 1998. Dietary guar gum and pectin stimulate intestinal microbial polyamine synthesis in rats. *J. Nutr.* **128**: 1385–91.
 70. Ohashi, Y., K. Sumitani, M. Tokunaga, N. Ishihara, T. Okubo, and T. Fujisawa. 2015. Consumption of partially hydrolysed guar gum stimulates Bifidobacteria and butyrate-producing bacteria in the human large intestine. *Benef. Microbes*. **6**: 451–455.
 71. Begley, M., C. Hill, and C. G. M. Gahan. 2006. Bile Salt Hydrolase Activity in Probiotics Bile Salt Hydrolase Activity in Probiotics. *Appl. Environ. Microbiol.* **72**: 1729–1738.
 72. Mudgil, D., S. Barak, and B. S. Khatkar. 2011. Guar gum: processing, properties and food applications—A Review. *J. Food Sci. Technol.* **51**: 409–418.

Supplemental figures and tables



Supplemental figure 1. Guar gum alters IL-8 signaling and complement system activation
(A) Volcano plot displaying relative changes in expression of 21115 genes (x axis) plotted against statistical significance (y axis) upon GG feeding. Dotted line represents cut-off for $p < 0.01$. (B) Heat map showing significant changes in expression of genes involved in IL-8 signaling and complement system activation in the livers of CTRL and GG mice. The Log2 expression signals of the CTRL group was arbitrarily set at 0.

Hepatic fibrosis / Hepatic stellate cell activation**IL-8 signaling****Acute phase response signaling****Supplemental figure 2. Effect of cholic acid and deoxycholic acid on hepatic genome-wide expression**

Heat maps showing changes in expression of genes involved in hepatic fibrosis/hepatic stellate cell activation, IL-8 signaling and acute phase response signalling in the livers of germ-free and conventionalized mice fed either a CTRL diet or supplemented with 0.5% CA or 0.5% DCA for two weeks. The Log2 expression signals of CTRL was arbitrarily set at 0.

Supplemental table 1. Macronutrient and ingredient composition of various diets based on formula D12451 study 1

	Control		Resistant starch		Guar Gum	
	g%	kcal%	g%	kcal%	g%	kcal%
Protein	24	20	24	21	24	20
Carbohydrate	41	35	41	32	41	35
Fat	24	45	24	47	24	45
Total		100		100		100
kcal/g	4.7		4.7		4.7	
Ingredient	g	kcal	g	kcal	g	kcal
Casein, 30 Mesh	200	800	200	800	200	800
L-Cystine	3	12	3	12	3	12
Corn Starch	72.8	291	0	0	0	0
Resistant Starch	0	0	86.7	173.4	0	0
Guar Gum	0	0	0	0	86.7	346.8
Maltodextrin 10	100	400	86.1	344.4	86.1	344.4
Sucrose	172.8	691	172.8	691	172.8	691
Cellulose, BW200	50	0	50	0	50	0
Soybean Oil	25	225	25	225	25	225
Safflower Oil	177.5	1598	177.5	1598	177.5	1598
Cholesterol	8.66	0	8.66	0	8.66	0
Mineral Mix S10026	10	0	10	0	10	0
DiCalcium Phosphate	13	0	13	0	13	0
Calcium Carbonate	5.5	0	5.5	0	5.5	0
Patassium Citrate	16.5	0	16.5	0	16.5	0
Vitamin Mix V10001	10	40	10	40	10	40
Choline Bitartrate	2	0	2	0	2	0
Total	866.8	4057	866.8	3884	866.8	4057

Supplemental table 2. Primer sequences used for qPCR

Name	Primer Sequence	
	Forward	Reverse
<i>m36b4</i>	ATGGGTACAAGCGCGTCCTG	GCCTTGACCTTTTCAGTAAG
<i>mβ-actin</i>	GATCTGGCACCACACCTTCT	GGGGTGTTGAAGGTCTCAAA
<i>mCd68</i>	CCAATTCAGGGTGGAAGAAA	CTCGGGCTCTGATGTAGGTC
<i>mF4/80</i>	CTTTGGCTATGGGCTTCCAGTC	GCAAGGAGGACAGAGTTTATCGTG
<i>mCd11c</i>	CTGGATAGCCTTTCTTCTGCTG	GCACACTGTGTCGGAACCTCA
<i>mCd206</i>	GCTTCCGTCAACCCTGTATGC	GTGTGTCATTCTTACACTCCC
<i>mMcp-1</i>	CCCAATGAGTAGGCTGGAGA	TCTGGACCCATTCTTCTTG
<i>mTnfa</i>	CAACCTCCTCTCTGCCGTCAA	TGACTCCAAAGTAGACCTGCCC
<i>mIl-10</i>	CTGGACAACATACTGCTAACCG	GGGCATCACTTCTACCAGGTAA
<i>mCol1a1</i>	TGTGTGCGATGACGTGCAAT	GGGTCCCTCGACTCCTACA
<i>maSma</i>	GTCCAGACATCAGGGAGTAA	TCGGATACTTCAGCGTCAGGA
<i>mTimp1</i>	GCAACTCGGACCTGGTCATAA	CGGCCCGTGATGAGAACT
<i>mCyp7a1</i>	CAGGGAGATGCTCTGTGTTCA	AGGCATACATCCCTTCCGTGA
<i>mCyp27a1</i>	GCCTTGCAACAAGGAAGTGA	CGCAGGGTCTCCTTAATCACA
<i>mCyp8b1</i>	CCTCTGGACAAGGGTTTGTG	GCACCGTGAAGACATCCCC
<i>mSlc51b</i>	AGATGCGGCTCCTTGAATTA	TGGCTGCTTCTTTCGATTCTG
<i>mNtcp</i>	ATGACCACCTGCTCCAGCTT	GCCTTTGTAGGGCACCTTGT
<i>mBsep</i>	CTGCCAAGGATGCTAATGCA	CGATGGCTACCTTTTGCTTCT
<i>mFgf15</i>	GCTCTGAAGACGATTGCCATC	TTCCTCCCTGAAGGTACAGTC
<i>mAsbt</i>	ATGGCGACATGGACCTCAGT	CCCGAGTCAACCCACATCTTG
<i>mIbabp</i>	CTTCCAGGAGACGTGATTGAAA	CCTCCGAAGTCTGGTGATAGTTG
<i>mSlc51a</i>	GTTCCAGGTGCTTGTCATCC	CCACTGTTAGCCAAGATGGAGAA

Supplemental table 3. Relative abundance of microbiota in colonic luminal content study 1

Phylum	Class	Order	Family	Genus	Species	CTRL (%)	RS (%)	GG (%)	FC RS*	P-value RS**	FC GG*	P-value GG**
Actinobacteria						0.26	1.54	15.63	5.9	0.012	59.2	p<0,001
	Actinobacteria					0.26	1.54	15.63	5.9	0.012	59.2	p<0,001
		Bifidobacteriales				0.26	1.54	15.63	5.9	0.012	59.2	p<0,001
			Bifidobacteriaceae			0.26	1.54	15.63	5.9	0.012	59.2	p<0,001
				<i>Bifidobacterium</i>		0.26	1.54	15.63	5.9	0.012	59.2	p<0,001
Bacteroidetes						4.51	17.16	14.49	3.8	0.002	3.2	p<0,001
	Bacteroidia					4.51	17.16	14.49	3.8	0.002	3.2	p<0,001
		Bacteroidales				4.51	17.16	14.49	3.8	0.002	3.2	p<0,001
			Unidentified			2.18	5.70	0.52	2.6	0.038	-4.2	0.002
			Paraprevotellaceae			0.12	0.09	3.24	-1.3	0.046	27.2	p<0,001
			<i>Prevotella</i>			0.12	0.09	3.24	-1.3	0.046	27.2	p<0,001
			Bacteroidaceae			1.21	3.94	5.26	3.2	0.01	4.3	0.002
			<i>Bacteroides</i>			1.21	3.94	5.26	3.2	0.01	4.3	0.002
			S24-7			0.99	7.43	5.47	7.5	0.001	5.5	p<0,001
			<i>Unidentified</i>			0.99	7.43	5.47	7.5	0.001	5.5	p<0,001
Deferribacteres						4.95	1.71	1.12	-2.9	0.038	-4.4	0.006
	Deferribacteres					4.95	1.71	1.12	-2.9	0.038	-4.4	0.006
		Deferribacterales				4.95	1.71	1.12	-2.9	0.038	-4.4	0.006
			Deferribacteraceae			4.95	1.71	1.12	-2.9	0.038	-4.4	0.006
			<i>Mucispirillum</i>			4.95	1.71	1.12	-2.9	0.038	-4.4	0.006
			<i>Mucispirillum schaedleri</i>			4.95	1.71	1.12	-2.9	0.038	-4.4	0.006
Firmicutes						84.63	74.76	55.43	-1.1	0.016	-1.5	p<0,001
	Bacilli					9.99	1.88	0.62	-5.3	0.012	-16.1	p<0,001
		Lactobacillales				9.99	1.88	0.62	-5.3	0.012	-16.1	p<0,001
			Lactobacillaceae			9.99	1.88	0.62	-5.3	0.012	-16.1	p<0,001
			<i>Lactobacillus</i>			9.99	1.88	0.62	-5.3	0.012	-16.1	p<0,001
	Clostridia					26.58	9.61	9.94	-2.8	0.002	-2.7	0.001
		Clostridiales				26.58	9.61	9.94	-2.8	0.002	-2.7	0.001
			Unidentified			17.87	3.99	6.34	-4.5	0.001	-2.8	0.006
			Clostridiaceae			4.09	3.03	0.00	-1.3	ns	-2275.9	0.001
			<i>SMB53</i>			4.09	3.03	0.00	-1.3	ns	-2275.9	0.001
			Lachnospiraceae			1.70	1.56	3.19	-1.1	ns	1.9	ns
			<i>Unidentified</i>			1.40	1.28	2.16	-1.1	ns	1.5	ns
			<i>Ruminococcus</i>			0.30	0.27	1.03	-1.1	ns	3.4	ns
			<i>Ruminococcus gnavus</i>			0.30	0.27	1.03	-1.1	ns	3.4	ns
			Ruminococcaceae			2.92	1.04	0.41	-2.8	ns	-7.2	p<0,001
			<i>Oscillospira</i>			2.92	1.04	0.41	-2.8	ns	-7.2	p<0,001
	Erysipelotrichi					48.06	63.27	44.87	1.3	ns	-1.1	ns
		Erysipelotrichales				48.06	63.27	44.87	1.3	ns	-1.1	ns
			Erysipelotrichaceae			48.06	63.27	44.87	1.3	ns	-1.1	ns
			<i>Allobaculum</i>			48.06	63.27	44.87	1.3	ns	-1.1	ns
Proteobacteria						5.51	4.81	5.10	-1.1	ns	-1.1	ns
	Deltaproteobacteria					5.51	4.81	5.10	-1.1	ns	-1.1	ns
		Desulfotribionales				5.51	4.81	5.10	-1.1	ns	-1.1	ns
			Desulfotribionaceae			5.51	4.81	5.10	-1.1	ns	-1.1	ns
			<i>Bilophila</i>			3.08	2.22	1.53	-1.4	ns	-2.0	ns
			<i>Desulfovibrio</i>			2.43	2.59	3.56	1.1	ns	1.5	ns
			<i>Unidentified</i>			2.42	2.47	1.60	1.0	ns	-1.5	ns
			<i>Desulfovibrio C21_c20</i>			0.00	0.12	1.97	83.2	ns	1308.8	0.002
Verrucomicrobia						0.14	0.01	8.23	-17.3	ns	60.8	p<0,001
	Verrucomicrobiae					0.14	0.01	8.23	-17.3	ns	60.8	p<0,001
		Verrucomicrobiales				0.14	0.01	8.23	-17.3	ns	60.8	p<0,001
			Verrucomicrobiaceae			0.14	0.01	8.23	-17.3	ns	60.8	p<0,001
			<i>Akkermansia</i>			0.14	0.01	8.23	-17.3	ns	60.8	p<0,001
			<i>Akkermansia muciniphila</i>			0.14	0.01	8.23	-17.3	ns	60.8	p<0,001

Abundance threshold for presentation in the table >0.5% in at least one of the three diet groups

* fold change (FC) compared with CTRL

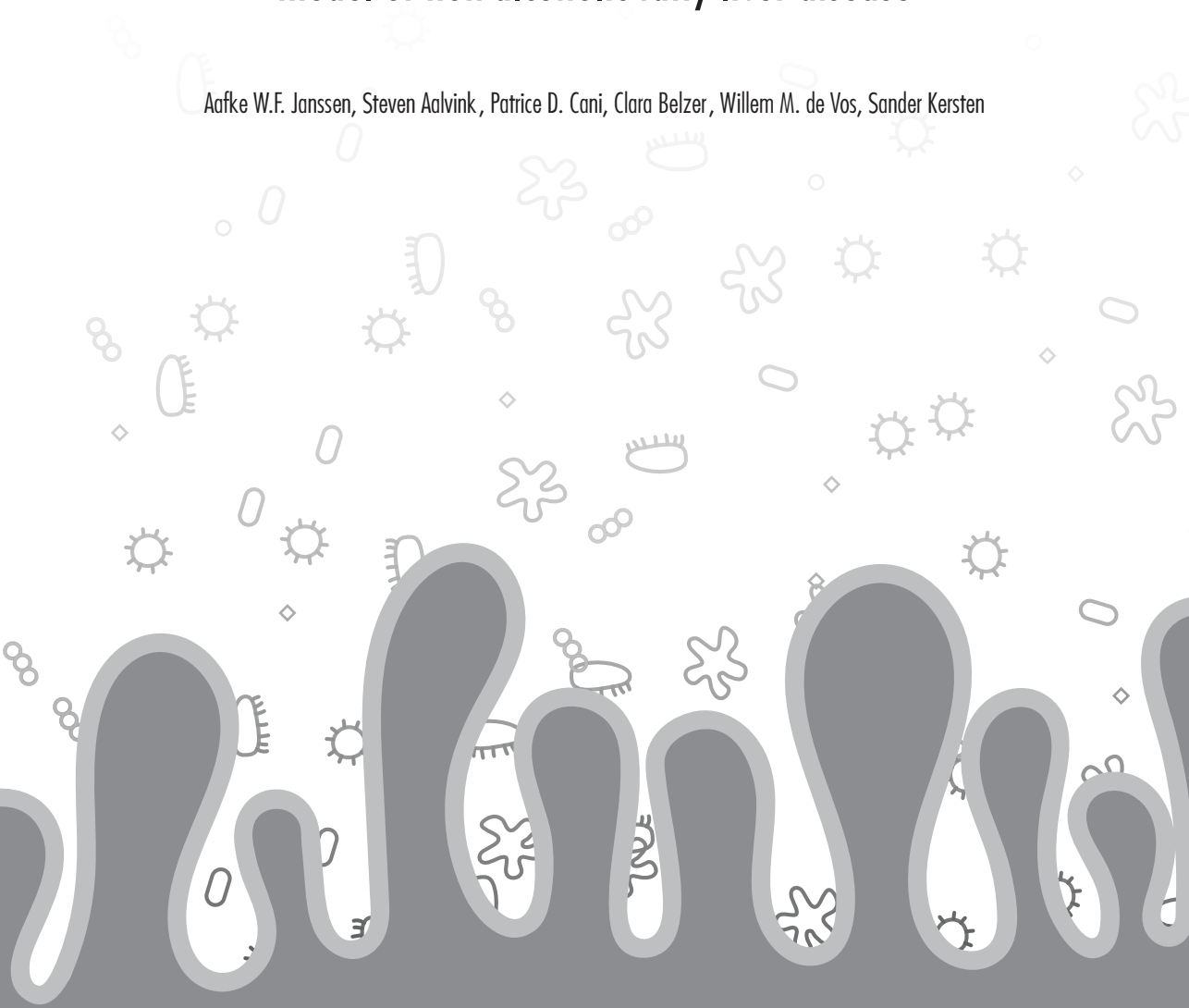
** significance according to Kruskal-Wallis test followed by unpaired Wilcoxon rank-sum test to test significance compared with CTRL

5



The mucin-degrading bacteria *A. muciniphila* and *B. thetaiotaomicron* have no effect in an obese mouse model of non-alcoholic fatty liver disease

Aafke W.F. Janssen, Steven Aalvink, Patrice D. Cani, Clara Belzer, Willem M. de Vos, Sander Kersten



Manuscript in preparation

Abstract

Recently, the administration of the mucin-degrading bacteria *Akkermansia muciniphila* was shown to protect against diet-induced obesity and glucose intolerance in mice. However, whether *A. muciniphila* or other mucin-degrading bacteria influence non-alcoholic fatty liver disease (NAFLD) in obese mice is currently unknown. To resolve this question, mice were fed a high fat/high cholesterol/high fructose diet for 13 weeks to induce NAFLD, followed by daily oral gavage of either live *A. muciniphila*, heat-killed *A. muciniphila*, live *Bacteroides thetaiotaomicron*, heat-killed *B. thetaiotaomicron*, or control gavage, for a total of 5 weeks.

Daily administration of viable *A. muciniphila* effectively increased the abundance of *A. muciniphila* in the colon, whereas administration of viable *B. thetaiotaomicron* had no effect on *B. thetaiotaomicron* abundance. All treatments caused a substantial decrease in bodyweight during the first week of oral gavages, which stabilized the remaining 4 weeks. No significant differences in bodyweight gain could be observed among the different treatments. Treatment of obese mice with *A. muciniphila* or *B. thetaiotaomicron* did not affect hepatic steatosis, inflammation or fibrosis. Finally, gut permeability and portal serum LPS levels were also not altered by treatment with *A. muciniphila* or *B. thetaiotaomicron*.

Taken together, treatment of obese mice with live or heat-killed *A. muciniphila* or *B. thetaiotaomicron* for 5 weeks did not significantly affect obesity, gut barrier function or features of NAFLD. Whether a higher dose or longer duration of *A. muciniphila* treatment may affect hepatic fibrosis remains to be investigated.

Introduction

In the past two decades, it has become increasingly apparent that the intestinal microbiota are involved in mediating the effects of host genetics and environment on the health status of the host. Numerous studies have shown that by modulating the intestinal microbiota, changes in gut microbial composition may have a causal role in various diseases (1–4). For example, mice harbouring no microbiota in the gut —so-called germ-free mice— do not develop diet-induced obesity and related metabolic disturbances, whereas conventionally-raised mice do (5, 6). Similarly, the administration of specific bacterial communities has been shown to confer beneficial health effects, such as attenuating non-alcoholic fatty liver disease (NAFLD) and reducing atherosclerosis (7–9). We recently demonstrated that modulation of the gut microbiota can be protective against diet-induced obesity, while at the same time promote NAFLD (10). Understanding how and which microbial species impact host health may provide useful insights into the role of the gut bacteria in metabolic diseases and may pave the way for new therapeutic targets in metabolic diseases.

One bacterium that gained a lot of interest in the last decade is the gram-negative anaerobic *Akkermansia muciniphila*. *A. muciniphila* is the only cultivable member of the Verrucomicrobia phylum and resides in the mucus layer of the intestinal tract (11, 12). With a relative abundance of 1–4%, *A. muciniphila* constitutes one of the most abundant species in the colon of human subjects (13, 14). Multiple studies have shown that the relative abundance of *A. muciniphila* inversely correlates with bodyweight and blood glucose levels in mice (15–17), as well as in humans (18–21). Moreover, weight loss has been shown to be associated with an increase in *A. muciniphila* (22, 23). By supplementing *A. muciniphila* to mice, it was demonstrated that *A. muciniphila* may be causally linked to obesity and glucose tolerance. Daily oral gavage of *A. muciniphila* to mice fed a chow diet or a high fat diet (15, 24–26) reduced bodyweight gain and improved glucose homeostasis, and was shown to reduce atherosclerosis (27). The improvement in metabolic status upon *A. muciniphila* treatment is suggested to be related to an improved integrity of the gut barrier. *A. muciniphila* degrades mucins in the mucus layer to obtain energy and as the sole source of carbon and nitrogen required for their growth (28). As a result, the mucus layer is constantly refreshed, which prevents thinning of the mucus layer and leakage of LPS into the circulation (15). Since entry of LPS into the circulating has been linked to weight gain and glucose intolerance (29), the counteracting effect of *A. muciniphila* on obesity and associated disorders might be explained by decreased plasma LPS levels (15, 24, 25, 27).

Another gram-negative anaerobic bacterium that is also able to degrade mucins is *Bacteroides thetaiotaomicron*. *B. thetaiotaomicron* is a dominant member of the intestinal microbiota of human and mice, and belongs to the phylum Bacteroidetes (30). *B.*

thetaitaomicron obtains energy by the degradation of complex dietary polysaccharides, but is able to switch its gene expression to metabolize host mucus polysaccharides when dietary polysaccharides are scarce (31). Recently, it was shown that the relative abundance of *B. thetaiotaomicron* is significantly lower in patients with the metabolic syndrome (32). Although the effect of *B. thetaiotaomicron* on host metabolism is less well studied than *A. muciniphila*, two studies have reported that *B. thetaiotaomicron* promotes fat storage in germ-free mice (1, 33). In addition, it is also suggested that *B. thetaiotaomicron* can modulate host immune responses (34, 35). As *B. thetaiotaomicron* has been suggested to promote goblet cell differentiation and thereby induce mucin synthesis (36), it can be hypothesized that *B. thetaiotaomicron* may affect host metabolism via changes in the gut barrier.

NAFLD is a liver disease commonly seen in overweight and obese individuals. NAFLD is characterized by excessive fat accumulation in the liver, and varies from simple steatosis to non-alcoholic steatohepatitis and cirrhosis. Key features of non-alcoholic steatohepatitis are lobular inflammation and ballooning of hepatocytes, which may progress towards fibrosis (37). Changes in the gut microbiota and subsequent alterations in gut barrier function have been suggested to be involved in the pathogenesis of NAFLD (38, 39). Taking into account the reported protective effect of *A. muciniphila* and *B. thetaiotaomicron* on gut barrier function, we hypothesized that treatment of obese mice with *A. muciniphila* and *B. thetaiotaomicron* may attenuate NAFLD development. To investigate this hypothesis, obesity and NAFLD were elicited in mice by feeding a diet rich in fat, cholesterol and fructose, followed by administration of live or heat-killed *A. muciniphila* and *B. thetaiotaomicron* for 5 weeks.

Materials and methods

Animals and diet

10-week-old C57Bl/6 male mice were maintained on a 12 hr light-dark cycle under specific pathogen-free conditions. The mice had ad libitum access to a high fat/high cholesterol/high fructose diet (HFCFD), providing 45% energy as triglycerides (formula 58V8 manufactured by TestDiet, St. Louis, USA) for 18 weeks. To promote the development of NAFLD, the diet was supplemented with 1% cholesterol (Dishman, Veenendaal, Netherlands) and the mice received 20% fructose in their drinking water (wt/vol) (10). After 13 weeks HFCFD we started with daily oral gavage of 2×10^8 cfu/0.2ml of either live or pasteurized *A. muciniphila* or *B. thetaiotaomicron* for a period of 5 weeks. Control mice received an equivalent volume of sterile anaerobic PBS containing 5% glycerol.

Bodyweight and food intake were assessed weekly. 6 mice died during the bacterial administration period for unknown reasons. These mice were inspected and no abnormalities were found. At the end of the study, mice were anesthetized with isoflurane and portal blood was collected. After euthanization, tissues and intestinal content was collected for further analysis. This animal study was approved by the local animal ethics committee of Wageningen University.

Culture and pasteurization of *A. muciniphila* and *B. thetaiotaomicron*

Akkermansia muciniphila cells were prepared as described before (25). *B. thetaiotaomicron* cells were grown on BHIS (40) till mid exponential phase. The cells were harvested and washed with PBS and then concentrated in PBS with 10% glycerol to 2×10^9 CFU/ml and stored at -80°C. Additionally, a separate batch of *A. muciniphila* and *B. thetaiotaomicron* at a concentration of 2×10^9 CFU/ml was inactivated by pasteurization for 30 min at 70°C. Shortly before gavage the cells were diluted in anaerobic PBS to an end concentration of 2×10^8 CFU/0.2 ml.

DNA extraction

DNA was extracted from fecal samples, as previously described (10). Briefly, 15-40 mg of fecal samples were lysed using a bead beater (BioSpec, Bartlesville, USA) and DNA was subsequently extracted and purified using a Maxwell 16 System (Promega).

Bacteria quantification

Standard curves were prepared by amplifying 16S rRNA gene using fecal DNA of the control group or genomic DNA of *A. muciniphila* or *B. thetaiotaomicron* using the universal 16S primers 27F (5'-GTTTGATCCTGGCTCAG-3') and 1492R (5'-CGGCTACCTTGTACGAC-3'). The

cycling conditions consisted of an initial denaturation of 95°C for 5 min, followed by 35 cycles of denaturation at 95°C for 30 sec, annealing at 52°C for 40 sec and extension at 72°C for 90 sec, and a final extension at 72°C for 7 min. After verifying the amplicon size by agarose electrophoresis, the amplicon was purified using a commercial available PCR purification kit (ThermoScientific) and diluted in series ranging from 10⁸ to 10¹ 16S rRNA gene copies/μl was generated.

Real-time PCR was performed using SensiMix (Bioline, GC biotech, Alphen aan den Rijn, Netherlands) on a CFX384 Real-Time PCR detection system (Bio-Rad Laboratories, Veenendaal, Netherlands). Amplification conditions were 95°C for 5 min, followed by 40 cycles of 95°C (15 sec), 60°C (30 sec) and 72°C (30 sec). For 16S rRNA gene the primers 1369F (5'-CGGTGAATACGTTTCYCGG-3') (41) and 1492R (5'-GGWTACCTTGTTACGACTT-3') (42) were used, for *A. muciniphila* AM1 (5'-CAGCACGTGAAGGTGGGGAC-3') and AM2 (5'-CCTTGCGGTTGGCTTCAGAT-3') (13) and for *B. thetaiotaomicron* Bt.1F (5'-ATAGCCTTTCGAAAGRAAGAT-3') and Bt.1R (5'-CCAGTATCAACTGCAATTTTA-3') (33).

Plasma parameters

Plasma concentrations of triglycerides (HUMAN Diagnostics, Wiesbaden, Germany), glucose and cholesterol (DiaSys Diagnostic Systems, Holzheim, Germany) were determined according to manufacturers' instructions. Plasma alanine aminotransferase activity was measured with a kit from Abcam (Cambridge, UK).

Portal serum LPS levels

Portal vein plasma LPS concentration was measured using an Endosafe-Multi-Cartridge System (Charles River Laboratories, MA, USA), as previously described (15).

Liver triglyceride quantification

Liver samples were homogenized in a buffer containing 10mM Tris, 2mM EDTA and 250mM sucrose at pH 7.5 with a Tissue Lyser II (Qiagen, Hilden, Germany). Triglycerides were subsequently quantified using Triglycerides liquicolor^{mono} kit from HUMAN Diagnostics (Wiesbaden, Germany). Protein concentration was determined using a BCA protein assay kit (Pierce, Rockford, USA).

Intestinal permeability assay

After 4 weeks bacterial administration an intestinal permeability assay was performed using 4 kilodalton fluorescein isothiocyanate (FITC)-dextran (600 mg/kg bodyweight, 40mg/ml). Blood was drawn from the tail vein prior to administration to correct for autofluorescence

and 1 hour after oral gavage. Blood was stored on ice in the dark and centrifuged for 15 minutes at 3000 rpm to obtain plasma. Plasma was diluted in PBS and fluorescent intensity was measured using a Fluorescence Spectrophotometer (excitation at 485nm and emission at 538nm). FITC-dextran concentrations were determined from a standard curve generated by diluting FITC-dextran in PBS.

RNA isolation and qPCR

TRIzol reagent (Life technologies, Bleiswijk, Netherlands) was used to extract RNA from liver and scrapings of the colon. 500ng RNA was reverse transcribed to cDNA using a iScript cDNA synthesis kit (Bio-Rad Laboratories, Veenendaal, Netherlands). Real-time PCR was performed using SensiMix (Bioline, GC biotech, Alphen aan den Rijn, Netherlands) on a CFX384 Real-Time PCR detection system (Bio-Rad Laboratories, Veenendaal, Netherlands). 36B4 was used as a housekeeping gene. Sequences of the used primers are listed in **Supplemental Table 1**.

¹H NMR spectroscopy

Short-chain fatty acids levels in the content of the cecum were measured in an Avance III NMR spectrometer, as previously described (10).

Histology

The liver and colon, rolled as a 'Swiss roll', were fixed in 4% formaldehyde and embedded in paraffin. Paraffin-embedded liver sections (5µm) were stained with hematoxylin and eosin (H&E) using standard protocols and for collagen using fast green FCF/Sirius Red F3B. Cross-sections of the colon (5µm) were stained with H&E and Alcian Blue according to standard protocols.

Statistics

Results are presented as mean ± SEM. Analysis of variance followed by a Tukey's post hoc multiple comparison test was performed to evaluate differences (GraphPad Software, Inc., La Jolla, USA). P<0.05 was considered as statistically significant.

Results

Administration of *A. muciniphila* and *B. thetaiotaomicron* had no effect on obesity

Supplementing mice fed a high fat diet with *A. muciniphila* has been shown to lead to beneficial metabolic health effects (15, 25–27). However, the effect of *A. muciniphila* supplementation or other mucin-degrading bacteria in obese mice is currently unknown. Accordingly, mice were fed a high fat/high cholesterol/high fructose diet for 13 weeks to induce NAFLD, followed by daily oral gavage of either live *A. muciniphila*, heat-killed *A.*

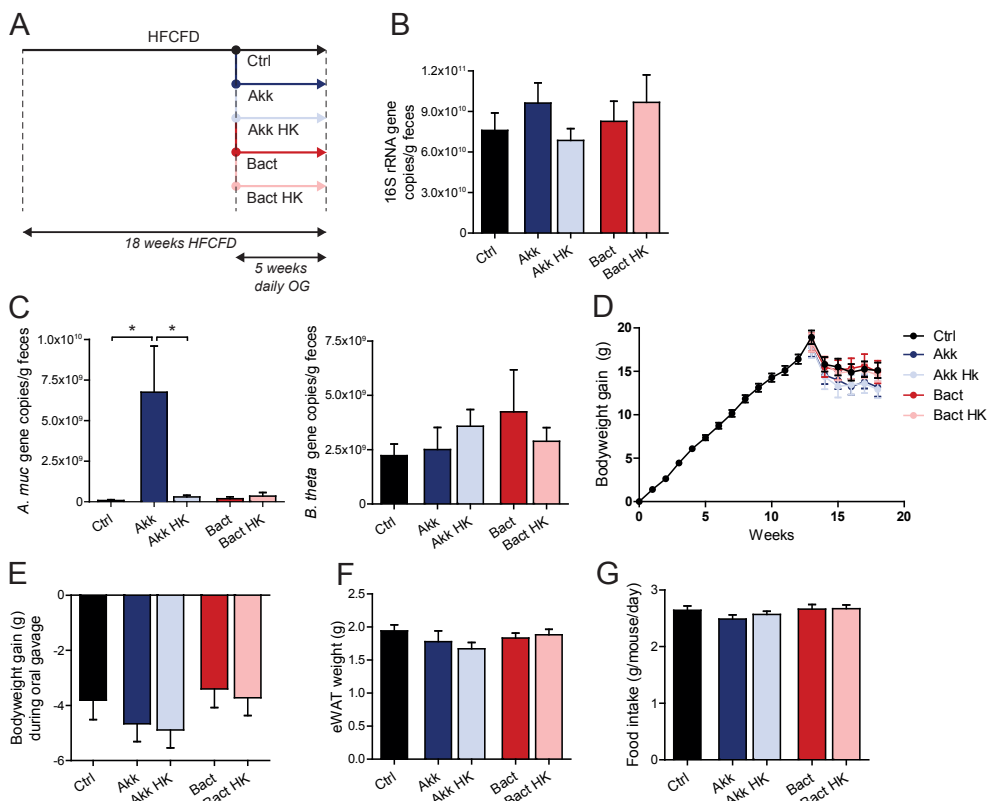


Figure 1. Administration of *A. muciniphila* and *B. thetaiotaomicron* has no effect on obesity

(A) Study design. Mice were fed a high fat/high cholesterol/high fructose diet (HFCFD) for 13 weeks followed by daily oral gavage (OG) of live or heat-killed (HK) *Akkermansia muciniphila* (Akk) or *Bacteroides thetaiotaomicron* (Bact) for 5 weeks. The control group received an oral gavage of sterile anaerobic PBS. (B) 16S rRNA and (C) *A. muciniphila* and *B. thetaiotaomicron* gene copies per gram feces. (D) Course of the bodyweight gain during entire study and (E) changes in bodyweight gain during oral administration of the different bacteria. (F) Weight of epididymal white adipose tissue depot. (G) Mean food intake per mouse per day. Data are presented as mean \pm SEM. Differences were evaluated for statistical significance by one-way ANOVA followed by Tukey's post hoc multiple comparison test. * $p < 0.05$.

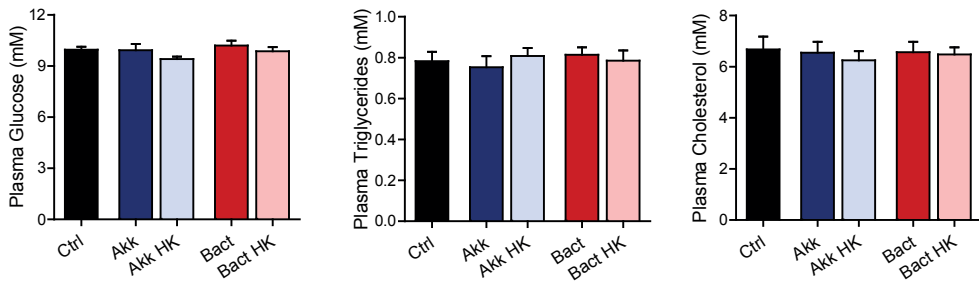


Figure 2. Administration of *A. muciniphila* and *B. thetaiotaomicron* has no effect on plasma parameters Plasma glucose, triglyceride and cholesterol levels upon the administration of viable or heat-killed *A. muciniphila* or *B. thetaiotaomicron* to high fat diet-fed mice. Data are presented as mean ± SEM. Differences were evaluated for statistical significance by one-way ANOVA followed by Tukey's post hoc multiple comparison test.

*mu*ciniphila, live *Bacteroides thetaiotaomicron*, heat-killed *Bacteroides thetaiotaomicron*, or control gavage, for a total of 5 weeks (**Figure 1A**). Treatment of obese mice with live *A. muciniphila* significantly increased the abundance of *A. muciniphila* as compared with treatment of mice with PBS or heat-killed *A. muciniphila*, whereas total bacterial numbers in the feces were comparable between the groups (**Figure 1B-C**). Daily supplementation of *B. thetaiotaomicron* resulted in a trend, though not-significant, towards increased fecal amounts of *B. thetaiotaomicron* (**Figure 1C**).

Bodyweight went up steadily in the first 13 weeks of high fat/high cholesterol/high fructose. By contrast, bodyweight declined during the first week of daily oral gavage, which stabilized during the remaining 4 weeks (**Figure 1D**). Administration of *A. muciniphila* or *B. thetaiotaomicron*, viable or heat-killed, had no effect on bodyweight gain or epididymal fat mass (**Figure 1E-F**). Levels of food intake were also similar between the groups (**Figure 1G**). At the end of the dietary intervention, all mice were hyperglycemic, with plasma glucose levels being slightly but not significantly lower in the mice supplemented with heat-killed *A. muciniphila*. Plasma triglyceride and cholesterol levels were not different between the 5 groups (**Figure 2**). Together, these findings indicate that supplementation of obese mice with *A. muciniphila* or *B. thetaiotaomicron* does not affect bodyweight, plasma glucose, plasma cholesterol, and plasma triglyceride levels.

Administration of *A. muciniphila* and *B. thetaiotaomicron* had no effect on features of NAFLD

We previously demonstrated that feeding mice a HFCFD induces many features of NAFLD and is therefore a suitable mouse model to study obesity-related NAFLD (10). Treatment of obese mice with *A. muciniphila* or *B. thetaiotaomicron* had no effect on liver weight (**Figure 3A**). In addition, treatment with *A. muciniphila* or *B. thetaiotaomicron* did not influence

hepatic steatosis, as indicated by liver triglyceride concentration and H&E staining (**Figure 3B-C**), nor plasma alanine transferase activity, indicating that bacterial administration did not protect against liver damage (**Figure 4A**). Further analysis of the liver revealed that the expression of several macrophage markers and cytokines, including *Mcp-1*, *Tnfa*, *Il-1 β* and *Il-1ra*, was not different between the 5 groups (**Figure 4B-C**). Treatment with viable *A. muciniphila* or *B. thetaiotaomicron* also did not affect hepatic fibrosis, as the expression of fibrosis markers and collagen deposition were similar to that of the control mice (**Figure 4D-E**). These data show that treatment of obese mice with either *A. muciniphila* or *B. thetaiotaomicron* had no effect on features of NAFLD.

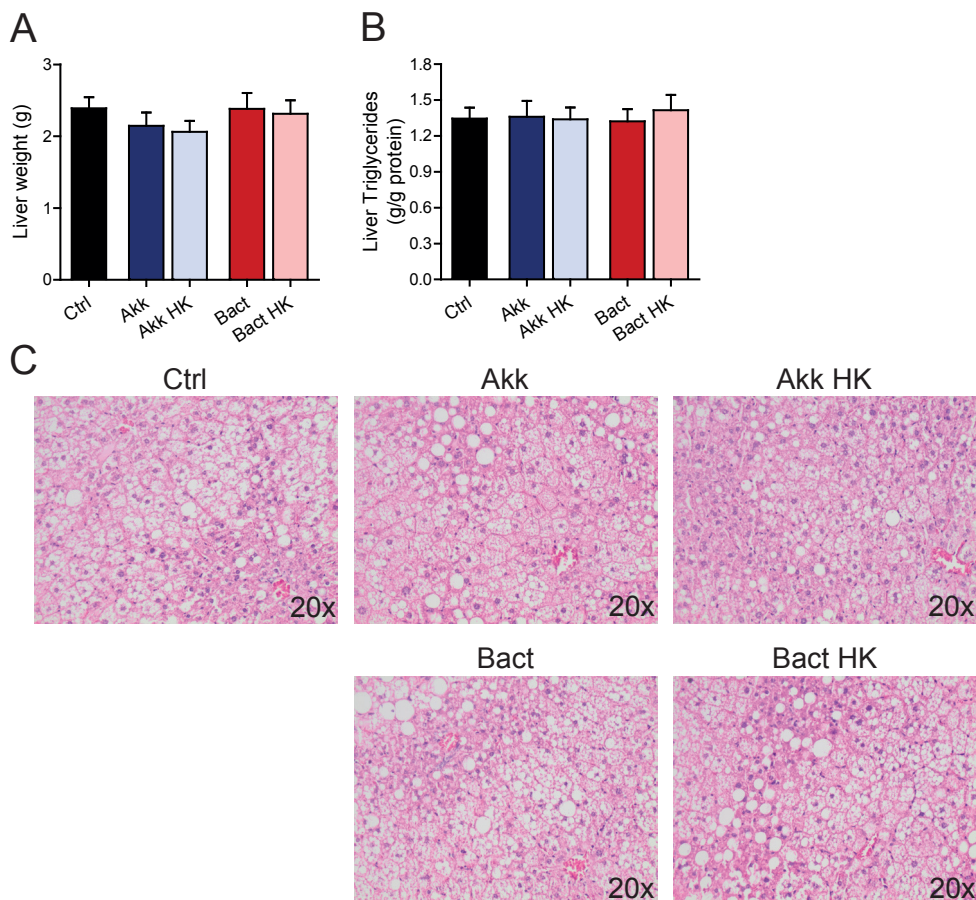


Figure 3. Administration of *A. muciniphila* and *B. thetaiotaomicron* has no effect on hepatic steatosis (A) Weight of the liver. (B) Quantification of liver triglyceride levels. Data are presented as mean \pm SEM. Differences were evaluated for statistical significance by one-way ANOVA followed by Tukey's post hoc multiple comparison test. (C) Representative pictures of the liver stained with H&E.

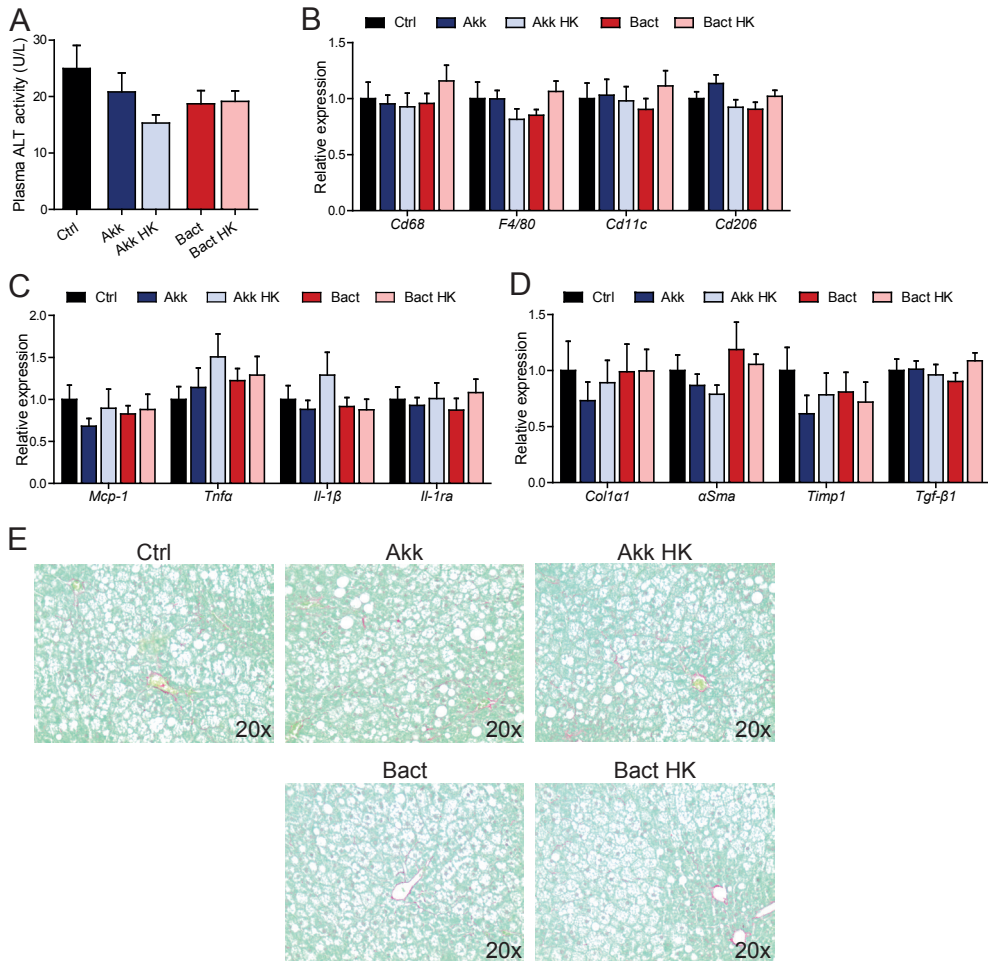


Figure 4. Administration of *A. muciniphila* and *B. thetaiotaomicron* has no effect on hepatic inflammation and fibrosis (A) Activity of alanine aminotransferase (ALT) in plasma. Relative expression of (B) macrophage markers, (C) cytokines and (D) fibrosis-related genes in the liver. Gene expression levels in CTRL mice were set at 1. Data are presented as mean \pm SEM. Differences were evaluated for statistical significance by one-way ANOVA followed by Tukey's post hoc multiple comparison test. (E) Representative pictures of the liver stained for collagen using fast green FCF/Sirius Red F3B.

Administration of *A. muciniphila* and *B. thetaiotaomicron* did not alter gut permeability and LPS levels in portal serum

Considering that the beneficial effects of *A. muciniphila* treatment on bodyweight and glucose homeostasis in mice fed a high fat diet were associated with improved gut barrier integrity (15, 27) and since *A. muciniphila* and *B. thetaiotaomicron* are mucin-degrading bacteria, we investigated whether *A. muciniphila* or *B. thetaiotaomicron* altered gut permeability in obese

mice. Gut permeability was determined by measuring levels of plasma FITC-dextran in the circulation after oral administration. Plasma FITC-dextran levels were similar between the groups, indicating that gut permeability was not affected by the different bacteria (**Figure 5A**). The lack of an effect on gut permeability was accompanied by similar expression levels of the tight junction proteins *Occludin* and *ZO-1*. (**Figure 5B**). Despite the absence of an effect on gut permeability, expression of the main secreted mucin, *Muc2*, was significantly lower in the colon of mice treated with live *B. thetaiotaomicron*. Colonic expression of *Muc3*, a membrane-bound mucin, was similar in all groups (**Figure 5C**). Based on H&E and Alcian Blue stainings of the colon, no difference in the goblet cell number could be observed (**Figure 5D-E**). As *A. muciniphila* supplementation has been associated with a reduction in plasma LPS levels, we also quantified LPS levels in portal blood. No difference in portal LPS levels was found between the groups (**Figure 5F**). In conclusion, treatment of obese mice with *A.*

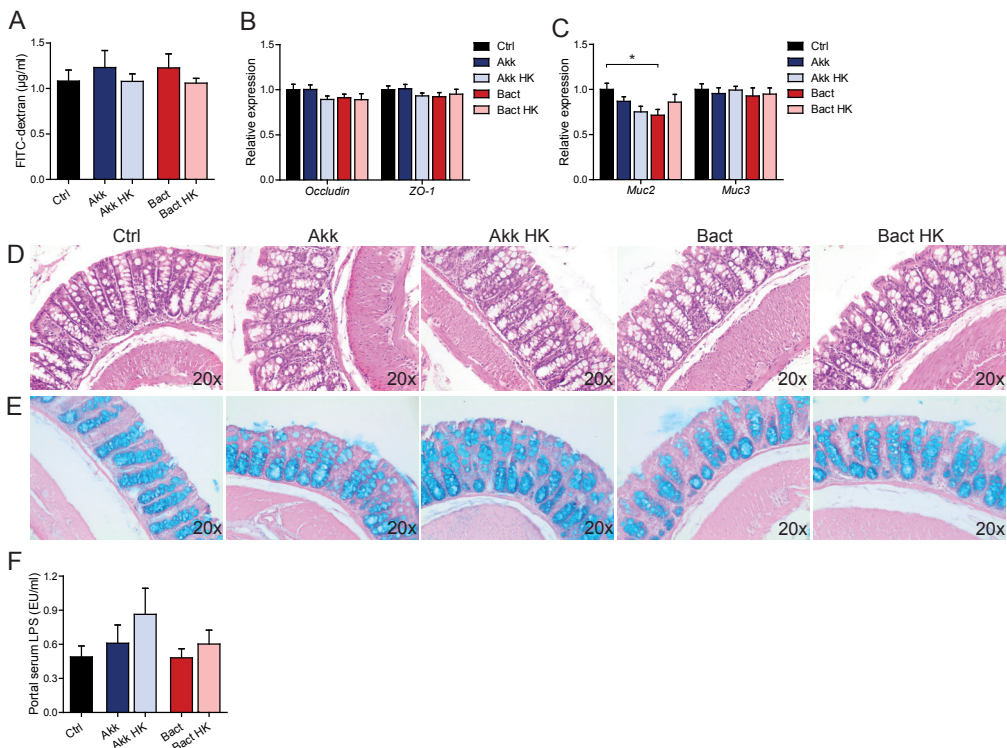


Figure 5. Administration of *A. muciniphila* and *B. thetaiotaomicron* does not alter gut permeability and LPS levels in portal serum

(A) Intestinal permeability as assessed by plasma FITC-dextran concentration 1 hour after oral administration. Relative expression of (B) tight junction and (C) mucin genes. Gene expression levels in CTRL mice were set at 1. Representative pictures of the colon stained with (D) H&E and (E) Alcian blue. (F) LPS concentration in portal serum. Data are presented as mean \pm SEM. Differences were evaluated for statistical significance by one-way ANOVA followed by Tukey's post hoc multiple comparison test. * $p < 0.05$.

muciniphila or *B. thetaiotaomicron* did not significantly affect obesity, features of NAFLD, gut permeability, and portal LPS levels.

Discussion

Previously, the effect of *A. muciniphila* supplementation was studied in lean mice that were fed a high-fat diet in a parallel with supplementation with *A. muciniphila* (15, 25–27). To our knowledge, this is the first time that the metabolic effects of *A. muciniphila* or *B. thetaiotaomicron* are investigated in obese mice. In our study, mice were first fed a high fat/high cholesterol/high fructose diet for 13 weeks to induce obesity-related NAFLD, followed by daily administration of live or heat-killed *A. muciniphila* or *B. thetaiotaomicron*. It was observed that treatment of mice with *A. muciniphila* or *B. thetaiotaomicron* did not affect bodyweight, gut barrier function, or features of NAFLD.

In several studies, obesity was shown to be associated with a decrease in the relative abundance of *A. muciniphila* (17, 22, 43). Treatment of mice on a high-fat diet with live *A. muciniphila* was shown to suppress diet-induced obesity (15, 26). Recently, Plovier *et al.* (25) demonstrated that pasteurized, but not autoclaved *A. muciniphila*, has a stronger effect on bodyweight and glucose homeostasis than live *A. muciniphila* (25). The reduction in bodyweight was associated with an increase in fecal energy excretion and was suggested to be mediated by Amuc_1100, a protein located on the outer membrane of *A. muciniphila* that resists denaturation at temperatures of pasteurization (25). In our study, we also made use of pasteurized *A. muciniphila* as control for the treatment of live *A. muciniphila*. However, neither live or pasteurized *A. muciniphila* significantly affected bodyweight. Several factors may explain the difference in effect of *A. muciniphila* on bodyweight in obese mice as compared to lean mice, despite live *A. muciniphila* administration effectively increasing the number of *A. muciniphila* in the colon. First, obese mice have a much thinner mucus layer than lean mice (15). As *A. muciniphila* usually resides in the mucus layer and obtains energy from the mucus layer, it is very likely that colonization in a gut with a thin mucus layer is more difficult and takes more time than in a gut with a thicker mucus layer. Secondly, the gut microbial composition is profoundly different between obese and lean mice (44, 45). Therefore, *A. muciniphila* has to compete with other microbes than in lean mice. Since the exact mechanism by which *A. muciniphila* exerts beneficial effects on host metabolism in lean mice is currently unknown, it cannot be excluded that the effects of *A. muciniphila* may be (partly) mediated by other microbial communities that either directly or indirectly affect host metabolism. The absence of an effect of *A. muciniphila* administration on bodyweight gain and glucose tolerance in *Apoe*^{-/-} mice (27) could therefore possibly also be explained by differences in the gut microbial composition between different mice strains (26, 46).

In comparison to *A. muciniphila*, *B. thetaiotaomicron* was not able to colonize the colon in 5 weeks of *B. thetaiotaomicron* administration. Whereas two studies reported that *B. thetaiotaomicron* administration promotes adiposity (1, 33), *B. thetaiotaomicron* had no effect on bodyweight in our study. Since the promotion of adiposity upon *B. thetaiotaomicron*

treatment was observed in germ-free mice, it can be speculated that in our study, other microbes may have hampered the effect of *B. thetaiotaomicron*. Future studies should address whether *B. thetaiotaomicron* may affect bodyweight in conventionally-raised lean mice, which have a different gut microbiota as compared to obese mice.

In our study, we did not find a significant effect of either *A. muciniphila* or *B. thetaiotaomicron* administration on features of NAFLD, using a protocol of daily administration of 2×10^8 cells for 7 days a week during 5 weeks. Interestingly, in a recent study, three times administration of 1.5×10^9 cells *A. muciniphila* to mice with alcoholic fatty liver disease led to improved liver injury markers and hepatic inflammation (47). Accordingly, it is possible that higher doses of *A. muciniphila* are needed to show an effect on hepatic fibrosis or possibly for a longer treatment duration.

A. muciniphila and *B. thetaiotaomicron* are mucin-degrading bacteria. Accordingly, the effects of *A. muciniphila* on the host are suggested to be mediated by improvements in the gut barrier. The gut barrier physically separates the gut lumen from the underlying tissues of the body and is composed of a mucus layer, epithelial cells and the lamina propria. The gut barrier integrity is mainly maintained by tight junction protein complexes that seal adjacent epithelial cells, which is complemented by the overlying mucus layer to add further protection. The expression of tight junctions proteins and the quantitation of mucus layer thickness are indirect measures for gut barrier function. To directly assess the functionality of the gut barrier, gut permeability tests have been developed (48, 49). A commonly used strategy to assess gut permeability is by administering a non-digestible marker, such as FITC-dextran, which will only end up in the circulation when the gut barrier function is diminished. In our study, plasma FITC-dextran levels were not altered upon administration of live *A. muciniphila* or *B. thetaiotaomicron*. Although we did find a significant reduction in the expression of the main secretory mucin *Muc2* upon live *B. thetaiotaomicron* administration, this result did not translate in a different gut barrier function. The lack of an effect of *A. muciniphila* on gut permeability is in accordance with a recently published study in which mice were first fed a high fat diet for 4 weeks and then treated with live *A. muciniphila* for 6 weeks (16). In contrast, Li *et al.* showed that 8 weeks of *A. muciniphila* treatment significantly improved gut permeability in mice fed a high fat diet (27). Considering the high dose and the long treatment duration used by Li *et al.*, it is possible that higher doses and longer treatment durations are needed for an effect of *A. muciniphila* on gut barrier function in obese mice.

Disruption of the gut barrier may lead to increased translocation of harmful substances, such as LPS, to the circulation. Previously, it has been shown that elevated plasma LPS levels may be involved in mediating the harmful effect of high-fat induced obesity on insulin resistance (29). In addition, LPS has also been suggested to mediate the effects of the gut microbiota on NAFLD (50, 51). While administration of *A. muciniphila* to lean mice caused

a reduction in portal LPS levels (15, 25, 27), in obese mice we did not find a difference in portal LPS levels, possible due to the lack of an effect on gut barrier function.

In our study, all treatments caused a substantial decrease in bodyweight during the first week of oral gavage. Oral gavage is considered as a potentially stressful procedure to mice and may therefore explain the bodyweight loss. Though, since this reduction in bodyweight occurred in all groups, we do not believe that this may have influenced the outcome of the study.

In conclusion, treatment of obese mice with 2×10^8 CFU of *A. muciniphila* or *B. thetaiotaomicron* for 5 weeks did not affect obesity, gut barrier function, or features of NAFLD. Whether a higher dose or longer duration of *A. muciniphila* treatment may affect hepatic fibrosis remains to be investigated.

Acknowledgements

This research was supported by The Netherlands Cardiovascular Research Committee IN-CONTROL grant (CVON 2012-03).

References

1. Bäckhed, F., H. Ding, T. Wang, L. V Hooper, G. Y. Koh, A. Nagy, C. F. Semenkovich, and J. I. Gordon. 2004. The gut microbiota as an environmental factor that regulates fat storage. *Proc. Natl. Acad. Sci. U. S. A.* **101**: 15718–15723.
2. Cani, P. D., R. Bibiloni, C. Knauf, A. M. Neyrinck, and N. M. Delzenne. 2008. Changes in Gut Microbiota Control Metabolic Endotoxemia-Induced Inflammation in High-Fat Diet – Induced Obesity and Diabetes in Mice. *Diabetes*. **57**: 1470–1481.
3. Janssen, A. W. F., and S. Kersten. 2015. The role of the gut microbiota in metabolic health. *FASEB J.* **29**: 3111–3123.
4. Ridaura, V. K., J. J. Faith, F. E. Rey, J. Cheng, A. E. Duncan, A. L. Kau, N. W. Griffin, V. Lombard, B. Henrissat, J. R. Bain, M. J. Muehlbauer, O. Ilkayeva, C. F. Semenkovich, K. Funai, D. K. Hayashi, B. J. Lyle, M. C. Martini, L. K. Ursell, J. C. Clemente, W. Van Treuren, W. a Walters, R. Knight, C. B. Newgard, A. C. Heath, and J. I. Gordon. 2013. Gut microbiota from twins discordant for obesity modulate metabolism in mice. *Science*. **341**: 1241214.
5. Bäckhed, F., J. K. Manchester, C. F. Semenkovich, and J. I. Gordon. 2007. Mechanisms underlying the resistance to diet-induced obesity in germ-free mice. *Proc. Natl. Acad. Sci. U. S. A.* **104**: 979–84.
6. Rabot, S., M. Membrez, A. Bruneau, P. Gérard, T. Harach, M. Moser, F. Raymond, R. Mansourian, and C. J. Chou. 2010. Germ-free C57BL/6J mice are resistant to high-fat-diet-induced insulin resistance and have altered cholesterol metabolism. *FASEB J.* **24**: 4948–59.
7. Mencarelli, A., S. Cipriani, B. Renga, A. Bruno, C. D'Amore, E. Distrutti, and S. Fiorucci. 2012. VSL#3 Resets Insulin Signaling and Protects against NASH and Atherosclerosis in a Model of Genetic Dyslipidemia and Intestinal Inflammation. *PLoS One*. **7**: e45425.
8. Chan, Y. K., H. El-Nezami, Y. Chen, K. Kinnunen, P. V. Kirjavainen, J. Baglione, J. Smith, C. Bian, Y. Wu, P. Chen, E. Blessing, M. Preusch, R. Kranzhofer, R. Kinscherf, N. Marx, M. Rosenfeld, B. Isermann, C. Weber, J. Kreuzer, J. Grafe, H. Katus, F. Bea, P. Cani, N. Delzenne, J. Amar, R. Burcelin, R. Dhiman, B. Rana, S. Agrawal, A. Garg, M. Chopra, K. Thumburu, A. Khattri, S. Malhotra, A. Duseja, Y. Chawla, F. Fak, F. Backhed, R. Fedorak, B. Feagan, N. Hotte, D. Leddin, L. Dieleman, D. Petrunia, R. Enns, A. Bitton, N. Chiba, P. Pare, A. Rostom, J. Marshall, et al. 2016. Probiotic mixture VSL#3 reduce high fat diet induced vascular inflammation and atherosclerosis in ApoE^{-/-} mice. *AMB Express*. **6**.
9. Alisi, A., G. Bedogni, G. Baviera, V. Giorgio, E. Porro, C. Paris, P. Giammaria, L. Reali, F. Anania, and V. Nobili. 2014. Randomised clinical trial: The beneficial effects of VSL#3 in obese children with non-alcoholic steatohepatitis. *Aliment. Pharmacol. Ther.* **39**: 1276–1285.
10. Janssen, A. W. F., T. Houben, S. Katiraei, W. Dijk, L. Boutens, N. van der Bolt, Z. Wang, M. J. Brown, S. L. Hazen, S. Mandard, R. Shiri-Sverdlov, F. Kuipers, K. W. van Dijk, J. Vervoort, and S. K. Rinke Stienstra, Guido JEJ Hooiveld. 2017. Modulation of the gut microbiota impacts non-alcoholic fatty liver disease: a potential role for bile acids. *J. Lipid Res.* **58**:1399-1416.
11. Belzer, C., and W. M. de Vos. 2012. Microbes inside--from diversity to function: the case of Akkermansia. *ISME J.* **6**: 1449–58.
12. Derrien, M., C. Belzer, and W. M. de Vos. 2016. Akkermansia muciniphila and its role in regulating host functions. *Microb. Pathog.*
13. Collado, M. C., M. Derrien, E. Isolauri, W. M. De Vos, and S. Salminen. 2007. Intestinal integrity and Akkermansia muciniphila, a mucin-degrading member of the intestinal microbiota present in infants, adults, and the elderly. *Appl. Environ. Microbiol.* **73**: 7767–7770.
14. Derrien, M., M. C. Collado, K. Ben-Amor, S. Salminen, and W. M. De Vos. 2008. The mucin degrader Akkermansia muciniphila is an abundant resident of the human intestinal tract. *Appl. Environ. Microbiol.* **74**: 1646–1648.
15. Everard, A., C. Belzer, L. Geurts, J. P. Ouwerkerk, C. Druart, L. B. Bindels, Y. Guiot, M. Derrien, G. G. Muccioli, N. M. Delzenne, W. M. de Vos, and P. D. Cani. 2013. Cross-talk between Akkermansia muciniphila and intestinal epithelium controls diet-induced obesity. *Proc. Natl. Acad. Sci. U. S. A.* **110**: 9066–71.
16. Shin, N. R., J. C. Lee, H. Y. Lee, M. S. Kim, T. W. Whon, M. S. Lee, and J. W. Bae. 2014. An increase in the Akkermansia spp. population induced by metformin treatment improves glucose homeostasis in diet-induced obese mice. *Gut*. **63**: 727–735.
17. Schneeberger, M., A. Everard, A. G. Gómez-Valadés, S. Matamoros, S. Ramírez, N. M. Delzenne, R. Gomis, M. Claret, and P. D. Cani. 2015. Akkermansia muciniphila inversely correlates with the onset of inflammation, altered adipose tissue metabolism and metabolic disorders during obesity in mice. *Sci. Rep.* **5**: 16643.
18. Dao, M. C., A. Everard, J. Aron-Wisniewsky, N. Sokolovska, E. Prifti, E. O. Verger, B. D. Kayser, F. Levenez, J. Chilloux, L. Hoyle, M. E. Dumas, S. W. Rizkalla, J. Dore, P. D. Cani, and K. Clement. 2016. Akkermansia muciniphila and improved metabolic health during a dietary intervention in obesity:

- relationship with gut microbiome richness and ecology. *Gut*. **65**: 426–436.
19. Karlsson, C. L. J., J. Onnerfält, J. Xu, G. Molin, S. Ahrné, and K. Thorngren-Jerneck. 2012. The microbiota of the gut in preschool children with normal and excessive body weight. *Obesity (Silver Spring)*. **20**: 2257–61.
 20. Santacruz, A., M. C. Collado, L. García-Valdés, M. T. Segura, J. A. Martín-Lagos, T. Anjos, M. Martí-Romero, R. M. Lopez, J. Florido, C. Campoy, and Y. Sanz. 2010. Gut microbiota composition is associated with body weight, weight gain and biochemical parameters in pregnant women. *Br. J. Nutr.* **104**: 83–92.
 21. de la Cuesta-Zuluaga, J., N. T. Mueller, V. Corrales-Agudelo, E. P. Velásquez-Mejía, J. A. Carmona, J. M. Abad, and J. S. Escobar. 2017. Metformin Is Associated With Higher Relative Abundance of Mucin-Degrading Akkermansia muciniphila and Several Short-Chain Fatty Acid – Producing Microbiota in the Gut. *Diabetes Care*. **40**: 1–9.
 22. Zhang, H., J. K. DiBaise, a Zuccolo, D. Kudrna, M. Braidotti, Y. Yu, P. Parameswaran, M. D. Crowell, R. Wing, B. E. Rittmann, and R. Krajmalnik-Brown. 2009. Human gut microbiota in obesity and after gastric bypass. *Proc Natl Acad Sci U S A*. **106**: 2365–2370.
 23. Remely, M., I. Tesar, B. Hippe, S. Gnauer, P. Rust, and A. G. Haslberger. 2015. Gut microbiota composition correlates with changes in body fat content due to weight loss. *Benef. Microbes*. **6**: 431–439.
 24. Zhao, S., W. Liu, J. Wang, J. Shi, Y. Sun, W. Wang, G. Ning, R. Liu, J. Hong, M. Diseases, and M. Diseases. 2017. Akkermansia muciniphila Improves Metabolic Profiles by Reducing Inflammation in Chow Diet-Fed Mice. *J. Mol. Endocrinol.* **58**: 1–14.
 25. Plovier, H., A. Everard, C. Druart, C. Depommier, M. Van Hul, L. Geurts, J. Chilloux, N. Ottman, T. Duparc, L. Lichtenstein, A. Myridakis, N. M. Delzenne, J. Klievink, A. Bhattacharjee, K. C. H. van der Ark, S. Aalvink, L. O. Martinez, M.-E. Dumas, D. Maiter, A. Loumaye, M. P. Hermans, J.-P. Thissen, C. Belzer, W. M. de Vos, and P. D. Cani. 2017. A purified membrane protein from Akkermansia muciniphila or the pasteurized bacterium improves metabolism in obese and diabetic mice. *Nat. Med.* **23**: 107–113.
 26. Org, E., B. W. Parks, J. W. J. Joo, B. Emert, W. Schwartzman, E. Y. Kang, M. Mehrabian, C. Pan, R. Knight, R. Gunsalus, T. A. Drake, E. Eskin, and A. J. Lusis. 2015. Genetic and environmental control of host-gut microbiota interactions. *Genome Res*. **25**: 1558–1569.
 27. Li, J., S. Lin, P. M. Vanhoutte, C. W. Woo, and A. Xu. 2016. Akkermansia Muciniphila Protects Against Atherosclerosis by Preventing Metabolic Endotoxemia-Induced Inflammation in Apoe ^{-/-} Mice. *Circulation*. **133**: 2434–2446.
 28. Derrien, M., E. E. Vaughan, C. M. Plugge, and W. M. de Vos. 2004. Akkermansia muciniphila gen. nov., sp. nov., a human intestinal mucin-degrading bacterium. *Int. J. Syst. Evol. Microbiol.* **54**: 1469–1476.
 29. Cani, P. D., J. Amar, M. A. Iglesias, M. Poggi, C. Knauf, D. Bastelica, A. M. Neyrinck, F. Fava, K. M. Tuohy, C. Chabo, T. Sulpice, B. Chamontin, G. R. Gibson, L. Casteilla, N. M. Delzenne, and M. C. Alessi. 2007. Metabolic endotoxemia initiates obesity and insulin resistance. *Diabetes*. **56**: 1761–1772.
 30. Maier, E., R. C. Anderson, and N. C. Roy. 2015. Understanding how commensal obligate anaerobic bacteria regulate immune functions in the large intestine. *Nutrients*. **7**: 45–73.
 31. Sonnenburg, J. L., J. Xu, D. D. Leip, C.-H. Chen, B. P. Westover, J. Weatherford, J. D. Buhler, and J. I. Gordon. 2005. Glycan foraging in vivo by an intestine-adapted bacterial symbiont. *Science*. **307**: 1955–9.
 32. Haro, C., S. Garcia-Carpintero, J. F. Alcalá-Díaz, F. Gomez-Delgado, J. Delgado-Lista, P. Perez-Martinez, O. a Rangel Zuniga, G. M. Quintana-Navarro, B. B. Landa, J. C. Clemente, J. Lopez-Miranda, A. Camargo, and F. Perez-Jimenez. 2015. The gut microbial community in metabolic syndrome patients is modified by diet. *J. Nutr. Biochem.* **27**: 27–31.
 33. Samuel, B. S., and J. I. Gordon. 2006. A humanized gnotobiotic mouse model of host-archaeal-bacterial mutualism. *Proc. Natl. Acad. Sci. U. S. A.* **103**: 10011–6.
 34. Kelly, D., J. I. Campbell, T. P. King, G. Grant, E. a Jansson, A. G. P. Coutts, S. Pettersson, and S. Conway. 2004. Commensal anaerobic gut bacteria attenuate inflammation by regulating nuclear-cytoplasmic shuttling of PPAR-gamma and RelA. *Nat. Immunol.* **5**: 104–12.
 35. Hooper, L. V., T. S. Stappenbeck, C. V. Hong, and J. I. Gordon. 2003. Angiogenins: a new class of microbicidal proteins involved in innate immunity. *Nat. Immunol.* **4**: 269–273.
 36. Wrzosek, L., S. Miquel, M.-L. Noordine, S. Bouet, M. Joncquel Chevalier-Curt, V. Robert, C. Philippe, C. Bridonneau, C. Cherbuy, C. Robbe-Masselot, P. Langella, and M. Thomas. 2013. Bacteroides thetaiotaomicron and Faecalibacterium prausnitzii influence the production of mucus glycans and the development of goblet cells in the colonic epithelium of a gnotobiotic model rodent. *BMC Biol.* **11**: 61.
 37. Takahashi, Y., and T. Fukusato. 2014. Histopathology of nonalcoholic fatty liver disease/nonalcoholic steatohepatitis. *World J. Gastroenterol.* **20**: 15539–15548.
 38. Bashiardes, S., H. Shapiro, S. Rozin, O. Shibolet, and E. Elinav. 2016. Non-alcoholic fatty liver and the gut microbiota. *Mol. Metab.* **5**: 782–794.
 39. Jiang, W., N. Wu, X. Wang, Y. Chi, Y. Zhang, X. Qiu, Y. Hu, J. Li, and Y. Liu. 2015. Dysbiosis gut microbiota

- associated with inflammation and impaired mucosal immune function in intestine of humans with non-alcoholic fatty liver disease. *Sci. Rep.* 5: 8096.
40. Smith, C. J., S. M. Markowitz, and F. L. Macrina. 1981. Transferable tetracycline resistance in *Clostridium difficile*. *Antimicrob. Agents Chemother.* 19: 997–1003.
41. Suzuki, M. T., L. T. Taylor, and E. F. DeLong. 2000. Quantitative analysis of small-subunit rRNA genes in mixed microbial populations via 5'-nuclease assays. *Appl. Environ. Microbiol.* 66: 4605–4614.
42. Weisburg, W. G., S. M. Barns, D. A. Pelletier, and D. J. Lane. 1991. 16S ribosomal DNA amplification for phylogenetic study. *J. Bacteriol.* 173: 697–703.
43. Borgo, F., E. Verduci, A. Riva, C. Lassandro, E. Riva, G. Morace, and E. Borghi. 2016. Relative Abundance in Bacterial and Fungal Gut Microbes in Obese Children: A Case Control Study. *Child. Obes.* 13: 78–84.
44. Ley, R. E., F. Bäckhed, P. Turnbaugh, C. a Lozupone, R. D. Knight, and J. I. Gordon. 2005. Obesity alters gut microbial ecology. *Proc. Natl. Acad. Sci. U. S. A.* 102: 11070–5.
45. Turnbaugh, P. J., F. Bäckhed, L. Fulton, and J. I. Gordon. 2008. Diet-Induced Obesity Is Linked to Marked but Reversible Alterations in the Mouse Distal Gut Microbiome. *Cell Host Microbe.* 3: 213–223.
46. Campbell, J. H., C. M. Foster, T. Vishnivetskaya, A. G. Campbell, Z. K. Yang, A. Wymore, A. V. Palumbo, E. J. Chesler, and M. Podar. 2012. Host genetic and environmental effects on mouse intestinal microbiota. *ISME J.* 6: 2033–2044.
47. Grander, C., T. E. Adolph, V. Wieser, P. Lowe, L. Wrzosek, B. Gyongyosi, D. V Ward, F. Grabherr, R. R. Gerner, A. Pfister, B. Enrich, D. Ciocan, S. Macheiner, L. Mayr, M. Drach, P. Moser, A. R. Moschen, G. Perlemuter, G. Szabo, A. M. Cassard, and H. Tilg. 2017. Recovery of ethanol-induced *Akkermansia muciniphila* depletion ameliorates alcoholic liver disease. *Gut.* 1–11.
48. Robinson, K., Z. Deng, Y. Hou, and G. Zhang. 2015. Regulation of the Intestinal Barrier Function by Host Defense Peptides. *Front. Vet. Sci.* 2: 1–17.
49. Bischoff, S. C., G. Barbara, W. Buurman, T. Ockhuizen, J.-D. Schulzke, M. Serino, H. Tilg, A. Watson, and J. M. Wells. 2014. Intestinal permeability – a new target for disease prevention and therapy. *BMC Gastroenterol.* 14: 189.
50. Douhara, A., K. Moriya, H. Yoshiji, R. Noguchi, T. Namisaki, M. Kitade, K. Kaji, Y. Aihara, N. Nishimura, K. Takeda, Y. Okura, H. Kawaratani, and H. Fukui. 2015. Reduction of endotoxin attenuates liver fibrosis through suppression of hepatic stellate cell activation and remission of intestinal permeability in a rat non-alcoholic steatohepatitis model. *Mol. Med. Rep.* 11: 1693–1700.
51. Lau, E., D. Carvalho, and P. Freitas. 2015. Gut Microbiota: Association with NAFLD and Metabolic Disturbances. *Biomed Res. Int.* 2015.

Supplemental table

Supplemental table 1. Primer sequences used for qPCR

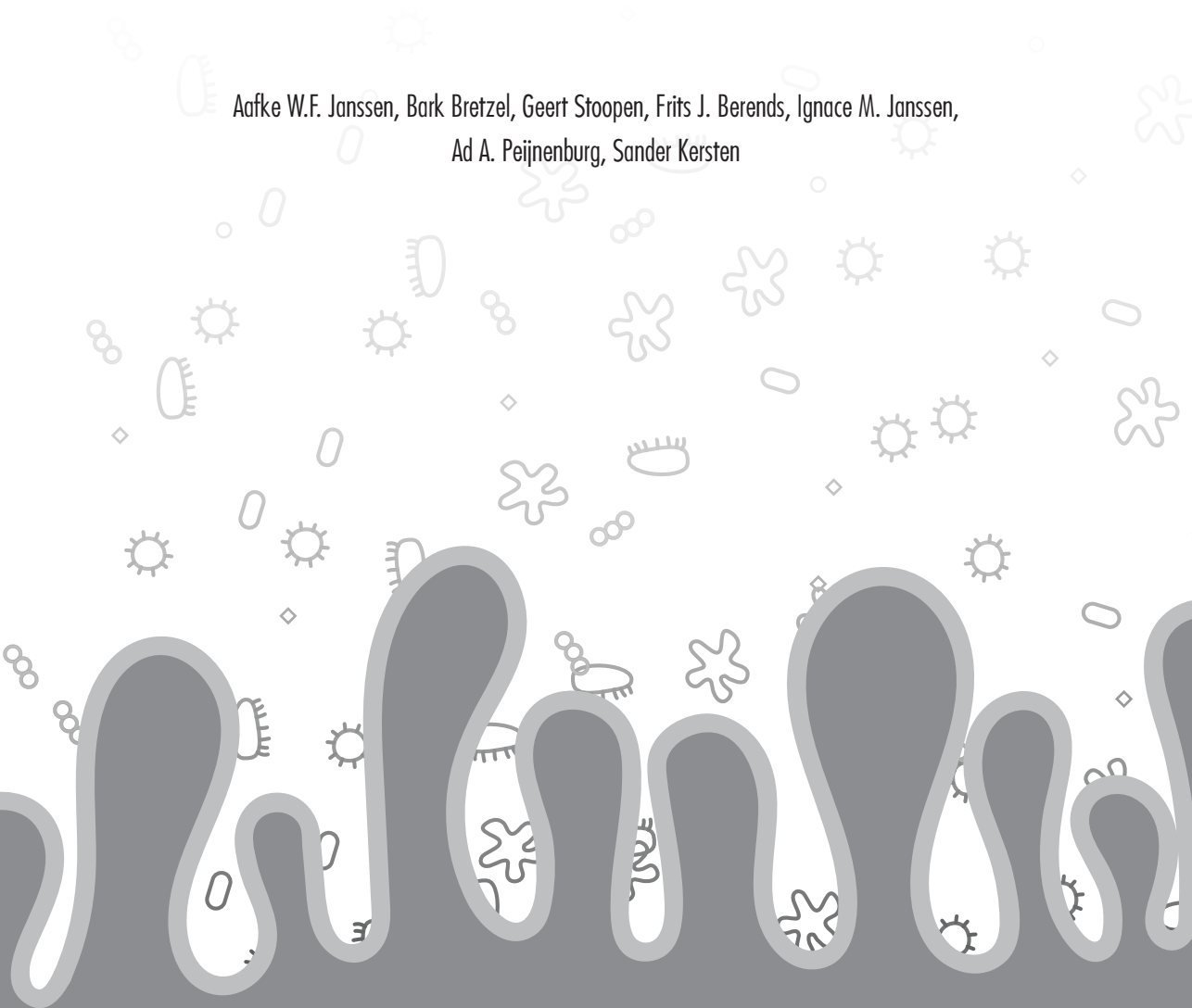
Name	Primer Sequence	
	Forward	Reverse
<i>m36b4</i>	ATGGGTACAAGCGCGTCCTG	GCCTTGACCTTTTCAGTAAG
<i>mCd68</i>	CCAATTCAGGTGGAAGAAA	CTCGGGCTCTGATGTAGGTC
<i>mF4/80</i>	CTTTGGCTATGGGCTTCCAGTC	GCAAGGAGGACAGAGTTTATCGTG
<i>mCd11c</i>	CTGGATAGCCTTTCTTCTGCTG	GCACACTGTGTCCGAActCA
<i>mCd206</i>	GCTTCCGTCACCCTGTATGC	GTGTGTcATTCTTACACTCCC
<i>mMcp-1</i>	CCCAATGAGTAGGCTGGAGA	TCTGGACCCATTcCTTCTTG
<i>mTnfa</i>	CAACCTCCTCTCTGCCGTCAA	TGACTCCAAAGTAGACCTGCCC
<i>mIl-1β</i>	CAGGCAGGCAGTATCACTCA	AGGTGCTCATGTCCCTCATCC
<i>mIl-1ra</i>	AAATCTGCTGGGGACCTTAC	TGAGCTGGTTGTTTCTCAGG
<i>mCol1a1</i>	TGTGTGCGATGACGTGCAAT	GGGTCCCTCGACTCCTACA
<i>mαSma</i>	GTCCCAGACATCAGGGAGTAA	TCGGATACTTCAGCGTCAGGA
<i>mTimp1</i>	GCAACTCGGACCTGGTCATAA	CGGCCCGTGATGAGAAACT
<i>mTgf-β1</i>	CCGCAACAACGCCATCTATG	CTCTGCACGGGACAGCAAT
<i>mOccludin</i>	CTGGATCTATGTACGGCTCACA	TCCACGTAGAGACCAGTACCT
<i>mZO-1</i>	GAGCGGGCTACCTTACTGAAC	GTCATCTCTTTCCGAGGCATTAG
<i>mMuc2</i>	AGGGCTCGGAACTCCAGAAA	CCAGGGAATCGGTAGACATCG
<i>mMuc3</i>	AGCGTAGAGATAGAGCCGACA	TCTTCAGACTTTCGGTCCTGTAG

6



The impact of PPAR α activation on whole genome gene expression in human precision cut liver slices

Aafke W.F. Janssen, Bark Bretzel, Geert Stoopen, Frits J. Berends, Ignace M. Janssen,
Ad A. Peijnenburg, Sander Kersten



Abstract

Background

Studies in mice have shown that PPAR α is an important regulator of lipid metabolism in liver and key transcription factor involved in the adaptive response to fasting. However, much less is known about the role of PPAR α in human liver.

Methods

Here we set out to study the function of PPAR α in human liver via analysis of whole genome gene regulation in human liver slices treated with the PPAR α agonist Wy14643.

Results

Quantitative PCR indicated that PPAR α is well expressed in human liver and human liver slices and that the classical PPAR α targets PLIN2, VLDLR, ANGPTL4, CPT1A and PDK4 are robustly induced by PPAR α activation. Transcriptomics analysis indicated that 617 genes were upregulated and 665 genes were downregulated by PPAR α activation (q value<0.05). Many genes induced by PPAR α activation were involved in lipid metabolism (ACSL5, AGPAT9, FADS1, SLC27A4), xenobiotic metabolism (POR, ABCC2, CYP3A5) or the unfolded protein response, whereas most of the downregulated genes were involved in immune-related pathways. Among the most highly repressed genes upon PPAR α activation were several chemokines (e.g. CXCL9-11, CCL8, CX3CL1, CXCL6), interferon γ -induced genes (e.g. IFITM1, IFIT1, IFIT2, IFIT3) and numerous other immune-related genes (e.g. TLR3, NOS2, and LCN2). Comparative analysis of gene regulation by Wy14643 between human liver slices and primary human hepatocytes showed that down-regulation of gene expression by PPAR α is much better captured by liver slices as compared to primary hepatocytes. In particular, PPAR α activation markedly suppressed immunity/inflammation-related genes in human liver slices but not in primary hepatocytes. Finally, several putative new target genes of PPAR α were identified that were commonly induced by PPAR α activation in the two human liver model systems, including TSKU, RHOF, CA12 and VSIG10L.

Conclusion

Our manuscript demonstrates the suitability and superiority of human liver slices over primary hepatocytes for studying the functional role of PPAR α in human liver. Our data underscore the major role of PPAR α in regulation of hepatic lipid and xenobiotic metabolism in human liver and reveal a marked immuno-suppressive/anti-inflammatory effect of PPAR α in human liver slices that may be therapeutically relevant for non-alcoholic fatty liver disease.

Introduction

The Peroxisome Proliferator Activated Receptors (PPARs) represent an important group of receptors involved in mediating the pleiotropic effects of various environmental contaminants, food components, and drugs [1]. PPARs are members of the nuclear receptor superfamily and induce the expression of numerous genes by functioning as ligand-activated transcription factors. The ligands for PPARs encompass a range of synthetic compounds and endogenous lipids, including various fatty acids and eicosanoids. Three different PPARs can be distinguished: PPAR α , PPAR δ , and PPAR γ , each characterized by a distinct tissue expression profile and set of functions [2, 3]. Multiple functions have been assigned to PPAR δ , including roles in inflammation, lipid metabolism and cancer [4]. Due to the ubiquitous expression pattern and diverse cellular actions of PPAR δ , there is no single descriptor that appropriately captures its biological function. PPAR γ is known as the key transcriptional regulator that drives adipogenesis [5], the process by which fat cells differentiate from pre-adipocytes into mature adipose cells. Apart from adipocytes, PPAR γ is also expressed in a limited number of other cell types where it exerts anti-inflammatory actions and promotes lipid storage [6]. By serving as the molecular target of the insulin-sensitizing drugs pioglitazone and rosiglitazone, PPAR γ is one of the key receptors in the pharmacological treatment of type 2 diabetes [7].

PPAR α is best known for its role in the liver, where it acts as the master regulator of lipid metabolism, especially during fasting [8-10]. Fasting is associated with dramatic changes in lipid handling in liver, which is coordinated by PPAR α . Specifically, low and high throughput gene expression analyses have demonstrated that PPAR α governs expression of numerous genes involved in nearly every single aspect of lipid metabolism, including fatty acid uptake, mitochondrial and peroxisomal fatty acid oxidation, ketogenesis, and formation and breakdown of triglycerides and lipid droplets [11].

Similar to other members of the PPAR family, PPAR α is activated by a range of different fatty acids and eicosanoids [12-16]. In addition, PPAR α serves as receptor for a diverse array of synthetic compounds collectively referred to as peroxisome proliferators [17]. These include phthalates, insecticides, herbicides, surfactants, organic solvents, and hypolipidemic fibrate drugs. Fibrates have been used for several decades mainly for their ability to lower circulating triglycerides [18]. More recently, pharmacological targeting of PPAR α has shown promise for the treatment of non-alcoholic fatty liver disease. Specifically, the dual PPAR α / δ agonist GFT505 was shown to improve liver dysfunction markers, decrease hepatic lipid accumulation, and reduce inflammatory gene expression in liver in several animal models of non-alcoholic fatty liver disease (NAFLD) [19]. Furthermore, GFT505 treatment lowered liver dysfunction markers and improved hepatic and peripheral insulin sensitivity in human

subjects [19, 20].

Most of our insights into the physiological, toxicological and pharmacological role of PPAR α has been derived from experiments in animals and in particular from rodent studies. These studies have revealed that PPAR α is not only involved in the adaptive response to fasting but also mediates the hepatocarcinogenic effects of peroxisome proliferators [21]. Whether PPAR α exerts similar functions in human liver has been the subject of controversy [22], which has been fueled by the perceived lack of effect of PPAR α agonists on peroxisomal fatty acid oxidation in humans [23], as well as due to the presumed low expression of PPAR α in human liver [24]. However, more recent studies have partly refuted those notions, showing that a) PPAR α expression is similar in mouse and human liver, b) in human hepatocytes PPAR α governs the expression of numerous genes in various lipid metabolic pathways, including peroxisomal fatty acid oxidation [25, 26].

Nevertheless, the absence of more complex human model systems has hampered our ability to gain insight into the molecular function of PPAR α in human liver, in particular with respect to target gene regulation. To overcome this limitation, we collected precision cut liver slices (PCLS) from human subjects and studied the effect of PPAR α activation on gene expression using whole genome expression profiling. In contrast to primary hepatocytes, PCLS mimic the multi-cellularity and structural organization of whole liver and thus represent a superior ex-vivo model system for human liver [27]. So far the use of PCLS for the study of nuclear receptors and specifically PPAR α function has been limited [28-30]. Here we report the use of PCLS in combination with whole genome gene expression profiling to gain insight into PPAR α -mediated gene regulation in human liver.

Materials and methods

Collection of liver biopsies

In all patients a laparoscopic Roux-en-Y Gastric Bypass was performed under general anesthesia as treatment for their morbid obesity. Patients were instructed to fasten for solid foods and liquids starting at the night before surgery. During surgery a biopsy of the liver was obtained with the help of ultrasound dissection (UltraCision®). The biopsy was collected from the liver edge. The majority of the liver biopsies collected (n=15) were immediately frozen in liquid nitrogen and stored at -80°C. The liver biopsies targeted for slicing (n=4) were immediately placed in ice-cold oxygenated Belzer UW Cold Storage Solution (Bridge to Life Ltd, Columbia, SC, USA) and quickly transferred to our laboratory for further processing of PCLS. Only healthy livers were used for slicing. Biopsies were provided by the biobank of the Rijnstate hospital. Collection of biopsies for research purposes into the biobank was approved by the local institutional review board on behalf of the medical ethics review committee of the Radboud University Medical Centre. All patients signed informed consent for collection of the biopsy prior to surgery. Donor characteristics of livers used for slicing are shown in **Table 1**.

Table 1. Donor characteristics of livers used for slicing

Patient	Gender	Age (years)	Body Mass Index (g/m ²)
1	Female	34	41
2	Female	46	43
3	Female	39	35
4	Female	41	38

Preparation and treatment of precision cut liver slices

PCLS were prepared and cultured as described previously [31]. 5 mm cylindrical liver cores were prepared with a surgical biopsy punch and sectioned to 200 μ m slices using a Krumdieck tissue slicer (Alabama Research and Development, Munford, AL, USA) filled with carbonated KHB (pH 7.4, supplemented with 25mM glucose). Liver slices were incubated in William's E Medium (Gibco, Paisley, Scotland) supplemented with penicillin/streptomycin in 6-well plates at 37°C/5% CO₂/80% O₂ under continuous shaking (70 rpm). Duplicate wells were used per donor with 3 liver slices per well. After 1 hour the media was replaced with fresh William's E Medium in the presence or absence of Wy14643 (100 μ M) dissolved in dimethyl sulfoxide (DMSO, final concentration 0.1%). This concentration was chosen based on the affinity of human PPAR α for Wy14643. [32]. After 24 h incubation, liver slices were snap-frozen in liquid nitrogen and stored in -80°C for RNA isolation.

Primary human hepatocytes

The treatment of primary human hepatocytes with Wy14643 has been previously described [26]. Briefly, human hepatocytes from six different donors were purchased from Lonza (Verviers, Belgium). Hepatocytes were isolated with two-step collagenase perfusion method. Cell viability was over 80%. The cells were incubated for 24h in the presence or absence of Wy14643 (50 μ M) dissolved in DMSO, followed by RNA isolation.

RNA isolation and qPCR

Total RNA was isolated using TRIzol reagent (Invitrogen). RNA integrity number was found to be above 7.1 for all samples suggesting that the human liver slices were of good quality. The RNA integrity number is based on a digital electropherogram generated using a Agilent bioanalyzer. It describes the degree of degradation of RNA with level 10 representing completely intact RNA. RNA was reverse transcribed using a iScript cDNA Synthesis Kit (Bio-Rad Laboratories BV, Veenendaal, The Netherlands). Real-time PCR was carried out using SensiMiX (Bioline) on a CFX 384 Bio-Rad thermal cycler (Bio-Rad). 36B4 was used as housekeeping gene. Primers sequences used are shown in **Table 2**.

Table 2. Primer sequences used for qPCR

Name	Primer Sequence	
	Forward	Reverse
<i>36B4</i>	CGGGAAGGCTGTGGTGCTG	GTGAACACAAAGCCCACATTCC
<i>ANGPTL4</i>	CACAGCCTGCAGACACAACCTC	GGAGGCCAAACTGGCTTTGC
<i>PLIN2</i>	ATGGCATCCGTTGCAGTTGAT	GATGGTCTTCACACCGTTCTC
<i>PDK4</i>	TGGAGCATTTCTCGCGCTAC	ACAGGCAATTCTGTGCGCAAA
<i>CPT1A</i>	TCCAGTTGGCTTATCGTGGTG	CTAACGAGGGGTCGATCTTGG
<i>VLDLR</i>	GGTGAAATGATTGTGACAGTGG	GTGAACCTCGTCGGGACTACA

Microarray analysis

Total RNA was purified with RNeasy Minikit columns (Qiagen) and RNA quality was assessed using RNA 6000 Nano chips on the Agilent 2100 Bioanalyzer (Agilent Technologies, Amsterdam, The Netherlands). Purified RNA (100 ng) was labeled with the Ambion WT expression kit (Invitrogen) and hybridized to an Affymetrix Human Gene 1.1 ST array plate (Affymetrix, Santa Clara, CA). Hybridization, washing, and scanning were carried out on an Affymetrix GeneTitan platform according to the instruction by the manufacturer. Arrays were normalized using the Robust Multiarray Average method [33, 34]. Probe sets were defined according to Dai et al.[35]. In this method probes are assigned to Entrez IDs as an unique gene identifier. The P values for the effect of Wy14643 treatment were calculated using an Intensity-Based Moderated T-statistic (IBMT) [36]. The q value was calculated as measure of significance for false discovery rate [37]. The microarray data for the human liver

slices were submitted to the Gene Expression Omnibus (GSE71731). The microarray data for the human primary hepatocytes have been previously submitted to Gene Expression Omnibus (GSE17251).

Gene set enrichment analysis (GSEA) was used to find enriched gene sets in the induced or suppressed genes [38]. Genes were ranked based on the paired IBMT-statistic and subsequently analyzed for over- or underrepresentation in predefined gene sets derived from Gene Ontology, KEGG, National Cancer Institute, PFAM, Biocarta, Reactome and WikiPathways pathway databases. Only gene sets consisting of more than 15 and fewer than 500 genes were taken into account. Statistical significance of GSEA results was determined using 1,000 permutations.

Results

First, we determined the relative expression level of PPAR α in PCLS in comparison with human liver. After correcting for the housekeeping gene 36B4, mRNA levels of PPAR α in human PCLS after 24h incubation were about ten-fold lower as compared to snap-frozen human liver biopsies (**Figure 1A**). To verify that the human liver slices maintain their ability to respond to PPAR α activation, we exposed the PCLS to 100 μ M Wy14643, isolated total RNA and performed qPCR to determine the expression of a number of well-established PPAR α target genes, including PLIN2, VLDLR, ANGPTL4, CPT1A and PDK4 (**Figure 1B**). All PPAR α target genes analyzed showed significant induction following Wy14643 treatment, indicating the validity of our model to study PPAR α -mediated gene regulation.

To study the effect of PPAR α activation on whole genome gene expression we performed microarray analysis. Wy14643-induced changes in expression of the selected PPAR α target genes were very similar between the microarray and qPCR analysis (**Figure 1C**). Using

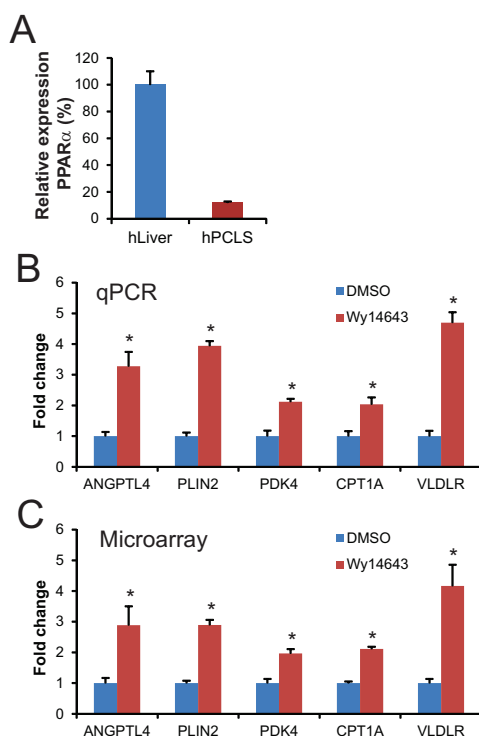


Figure 1. Classical PPAR α targets genes are robustly induced by PPAR α activation in human PCLS

(A) Expression level of PPAR α in human liver biopsies (n=15) and human PCLS (n=5). (B) Gene expression changes of selected PPAR α target genes in human PCLS in response to 24h Wy14643 treatment as determined by quantitative real-time PCR. (C) Gene expression changes of the same genes according to microarray. Error bars represent SEM. Asterisk indicates statistically significant ($P < 0.05$, Students t-test).

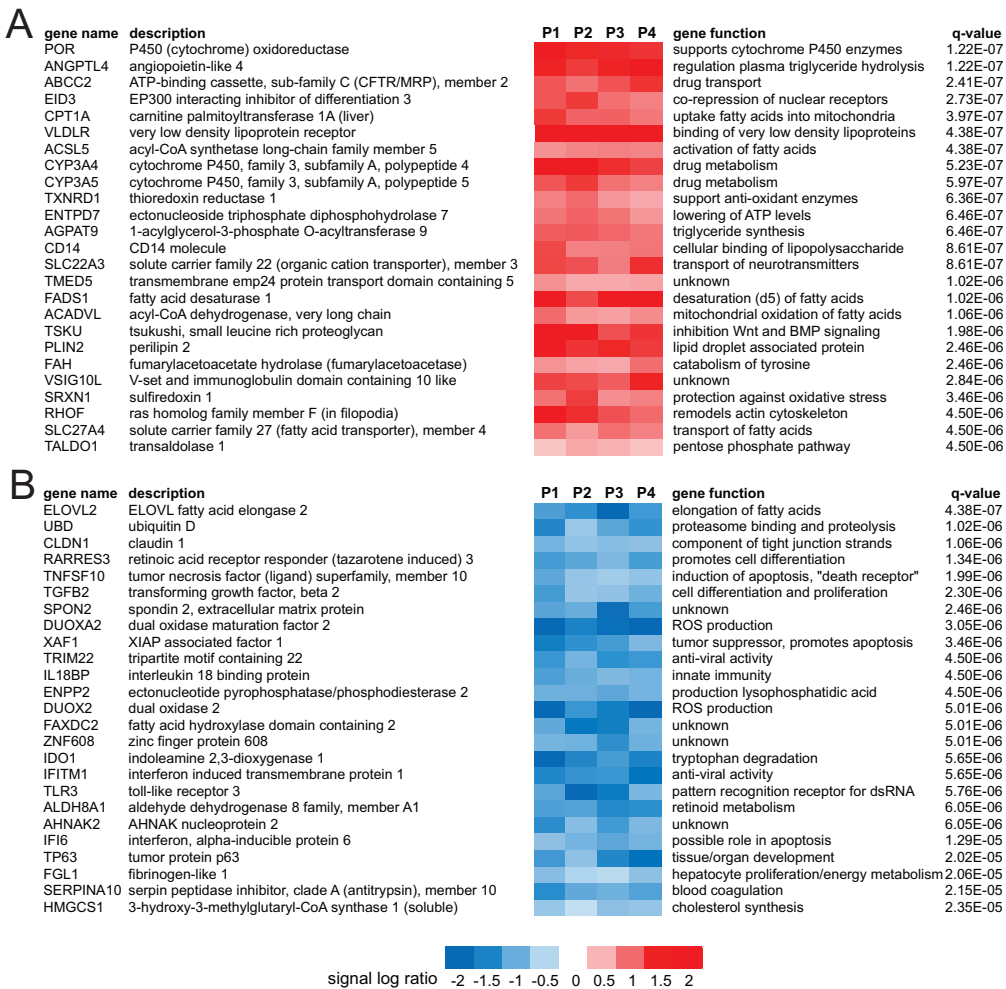


Figure 2. Top 25 genes induced or repressed by Wy14643 in human PCLS

Heatmap showing gene expression changes of the top 25 most significantly induced (A) and repressed (B) genes in human PCLS treated with Wy14643 for 24h, as determined by microarray analysis. Genes were ranked based on statistical significance in the form of q-value (IBMT regularised paired t-test). P1 to P4 represent the four human subjects that donated a liver specimen for preparation of PCLS.

a FDR q-value of 0.05 as cut-off (IBMT regularised paired t-test), the expression of 1282 genes (out of 19654 genes on the array) was found to be significantly altered by Wy14643 treatment, of which 617 genes were upregulated and 665 genes were downregulated. The top 25 of most significantly induced genes, ranked according to statistical significance, are shown in **Figure 2A**. The full list is available as **Supplemental Table 1**. The list includes many well-known PPARα target genes involved in lipid metabolism (e.g. VLDLR, ACADVL, PLIN2, ANGPTL4, CPT1A), as well as many other genes covering a wide variety of biological

functions. In addition, the list includes a number of genes with unknown function. **Figure 2B** shows the top 25 of most significantly repressed genes, many of which are related to immune function and inflammation. The full list of significantly downregulated genes is available as **Supplemental Table 2**.

To gain better insight into the biological function of genes regulated by PPAR α activation in human liver slices, we performed gene set enrichment analysis (GSEA). Pathways related to lipid metabolism or directly involving PPAR α featured prominently among the gene sets induced by Wy14643 (**Figure 3**). Also, several gene sets induced by Wy14643 were related to the unfolded protein response and UPR signaling by IRE1 α and XBP1. Finally, we observed significant enrichment of genes related to oxidative stress and xenobiotic/drug metabolism. Gene sets downregulated by PPAR α activation were all related to immune function and inflammation, illustrating a potent anti-inflammatory/immuno-suppressive action of PPAR α in human liver.

An important goal of the present work was to test the suitability of liver slices as a model to study PPAR α dependent gene regulation and compare it with other available model systems for human liver. To that end, we compared the whole genome expression profiles of human liver slices treated with Wy14643 with the expression profiles of primary human hepatocytes treated with Wy14643. The expression profiles of primary human hepatocytes have been previously published but were re-analyzed [26]. The primary human hepatocytes were treated for the same duration and microarray analysis was performed in the same laboratory on the same microarray platform.

The comparative analysis between primary human hepatocytes and human liver slices was performed on a common gene set of 17351 genes. Using a statistical cut-off of $P < 0.001$ (IBMT regularised paired t-test) combined with a fold-change cut-off of 1.2, we found 347 genes to be upregulated in human liver slices, as compared to 121 genes in the hepatocytes (**Figure 4A**), with an overlap of 47 genes. Remarkably, whereas 401 genes were downregulated by Wy14643 in the liver slices, only 25 genes were downregulated by Wy14643 in the human hepatocytes, with an overlap of only 4 genes. The data indicate that the human liver slices are much more sensitive towards especially downregulation of gene expression by Wy14643 as compared to human hepatocytes. This notion was further supported by correlation analysis in the form of a scatter plot (**Figure 4B**). The upper right portion of the scatter plot was well filled (**Figure 4B**), reflecting common induction by Wy14643 in PCLS and primary hepatocytes, including well-known PPAR α targets such as FABP1, PLIN2, PDK4 and ANGPTL4. In contrast, the lower left portion of the scatter plot was much less filled (**Figure 4B**), reflecting little agreement between PCLS and primary hepatocytes with respect to downregulation of gene expression by Wy14643. In fact, many genes were markedly downregulated by Wy14643 in the liver slices but showed no change in expression

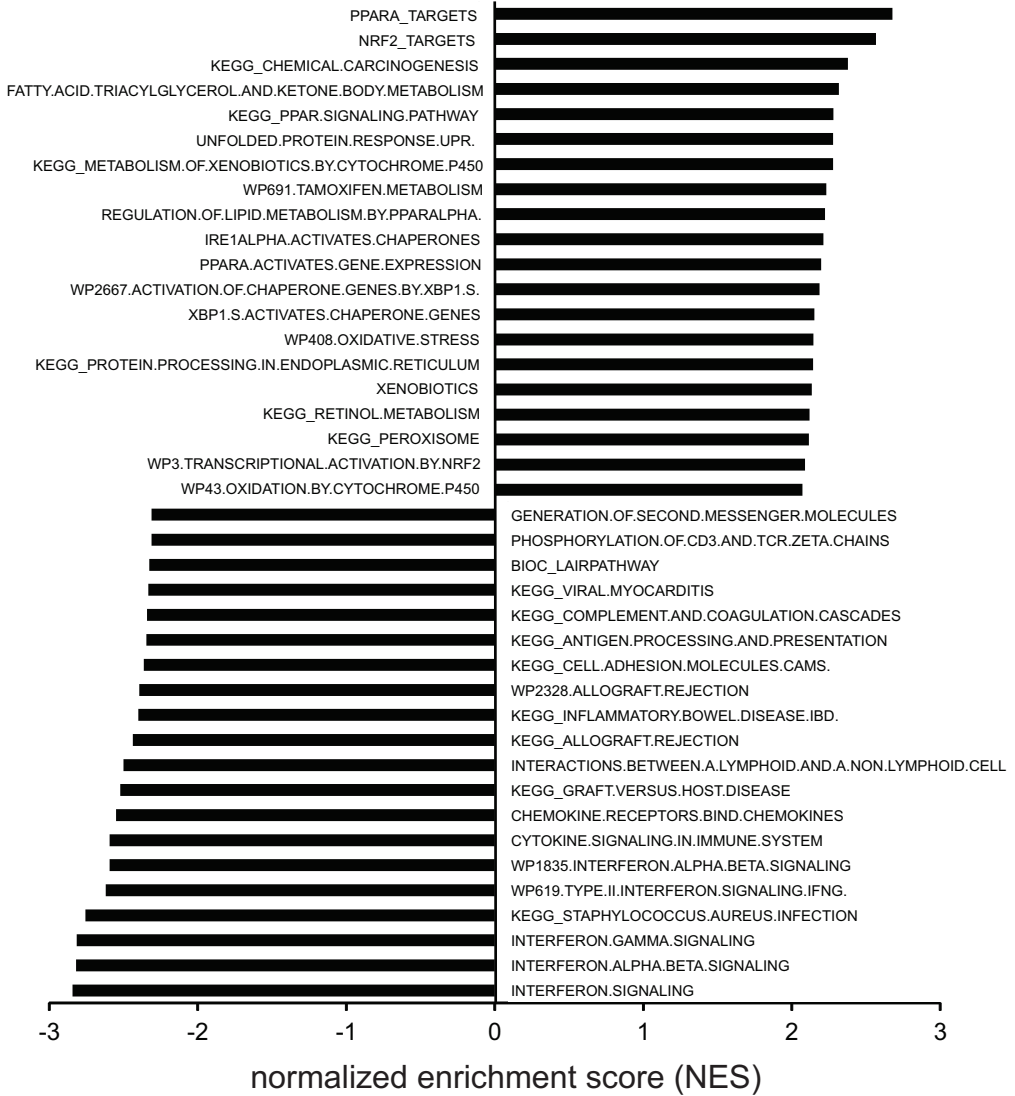


Figure 3. Top 20 gene sets induced or repressed by Wyl4643 in human PCLS

The top 20 most significantly induced or repressed pathways in human PCLS in response to 24h Wyl4643 treatment were determined by gene set enrichment analysis. Gene sets were ranked according to normalized enrichment score (NES).

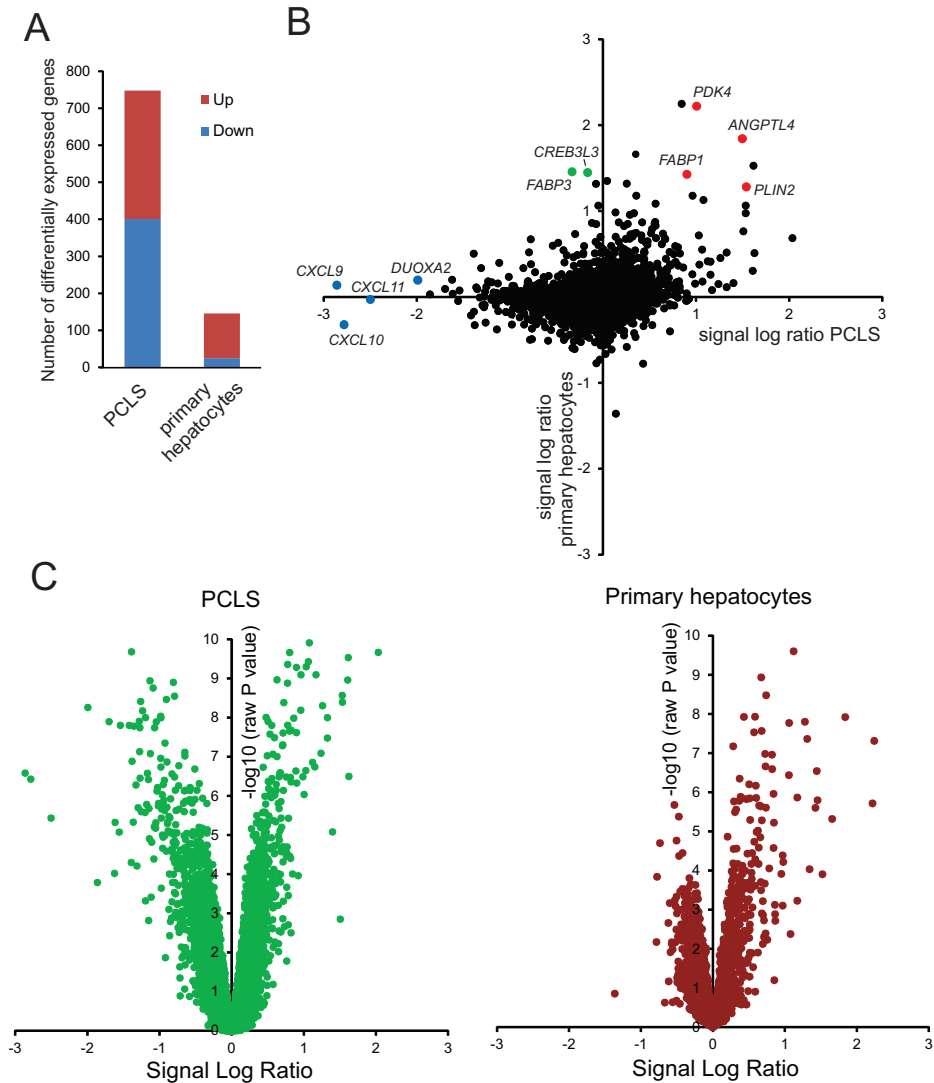


Figure 4. Comparative analysis of effect Wy14643 on gene expression in human PCLS and primary hepatocytes

(A) The number of differentially expressed genes in human PCLS and human primary hepatocytes in response to 24h Wy14643 treatment in a common geneset of 17351 genes was calculated based on a statistical significance cut-off of $P < 0.001$ (IBMT regularised paired t-test) and fold-change > 1.20 . Genes were separated according to up- or down-regulation. (B) Correlation plot showing changes in gene expression in response to Wy14643 (expressed as signal log ratio) in human PCLS (x-axis) and primary human hepatocytes (y-axis). Selected PPAR α target genes commonly induced by Wy14643 in PCLS and hepatocytes are highlighted in red. Selected inflammation-related genes specifically repressed by Wy14643 in PCLS are highlighted in blue. Selected lipid metabolism-related genes specifically induced by Wy14643 in primary hepatocytes are highlighted in green. (C) Volcano plot showing relative changes in gene expression in response to Wy14643 (expressed as signal log ratio, x-axis) plotted against statistical significance (expressed as IBMT regularised paired t-test P-value, y-axis) for the PCLS and primary hepatocytes.

in the hepatocytes. Nearly all genes conforming to this type of expression were involved in immune-related function, as illustrated by the chemokines CXCL9, CXCL10, and CXCL11. Interestingly, a number of genes was explicitly induced by PPARα activation in primary hepatocytes but not in liver slices, including FABP3 as well as CREB3L3, a possible mediator of the stimulatory effects of PPARα on hepatic gene expression [11]. Subsequent analysis by Volcano plot confirmed the overall more pronounced effect of PPARα activation on gene expression in liver slices as compared to primary hepatocytes and also corroborated the relatively minor down-regulation of gene expression by PPARα activation in primary hepatocytes (**Figure 4C**).

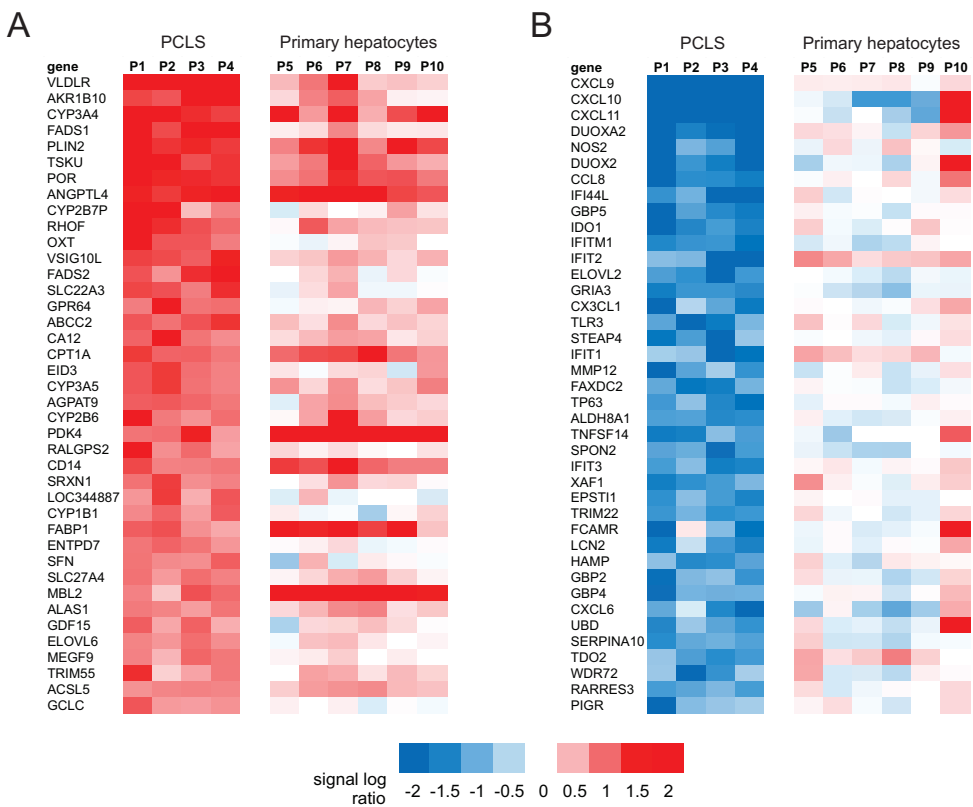


Figure 5. Comparative heatmap analysis of effect Wy14643 on gene expression in human PCLS and primary hepatocytes

Genes that were statistically significantly regulated by Wy14643 in human PCLS ($P < 0.001$, IBMT regularised paired t-test) were ranked according to fold-change in expression. The top 40 genes with highest fold-induction (**A**) or fold-repression (**B**) are shown. Expression changes of the same gene set in primary hepatocytes is shown in the right panel. P1 to P4 represent the four human subjects that donated a liver specimen for preparation of PCLS. P5 to P10 represent the six human subjects that donated a liver specimen for preparation of human hepatocytes.

To further investigate this observation, we took the 40 genes most highly induced or repressed by Wy14643 in the liver slices ($P < 0.001$ and ranked according to fold-change) and studied the response to Wy14643 of the same genes in the primary hepatocytes. Whereas the majority of genes induced by Wy14643 in liver slices were also induced by Wy14643 in the hepatocytes (**Figure 5A**) – as illustrated by the common induction of well-known targets such as FABP1, PLIN2, FADS1 and ANGPTL4 – few genes that were downregulated by Wy14643 in liver slices were also consistently downregulated by Wy14643 in primary hepatocytes (**Figure 5B**). Also, the magnitude of gene suppression by Wy14643 was generally much less pronounced in primary hepatocytes. Confirming the GSEA results, the majority of the most highly repressed genes were related to immunity and inflammation, including the aforementioned chemokines (CXCL9-11, CCL8, CX3CL1, CXCL6), interferon γ -induced genes (IFITM1, IFIT1, IFIT2, IFIT3) and other immune-related genes (TLR3, NOS2, and LCN2).

To further explore the similarity in gene regulation by Wy14643 between PCLS and primary hepatocytes, we took the enriched genes within the positively or negatively enriched gene sets “IRE1 α activated chaperones”, “metabolism of xenobiotics by cytochrome P450”, and “Interferon alpha beta signaling” (**Figure 3**), and compared gene expression changes between PCLS and primary hepatocytes. Induction of most genes part of “metabolism of xenobiotics by cytochrome P450” was more pronounced in PCLS than in primary hepatocytes but reasonably well conserved between the two model systems (**Figure 6A**). A limited number of genes (i.e. CYP2J2) showed higher fold-inductions in the primary hepatocytes as compared to PCLS. Induction of genes part of “IRE1 α activated chaperones” was generally less pronounced in comparison with genes part of “metabolism of xenobiotics by cytochrome P450”, and was relatively weakly conserved between PCLS and primary hepatocytes (**Figure 6B**). An exception is ACADVL. However, the inclusion of ACADVL (very long chain acyl-CoA dehydrogenase = fatty acid oxidation) within “IRE1 α activated chaperones” may be questioned. Consistent with the other data showing potent downregulation of immune- and inflammation-related genes by PPAR α activation in PCLS but not primary hepatocytes, suppression of genes part of “Interferon alpha beta signaling” was exclusively observed in PCLS (**Figure 6C**).

Finally, we used the microarray data of the human primary hepatocytes and human PCLS treated with Wy14643 to generate a detailed gene map of known and putative PPAR α target genes involved in lipid metabolic pathways (**Figure 7**). The map illustrates that regulation of bile acid synthesis and secretion, which is a well-established PPAR α target pathway in mouse, was only evident in primary hepatocytes and not in liver slices. Conversely, genes involved in fatty acid elongation and desaturation were clearly induced by PPAR α activation in human liver slices but not in primary hepatocytes.

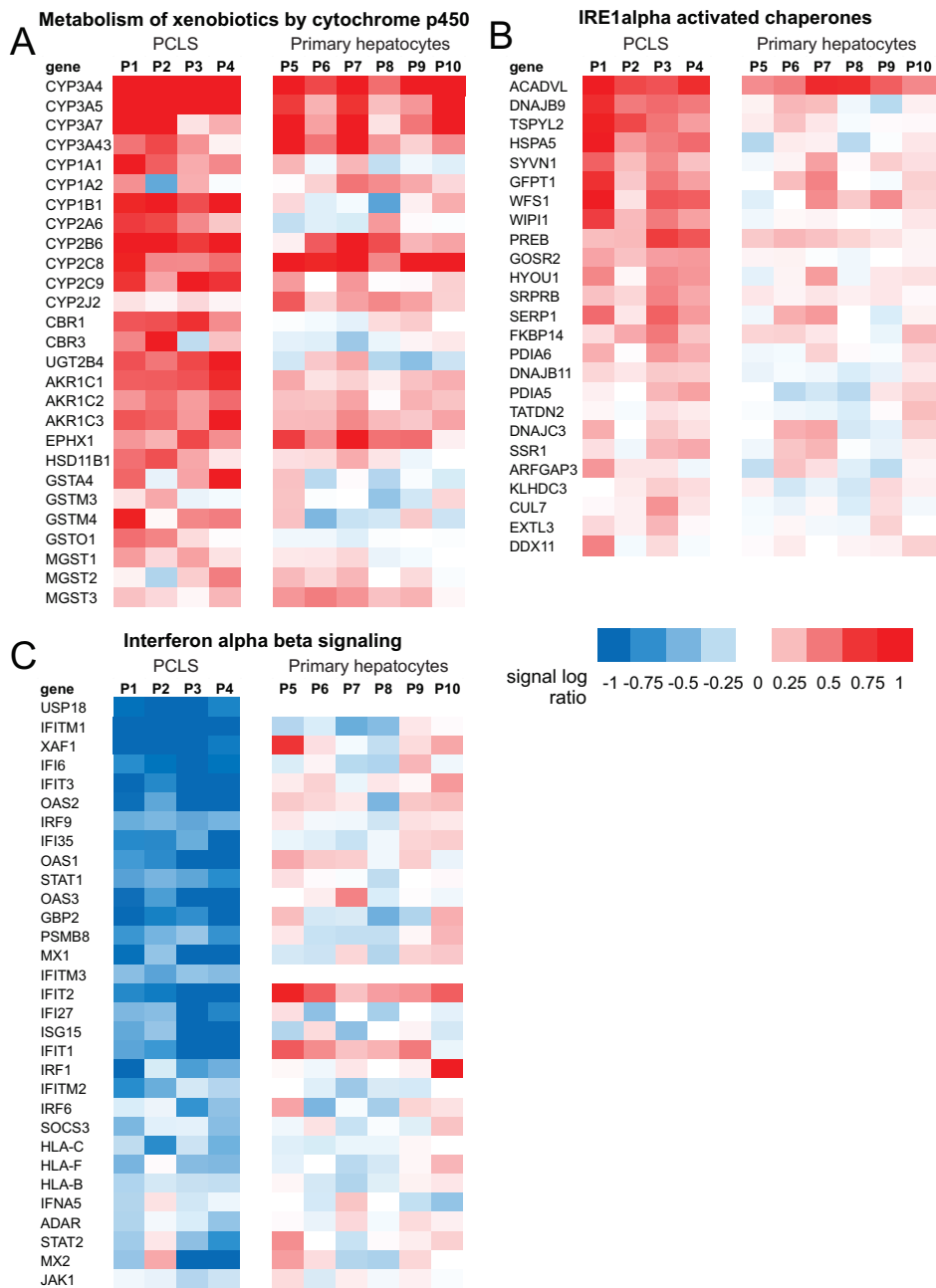


Figure 6. Regulation of selected gene sets by Wy14643 in human PCLS and primary hepatocytes
Heatmap showing gene expression changes of enriched genes that are part of the gene sets “metabolism of xenobiotics by cytochrome P450” (A), “IRE1a activated chaperones” (B), and “Interferon alpha beta signaling” (C) in human PCLS and primary hepatocytes. P1 to P4 represent the four human subjects that donated a liver specimen for preparation of PCLS. P5 to P10 represent the six human subjects that donated a liver specimen for preparation of human hepatocytes.

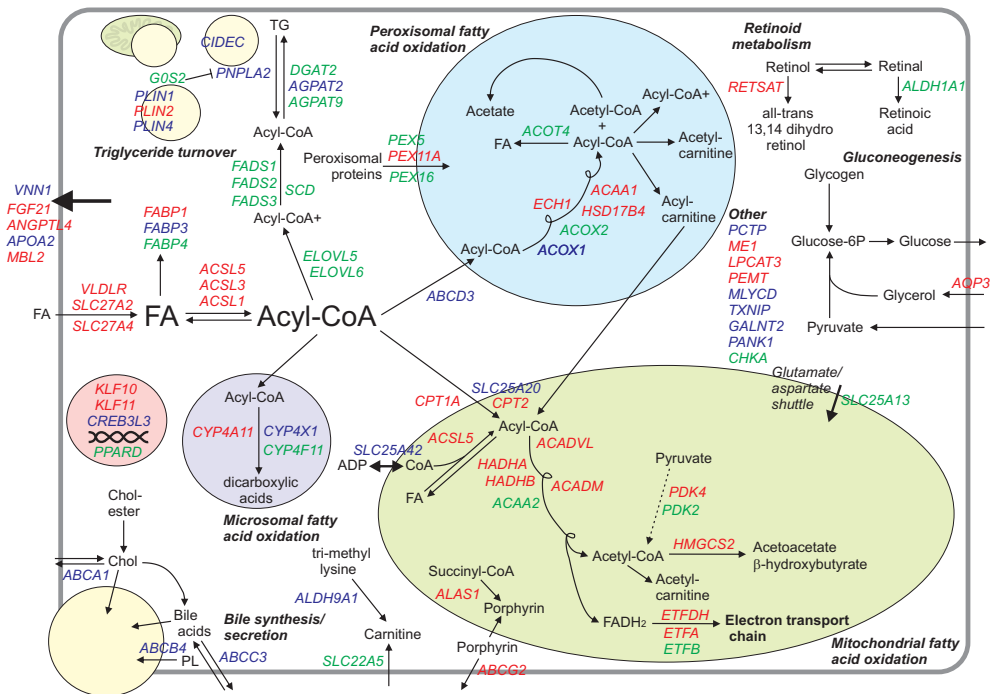


Figure 7. Overview of regulation of lipid metabolism by PPARα in human liver

A detailed overview map was created of metabolic genes upregulated by PPARα in human liver based on transcriptomics analysis of human PCLS and primary hepatocytes treated with Wy14643. Genes indicated in red are significantly induced by Wy14643 in human PCLS and primary hepatocytes. Genes indicated in green are significantly induced by Wy14643 in human PCLS but not primary hepatocytes. Genes indicated in blue are significantly induced by Wy14643 in human primary hepatocytes but not PCLS. Statistical significance was determined by IBMT regularised paired t-test ($P < 0.01$).

Discussion

The main conclusion of our study is that induction of gene expression by PPAR α activation is generally well captured and shows significant overlap between human liver slices and primary human hepatocytes, showing consistent upregulation of genes involved in lipid and xenobiotic metabolism in the two model systems. In contrast, downregulation of gene expression by PPAR α activation is almost exclusively observed in human liver slices. A previous study comparing mouse primary hepatocytes, mouse liver slices and mouse liver reached a similar conclusion [30]. Overall, our data indicate that human PCLS are a superior model to study PPAR α -dependent gene regulation and PPAR α functions in human liver.

As indicated above, PPAR α activation caused major downregulation of gene expression in human liver slices but not in primary hepatocytes. A key difference between primary hepatocytes and liver slices is that the primary hepatocyte culture consists of only hepatocytes, whereas the liver slices include other cell types, including stellate cells and Kupffer cells. A large portion of the downregulated genes and pathways in the liver slices was found to be connected to the immune system. Genes that were highly repressed upon PPAR α activation included several chemokines (e.g. CXCL9-11, CCL8, CX3CL1, CXCL6), interferon γ -induced genes (e.g. IFITM1, IFIT1, IFIT2, IFIT3) and numerous other immune-related genes (e.g. TLR3, NOS2, and LCN2). Downregulation of gene expression is unlikely to be mediated by PPAR α present in non-parenchymal cells, as PPAR α expression in these cells is very low [30, 39]. Instead we prefer a scenario in which the immuno-suppressive action of PPAR α activation in hepatocytes is dependent on (inflammatory) signals emanating from non-parenchymal cells. Indeed, downregulation of inflammatory gene expression in primary hepatocytes and mouse liver by PPAR α activation is sensitive to the presence of pro-inflammatory stimuli [40, 41]. Previously, we and others already demonstrated that Kupffer cells promote fat storage in hepatocytes by releasing inflammatory signals such as IL-1 β , causing downregulation of PPAR α gene expression [42, 43]. Overall, these data suggest that the full scope of functions of PPAR α in hepatocytes is critically dependent on the interaction with other liver cell types. It is of interest to note that recently the anti-inflammatory action of PPAR α in mouse liver was unequivocally attributed to the ability of PPAR α to interact with other transcription factor pathways – a property referred to as transrepression – independent of the DNA-binding ability of PPAR α , as shown in the context of steatohepatitis [44].

Despite the clear clinical efficacy of fibrates towards lowering of circulating triglycerides, the lack of peroxisome proliferation in human primary hepatocytes following PPAR α activation has fed the idea that humans are largely insensitive to peroxisome-proliferator-induced hepatic effects and that the functional role of PPAR α in human liver may be limited [45-47]. Subsequent whole genome expression profiling studies in primary human

hepatocytes have mostly discounted these notions [25, 26]. We found that PPAR α is highly expressed in human liver with Ct values ranging from 22 to 26, which is similar to the values observed in mouse liver (data not shown). Importantly, despite the markedly lower expression of PPAR α in human PCLS as compared to human liver, activation of PPAR α in PCLS caused pronounced upregulation or downregulation of numerous genes, including many known PPAR α targets, strongly supporting the functionality of PPAR α in human PCLS and giving even more credibility to an important *in vivo* role of PPAR α in human liver. Recently, it was found that human liver PPAR α gene expression correlates negatively with the severity of steatohepatitis and with measures of insulin resistance. Furthermore, histological improvement in a follow-up biopsy was associated with increased expression of PPAR α and its target genes, suggesting that PPAR α is involved in and may be therapeutically targeted for human steatohepatitis [48].

The majority of gene sets enriched among the upregulated genes were related to lipid and xenobiotic metabolism, which are well-established target pathways of PPAR α . Intriguingly, several highly enriched gene sets were part of the unfolded protein response and IRE1 α -XBP1 signaling, two key factors involved in governing UPR. Currently, there are no published data linking PPAR α to IRE1 α -XBP1 signaling and regulation of UPR, though it has been observed that PPAR α is involved in regulating proteome maintenance by inducing numerous heat shock proteins [49]. Surprisingly, recently it was demonstrated that IRE1 α -XBP1 signaling leads to activation of PPAR α via direct binding of XBP1s to the promoter of PPAR α , thereby stimulating mitochondrial β -oxidation and ketogenesis [50]. Thus, there appear to be reciprocal interactions between PPAR α and UPR. The wider biological framework for regulation of UPR requires further clarification.

Our analysis reveals differential regulation of a number of PPAR α targets between liver slices and primary hepatocytes. For instance, VNN1 was significantly upregulated by PPAR α activation in primary hepatocytes but showed no change in expression in liver slices. Conversely, expression of FADS2 was significantly increased in human liver slices but showed no change in primary hepatocytes. The differential regulation of specific PPAR α target genes by Wyl4643 between primary hepatocytes and liver slices may be a reflection of the different cellular context in the two models systems, with non-hepatocytes potentially exerting a stimulatory or inhibitory influence on PPAR α -dependent gene induction. However, it should be realized that for a number of genes the seemingly differential regulation may reflect a quantitative difference rather than a true qualitative difference. For example, SLC25A20 was induced significantly by 1.58-fold in primary hepatocytes as compared to a non-significant 1.34-fold induction in liver slices, barely missing the statistical significance cut-off.

Our analysis yielded a number of relatively poorly characterized genes that showed a pronounced and consistent upregulation upon PPAR α activation in the two human liver

model systems. These include TSKU, RHOF, CA12 and VSIG10L. Interestingly, many genes that were found to be induced by PPAR α in early microarray analyses and which did not have an assigned function at the time were later shown to be involved in some aspect of lipid metabolism. Accordingly, it can be hypothesized that the above mentioned genes as well as other poorly characterized genes that are commonly induced by Wy14643 in various liver model systems may be directly or indirectly connected to lipid metabolism.

The comparative microarray analysis of the effect of PPAR α activation in primary human hepatocytes and human liver slices is somewhat hampered by a number of different factors, including the use of different types of Affymetrix gene chips, different human donors, and an unequal number of biological replicates per group. However, treatments of liver slices and hepatocytes were carried out for the same duration and with the same PPAR α agonist. Furthermore, RNA was isolated and labeled via the same technique, hybridizations were performed on the same platform by the same technician, and the microarray data were processed in parallel using the same analysis methods.

On a final note, the data collected in this paper were added to a publicly available overview map of known (lipid) metabolic genes upregulated by PPAR α in human liver (accessible via: http://en.wikipedia.org/wiki/Peroxisome_proliferator-activated_receptor_alpha), which was generated largely by using published transcriptome datasets.

In conclusion, our manuscript demonstrates the suitability and superiority of PCLS over primary human hepatocytes for studying the functional role of PPAR α in human liver. Our data underscore the major role of PPAR α in regulation of hepatic lipid and xenobiotic metabolism and reveal a marked immuno-suppressive/anti-inflammatory effect of PPAR α in human liver that may be therapeutically relevant for NAFLD. The data add to our growing understanding of the critical role of PPAR α in gene regulation in human liver.

Acknowledgements

This research was supported by The Netherlands Cardiovascular Research Committee IN-CONTROL Grant (CVON 2012-03).

References

1. Kersten S, Desvergne B, Wahli W: Roles of PPARs in health and disease. *Nature* 2000, **405**(6785):421-424.
2. Dreyer C, Krey G, Keller H, Givel F, Helftenbein G, Wahli W: Control of the peroxisomal beta-oxidation pathway by a novel family of nuclear hormone receptors. *Cell* 1992, **68**(5):879-887.
3. Braissant O, Foulle F, Scotto C, Dauca M, Wahli W: Differential expression of peroxisome proliferator-activated receptors (PPARs): tissue distribution of PPAR-alpha, -beta, and -gamma in the adult rat. *Endocrinology* 1996, **137**(1):354-366.
4. Wagner KD, Wagner N: Peroxisome proliferator-activated receptor beta/delta (PPARbeta/delta) acts as regulator of metabolism linked to multiple cellular functions. *Pharmacol Ther* 2010, **125**(3):423-435.
5. Tontonoz P, Hu E, Spiegelman BM: Stimulation of adipogenesis in fibroblasts by PPAR gamma 2, a lipid-activated transcription factor. *Cell* 1994, **79**(7):1147-1156.
6. Tontonoz P, Spiegelman BM: Fat and beyond: the diverse biology of PPARgamma. *Annu Rev Biochem* 2008, **77**:289-312.
7. Lehmann JM, Moore LB, Smith-Oliver TA, Wilkison WO, Willson TM, Kliewer SA: An antidiabetic thiazolidinedione is a high affinity ligand for peroxisome proliferator-activated receptor gamma (PPAR gamma). *J Biol Chem* 1995, **270**(22):12953-12956.
8. Hashimoto T, Cook WS, Qi C, Yeldandi AV, Reddy JK, Rao MS: Defect in peroxisome proliferator-activated receptor alpha-inducible fatty acid oxidation determines the severity of hepatic steatosis in response to fasting. *J Biol Chem* 2000, **275**(37):28918-28928.
9. Kersten S, Seydoux J, Peters JM, Gonzalez FJ, Desvergne B, Wahli W: Peroxisome proliferator-activated receptor alpha mediates the adaptive response to fasting. *J Clin Invest* 1999, **103**(11):1489-1498.
10. Leone TC, Weinheimer CJ, Kelly DP: A critical role for the peroxisome proliferator-activated receptor alpha (PPARalpha) in the cellular fasting response: the PPARalpha-null mouse as a model of fatty acid oxidation disorders. *Proc Natl Acad Sci U S A* 1999, **96**(13):7473-7478.
11. Kersten S: Integrated physiology and systems biology of PPARalpha. *Molecular metabolism* 2014, **3**(4):354-371.
12. Dreyer C, Keller H, Mahfoudi A, Laudet V, Krey G, Wahli W: Positive regulation of the peroxisomal beta-oxidation pathway by fatty acids through activation of peroxisome proliferator-activated receptors (PPAR). *Biology of the cell / under the auspices of the European Cell Biology Organization* 1993, **77**(1):67-76.
13. Forman BM, Chen J, Evans RM: Hypolipidemic drugs, polyunsaturated fatty acids, and eicosanoids are ligands for peroxisome proliferator-activated receptors alpha and delta. *Proc Natl Acad Sci U S A* 1997, **94**(9):4312-4317.
14. Gottlicher M, Widmark E, Li Q, Gustafsson JA: Fatty acids activate a chimera of the clofibrate acid-activated receptor and the glucocorticoid receptor. *Proc Natl Acad Sci U S A* 1992, **89**(10):4653-4657.
15. Kliewer SA, Sundseth SS, Jones SA, Brown PJ, Wisely GB, Koble CS, Devchand P, Wahli W, Willson TM, Lenhard JM *et al*: Fatty acids and eicosanoids regulate gene expression through direct interactions with peroxisome proliferator-activated receptors alpha and gamma. *Proc Natl Acad Sci U S A* 1997, **94**(9):4318-4323.
16. Krey G, Braissant O, L'Hors F, Kalkhoven E, Perroud M, Parker MG, Wahli W: Fatty acids, eicosanoids, and hypolipidemic agents identified as ligands of peroxisome proliferator-activated receptors by coactivator-dependent receptor ligand assay. *Mol Endocrinol* 1997, **11**(6):779-791.
17. Issemann I, Green S: Activation of a member of the steroid hormone receptor superfamily by peroxisome proliferators. *Nature* 1990, **347**(6294):645-650.
18. Staels B, Fruchart JC: Therapeutic roles of peroxisome proliferator-activated receptor agonists. *Diabetes* 2005, **54**(8):2460-2470.
19. Staels B, Rubenstrunk A, Noel B, Rigou G, Delataille P, Millatt LJ, Baron M, Lucas A, Tailleux A, Hum DW *et al*: Hepatoprotective effects of the dual peroxisome proliferator-activated receptor alpha/delta agonist, GFT505, in rodent models of nonalcoholic fatty liver disease/nonalcoholic steatohepatitis. *Hepatology* 2013, **58**(6):1941-1952.
20. Cariou B, Hanf R, Lambert-Porcheron S, Zair Y, Sauvinet V, Noel B, Flet L, Vidal H, Staels B, Laville M: Dual peroxisome proliferator-activated receptor alpha/delta agonist GFT505 improves hepatic and peripheral insulin sensitivity in abdominally obese subjects. *Diabetes Care* 2013, **36**(10):2923-2930.
21. Lee SS, Pineau T, Drago J, Lee EJ, Owens JW, Kroetz DL, Fernandez-Salguero PM, Westphal H, Gonzalez FJ: Targeted disruption of the alpha isoform of the peroxisome proliferator-activated receptor gene in mice results in abolishment of the pleiotropic effects of peroxisome proliferators. *Mol Cell Biol* 1995, **15**(6):3012-3022.
22. Corton JC, Cunningham ML, Hummer BT, Lau C, Meek B, Peters JM, Popp JA, Rhomberg L, Seed J, Klaunig JE: Mode of action framework analysis for receptor-mediated toxicity: The peroxisome

- proliferator-activated receptor alpha (PPAR α) as a case study. *Crit Rev Toxicol* 2014, **44**(1):1-49.
23. Blaauboer BJ, van Holsteijn CW, Bleumink R, Mennes WC, van Pelt FN, Yap SH, van Pelt JF, van Iersel AA, Timmerman A, Schmid BP: The effect of bezafibrate and fenofibrate on peroxisomal β -oxidation and peroxisome proliferation in primary cultures of rat, monkey and human hepatocytes. *Biochem Pharmacol* 1990, **40**(3):521-528.
24. Cattley RC, DeLuca J, Elcombe C, Fenner-Crisp P, Lake BG, Marsman DS, Pastoor TA, Popp JA, Robinson DE, Schwetz B *et al*: Do peroxisome proliferating compounds pose a hepatocarcinogenic hazard to humans? *Regulatory toxicology and pharmacology : RTP* 1998, **27**(1 Pt 1):47-60.
25. McMullen PD, Bhattacharya S, Woods CG, Sun B, Yarborough K, Ross SM, Miller ME, McBride MT, Lecluyse EL, Clewell RA *et al*: A map of the PPAR α transcription regulatory network for primary human hepatocytes. *Chemico-biological interactions* 2013, **209C**:14-24.
26. Rakhshandehroo M, Hooiveld G, Muller M, Kersten S: Comparative analysis of gene regulation by the transcription factor PPAR α between mouse and human. *PLoS One* 2009, **4**(8):e6796.
27. Smith PF, Gandolfi AJ, Krumdieck CL, Putnam CW, Zukoski CF, 3rd, Davis WM, Brendel K: Dynamic organ culture of precision liver slices for in vitro toxicology. *Life Sci* 1985, **36**(14):1367-1375.
28. Jung D, Elferink MG, Stellaard F, Groothuis GM: Analysis of bile acid-induced regulation of FXR target genes in human liver slices. *Liver Int* 2007, **27**(1):137-144.
29. Mattijssen F, Georgiadi A, Andasari T, Szalowska E, Zota A, Kronen-Herzig A, Heier C, Ratman D, De Bosscher K, Qi L *et al*: Hypoxia-inducible lipid droplet-associated (HILPDA) is a novel peroxisome proliferator-activated receptor (PPAR) target involved in hepatic triglyceride secretion. *J Biol Chem* 2014, **289**(28):19279-19293.
30. Szalowska E, Tesfay HA, van Hijum SA, Kersten S: Transcriptomic signatures of peroxisome proliferator-activated receptor alpha (PPAR α) in different mouse liver models identify novel aspects of its biology. *BMC genomics* 2014, **15**:1106.
31. Szalowska E, van der Burg B, Man HY, Hendriksen PJ, Peijnenburg AA: Model steatogenic compounds (amiodarone, valproic acid, and tetracycline) alter lipid metabolism by different mechanisms in mouse liver slices. *PLoS One* 2014, **9**(1):e86795.
32. Willson TM, Brown PJ, Sternbach DD, Henke BR: The PPARs: from orphan receptors to drug discovery. *J Med Chem* 2000, **43**(4):527-550.
33. Bolstad BM, Irizarry RA, Astrand M, Speed TP: A comparison of normalization methods for high density oligonucleotide array data based on variance and bias. *Bioinformatics* 2003, **19**(2):185-193.
34. Irizarry RA, Bolstad BM, Collin F, Cope LM, Hobbs B, Speed TP: Summaries of Affymetrix GeneChip probe level data. *Nucleic Acids Res* 2003, **31**(4):e15.
35. Dai M, Wang P, Boyd AD, Kostov G, Athey B, Jones EG, Bunney WE, Myers RM, Speed TP, Akil H *et al*: Evolving gene/transcript definitions significantly alter the interpretation of GeneChip data. *Nucleic Acids Res* 2005, **33**(20):e175.
36. Sartor MA, Tomlinson CR, Wesselkamper SC, Sivaganesan S, Leikauf GD, Medvedovic M: Intensity-based hierarchical Bayes method improves testing for differentially expressed genes in microarray experiments. *BMC Bioinformatics* 2006, **7**:538.
37. Storey JD, Tibshirani R: Statistical significance for genomewide studies. *Proc Natl Acad Sci U S A* 2003, **100**(16):9440-9445.
38. Subramanian A, Tamayo P, Mootha VK, Mukherjee S, Ebert BL, Gillette MA, Paulovich A, Pomeroy SL, Golub TR, Lander ES *et al*: Gene set enrichment analysis: a knowledge-based approach for interpreting genome-wide expression profiles. *Proc Natl Acad Sci U S A* 2005, **102**(43):15545-15550.
39. Peters JM, Rusyn I, Rose ML, Gonzalez FJ, Thurman RG: Peroxisome proliferator-activated receptor alpha is restricted to hepatic parenchymal cells, not Kupffer cells: implications for the mechanism of action of peroxisome proliferators in hepatocarcinogenesis. *Carcinogenesis* 2000, **21**(4):823-826.
40. Gervois P, Kleemann R, Pilon A, Percevault F, Koenig W, Staels B, Kooistra T: Global suppression of IL-6-induced acute phase response gene expression after chronic in vivo treatment with the peroxisome proliferator-activated receptor-alpha activator fenofibrate. *J Biol Chem* 2004, **279**(16):16154-16160.
41. Gervois P, Vu-Dac N, Kleemann R, Kockx M, Dubois G, Laine B, Kosykh V, Fruchart JC, Kooistra T, Staels B: Negative regulation of human fibrinogen gene expression by peroxisome proliferator-activated receptor alpha agonists via inhibition of CCAAT box/enhancer-binding protein beta. *J Biol Chem* 2001, **276**(36):33471-33477.
42. Fang X, Zou S, Zhao Y, Cui R, Zhang W, Hu J, Dai J: Kupffer cells suppress perfluorononanoic acid-induced hepatic peroxisome proliferator-activated receptor alpha expression by releasing cytokines. *Archives of toxicology* 2012, **86**(10):1515-1525.
43. Stienstra R, Saudale F, Duval C, Keshtkar S, Groener JE, van Rooijen N, Staels B, Kersten S, Muller M: Kupffer cells promote hepatic steatosis via interleukin-1 β -dependent suppression of peroxisome proliferator-activated receptor alpha activity. *Hepatology* 2010, **51**(2):511-522.

44. Pawlak M, Bauge E, Bourguet W, De Bosscher K, Lalloyer F, Tailleux A, Lebherz C, Lefebvre P, Staels B: The transrepressive activity of peroxisome proliferator-activated receptor alpha is necessary and sufficient to prevent liver fibrosis in mice. *Hepatology* 2014, **60**(5):1593-1606.
45. Bentley P, Calder I, Elcombe C, Grasso P, Stringer D, Wiegand HJ: Hepatic peroxisome proliferation in rodents and its significance for humans. *Food and chemical toxicology : an international journal published for the British Industrial Biological Research Association* 1993, **31**(11):857-907.
46. Palmer CN, Hsu MH, Griffin KJ, Raucy JL, Johnson EF: Peroxisome proliferator activated receptor-alpha expression in human liver. *Mol Pharmacol* 1998, **53**(1):14-22.
47. Holden PR, Tugwood JD: Peroxisome proliferator-activated receptor alpha: role in rodent liver cancer and species differences. *J Mol Endocrinol* 1999, **22**(1):1-8.
48. Francque S, Verrijken A, Caron S, Prawitt J, Paumelle R, Derudas B, Lefebvre P, Taskinen MR, Van Hul W, Mertens I *et al*: PPARalpha gene expression correlates with severity and histological treatment response in patients with Non-alcoholic Steatohepatitis. *J Hepatol* 2015, **63**(1):164-173.
49. Vallanat B, Anderson SP, Brown-Borg HM, Ren H, Kersten S, Jonnalagadda S, Srinivasan R, Corton JC: Analysis of the heat shock response in mouse liver reveals transcriptional dependence on the nuclear receptor peroxisome proliferator-activated receptor alpha (PPARalpha). *BMC genomics* 2010, **11**:16.
50. Shao M, Shan B, Liu Y, Deng Y, Yan C, Wu Y, Mao T, Qiu Y, Zhou Y, Jiang S *et al*: Hepatic IRE1alpha regulates fasting-induced metabolic adaptive programs through the XBP1s-PPARalpha axis signalling. *Nature communications* 2014, **5**:3528.

Supplemental tables

Supplemental table 1. Full list of genes induced by Wy14643 in human PCLS

Entrez ID	Gene name	Fold change	q-value	Description
7436	VLDLR	4.11	4.38E-07	very low density lipoprotein receptor
57016	AKR1B10	3.09	6.09E-05	aldo-keto reductase family 1, member B10 (aldose reductase)
1576	CYP3A4	3.07	5.23E-07	cytochrome P450, family 3, subfamily A, polypeptide 4
3992	FADS1	3.06	1.02E-06	fatty acid desaturase 1
123	PLIN2	2.91	2.46E-06	perilipin 2
25987	TSKU	2.90	1.98E-06	tsukushi, small leucine rich proteoglycan
5447	POR	2.90	1.22E-07	P450 (cytochrome) oxidoreductase
1551	CYP3A7	2.85	2.50E-02	cytochrome P450, family 3, subfamily A, polypeptide 7
51129	ANGPTL4	2.82	1.22E-07	angiopoietin-like 4
1556	CYP2B7P	2.64	6.79E-04	cytochrome P450, family 2, subfamily B, polypeptide 7, pseudogene
54509	RHOF	2.52	4.50E-06	ras homolog family member F (in filopodia)
5020	OXT	2.52	9.73E-06	oxytocin/neurophysin I prepropeptide
147645	VSIG10L	2.40	2.84E-06	V-set and immunoglobulin domain containing 10 like
9415	FADS2	2.37	2.15E-05	fatty acid desaturase 2
6581	SLC22A3	2.26	8.61E-07	solute carrier family 22 (organic cation transporter), member 3
10149	GPR64	2.23	4.02E-05	G protein-coupled receptor 64
1244	ABCC2	2.23	2.41E-07	ATP-binding cassette, sub-family C (CFTR/MRP), member 2
771	CA12	2.18	3.21E-05	carbonic anhydrase XII
1374	CPT1A	2.12	3.97E-07	carnitine palmitoyltransferase 1A (liver)
493861	EID3	2.10	2.73E-07	EP300 interacting inhibitor of differentiation 3
1577	CYP3A5	2.09	5.97E-07	cytochrome P450, family 3, subfamily A, polypeptide 5
84803	AGPAT9	2.05	6.46E-07	1-acylglycerol-3-phosphate O-acyltransferase 9
1555	CYP2B6	2.04	4.78E-05	cytochrome P450, family 2, subfamily B, polypeptide 6
5166	PKD4	2.01	1.28E-04	pyruvate dehydrogenase kinase, isozyme 4
55103	RALGPS2	1.99	6.09E-05	Ral GEF with PH domain and SH3 binding motif 2
929	CD14	1.95	8.61E-07	CD14 molecule
140809	SRXN1	1.95	3.46E-06	sulfiredoxin 1
344887	LOC344887	1.90	4.01E-03	NmrA-like family domain containing 1 pseudogene
1545	CYP1B1	1.87	7.74E-05	cytochrome P450, family 1, subfamily B, polypeptide 1
2168	FABP1	1.87	7.58E-06	fatty acid binding protein 1, liver
57089	ENTPD7	1.87	6.46E-07	ectonucleoside triphosphate diphosphohydrolase 7
2810	SFN	1.86	4.82E-05	stratifin
10999	SLC27A4	1.82	4.50E-06	solute carrier family 27 (fatty acid transporter), member 4
4153	MBL2	1.80	3.76E-03	mannose-binding lectin (protein C) 2, soluble
211	ALAS1	1.78	6.88E-06	aminolevulinatase, delta-, synthase 1
135656	DPCR1	1.77	4.24E-02	diffuse panbronchiolitis critical region 1
9518	GDF15	1.77	7.30E-05	growth differentiation factor 15
79071	ELOVL6	1.77	1.94E-03	ELOVL fatty acid elongase 6
1955	MEGF9	1.76	6.13E-05	multiple EGF-like-domains 9
84675	TRIM55	1.75	1.78E-03	tripartite motif containing 55
51703	ACSL5	1.75	4.38E-07	acyl-CoA synthetase long-chain family member 5
2729	GCLC	1.75	7.08E-06	glutamate-cysteine ligase, catalytic subunit
28449	IGHV3-13	1.75	2.94E-02	immunoglobulin heavy variable 3-13
54210	TREM1	1.73	3.69E-04	triggering receptor expressed on myeloid cells 1
2151	F2RL2	1.73	3.11E-02	coagulation factor II (thrombin) receptor-like 2
10786	SLC17A3	1.73	9.39E-03	solute carrier family 17 (organic anion transporter), member 3
6974	TRGV2	1.72	4.52E-02	T cell receptor gamma variable 2
7296	TXNRD1	1.72	6.36E-07	thioredoxin reductase 1
4835	NQO2	1.72	5.65E-06	NAD(P)H dehydrogenase, quinone 2
37	ACADVL	1.72	1.06E-06	acyl-CoA dehydrogenase, very long chain
23657	SLC7A11	1.71	1.25E-03	solute carrier family 7 (anionic amino acid transporter light chain, xc- system), member 11
552	AVPR1A	1.71	1.56E-03	arginine vasopressin receptor 1A
3131	HLF	1.70	6.58E-03	hepatic leukemia factor
11069	RAPGEF4	1.70	1.78E-03	Rap guanine nucleotide exchange factor (GEF) 4
10058	ABCB6	1.70	6.09E-05	ATP-binding cassette, sub-family B (MDR/TAP), member 6
1591	CYP24A1	1.66	3.37E-02	cytochrome P450, family 24, subfamily A, polypeptide 1
2184	FAH	1.66	2.46E-06	fumarylacetoacetate hydrolase (fumarylacetoacetase)
13	AADAC	1.65	1.04E-04	arylacetamide deacetylase
8431	NR0B2	1.65	1.18E-02	nuclear receptor subfamily 0, group B, member 2
3148	HMGB2	1.65	1.24E-03	high mobility group box 2
89866	SEC16B	1.64	2.22E-03	SEC16 homolog B (S. cerevisiae)
7363	UGT2B4	1.64	7.62E-06	UDP glucuronosyltransferase 2 family, polypeptide B4
23189	KANK1	1.64	1.40E-05	KN motif and ankyrin repeat domains 1
990	CDC6	1.64	2.47E-02	cell division cycle 6
2730	GCLM	1.63	1.44E-05	glutamate-cysteine ligase, modifier subunit
54346	UNC93A	1.63	1.38E-03	unc-93 homolog A (C. elegans)
57761	TRIB3	1.62	5.48E-04	tribbles pseudokinase 3
7378	UPP1	1.62	1.47E-03	uridine phosphorylase 1
168620	BHLHA15	1.61	1.30E-03	basic helix-loop-helix family, member a15
1528	CYB5A	1.61	3.69E-04	cytochrome b5 type A (microsomal)

Entrez ID	Gene name	Fold change	q-value	Description
2167	FABP4	1.61	4.10E-02	fatty acid binding protein 4, adipocyte
1559	CYP2C9	1.61	1.76E-04	cytochrome P450, family 2, subfamily C, polypeptide 9
4862	NPAS2	1.60	5.28E-03	neuronal PAS domain protein 2
6584	SLC22A5	1.60	3.82E-03	solute carrier family 22 (organic cation/carnitine transporter), member 5
54518	APBB1IP	1.60	6.47E-04	amyloid beta (A4) precursor protein-binding, family B, member 1 interacting protein
1891	ECH1	1.59	5.33E-05	enoyl CoA hydratase 1, peroxisomal
65084	TMEM135	1.59	9.41E-04	transmembrane protein 135
1645	AKR1C1	1.58	6.09E-05	aldo-keto reductase family 1, member C1
11153	FICD	1.58	2.38E-04	FIC domain containing
11200	CHEK2	1.58	4.83E-02	checkpoint kinase 2
54551	MAGEL2	1.58	3.94E-02	MAGE-like 2
2852	GPFR1	1.57	4.80E-03	G protein-coupled estrogen receptor 1
79729	SH3D21	1.57	7.73E-04	SH3 domain containing 21
164832	LONRF2	1.57	1.39E-02	LON peptidase N-terminal domain and ring finger 2
8644	AKR1C3	1.57	3.76E-03	aldo-keto reductase family 1, member C3
8462	KLF11	1.57	1.86E-04	Kruppel-like factor 11
4882	NPR2	1.56	3.72E-03	natriuretic peptide receptor 2
84263	HSDL2	1.55	2.41E-05	hydroxysteroid dehydrogenase like 2
50999	TMED5	1.55	1.02E-06	transmembrane emp24 protein transport domain containing 5
6319	SCD	1.54	1.17E-03	stearoyl-CoA desaturase (delta-9-desaturase)
55532	SLC30A10	1.54	8.22E-05	solute carrier family 30, member 10
1271	CNTFR	1.53	5.22E-03	ciliary neurotrophic factor receptor
51076	CUTC	1.53	4.39E-04	cutC copper transporter
133746	JMY	1.53	9.05E-03	junction mediating and regulatory protein, p53 cofactor
3024	HIST1H1A	1.53	5.74E-03	histone cluster 1, H1a
193629	LINC00189	1.52	9.60E-03	long intergenic non-protein coding RNA 189
84883	AIFM2	1.52	1.30E-04	apoptosis-inducing factor, mitochondrion-associated, 2
64061	TSPYL2	1.52	1.55E-03	TSPY-like 2
5226	PGD	1.51	9.62E-06	phosphogluconate dehydrogenase
7466	WFS1	1.51	1.59E-03	Wolfram syndrome 1 (wolframin)
3613	IMPA2	1.51	1.47E-02	inositol(myo)-1-(or 4)-monophosphatase 2
91614	DEPDC7	1.50	3.03E-03	DEP domain containing 7
275	AMT	1.50	1.20E-03	aminomethyltransferase
5652	PRSS8	1.50	9.97E-03	protease, serine, 8
1647	GADD45A	1.50	1.00E-02	growth arrest and DNA-damage-inducible, alpha
4189	DNAJB9	1.50	4.13E-04	DnaJ (Hsp40) homolog, subfamily B, member 9
79631	EFTUD1	1.49	1.39E-02	elongation factor Tu GTP binding domain containing 1
65124	SOWAHC	1.49	1.28E-03	soosondawah ankyrin repeat domain family member C
161436	EML5	1.49	1.55E-02	echinoderm microtubule associated protein like 5
3309	HSPA5	1.49	2.20E-05	heat shock 70kDa protein 5 (glucose-regulated protein, 78kDa)
51083	GAL	1.49	2.56E-02	galanin/GMAP prepropeptide
1376	CPT2	1.49	7.56E-03	carnitine palmitoyltransferase 2
10110	SGK2	1.48	3.63E-02	serum/glucocorticoid induced regulated kinase 2
26291	FGF21	1.48	3.54E-02	fibroblast growth factor 21
1558	CYP2C8	1.48	6.39E-05	cytochrome P450, family 2, subfamily C, polypeptide 8
2936	GSR	1.47	5.65E-06	glutathione reductase
10166	SLC25A15	1.47	5.23E-03	solute carrier family 25 (mitochondrial carrier // ornithine transporter) member 15
83667	SESN2	1.47	4.17E-03	sestrin 2
83699	SH3BGR2	1.47	3.83E-03	SH3 domain binding glutamate-rich protein like 2
734	OSGIN2	1.47	8.41E-04	oxidative stress induced growth inhibitor family member 2
132299	OCIA2	1.47	1.48E-04	OCIA domain containing 2
114038	LINC00313	1.46	6.80E-03	long intergenic non-protein coding RNA 313
54825	CDHR2	1.45	1.27E-03	cadherin-related family member 2
444	ASPH	1.45	1.04E-04	aspartate beta-hydroxylase
3242	HPD	1.45	7.99E-06	4-hydroxyphenylpyruvate dioxygenase
51117	COQ4	1.45	6.58E-03	coenzyme Q4
144423	GLT1D1	1.45	1.31E-03	glycosyltransferase 1 domain containing 1
6505	SLC1A1	1.45	3.87E-03	solute carrier family 1 (neuronal/epithelial high affinity glutamate transporter, system Xag), member 1
84243	ZDHC18	1.45	7.30E-05	zinc finger, DHHC-type containing 18
9540	TP53I3	1.44	9.80E-03	tumor protein p53 inducible protein 3
8517	IKBK	1.44	3.37E-03	inhibitor of kappa light polypeptide gene enhancer in B-cells, kinase gamma
8800	PEX11A	1.44	8.67E-03	peroxisomal biogenesis factor 11 alpha
201161	CENPV	1.44	1.23E-02	centromere protein V
389432	SAMD5	1.44	2.20E-03	sterile alpha motif domain containing 5
54884	RETSAT	1.43	3.62E-03	retinol saturase (all-trans-retinol 13,14-reductase)
730102	LOC730102	1.43	2.76E-02	quinone oxidoreductase-like protein 2 pseudogene
1548	CYP2A6	1.43	3.35E-04	cytochrome P450, family 2, subfamily A, polypeptide 6
2632	GBE1	1.43	9.92E-05	glucan (1,4-alpha)-, branching enzyme 1
127845	GOLT1A	1.43	7.42E-03	golgi transport 1A
22949	PTGR1	1.43	1.36E-04	prostaglandin reductase 1
9709	HERPUD1	1.42	9.37E-03	homocysteine-inducible, endoplasmic reticulum stress-inducible, ubiquitin-like domain member 1
5238	PGM3	1.42	7.30E-05	phosphoglucomutase 3
114883	OSBPL9	1.42	5.01E-06	oxysterol binding protein-like 9
7498	XDH	1.42	1.13E-02	xanthine dehydrogenase

Entrez ID	Gene name	Fold change	q-value	Description
8501	SLC43A1	1.42	1.98E-03	solute carrier family 43 (amino acid system L transporter), member 1
54978	SLC35F6	1.42	2.47E-03	solute carrier family 35, member F6
51302	CYP39A1	1.42	1.21E-02	cytochrome P450, family 39, subfamily A, polypeptide 1
133686	NADK2	1.42	4.50E-04	NAD kinase 2, mitochondrial
25998	IBTK	1.41	2.35E-05	inhibitor of Bruton agammaglobulinemia tyrosine kinase
4337	MOCS1	1.41	6.77E-03	molybdenum cofactor synthesis 1
3690	ITGB3	1.41	5.11E-04	integrin, beta 3 (platelet glycoprotein IIIa, antigen CD61)
55323	LARP6	1.41	2.16E-03	La ribonucleoprotein domain family, member 6
79605	PGBD5	1.41	2.11E-02	piggyBac transposable element derived 5
65009	NDRG4	1.41	3.79E-02	NDRG family member 4
152189	CMTM8	1.40	1.97E-03	CKLF-like MARVEL transmembrane domain containing 8
30061	SLC40A1	1.40	3.68E-02	solute carrier family 40 (iron-regulated transporter), member 1
79922	MRM1	1.40	4.56E-02	mitochondrial rRNA methyltransferase 1 homolog (S. cerevisiae)
51559	NTSDC3	1.40	2.51E-02	5'-nucleotidase domain containing 3
54893	MTMR10	1.40	6.83E-04	myotubularin related protein 10
343099	CCDC18	1.40	6.00E-03	coiled-coil domain containing 18
51533	PHF7	1.40	6.39E-03	PHD finger protein 7
10162	LPCAT3	1.40	1.45E-02	lysophosphatidylcholine acyltransferase 3
6888	TALDO1	1.39	4.50E-06	transaldolase 1
2110	ETFDH	1.39	8.52E-04	electron-transferring-flavoprotein dehydrogenase
997	CDC34	1.39	3.37E-03	cell division cycle 34
10486	CAP2	1.39	3.43E-03	CAP, adenylate cyclase-associated protein, 2 (yeast)
23327	NEDD4L	1.39	1.30E-03	neural precursor cell expressed, developmentally down-regulated 4-like, E3 ubiquitin protein ligase
847	CAT	1.39	1.91E-04	catalase
89894	TMEM116	1.39	1.75E-02	transmembrane protein 116
345757	FAM174A	1.39	1.00E-02	family with sequence similarity 174, member A
220108	FAM124A	1.39	3.84E-02	family with sequence similarity 124A
124512	METTL23	1.39	1.38E-02	methyltransferase like 23
4925	NUCB2	1.39	8.11E-03	nucleobindin 2
10113	PREB	1.38	1.25E-02	prolactin regulatory element binding
57406	ABHD6	1.38	1.32E-02	abhydrolase domain containing 6
51567	TDP2	1.38	2.79E-04	tyrosyl-DNA phosphodiesterase 2
84719	LINC00260	1.38	2.72E-02	long intergenic non-protein coding RNA 260
56605	ERO1LB	1.38	1.76E-03	ERO1-like beta (S. cerevisiae)
64093	SMOC1	1.38	1.04E-02	SPARC related modular calcium binding 1
63874	ABHD4	1.38	4.43E-04	abhydrolase domain containing 4
1646	AKR1C2	1.38	2.78E-04	aldo-keto reductase family 1, member C2
100272147	CMC4	1.38	1.15E-02	C-x(9)-C motif containing 4
2108	ETFA	1.38	1.38E-04	electron-transfer-flavoprotein, alpha polypeptide
3708	ITPR1	1.38	8.27E-04	inositol 1,4,5-trisphosphate receptor, type 1
11001	SLC27A2	1.38	1.29E-03	solute carrier family 27 (fatty acid transporter), member 2
57149	LYRM1	1.38	2.82E-03	LYR motif containing 1
2673	GFPT1	1.38	2.35E-03	glutamine-fructose-6-phosphate transaminase 1
112849	L3HYPDH	1.38	2.11E-02	L-3-hydroxyproline dehydratase (trans-)
9601	PDIA4	1.38	1.20E-03	protein disulfide isomerase family A, member 4
100033432	SNORD116-21	1.37	3.54E-02	small nucleolar RNA, C/D box 116-21
10449	ACAA2	1.37	7.03E-04	acetyl-CoA acyltransferase 2
8856	NR1I2	1.37	1.17E-02	nuclear receptor subfamily 1, group I, member 2
10891	PPARGC1A	1.37	3.61E-03	peroxisome proliferator-activated receptor gamma, coactivator 1 alpha
257364	SNX33	1.37	1.03E-02	sorting nexin 33
29948	OSGIN1	1.37	7.07E-04	oxidative stress induced growth inhibitor 1
101928229	NA	1.37	1.96E-02	NA
11080	DNAJB4	1.37	3.84E-02	DnaJ (Hsp40) homolog, subfamily B, member 4
55062	WIPI1	1.37	4.74E-04	WD repeat domain, phosphoinositide interacting 1
5603	MAPK13	1.37	3.20E-02	mitogen-activated protein kinase 13
9871	SEC24D	1.37	9.59E-04	SEC24 family member D
22885	ABLIM3	1.37	1.30E-03	actin binding LIM protein family, member 3
84561	SLC12A8	1.37	4.05E-03	solute carrier family 12, member 8
79746	ECHDC3	1.37	4.97E-03	enoyl CoA hydratase domain containing 3
2948	GSTM4	1.37	1.21E-02	glutathione S-transferase mu 4
2651	GCNT2	1.37	1.55E-02	glucosaminyl (N-acetyl) transferase 2, I-branching enzyme (I blood group)
81539	SLC38A1	1.37	1.83E-03	solute carrier family 38, member 1
5256	PKA2	1.36	1.59E-03	phosphorylase kinase, alpha 2 (liver)
22853	LMTK2	1.36	4.74E-04	lemur tyrosine kinase 2
2052	EPHX1	1.36	2.78E-04	epoxide hydrolase 1, microsomal (xenobiotic)
79935	CNTD2	1.36	3.61E-02	cyclin N-terminal domain containing 2
27242	TNFRSF21	1.36	1.29E-02	tumor necrosis factor receptor superfamily, member 21
3625	INHBB	1.36	4.83E-02	inhibin, beta B
375757	SWI5	1.36	4.25E-03	SWI5 recombination repair homolog (yeast)
203228	C9orf72	1.36	3.67E-03	chromosome 9 open reading frame 72
3251	HPRT1	1.36	4.70E-04	hypoxanthine phosphoribosyltransferase 1
7873	MANF	1.36	1.02E-03	mesencephalic astrocyte-derived neurotrophic factor
100130742	LRRRC69	1.36	2.85E-02	leucine rich repeat containing 69
493	ATP2B4	1.36	6.31E-03	ATPase, Ca+++ transporting, plasma membrane 4
168451	THAP5	1.36	3.53E-02	THAP domain containing 5

Entrez ID	Gene name	Fold change	q-value	Description
9942	XYLB	1.36	5.23E-03	xylulokinase homolog (H. influenzae)
8878	SQSTM1	1.36	4.02E-05	sequestosome 1
3159	HMGAI	1.35	8.87E-03	high mobility group AT-hook 1
128853	DUSP15	1.35	1.74E-02	dual specificity phosphatase 15
27090	ST6GALNAC4	1.35	8.74E-04	ST6 (alpha-N-acetyl-neuraminyl-2,3-beta-galactosyl-1,3)-N-acetylglactosaminide alpha-2,6-sialyltransferase 4
5009	OTC	1.35	3.01E-02	ornithine carbamoyltransferase
6520	SLC3A2	1.35	2.79E-04	solute carrier family 3 (amino acid transporter heavy chain), member 2
26064	RAH14	1.35	9.97E-04	retinoic acid induced 14
400798	C1orf220	1.35	1.05E-02	chromosome 1 open reading frame 220
54700	RRN3	1.35	2.47E-02	RRN3 RNA polymerase I transcription factor homolog (S. cerevisiae)
122970	ACOT4	1.35	3.11E-02	acyl-CoA thioesterase 4
84681	HINT2	1.35	1.56E-02	histidine triad nucleotide binding protein 2
6482	ST3GAL1	1.35	1.10E-03	ST3 beta-galactoside alpha-2,3-sialyltransferase 1
901	CCNG2	1.35	2.46E-02	cyclin G2
55728	N4BP2	1.35	1.81E-02	NEDD4 binding protein 2
8209	C21orf33	1.34	1.10E-03	chromosome 21 open reading frame 33
548645	DNAJC25	1.34	2.31E-03	DnaJ (Hsp40) homolog, subfamily C, member 25
6675	UAP1	1.34	3.83E-03	UDP-N-acetylglucosamine pyrophosphorylase 1
2274	FHL2	1.34	8.81E-03	four and a half LIM domains 2
91050	CCDC149	1.34	2.69E-02	coiled-coil domain containing 149
8309	ACOX2	1.34	3.84E-02	acyl-CoA oxidase 2, branched chain
645	BLVRB	1.34	1.52E-03	biliverdin reductase B (flavin reductase (NADPH))
55219	TMEM57	1.34	5.79E-03	transmembrane protein 57
7754	ZNF204P	1.34	3.85E-02	zinc finger protein 204, pseudogene
692099	FAM86DP	1.34	8.01E-04	family with sequence similarity 86, member D, pseudogene
10126	DNAL4	1.34	3.22E-02	dynein, axonemal, light chain 4
5243	ABCB1	1.34	9.46E-03	ATP-binding cassette, sub-family B (MDR/TAP), member 1
1119	CHKA	1.34	2.72E-02	choline kinase alpha
58510	PRODH2	1.34	1.24E-02	proline dehydrogenase (oxidase) 2
643246	MAP1LC3B2	1.34	4.21E-02	microtubule-associated protein 1 light chain 3 beta 2
9532	BAG2	1.34	1.94E-03	BCL2-associated athanogene 2
27440	CECR5	1.34	3.17E-02	cat eye syndrome chromosome region, candidate 5
4359	MPZ	1.34	2.74E-02	myelin protein zero
79739	TTL7	1.33	2.93E-02	tubulin tyrosine ligase-like family, member 7
64816	CYP3A43	1.33	4.90E-02	cytochrome P450, family 3, subfamily A, polypeptide 43
271	AMPD2	1.33	7.37E-03	adenosine monophosphate deaminase 2
8027	STAM	1.33	1.78E-03	signal transducing adaptor molecule (SH3 domain and ITAM motif) 1
9955	HS3ST3A1	1.33	3.49E-02	heparan sulfate (glucosamine) 3-O-sulfotransferase 3A1
23753	SDF2L1	1.33	6.72E-03	stromal cell-derived factor 2-like 1
6786	STIM1	1.33	1.21E-03	stromal interaction molecule 1
135398	C6orf141	1.33	5.22E-03	chromosome 6 open reading frame 141
1373	CP51	1.33	5.09E-03	carbamoyl-phosphate synthase 1, mitochondrial
26995	TRUB2	1.32	5.56E-04	TruB pseudouridine (psi) synthase family member 2
27230	SERP1	1.32	1.22E-03	stress-associated endoplasmic reticulum protein 1
8165	AKAP1	1.32	1.75E-03	A kinase (PRKA) anchor protein 1
256987	SERINC5	1.32	2.67E-03	serine incorporator 5
3290	HSD11B1	1.32	2.87E-03	hydroxysteroid (11-beta) dehydrogenase 1
189	AGXT	1.32	1.48E-03	alanine-glyoxylate aminotransferase
23743	BHMT2	1.32	4.30E-04	betaine-homocysteine S-methyltransferase 2
27347	STK39	1.32	3.73E-02	serine threonine kinase 39
171586	ABHD3	1.32	6.31E-03	abhydrolase domain containing 3
3081	HGD	1.32	2.11E-02	homogentisate 1,2-dioxygenase
8412	BCAR3	1.32	1.69E-02	breast cancer anti-estrogen resistance 3
79003	MIS12	1.32	1.07E-02	MIS12 kinetochore complex component
493856	CISD2	1.31	1.83E-02	CDGSH iron sulfur domain 2
10726	NUDC	1.31	1.28E-03	nudC nuclear distribution protein
84288	EFCAB2	1.31	3.61E-02	EF-hand calcium binding domain 2
55974	SLC50A1	1.31	7.27E-03	solute carrier family 50 (sugar efflux transporter), member 1
79701	OGFOD3	1.31	1.23E-02	2-oxoglutarate and iron-dependent oxygenase domain containing 3
114907	FBXO32	1.30	3.00E-02	F-box protein 32
399665	FAM102A	1.30	1.71E-02	family with sequence similarity 102, member A
1050	CEBPA	1.30	2.46E-02	CCAAT/enhancer binding protein (C/EBP), alpha
6836	SURF4	1.30	4.36E-04	surfeit 4
2878	GPX3	1.30	2.47E-03	glutathione peroxidase 3 (plasma)
51651	PTRH2	1.30	1.83E-02	peptidyl-tRNA hydrolase 2
84513	PPAPDC1B	1.30	6.39E-03	phosphatidic acid phosphatase type 2 domain containing 1B
7068	THRB	1.30	4.82E-02	thyroid hormone receptor, beta
202915	TMEM184A	1.30	1.54E-02	transmembrane protein 184A
84447	SYVN1	1.30	5.23E-03	synovial apoptosis inhibitor 1, synoviolin
8565	YARS	1.30	1.34E-03	tyrosyl-tRNA synthetase
2770	GNAI1	1.30	4.79E-02	guanine nucleotide binding protein (G protein), alpha inhibiting activity polypeptide 1
83752	LONP2	1.30	1.30E-03	ion peptidase 2, peroxisomal
56261	GPCPD1	1.30	4.59E-02	glycerophosphocholine phosphodiesterase GDE1 homolog (S. cerevisiae)
157922	CAMSAP1	1.30	5.74E-03	calmodulin regulated spectrin-associated protein 1
25791	NGEF	1.30	3.85E-02	neuronal guanine nucleotide exchange factor

Entrez ID	Gene name	Fold change	q-value	Description
219743	TYSDN1	1.30	1.00E-02	trypsin domain containing 1
29968	PSAT1	1.30	3.16E-02	phosphoserine aminotransferase 1
286343	LURAP1L	1.29	2.66E-02	leucine rich adaptor protein 1-like
3775	KCNK1	1.29	2.11E-02	potassium channel, subfamily K, member 1
2035	EPB41	1.29	1.00E-02	erythrocyte membrane protein band 4.1 (elliptocytosis 1, RH-linked)
3655	ITGA6	1.29	2.42E-03	integrin, alpha 6
11162	NUDT6	1.29	3.01E-02	nudix (nucleoside diphosphate linked moiety X)-type motif 6
10165	SLC25A13	1.29	3.83E-03	solute carrier family 25 (aspartate/glutamate carrier), member 13
2717	GLA	1.29	1.78E-03	galactosidase, alpha
55343	SLC35C1	1.29	4.90E-02	solute carrier family 35 (GDP-fucose transporter), member C1
79161	TMEM243	1.29	3.00E-02	transmembrane protein 243, mitochondrial
2109	ETFB	1.29	5.58E-03	electron-transfer-flavoprotein, beta polypeptide
27304	MOCS3	1.29	4.82E-02	molybdenum cofactor synthesis 3
51136	RNFT1	1.29	1.17E-02	ring finger protein, transmembrane 1
114818	KLHL29	1.29	1.24E-02	kelch-like family member 29
3693	ITGB5	1.29	2.71E-03	integrin, beta 5
283464	GXYLT1	1.29	2.17E-03	glucoside xylosyltransferase 1
23576	DDAH1	1.29	2.09E-03	dimethylarginine dimethylaminohydrolase 1
79594	MUL1	1.29	1.48E-02	mitochondrial E3 ubiquitin protein ligase 1
1491	CTH	1.29	3.96E-02	cystathionase (cystathionine gamma-lyase)
11260	XPOT	1.28	9.69E-03	exportin, tRNA
7371	UCK2	1.28	6.56E-03	uridine-cytidine kinase 2
9821	RB1CC1	1.28	2.28E-03	RB1-inducible coiled-coil 1
196410	METTL7B	1.28	1.53E-02	methyltransferase like 7B
9697	TRAM2	1.28	2.19E-03	translocation associated membrane protein 2
200933	FBXO45	1.28	2.35E-02	F-box protein 45
3032	HADHB	1.28	1.95E-03	hydroxyacyl-CoA dehydrogenase/3-ketoacyl-CoA thiolase/enoyl-CoA hydratase (trifunctional protein), beta subunit
152641	WWC2-AS2	1.28	2.03E-02	WWC2 antisense RNA 2
9975	NR1D2	1.28	4.04E-03	nuclear receptor subfamily 1, group D, member 2
29958	DMGDH	1.28	3.89E-02	dimethylglycine dehydrogenase
57161	PELI2	1.28	1.03E-02	pellino E3 ubiquitin protein ligase family member 2
51099	ABHD5	1.28	3.68E-02	abhydrolase domain containing 5
8366	HIST1H4B	1.28	4.05E-02	histone cluster 1, H4b
10397	NDRG1	1.28	1.32E-02	N-myc downstream regulated 1
29925	GMPPB	1.28	1.33E-02	GDP-mannose pyrophosphorylase B
5795	PTPRJ	1.28	7.07E-03	protein tyrosine phosphatase, receptor type, J
85377	MICAL1	1.28	4.87E-02	MICAL-like 1
6249	CLIP1	1.28	9.72E-04	CAP-GLY domain containing linker protein 1
7922	SLC39A7	1.28	3.02E-03	solute carrier family 39 (zinc transporter), member 7
9093	DNAJA3	1.28	2.42E-03	DnaJ (Hsp40) homolog, subfamily A, member 3
80218	NAA50	1.28	3.30E-04	N(alpha)-acetyltransferase 50, NatE catalytic subunit
55605	KIF21A	1.28	4.19E-03	kinesin family member 21A
25850	ZNF345	1.28	4.54E-02	zinc finger protein 345
84725	PLEKHA8	1.28	3.54E-02	pleckstrin homology domain containing, family A (phosphoinositide binding specific) member 8
55435	AP1AR	1.28	4.96E-03	adaptor-related protein complex 1 associated regulatory protein
10560	SLC19A2	1.27	3.17E-02	solute carrier family 19 (thiamine transporter), member 2
84818	IL17RC	1.27	2.95E-02	interleukin 17 receptor C
23277	CLUH	1.27	1.55E-03	clustered mitochondria (cluA/CLU1) homolog
216	ALDH1A1	1.27	8.23E-03	aldehyde dehydrogenase 1 family, member A1
5053	PAH	1.27	4.16E-02	phenylalanine hydroxylase
133	ADM	1.27	2.75E-02	adrenomedullin
28955	DEXI	1.27	3.71E-02	Dexi homolog (mouse)
91526	ANKRD44	1.27	8.26E-03	ankyrin repeat domain 44
9980	DOPEY2	1.27	2.80E-02	dopey family member 2
2247	FGF2	1.27	1.70E-02	fibroblast growth factor 2 (basic)
83606	GUCD1	1.27	8.74E-04	guanylyl cyclase domain containing 1
64755	C16orf58	1.27	8.02E-03	chromosome 16 open reading frame 58
2646	GCKR	1.27	2.82E-02	glucokinase (hexokinase 4) regulator
5062	PAK2	1.27	8.74E-04	p21 protein (Cdc42/Rac)-activated kinase 2
1843	DUSP1	1.27	4.50E-04	dual specificity phosphatase 1
5217	PFN2	1.27	4.91E-03	profilin 2
51114	ZDHHC9	1.27	2.55E-03	zinc finger, DHHC-type containing 9
64216	TFB2M	1.27	7.34E-03	transcription factor B2, mitochondrial
201232	SLC16A13	1.27	1.42E-02	solute carrier family 16, member 13
57414	RHBDD2	1.27	7.75E-03	rhomboid domain containing 2
56288	PARD3	1.27	7.37E-04	par-3 family cell polarity regulator
3741	KCNA5	1.27	4.52E-02	potassium voltage-gated channel, shaker-related subfamily, member 5
2872	MKNK2	1.27	3.98E-02	MAP kinase interacting serine/threonine kinase 2
10483	SEC23B	1.26	3.44E-03	Sec23 homolog B (S. cerevisiae)
56997	ADCK3	1.26	4.95E-02	aarF domain containing kinase 3
22928	SEPHS2	1.26	3.48E-03	selenophosphate synthetase 2
5387	PMS2P3	1.26	1.24E-02	postmeiotic segregation increased 2 pseudogene 3
4953	ODC1	1.26	1.79E-03	ornithine decarboxylase 1
57834	CYP4F11	1.26	2.04E-02	cytochrome P450, family 4, subfamily F, polypeptide 11

Entrez ID	Gene name	Fold change	q-value	Description
5621	PRNP	1.26	3.26E-03	prion protein
29088	MRPL15	1.26	4.38E-02	mitochondrial ribosomal protein L15
79144	PPDPF	1.26	1.78E-02	pancreatic progenitor cell differentiation and proliferation factor
29926	GMPPA	1.26	8.97E-03	GDP-mannose pyrophosphorylase A
23223	RRP12	1.26	4.19E-03	ribosomal RNA processing 12 homolog (S. cerevisiae)
55330	BLOC1S4	1.26	4.91E-02	biogenesis of lysosomal organelles complex-1, subunit 4, cappuccino
10525	HYOU1	1.26	1.19E-02	hypoxia up-regulated 1
1978	EIF4EBP1	1.26	2.50E-02	eukaryotic translation initiation factor 4E binding protein 1
1579	CYP4A11	1.26	3.27E-02	cytochrome P450, family 4, subfamily A, polypeptide 11
51058	ZNF691	1.26	4.33E-02	zinc finger protein 691
54929	TMEM161A	1.26	4.43E-02	transmembrane protein 161A
63893	UBE2O	1.26	1.42E-02	ubiquitin-conjugating enzyme E2O
10400	PEMT	1.26	1.11E-02	phosphatidylethanolamine N-methyltransferase
6782	HSPA13	1.26	2.76E-03	heat shock protein 70kDa family, member 13
22809	ATF5	1.26	1.18E-02	activating transcription factor 5
254887	ZDHHC23	1.26	1.05E-02	zinc finger, DHHC-type containing 23
9570	GOSR2	1.26	6.56E-03	golgi SNAP receptor complex member 2
84649	DGAT2	1.25	3.46E-02	diacylglycerol O-acyltransferase 2
79875	THSD4	1.25	3.73E-02	thrombospondin, type I, domain containing 4
55884	WSB2	1.25	4.75E-03	WD repeat and SOCS box containing 2
7923	HSD17B8	1.25	9.05E-03	hydroxysteroid (17-beta) dehydrogenase 8
134147	CMBL	1.25	1.03E-02	carboxymethylglutaminylase homolog (Pseudomonas)
8608	RDH16	1.25	3.60E-02	retinol dehydrogenase 16 (all-trans)
2669	GEM	1.25	1.83E-02	GTP binding protein overexpressed in skeletal muscle
144811	LACC1	1.25	1.29E-02	laccase (multicopper oxidoreductase) domain containing 1
221756	SERPINF9P1	1.25	4.95E-02	serpin peptidase inhibitor, clade B (ovalbumin), member 9, pseudogene 1
7132	TNFRSF1A	1.25	2.76E-03	tumor necrosis factor receptor superfamily, member 1A
8439	NSMAF	1.25	1.97E-02	neutral sphingomyelinase (N-SMase) activation associated factor
55132	LARP1B	1.25	3.17E-02	La ribonucleoprotein domain family, member 1B
9429	ABCG2	1.25	3.67E-02	ATP-binding cassette, sub-family G (WHITE), member 2
200844	C3orf67	1.25	2.98E-02	chromosome 3 open reading frame 67
29914	UBIAD1	1.25	1.47E-02	UbiA prenyltransferase domain containing 1
56947	MFF	1.24	9.39E-03	mitochondrial fission factor
9689	BZW1	1.24	1.29E-02	basic leucine zipper and W2 domains 1
10099	TSPAN3	1.24	3.96E-03	tetraspanin 3
10933	MORF4L1	1.24	1.62E-02	mortality factor 4 like 1
8187	ZNF239	1.24	4.52E-02	zinc finger protein 239
30836	DNTTIP2	1.24	7.07E-03	deoxynucleotidyltransferase, terminal, interacting protein 2
5565	PRKAB2	1.24	2.10E-02	protein kinase, AMP-activated, beta 2 non-catalytic subunit
84085	FBXO30	1.24	1.77E-03	F-box protein 30
5830	PEX5	1.24	7.83E-03	peroxisomal biogenesis factor 5
54867	TMEM214	1.24	1.66E-02	transmembrane protein 214
347735	SERINC2	1.24	1.54E-02	serine incorporator 2
5164	PKD2	1.24	3.99E-02	pyruvate dehydrogenase kinase, isozyme 2
26777	SNORA71A	1.24	2.47E-02	small nucleolar RNA, H/ACA box 71A
23483	TGDS	1.24	8.81E-03	TDP-glucose 4,6-dehydratase
7184	HSP90B1	1.24	1.56E-03	heat shock protein 90kDa beta (Grp94), member 1
60314	C12orf10	1.24	1.55E-02	chromosome 12 open reading frame 10
51582	AZIN1	1.23	7.57E-04	antizyme inhibitor 1
221656	KDM1B	1.23	1.34E-02	lysine (K)-specific demethylase 1B
84336	TMEM101	1.23	4.08E-02	transmembrane protein 101
10613	ERLIN1	1.23	2.22E-02	ER lipid raft associated 1
3998	LMAN1	1.23	1.55E-02	lectin, mannose-binding, 1
162989	DEDD2	1.23	4.10E-02	death effector domain containing 2
23139	MAST2	1.23	8.15E-03	microtubule associated serine/threonine kinase 2
10598	AHA1	1.23	1.84E-03	AHA1, activator of heat shock 90kDa protein ATPase homolog 1 (yeast)
64795	RMND5A	1.23	4.95E-02	required for meiotic nuclear division 5 homolog A (S. cerevisiae)
64425	POLR1E	1.23	2.08E-02	polymerase (RNA) I polypeptide E, 53kDa
54676	GTPBP2	1.23	2.92E-02	GTP binding protein 2
153241	CEP120	1.23	4.82E-02	centrosomal protein 120kDa
360023	ZBTB41	1.23	3.01E-02	zinc finger and BTB domain containing 41
63971	KIF13A	1.23	1.16E-02	kinesin family member 13A
79018	GID4	1.23	4.71E-02	GID complex subunit 4
55313	CPPED1	1.23	2.45E-03	calcineurin-like phosphoesterase domain containing 1
58477	SRPRB	1.23	2.54E-03	signal recognition particle receptor, B subunit
51649	MRPS23	1.23	3.70E-02	mitochondrial ribosomal protein S23
7514	XPO1	1.23	7.72E-03	exportin 1
64175	LEPRE1	1.23	3.41E-02	leucine proline-enriched proteoglycan (leprecan) 1
978	CDA	1.22	1.86E-02	cytidine deaminase
11108	PRDM4	1.22	1.28E-02	PR domain containing 4
7071	KLF10	1.22	5.44E-03	Kruppel-like factor 10
96610	BMS1P20	1.22	2.96E-02	BMS1 pseudogene 20
90411	MCFD2	1.22	6.31E-03	multiple coagulation factor deficiency 2
7165	TPD52L2	1.22	4.91E-03	tumor protein D52-like 2
3030	HADHA	1.22	1.70E-02	hydroxyacyl-CoA dehydrogenase/3-ketoacyl-CoA thiolase/enoyl-CoA hydratase (trifunctional protein), alpha subunit

Entrez ID	Gene name	Fold change	q-value	Description
5167	ENPP1	1.22	1.11E-02	ectonucleotide pyrophosphatase/phosphodiesterase 1
50640	PNPLA8	1.22	2.19E-02	patatin-like phospholipase domain containing 8
64771	C6orf106	1.22	8.02E-03	chromosome 6 open reading frame 106
375035	SFT2D2	1.22	1.94E-02	SFT2 domain containing 2
26207	PITPNC1	1.22	9.59E-03	phosphatidylinositol transfer protein, cytoplasmic 1
26151	NAT9	1.22	2.75E-02	N-acetyltransferase 9 (GCN5-related, putative)
5412	UBL3	1.22	9.85E-03	ubiquitin-like 3
27248	ERLEC1	1.22	2.49E-02	endoplasmic reticulum lectin 1
91252	SLC39A13	1.22	2.42E-02	solute carrier family 39 (zinc transporter), member 13
9557	CHD1L	1.22	3.63E-02	chromodomain helicase DNA binding protein 1-like
54469	ZFAND6	1.22	3.09E-02	zinc finger, AN1-type domain 6
10196	PRMT3	1.22	2.69E-02	protein arginine methyltransferase 3
80273	GRPEL1	1.22	7.67E-03	GrpE-like 1, mitochondrial (E. coli)
10838	ZNF275	1.22	2.47E-02	zinc finger protein 275
51566	ARMKC3	1.22	3.95E-02	armadillo repeat containing, X-linked 3
26608	TBL2	1.22	4.81E-02	transducin (beta)-like 2
9917	FAM20B	1.21	1.10E-02	family with sequence similarity 20, member B
7419	VDAC3	1.21	5.82E-04	voltage-dependent anion channel 3
54517	PUS7	1.21	1.76E-02	pseudouridylate synthase 7 (putative)
3295	HSD17B4	1.21	1.41E-02	hydroxysteroid (17-beta) dehydrogenase 4
400	ARL1	1.21	2.02E-02	ADP-ribosylation factor-like 1
8907	AP1M1	1.21	3.82E-02	adaptor-related protein complex 1, mu 1 subunit
5054	SERPINE1	1.21	2.61E-02	serpin peptidase inhibitor, clade E (nexin, plasminogen activator inhibitor type 1), member 1
8100	IFT88	1.21	2.46E-02	intraflagellar transport 88 homolog (Chlamydomonas)
85379	KIAA1671	1.21	1.10E-02	KIAA1671
2801	GOLGA2	1.21	1.67E-02	golgin A2
10322	SMYD5	1.21	2.74E-02	SMYD family member 5
4780	NFE2L2	1.21	1.39E-02	nuclear factor, erythroid 2-like 2
84919	PPP1R15B	1.21	2.14E-02	protein phosphatase 1, regulatory subunit 15B
57222	ERGIC1	1.21	4.17E-03	endoplasmic reticulum-golgi intermediate compartment (ERGIC) 1
27075	TSPAN13	1.20	3.73E-02	tetraspanin 13
4199	ME1	1.20	1.04E-02	malic enzyme 1, NADP(+)-dependent, cytosolic
91272	BOD1	1.20	1.49E-02	biorientation of chromosomes in cell division 1
5467	PPARD	1.20	3.13E-02	peroxisome proliferator-activated receptor delta
9146	HGS	1.20	1.70E-02	hepatocyte growth factor-regulated tyrosine kinase substrate
56647	BCCIP	1.20	3.36E-02	BRCA2 and CDKN1A interacting protein
1979	EIF4EBP2	1.20	2.57E-03	eukaryotic translation initiation factor 4E binding protein 2
56683	C21orf59	1.20	1.20E-02	chromosome 21 open reading frame 59
6746	SSR2	1.20	1.11E-02	signal sequence receptor, beta (translocon-associated protein beta)
4233	MET	1.20	3.45E-02	met proto-oncogene
7965	AIMP2	1.20	1.70E-02	aminoacyl tRNA synthetase complex-interacting multifunctional protein 2
6683	SPAST	1.20	1.56E-02	spastin
1317	SLC31A1	1.20	2.19E-02	solute carrier family 31 (copper transporter), member 1
7295	TXN	1.20	1.00E-02	thioredoxin
6780	STAU1	1.20	3.62E-03	staufen double-stranded RNA binding protein 1
134553	C5orf24	1.20	3.17E-02	chromosome 5 open reading frame 24
81671	VMP1	1.20	1.94E-03	vacuole membrane protein 1
56910	STARD7	1.20	3.38E-03	STAR-related lipid transfer (START) domain containing 7
1497	CTNS	1.20	2.93E-02	cystinosis, lysosomal cystine transporter
5686	PSMA5	1.20	3.64E-02	proteasome (prosome, macropain) subunit, alpha type, 5
55829	VIMP	1.20	3.25E-02	VCP-interacting membrane protein
11046	SLC35D2	1.20	2.81E-02	solute carrier family 35 (UDP-GlcNAc/UDP-glucose transporter), member D2
10455	ECI2	1.19	9.14E-03	enoyl-CoA delta isomerase 2
6732	SRPK1	1.19	2.45E-02	SRSF protein kinase 1
7764	ZNF217	1.19	3.37E-02	zinc finger protein 217
51061	TXNDC11	1.19	3.67E-02	thioredoxin domain containing 11
8772	FADD	1.19	3.69E-02	Fas (TNFRSF6)-associated via death domain
10953	TOMM34	1.19	1.34E-02	translocase of outer mitochondrial membrane 34
63929	XPNPEP3	1.19	4.99E-02	X-prolyl aminopeptidase (aminopeptidase P) 3, putative
10130	PDIA6	1.19	2.18E-02	protein disulfide isomerase family A, member 6
29855	UBN1	1.19	4.92E-02	ubiquitin 1
7813	EVI5	1.19	3.70E-02	ecotropic viral integration site 5
10728	PTGES3	1.19	1.75E-02	prostaglandin E synthase 3 (cytosolic)
9184	BUB3	1.19	3.57E-02	BUB3 mitotic checkpoint protein
10120	ACTR1B	1.19	3.47E-02	ARP1 actin-related protein 1 homolog B, contractin beta (yeast)
4257	MGST1	1.19	5.78E-03	microsomal glutathione S-transferase 1
613	BCR	1.19	4.16E-02	breakpoint cluster region
8630	HSD17B6	1.19	2.10E-02	hydroxysteroid (17-beta) dehydrogenase 6
23230	VPS13A	1.19	2.88E-02	vacuolar protein sorting 13 homolog A (S. cerevisiae)
26354	GNL3	1.19	1.40E-02	guanine nucleotide binding protein-like 3 (nucleolar)
10885	WDR3	1.19	2.75E-02	WD repeat domain 3
25923	ATL3	1.19	6.77E-03	atlastin GTPase 3
84522	JAGN1	1.19	3.31E-02	jagunal homolog 1 (Drosophila)
25888	ZNF473	1.19	3.55E-02	zinc finger protein 473
55907	CMAS	1.19	4.84E-02	cytidine monophosphate N-acetylneuraminic acid synthetase

Entrez ID	Gene name	Fold change	q-value	Description
127262	TPRG1L	1.19	4.14E-02	tumor protein p63 regulated 1-like
22931	RAB18	1.18	8.02E-03	RAB18, member RAS oncogene family
85021	REPS1	1.18	5.26E-03	RALBP1 associated Eps domain containing 1
9950	GOLGA5	1.18	4.72E-02	golgin A5
142891	SAMD8	1.18	1.56E-02	sterile alpha motif domain containing 8
8886	DDX18	1.18	1.29E-02	DEAD (Asp-Glu-Ala-Asp) box polypeptide 18
58513	EPS15L1	1.18	3.86E-02	epidermal growth factor receptor pathway substrate 15-like 1
7342	UBP1	1.18	2.89E-02	upstream binding protein 1 (LBP-1a)
7267	TTC3	1.18	3.24E-02	tetratricopeptide repeat domain 3
50865	HEBP1	1.18	4.12E-02	heme binding protein 1
51430	SUCO	1.18	2.47E-02	SUN domain containing ossification factor
6868	ADAM17	1.18	3.15E-02	ADAM metalloproteinase domain 17
116064	LRRC58	1.18	3.71E-02	leucine rich repeat containing 58
9921	RNF10	1.18	1.38E-02	ring finger protein 10
9043	SPAG9	1.18	4.48E-02	sperm associated antigen 9
22937	SCAP	1.18	2.98E-02	SREBF chaperone
92140	MTDH	1.18	6.72E-03	metadherin
30	ACAA1	1.18	1.15E-02	acetyl-CoA acyltransferase 1
8882	ZPR1	1.18	2.36E-02	ZPR1 zinc finger
57587	KIAA1430	1.18	1.97E-02	KIAA1430
200734	SPRED2	1.18	3.34E-02	sprouty-related, EVH1 domain containing 2
8476	CDC42BPA	1.18	3.17E-02	CDC42 binding protein kinase alpha (DMPK-like)
55760	DXH32	1.17	1.49E-02	DEAH (Asp-Glu-Ala-His) box polypeptide 32
55003	PAK1IP1	1.17	1.97E-02	PAK1 interacting protein 1
2288	FKBP4	1.17	2.65E-02	FK506 binding protein 4, 59kDa
262	AMD1	1.17	2.30E-02	adenosylmethionine decarboxylase 1
80854	SETD7	1.17	7.61E-03	SET domain containing (lysine methyltransferase) 7
7110	TMF1	1.17	1.86E-02	TATA element modulatory factor 1
51012	SLMO2	1.17	2.96E-02	slowmo homolog 2 (Drosophila)
10105	PIIF	1.17	2.82E-02	peptidylprolyl isomerase F
84246	MED10	1.17	2.83E-02	mediator complex subunit 10
3633	INPP5B	1.17	4.68E-02	inositol polyphosphate-5-phosphatase, 75kDa
169200	TMEM64	1.17	2.18E-02	transmembrane protein 64
85403	EAF1	1.17	1.70E-02	ELL associated factor 1
9731	CEP104	1.17	3.01E-02	centrosomal protein 104kDa
7106	TSPAN4	1.17	2.74E-02	tetraspanin 4
9475	ROCK2	1.17	1.93E-02	Rho-associated, coiled-coil containing protein kinase 2
55127	HEATR1	1.17	4.95E-02	HEAT repeat containing 1
55667	DENN4D4C	1.17	2.81E-02	DENN/MADD domain containing 4C
58472	SQRDL	1.17	4.00E-02	sulfide quinone reductase-like (yeast)
5929	RBBP5	1.17	4.78E-02	retinoblastoma binding protein 5
22870	PPP6R1	1.17	3.57E-02	protein phosphatase 6, regulatory subunit 1
3459	IFNGR1	1.17	2.76E-03	interferon gamma receptor 1
9654	TTL4	1.17	3.20E-02	tubulin tyrosine ligase-like family, member 4
1604	CD55	1.17	3.17E-02	CD55 molecule, decay accelerating factor for complement (Cromer blood group)
3692	EIF6	1.17	5.00E-02	eukaryotic translation initiation factor 6
5352	PLOD2	1.16	4.45E-02	procollagen-lysine, 2-oxoglutarate 5-dioxygenase 2
4170	MCL1	1.16	1.08E-02	myeloid cell leukemia 1
26003	GORASP2	1.16	1.54E-02	golgi reassembly stacking protein 2, 55kDa
2317	FLNB	1.16	2.14E-02	filamin B, beta
4927	NUP88	1.16	3.98E-02	nucleoporin 88kDa
2803	GOLGA4	1.16	8.74E-03	golgin A4
155061	ZNF746	1.16	3.54E-02	zinc finger protein 746
55054	ATG16L1	1.16	4.94E-02	autophagy related 16-like 1 (S. cerevisiae)
1983	EIF5	1.16	2.47E-02	eukaryotic translation initiation factor 5
26100	WIPI2	1.16	4.90E-02	WD repeat domain, phosphoinositide interacting 2
5092	PCBD1	1.16	2.95E-02	pterin-4 alpha-carbinolamine dehydratase/dimerization cofactor of hepatocyte nuclear factor 1 alpha
5203	PFDN4	1.16	4.65E-02	prefoldin subunit 4
51181	DCXR	1.16	4.12E-02	dicarbonyl/L-xylulose reductase
571	BACH1	1.16	4.56E-02	BTB and CNC homology 1, basic leucine zipper transcription factor 1
3312	HSPA8	1.16	9.45E-03	heat shock 70kDa protein 8
4799	NFX1	1.16	3.95E-02	nuclear transcription factor, X-box binding 1
79691	QTRTD1	1.16	4.75E-02	queuine tRNA-ribosyltransferase domain containing 1
3376	IARS	1.16	2.42E-02	isoleucyl-tRNA synthetase
3313	HSPA9	1.16	1.31E-02	heat shock 70kDa protein 9 (mortalin)
6856	SYPL1	1.16	3.57E-02	synaptophysin-like 1
27339	PRPF19	1.15	4.77E-02	pre-mRNA processing factor 19
8615	USO1	1.15	2.81E-02	USO1 vesicle transport factor
221749	PXDC1	1.15	3.71E-02	PX domain containing 1
5264	PHYH	1.15	3.01E-02	phytanoyl-CoA 2-hydroxylase
1650	DDOST	1.15	4.85E-02	dolichyl-diphosphoglycosaccharide--protein glycosyltransferase subunit (non-catalytic)
1212	CLTB	1.15	3.72E-02	clathrin, light chain B
10969	EBNA1BP2	1.15	2.73E-02	EBNA1 binding protein 2
10857	PGRMC1	1.15	6.31E-03	progesterone receptor membrane component 1
8833	GMPS	1.15	4.25E-02	guanine monophosphate synthase

Entrez ID	Gene name	Fold change	q-value	Description
8454	CUL1	1.15	1.03E-02	cullin 1
60481	ELOVL5	1.15	1.40E-02	ELOVL fatty acid elongase 5
201627	DENND6A	1.14	3.19E-02	DENN/MADD domain containing 6A
7415	VCP	1.14	4.53E-03	valosin containing protein
23214	XPO6	1.14	2.63E-02	exportin 6
7763	ZFAND5	1.14	1.48E-02	zinc finger, AN1-type domain 5
7358	UGDH	1.14	8.38E-03	UDP-glucose 6-dehydrogenase
5007	OSBP	1.14	4.78E-02	oxysterol binding protein
3069	HDLBP	1.14	4.45E-02	high density lipoprotein binding protein
23074	UHRF1BP1L	1.14	3.84E-02	UHRF1 binding protein 1-like
3326	HSP90AB1	1.14	1.56E-02	heat shock protein 90kDa alpha (cytosolic), class B member 1
92856	IMP4	1.14	1.33E-02	IMP4, U3 small nucleolar ribonucleoprotein
55970	GNG12	1.13	2.98E-02	guanine nucleotide binding protein (G protein), gamma 12
9275	BCL7B	1.13	3.34E-02	B-cell CLL/lymphoma 7B
4259	MGST3	1.13	4.79E-02	microsomal glutathione S-transferase 3
1635	DCTD	1.13	3.73E-02	dCMP deaminase
3416	IDE	1.13	3.17E-02	insulin-degrading enzyme
94056	SYAP1	1.13	2.35E-02	synapse associated protein 1
821	CANX	1.12	2.87E-02	calnexin
3267	AGFG1	1.12	3.58E-02	ArfGAP with FG repeats 1
5052	PRDX1	1.11	4.10E-02	peroxiredoxin 1

Supplemental table 2. Full list of genes repressed by Wy14643 in human PCLS

Entrez ID	Gene name	Fold change	q-value	Description
4283	CXCL9	-7.25	5.28E-05	chemokine (C-X-C motif) ligand 9
3627	CXCL10	-6.88	6.58E-05	chemokine (C-X-C motif) ligand 10
6373	CXCL11	-5.65	3.69E-04	chemokine (C-X-C motif) ligand 11
405753	DUOX2	-3.97	3.05E-06	dual oxidase maturation factor 2
4843	NOS2	-3.62	5.43E-03	nitric oxide synthase 2, inducible
50506	DUOX2	-3.24	5.01E-06	dual oxidase 2
6355	CCL8	-3.07	3.67E-03	chemokine (C-C motif) ligand 8
10964	IFI44L	-3.06	4.43E-04	interferon-induced protein 44-like
115362	GBP5	-2.94	6.83E-04	guanylate binding protein 5
3620	IDO1	-2.91	5.65E-06	indoleamine 2,3-dioxygenase 1
8519	IFITM1	-2.67	5.65E-06	interferon induced transmembrane protein 1
3433	IFIT2	-2.61	2.28E-03	interferon-induced protein with tetratricopeptide repeats 2
54898	ELOVL2	-2.61	4.38E-07	ELOVL fatty acid elongase 2
2892	GRIA3	-2.60	3.06E-05	glutamate receptor, ionotropic, AMPA 3
6376	CX3CL1	-2.57	4.43E-04	chemokine (C-X3-C motif) ligand 1
7098	TLR3	-2.55	5.76E-06	toll-like receptor 3
79689	STEAP4	-2.50	8.35E-05	STEAP family member 4
3434	IFIT1	-2.48	2.64E-03	interferon-induced protein with tetratricopeptide repeats 1
4321	MMP12	-2.45	2.30E-04	matrix metalloproteinase 12 (macrophage elastase)
10826	FAXDC2	-2.42	5.01E-06	fatty acid hydroxylase domain containing 2
8626	TP63	-2.41	2.02E-05	tumor protein p63
64577	ALDH8A1	-2.41	6.05E-06	aldehyde dehydrogenase 8 family, member A1
8740	TNFSF14	-2.40	6.35E-05	tumor necrosis factor (ligand) superfamily, member 14
10417	SPON2	-2.39	2.46E-06	spondin 2, extracellular matrix protein
3437	IFIT3	-2.38	2.74E-04	interferon-induced protein with tetratricopeptide repeats 3
54739	XAF1	-2.35	3.46E-06	XIAP associated factor 1
94240	EPSTI1	-2.29	2.79E-04	epithelial stromal interaction 1 (breast)
10346	TRIM22	-2.28	4.50E-06	tripartite motif containing 22
83953	FCAMR	-2.28	1.16E-02	Fc receptor, IgA, IgM, high affinity
3934	LCN2	-2.26	1.95E-04	lipocalin 2
388646	GBP7	-2.25	1.82E-04	guanylate binding protein 7
57817	HAMP	-2.24	5.28E-05	hepcidin antimicrobial peptide
2634	GBP2	-2.22	6.65E-05	guanylate binding protein 2, interferon-inducible
9288	TAAR3	-2.22	2.65E-02	trace amine associated receptor 3 (gene/pseudogene)
115361	GBP4	-2.21	2.38E-04	guanylate binding protein 4
6372	CXCL6	-2.20	8.74E-04	chemokine (C-X-C motif) ligand 6
10537	UBD	-2.19	1.02E-06	ubiquitin D
11274	USP18	-2.18	3.82E-04	ubiquitin specific peptidase 18
51156	SERPINA10	-2.18	2.15E-05	serpin peptidase inhibitor, clade A (alpha-1 antiproteinase, antitrypsin), member 10
6999	TDO2	-2.16	9.97E-03	tryptophan 2,3-dioxygenase
256764	WDR72	-2.15	1.02E-03	WD repeat domain 72
5920	RARRES3	-2.12	1.34E-06	retinoic acid receptor responder (tazarotene induced) 3
5284	PIGR	-2.11	1.97E-03	polymeric immunoglobulin receptor
4939	OAS2	-2.10	5.36E-04	2'-5'-oligoadenylate synthetase 2, 69/71kDa
113146	AHNAK2	-2.09	6.05E-06	AHNAK nucleoprotein 2
4599	MX1	-2.07	5.70E-04	myxovirus (influenza virus) resistance 1, interferon-inducible protein p78 (mouse)
4940	OAS3	-2.06	4.49E-04	2'-5'-oligoadenylate synthetase 3, 100kDa

Entrez ID	Gene name	Fold change	q-value	Description
57507	ZNF608	-2.06	5.01E-06	zinc finger protein 608
2633	GBP1	-2.04	1.05E-04	guanylate binding protein 1, interferon-inducible
3626	INHBC	-2.03	9.40E-05	inhibin, beta C
117153	MIA2	-2.02	2.07E-04	melanoma inhibitory activity 2
80833	APOL3	-2.01	1.86E-04	apolipoprotein L, 3
10068	IL18BP	-1.97	4.50E-06	interleukin 18 binding protein
54809	SAMD9	-1.97	2.61E-05	sterile alpha motif domain containing 9
84873	GPR128	-1.97	4.02E-05	G protein-coupled receptor 128
5168	ENPP2	-1.97	4.50E-06	ectonucleotide pyrophosphatase/phosphodiesterase 2
5207	PFKFB1	-1.96	3.69E-04	6-phosphofructo-2-kinase/fructose-2,6-bisphosphatase 1
10272	FSTL3	-1.96	6.80E-03	folistatin-like 3 (secreted glycoprotein)
6289	SAA2	-1.96	1.46E-03	serum amyloid A2
10561	IFI44	-1.95	2.40E-04	interferon-induced protein 44
420	ART4	-1.94	1.30E-04	ADP-ribosyltransferase 4 (Dombrock blood group)
219285	SAMD9L	-1.94	7.48E-04	sterile alpha motif domain containing 9-like
4938	OAS1	-1.94	1.86E-04	2'-5'-oligoadenylate synthetase 1, 40/46kDa
80380	PDCD1LG2	-1.93	1.30E-03	programmed cell death 1 ligand 2
23586	DDX58	-1.93	8.22E-05	DEAD (Asp-Glu-Ala-Asp) box polypeptide 58
9636	ISG15	-1.92	8.26E-04	ISG15 ubiquitin-like modifier
4547	MTTP	-1.91	1.65E-04	microsomal triglyceride transfer protein
343450	KCNT2	-1.90	6.93E-05	potassium channel, subfamily T, member 2
5288	PIK3C2G	-1.90	2.58E-04	phosphatidylinositol-4-phosphate 3-kinase, catalytic subunit type 2 gamma
2537	IFI6	-1.89	1.29E-05	interferon, alpha-inducible protein 6
1592	CYP26A1	-1.89	7.57E-04	cytochrome P450, family 26, subfamily A, polypeptide 1
342372	PKD1L3	-1.89	2.15E-03	polycystic kidney disease 1-like 3
353514	LILRA5	-1.87	1.46E-03	leukocyte immunoglobulin-like receptor, subfamily A (with TM domain), member 5
7042	TGFB2	-1.87	2.30E-06	transforming growth factor, beta 2
23767	FLRT3	-1.86	2.25E-04	fibronectin leucine rich transmembrane protein 3
83666	PARP9	-1.86	3.18E-05	poly (ADP-ribose) polymerase family, member 9
412	STS	-1.85	4.62E-04	steroid sulfatase (microsomal), isozyme S
10677	AVIL	-1.84	4.43E-04	advillin
83729	INHBE	-1.84	6.47E-04	inhibin, beta E
163351	GBP6	-1.82	1.65E-02	guanylate binding protein family, member 6
2635	GBP3	-1.82	3.43E-04	guanylate binding protein 3
55008	HERC6	-1.81	3.76E-03	HECT and RLD domain containing E3 ubiquitin protein ligase family member 6
6274	S100A3	-1.81	4.79E-02	S100 calcium binding protein A3
55601	DDX60	-1.81	3.68E-04	DEAD (Asp-Glu-Ala-Asp) box polypeptide 60
114899	C1QTNF3	-1.80	2.75E-02	C1q and tumor necrosis factor related protein 3
27289	RND1	-1.79	1.56E-04	Rho family GTPase 1
952	CD38	-1.78	6.84E-04	CD38 molecule
9510	ADAMTS1	-1.78	2.41E-02	ADAM metalloproteinase with thrombospondin type 1 motif, 1
5737	PTGFR	-1.78	7.03E-04	prostaglandin F receptor (FP)
51056	LAP3	-1.78	1.46E-03	leucine aminopeptidase 3
64108	RTP4	-1.77	1.33E-03	receptor (chemosensory) transporter protein 4
6363	CCL19	-1.77	5.33E-05	chemokine (C-C motif) ligand 19
4068	SH2D1A	-1.77	1.20E-02	SH2 domain containing 1A
7127	TNFAIP2	-1.76	5.43E-03	tumor necrosis factor, alpha-induced protein 2
28951	TRIB2	-1.75	1.94E-03	tribbles pseudokinase 2
222643	UNC5CL	-1.75	1.02E-03	unc-5 homolog C (C. elegans)-like
9076	CLDN1	-1.75	1.06E-06	claudin 1
6690	SPINK1	-1.74	3.81E-03	serine peptidase inhibitor, Kazal type 1
200373	PCDP1	-1.74	1.56E-03	primary ciliary dyskinesia protein 1
6352	CCL5	-1.74	6.93E-04	chemokine (C-C motif) ligand 5
8875	VNN2	-1.73	7.42E-04	vanin 2
11074	TRIM31	-1.73	6.09E-05	tripartite motif containing 31
8743	TNFSF10	-1.73	1.99E-06	tumor necrosis factor (ligand) superfamily, member 10
118932	ANKRD22	-1.73	8.29E-03	ankyrin repeat domain 22
3430	IFI35	-1.72	5.43E-03	interferon-induced protein 35
3560	IL2RB	-1.72	2.29E-03	interleukin 2 receptor, beta
8470	SORBS2	-1.72	9.72E-04	sorbin and SH3 domain containing 2
60489	APOBEC3G	-1.72	2.10E-02	apolipoprotein B mRNA editing enzyme, catalytic polypeptide-like 3G
5698	PSMB9	-1.72	1.20E-03	proteasome (prosome, macropain) subunit, beta type, 9
7045	TGFB1	-1.71	1.04E-04	transforming growth factor, beta-induced, 68kDa
2877	GPX2	-1.71	8.74E-03	glutathione peroxidase 2 (gastrointestinal)
51513	ETV7	-1.71	1.86E-02	ets variant 7
284111	SLC13A5	-1.71	4.83E-04	solute carrier family 13 (sodium-dependent citrate transporter), member 5
6288	SAA1	-1.71	3.91E-04	serum amyloid A1
5320	PLA2G2A	-1.70	1.06E-03	phospholipase A2, group IIA (platelets, synovial fluid)
4212	MEIS2	-1.70	2.58E-04	Meis homeobox 2
64127	NOD2	-1.70	2.34E-02	nucleotide-binding oligomerization domain containing 2
6906	SERPINA7	-1.69	1.77E-03	serpin peptidase inhibitor, clade A (alpha-1 antiproteinase, antitrypsin), member 7
64902	AGXT2	-1.69	1.93E-02	alanine-glyoxylate aminotransferase 2
6362	CCL18	-1.69	7.01E-04	chemokine (C-C motif) ligand 18 (pulmonary and activation-regulated)
56521	DNAJC12	-1.69	2.28E-03	DnaJ (Hsp40) homolog, subfamily C, member 12
100423062	IGLL5	-1.69	4.02E-02	immunoglobulin lambda-like polypeptide 5
7274	TPPA	-1.68	1.32E-02	tocopherol (alpha) transfer protein

Entrez ID	Gene name	Fold change	q-value	Description
29760	BLNK	-1.68	2.88E-03	B-cell linker
6335	SCN9A	-1.68	2.84E-03	sodium channel, voltage-gated, type IX, alpha subunit
126410	CYP4F22	-1.68	2.94E-03	cytochrome P450, family 4, subfamily F, polypeptide 22
126	ADH1C	-1.67	3.50E-02	alcohol dehydrogenase 1C (class I), gamma polypeptide
10351	ABCA8	-1.67	1.30E-02	ATP-binding cassette, sub-family A (ABC1), member 8
3003	GZMK	-1.66	6.15E-03	granzyme K (granzyme 3 /// tryptase II)
9971	NR1H4	-1.66	8.69E-05	nuclear receptor subfamily 1, group H, member 4
5629	PROX1	-1.66	3.84E-05	prospero homeobox 1
388403	YPEL2	-1.65	2.42E-04	yippee-like 2 (Drosophila)
84072	HORMAD1	-1.65	4.16E-02	HORMA domain containing 1
347051	SLC10A5	-1.65	8.97E-03	solute carrier family 10, member 5
6318	SERPINB4	-1.63	2.98E-02	serpin peptidase inhibitor, clade B (ovalbumin), member 4
5858	PZP	-1.63	2.91E-03	pregnancy-zone protein
4982	TNFRSF11B	-1.63	1.41E-03	tumor necrosis factor receptor superfamily, member 11b
3429	IFI27	-1.62	1.42E-03	interferon, alpha-inducible protein 27
2621	GAS6	-1.62	1.94E-03	growth arrest-specific 6
7447	VSNL1	-1.61	1.36E-03	visinin-like 1
834	CASP1	-1.61	2.46E-02	caspase 1, apoptosis-related cysteine peptidase
6366	CCL21	-1.60	1.76E-02	chemokine (C-C motif) ligand 21
6775	STAT4	-1.60	2.49E-03	signal transducer and activator of transcription 4
84171	LOXL4	-1.60	3.32E-02	lysyl oxidase-like 4
2212	FCGR2A	-1.60	3.96E-03	Fc fragment of IgG, low affinity IIa, receptor (CD32)
10158	PDZK1IP1	-1.60	2.84E-02	PDZK1 interacting protein 1
4316	MMP7	-1.60	2.24E-02	matrix metallopeptidase 7 (matrilysin, uterine)
7097	TLR2	-1.59	2.26E-03	toll-like receptor 2
8736	MYOM1	-1.59	1.24E-02	myomesin 1
401474	SAMD12	-1.59	2.02E-02	sterile alpha motif domain containing 12
64135	IFIH1	-1.59	2.98E-03	interferon induced with helicase C domain 1
958	CD40	-1.59	1.20E-02	CD40 molecule, TNF receptor superfamily member 5
27074	LAMP3	-1.58	1.86E-04	lysosomal-associated membrane protein 3
10261	IGSF6	-1.58	2.81E-03	immunoglobulin superfamily, member 6
6890	TAP1	-1.58	3.37E-03	transporter 1, ATP-binding cassette, sub-family B (MDR/TAP)
1080	CFTR	-1.58	7.70E-04	cystic fibrosis transmembrane conductance regulator (ATP-binding cassette sub-family C, member 7)
117247	SLC16A10	-1.57	1.05E-04	solute carrier family 16 (aromatic amino acid transporter), member 10
10906	TRAFD1	-1.57	8.33E-03	TRAF-type zinc finger domain containing 1
6716	SRD5A2	-1.57	2.74E-04	steroid-5-alpha-reductase, alpha polypeptide 2 (3-oxo-5 alpha-steroid delta 4-dehydrogenase alpha 2)
400986	ANKRD36C	-1.57	4.91E-04	ankyrin repeat domain 36C
6696	SPP1	-1.57	1.41E-03	secreted phosphoprotein 1
719	C3AR1	-1.57	4.19E-03	complement component 3a receptor 1
10903	MTMR11	-1.56	2.31E-03	myotubularin related protein 11
4739	NEDD9	-1.56	1.28E-03	neural precursor cell expressed, developmentally down-regulated 9
30835	CD209	-1.56	5.51E-03	CD209 molecule
2267	FGL1	-1.56	2.06E-05	fibrinogen-like 1
3157	HMGCS1	-1.56	2.35E-05	3-hydroxy-3-methylglutaryl-CoA synthase 1 (soluble)
389197	C4orf50	-1.56	6.25E-03	chromosome 4 open reading frame 50
114836	SLAMF6	-1.56	3.72E-02	SLAM family member 6
3175	ONECUT1	-1.55	1.98E-03	one cut homeobox 1
2690	GHR	-1.55	3.72E-03	growth hormone receptor
3659	IRF1	-1.55	6.31E-03	interferon regulatory factor 1
7078	TIMP3	-1.55	9.19E-04	TIMP metallopeptidase inhibitor 3
80310	PDGFD	-1.55	9.79E-03	platelet derived growth factor D
5359	PLSCR1	-1.55	1.73E-04	phospholipid scramblase 1
4837	NNMT	-1.55	2.35E-03	nicotinamide N-methyltransferase
55013	CCDC109B	-1.55	1.04E-04	coiled-coil domain containing 109B
55076	TMEM45A	-1.55	1.12E-02	transmembrane protein 45A
3383	ICAM1	-1.55	2.24E-03	intercellular adhesion molecule 1
28755	TRAC	-1.55	1.75E-03	T cell receptor alpha constant
9627	SNCAIP	-1.54	8.39E-03	synuclein, alpha interacting protein
6772	STAT1	-1.54	1.28E-03	signal transducer and activator of transcription 1, 91kDa
994	CDC25B	-1.54	7.05E-04	cell division cycle 25B
3001	GZMA	-1.54	1.99E-02	granzyme A (granzyme 1, cytotoxic T-lymphocyte-associated serine esterase 3)
221468	TMEM217	-1.54	6.07E-03	transmembrane protein 217
117283	IP6K3	-1.54	1.18E-02	inositol hexakisphosphate kinase 3
597	BCL2A1	-1.53	8.77E-03	BCL2-related protein A1
10568	SLC34A2	-1.53	4.17E-03	solute carrier family 34 (type II sodium/phosphate cotransporter), member 2
57393	TMEM27	-1.53	1.51E-02	transmembrane protein 27
10866	HCP5	-1.53	3.84E-03	HLA complex P5 (non-protein coding)
5721	PSME2	-1.53	1.29E-02	proteasome (prosome, macropain) activator subunit 2 (PA28 beta)
8564	KMO	-1.53	2.47E-03	kynurenine 3-monooxygenase (kynurenine 3-hydroxylase)
7453	WARS	-1.52	6.26E-03	tryptophanyl-tRNA synthetase
5341	PLEK	-1.52	3.76E-03	pleckstrin
55304	SPTLC3	-1.52	1.76E-03	serine palmitoyltransferase, long chain base subunit 3
2	A2M	-1.52	2.84E-02	alpha-2-macroglobulin
54625	PARP14	-1.52	6.41E-03	poly (ADP-ribose) polymerase family, member 14

Entrez ID	Gene name	Fold change	q-value	Description
338809	C12orf74	-1.51	1.54E-02	chromosome 12 open reading frame 74
9563	H6PD	-1.50	1.86E-02	hexose-6-phosphate dehydrogenase (glucose 1-dehydrogenase)
727	C5	-1.50	1.29E-02	complement component 5
9332	CD163	-1.50	1.63E-02	CD163 molecule
5696	PSMB8	-1.50	1.10E-03	proteasome (prosome, macropain) subunit, beta type, 8
80323	CCDC68	-1.50	2.66E-02	coiled-coil domain containing 68
6351	CCL4	-1.50	3.85E-02	chemokine (C-C motif) ligand 4
145864	HAPLN3	-1.49	4.00E-02	hyaluronan and proteoglycan link protein 3
54757	FAM20A	-1.49	1.00E-02	family with sequence similarity 20, member A
3075	CFH	-1.49	1.61E-04	complement factor H
59269	HIVEP3	-1.49	2.14E-03	human immunodeficiency virus type 1 enhancer binding protein 3
9830	TRIM14	-1.49	1.04E-04	tripartite motif containing 14
84174	SLA2	-1.49	6.31E-03	Src-like-adaptor 2
338821	SLCO1B7	-1.49	3.54E-02	solute carrier organic anion transporter family, member 1B7 (non-functional)
39	ACAT2	-1.49	9.40E-05	acetyl-CoA acetyltransferase 2
150864	FAM117B	-1.48	1.47E-03	family with sequence similarity 117, member B
1824	DSC2	-1.48	1.79E-04	desmocollin 2
64116	SLC39A8	-1.48	2.14E-03	solute carrier family 39 (zinc transporter), member 8
81788	NUAK2	-1.48	1.72E-02	NUAK family, SNF1-like kinase, 2
4261	CIITA	-1.47	2.11E-02	class II, major histocompatibility complex, transactivator
3128	HLA-DRB6	-1.47	3.96E-02	major histocompatibility complex, class II, DR beta 6 (pseudogene)
54463	FAM134B	-1.47	1.94E-03	family with sequence similarity 134, member B
50604	IL20	-1.47	4.13E-02	interleukin 20
116071	BATF2	-1.47	4.24E-02	basic leucine zipper transcription factor, ATF-like 2
8854	ALDH1A2	-1.47	2.03E-02	aldehyde dehydrogenase 1 family, member A2
6446	SGK1	-1.47	2.21E-03	serum/glucocorticoid regulated kinase 1
10384	BTN3A3	-1.47	6.77E-03	butyrophilin, subfamily 3, member A3
127733	UBXN10	-1.47	1.09E-02	UBX domain protein 10
94241	TP53INP1	-1.47	1.10E-03	tumor protein p53 inducible nuclear protein 1
5699	PSMB10	-1.46	2.00E-03	proteasome (prosome, macropain) subunit, beta type, 10
25939	SAMHD1	-1.46	1.19E-02	SAM domain and HD domain 1
843	CASP10	-1.46	1.96E-02	caspase 10, apoptosis-related cysteine peptidase
129607	CMPK2	-1.46	2.91E-02	cytidine monophosphate (UMP-CMP) kinase 2, mitochondrial
10993	SDS	-1.46	2.10E-03	serine dehydratase
158584	FAAH2	-1.46	8.28E-03	fatty acid amide hydrolase 2
113263	GLCC1	-1.46	1.47E-03	glucocorticoid induced transcript 1
1723	DHODH	-1.46	4.59E-02	dihydroorotate dehydrogenase (quinone)
1806	DPYD	-1.46	2.10E-03	dihydropyrimidine dehydrogenase
4494	MT1F	-1.46	1.86E-04	metallothionein 1F
158219	TTC39B	-1.46	6.77E-03	tetratricopeptide repeat domain 39B
55603	FAM46A	-1.46	8.97E-03	family with sequence similarity 46, member A
81794	ADAMTS10	-1.46	7.03E-04	ADAM metalloproteinase with thrombospondin type 1 motif, 10
28638	TRBC2	-1.46	2.60E-02	T cell receptor beta constant 2
128439	SNHG11	-1.46	1.72E-02	small nucleolar RNA host gene 11 (non-protein coding)
51313	FAM198B	-1.46	4.69E-03	family with sequence similarity 198, member B
8600	TNFSF11	-1.46	2.18E-03	tumor necrosis factor (ligand) superfamily, member 11
10154	PLXNC1	-1.45	1.31E-02	plexin C1
168537	GIMAP7	-1.45	4.60E-03	GTPase, IMAP family member 7
57674	RNF213	-1.45	2.89E-03	ring finger protein 213
10225	CD96	-1.45	5.43E-03	CD96 molecule
55075	UACA	-1.45	3.09E-03	uveal autoantigen with coiled-coil domains and ankyrin repeats
2272	FHIT	-1.45	4.50E-02	fragile histidine triad
84419	C15orf48	-1.45	2.99E-02	chromosome 15 open reading frame 48
10379	IRF9	-1.45	7.70E-04	interferon regulatory factor 9
3431	SP110	-1.45	2.58E-03	SP110 nuclear body protein
100133315	LOC100133315	-1.44	2.60E-02	transient receptor potential cation channel, subfamily C, member 2-like
406	ARNTL	-1.44	5.20E-03	aryl hydrocarbon receptor nuclear translocator-like
3005	H1FO	-1.44	7.10E-04	H1 histone family, member 0
337972	KRTAP19-5	-1.44	4.67E-02	keratin associated protein 19-5
3728	JUP	-1.44	2.78E-04	junction plakoglobin
2160	F11	-1.44	6.75E-04	coagulation factor XI
23213	SULF1	-1.44	1.39E-02	sulfatase 1
953	ENTPD1	-1.44	4.64E-03	ectonucleoside triphosphate diphosphohydrolase 1
6385	SDC4	-1.44	1.78E-03	syndecan 4
1520	CTSS	-1.44	2.65E-03	cathepsin S
259307	IL4I1	-1.44	8.20E-03	interleukin 4 induced 1
3929	LBP	-1.44	1.77E-03	lipopolysaccharide binding protein
440836	ODF3B	-1.44	3.11E-02	outer dense fiber of sperm tails 3B
6590	SLPI	-1.43	2.71E-03	secretory leukocyte peptidase inhibitor
6499	SKIV2L	-1.43	1.12E-02	superkiller viralicidal activity 2-like (S. cerevisiae)
199	AIF1	-1.43	1.64E-02	allograft inflammatory factor 1
4008	LMO7	-1.42	1.97E-03	LIM domain 7
23460	ABCA6	-1.42	1.08E-02	ATP-binding cassette, sub-family A (ABC1), member 6
4318	MMP9	-1.42	6.31E-03	matrix metalloproteinase 9 (gelatinase B, 92kDa gelatinase, 92kDa type IV collagenase)
8832	CD84	-1.42	5.45E-03	CD84 molecule
5031	P2RY6	-1.42	3.42E-02	pyrimidineric receptor P2Y, G-protein coupled, 6

Entrez ID	Gene name	Fold change	q-value	Description
79132	DHX58	-1.42	3.43E-02	DEXH (Asp-Glu-X-His) box polypeptide 58
8013	NR4A3	-1.42	4.19E-03	nuclear receptor subfamily 4, group A, member 3
23012	STK38L	-1.42	4.42E-05	serine/threonine kinase 38 like
2766	GMFR	-1.42	4.93E-02	guanosine monophosphate reductase
6892	TAPBP	-1.42	1.59E-04	TAP binding protein (tapasin)
25816	TNFAIP8	-1.42	8.39E-03	tumor necrosis factor, alpha-induced protein 8
91351	DDX60L	-1.42	2.46E-02	DEAD (Asp-Glu-Ala-Asp) box polypeptide 60-like
1643	DDB2	-1.42	2.30E-03	damage-specific DNA binding protein 2, 48kDa
23780	APOL2	-1.42	4.60E-03	apolipoprotein L, 2
7412	VCAM1	-1.41	4.45E-02	vascular cell adhesion molecule 1
3113	HLA-DPA1	-1.41	5.99E-03	major histocompatibility complex, class II, DP alpha 1
132321	C4orf33	-1.41	2.50E-02	chromosome 4 open reading frame 33
51348	KLRF1	-1.41	1.38E-02	killer cell lectin-like receptor subfamily F, member 1
58476	TP53INP2	-1.41	6.07E-03	tumor protein p53 inducible nuclear protein 2
976	CD97	-1.41	4.10E-02	CD97 molecule
3176	HNMT	-1.41	6.89E-04	histamine N-methyltransferase
83875	BCO2	-1.41	2.47E-02	beta-carotene oxygenase 2
3140	MR1	-1.41	4.81E-03	major histocompatibility complex, class I-related
1236	CCR7	-1.41	4.59E-02	chemokine (C-C motif) receptor 7
166336	PRICKLE2	-1.40	3.02E-02	prickle homolog 2 (Drosophila)
56892	C8orf4	-1.40	1.14E-03	chromosome 8 open reading frame 4
83593	RASSF5	-1.40	2.72E-02	Ras association (RalGDS/AF-6) domain family member 5
79668	PARP8	-1.40	4.01E-03	poly (ADP-ribose) polymerase family, member 8
10410	IFITM3	-1.39	4.62E-04	interferon induced transmembrane protein 3
9235	IL32	-1.39	1.01E-03	interleukin 32
55064	SPATA6L	-1.39	1.86E-02	spermatogenesis associated 6-like
6480	ST6GAL1	-1.39	6.72E-03	ST6 beta-galactosamide alpha-2,6-sialyltransferase 1
9746	CLSTN3	-1.39	1.04E-04	calsynenin 3
4343	MOV10	-1.39	1.30E-03	Mov10, Moloney leukemia virus 10, homolog (mouse)
255231	MCOLN2	-1.39	3.34E-02	mucolipin 2
6695	SPOCK1	-1.39	8.47E-03	sparc/osteonectin, cwcv and kazal-like domains proteoglycan (testican) 1
6718	AKR1D1	-1.39	2.41E-03	aldo-keto reductase family 1, member D1
10100	TSPAN2	-1.38	3.56E-02	tetraspanin 2
30817	EMR2	-1.38	9.46E-03	egf-like module containing, mucin-like, hormone receptor-like 2
3717	JAK2	-1.38	2.08E-02	Janus kinase 2
79776	ZFXH4	-1.38	6.71E-03	zinc finger homeobox 4
348645	C22orf34	-1.38	4.61E-02	chromosome 22 open reading frame 34
91937	TIMD4	-1.38	1.30E-02	T-cell immunoglobulin and mucin domain containing 4
1033	CDKN3	-1.38	4.83E-02	cyclin-dependent kinase inhibitor 3
10863	ADAM28	-1.38	2.08E-02	ADAM metalloproteinase domain 28
93663	ARHGAP18	-1.38	4.55E-03	Rho GTPase activating protein 18
1073	CFL2	-1.38	7.21E-04	cofilin 2 (muscle)
64218	SEMA4A	-1.38	1.89E-03	sema domain, immunoglobulin domain(Ig), transmembrane domain(TM) and short cytoplasmic domain, (semaphorin) 4A
26031	OSBPL3	-1.38	1.69E-02	oxysterol binding protein-like 3
148213	ZNF681	-1.38	2.66E-02	zinc finger protein 681
26191	PTPN22	-1.38	4.51E-02	protein tyrosine phosphatase, non-receptor type 22 (lymphoid)
140564	APOBEC3D	-1.38	3.00E-02	apolipoprotein B mRNA editing enzyme, catalytic polypeptide-like 3D
401494	PTPLA2D	-1.37	3.49E-02	protein tyrosine phosphatase-like A domain containing 2
6653	SORL1	-1.37	1.38E-02	sortilin-related receptor, L(DLR class) A repeats containing
7903	ST8SIA4	-1.37	1.62E-02	ST8 alpha-N-acetyl-neuraminidase alpha-2,8-sialyltransferase 4
55824	PAG1	-1.37	1.82E-02	phosphoprotein associated with glycosphingolipid microdomains 1
9246	UBE2L6	-1.37	1.62E-02	ubiquitin-conjugating enzyme E2L 6
6347	CCL2	-1.37	1.39E-02	chemokine (C-C motif) ligand 2
145957	NRG4	-1.37	2.78E-02	neuregulin 4
6891	TAP2	-1.37	4.26E-02	transporter 2, ATP-binding cassette, sub-family B (MDR/TAP)
3026	HABP2	-1.37	1.59E-03	hyaluronan binding protein 2
81704	DOCK8	-1.37	8.38E-03	dedicator of cytokinesis 8
9175	MAP3K13	-1.37	4.25E-02	mitogen-activated protein kinase kinase kinase 13
10457	GNPMB	-1.37	3.71E-02	glycoprotein (transmembrane) nmb
79370	BCL2L14	-1.37	2.73E-02	BCL2-like 14 (apoptosis facilitator)
4084	MXD1	-1.37	9.72E-04	MAX dimerization protein 1
3070	HELLS	-1.37	4.87E-02	helicase, lymphoid-specific
5880	RAC2	-1.37	9.40E-03	ras-related C3 botulinum toxin substrate 2 (rho family, small GTP binding protein Rac2)
5027	P2RX7	-1.37	8.81E-03	purinergic receptor P2X, ligand-gated ion channel, 7
857	CAV1	-1.36	1.64E-02	caveolin 1, caveolae protein, 22kDa
10203	CALCRL	-1.36	1.77E-02	calcitonin receptor-like
2207	FCER1G	-1.36	9.73E-03	Fc fragment of IgE, high affinity I, receptor for III gamma polypeptide
8502	PKP4	-1.36	5.46E-04	plakophilin 4
8836	GGH	-1.36	2.47E-02	gamma-glutamyl hydrolase (conjugase, folylpolyglutammaglutamyl hydrolase)
90527	DUOXA1	-1.36	7.43E-03	dual oxidase maturation factor 1
8673	VAMP8	-1.36	7.98E-05	vesicle-associated membrane protein 8
3122	HLA-DRA	-1.36	3.73E-03	major histocompatibility complex, class II, DR alpha
123803	NTAN1	-1.36	4.53E-03	N-terminal asparagine amidase
94015	TTYH2	-1.36	2.56E-03	tweet family member 2
3604	TNFRSF9	-1.36	1.83E-02	tumor necrosis factor receptor superfamily, member 9

Entrez ID	Gene name	Fold change	q-value	Description
10288	LILRB2	-1.36	4.75E-02	leukocyte immunoglobulin-like receptor, subfamily B (with TM and ITIM domains), member 2
481	ATP1B1	-1.36	2.68E-03	ATPase, Na ⁺ /K ⁺ transporting, beta 1 polypeptide
10581	IFITM2	-1.36	1.13E-02	interferon induced transmembrane protein 2
23648	SSBP3	-1.36	1.11E-02	single stranded DNA binding protein 3
64092	SAMSN1	-1.35	5.45E-03	SAM domain, SH3 domain and nuclear localization signals 1
342132	ZNF774	-1.35	4.35E-02	zinc finger protein 774
57169	ZNFX1	-1.35	8.82E-03	zinc finger, NFX1-type containing 1
4588	MUC6	-1.35	4.84E-02	mucin 6, oligomeric mucus/gel-forming
10133	OPTN	-1.35	1.06E-03	optineurin
55509	BATF3	-1.35	7.56E-03	basic leucine zipper transcription factor, ATF-like 3
23768	FLRT2	-1.35	5.43E-03	fibronectin leucine rich transmembrane protein 2
961	CD47	-1.35	5.96E-03	CD47 molecule
1767	DNAH5	-1.35	3.89E-02	dynein, axonemal, heavy chain 5
84166	NLRCS	-1.35	3.43E-02	NLR family, CARD domain containing 5
241	ALOX5AP	-1.35	8.51E-03	arachidonate 5-lipoxygenase-activating protein
2627	GATA6	-1.35	1.44E-02	GATA binding protein 6
50515	CHST11	-1.34	7.48E-04	carbohydrate (chondroitin 4) sulfotransferase 11
1519	CTSO	-1.34	1.64E-02	cathepsin O
669	BPGM	-1.34	1.06E-03	2,3-bisphosphoglycerate mutase
7111	TMOD1	-1.34	2.87E-02	tropomodulin 1
6367	CCL22	-1.34	1.96E-02	chemokine (C-C motif) ligand 22
51704	GPRCSB	-1.34	1.34E-03	G protein-coupled receptor, class C, group 5, member B
38	ACAT1	-1.34	1.27E-03	acetyl-CoA acetyltransferase 1
725	C4BPB	-1.34	3.36E-02	complement component 4 binding protein, beta
972	CD74	-1.34	7.61E-03	CD74 molecule, major histocompatibility complex, class II invariant chain
89870	TRIM15	-1.34	3.61E-02	tripartite motif containing 15
1004	CDH6	-1.34	9.60E-03	cadherin 6, type 2, K-cadherin (fetal kidney)
25903	OLFML2B	-1.34	4.67E-02	olfactomedin-like 2B
9223	MAGI1	-1.34	4.24E-03	membrane associated guanylate kinase, WW and PDZ domain containing 1
164656	TMPSRSS6	-1.33	1.44E-03	transmembrane protease, serine 6
85441	HELZ2	-1.33	2.85E-02	helicase with zinc finger 2, transcriptional coactivator
7456	WIPF1	-1.33	2.23E-02	WAS/WASL interacting protein family, member 1
55619	DOCK10	-1.33	1.64E-02	dedicator of cytokinesis 10
57530	CGN	-1.33	6.26E-03	cingulin
3108	HLA-DMA	-1.33	1.63E-02	major histocompatibility complex, class II, DM alpha
57619	SHROOM3	-1.33	2.47E-02	shroom family member 3
1880	GPR183	-1.33	1.17E-02	G protein-coupled receptor 183
1890	TYMP	-1.33	6.65E-03	thymidine phosphorylase
7743	ZNF189	-1.33	4.89E-03	zinc finger protein 189
4300	MLLT3	-1.33	3.98E-02	myeloid/lymphoid or mixed-lineage leukemia (trithorax homolog, Drosophila) /// translocated to, 3
728411	GUSBP1	-1.33	6.77E-03	glucuronidase, beta pseudogene 1
57655	GRAMD1A	-1.32	2.19E-02	GRAM domain containing 1A
151636	DTX3L	-1.32	6.37E-03	deltex 3 like, E3 ubiquitin ligase
3937	LCP2	-1.32	1.93E-02	lymphocyte cytosolic protein 2 (SH2 domain containing leukocyte protein of 76kDa)
11199	ANXA10	-1.32	2.97E-02	annexin A10
5734	PTGER4	-1.32	1.75E-02	prostaglandin E receptor 4 (subtype EP4)
920	CD4	-1.32	2.47E-02	CD4 molecule
64393	ZMAT3	-1.32	1.59E-03	zinc finger, matrin-type 3
80765	STARD5	-1.32	4.37E-02	STAR-related lipid transfer (START) domain containing 5
23338	JADE2	-1.32	3.53E-02	jade family PHD finger 2
717	C2	-1.32	5.70E-04	complement component 2
694	BTG1	-1.32	1.52E-04	B-cell translocation gene 1, anti-proliferative
5552	SRGN	-1.32	1.46E-03	serglycin
64167	ERAP2	-1.32	3.83E-02	endoplasmic reticulum aminopeptidase 2
7104	TM4SF4	-1.32	3.42E-02	transmembrane 4 L six family member 4
8869	ST3GAL5	-1.32	4.11E-02	ST3 beta-galactoside alpha-2,3-sialyltransferase 5
18	ABAT	-1.32	1.29E-02	4-aminobutyrate aminotransferase
11067	C10orf10	-1.31	1.35E-03	chromosome 10 open reading frame 10
359845	FAM101B	-1.31	6.38E-03	family with sequence similarity 101, member B
1030	CDKN2B	-1.31	8.76E-03	cyclin-dependent kinase inhibitor 2B (p15, inhibits CDK4)
5294	PIK3CG	-1.31	3.94E-02	phosphatidylinositol-4,5-bisphosphate 3-kinase, catalytic subunit gamma
133308	SLC9B2	-1.31	2.05E-03	solute carrier family 9, subfamily B (NHA2, cation proton antiporter 2), member 2
51312	SLC25A37	-1.31	9.47E-03	solute carrier family 25 (mitochondrial iron transporter), member 37
5918	RARRES1	-1.31	2.04E-02	retinoic acid receptor responder (tazarotene induced) 1
126917	IFFO2	-1.31	2.58E-02	intermediate filament family orphan 2
135112	NCOA7	-1.31	7.35E-03	nuclear receptor coactivator 7
9873	FCHSD2	-1.31	5.67E-03	FCH and double SH3 domains 2
64856	VWA1	-1.31	3.68E-02	von Willebrand factor A domain containing 1
5788	PTPRC	-1.31	4.67E-02	protein tyrosine phosphatase, receptor type, C
1356	CP	-1.31	5.03E-03	ceruloplasmin (ferroxidase)
4524	MTHFR	-1.31	1.86E-02	methylenetetrahydrofolate reductase (NAD(P)H)
6609	SMPD1	-1.30	1.40E-02	sphingomyelin phosphodiesterase 1, acid lysosomal
79895	ATP8B4	-1.30	5.00E-02	ATPase, class I, type 8B, member 4
2595	GANC	-1.30	2.92E-02	glucosidase, alpha /// neutral C

Entrez ID	Gene name	Fold change	q-value	Description
51279	C1RL	-1.30	5.89E-03	complement component 1, r subcomponent-like
732	C8B	-1.30	4.99E-03	complement component 8, beta polypeptide
1500	CTNND1	-1.30	5.77E-03	catenin (cadherin-associated protein), delta 1
6567	SLC16A2	-1.30	1.86E-02	solute carrier family 16, member 2 (thyroid hormone transporter)
57185	NIPAL3	-1.30	2.98E-02	NIPA-like domain containing 3
2040	STOM	-1.30	3.61E-03	stomatin
6387	CXCL12	-1.30	1.30E-03	chemokine (C-X-C motif) ligand 12
200316	APOBEC3F	-1.30	1.49E-02	apolipoprotein B mRNA editing enzyme, catalytic polypeptide-like 3F
3115	HLA-DPB1	-1.30	3.01E-02	major histocompatibility complex, class II, DP beta 1
118788	PIK3AP1	-1.29	2.62E-02	phosphoinositide-3-kinase adaptor protein 1
23094	SIPA1L3	-1.29	3.83E-03	signal-induced proliferation-associated 1 like 3
118429	ANTXR2	-1.29	6.39E-04	anthrax toxin receptor 2
4430	MYO1B	-1.29	1.60E-03	myosin IB
63901	FAM111A	-1.29	2.75E-02	family with sequence similarity 111, member A
5796	PTPRK	-1.29	1.30E-03	protein tyrosine phosphatase, receptor type, K
5519	PPP2R1B	-1.29	1.27E-03	protein phosphatase 2, regulatory subunit A, beta
55902	ACSS2	-1.29	1.23E-02	acyl-CoA synthetase short-chain family member 2
53	ACP2	-1.29	5.23E-03	acid phosphatase 2, lysosomal
9881	TRANK1	-1.29	2.08E-02	tetratricopeptide repeat and ankyrin repeat containing 1
27106	ARRDC2	-1.29	1.00E-02	arrestin domain containing 2
2266	FGG	-1.28	6.80E-03	fibrinogen gamma chain
10039	PARP3	-1.28	1.30E-02	poly (ADP-ribose) polymerase family, member 3
23424	TDRD7	-1.28	3.10E-02	tudor domain containing 7
9674	KIAA0040	-1.28	1.07E-02	KIAA0040
10026	PIGK	-1.28	3.82E-02	phosphatidylinositol glycan anchor biosynthesis, class K
11221	DUSP10	-1.28	8.93E-03	dual specificity phosphatase 10
822	CAPG	-1.28	2.50E-02	capping protein (actin filament), gelsolin-like
54557	SGTB	-1.28	4.05E-02	small glutamine-rich tetratricopeptide repeat (TPR)-containing, beta
285830	HLA-F-AS1	-1.28	4.86E-02	HLA-F antisense RNA 1
2028	ENPEP	-1.28	3.11E-02	glutamyl aminopeptidase (aminopeptidase A)
23235	SIK2	-1.28	3.77E-02	salt-inducible kinase 2
1959	EGR2	-1.28	1.61E-02	early growth response 2
11151	CORO1A	-1.28	1.86E-02	coronin, actin binding protein, 1A
55620	STAP2	-1.28	2.36E-02	signal transducing adaptor family member 2
5045	FURIN	-1.28	6.20E-03	furin (paired basic amino acid cleaving enzyme)
10437	IFI30	-1.28	4.21E-02	interferon, gamma-inducible protein 30
726	CAPN5	-1.28	2.02E-02	calpain 5
3134	HLA-F	-1.28	3.22E-02	major histocompatibility complex, class I, F
9032	TM4SF5	-1.28	2.96E-02	transmembrane 4 L six family member 5
23705	CADM1	-1.28	4.25E-03	cell adhesion molecule 1
54464	XRN1	-1.28	1.55E-02	5'-3' exonuclease 1
5720	PSME1	-1.27	6.25E-03	proteasome (prosome, macropain) activator subunit 1 (PA28 alpha)
3096	HIVEP1	-1.27	1.18E-03	human immunodeficiency virus type 1 enhancer binding protein 1
5345	SERPINF2	-1.27	2.14E-02	serpin peptidase inhibitor, clade F (alpha-2 antiplasmin, pigment epithelium derived factor), member 2
1512	CTSH	-1.27	2.57E-03	cathepsin H
1803	DPP4	-1.27	2.41E-02	dipeptidyl-peptidase 4
90139	TSPAN18	-1.27	3.62E-02	tetraspanin 18
6615	SNAI1	-1.27	4.10E-02	snail family zinc finger 1
51542	VP54	-1.27	3.68E-02	vacuolar protein sorting 54 homolog (S. cerevisiae)
5058	PAK1	-1.27	1.28E-02	p21 protein (Cdc42/Rac)-activated kinase 1
11161	C14orf1	-1.27	1.39E-02	chromosome 14 open reading frame 1
5610	EIF2AK2	-1.27	1.93E-02	eukaryotic translation initiation factor 2-alpha kinase 2
115825	WDFY2	-1.27	3.42E-03	WD repeat and FYVE domain containing 2
5337	PLD1	-1.27	4.48E-02	phospholipase D1, phosphatidylcholine-specific
8542	APOL1	-1.27	3.17E-02	apolipoprotein L, 1
9926	LPGAT1	-1.27	2.96E-02	lysophosphatidylglycerol acyltransferase 1
11278	KLF12	-1.27	3.84E-02	Kruppel-like factor 12
374378	GALNT18	-1.27	3.42E-02	UDP-N-acetyl-alpha-D-galactosamine:polypeptide N-acetylgalactosaminyltransferase 18
23654	PLXNB2	-1.27	1.86E-04	plexin B2
56829	ZC3HAV1	-1.27	1.77E-03	zinc finger CCCH-type, antiviral 1
6240	RRM1	-1.27	4.26E-02	ribonucleotide reductase M1
5641	LGMM	-1.26	7.37E-03	legumain
8148	TAF15	-1.26	7.03E-04	TAF15 RNA polymerase II, TATA box binding protein (TBP)-associated factor, 68kDa
84159	ARID5B	-1.26	2.67E-03	AT rich interactive domain 5B (MRF1-like)
3587	IL10RA	-1.26	2.51E-02	interleukin 10 receptor, alpha
221895	JAZF1	-1.26	4.96E-02	JAZF zinc finger 1
124540	MSI2	-1.26	1.18E-02	musashi RNA-binding protein 2
3683	ITGAL	-1.26	4.54E-02	integrin, alpha L (antigen CD11A (p180), lymphocyte function-associated antigen 1 /// alpha polypeptide)
2934	GSN	-1.26	1.71E-02	gelsolin
8530	CST7	-1.26	3.33E-02	cystatin F (leukocystatin)
6768	ST14	-1.26	2.41E-02	suppression of tumorigenicity 14 (colon carcinoma)
285440	CYP4V2	-1.26	1.17E-03	cytochrome P450, family 4, subfamily V, polypeptide 2
64780	MICAL1	-1.26	4.29E-02	microtubule associated monooxygenase, calponin and LIM domain containing 1
629	CFB	-1.26	6.18E-04	complement factor B

Entrez ID	Gene name	Fold change	q-value	Description
3732	CD82	-1.26	1.53E-02	CD82 molecule
9945	GFPT2	-1.26	4.62E-02	glutamine-fructose-6-phosphate transaminase 2
64761	PARP12	-1.26	6.07E-03	poly (ADP-ribose) polymerase family, member 12
6307	MSMO1	-1.26	3.17E-02	methylsterol monooxygenase 1
85461	TANC1	-1.26	8.85E-03	tetratricopeptide repeat, ankyrin repeat and coiled-coil containing 1
81553	FAM49A	-1.26	4.31E-02	family with sequence similarity 49, member A
407018	MIR27A	-1.26	3.53E-02	microRNA 27a
9414	TJP2	-1.26	1.15E-02	tight junction protein 2
3684	ITGAM	-1.26	1.83E-02	integrin, alpha M (complement component 3 receptor 3 subunit)
10018	BCL2L11	-1.26	1.86E-02	BCL2-like 11 (apoptosis facilitator)
5654	HTRA1	-1.26	1.83E-02	HtrA serine peptidase 1
2995	GYPE	-1.26	4.35E-03	glycophorin C (Gerbich blood group)
718	C3	-1.26	1.59E-03	complement component 3
51474	LIMA1	-1.26	1.00E-02	LIM domain and actin binding 1
51667	NUB1	-1.25	8.02E-03	negative regulator of ubiquitin-like proteins 1
2037	EPB41L2	-1.25	4.73E-02	erythrocyte membrane protein band 4.1-like 2
3507	IGHM	-1.25	3.73E-02	immunoglobulin heavy constant mu
10982	MAPRE2	-1.25	2.70E-02	microtubule-associated protein, RP/EB family, member 2
716	C1S	-1.25	3.37E-03	complement component 1, s subcomponent
84885	ZDHHC12	-1.25	2.65E-02	zinc finger, DHHC-type containing 12
10157	AASS	-1.25	3.95E-02	aminoadipate-semialdehyde synthase
10420	TESK2	-1.25	3.36E-02	testis-specific kinase 2
23136	EPB41L3	-1.25	2.40E-02	erythrocyte membrane protein band 4.1-like 3
4853	NOTCH2	-1.25	1.08E-02	notch 2
80830	APOL6	-1.25	3.44E-02	apolipoprotein L, 6
51768	TM7SF3	-1.25	8.33E-03	transmembrane 7 superfamily member 3
5993	RFX5	-1.25	4.03E-02	regulatory factor X, 5 (influences HLA class II expression)
3426	CFI	-1.25	2.51E-02	complement factor I
868	CBLB	-1.25	2.22E-03	Cbl proto-oncogene B, E3 ubiquitin protein ligase
55281	TMEM140	-1.25	2.80E-02	transmembrane protein 140
4067	LYN	-1.25	4.68E-03	v-yes-1 Yamaguchi sarcoma viral related oncogene homolog
5538	PPT1	-1.25	2.81E-02	palmitoyl-protein thioesterase 1
4818	NKG7	-1.25	4.68E-02	natural killer cell granule protein 7
7277	TUBA4A	-1.24	2.91E-02	tubulin, alpha 4a
55337	C19orf66	-1.24	1.36E-02	chromosome 19 open reading frame 66
93349	SP140L	-1.24	4.37E-02	SP140 nuclear body protein-like
3371	TNC	-1.24	2.34E-02	tenascin C
330	BIRC3	-1.24	3.31E-02	baculoviral IAP repeat containing 3
123036	TC2N	-1.24	3.98E-02	tandem C2 domains, nuclear
3601	IL15RA	-1.24	7.43E-03	interleukin 15 receptor, alpha
23253	ANKRD12	-1.24	4.68E-03	ankyrin repeat domain 12
2224	FDP5	-1.24	4.91E-02	farnesyl diphosphate synthase
134429	STARD4	-1.24	2.67E-03	StAR-related lipid transfer (START) domain containing 4
57381	RHOJ	-1.24	2.10E-02	ras homolog family member J
4891	SLC11A2	-1.24	9.74E-03	solute carrier family 11 (proton-coupled divalent metal ion transporter), member 2
4647	MYO7A	-1.24	2.91E-02	myosin VIIA
89796	NAV1	-1.24	1.03E-02	neuron navigator 1
8728	ADAM19	-1.24	1.06E-02	ADAM metalloproteinase domain 19
23157	6/sep	-1.24	1.54E-02	sepin 6
12	SERPINA3	-1.24	1.80E-02	serpin peptidase inhibitor, clade A (alpha-1 antiproteinase, antitrypsin), member 3
84230	LRRC8C	-1.23	9.60E-03	leucine rich repeat containing 8 family, member C
4124	MAN2A1	-1.23	3.37E-03	mannosidase, alpha, class 2A, member 1
10046	MAMLD1	-1.23	8.96E-03	mastermind-like domain containing 1
3588	IL10RB	-1.23	1.10E-02	interleukin 10 receptor, beta
3017	HIST1H2BD	-1.23	2.26E-02	histone cluster 1, H2bd
260425	MAGI3	-1.23	1.77E-02	membrane associated guanylate kinase, WW and PDZ domain containing 3
123096	SLC25A29	-1.23	3.85E-02	solute carrier family 25 (mitochondrial carnitine/acylcarnitine carrier), member 29
23635	SSBP2	-1.23	2.26E-02	single-stranded DNA binding protein 2
22920	KIFAP3	-1.23	1.16E-02	kinesin-associated protein 3
3398	ID2	-1.23	1.82E-02	inhibitor of DNA binding 2, dominant negative helix-loop-helix protein
9766	KIAA0247	-1.23	2.65E-02	KIAA0247
214	ALCAM	-1.23	2.19E-02	activated leukocyte cell adhesion molecule
23406	COTL1	-1.23	4.73E-02	coactosin-like F-actin binding protein 1
10957	PNRC1	-1.23	6.43E-03	proline-rich nuclear receptor coactivator 1
8613	PPAP2B	-1.23	3.98E-02	phosphatidic acid phosphatase type 2B
140606	SELM	-1.23	3.77E-03	selenoprotein M
23033	DOPEY1	-1.23	3.17E-02	dopey family member 1
178	AGL	-1.23	3.00E-02	amylase-like 1, 6-glucosidase, 4-alpha-glucanotransferase
4704	NDUF9A	-1.23	3.61E-02	NADH dehydrogenase (ubiquinone) 1 alpha subcomplex, 9, 39kDa
27244	SESN1	-1.22	4.68E-02	sestrin 1
7263	TST	-1.22	3.46E-02	thiosulfate sulfurtransferase (rhodanese)
23293	SMG6	-1.22	3.47E-02	SMG6 nonsense mediated mRNA decay factor
8844	KSR1	-1.22	1.41E-02	kinase suppressor of ras 1
2683	B4GALT1	-1.22	4.54E-02	UDP-Gal:betaGlcNAc beta 1,4- galactosyltransferase, polypeptide 1
659	BMPR2	-1.22	1.23E-02	bone morphogenetic protein receptor, type II (serine/threonine kinase)
9021	SOC3	-1.22	2.80E-02	suppressor of cytokine signaling 3

Entrez ID	Gene name	Fold change	q-value	Description
11031	RAB31	-1.22	1.03E-02	RAB31, member RAS oncogene family
114569	MAL2	-1.22	6.25E-03	mal, T-cell differentiation protein 2 (gene/pseudogene)
5156	PDGFRA	-1.22	3.54E-02	platelet-derived growth factor receptor, alpha polypeptide
51170	HSD17B11	-1.22	3.96E-02	hydroxysteroid (17-beta) dehydrogenase 11
29992	PILRA	-1.22	2.80E-02	paired immunoglobulin-like type 2 receptor alpha
56927	GPR108	-1.22	4.31E-02	G protein-coupled receptor 108
79815	NIPAL2	-1.22	4.96E-02	NIPA-like domain containing 2
23604	DAPK2	-1.21	4.96E-02	death-associated protein kinase 2
80344	DCAF11	-1.21	1.86E-02	DDB1 and CUL4 associated factor 11
2647	BLOC1S1	-1.21	2.97E-02	biogenesis of lysosomal organelles complex-1, subunit 1
3428	IFI16	-1.21	4.83E-02	interferon, gamma-inducible protein 16
55803	ADAP2	-1.21	3.48E-02	ArfGAP with dual PH domains 2
196527	ANO6	-1.21	6.48E-03	anoctamin 6
307	ANXA4	-1.21	4.24E-02	annexin A4
285513	GPRIN3	-1.21	3.34E-02	GPRIN family member 3
9770	RASSF2	-1.21	1.06E-02	Ras association (RalGDS/AF-6) domain family member 2
647135	SRGAP2B	-1.21	9.80E-03	SLIT-ROBO Rho GTPase activating protein 2B
355	FAS	-1.21	2.11E-02	Fas cell surface death receptor
3087	HHEX	-1.21	1.57E-02	hematopoietically expressed homeobox
91452	ACBD5	-1.21	2.80E-02	acyl-CoA binding domain containing 5
55748	CNDP2	-1.21	3.73E-02	CNDP dipeptidase 2 (metallopeptidase M20 family)
6672	SP100	-1.20	1.99E-02	SP100 nuclear antigen
11329	STK38	-1.20	1.79E-02	serine/threonine kinase 38
88455	ANKRD13A	-1.20	4.01E-03	ankyrin repeat domain 13A
4478	MSN	-1.20	7.81E-03	moesin
2581	GALC	-1.20	4.37E-02	galactosylceramidase
80021	TMEM62	-1.20	4.23E-02	transmembrane protein 62
10769	PLK2	-1.20	1.32E-02	polo-like kinase 2
79056	PRRG4	-1.20	2.81E-02	proline rich Gla (G-carboxyglutamic acid) 4 (transmembrane)
900	CCNG1	-1.20	2.47E-03	cyclin G1
25937	WWTR1	-1.20	3.42E-02	WW domain containing transcription regulator 1
9124	PDLIM1	-1.19	3.67E-02	PDZ and LIM domain 1
722	C4BPA	-1.19	9.29E-03	complement component 4 binding protein, alpha
57186	RALGAP2	-1.19	2.91E-02	Ral GTPase activating protein, alpha subunit 2 (catalytic)
7052	TGM2	-1.19	3.50E-02	transglutaminase 2
23102	TBC1D2B	-1.19	4.98E-02	TBC1 domain family, member 2B
6709	SPTAN1	-1.19	1.15E-02	spectrin, alpha, non-erythrocytic 1
1730	DIAPH2	-1.19	2.42E-02	diaphanous-related formin 2
6282	S100A11	-1.19	3.86E-02	S100 calcium binding protein A11
6934	TCF7L2	-1.19	1.14E-02	transcription factor 7-like 2 (T-cell specific, HMG-box)
23516	SLC39A14	-1.18	4.82E-02	solute carrier family 39 (zinc transporter), member 14
4646	MYO6	-1.18	1.55E-02	myosin VI
223082	ZNRF2	-1.18	3.89E-02	zinc and ring finger 2
59338	PLEKHA1	-1.18	2.64E-02	pleckstrin homology domain containing, family A (phosphoinositide binding specific) member 1
7538	ZFP36	-1.18	2.60E-02	ZFP36 ring finger protein
23646	PLD3	-1.18	2.50E-02	phospholipase D family, member 3
3065	HDAC1	-1.18	6.61E-03	histone deacetylase 1
55014	STX17	-1.18	2.47E-02	syntaxin 17
6774	STAT3	-1.18	1.00E-02	signal transducer and activator of transcription 3 (acute-phase response factor)
9500	MAGED1	-1.18	3.11E-02	melanoma antigen family D, 1
5446	PON3	-1.18	3.44E-02	paraoxonase 3
115548	FCHO2	-1.17	2.96E-02	FCH domain only 2
51088	KLHL5	-1.17	4.52E-02	kelch-like family member 5
3985	LIMK2	-1.17	2.46E-02	LIM domain kinase 2
25865	PRKD2	-1.17	2.58E-02	protein kinase D2
27436	EML4	-1.17	2.23E-02	echinoderm microtubule associated protein like 4
1021	CDK6	-1.17	4.10E-02	cyclin-dependent kinase 6
808	CALM3	-1.17	4.03E-02	calmodulin 3 (phosphorylase kinase, delta)
3699	ITIH3	-1.17	2.03E-02	inter-alpha-trypsin inhibitor heavy chain 3
8892	EIF2B2	-1.17	1.37E-02	eukaryotic translation initiation factor 2B, subunit 2 beta, 39kDa
6558	SLC12A2	-1.17	4.60E-02	solute carrier family 12 (sodium/potassium/chloride transporter), member 2
6594	SMARCA1	-1.17	3.84E-02	SWI/SNF related, matrix associated, actin dependent regulator of chromatin, subfamily a, member 1
3106	HLA-B	-1.17	3.84E-02	major histocompatibility complex, class I, B
800	CALD1	-1.17	2.52E-02	caldesmon 1
51571	FAM49B	-1.17	2.77E-02	family with sequence similarity 49, member B
731	C8A	-1.17	3.49E-02	complement component 8, alpha polypeptide
5562	PRKAA1	-1.17	2.65E-02	protein kinase, AMP-activated, alpha 1 catalytic subunit
567	B2M	-1.17	4.48E-02	beta-2-microglobulin
3611	ILK	-1.16	1.32E-02	integrin-linked kinase
23530	NNT	-1.16	2.53E-02	nicotinamide nucleotide transhydrogenase
667	DST	-1.16	2.80E-02	dystonin
30844	EHD4	-1.16	2.98E-02	EH-domain containing 4
11059	WWP1	-1.15	3.49E-02	WW domain containing E3 ubiquitin protein ligase 1
48	ACO1	-1.15	4.78E-02	aconitase 1, soluble

Entrez ID	Gene name	Fold change	q-value	Description
7317	UBA1	-1.15	2.60E-02	ubiquitin-like modifier activating enzyme 1
1282	COL4A1	-1.15	4.54E-02	collagen, type IV, alpha 1
9879	DDX46	-1.15	4.03E-02	DEAD (Asp-Glu-Ala-Asp) box polypeptide 46
4670	HNRNPM	-1.15	2.10E-02	heterogeneous nuclear ribonucleoprotein M
23607	CD2AP	-1.15	2.74E-02	CD2-associated protein
309	ANXA6	-1.15	3.69E-02	annexin A6
2244	FGB	-1.15	3.69E-02	fibrinogen beta chain
1431	CS	-1.15	4.02E-02	citrate synthase
715	C1R	-1.14	2.63E-02	complement component 1, r subcomponent
3263	HPX	-1.14	1.62E-02	hemopexin
1389	CREBL2	-1.14	3.42E-02	cAMP responsive element binding protein-like 2
51585	PCF11	-1.14	4.89E-02	PCF11 cleavage and polyadenylation factor subunit
10096	ACTR3	-1.13	3.46E-02	ARP3 actin-related protein 3 homolog (yeast)
6314	ATXN7	-1.12	3.47E-02	ataxin 7
805	CALM2	-1.12	3.33E-02	calmodulin 2 (phosphorylase kinase, delta)
8553	BHLHE40	-1.12	4.29E-02	basic helix-loop-helix family, member e40
3315	HSPB1	-1.12	4.45E-02	heat shock 27kDa protein 1
7533	YWHAH	-1.12	4.62E-02	tyrosine 3-monooxygenase/tryptophan 5-monooxygenase activation protein, eta
975	CD81	-1.12	2.43E-02	CD81 molecule

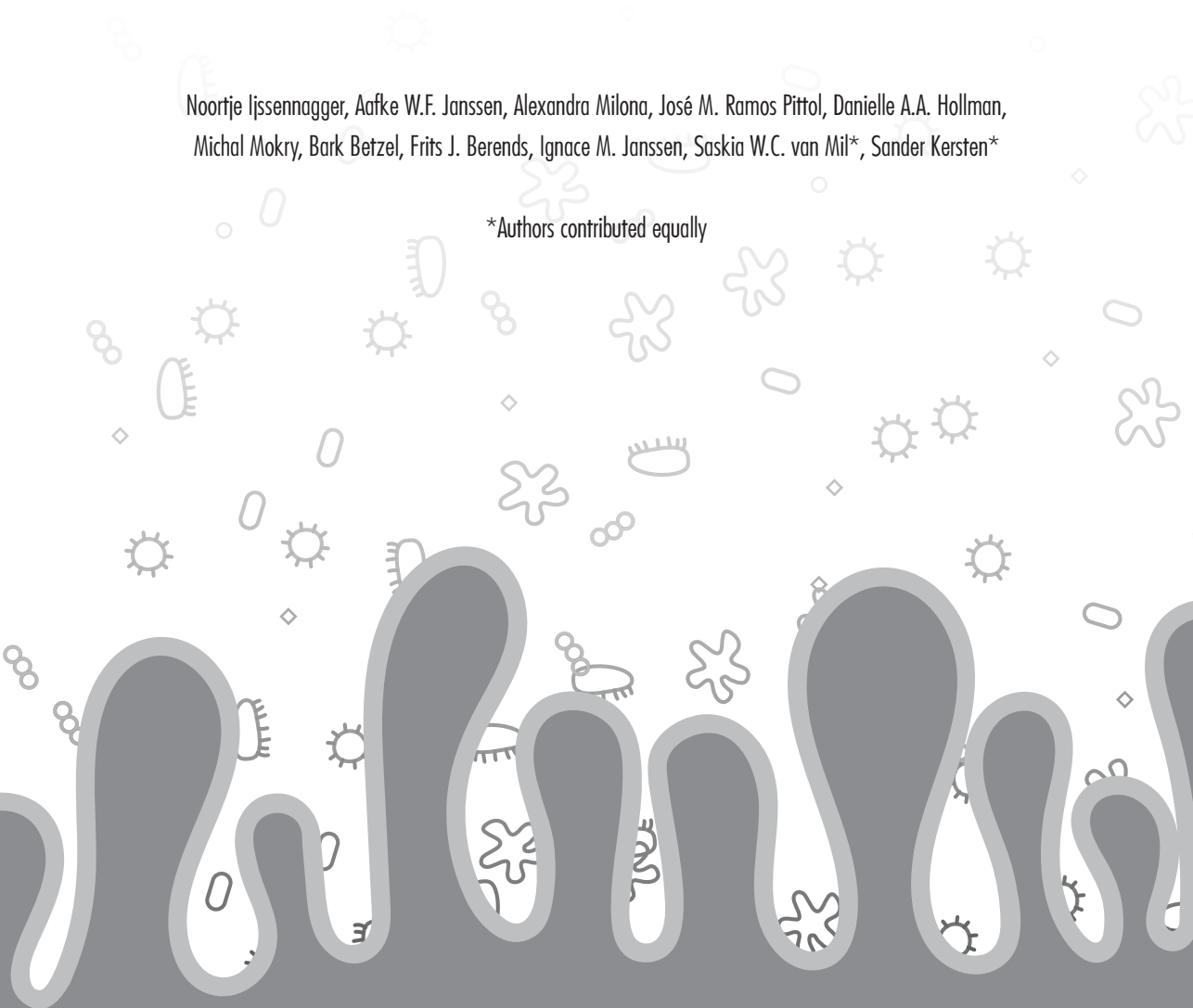
7



Gene expression profiling in human precision cut liver slices in response to the FXR agonist obeticholic acid

Noortje Ijssennagger, Aafke W.F. Janssen, Alexandra Milona, José M. Ramos Pittol, Danielle A.A. Hollman, Michal Mokry, Bark Betzel, Frits J. Berends, Ignace M. Janssen, Saskia W.C. van Mil*, Sander Kersten*

*Authors contributed equally



Abstract

Background

The bile acid-activated farnesoid X receptor (FXR) is a nuclear receptor regulating bile acid, glucose and cholesterol homeostasis. Obeticholic acid (OCA), a promising drug for the treatment of non-alcoholic steatohepatitis (NASH) and type 2 diabetes, activates FXR. Mouse studies demonstrated that FXR activation by OCA alters hepatic expression of many genes. However, no data are available on the effects of OCA in human liver. Here we generated gene expression profiles in human precision cut liver slices (hPCLS) after treatment with OCA.

Methods

hPCLS were incubated with OCA for 24 h. WT or FXR^{-/-} mice received OCA or vehicle by oral gavage for 7 days.

Results

Transcriptomic analysis showed that well-known FXR target genes, including *NR0B2* (SHP), *ABCB11* (BSEP), *SLC51A* (OST α) and *SLC51B* (OST β), and *ABCB4* (MDR3) are regulated by OCA in hPCLS. Ingenuity pathway analysis confirmed that 'FXR/RXR activation' is the most significantly changed pathway upon OCA treatment. Comparison of gene expression profiles in hPCLS and mouse livers identified 18 common potential FXR targets. ChIP-sequencing in mouse liver confirmed FXR binding to IR1 sequences of *Akap13*, *Cgntl1*, *Dyrk3*, *Pdia5*, *PPP1R3B* and *Tbx6*.

Conclusions

Our study shows that hPCLS respond to OCA treatment by upregulating well-known FXR target genes, demonstrating its suitability to study FXR-mediated gene regulation. We identified 6 novel bona-fide FXR target genes in both mouse and human liver. Finally, we discuss a possible explanation for changes in HDL/LDL observed in NASH and primary biliary cirrhosis patients treated with OCA based on the genomic expression profile in hPCLS.

Introduction

In many countries, non-alcoholic fatty liver disease (NAFLD) has become the most common liver disorder, surpassing viral hepatitis. NAFLD is frequently accompanied by obesity and is sometimes referred to as the hepatic manifestation of the metabolic syndrome. The main initial feature of NAFLD is hepatic steatosis. In some cases steatosis progresses to non-alcoholic steatohepatitis (NASH), which is characterized by fatty infiltration along with liver inflammation. In Western countries, the prevalence of NASH is about 2-3% and is expected to further increase in parallel with the global expansion in the prevalence of obesity [1]. If left untreated, NASH will worsen with time and may eventually proceed to liver cirrhosis and liver cancer. Presently, the only effective treatment for NASH is weight loss combined with other lifestyle modifications, but the long term compliance to these changes is disappointing. A promising new drug-based approach to NASH consists of treatment with obeticholic acid (OCA, INT-747, 6 α -ethyl-chenodeoxycholic acid), a semi-synthetic agonist of the nuclear receptor FXR [2]. FXR is a ligand-activated transcription factor that is considered as the master regulator of bile acid metabolism in liver and intestine. FXR is activated by bile acids and — once activated — stimulates transcription of genes involved in synthesis, transport and metabolism of bile acids [3]. A major target of FXR is *NR0B2*, encoding SHP, acting as a transcriptional repressor of bile acid synthesis via downregulation of *CYP7A1* and *CYP8B1* [4]. FXR also induces transcription of *BAAT*, *ABCB11* (BSEP), and *ABCB4* (MDR3), thereby inducing bile acid conjugation and export of bile acids and phospholipids from hepatocytes into the bile canaliculus, respectively [5-7].

As indicated above, FXR can be activated by the clinically relevant compound OCA. In studies using murine disease models for hepatic inflammation and renal dysfunction, it has been shown that OCA can resolve disease symptoms in wild type mice, but not FXR knockout mice, indicating that OCA acts mainly via FXR [8-10]. In a recent proof of concept study in NAFLD and type 2 diabetic patients, OCA was shown to increase insulin sensitivity and reduce markers of liver inflammation and fibrosis [11]. In a larger clinical study in NASH patients, OCA improved biochemical and histological features of NASH [2]. However, OCA treatment also decreased hepatic insulin sensitivity and raised serum concentrations of total and LDL cholesterol, while lowering HDL cholesterol. Currently, most insights into the effect of OCA and FXR activation are derived from animal experiments or cell lines. The lack of a more complex human model system has hampered our ability to investigate the impact of FXR activation by OCA in human liver. Therefore, in this study, we tested the effect of FXR activation by OCA on gene regulation in human Precision Cut Liver Slices (hPCLS). The advantage of hPCLS over primary human hepatocytes is that their preparation does not require any proteolytic enzymes that might disturb cell-cell interactions and can induce

cell damage. Moreover, because cell-cell interactions and cell heterogeneity are maintained within the original tissue matrix, the hPCLS better reflect the high level of biological organization of the liver [12].

Materials and methods

Collection of human liver biopsies

Liver biopsies were taken from 15 patients undergoing laparoscopic Roux-en-Y Gastric Bypass and were immediately frozen in liquid nitrogen and stored at -80°C . Precision cut liver slices (PCLS) were generated from fresh liver biopsies of 3 patients as described before [13]. Biopsies were stained with H&E and Sirius Red to determine steatosis and fibrosis, respectively. Slides were blindly scored by a pathologist. All 3 livers were scored with a Brunt score for steatosis of 0 ($<5\%$ steatosis) and an F score of 0 (no fibrosis) [14, 15], indicating no signs of liver disease (see **Supplemental Figure 1A**). Biopsies were provided by the biobank of the Rijnstate hospital. Collection of biopsies for research purposes into the biobank was approved by the local institutional review board on behalf of the medical ethics review committee of the Radboud University Medical Centre. All patients signed informed consent for collection of the biopsies prior to surgery.

Preparation and treatment of precision cut liver slices

Human and mouse (C57Bl6) PCLS were prepared and cultured as described previously [16]. Briefly, 5 mm cylindrical liver cores were prepared with a surgical biopsy punch and sectioned to 200 μm slices using a Krumdieck tissue slicer (Alabama Research and Development, Munford, AL, USA) filled with carbonated KHB (pH 7.4, supplemented with 25mM glucose). Liver slices were incubated in William's E Medium (Gibco, Paisley, Scotland) supplemented with pen/strep in 6-well plates at $37^{\circ}\text{C}/5\% \text{CO}_2/80\% \text{O}_2$ under continuous shaking (70 rpm). Duplicate wells were used per donor with 3 liver slices per well. After 1 hour medium was replaced with fresh William's E Medium in the presence or absence of OCA (1 μM) dissolved in dimethyl sulfoxide (DMSO, final concentration 0.1%). OCA was kindly provided by Luciano Adorini (Intercept Pharmaceuticals Inc., San Diego, California, USA). After 24 h incubation, liver slices were snap-frozen in liquid nitrogen and stored in -80°C for RNA isolation.

Animal experiment

The experiment was approved by the ethics committee of the University Medical Center Utrecht and was in accordance with European law. 9-12 weeks old male C57BL/6 wild-type (WT) and FXR^{-/-} mice [17] were housed in a room with controlled temperature (20-24°C), relative humidity (55% \pm 15%) and a 12h light dark cycle. Mice were fed chow and demineralized water ad libitum. Mice received either a treatment with OCA (10 mg/kg/day) to pharmacologically activate FXR, or vehicle (1% methyl cellulose) daily by oral gavage for 7 days. On the last day, mice were starved and received a final dose of OCA or vehicle. After

4h, mice were sacrificed, livers were collected, snap-frozen in liquid nitrogen and stored at -80°C.

RNA isolation and qPCR

Total RNA of human and mouse tissue was isolated using TRIzol reagent (Invitrogen). RNA was reverse transcribed using the iScript cDNA Synthesis Kit (Bio-Rad Laboratories BV, Veenendaal, The Netherlands). Real-time PCR was carried out using SensiMiX (Bioline) on a CFX 384 Bio-Rad thermal cycler (Bio-Rad). mRNA expression of genes of interest were normalized to Cyclophilin and 36B4. Primers sequences are shown in **Supplemental Table 1**.

Microarray analysis

For microarray hybridization, the isolated human and mouse RNA was further purified using RNeasy Minikit columns (Qiagen). RNA concentrations were measured on a nanodrop ND-1000 UV-Vis spectrophotometer (Isogen, Maarssen, The Netherlands) and analyzed on an Agilent 2100 bioanalyzer (Agilent Technologies, Amsterdam, The Netherlands) with 6000 Nano Chips, according to the manufacturer's protocol. RNA was judged suitable for array hybridization only if samples exhibited intact bands corresponding to the 18S and 28S ribosomal RNA subunits, and displayed no chromosomal peaks or RNA degradation products.

Purified RNA (100 ng) was labeled with the Ambion WT expression kit (Invitrogen) and hybridized to either Affymetrix Human Gene 1.1 ST arrays or to Affymetrix Mouse Gene 1.1 ST arrays, provided in plate format (Affymetrix, Santa Clara, CA). Hybridization, washing and scanning of the array plates was performed on an Affymetrix GeneTitan instrument, according to the manufacturer's recommendations. Normalized expression estimates were obtained from the raw intensity values applying the robust multi-array analysis (RMA) [18,19] preprocessing algorithm available in the Bioconductor library AffyPLM with default settings. Probe sets were defined according to Dai et al. [20]. In this method probes are assigned to Entrez IDs as a unique gene identifier. In this study, probes were reorganized based on the Entrez Gene database, build 37, version 1 (remapped CDF v19). The P values were calculated using an Intensity-Based Moderated T-statistic (IBMT) [21]. Probe sets that satisfied the criterion of a P value < 0.01 were considered significantly regulated and used for further bioinformatics analysis. In total 6 human arrays (3 patients, per patient 1 DMSO control and 1 treated with OCA) and 24 mouse arrays were performed (6/group, 4 groups; WT vehicle, WT OCA, FXR^{-/-} vehicle and FXR^{-/-} OCA). Microarray datasets have been submitted to Gene Expression Omnibus, accession number GSE76163.

To identify biological processes influenced by FXR activation and ablation pathway

analysis was performed using Ingenuity Canonical Pathway Analysis (Ingenuity® Systems, www.ingenuity.com). This analysis identifies the pathways from the Ingenuity Pathway Analysis library of canonical pathways that are most significant to a microarray dataset. Fisher's exact test was used to calculate a p-value determining the probability that the association between the genes in the dataset and the canonical pathway is explained by chance alone.

Chromatin immunoprecipitation

30 mg of snap-frozen liver tissue from vehicle or OCA treated WT mice was cross-linked using DSG and formaldehyde, as described by Nowak et al [22]. The nuclei were extracted and sonicated to yield 500-1,000 basepair (bp) DNA fragments. ChIP was performed according to Sacconi et al [23], using an anti-FXR antibody (sc-13063, SantaCruz, CA).

ChIP-sequencing

Immunoprecipitated material and input DNA from each sample was re-sonicated to achieve an average fragment size of around 300bp; DNA was processed using the SOLiD ChIP-seq kit, and sequenced on a SOLiD 5500 WF platform. Alignment to the mm9 reference genome was carried out using BWA allowing for up to 2 mismatches. For display, mapped reads from ChIP datasets were extended to 200bp and summed in 50 bp bins using standard perl scripts. Regions of 15 kb around the detected peaks are shown from livers collected from 2 mice. FXR peaks were identified using MACS 1.4 (with parameters: pvalue=1e-4, nomodel, nolambda, shiftsize=150). Peaks located within 10 kb up and downstream annotated genes according to the mm9 refGene table of RefSeq genes (UCSC genome browser) were considered for further analysis. Genomic distances were calculated using BEDtools [24]. IR1 motifs [25] were searched in peak regions proximal to target genes using the HOMER suite [26] and qPCR primers were designed in proximity to these motifs. Results from representative FXR ChIP experiments are shown at the following coordinates (mm9): Akap13 (chr7: 82892181-82907181), Cgln1 (chr9: 71566626-71581626), Dyrk3 (chr1: 133015491-133030491), Pdia5 (chr16: 35482324-35497324), Ppp1r3b (chr8: 36431025-36446025) and Tbx6 (chr7: 133918281-133933281). Primer sequences can be found in **Supplemental Table 1**. ChIP sequencing datasets have been submitted to Gene Expression Omnibus, accession number GSE73624.

Results

FXR expression and target gene induction in hPCLS

Apart from human liver biopsies from patients treated with OCA, which are unavailable for experimental studies, hPCLS are the next best model to study gene regulation in human liver. To characterize hPCLS with respect to FXR and FXR target genes, we determined the relative expression of FXR in hPCLS after 24h in culture medium in comparison with human liver biopsies immediately snap-frozen after collection. FXR is well expressed in hPCLS at Ct values ranging from 23-26, which is about 6.5-fold lower as compared to frozen biopsies (**Supplementary Figure 1B**). To verify that hPCLS maintain their ability to respond to FXR activation, we exposed the slices to 1 μ M OCA for 24h. The expression level of the known FXR target genes *NR0B2* (SHP), *ABCB11* (BSEP), *SLC51A* (OSTa) was significantly induced upon OCA treatment, indicating the validity of our model to study FXR-mediated gene regulation (**Figure 1A**). Induction of *ABCB4* (MDR3) did not reach significance.

Differentially expressed genes upon FXR activation in hPCLS

To study genome-wide effects of FXR activation on human liver slices, we performed microarray analysis. The OCA-induced upregulation of selected FXR target genes was similar between microarray and qPCR analysis. Using $p < 0.01$ as cut-off (IBMT regularized paired t-test), OCA treatment altered the expression of 627 genes in hPCLS. Of these 627 genes, 299 genes were upregulated and 328 genes were downregulated. The 25 most highly

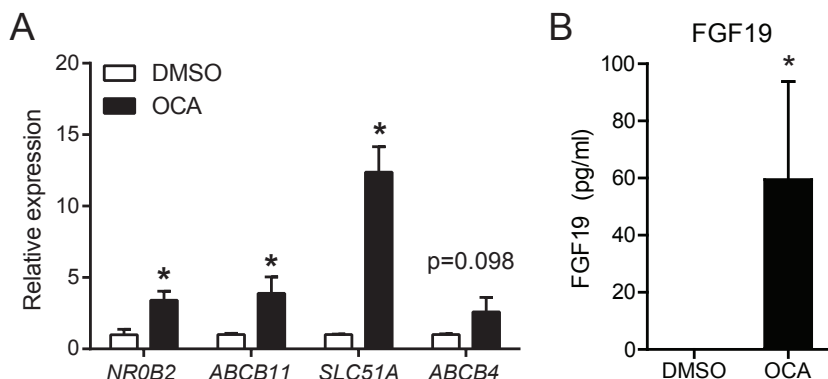


Figure 1. Classical FXR target genes are robustly induced by the FXR agonist OCA in human liver slices (A) Gene expression of selected FXR target genes in hPCLS (n=3/group) in response to a 24h treatment with OCA as determined by qPCR. Expression of DMSO is set at 1 and OCA treatment is relative to DMSO. Data are shown as mean \pm SEM, * $p < 0.05$ by a Students t-test (one sided). (B) Release of FGF19 in the medium of OCA-treated hPCLS as measured by ELISA (n=3/group). Data are shown as mean \pm SEM, * $p < 0.05$ by a Students t-test.

induced genes can be found in **Table 1** and contained the well-known FXR target genes *NR0B2* (SHP), *ABCB11* (BSEP), *SLC51A* (OST α) and *SLC51B* (OST β), and *ABCB4* (MDR3), all of which are involved in bile acid metabolism. Remarkably, the most highly upregulated gene upon OCA treatment in hPCLS was *FGF19*. *FGF19* is known as FXR target gene in the ileum and encodes a hormone produced in the ileum upon bile acid absorption. Release of FGF19 into the medium was markedly stimulated by OCA treatment (**Figure 1B**).

Table 2 shows the most highly repressed genes in hPCLS upon OCA treatment. The list of downregulated genes does not contain any well-known FXR targets. CYP7A1 and CYP8B1, normally downregulated upon FXR activation, were not expressed in hPCLS, presumably because their expression is rapidly lost upon culturing (**Supplemental Figure 1C**). Loss of expression of P450 enzymes is also observed in other liver-derived *in vitro* systems, such as HepG2 cells [27]. Genes downregulated by OCA were mainly involved in inflammatory responses (*CHI3L1*, *IL18BP*), cilium morphogenesis (*PCDPI*, *AVIL1*), cholesterol and triglycerides homeostasis (*MIA2*) and signal transduction (*CXCL10*, *RAP1GAP*).

Table 1. The 25 highest upregulated genes (p<0.01) in hPCLS upon treatment with OCA

Human Gene name	Description	FC
<i>FGF19</i>	fibroblast growth factor 19	20.0
<i>RHCG</i>	Rh family, C glycoprotein	3.6
<i>PALMD</i>	palmdelphin	3.2
<i>TRAV14DV4</i>	T cell receptor alpha variable 14/delta variable 4	3.2
<i>FNDC5</i>	fibronectin type III domain containing 5	3.1
<i>NR0B2</i>	nuclear receptor subfamily 0, group B, member 2	2.8
<i>RHOF</i>	ras homolog family member F	2.7
<i>ABCB11</i>	ATP-binding cassette, sub-family B (MDR/TAP), member 11	2.6
<i>OR2L8</i>	olfactory receptor, family 2, subfamily L, member 8	2.5
<i>HSPA12A</i>	heat shock 70kDa protein 12A	2.5
<i>SLC51A</i>	solute carrier family 51, alpha subunit	2.5
<i>CYP2A13</i>	cytochrome P450, family 2, subfamily A, polypeptide 13	2.2
<i>RTP3</i>	receptor (chemosensory) transporter protein 3	2.1
<i>PEG10</i>	paternally expressed 10	2.1
<i>SLC51B</i>	solute carrier family 51, beta subunit	2.1
<i>MFSD2A</i>	major facilitator superfamily domain containing 2A	2.1
<i>LOXL4</i>	lysyl oxidase-like 4	2.0
<i>CCL15</i>	chemokine (C-C motif) ligand 15	1.9
<i>TRGV2</i>	T cell receptor gamma variable 2	1.9
<i>IGHG3</i>	immunoglobulin heavy constant gamma 3	1.9
<i>G6PC</i>	glucose-6-phosphatase, catalytic subunit	1.9
<i>PHKA1</i>	phosphorylase kinase, alpha 1 (muscle)	1.9
<i>ABCB4</i>	ATP-binding cassette, sub-family B (MDR/TAP), member 4	1.9
<i>IGLON5</i>	IgLON family member 5	1.8
<i>ACTA2-AS1</i>	ACTA2 antisense RNA 1	1.8

FC, fold change.

Table 2. The 25 highest downregulated genes (p<0.01) in hPCLS upon treatment with OCA

Human		
Gene name	Description	FC
LOC728554	THO complex 3 pseudogene	-2.6
LOC100130207	uncharacterized LOC100130207	-2.4
CHI3L1	chitinase 3-like 1 (cartilage glycoprotein-39)	-2.0
MAGEA3	melanoma antigen family A, 3	-2.0
SERPINB4	serpin peptidase inhibitor, clade B (ovalbumin), member 4	-1.9
CXCL10	chemokine (C-X-C motif) ligand 10	-1.9
WDR72	WD repeat domain 72	-1.8
MTMR11	myotubularin related protein 11	-1.7
ESPNP	espin pseudogene	-1.7
TRIB2	tribbles pseudokinase 2	-1.7
DUOX2	dual oxidase 2	-1.7
PCDP1	primary ciliary dyskinesia protein 1	-1.7
RAP1GAP	RAP1 GTPase activating protein	-1.7
DTWD2	DTW domain containing 2	-1.7
ENKUR	enkurin, TRPC channel interacting protein	-1.6
DUOXA2	dual oxidase maturation factor 2	-1.6
AHNAK2	AHNAK nucleoprotein 2	-1.6
MIA2	melanoma inhibitory activity 2	-1.6
NIPAL3	NIPA-like domain containing 3	-1.6
SPATA6L	spermatogenesis associated 6-like	-1.6
AVIL	advillin	-1.6
DHODH	dihydroorotate dehydrogenase (quinone)	-1.6
GBP4	guanylate binding protein 4	-1.6
IL18BP	interleukin 18 binding protein	-1.6
FASTKD3	FAST kinase domains 3	-1.6

FC, fold change.

Biological pathways in human and mouse tissue upon OCA treatment

To gain better insight into the biological function of genes regulated by FXR activation in hPCLS, we performed Ingenuity Pathway Analysis on all differentially expressed genes (p<0.01). The most significantly changed pathway in hPCLS by OCA treatment was ‘FXR/RXR activation’ (**Figure 2A**). In addition, pathways involving RXR, the heterodimeric partner of FXR, feature prominently among the most changed pathways.

Whereas hPCLS represents the most suitable *in vitro* model system to study gene regulation by OCA in human liver, treatment of mice with OCA followed by harvesting of livers represent the most feasible and suitable *in vivo* model system. Therefore, we studied the effect of orally-provided OCA on hepatic gene expression in WT and FXR^{-/-} mice. In WT mice, OCA treatment significantly changed the expression of 619 genes (p<0.01, 333 up- and 286 genes downregulated). Ingenuity Pathway Analysis showed that the most significantly changed pathways were related to cholesterol and fatty acid metabolism (**Figure 2B**).

Differential expression of FXR target genes in hPCLS and mouse liver

To gain more insight into the commonality of gene regulation by OCA in hPCLS and mouse liver, we analyzed the expression of known FXR target genes [28-30] in hPCLS and

compared it to mouse liver. OCA treatment significantly increased the expression of the FXR target genes *ABCB11*, *ABCB4*, *ABCG5*, *ABCG8*, *ALAS1*, *FETUB*, *FGF19*, *ICAM1*, *KNGL1*, *NR0B2*, *SLC51A* and *SLC51B* in hPCLS, whereas the expression of *ABCC2* was significantly decreased (**Figure 3**).

In WT mice, OCA treatment significantly induced the expression of *Fasn*, *Nr0b2*, *Nr1i2* and *Slc51b* and reduced the expression of *Csad* and *Cyp8b1* (**Figure 3**). As expected, the stimulatory effect of OCA treatment on FXR targets was abolished in *FXR^{-/-}* mice, except for a significant downregulation of *Apoa5*, indicating that the regulation of bile acid metabolism genes by OCA is mediated by FXR. Furthermore, baseline expression of most FXR target genes was decreased in the *FXR^{-/-}* mice as compared to the WT mice.

Identification of putative novel FXR target genes

To focus on FXR-dependent gene regulation, we excluded genes up- or downregulated by

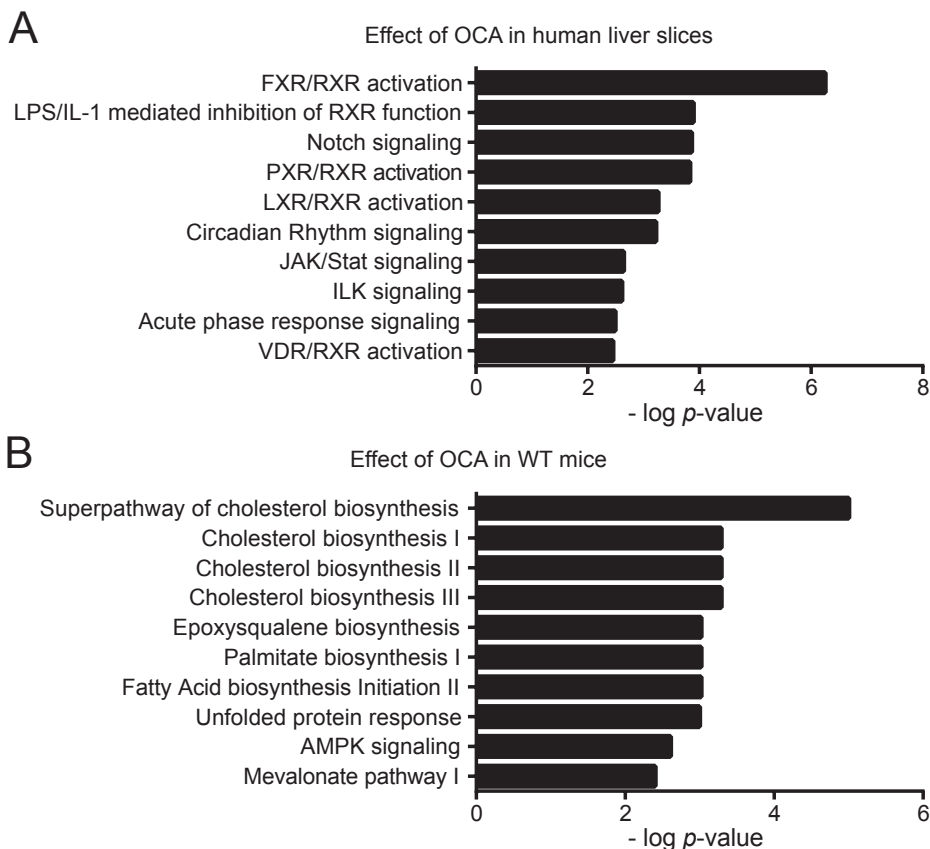


Figure 2. Top 10 canonical pathways from Ingenuity Pathway Analysis changed by OCA treatment
The 10 most significantly changed pathways ($p < 0.01$) for hPCLS (A) and in mouse WT livers (B).

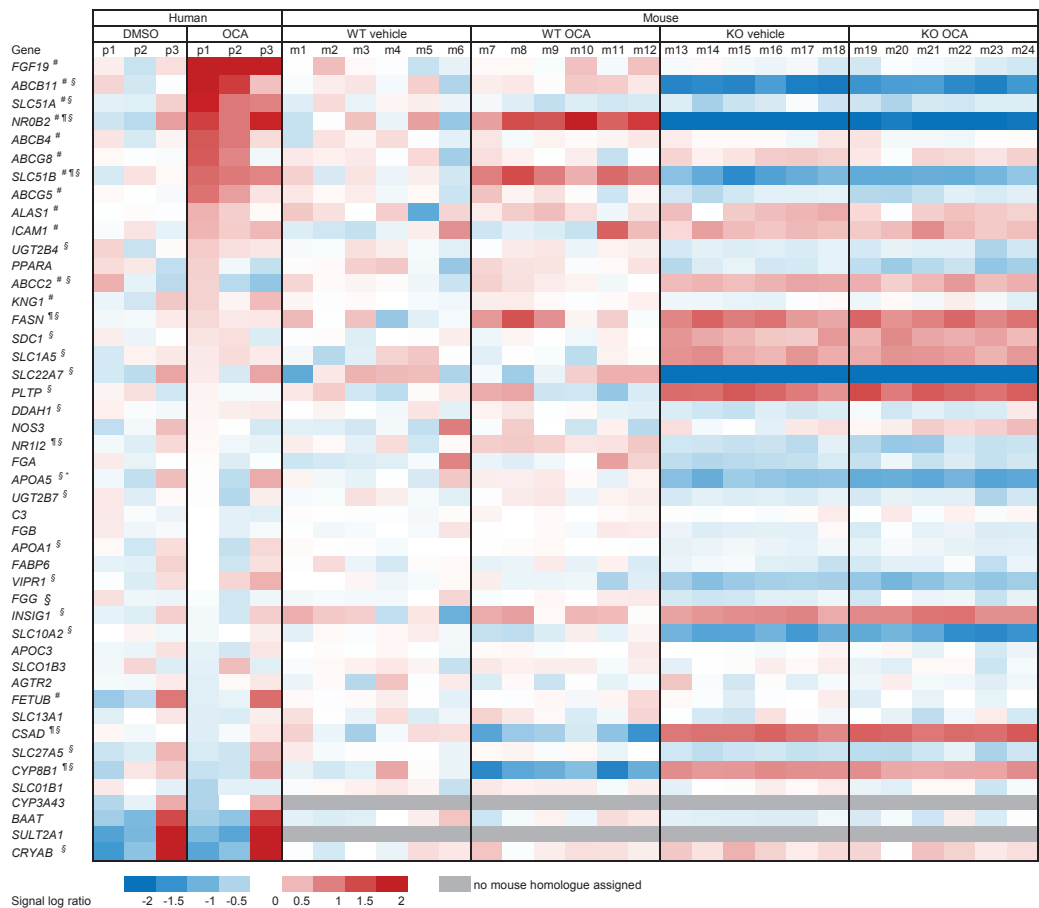


Figure. 3. Comparative heatmap analysis of the effect of OCA on FXR target genes [28-30] in hPCLS and mouse liver

P1 to P3 represent the 3 human subjects that donated a liver specimen for preparation of hPCLS. hPCLS were incubated with DMSO (control) and OCA, and # indicates significant changed genes, $p < 0.01$. Regarding the mouse data, the effect of OCA on gene expression in the WT mice (m7-m12) was compared to the WT vehicle-treated mice (m1-6) and significant genes ($p < 0.01$) are indicated by ¶. The effect of FXR ablation was studied by comparing FXR^{-/-} vehicle-treated mice (m13-18) to the WT vehicle-treated mice and significant differences ($p < 0.01$) are indicated with §. The effect of OCA in FXR^{-/-} mice (m19-24) compared to FXR^{-/-} vehicle treated mice yield 1 significant different gene ($p < 0.01$) indicated by *.

OCA in a similar direction in WT and FXR^{-/-} livers (**Figure 4A**). Of the 11 genes that were significantly regulated in both WT and KO mice, 8 genes were excluded because they changed in the same direction. The remaining 3 genes were not excluded as they were regulated in the opposite direction. In total, 611 genes were regulated in an FXR dependent manner in mouse liver tissue, and 235 genes were regulated independently of FXR.

When comparing all genes significantly induced by OCA ($p < 0.01$) in hPCLS ($n = 627$) and

mouse liver (n=611), only a small overlap of 31 overlapping genes was found (**Figure 4B**). We tested whether the small overlap was due to experimental differences (human liver slices vs whole mouse tissue) by validating FXR target gene expression changes in mouse precision cut liver slices. The FXR target genes *Abcb11*, *Slc51a* and *Abcb4* were not regulated in mouse liver tissue and were also not regulated in the mouse liver slices (**Supplemental Figure 2**). *Slc51b* was upregulated in mouse liver tissue and was also upregulated in the mouse liver slices. We therefore conclude that experimental differences in the setup of the study are probably not responsible for the small overlap in human and mouse OCA- regulated genes, but that the limited overlap is most probably due to species differences.

Within this overlap of 31 genes, 20 genes changed expression in the same direction in both models (**Figure 4C**). Among those 20 genes were the known FXR targets *NR0B2* and *SLC51B* (OST β) and 18 genes not yet described as FXR targets. The 11 genes that were regulated oppositely in mouse and human were not considered further, because we reasoned that target genes should be regulated similarly in human and mouse liver.

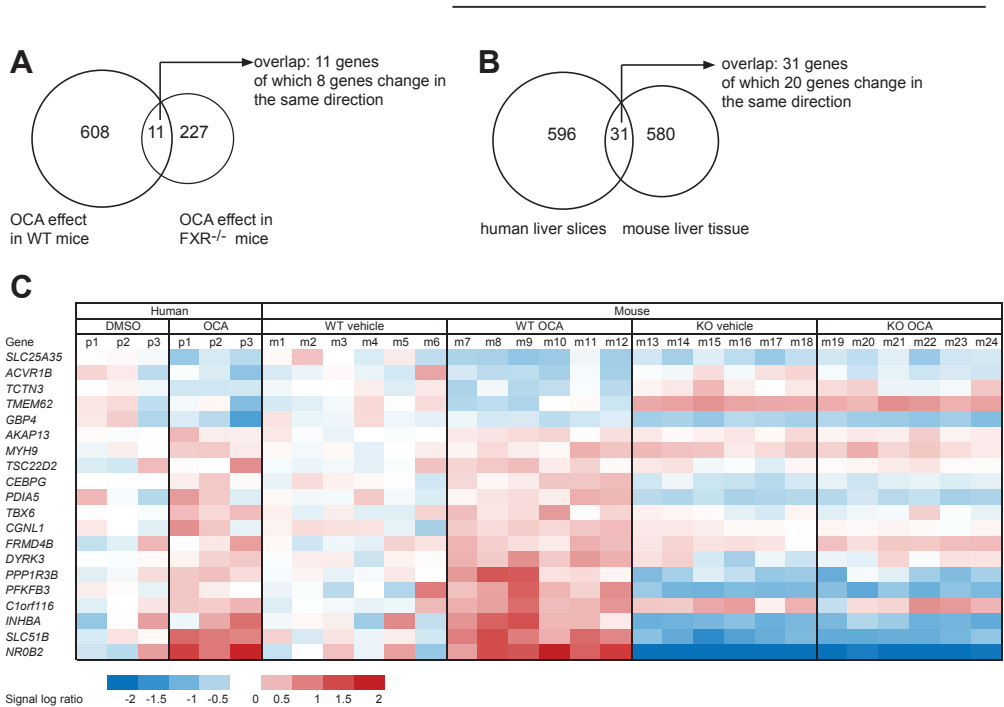


Figure 4. Comparative analysis of the effect of OCA on gene expression in human liver slices and mouse liver

(A) Venn diagram showing the number of genes regulated by OCA in WT mice, in FXR^{-/-} mice and the number of overlapping genes (p<0.01). (B) Venn diagram showing the number of genes regulated in hPCLS, in mouse liver and the number of overlapping genes (p<0.01). (C) Comparative heatmap analysis of the overlapping genes, which were significantly changed (p<0.01) in the hPCLS as well as in mouse liver.

Confirmation of novel FXR targets by ChIP-seq

To examine whether these 18 genes may be novel FXR targets, we generated genome-wide FXR binding profiles by ChIP-seq in mouse liver. Binding of FXR was observed for *Akap13*, *Cgnl1*, *Dyrk3*, *Pdia5*, *Ppp1r3b* and *Tbx6* genes within 10kb distance to the genes. Binding was observed close to the transcription start site (TSS) for *Akap13*, in introns 1 or 2 (*Cgnl1*, *Pdia5*, *Pfkfb3*, *Ppp1r3b*, *Tbx6*) regions, or intergenic (*Dyrk3*) (Figure 5A). Since

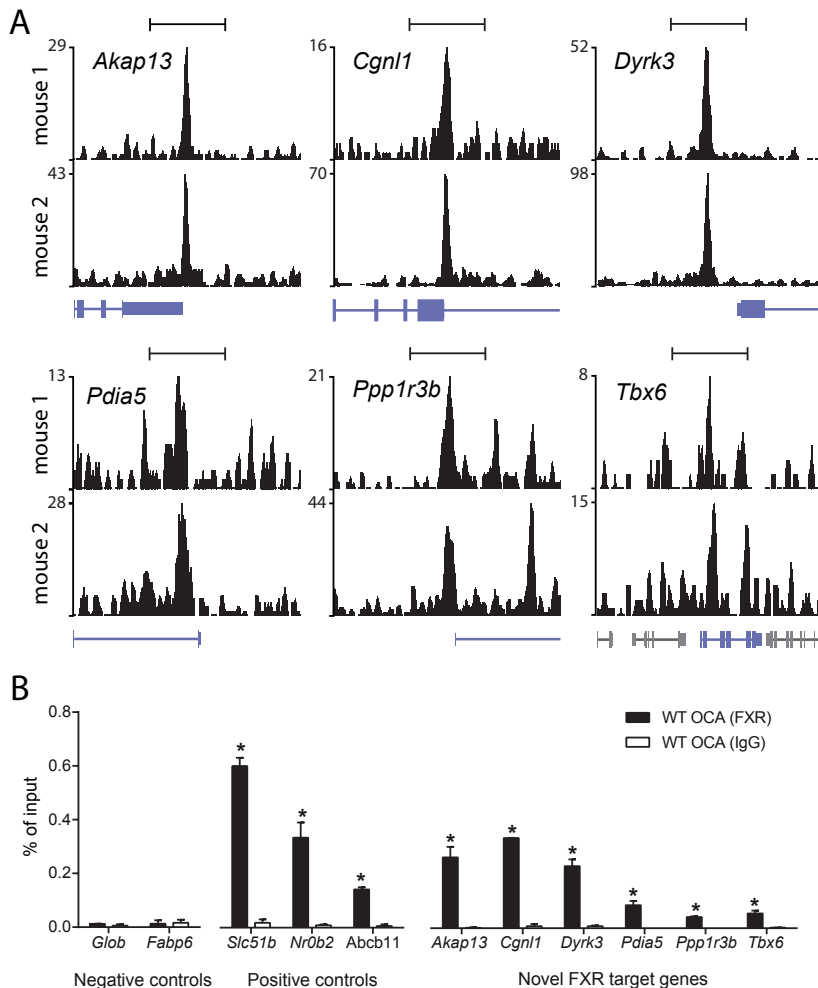


Figure 5. Identification of 6 novel FXR target genes

(A) FXR ChIPseq tracks from 2 independent mouse livers (WT) showing 15Kb around FXR peaks proximal to putative target genes. The IR-1 motif was found in all cases at the peak's summit. (B) Validation of candidate peaks by ChIP-qPCR. *Globin* and *Fabp6* were used as negative controls for FXR in the liver; *Slc51b*, *Nr0b2* and *Abcb11* were used as positive controls. Data are shown as mean \pm SEM, n=2, *p<0.05 by a Student's t-test.

FXR is known to bind a consensus sequence comprising an inverted NR-hexamer sequence (IR1) [25], we looked for IR1 sites in the selected peaks and found them being present in the analyzed regions (**Table 3**). Next, primers were designed in the region surrounding the IR1 sites, and ChIP-qPCR was performed to validate FXR binding in these regions (**Figure 5B**). *Globin* and *Fabp6* promoters were used as negative control regions, since they have been described to be depleted of FXR in liver tissue [31], whereas *Slc51b*, *Nr0b2* and *Abcb11* were used as positive controls for FXR binding. Of the putative novel FXR target genes, we confirmed that FXR binds to *Akap13*, *Cgnl1*, *Dyrk3*, *Pdia5*, *Ppp1r3b* and *Tbx6* promoters in mouse liver. FXR binding was similar in OCA and vehicle treated mice (**Supplemental Figure 3**), which is line with the previous observation that treatment of mice with an FXR agonist does not result in an increase in FXR binding in liver tissue [22].

Table 3. IR1-like motifs found in 2 known FXR target genes and 8 putative novel FXR target genes

Gene	Annotation	Distance to target gene	Distance to transcription start site	IR1 motif sequence
Homer motif				
<i>FXR(NR)</i> , <i>IR1</i>				AGGTCANTGACCTB
Known targets				
<i>Nr0b2</i>	Promotor-TSS	-272	-272	GGGTTAATGACCCT
<i>Slc51b</i>	Promotor-TSS	-193	-193	GGGTGAATGACCCC
Putative targets				
<i>Akap13</i>	TTS	187	-93544	GGGTCAGTACCCCA
<i>Cgnl1</i>	Intron 1 out of 18	0	45284	GGTGTAATGACCTC
<i>Dyrk3</i>	Intergenic	2026	11821	AGGGTAATGACCCT
<i>Pdia5</i>	Intron 1 out of 16	0	636	AGGTCAGTCCCCTG
<i>Ppp1r3b</i>	Intron 1 out of 1	0	3143	AGGGCACTGACTGC
<i>Tbx6</i>	Intron 2 out of 7	0	783	GGGTCAAGGACCAG

Motifs were located in the summit of the peak.

TSS, transcription start site; TTS; transcription termination site.

Discussion

This is the first study to investigate the effect of the novel drug OCA, now in phase 3 clinical trials for NASH, on liver gene expression using hPCLS as a model system for human liver. Using whole genome profiling, we show that multiple genes are highly and consistently responsive to FXR activation in hPCLS, including many established FXR target genes, thereby providing valuable new insights into the potential mechanisms underlying the therapeutic efficacy of OCA in humans. Our data suggest that hPCLS are an excellent model to study the impact of FXR activation on gene expression in human liver.

In our study, the number of FXR target genes commonly regulated in mouse liver and hPCLS was relatively small. The small overlap might be explained by several factors. First, the human donors were females, whereas we used male mice. Second, hPCLS were incubated for 24h with OCA, whereas mice received a daily oral gavage with OCA for 7 days with the last dose provided 4h before sacrifice. Thirdly, orally provided OCA circulates in the enterohepatic cycle and accumulates in the bile acid pool. Therefore, the exact amount of OCA reaching the liver in mice is not known. In contrast, the concentration of OCA that hPCLS are exposed to can be very carefully controlled. Finally, some genes altered by OCA in mouse livers may be regulated secondary to FXR activation in the ileum or even other tissues, which is not a concern in hPCLS. Along the same lines, we previously found limited overlap in gene regulation upon activation of the PPAR α nuclear receptor between primary mouse hepatocytes and human hepatocytes [32]. This is in contrast to comparative ChIP-sequencing studies for PPAR γ , where approximately 50% of regulated genes between mouse and human match in adipose tissue [33, 34]. However, these comparative ChIP-Seq studies do not measure regulation of gene expression but rather genomic binding. These studies, although useful, provide no information on conservation of gene regulation between species (for instance, binding sites may be conserved but may not result in gene regulation). In addition, the overall number of genes regulated by FXR is substantially lower as compared to PPARs, making a direct comparison difficult. We therefore believe that the small overlap is probably mainly due to species differences and not to experimental differences, as FXR target gene regulation was similar between mouse livers and mouse liver slices.

OCA caused a marked increase in mRNA levels of the gene encoding fibroblast growth factor 19 (*FGF19*) in hPCLS. Expression of *FGF19* is known to be induced by FXR in the ileum but has been reported to remain below detection in mouse liver [35]. In humans a liver-specific upregulation of *FGF19* was described in patients with extrahepatic cholestasis [36] and in primary biliary cirrhosis [37], but no *FGF19* mRNA was detected in healthy human livers [36-38]. Consistent with these data, *FGF19* was not expressed in untreated hPCLS, as judged by the intensity of the *FGF19* signal on the microarray. However, *FGF19*

mRNA expression and release of protein were dramatically induced by OCA. While it has been reported that *FGF19* is expressed in cholangiocytes [39], it is unlikely that this cell type is responsible for the 20-fold induction in *FGF19* gene expression, as only ~2% of liver tissue consists of cholangiocytes. At this moment we do not know if the upregulation of *FGF19* is a consequence of the model—because of the absence of the enterohepatic circulation—or that this upregulation also occurs in humans treated with OCA.

By comparing the effects of OCA in the two model systems, we were able to identify several novel target genes of FXR. These novel targets induced by FXR activation in both human and mouse liver include *Akap13*, *Cgnl1*, *Dyrk3*, *Pdia5*, *Ppp1r3b* and *Tbx6*. *Akap13* (also Lymphoid Blast Crisis) is a Rho guanine-nucleotide exchange factor that activates Rho GTPase implicated in cancer and metastasis [40]. *Cgnl1* (Cingulin-like1 or paracingulin) is also involved in regulating the activity of GTPases Rho and Rac1, thereby mediating cell-cell junction assembly [41]. Interestingly, the anti-apoptotic DYRK3 (dual-specificity tyrosine-(Y)-phosphorylation regulated kinase 3) promotes cell survival through phosphorylation and activation of SIRT1, a protein deacetylase essential in a variety of physiological processes including stress response and energy metabolism [42]. Mice overexpressing SIRT1 have an impaired farnesoid X receptor (FXR) activity due to persistent deacetylation and lower protein expression that was shown to lead to decreased expression of the FXR targets *Shp* and *Bsep*, and increased expression of *Cyp7A1* [43]. In our studies, *Dyrk3* was upregulated by FXR activation in mouse liver and hPCLS, which might be indicative of a negative feedback mechanism of FXR function. Not much is known about *Tbx6* and *Pdia5*, other than that *Tbx6* is a T-box gene encoding for transcription factors regulating developmental processes, and *Pdia5* encodes for a protein with disulfide isomerase activity.

Another gene that was identified as a novel FXR target gene in our study is *PPP1R3B*, encoding a regulatory subunit of the glycogen-associated protein phosphatase-1 (PP-1). PP-1 has been shown to play an important role in the regulation of glycogen synthase activity and as such promotes glycogen synthesis. A substitution in the 3'-untranslated region (UTR) detected in Pima Indians results in destabilization of *PPP1R3B* mRNA and concomitant decreased protein levels, and is associated with insulin resistance and type 2 diabetes in the Pimas [44]. Another polymorphism, Asp905Tyr, was shown to be associated with decreased glycogen synthesis and an increased basal glucose oxidation rate when compared with wild type carriers [45]. Association studies suggest that genetic variants in or near *PPP1R3B* are associated with insulin resistance and type 2 diabetes [44-48], hepatic steatosis and altered serum lipids [49] and with increased hepatic triglyceride content [50]. Also, the hepatic steatosis increasing variant in *PPP1R3B* is associated with increased HDL- and LDL cholesterol levels and decreased fasting glucose [49]. In line with these findings, overexpression of mouse *Ppp1r3b* in mouse liver resulted in significantly lower plasma

HDL-levels as well as total cholesterol [51]. We find PPP1R3B upregulated in mouse liver and human PCLS which is consistent with decreased HDL levels in patients treated with OCA [2, 52]. The mechanism by which PPP1R3B affects HDL concentrations is currently unclear, and might be secondary to changes in energy metabolism.

NASH patients treated with OCA exhibit increased total and LDL cholesterol levels [2]. It was suggested that these changes are mediated by decreased expression of Cyp7A1, which converts cholesterol to bile acids. However, in a recent study in PBC patients, LDL cholesterol was not significantly changed upon OCA-treatment, while total cholesterol was decreased [52]. The discrepancy in regulation of total cholesterol and LDL cholesterol between these two patient groups raises the question whether LDL levels are mediated directly by FXR, or may rather be a consequence of the high fat/cholesterol environment in livers of NASH patients. It should be noted here that although no steatosis and fibrosis were observed, the hPCLS used for this study were obtained from patients with a high BMI (35-43 kg/m²),

A decrease in HDL levels after treatment with OCA was found in both NASH and PBC patients [2, 52]. In a further attempt to understand the decreased HDL levels in both studies, we reviewed the literature for mouse knockout models associated with this feature and compared them to the expression data in hPCLS. It has been shown that knock out models of *Abca1* (cholesterol efflux pump) and *Tgm2* [53], *Fgl1* [54], *Npc1l1* (uptake free cholesterol) [55], *Angptl4* [56], *Hif1an* [57] and *Ghr* [58], which were all downregulated in hPCLS ($p < 0.03$) upon OCA treatment, are associated with decreased HDL levels. Furthermore, knockout mice for *Ldlr* (low density lipoprotein receptor) [59], *Gpr12* [60], and *Scp2* [61] have increased plasma HDL levels. In line with this observation, hPCLS treated with OCA showed a significant upregulation of *LDLR*, *SCP2* ($p < 0.01$) and a trend for increased *GPR12* ($p = 0.06$). Altogether, these genes may be suggested to possibly contribute to the decreased HDL plasma levels of patients treated with OCA. The relation of these genes to FXR activity, via direct or indirect regulation, should be investigated further.

In conclusion, our study shows that hPCLS respond to OCA treatment by upregulating many well-known FXR target genes, demonstrating the suitability of hPCLS to study FXR-mediated gene regulation. By comparing human and mouse liver gene expression profiles, *Akap13*, *Cgnl1*, *Dyrk3*, *Pdia5*, *Ppp1r3b* and *Tbx6* were identified as bona-fide FXR target genes in mouse and human liver. Overall, our study provides novel insights into the mechanisms of action of OCA and a possible explanation for decreased HDL and increased LDL levels observed in patients treated with OCA.

Acknowledgements

The authors would like to thank Ewa Szalowska, Geert Stoop and Ad A. Peijnenburg for their help with the preparation of the liver slices, and Ellen C.L. Willemsen, Ingrid T.G.W. Bijmans and Vittoria Massafra for technical assistance. This research was supported by The Netherlands Cardiovascular Research Committee IN-CONTROL grant (CVON 2012-03) and by the Netherlands Organization for Scientific Research (NWO) Project VIDI (917.11.365), FP7 Marie Curie Actions IAPP (FXR-IBD, 611979), the Utrecht University Support Grant, Wilhelmina Children's Hospital Research Fund.

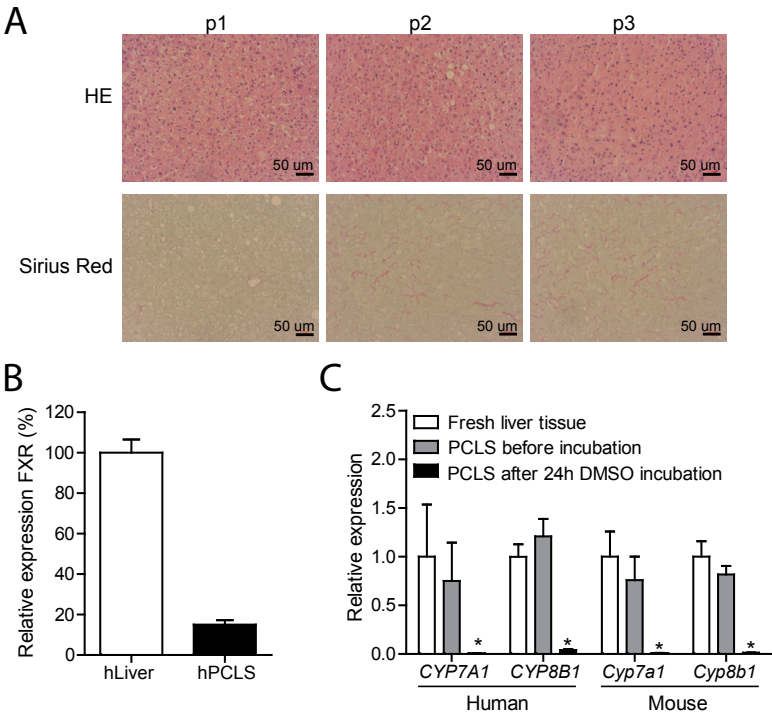
References

1. Bellentani S, Scaglioni F, Marino M, Bedogni G. Epidemiology of non-alcoholic fatty liver disease. *Dig Dis* 2010;28:155-161.
2. Neuschwander-Tetri BA, Loomba R, Sanyal AJ, Lavine JE, Van Natta ML, Abdelmalek MF, et al. Farnesoid X nuclear receptor ligand obeticholic acid for non-cirrhotic, non-alcoholic steatohepatitis (FLINT): a multicentre, randomised, placebo-controlled trial. *Lancet* 2015;385:956-965.
3. Wang YD, Chen WD, Moore DD, Huang W. FXR: a metabolic regulator and cell protector. *Cell Res* 2008;18:1087-1095.
4. Goodwin B, Jones SA, Price RR, Watson MA, McKee DD, Moore LB, et al. A regulatory cascade of the nuclear receptors FXR, SHP-1, and LRH-1 represses bile acid biosynthesis. *Mol Cell* 2000;6:517-526.
5. Ananthanarayanan M, Balasubramanian N, Makishima M, Mangelsdorf DJ, Suchy FJ. Human bile salt export pump promoter is transactivated by the farnesoid X receptor/bile acid receptor. *J Biol Chem* 2001;276:28857-28865.
6. Huang L, Zhao A, Lew JL, Zhang T, Hrywna Y, Thompson JR, et al. Farnesoid X receptor activates transcription of the phospholipid pump MDR3. *J Biol Chem* 2003;278:51085-51090.
7. Pircher PC, Kitto JL, Petrowski ML, Tangirala RK, Bischoff ED, Schulman IG, et al. Farnesoid X receptor regulates bile acid-amino acid conjugation. *J Biol Chem* 2003;278:27703-27711.
8. Wang XX, Jiang T, Shen Y, Adorini L, Pruzanski M, Gonzalez FJ, et al. The farnesoid X receptor modulates renal lipid metabolism and diet-induced renal inflammation, fibrosis, and proteinuria. *Am J Physiol Renal Physiol* 2009;297:F1587-1596.
9. Wang XX, Jiang T, Shen Y, Caldas Y, Miyazaki-Anzai S, Santamaria H, et al. Diabetic nephropathy is accelerated by farnesoid X receptor deficiency and inhibited by farnesoid X receptor activation in a type 1 diabetes model. *Diabetes* 2010;59:2916-2927.
10. Wang YD, Chen WD, Wang M, Yu D, Forman BM, Huang W. Farnesoid X receptor antagonizes nuclear factor kappaB in hepatic inflammatory response. *Hepatology* 2008;48:1632-1643.
11. Mudaliar S, Henry RR, Sanyal AJ, Morrow L, Marshall HU, Kipnes M, et al. Efficacy and safety of the farnesoid X receptor agonist obeticholic acid in patients with type 2 diabetes and nonalcoholic fatty liver disease. *Gastroenterology* 2013;145:574-582 e571.
12. Lerche-Langrand C, Toutain HJ. Precision-cut liver slices: characteristics and use for in vitro pharmacotoxicology. *Toxicology* 2000;153:221-253.
13. Janssen AW, Betzel B, Stoopen G, Berends FJ, Janssen IM, Peijnenburg AA, et al. The impact of PPARalpha activation on whole genome gene expression in human precision cut liver slices. *BMC Genomics* 2015;16:760.
14. Brunt EM, Janney CG, Di Bisceglie AM, Neuschwander-Tetri BA, Bacon BR. Nonalcoholic steatohepatitis: a proposal for grading and staging the histological lesions. *Am J Gastroenterol* 1999;94:2467-2474.
15. Batts KP, Ludwig J. Chronic hepatitis. An update on terminology and reporting. *Am J Surg Pathol* 1995;19:1409-1417.
16. Szalowska E, Tesfay HA, van Hijum SA, Kersten S. Transcriptomic signatures of peroxisome proliferator-activated receptor alpha (PPARalpha) in different mouse liver models identify novel aspects of its biology. *BMC Genomics* 2014;15:1106.
17. Sinal CJ, Tohkin M, Miyata M, Ward JM, Lambert G, Gonzalez FJ. Targeted disruption of the nuclear receptor FXR/BAR impairs bile acid and lipid homeostasis. *Cell* 2000;102:731-744.
18. Bolstad BM, Irizarry RA, Astrand M, Speed TP. A comparison of normalization methods for high density oligonucleotide array data based on variance and bias. *Bioinformatics* 2003;19:185-193.
19. Irizarry RA, Bolstad BM, Collin F, Cope LM, Hobbs B, Speed TP. Summaries of Affymetrix GeneChip probe level data. *Nucleic acids research* 2003;31:e15.
20. Dai M, Wang P, Boyd AD, Kostov G, Athey B, Jones EG, et al. Evolving gene/transcript definitions significantly alter the interpretation of GeneChip data. *Nucleic acids research* 2005;33:e175.
21. Sartor MA, Tomlinson CR, Wesselkamper SC, Sivaganesan S, Leikauf GD, Medvedovic M. Intensity-based hierarchical Bayes method improves testing for differentially expressed genes in microarray experiments. *BMC Bioinformatics* 2006;7:538.
22. Nowak DE, Tian B, Brasier AR. Two-step cross-linking method for identification of NF-kappaB gene network by chromatin immunoprecipitation. *Biotechniques* 2005;39:715-725.
23. Saccani S, Pantano S, Natoli G. p38-Dependent marking of inflammatory genes for increased NF-kappaB recruitment. *Nat Immunol* 2002;3:69-75.
24. Quinlan AR, Hall IM. BEDTools: a flexible suite of utilities for comparing genomic features. *Bioinformatics* 2010;26:841-842.
25. Chong HK, Infante AM, Seo YK, Jeon TI, Zhang Y, Edwards PA, et al. Genome-wide interrogation of hepatic FXR reveals an asymmetric IR-1 motif and synergy with LRH-1. *Nucleic Acids Res* 2010;38:6007-6017.

26. Heinz S, Benner C, Spann N, Bertolino E, Lin YC, Laslo P, et al. Simple combinations of lineage-determining transcription factors prime cis-regulatory elements required for macrophage and B cell identities. *Mol Cell* 2010;38:579-589.
27. Donato MT, Lahoz A, Castell JV, Gomez-Lechon MJ. Cell lines: a tool for in vitro drug metabolism studies. *Curr Drug Metab* 2008;9:1-11.
28. Lefebvre P, Cariou B, Lien F, Kuipers F, Staels B. Role of bile acids and bile acid receptors in metabolic regulation. *Physiol Rev* 2009;89:147-191.
29. Lee FY, Lee H, Hubbert ML, Edwards PA, Zhang Y. FXR, a multipurpose nuclear receptor. *Trends Biochem Sci* 2006;31:572-580.
30. Kalaany NY, Mangelsdorf DJ. LXRS and FXR: the yin and yang of cholesterol and fat metabolism. *Annu Rev Physiol* 2006;68:159-191.
31. Thomas AM, Hart SN, Kong B, Fang J, Zhong XB, Guo GL. Genome-wide tissue-specific farnesoid X receptor binding in mouse liver and intestine. *Hepatology* 2010;51:1410-1419.
32. Rakhshandehroo M, Hooiveld G, Muller M, Kersten S. Comparative analysis of gene regulation by the transcription factor PPARalpha between mouse and human. *PLoS One* 2009;4:e6796.
33. Schmidt SF, Jorgensen M, Sandelin A, Mandrup S. Cross-species ChIP-seq studies provide insights into regulatory strategies of PPARgamma in adipocytes. *Transcription* 2012;3:19-24.
34. Soccio RE, Tuteja G, Everett LJ, Li Z, Lazar MA, Kaestner KH. Species-specific strategies underlying conserved functions of metabolic transcription factors. *Molecular endocrinology* 2011;25:694-706.
35. Fon Tacer K, Bookout AL, Ding X, Kurosu H, John GB, Wang L, et al. Research resource: Comprehensive expression atlas of the fibroblast growth factor system in adult mouse. *Mol Endocrinol* 2010;24:2050-2064.
36. Schaap FG, van der Gaag NA, Gouma DJ, Jansen PL. High expression of the bile salt-homeostatic hormone fibroblast growth factor 19 in the liver of patients with extrahepatic cholestasis. *Hepatology* 2009;49:1228-1235.
37. Wunsch E, Milkiewicz M, Wasik U, Trottier J, Kempinska-Podhorodecka A, Elias E, et al. Expression of hepatic Fibroblast Growth Factor 19 is enhanced in Primary Biliary Cirrhosis and correlates with severity of the disease. *Sci Rep* 2015;5:13462.
38. Nishimura T, Utsunomiya Y, Hoshikawa M, Ohuchi H, Itoh N. Structure and expression of a novel human FGF, FGF-19, expressed in the fetal brain. *Biochim Biophys Acta* 1999;1444:148-151.
39. Jung D, York JP, Wang L, Yang C, Zhang A, Francis HL, et al. FXR-induced secretion of FGF15/19 inhibits CYP27 expression in cholangiocytes through p38 kinase pathway. *Pflugers Arch* 2014;466:1011-1019.
40. Sterpetti P, Marucci L, Candelaresi C, Toksoz D, Alpini G, Ugili L, et al. Cell proliferation and drug resistance in hepatocellular carcinoma are modulated by Rho GTPase signals. *Am J Physiol Gastrointest Liver Physiol* 2006;290:G624-632.
41. Guillemot L, Paschoud S, Jond L, Foglia A, Citi S. Paracrine regulates the activity of Rac1 and RhoA GTPases by recruiting Tiam1 and GEF-H1 to epithelial junctions. *Mol Biol Cell* 2008;19:4442-4453.
42. Guo X, Williams JG, Schug TT, Li X. DYRK1A and DYRK3 promote cell survival through phosphorylation and activation of SIRT1. *J Biol Chem* 2010;285:13223-13232.
43. Garcia-Rodriguez JL, Barbier-Torres L, Fernandez-Alvarez S, Gutierrez-de Juan V, Monte MJ, Halilbasic E, et al. SIRT1 controls liver regeneration by regulating bile acid metabolism through farnesoid X receptor and mammalian target of rapamycin signaling. *Hepatology* 2014;59:1972-1983.
44. Xia J, Scherer SW, Cohen PT, Majer M, Xi T, Norman RA, et al. A common variant in PPP1R3 associated with insulin resistance and type 2 diabetes. *Diabetes* 1998;47:1519-1524.
45. Hansen L, Hansen T, Vestergaard H, Bjorbaek C, Echwald SM, Clausen JO, et al. A widespread amino acid polymorphism at codon 905 of the glycogen-associated regulatory subunit of protein phosphatase-1 is associated with insulin resistance and hypersecretion of insulin. *Hum Mol Genet* 1995;4:1313-1320.
46. Doney AS, Fischer B, Cecil JE, Cohen PT, Boyle DI, Leese G, et al. Male preponderance in early diagnosed type 2 diabetes is associated with the ARE insertion/deletion polymorphism in the PPP1R3A locus. *BMC Genet* 2003;4:11.
47. Maegawa H, Shi K, Hidaka H, Iwai N, Nishio Y, Egawa K, et al. The 3'-untranslated region polymorphism of the gene for skeletal muscle-specific glycogen-targeting subunit of protein phosphatase 1 in the type 2 diabetic Japanese population. *Diabetes* 1999;48:1469-1472.
48. Wang G, Qian R, Li Q, Niu T, Chen C, Xu X. The association between PPP1R3 gene polymorphisms and type 2 diabetes mellitus. *Chin Med J (Engl)* 2001;114:1258-1262.
49. Speliotes EK, Yerges-Armstrong LM, Wu J, Hernaez R, Kim LJ, Palmer CD, et al. Genome-wide association analysis identifies variants associated with nonalcoholic fatty liver disease that have distinct effects on metabolic traits. *PLoS Genet* 2011;7:e1001324.
50. Leon-Mimila P, Vega-Badillo J, Gutierrez-Vidal R, Villamil-Ramirez H, Villareal-Molina T, Larrieta-Carrasco E, et al. A genetic risk score is associated with hepatic triglyceride content and non-alcoholic

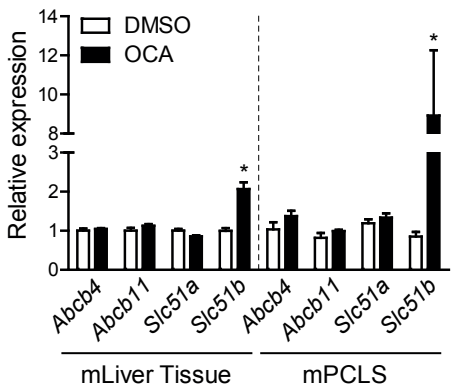
- steatohepatitis in Mexicans with morbid obesity. *Exp Mol Pathol* 2015;98:178-183.
51. Teslovich TM, Musunuru K, Smith AV, Edmondson AC, Stylianou IM, Koseki M, et al. Biological, clinical and population relevance of 95 loci for blood lipids. *Nature* 2010;466:707-713.
52. Hirschfield GM, Mason A, Luketic V, Lindor K, Gordon SC, Mayo M, et al. Efficacy of obeticholic acid in patients with primary biliary cirrhosis and inadequate response to ursodeoxycholic acid. *Gastroenterology* 2015;148:751-761 e758.
53. Iadevaia V, Rinaldi A, Falasca L, Pucillo LP, Alonzi T, Chimini G, et al. ATP-binding cassette transporter 1 and transglutaminase 2 act on the same genetic pathway in the apoptotic cell clearance. *Cell Death Differ* 2006;13:1998-2001.
54. Demchev V, Malana G, Vangala D, Stoll J, Desai A, Kang HW, et al. Targeted deletion of fibrinogen like protein 1 reveals a novel role in energy substrate utilization. *PLoS One* 2013;8:e58084.
55. Davies JP, Scott C, Oishi K, Liapis A, Ioannou YA. Inactivation of NPC1L1 causes multiple lipid transport defects and protects against diet-induced hypercholesterolemia. *J Biol Chem* 2005;280:12710-12720.
56. Desai U, Lee EC, Chung K, Gao C, Gay J, Key B, et al. Lipid-lowering effects of anti-angiopoietin-like 4 antibody recapitulate the lipid phenotype found in angiopoietin-like 4 knockout mice. *Proc Natl Acad Sci U S A* 2007;104:11766-11771.
57. Zhang N, Fu Z, Linke S, Chicher J, Gorman JJ, Visk D, et al. The asparaginyl hydroxylase factor inhibiting HIF-1 α is an essential regulator of metabolism. *Cell Metab* 2010;11:364-378.
58. Egecioglu E, Bjursell M, Ljungberg A, Dickson SL, Kopchick JJ, Bergstrom G, et al. Growth hormone receptor deficiency results in blunted ghrelin feeding response, obesity, and hypolipidemia in mice. *Am J Physiol Endocrinol Metab* 2006;290:E317-325.
59. Hasty AH, Shimano H, Osuga J, Namatame I, Takahashi A, Yahagi N, et al. Severe hypercholesterolemia, hypertriglyceridemia, and atherosclerosis in mice lacking both leptin and the low density lipoprotein receptor. *J Biol Chem* 2001;276:37402-37408.
60. Fuchs M, Hafer A, Munch C, Kannenberg F, Teichmann S, Scheibner J, et al. Disruption of the sterol carrier protein 2 gene in mice impairs biliary lipid and hepatic cholesterol metabolism. *J Biol Chem* 2001;276:48058-48065.
61. Bjursell M, Gerdin AK, Jonsson M, Surve VV, Svensson L, Huang XF, et al. G protein-coupled receptor 12 deficiency results in dyslipidemia and obesity in mice. *Biochem Biophys Res Commun* 2006;348:359-366.

Supplemental figures and tables

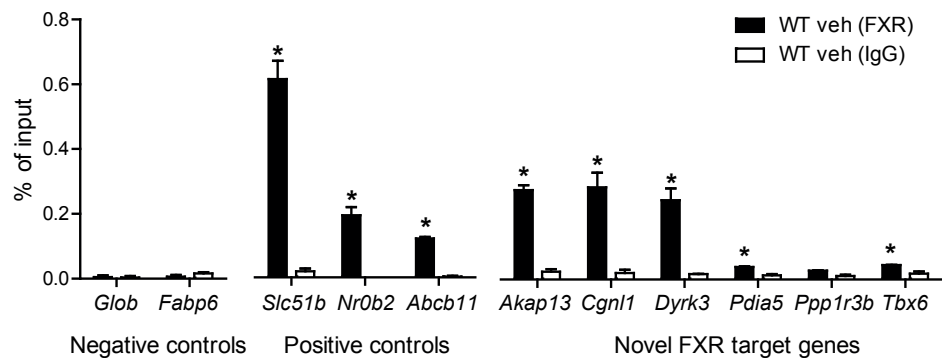


Supplemental figure 1. Characteristics of liver tissue and slices.

(A) Liver slices of p1-3 stained for HE to determine steatosis and Sirius Red to determine fibrosis. There were no signs of steatosis and fibrosis in these livers. (B) Expression level of FXR (%) in human liver biopsies (n=15) and human precision cut liver slices (n=3). (C) Relative expression levels of Cyp7a1 and Cyp8B1 in fresh liver tissue, in PCLS after cutting but before incubation, and after 24h of DMSO incubation (n=3).



Supplemental figure 2. Expression of FXR target genes in mouse liver tissue (n=6) and mouse PCLS (n=3) upon treatment with OCA shows a similar profile.



Supplemental figure 3. Identification of 6 novel FXR target genes.
Globin and *Fabp6* were used as negative controls for FXR in the liver; *Slc51b*, *Nr0b2* and *Abcb11* were used as positive controls. Data are shown as mean \pm SEM, n=2, *p<0.05 by a Students t-test.

Supplemental table 1. Primer sequences used for qPCR

Primer Sequence		
Name	Forward	Reverse
<i>h36B4</i>	CGGGAAGGCTGTGGTGCTG	GTGAACACAAAGCCCACATTCC
<i>hCYCLOPHILIN</i>	CCCACCGTGTTCTTCGACAT	TCTTTGGGACCTTGCTGCAA
<i>hFXR</i>	ACCAGCCTGAAAATCCTCAACAC	CTCTCCATGACATCAGCATCTCAG
<i>hNR0B2</i>	CCCAAGATGCTGTGACCTTTGAG	TGGGGTCTGTCTGGCAGTTG
<i>hABCB11</i>	GCAGAGGGAGCTACCAGGATAG	ACAACAGCTAATGGAGGTTCTGTG
<i>hSLC51A</i>	TTCCTCTAAAACCAGGTCTCAAGT	GCACAGTCATTAGAAAAGTCTCCA
<i>hABCB4</i>	TTTTCTTGTCGCTGCTAAATCC	AGCACCCAATCCTGAGTAGTAA
<i>m36b4</i>	ATGGGTACAAGCGCGTCCTG	GCCTTGACCTTTTTCAGTAAG
<i>mAbcb4</i>	TATCCGCTATGGCCGTGGGAA	ATCGGTGAGCTATCACAATGG
<i>mAbcb11</i>	CTGCCAAGGATGCTAATGCA	CGATGGCTACCTTTTGTCTTCT
<i>mSlc51a</i>	GTTCCAGGTGCTGTGCATCC	CCACTGTTAGCCAAGATGGAGAA
<i>mSlc51b</i>	AGATGCGGCTCCTTGAATTA	TGGCTGCTTCTTTTCGATTCTG
<i>mCyp7a1</i>	CAGGGAGATGCTCTGTGTTCA	AGGCATACATCCCTTCCGTGA
<i>mCyp8b1</i>	CCTCTGGACAAGGGTTTTGTG	GCACCGTGAAGACATCCCC
<i>mGlob</i> ChIP	CCTGCCCTCTCTATCCTGTG	GCAAATGTGTTGCCAAAAAG
<i>mFabp6</i> ChIP	ACACTCTGTGGCCGTCCT	GGAAAAACACCTACAATCCCACT
<i>mSlc51a</i> ChIP	CAGTGGAAGTGGCTTGAGTC	GGGCAGGAGAGGAAGCTAAG
<i>mSlc51b</i> ChIP	CCGCAATGGCAGATCATAC	GTGAATGACCCACGAATG
<i>mNr0b2</i> ChIP	CATGGAAATGGGCATCAATA	CGTGGCCTTGCTATCACTTT
<i>mAbcb11</i> ChIP	TCAATTCTCCATGAACTTTGG	GTGACATCCTGGGTTGCAG
<i>mAkap13</i> ChIP	GGGAGTAGGGTGTAAGGAGGA	CAGTGACCCCTGGAGGTTTG
<i>mCgnl1</i> ChIP	TGTCCTTGAGCCTGTGTGAC	ACACCAGAGACTGCCCTCAG
<i>mDyrk3</i> ChIP	TGACCCTTTCAACTGTCTGCT	GGTGGTTTTGCCTGTCTTA
<i>mPdia5</i> ChIP	ACTGAAGGGAGGGAAAAAGG	AGTTGGGCTGACTCCCATC
<i>mPpp1r3b</i> ChIP	TTAGCAGTGGGGAACCTTGC	AAGGTCCGGCTGTAGAGAGA
<i>mTbx6</i> ChIP	AGGGGCCGTGTGTGACTA	AGCTCACACGGTAGGCAATC

8



ANGPTL4 promotes bile acid absorption during taurocholic acid supplementation via a mechanism dependent on the gut microbiota

Aafke W.F. Janssen*, Wieneke Dijk*, Jos Boekhorst, Folkert Kuipers, Albert K. Groen, Sabina Lukovac,
Guido J.E.J. Hooiveld, Sander Kersten

* Authors contributed equally



Abstract

Angiopoietin-like 4 (ANGPTL4) raises plasma triglyceride levels by inhibiting lipoprotein lipase. A set of compounds that are able to reduce plasma triglyceride levels are bile acids (BA). Because BA have been shown to decrease ANGPTL4 secretion by intestinal cells, we hypothesized that BA lower plasma triglycerides (partly) via ANGPTL4. To test that hypothesis, wild-type and *Angptl4*^{-/-} mice were fed chow supplemented with taurocholic acid (TCA) for seven days. TCA supplementation effectively lowered plasma triglycerides in wild-type and *Angptl4*^{-/-} mice, indicating that ANGPTL4 is not required for plasma triglyceride-lowering by BA. Intriguingly, however, plasma and hepatic BA concentrations were significantly lower in TCA-supplemented *Angptl4*^{-/-} mice than in TCA-supplemented wild-type mice. These changes in the *Angptl4*^{-/-} mice were accompanied by lower BA levels in ileal scrapings and decreased expression of FXR-target genes in the ileum, including the BA transporter *Slc10a2*. By contrast, faecal excretion of specifically primary BA was higher in the *Angptl4*^{-/-} mice, suggesting that loss of ANGPTL4 impairs intestinal BA absorption. Since the gut microbiota convert primary BA into secondary BA, elevated excretion of primary BA in *Angptl4*^{-/-} mice may reflect differences in gut microbial composition and/or functionality. Indeed, colonic microbial composition was markedly different between *Angptl4*^{-/-} and wild-type mice. Suppression of the gut bacteria using antibiotics abolished differences in plasma, hepatic, and faecal BA levels between TCA-supplemented *Angptl4*^{-/-} and wild-type mice. In conclusion, 1) ANGPTL4 is not involved in the triglyceride-lowering effect of BA; 2) ANGPTL4 promotes BA absorption during TCA supplementation via a mechanism dependent on the gut microbiota.

Introduction

Dietary triglycerides are digested in the small intestine primarily via the action of the enzyme pancreatic lipase. The activity of pancreatic lipase and subsequent breakdown of triglycerides is supported by bile acids (BA). BA are amphipathic molecules that are able to emulsify triglycerides and stimulate pancreatic lipase activity. The resulting fatty acids are taken up by enterocytes and re-esterified into triglycerides, which in turn are packed in chylomicrons and secreted into the lymph (1–3). Circulating triglycerides—as intestine-derived chylomicrons or liver-derived very low-density lipoproteins—are cleared from the bloodstream by hydrolysis catalyzed by lipoprotein lipase (LPL), an enzyme attached to the capillary wall in adipose tissue and muscle (4, 5). The activity of LPL is regulated by a number of proteins, including the ubiquitously expressed angiopoietin-like 4 (ANGPTL4). Numerous studies have shown that ANGPTL4 potently inhibits the activity of LPL, likely by unfolding and thereby destabilizing LPL, leading to its degradation (6–9). Accordingly, mice lacking *Angptl4* have reduced plasma triglyceride levels, whereas mice overexpressing *Angptl4* have elevated plasma triglyceride levels as compared with wild-type mice (6, 10–12). Overall, it is becoming increasingly apparent that ANGPTL4 is the main factor governing the physiological changes in LPL activity in white adipose tissue during fasting, in brown adipose tissue during cold exposure, and in muscle during exercise (6, 13, 14).

In addition to supporting the function of pancreatic lipase in lipid digestion, BA also have major regulatory roles in the control of lipid, glucose and energy metabolism through activation of the bile acid receptors FXR and TGR5 (15). Importantly, the various BA species that are present in rodents and humans show differential potencies towards the different BA signaling pathways (16). In addition, BA may influence biological processes via interactions with the gut microbiota. An intricate interrelationship exists between the gut microbiota, BA, and host metabolism. While the gut microbiota influences BA composition by deconjugating BA and transforming primary BA into secondary BA, alterations in BA composition may in turn affect the gut microbiota (17–20). By modulating BA composition, the gut microbiota may significantly impact BA signaling and, thereby, host metabolism (15, 21).

An important manifestation of the regulatory role of BA in lipid metabolism is their ability to influence plasma triglyceride levels. The hypertriglyceridemic effect of BA-binding resins and the hypotriglyceridemic effects of oral BA therapies are well-documented in humans (22–26). Direct and dose-dependent suppression of the production of very low-density lipoproteins by BA has been demonstrated in cultured human and rat hepatocytes (27)(28). Evidence has also been presented indicating that the hypotriglyceridemic effect of BA is mediated by hepatic FXR activation, leading to up- and down-regulation of *Apoc2* and *Apoc3* expression, respectively, collectively resulting in enhanced triglyceride

clearance (29)(30). In addition, hepatic FXR activation has been suggested to lead to reduced hepatic lipogenesis via SREBP1c (25). Nevertheless, complete insight into the mechanisms underlying the triglyceride-lowering actions of BA is still lacking. Previously, we observed that BA potently lower ANGPTL4 secretion from the human duodenal cell line Hutu-80. Based on this observation and given the prominent role of ANGPTL4 in the regulation of plasma triglyceride levels, we hypothesized that the triglyceride-lowering effect of BA may, at least in part, be mediated *via* down-regulation of ANGPTL4 in intestine and/or liver (31).

To test this hypothesis, wild-type and *Angptl4*^{-/-} mice were supplemented with the primary BA taurocholic acid (TCA) for seven days by adding it to the feed. TCA effectively lowered circulating triglycerides in both wild-type and *Angptl4*^{-/-} mice, indicating that ANGPTL4 is not required for the plasma triglyceride-lowering action of BA. Interestingly, however, our studies revealed a novel and unexpected interaction between ANGPTL4 and BA metabolism that is dependent on the gut microbiota.

Materials and methods

Animals and diet

Animal studies were performed using pure-bred wild-type and *Angptl4*^{-/-} mice on a C57BL/6 background that were bred and maintained in the same facility for more than 20 generations. *Angptl4*^{-/-} mice have been obtained via homologous recombination of embryonic stem cells and lack part of the *Angptl4* gene, resulting in a non-functional ANGPTL4 protein (11, 32). Mice were individually housed in temperature- and humidity-controlled specific pathogen-free conditions. In study 1, 4 month-old male mice received either chow (control, n=8) or chow supplemented with 0.5% (wt/wt) taurocholic acid (TCA, n=8) (Calbiochem, La Jolla, CA) for 7 days. Chow was sterilized by γ -irradiation at 20-50kGy. TCA was added to the chow by crushing the chow pellets and mixing in the TCA. Diets were provided to the mice in a powdered form. In study 2, 12-week old male wild-type and *Angptl4*^{-/-} mice (n=10 per group) received a run-in diet for 3 weeks consisting of a powdered AIN-93G purified diet (TestDiet, St. Louis, USA, sterilized by γ -irradiation at 18-50kGy) and an antibiotic cocktail in the drinking water. The antibiotic cocktail consisted of 1g/l Ampicillin, 1g/l Neomycin sulphate and 0.5g/l Metronidazole. After 3 weeks the mice were switched to a powdered AIN-93G purified diet supplemented with 0.5% (wt/wt) TCA (Calbiochem) for 7 days, while still receiving the antibiotic cocktail in the drinking water. The mice had *ad libitum* access to food and water. Body weight and food intake were assessed daily. At the end of the study, mice were anesthetized using isoflurane and blood was collected by orbital puncture. Mice were euthanized *via* cervical dislocation after which tissues were excised and weighed. The small intestine was divided into three equal parts along the distal-to-proximal axis and epithelial cells were obtained by scraping the mucosal lining. All animal experiments were approved by the local animal ethics committee of Wageningen University.

Plasma parameters

Blood was collected in EDTA-coated tubes and centrifuged for 15 minutes at 3000 rpm to obtain plasma. Plasma free fatty acid and triglyceride concentrations were determined according to manufacturer's instructions using commercially available kits (Wako chemicals, Neuss, Germany and HUMAN Diagnostics, Wiesbaden, Germany). Plasma cholesterol was quantified using a kit from Elitech (Sees, France). Free and conjugated BA species were quantified by liquid chromatography tandem MS (LC-MS/MS) using a SHIMADZU liquid chromatography system (SHIMADZU, Kyoto, Japan) and tandem AB SCIEX API-3200 triple quadrupole mass spectrometer (AB SCIEX, Framingham, USA) as previously described (33).

RNA isolation and qPCR

Total RNA was extracted from scrapings of the distal small intestine and liver using TRIzol reagent (Life technologies, Bleiswijk, Netherlands). Subsequently, 500 ng RNA was used to synthesize cDNA using the iScript cDNA synthesis kit (Bio-Rad Laboratories, Veenendaal, the Netherlands). Changes in gene expression were determined by real-time PCR on a CFX384 Real-Time PCR detection system (Bio-Rad) by using SensiMix (Bioline, GC biotech, Alphen aan den Rijn, the Netherlands). The housekeeping genes *36b4* and *β-actin* were used for normalization. Sequences of the used primers are listed in **Supplemental Table 1**.

Bile acid quantification in liver and ileal scrapings

Total bile acids were quantified in the liver and scrapings of the ileum. Livers and ileal scrapings were homogenized in 75% ethanol, incubated at 50°C and centrifuged. After the collection of the supernatant, the concentration of total bile acids was determined using a colorimetric assay kit (Diazyme Laboratories, Poway, USA).

Faecal measurements

Prior to euthanasia, faeces were collected over a period of 48 hours. Total lipids were measured in the faecal samples as described by Govers *et al* (34). Briefly, 100 mg of faecal samples were weighed, dried and acidified using HCl. Lipids were then extracted using petroleum and diethyl ether. The ether fraction was collected, evaporated and total lipids were weighed. Faecal bile salt composition and faecal neutral sterols were determined by capillary gas chromatography (Agilent 6890, Amstelveen, the Netherlands) as described previously (35, 36).

Bacterial DNA extraction, 16S rRNA gene sequencing and analysis (Study 1)

In study 1, DNA was extracted from the freeze-dried luminal content of the colon as described previously (37). Universal primers were used for initial amplification of part of the 16S rRNA gene: forward primer, '5-TCGTCGGCAGCGTCAGATGTGTA TAAGAGACAGCCTACGGGAGGCAGCAG-3' (broadly conserved bacterial primer 357F) and reverse primer, '5-GTCTCGTGGGCTCGGAGATGTGTATAAGAGACAGTACNV GGGTATCTAAKCC' (broadly conserved bacterial primer 802R). To the purified PCR product, Illumina sequencing adapters were added and the 16S rRNA gene was subsequently sequenced on the Illumina MiSeq (PE300 cycles run) platform.

Sequences were analyzed using a workflow based on QIIME 1.8 (38). OTU clustering, taxonomic assignment and reference alignment were done with the `pick_open_reference_otus.py` workflow script of QIIME, using `uclust` as clustering method (97% identity) and GreenGenes v13.8 as reference database for taxonomic assignment. Reference-based

chimera removal was done with uchime. Redundancy analysis (RDA) was performed in Canoco version 5 (39).

Bacterial DNA extraction and 16S rRNA gene quantification (Study 2)

In study 2, fecal samples (~40-90mg), which were collected over a period of 48 hours, were suspended in 600µL S.T.A.R. buffer (Roche). After addition of 0.1mm zirconia and 2.5mm glass beads (BioSpec, Bartlesville, USA), cells were lysed by mechanical disruption using a bead beater (MP biomedical, Santa Ana, USA) for 3x1 minute. DNA was subsequently extracted and purified using Maxwell 16 System (Promega). In brief, homogenates (250 µL) were transferred to a prefilled reagent cartridge (Maxwell® 16 Tissue LEV Total RNA Purification Kit, Custom-made, Promega). Sixteen samples were processed at the same time. After 30 minutes the purification process was completed and DNA was eluted in 50 µL of water (Nuclease free)(Promega).

Real-time PCR was used to quantify 16S rRNA gene in equal amounts of extracted DNA on a CFX384 Real-Time PCR detection system (Bio-Rad Laboratories, Veenendaal, Netherlands) by using SensiMix (Bioline, GC biotech, Alphen aan den Rijn, Netherlands). 16S rRNA gene was amplified using the forward primer 1369F (5'-CGGTGAATACGTTTCYCGG-3')(40) and the reverse primer 1492R (5'-GGWTACCTTGTTACGACTT-3')(41). The cycling conditions consisted of an initial denaturation of 95°C for 5 min, followed by 40 cycles of denaturation at 95°C for 15 sec, annealing at 60 °C for 30 sec and extension at 72°C for 30 sec.

Statistical analysis

Data are presented as mean ± SEM. Statistical significant differences were determined with two-way analysis of variance with Bonferroni post-hoc tests or by Student's t-test where appropriate using GraphPad Prism (GraphPad Software, Inc., La Jolla, USA). $P < 0.05$ was considered as statistically significant. For microbiota analysis, false discovery rate (FDR)-corrected P-values were estimated for each taxon to correct for multiple testing. Bacterial taxa with a FDR-corrected P-value < 0.20 were considered significant. Significance of RDA analysis was determined using Monte-Carlo permutation (500 randomizations) as implemented in Canoco 5 (39).

Results

ANGPTL4 is not implicated in the triglyceride-lowering effects of BA

To investigate the potential role of ANGPTL4 in the lowering of plasma triglycerides by BA, wild-type and *Angptl4*^{-/-} mice were fed either chow or chow supplemented with taurocholic acid (TCA) for seven days (**Figure 1A**). The TCA-supplemented diet slightly reduced food intake and body weight. However, no differences were observed between the genotypes (**Supplemental Figure 1**). In contrast to our hypothesis that BA may down-regulate *Angptl4* expression, mRNA levels of *Angptl4* were either unchanged (liver; **Figure 1B**) or increased (ileum; **Figure 1C**) by TCA supplementation. As expected, TCA supplementation markedly

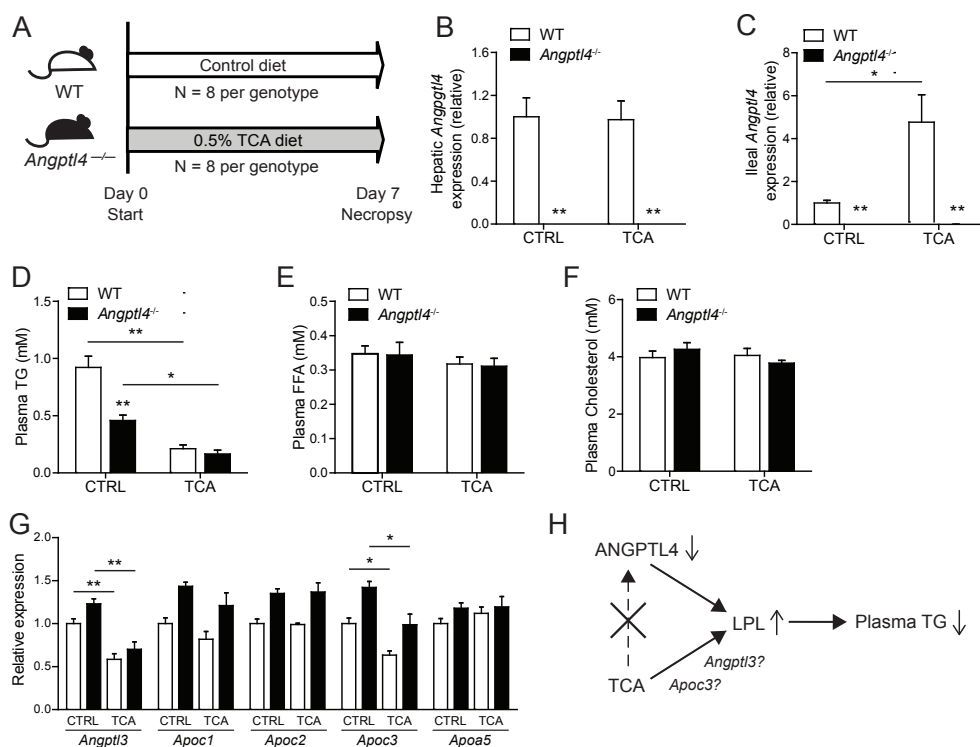


Figure 1. ANGPTL4 is not part of the triglyceride-lowering effects of bile acids

(A) Schematic representation of the dietary intervention with 0.5% w/w taurocholic acid (TCA) in wild-type and *Angptl4*^{-/-} mice. Relative gene expression of (B) hepatic *Angptl4*, (C) ileal *Angptl4* in wild-type and *Angptl4*^{-/-} mice fed chow (CTRL) or chow supplemented with TCA for 7 days. Gene expression levels in wild-type mice fed the control diet were set at 1. (D) Plasma triglycerides, (E) Plasma free fatty acids (FFA), and (F) Plasma cholesterol concentration. (G) Relative gene expression of *Angptl3* and the apolipoproteins *Apoc1*, *Apoc2*, *Apoc3* and *Apoa5* in the liver. Data are presented as mean \pm SEM. Asterisks indicate significant differences compared with wild-type mice or between groups as indicated by bars according to two-way ANOVA followed by a Bonferroni post-hoc test. * $p < 0.05$, ** $p < 0.001$. (H) Hypothetical model of how TCA may lower plasma triglyceride levels.

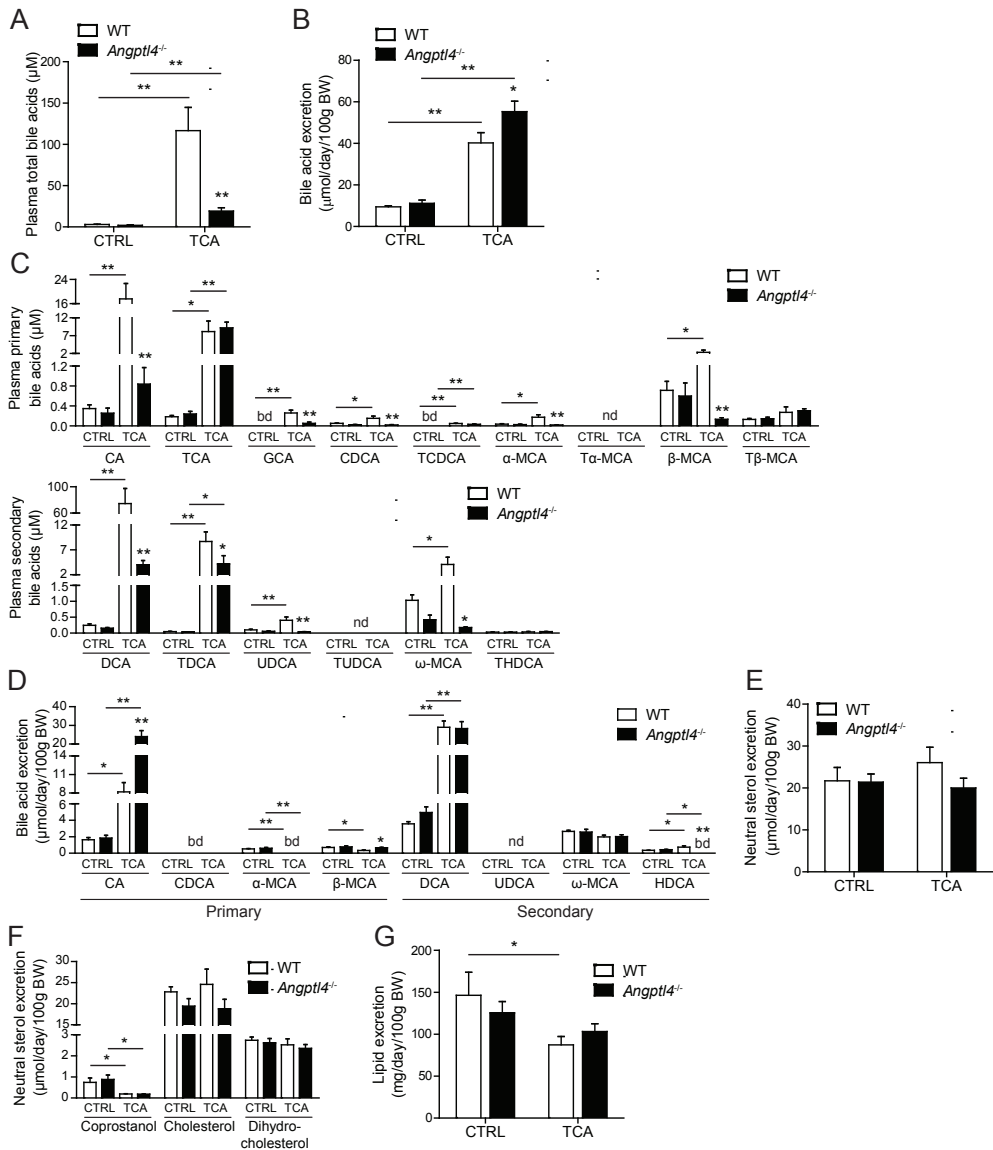


Figure 2. Loss of ANGPTL4 decreases plasma BA levels and increases faecal BA levels in TCA-supplemented mice

Total plasma BA concentration (A), total BA excretion (B), and plasma concentration of free and conjugated BA subspecies (C) in wild-type and *Angptl4*^{-/-} mice fed chow (CTRL) or chow supplemented with TCA for 7 days. (D) Mean excretion of free and conjugated BA subspecies. Nd indicates that this BA was not determined. Mean excretion of total neutral sterols (E), coprostanol, cholesterol, and dihydro-cholesterol (F), and lipids (G). Data are presented as mean \pm SEM. Asterisks indicate significant differences compared with wild-type mice or between groups as indicated by bars according to two-way ANOVA followed by a Bonferroni post-hoc test. * $p < 0.05$, ** $p < 0.001$

lowered plasma triglyceride levels in wild-type mice. Interestingly, however, TCA also effectively lowered plasma triglyceride levels in mice lacking ANGPTL4 (**Figure 1D**). Other plasma lipid parameters, including free fatty acids (**Figure 1E**) and cholesterol (**Figure 1F**) were not different between the genotypes and were also not affected by TCA supplementation. These data indicate that ANGPTL4 is not involved in the plasma triglyceride-lowering effect of BA. Since loss of ANGPTL4 did not lead to a further reduction in plasma triglycerides in TCA-supplemented mice, TCA likely lowers plasma triglyceride levels via a mechanism similar to loss of ANGPTL4 (e.g. enhanced LPL activity). Interestingly, the expression of *Angptl3* and *Apoc3*, two known inhibitors of LPL, was strongly reduced upon TCA supplementation in both wild-type and *Angptl4*^{-/-} mice, whereas the expression of *Apoc1*, *Apoc2* and *Apoa5* was not altered (**Figure 1G**), suggesting that TCA might lower plasma triglycerides by downregulating *Angptl3* and/or *Apoc3* expression (**Figure 1H**).

Loss of ANGPTL4 leads to reduced BA absorption in TCA-supplemented mice

As expected, the TCA-supplemented diet significantly increased total BA levels in plasma and total BA excretion in the faeces (**Figure 2A & 2B**). Intriguingly, the total plasma BA concentration was significantly lower in the TCA-supplemented *Angptl4*^{-/-} mice as compared to the TCA-supplemented wild-type mice, while faecal BA excretion was significantly higher in the *Angptl4*^{-/-} mice (**Figure 2A & 2B**). These observations suggest that the loss of ANGPTL4 reduces the absorption of BA. To further study the effect of *Angptl4* deletion on BA absorption, we quantified the levels of individual BA in plasma and faeces. In wild-type mice, TCA supplementation significantly increased plasma levels of primary BA, including cholic acid, taurocholic acid, glycocholic acid, chenodeoxycholic acid, taurochenodeoxycholic acid and unconjugated muricholic acids, as well as secondary BA, including deoxycholic acid, taurodeoxycholic acid, ursodeoxycholic acid and ω -muricholic acid. The lower levels of total plasma BA in TCA-supplemented *Angptl4*^{-/-} mice as compared to TCA-supplemented wild-type mice were primarily accounted for by lower plasma levels of the primary BA cholic acid and β -muricholic acid, and the secondary BA deoxycholic acid and ω -muricholic acid (**Figure 2C**). With respect to faecal BA levels, TCA supplementation in wild-type mice markedly increased the excretion of the primary BA cholic acid and deoxycholic acid, and the secondary BA hyodeoxycholic acid. The increased excretion of BA in the TCA-supplemented *Angptl4*^{-/-} mice as compared to TCA-supplemented wild-type mice was mainly accounted for by an increase in excretion of cholic acid and β -muricholic acid, whereas faecal excretion of the secondary BA deoxycholic acid and ω -muricholic acid, as well as the excretion of neutral sterols and lipids, was not different between the genotypes (**Figure 2D – 2G**). The observation that differences in plasma BA between *Angptl4*^{-/-} and wild-type mice after TCA-supplementation were caused by differences in unconjugated cholic

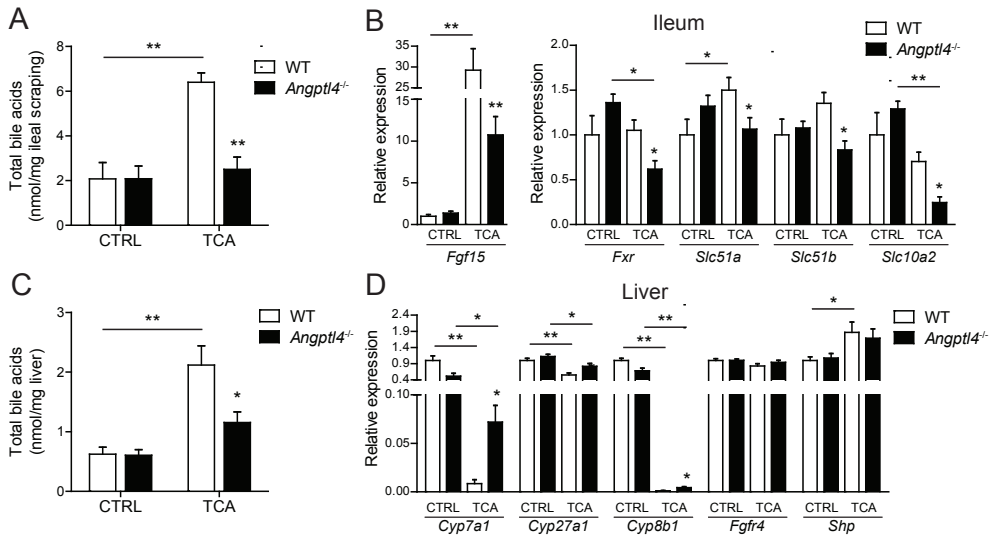


Figure 3. Levels of BA in liver and ileal scrapings after TCA supplementation are lower in *Angptl4*^{-/-} mice as compared to wild-type mice

(A) Total BA levels in ileal scraping of wild-type and *Angptl4*^{-/-} mice fed chow (CTRL) or chow supplemented with TCA for 7 days. (B) Relative expression of ileal BA transporters and BA-responsive genes, *Fgf15*, *Fxr*, *Slc51a*, *Slc51b* and *Slc10a2*. Gene expression levels in wild-type mice fed the CTRL diet were set at 1. (C) Total BA levels in the liver. (D) Relative hepatic expression of genes involved in BA synthesis and metabolism. Data are presented as mean ± SEM. Asterisks indicate significant differences compared with wild-type mice or between groups as indicated by bars according to two-way ANOVA followed by a Bonferroni post-hoc test. **p*<0.05, ***p*<0.001

acid and deoxycholic acid, without significant differences in tauroconjugates, is indicative of decreased ileal BA absorption in the *Angptl4*^{-/-} mice. Overall, these data indicate that the loss of ANGPTL4 in mice supplemented with TCA reduces BA absorption, leading to lower levels of BA in the circulation and higher faecal BA loss.

The lower absorption of BA in the *Angptl4*^{-/-} mice is expected to significantly impact ileal and hepatic BA levels, as well as BA signaling via FXR. Consistent with this notion, total BA levels in ileal scraping were increased in TCA-supplemented wild-type but not *Angptl4*^{-/-} mice (Figure 3A). Moreover, ileal expression of several FXR target genes, including *Fgf15*, *Slc51a* (*Osta*), and *Slc51b* (*Ostβ*), as well as expression of *Fxr* itself, was significantly lower in TCA-supplemented *Angptl4*^{-/-} mice than TCA-supplemented wild-type mice (Figure 3B, Supplemental Figure 2). Interestingly, ileal expression of the BA transporter *Slc10a2* (*Asbt*) was markedly lower in the *Angptl4*^{-/-} mice as compared to wild-type mice after TCA supplementation, potentially contributing to the lower BA absorption (Figure 3B).

In the liver, total BA levels were also significantly lower in the TCA-supplemented *Angptl4*^{-/-} mice as compared to TCA-supplemented wild-type mice (Figure 3C). The lower

hepatic BA levels and the reduced expression of *Fgf15* in the ileum of *Angptl4*^{-/-} mice were associated with markedly higher hepatic expression of genes involved in BA synthesis, including *Cyp7a1* and *Cyp8b1*, whereas hepatic expression of other genes involved in BA metabolism was not or only slightly different between the *Angptl4*^{-/-} and wild-type mice (Figure 3D, Supplemental Figure 2). Taken together, the TCA-supplemented *Angptl4*^{-/-} mice display reduced bile acid absorption as compared to TCA-supplemented wild-type mice, consequently leading to lower total bile acids levels in the plasma and liver and subsequently to the induction of genes involved in bile acid synthesis.

ANGPTL4 affects TCA-induced changes in gut microbial composition

As pointed out above, the excretion of the primary BA cholic acid and β -muricholic acid was significantly higher in *Angptl4*^{-/-} mice, whereas the excretion of secondary BA and neutral sterols was not different between the genotypes. Inasmuch as the conversion of primary BA into secondary BA is mediated by the gut microbiota, the higher excretion of specifically primary BA in the faeces of *Angptl4*^{-/-} mice suggests that loss of ANGPTL4 may impact gut microbial composition. Analysis of the colonic microbial composition by 16S rRNA gene sequencing revealed substantial differences between *Angptl4*^{-/-} and wild-type mice, both on the control diet and on the TCA-supplemented diet. Redundancy analysis (RDA) showed that the explanatory variables diet and genotype explained 34.9% of the total variation in the colonic microbiota composition (Figure 4). To determine which variable was the most important determinant of colonic microbial composition, a partial RDA was performed.

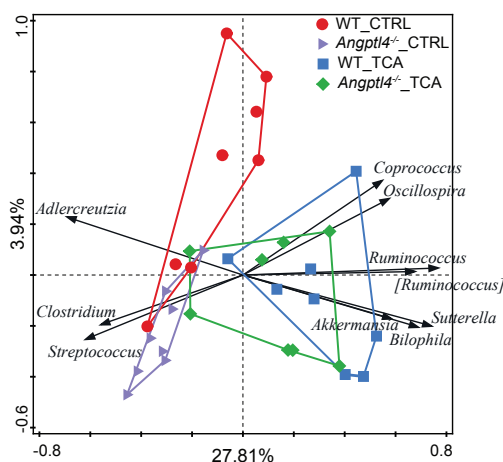


Figure 4. TCA supplementation and *Angptl4* genotype affect gut microbial composition

Redundancy analysis (RDA) correlation biplot describing the relationship between colonic luminal microbiota composition and the differences caused by genotype and diet. The explanatory variables diet and genotype explained 34.9% of the total variation in the microbiota composition.

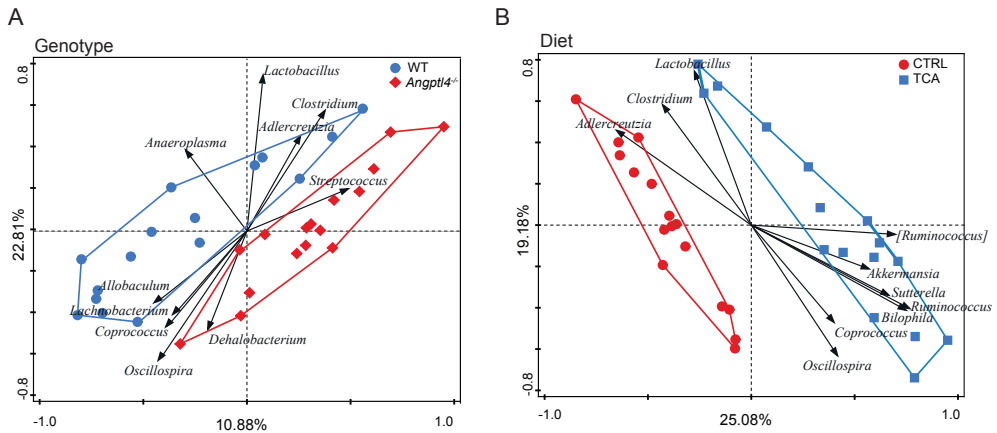


Figure 5. Bile acid feeding has more impact on gut microbial composition than *Angptl4* genotype
 (A-B) Partial RDA correlation biplot describing the relationship between colonic luminal microbiota composition and explanatory variables (A) genotype and (B) diet. Genotype explained 10.9% and diet 25.1% of total variation in microbiota composition.

While genotype explained 10.9% of the total variation in microbial composition, diet was more important and explained 25.1% of the microbial variation (Figure 5A & 5B).

Since the differences in BA metabolism between *Angptl4*^{-/-} and wild-type mice were most evident after TCA supplementation, the composition of the colonic microbiota of wild-type and *Angptl4*^{-/-} mice fed the TCA-supplemented diet was compared in more detail. At the phylum level, the relative abundance of Actinobacteria was significantly higher in the *Angptl4*^{-/-} mice than in the wild-type mice, whereas the relative abundance of Bacteroidetes and Cyanobacteria followed an opposite pattern (Figure 6, Supplemental Table 2). The increased abundance of the phylum Actinobacteria was largely explained by a significant increase within the genus *Adlercreutzia*. Concurrently, the decrease in the phylum Bacteroidetes was mainly accounted for by a significant decrease in the genus *Prevotella* (Figure 6, Supplemental Table 2). Interestingly, while the relative abundance of the phylum Proteobacteria was comparable between the genotypes, the family of Enterobacteriaceae was, with a relative abundance of 3.6%, 158-fold (FDR-corrected p-value = 0.188) more abundant in the colon of the *Angptl4*^{-/-} mice as compared with wild-type mice (Figure 6, Supplemental Table 2). Conversely, the abundance of *Bilophila* was significantly lower in the colonic luminal content of *Angptl4*^{-/-} mice as compared with wild-type mice. Finally, the species *Lactobacillus reuteri* was present in the colonic luminal content of wild-type mice, whereas it was almost absent in the *Angptl4*^{-/-} mice (Figure 6, Supplemental Table 2). These data reveal pronounced differences in gut microbiota composition between wild-type and *Angptl4*^{-/-} mice supplemented with TCA.

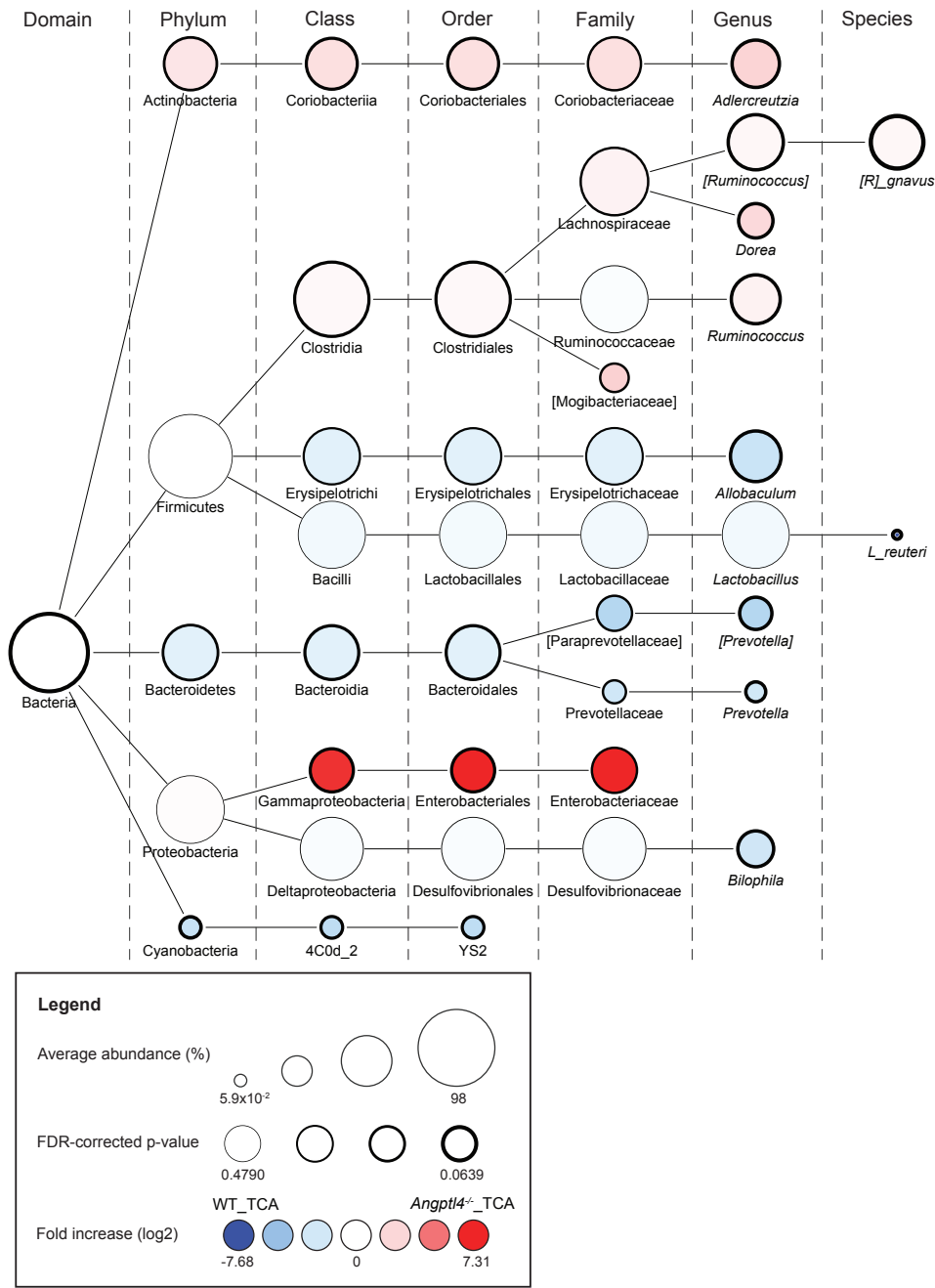


Figure 6. Differences in microbial composition between wild-type and *Angptl4*^{-/-} mice after TCA supplementation

Nodes represent taxa and the edges link the different taxonomic levels. The fold increase is calculated as the ³log of the ratio of the relative abundance in *Angptl4*^{-/-} and wild-type mice after TCA supplementation. Significance is expressed as the FDR-corrected p-value.

Suppression of the gut microbiota abolishes the decrease in BA absorption in *Angptl4*^{-/-} mice after TCA supplementation

To investigate if the reduction in BA absorption in the *Angptl4*^{-/-} mice supplemented with TCA is dependent on the gut microbiota, wild-type and *Angptl4*^{-/-} mice fed the TCA-supplemented diet were given antibiotics via the drinking water for 7 days. Oral antibiotics markedly reduced DNA levels in the faeces and decreased 16S rRNA gene amplification (**Figure 7A**), indicating an effective suppression of bacteria numbers in the colon. After treatment with antibiotics, plasma triglyceride levels were markedly lower in TCA-supplemented *Angptl4*^{-/-} mice as compared to TCA-supplemented wild-type mice,

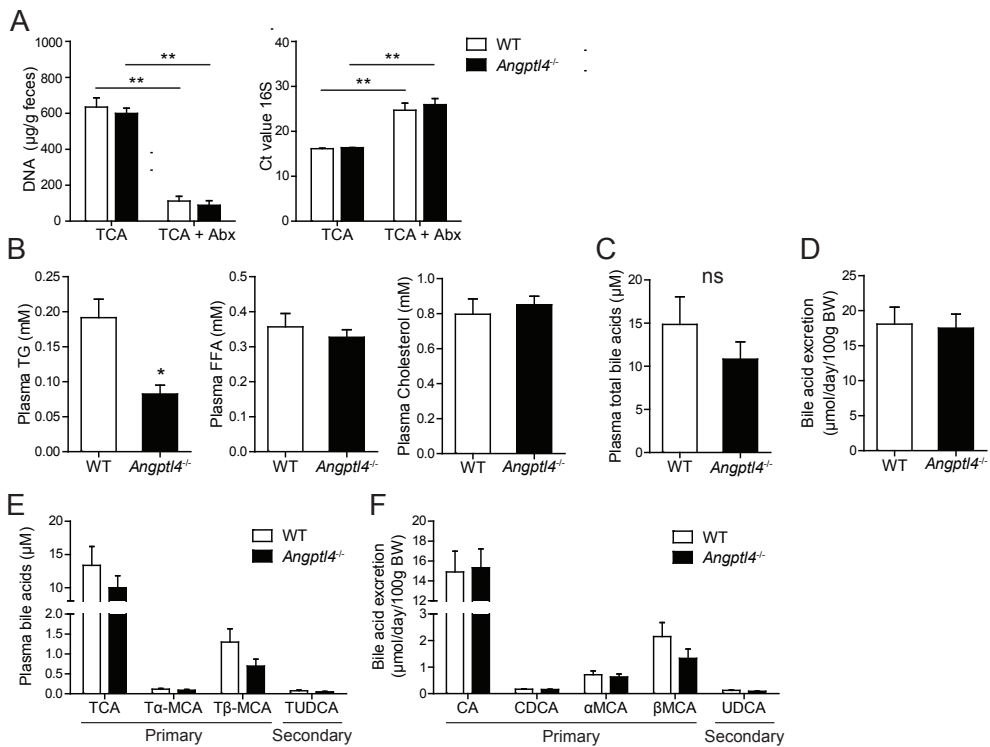


Figure 7. Antibiotics abolish the difference in BA (re)absorption between TCA-supplemented *Angptl4*^{-/-} and wild-type mice

(A) Quantitative analysis of faecal DNA levels and Ct values of qPCR amplification of 16S rRNA gene in equal amounts of faecal DNA. Data are presented as mean ± SEM. Asterisks indicate significant differences according to two-way ANOVA followed by a Bonferroni post-hoc test. (B) Plasma triglycerides (TG), free fatty acid (FFA) and cholesterol concentration in wild-type and *Angptl4*^{-/-} mice fed the TCA-supplemented diet for 7 days with antibiotics provided via the drinking water. (C) Total plasma BA concentration. (D) total BA excretion. Ns indicates not significant. (E) Plasma concentration of free and conjugated BA subspecies. (F) Mean excretion of free and conjugated BA subspecies. Data are presented as mean ± SEM. Asterisks indicate significant differences compared with wild-type mice according to a Student's t-test. *p<0.05, **p<0.001.

consistent with the function of ANGPTL4 as LPL inhibitor, whereas plasma free fatty acids and cholesterol were not different between the genotypes (**Figure 7B**). In contrast to the observations made in mice not given antibiotics, after antibiotics treatment, total plasma BA levels (**Figure 7C**) and faecal BA excretion (**Figure 7D**) were similar in TCA-supplemented *Angptl4*^{-/-} and TCA-supplemented wild-type mice. Although several BA species fell below the detection limit after antibiotics treatment, levels of individual primary and secondary BA in plasma (**Figure 7E**) and in faeces (**Figure 7F**) were similar in the two sets of mice. Also, after antibiotics treatment, ileal expression of *Fxr* and *Slc51b* were higher in TCA-supplemented *Angptl4*^{-/-} mice than TCA-supplemented wild-type mice, while the expression of *Fgf15*, *Slc51a* or *Slc10a2* was not different between the two genotypes (**Figure 8A**). The latter result contrasts with the lower ileal expression of *Fgf15*, *Fxr*, *Slc51a* (*Osta*), *Slc51b* (*Ostβ*), and *Slc10a2* (*Asbt*) in the TCA-supplemented *Angptl4*^{-/-} mice as compared to TCA-supplemented wild-type mice in the absence of antibiotics (**Figure 3A**). After antibiotics treatment, BA levels in the ileal scrapings were still significantly lower in TCA-supplemented

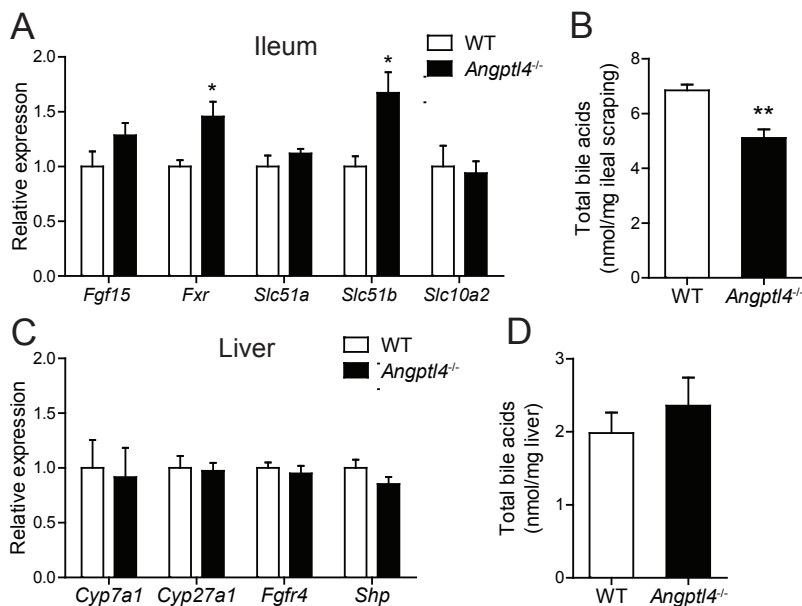


Figure 8. Antibiotics largely abolish the difference in ileal and hepatic bile acid levels and gene expression between TCA-supplemented *Angptl4*^{-/-} and wild-type mice

(A) Relative expression of ileal BA transporters and BA-responsive genes *Fgf15*, *Fxr*, *Slc51a*, *Slc51b* and *Slc10a2*, in wild-type and *Angptl4*^{-/-} mice fed the TCA-supplemented diet for 7 days with antibiotics provided via the drinking water. Gene expression levels in wild-type mice were set at 1. (B) Total BA levels in ileal scraping. (C) Relative hepatic expression of genes involved in BA synthesis and metabolism. (D) Total BA levels in the liver. Data are presented as mean \pm SEM. Asterisks indicate significant differences compared with wild-type mice according to a Student's t-test. * $p < 0.05$, ** $p < 0.001$.

Angptl4^{-/-} mice as compared to TCA-supplemented wild-type mice (**Figure 8B**), though less pronounced than in the absence of antibiotics (**Figure 3A**). Furthermore, after antibiotics treatment, no differences in hepatic BA levels and hepatic expression of genes related to BA synthesis and metabolism could be observed between the two sets of mice (**Figure 8C-D**), which is in line with the lack of difference in plasma BA levels between the two genotypes after antibiotics treatment. Overall, these data suggest that loss of ANGPTL4 reduces BA absorption via a mechanism that is dependent on the gut microbiota.

Discussion

Oral administration of BA has been shown to lower plasma triglyceride levels in mice and humans. In contrast, promoting BA excretion via resin treatment has the opposite effect (22–26). In the present paper, we found that TCA supplementation caused a marked reduction in plasma triglycerides in both wild-type and *Angptl4*^{-/-} mice, suggesting that ANGPTL4 is not involved in the triglyceride-lowering effect of BA. Interestingly, however, we found that plasma and hepatic BA concentrations were significantly lower in TCA-supplemented *Angptl4*^{-/-} mice than in TCA-supplemented wild-type mice. Moreover, after TCA-supplementation, BA levels in ileal scrapings were lower in *Angptl4*^{-/-} mice compared to wild-type mice, whereas faecal excretion of specifically primary BA was significantly higher in *Angptl4*^{-/-} mice, suggesting that loss of ANGPTL4 leads to impaired intestinal BA absorption. Changes in ileal and hepatic gene expression in *Angptl4*^{-/-} mice were consistent with this scenario. Furthermore, we found that suppression of the gut bacteria via oral antibiotics abolished the lower BA absorption in TCA-supplemented *Angptl4*^{-/-} mice as compared to wild-type mice. Overall, our data indicate that ANGPTL4 promotes BA absorption via a mechanism dependent on the gut microbiota.

The observation that loss of ANGPTL4 does not further reduce plasma triglyceride levels in mice supplemented with TCA may imply that ANGPTL4 and TCA decrease plasma triglycerides via similar non-additive mechanisms. Since loss of ANGPTL4 lowers plasma triglycerides by stimulating LPL-dependent plasma triglyceride clearance, TCA supplementation likely has a similar mode of action. By contrast, if TCA would lower plasma triglyceride levels by reducing VLDL-TG production in the liver, loss of ANGPTL4 may be expected to lead to a further decrease in plasma triglycerides in TCA-supplemented mice. Previous studies have provided evidence that the hypotriglyceridemic effect of BA occurs via activation of FXR, either via enhanced triglyceride clearance via regulation of APOC2 and/or APOC3, and/or reduced hepatic triglyceride production via SREBP1c (25, 29, 30). Additionally, triglyceride-lowering by BA may be mediated by downregulation of *Angptl3*, which akin to *Angptl4* encodes an inhibitor of LPL (25). Consistent with these studies, we found that the expression of *Apoc3* and *Angptl3* was markedly reduced by TCA supplementation, lending credence to the notion that the triglyceride-lowering effect of BA may be mediated by downregulation of the LPL inhibitors ANGPTL3 and APOC3.

An interesting new observation is the markedly lower concentration of plasma BA in *Angptl4*^{-/-} mice as compared to wild-type mice after TCA supplementation. This finding may be explained by the decreased expression of *Slc10a2*—the main active transporter for BA absorption—in the ileum of *Angptl4*^{-/-} mice (42). Expression of *Slc10a2* in the ileum is down-regulated by FXR via a negative feedback mechanism that involves activation of the small

heterodimer partner (SHP) and subsequent repression of liver related homolog-1 (LRH-1) (42–44). Various BA activate intestinal FXR, but their potency to activate FXR varies greatly (43, 45). Indeed, a recent study demonstrated that different BA species differentially affect the expression of *Fxr* and FXR-target genes such as *Fgf15* and *Slc10a2* (46). More hydrophilic BA such as tauro- β -muricholic acid have been suggested to act as antagonists of FXR (47). Since *Angptl4*^{-/-} mice had a significantly higher excretion of specifically primary BA, it can be hypothesized that the lower ileal expression of *Slc10a2* in *Angptl4*^{-/-} mice may be explained by differences in intestinal BA composition between *Angptl4*^{-/-} and wild-type mice.

Gut microbial composition potently influences intestinal BA metabolism and BA composition. Indeed, the gut microbiota converts primary BA to secondary BA via 7 α -dehydroxylation activity, thereby increasing the hydrophobicity of BA. In addition, the gut microbiota promote the deconjugation of BA, thereby preventing the active absorption of BA by SLC10A2 (15, 17, 20). As a result, alterations in gut microbial composition, for example by treatment with antibiotics, probiotics or a high-fat diet, significantly impact the abundance of secondary BA and overall BA homeostasis (19, 46–49). In addition to promoting 7 α -dehydroxylation and deconjugation of BA, the gut microbiota may influence BA metabolism via other mechanisms. For example, a recent study has shown that bacterial metabolites can modulate FXR activity (50) and that conventionalization of germ-free mice increases the expression of FXR-target genes (47). Moreover, it was shown that suppression of the gut microbiota by antibiotics treatment reduced activation of GATA4, a transcription factor that negatively regulates the expression of the *Slc10a2* transporter, resulting in higher expression of *Slc10a2* and higher BA absorption, whereas conventionalization of germ-free mice lowered *Slc10a2* expression (51, 52).

Given the intricate relationship between the gut microbiota and BA metabolism, we hypothesized that differences in BA metabolism between wild-type and *Angptl4*^{-/-} mice after TCA supplementation are accounted for by differences in microbial composition between the two sets of mice. Indeed, we detected a higher abundance of the Enterobacteriaceae, a family that includes several pathogenic strains such as *Salmonella* and *E.Coli*, and a lower abundance of bile-loving, sulphite-reducing *Bilophila* in the colon of TCA-supplemented *Angptl4*^{-/-} mice as compared with TCA-supplemented wild-type mice (53). In human subjects, Enterobacteriaceae have been associated with the presence of primary BA in the faeces and have been linked to pathologies such as hepatic encephalopathy and Crohn's disease (54–56).

Importantly, suppression of the gut bacteria by antibiotics abolished the decrease in BA absorption in TCA-supplemented *Angptl4*^{-/-} mice compared to TCA-supplemented wild-type mice, suggesting that the difference in bile acid metabolism between *Angptl4*^{-/-} and wild-type mice is dependent on the gut bacteria. It remains to be investigated, however,

whether the microbial changes in the *Angptl4*^{-/-} mice are directly responsible for the difference in bile acid absorption or whether the microbial changes modulate a possible direct effect of ANGPTL4 on bile acid absorption (**Figure 9**).

Ideally, we should have used the same diet in the study without antibiotics and in the study with antibiotics. However, in our experience, it is impossible to give chow-fed mice antibiotics, as it leads to intestinal blockage and weight loss, likely due to the high fiber content in chow. For this reason, we switched to the semi-purified AIN-93G diet in the second study, which does not cause health problems when combined with antibiotics.

The difference in gut microbial composition between *Angptl4*^{-/-} and wild-type mice, which is already noticeable in the absence of TCA supplementation (**Supplemental Figure 3, Supplemental Table 3**), is quite remarkable. The origin of these differences is presently unclear, which is partly due to the partially unresolved function(s) of intestinal ANGPTL4. In human intestine, immunofluorescent staining showed that ANGPTL4 is particularly abundant in entero-endocrine cells (31). However, it is evident that *Angptl4* expression is not restricted to entero-endocrine cells, as several enterocyte cell lines produce and secrete ample amounts of ANGPTL4 (57). Expression of ANGPTL4 in a number of intestinal cell lines is highly sensitive to various stimuli such as BA, fatty acids, bacteria, and bacterial metabolites (31, 57–60). One of the key issues is whether ANGPTL4 produced by enterocytes is secreted into the blood stream and/or into the intestinal tract (31, 61).

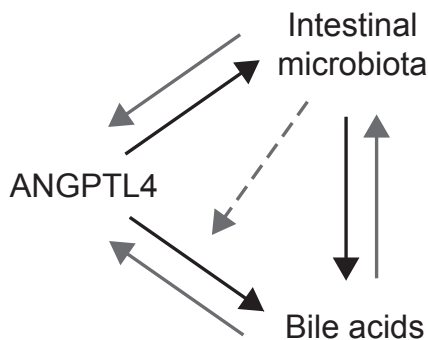


Figure 9. Hypothetical model of how ANGPTL4 may influence bile acid metabolism

An intricate relationship exists between ANGPTL4, the intestinal microbiota, and bile acid metabolism. ANGPTL4 influences the gut microbiota and vice versa. The gut microbiota influence intestinal bile acids and vice versa. Previous studies have shown that bile acids may influence ANGPTL4 secretion. Data presented in this manuscript suggest that ANGPTL4 may influence bile acid metabolism. It can be hypothesized that the changes in gut microbial composition caused by loss of ANGPTL4 directly impact bile acid metabolism, implying that ANGPTL4 influences bile acid metabolism via the gut microbiota. Alternatively, it is possible that (loss of) ANGPTL4 directly influences bile acid metabolism via a mechanism that is dependent on the gut microbiota.

Bäckhed *et al.* showed that conventionalization of germ-free mice suppressed intestinal *Angptl4* expression. In some though not all studies, conventionalization increased adiposity in wild-type but not *Angptl4*^{-/-} mice *via* the purported loss of endocrine inhibition on adipose tissue LPL activity (62–65). In contrast, in line with observations that suggest a local instead of endocrine function of ANGPTL4, we found that intestinal ANGPTL4 has the capacity to inhibit pancreatic lipase, a family member of LPL and the main enzyme responsible for the hydrolysis of dietary triglycerides in the gastro-intestinal tract (8, 9, 61). Multiple studies indicate that elevated levels of lipids in the ileum and colon can markedly influence the gut microbial composition, indicating that the differences in gut microbial composition between wild-type and *Angptl4*^{-/-} mice may be explained by differences in dietary fat metabolism (66, 67). It can be speculated that the origin of the differences in gut microbial composition between wild-type and *Angptl4*^{-/-} mice may lie during suckling, when pups receive a high amount of lipid-containing milk. Differences in gut microbial composition may also be related to differences in intestinal immunity, as it was recently shown that *Angptl4*^{-/-} mice have increased leukocyte infiltration and inflammation in the colon upon DSS treatment, concurrent with differences in gut microbial composition (68). Future studies using intestine-specific *Angptl4*^{-/-} mice should investigate whether intestinal-derived ANGPTL4 is responsible for the changes in gut microbiota composition and clarify how ANGPTL4 influences the gut microbiota composition.

In conclusion, we demonstrate that loss of ANGPTL4 significantly reduces plasma, hepatic, and ileal BA levels and increases BA excretion in mice supplemented with TCA. Suppression of the gut bacteria by antibiotics largely abolished the decrease in bile acid absorption in *Angptl4*^{-/-} mice, suggesting that ANGPTL4 promotes bile acid absorption via a mechanism dependent on the gut microbiota. Our studies thus reveal a novel interaction between ANGPTL4 and BA metabolism that is dependent on the gut microbiota. Finally, we show that ANGPTL4 is not required for the plasma triglyceride lowering action of BA.

Acknowledgements

We thank Shohreh Keshtkar for help with DNA isolation from colonic content and Martijn Koehorst for the bile acid measurements. This research was supported by grant 12CVD04 from the Fondation Leducq and the IN-CONTROL grant CVON2012-03 from the Netherlands Cardiovascular Research Committee.

References

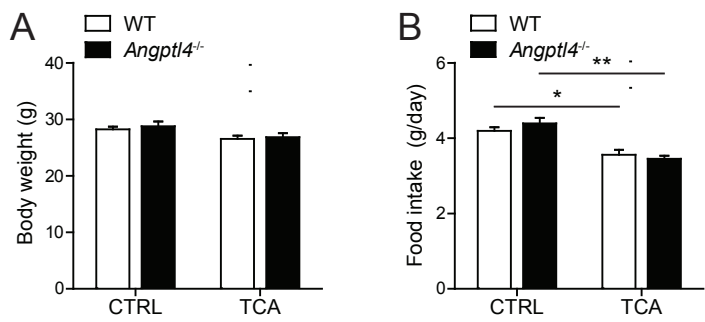
- Whitcomb, D. C., and M. E. Lowe. 2007. Human pancreatic digestive enzymes. *Dig. Dis. Sci.* **52**: 1–17.
- Iqbal, J., and M. M. Hussain. 2009. Intestinal lipid absorption. *AJP Endocrinol. Metab.* **296**: E1183–E1194.
- Demignot, S., F. Beilstein, and E. Morel. 2014. Triglyceride-rich lipoproteins and cytosolic lipid droplets in enterocytes: Key players in intestinal physiology and metabolic disorders. *Biochimie.* **96**: 48–55.
- Kersten, S. 2014. Physiological regulation of lipoprotein lipase. *Biochim. Biophys. Acta.* **1841**: 919–933.
- Goldberg, I. J., R. H. Eckel, and N. a Abumrad. 2009. Regulation of fatty acid uptake into tissues: lipoprotein lipase- and CD36-mediated pathways. *J. Lipid Res.* **50 Suppl**: S86–90.
- Kroupa, O., E. Vorrjö, R. Stienstra, F. Mattijssen, S. K. Nilsson, V. Sukonina, S. Kersten, G. Olivecrona, and T. Olivecrona. 2012. Linking nutritional regulation of Angptl4, Gpihbp1, and Lmf1 to lipoprotein lipase activity in rodent adipose tissue. *BMC Physiol.* **12**: 13.
- Sukonina, V., A. Lookene, T. Olivecrona, and G. Olivecrona. 2006. Angiopietin-like protein 4 converts lipoprotein lipase to inactive monomers and modulates lipase activity in adipose tissue. *Proc. Natl. Acad. Sci. U. S. A.* **103**: 17450–5.
- Dijk, W., and S. Kersten. 2014. Regulation of lipoprotein lipase by Angptl4. *Trends Endocrinol. Metab.* **25**: 146–55.
- Dijk, W., A. P. Beigneux, M. Larsson, A. Bensadoun, S. G. Young, and S. Kersten. 2016. Angiopietin-like 4 (ANGPTL4) promotes intracellular degradation of lipoprotein lipase in adipocytes. *J. Lipid Res.* **58**: 7250–7.
- Lichtenstein, L., J. F. P. Berbée, S. J. van Dijk, K. W. van Dijk, A. Bensadoun, I. P. Kema, P. J. Voshol, M. Müller, P. C. N. Rensen, and S. Kersten. 2007. Angptl4 upregulates cholesterol synthesis in liver via inhibition of LPL- and HL-dependent hepatic cholesterol uptake. *Arterioscler. Thromb. Vasc. Biol.* **27**: 2420–7.
- Köster, A., Y. B. Chao, M. Mosior, A. Ford, P. a Gonzalez-DeWhitt, J. E. Hale, D. Li, Y. Qiu, C. C. Fraser, D. D. Yang, J. G. Heuer, S. R. Jaskunas, and P. Eacho. 2005. Transgenic angiopietin-like (angptl)4 overexpression and targeted disruption of angptl4 and angptl3: regulation of triglyceride metabolism. *Endocrinology.* **146**: 4943–50.
- Mandard, S., F. Zandbergen, E. van Straten, W. Wahli, F. Kuipers, M. Müller, and S. Kersten. 2006. The fasting-induced adipose factor/angiopoietin-like protein 4 is physically associated with lipoproteins and governs plasma lipid levels and adiposity. *J. Biol. Chem.* **281**: 934–44.
- Dijk, W., M. Heine, L. Vergnes, M. R. Boon, G. Schaart, M. K. Hesselink, K. Reue, W. D. van Marken Lichtenbelt, G. Olivecrona, P. C. Rensen, J. Heeren, and S. Kersten. 2015. ANGPTL4 mediates shuttling of lipid fuel to brown adipose tissue during sustained cold exposure. *Elife.* **4**: e08428.
- Catoire, M., S. Alex, N. Paraskevopoulos, F. Mattijssen, I. Evers-van Gogh, G. Schaart, J. Jeppesen, A. Kneppers, M. Mensink, P. J. Voshol, G. Olivecrona, N. S. Tan, M. K. C. Hesselink, J. F. Berbée, P. C. N. Rensen, E. Kalkhoven, P. Schrauwen, and S. Kersten. 2014. Fatty acid-inducible ANGPTL4 governs lipid metabolic response to exercise. *Proc. Natl. Acad. Sci. U. S. A.* **111**: E1043–52.
- Wahlström, A., S. I. Sayin, H.-U. Marschall, and F. Bäckhed. 2016. Intestinal Crosstalk between Bile Acids and Microbiota and Its Impact on Host Metabolism. *Cell Metab.* 1–10.
- Kuipers, F., V. W. Bloks, and A. K. Groen. 2014. Beyond intestinal soap--bile acids in metabolic control. *Nat. Rev. Endocrinol.* **10**: 488–498.
- de Aguiar Vallim, T. Q., E. J. Tarling, and P. A. Edwards. 2013. Pleiotropic roles of bile acids in metabolism. *Cell Metab.* **17**: 657–669.
- Ridlon, J. M., D. J. Kang, P. B. Hylemon, and J. S. Bajaj. 2014. Bile acids and the gut microbiome. *Curr. Opin. Gastroenterol.*
- Vrieze, A., C. Out, S. Fuentes, L. Jonker, I. Reuling, R. S. Kootte, E. Van Nood, F. Holleman, M. Knaapen, J. A. Romijn, M. R. Soeters, E. E. Blaak, G. M. Dallinga-Thie, D. Reijnders, M. T. Ackermans, M. J. Serlie, F. K. Knop, J. J. Holst, C. Van Der Ley, I. P. Kema, E. G. Zoetendal, W. M. De Vos, J. B. L. Hoekstra, E. S. Strees, A. K. Groen, and M. Nieuwdorp. 2014. Impact of oral vancomycin on gut microbiota, bile acid metabolism, and insulin sensitivity. *J. Hepatol.* **60**: 824–831.
- Fiorucci, S., and E. Distrutti. 2015. Bile Acid-Activated Receptors, Intestinal Microbiota, and the Treatment of Metabolic Disorders. *Trends Mol. Med.* **21**: 702–714.
- Janssen, A. W. F., and S. Kersten. 2017. Potential mediators linking gut bacteria to metabolic health: a critical view. *J. Physiol.* **595**: 477–487.
- Elzinga, B. M., R. Havinga, J. F. W. Baller, H. Wolters, V. Bloks, A. R. Mensenkamp, F. Kuipers, and H. J. Verkade. 2002. The role of transhepatic bile salt flux in the control of hepatic secretion of triacylglycerol-rich lipoproteins in vivo in rodents. *Biochim. Biophys. Acta.* **1573**: 9–20.
- Carulli, N., M. Ponz de Leon, M. Podda, M. Zuin, A. Strata, G. Frigerio, and A. Digrisolo. 1981. Chenodeoxycholic acid and ursodeoxycholic acid effects in endogenous hypertriglyceridemias. A

- controlled double-blind trial. *J. Clin. Pharmacol.* **21**: 436–42.
24. Bateson, M. C., D. Maclean, J. R. Evans, and I. A. Bouchier. 1978. Chenodeoxycholic acid therapy for hypertriglyceridaemia in men. *Br. J. Clin. Pharmacol.* **5**: 249–54.
 25. Watanabe, M., S. M. Houten, L. Wang, A. Moschetta, D. J. Mangelsdorf, R. A. Heyman, D. D. Moore, and J. Auwerx. 2004. Bile acids lower triglyceride levels via a pathway involving FXR, SHP, and SREBP-1c. *J. Clin. Invest.* **113**: 1408–1418.
 26. Staels, B., and F. Kuipers. 2007. Bile acid sequestrants and the treatment of type 2 diabetes mellitus. *Drugs*. **67**: 1383–1392.
 27. Lin, Y., R. Havinga, H. J. Verkade, H. Moshage, M. J. H. Slooff, R. J. Vonk, and F. Kuipers. 1996. Bile acids suppress the secretion of very-low-density lipoprotein by human hepatocytes in primary culture. *Hepatology*. **23**: 218–228.
 28. Lin, Y., R. Havinga, I. J. Schippers, H. J. Verkade, R. J. Vonk, and F. Kuipers. 1996. Characterization of the inhibitory effects of bile acids on very-low-density lipoprotein secretion by rat hepatocytes in primary culture. *Biochem. J.* **316**: 531–538.
 29. Li, P., X. Ruan, L. Yang, K. Kiesewetter, Y. Zhao, H. Luo, Y. Chen, M. Gucek, J. Zhu, and H. Cao. 2015. A liver-enriched long non-coding RNA, lncLSTR, regulates systemic lipid metabolism in mice. *Cell Metab.* **21**: 455–67.
 30. Claudel, T., Y. Inoue, O. Barbier, D. Duran-Sandoval, V. Kosykh, J. Fruchart, J.-C. Fruchart, F. J. Gonzalez, and B. Staels. 2003. Farnesoid X receptor agonists suppress hepatic apolipoprotein CIII expression. *Gastroenterology*. **125**: 544–555.
 31. Alex, S., L. Lichtenstein, W. Dijk, R. P. Mensink, N. S. Tan, and S. Kersten. 2014. ANGPTL4 is produced by entero-endocrine cells in the human intestinal tract. *Histochem. Cell Biol.* **141**: 383–391.
 32. Lichtenstein, L., F. Mattijssen, N. J. de Wit, A. Georgiadi, G. J. Hooiveld, R. van der Meer, Y. He, L. Qi, A. Köster, J. T. Tamsma, N. S. Tan, M. Müller, and S. Kersten. 2010. Angptl4 protects against severe proinflammatory effects of saturated fat by inhibiting fatty acid uptake into mesenteric lymph node macrophages. *Cell Metab.* **12**: 580–92.
 33. Nagy, R. A., A. P. A. van Montfoort, A. Dijkers, J. van Echten-Arends, I. Homminga, J. A. Land, A. Hoek, and U. J. F. Tietge. 2015. Presence of bile acids in human follicular fluid and their relation with embryo development in modified natural cycle IVF. *Hum. Reprod.* **30**: 1102–1109.
 34. Govers, M. J., and R. Van der Meet. 1993. Effects of dietary calcium and phosphate on the intestinal interactions between calcium, phosphate, fatty acids, and bile acids. *Gut*. **34**: 365–370.
 35. Grefhorst, A., M. H. Oosterveer, G. Brufau, M. Boesjes, F. Kuipers, and A. K. Groen. 2012. Pharmacological LXR activation reduces presence of SR-B1 in liver membranes contributing to LXR-mediated induction of HDL-cholesterol. *Atherosclerosis*. **222**: 382–9.
 36. van Meer, H., G. Boehm, F. Stellaard, A. Vriesema, J. Knol, R. Havinga, P. J. Sauer, and H. J. Verkade. 2008. Prebiotic oligosaccharides and the enterohepatic circulation of bile salts in rats. *Am. J. Physiol. Gastrointest. Liver Physiol.* **294**: G540–G547.
 37. Steegenga, W. T., M. Mischke, C. Lute, M. V. Boekschoten, M. G. Pruis, A. Lendvai, H. J. Verkade, J. Boekhorst, H. M. Timmerman, T. Plösch, and M. Müller. 2014. Sexually dimorphic characteristics of the small intestine and colon of prepubescent C57BL/6 mice. *Biol. Sex Differ.* **5**: 11.
 38. Caporaso, J. G., J. Kuczynski, J. Stombaugh, K. Bittinger, F. D. Bushman, E. K. Costello, N. Fierer, A. G. Peña, J. K. Goodrich, J. I. Gordon, G. A. Huttley, S. T. Kelley, D. Knights, J. E. Koenig, R. E. Ley, C. A. Lozupone, D. McDonald, B. D. Muegge, M. Pirrung, J. Reeder, J. R. Sevinsky, P. J. Turnbaugh, W. A. Walters, J. Widmann, T. Yatsunenko, J. Zaneveld, and R. Knight. 2010. QIIME allows analysis of high-throughput community sequencing data. *Nat. Methods*. **7**: 335–6.
 39. Braak, C., and P. Šmilauer. 2012. CANOCO Reference Manual and User's Guide: Software for Ordination (version 5.0). *Ithaca: Biometris*.
 40. Suzuki, M. T., L. T. Taylor, and E. F. DeLong. 2000. Quantitative analysis of small-subunit rRNA genes in mixed microbial populations via 5'-nuclease assays. *Appl. Environ. Microbiol.* **66**: 4605–4614.
 41. Weisburg, W. G., S. M. Barns, D. A. Pelletier, and D. J. Lane. 1991. 16S ribosomal DNA amplification for phylogenetic study. *J. Bacteriol.* **173**: 697–703.
 42. Ferrebee, C. B., and P. A. Dawson. 2015. Metabolic effects of intestinal absorption and enterohepatic cycling of bile acids. *Acta Pharm. Sin. B*. **5**: 129–34.
 43. Matsubara, T., F. Li, and F. J. Gonzalez. 2013. FXR signaling in the enterohepatic system. *Mol. Cell. Endocrinol.* **368**: 17–29.
 44. Chen, F., L. Ma, P. A. Dawson, C. J. Sinal, E. Sehayek, F. J. Gonzalez, J. Breslow, M. Ananthanarayanan, and B. L. Shneider. 2003. Liver receptor homologue-1 mediates species- and cell line-specific bile acid-dependent negative feedback regulation of the apical sodium-dependent bile acid transporter. *J. Biol. Chem.* **278**: 19909–16.
 45. Parks, D. J., S. G. Blanchard, R. K. Bledsoe, G. Chandra, T. G. Consler, S. A. Kliewer, J. B. Stimmel, T. M. Willson, a M. Zavacki, D. D. Moore, and J. M. Lehmann. 1999. Bile acids: natural ligands for an orphan

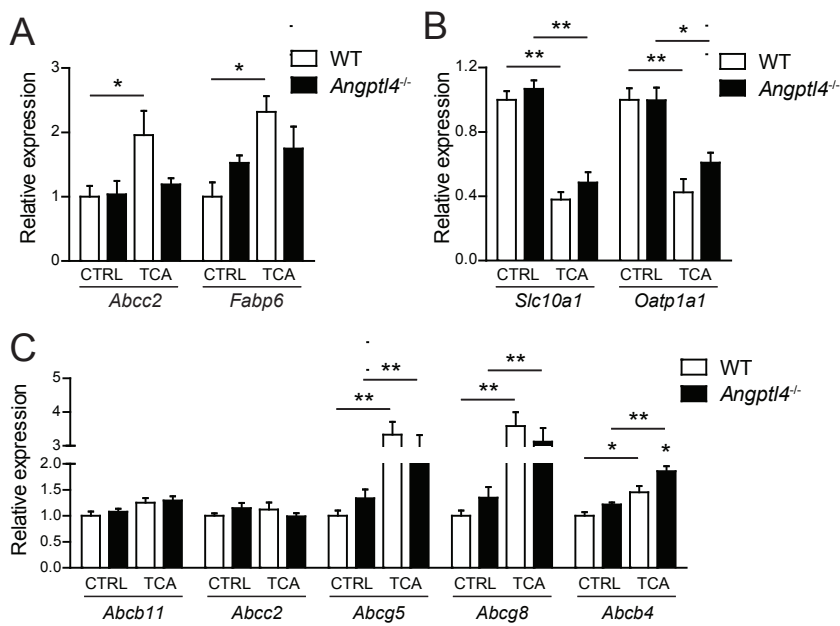
- nuclear receptor. *Science*. **284**: 1365–8.
46. Song, P., C. E. Rockwell, J. Y. Cui, and C. D. Klaassen. 2015. Individual bile acids have differential effects on bile acid signaling in mice. *Toxicol. Appl. Pharmacol.* **283**: 57–64.
 47. Sayin, S. I., A. Wahlström, J. Felin, S. Jäntti, H.-U. Marschall, K. Bamberg, B. Angelin, T. Hyötyläinen, M. Orešič, and F. Bäckhed. 2013. Gut microbiota regulates bile acid metabolism by reducing the levels of tauro-beta-muricholic acid, a naturally occurring FXR antagonist. *Cell Metab.* **17**: 225–235.
 48. Degirolamo, C., S. Rainaldi, F. Bovenga, S. Murzilli, and A. Moschetta. 2014. Microbiota Modification with Probiotics Induces Hepatic Bile Acid Synthesis via Downregulation of the Fxr-Fgf15 Axis in Mice. *Cell Rep.* **7**: 12–8.
 49. Yoshimoto, S., T. M. Loo, K. Atarashi, H. Kanda, S. Sato, S. Oyadomari, Y. Iwakura, K. Oshima, H. Morita, M. Hattori, K. Honda, Y. Ishikawa, E. Hara, and N. Ohtani. 2013. Obesity-induced gut microbial metabolite promotes liver cancer through senescence secretome. *Nature*. **499**: 97–101.
 50. Zhang, X., T. Osaka, and S. Tsuneda. 2015. Bacterial metabolites directly modulate farnesoid X receptor activity. *Nutr. Metab. (Lond)*. **12**: 48.
 51. Beuling, E., I. M. Kerkhof, G. A. Nicksa, M. J. Giuffrida, J. Haywood, D. J. aan de Kerk, C. M. Piaseckij, W. T. Pu, T. L. Buchmiller, P. A. Dawson, and S. D. Krasinski. 2010. Conditional Gata4 deletion in mice induces bile acid absorption in the proximal small intestine. *Gut*. **59**: 888–95.
 52. Out, C., J. V. Patankar, M. Doktorova, M. Boesjes, T. Bos, S. de Boer, R. Havinga, H. Wolters, R. Boverhof, T. H. van Dijk, A. Smoczek, A. Bleich, V. Sachdev, D. Kratky, F. Kuipers, H. J. Verkade, and A. K. Groen. 2015. Gut microbiota inhibit Asbt-dependent intestinal bile acid reabsorption via Gata4. *J. Hepatol.* **63**: 697–704.
 53. Devkota, S., Y. Wang, M. W. Musch, V. Leone, H. Fehlner-Peach, A. Nadimpalli, D. A. Antonopoulos, B. Jabri, and E. B. Chang. 2012. Dietary-fat-induced taurocholic acid promotes pathobiont expansion and colitis in IL10-/- mice. *Nature*. **487**: 104–8.
 54. Rai, R., V. A. Saraswat, and R. K. Dhiman. 2015. Gut microbiota: its role in hepatic encephalopathy. *J. Clin. Exp. Hepatol.* **5**: S29–36.
 55. Wright, E. K., M. A. Kamm, S. M. Teo, M. Inouye, J. Wagner, and C. D. Kirkwood. 2015. Recent advances in characterizing the gastrointestinal microbiome in Crohn's disease: a systematic review. *Inflamm Bowel Dis.* **21**: 1219–1228.
 56. Kakiyama, G., W. M. Pandak, P. M. Gillevet, P. B. Hylemon, D. M. Heuman, K. Daita, H. Takei, A. Muto, H. Nittono, J. M. Ridlon, M. B. White, N. A. Noble, P. Monteith, M. Fuchs, L. R. Thacker, M. Sikaroodi, and J. S. Bajaj. 2013. Modulation of the fecal bile acid profile by gut microbiota in cirrhosis. *J. Hepatol.* **58**: 949–55.
 57. Alex, S., K. Lange, T. Amolo, J. S. Grinstead, A. K. Haakonsson, E. Szalowska, A. Koppen, K. Mudde, D. Haenen, S. Al-Lahham, H. Roelofsen, R. Houtman, B. van der Burg, S. Mandrup, A. M. J. J. Bonvin, E. Kalkhoven, M. Müller, G. J. Hooiveld, and S. Kersten. 2013. Short-chain fatty acids stimulate angiopoietin-like 4 synthesis in human colon adenocarcinoma cells by activating peroxisome proliferator-activated receptor γ . *Mol. Cell. Biol.* **33**: 1303–16.
 58. Mattijssen, F., A. Georgiadi, T. Andasarie, E. Szalowska, A. Zota, A. Krones-Herzig, C. Heier, D. Ratman, K. De Bosscher, L. Qi, R. Zechner, S. Herzig, and S. Kersten. 2014. Hypoxia-inducible Lipid Droplet-associated (HILPDA) is a novel Peroxisome Proliferator-activated Receptor (PPAR) target involved in hepatic triglyceride secretion. *J. Biol. Chem.* **289**: 19279–19293.
 59. Korecka, A., T. de Wouters, A. Cultrone, N. Lapaque, S. Pettersson, J. Doré, H. M. Blottière, and V. Arulampalam. 2013. ANGPTL4 expression induced by butyrate and rosiglitazone in human intestinal epithelial cells utilizes independent pathways. *Am. J. Physiol. Gastrointest. Liver Physiol.* **304**: G1025–37.
 60. Aronsson, L., Y. Huang, P. Parini, M. Korach-André, J. Håkansson, J. Å. Gustafsson, S. Pettersson, V. Arulampalam, and J. Rafter. 2010. Decreased fat storage by *Lactobacillus paracasei* is associated with increased levels of angiopoietin-like 4 protein (ANGPTL4). *PLoS One*. **5**: e13087.
 61. Mattijssen, F., S. Alex, H. J. Swarts, A. K. Groen, E. M. van Schothorst, and S. Kersten. 2014. Angptl4 serves as an endogenous inhibitor of intestinal lipid digestion. *Mol. Metab.* **3**: 135–144.
 62. Fleissner, C. K., N. Huebel, M. M. Abd El-Bary, G. Loh, S. Klaus, and M. Blaut. 2010. Absence of intestinal microbiota does not protect mice from diet-induced obesity. *Br. J. Nutr.* **104**: 919–29.
 63. Bäckhed, F., H. Ding, T. Wang, L. V. Hooper, G. Y. Koh, A. Nagy, C. F. Semenkovich, and J. I. Gordon. 2004. The gut microbiota as an environmental factor that regulates fat storage. *Proc. Natl. Acad. Sci. U. S. A.* **101**: 15718–15723.
 64. Bäckhed, F., J. K. Manchester, C. F. Semenkovich, and J. I. Gordon. 2007. Mechanisms underlying the resistance to diet-induced obesity in germ-free mice. *Proc. Natl. Acad. Sci. U. S. A.* **104**: 979–84.
 65. El Aidy, S., C. a Merrifield, M. Derrien, P. van Baaren, G. Hooiveld, F. Levenez, J. Doré, J. Dekker, E. Holmes, S. P. Claus, D.-J. Reijngoud, and M. Kleerebezem. 2013. The gut microbiota elicits a profound metabolic reorientation in the mouse jejunal mucosa during conventionalisation. *Gut*. **62**: 1306–14.
 66. Robinson, D. T., and M. S. Caplan. 2015. Linking fat intake, the intestinal microbiome, and necrotizing

- enterocolitis in premature infants. *Pediatr. Res.* 77: 121–6.
67. Huang, E. Y., V. A. Leone, S. Devkota, Y. Wang, M. J. Brady, and E. B. Chang. 2013. Composition of dietary fat source shapes gut microbiota architecture and alters host inflammatory mediators in mouse adipose tissue. *JPEN. J. Parenter. Enteral Nutr.* 37: 746–54.
68. Phua, T., M. K. Sng, E. H. P. Tan, D. S. L. Chee, Y. Li, J. W. K. Wee, Z. Teo, J. S. K. Chan, M. M. K. Lim, C. K. Tan, P. Zhu, V. Arulampalam, and N. S. Tan. 2017. Angiopoietin-like 4 Mediates Colonic Inflammation by Regulating Chemokine Transcript Stability via Tristetraprolin. *Sci. Rep.* 7: 44351.

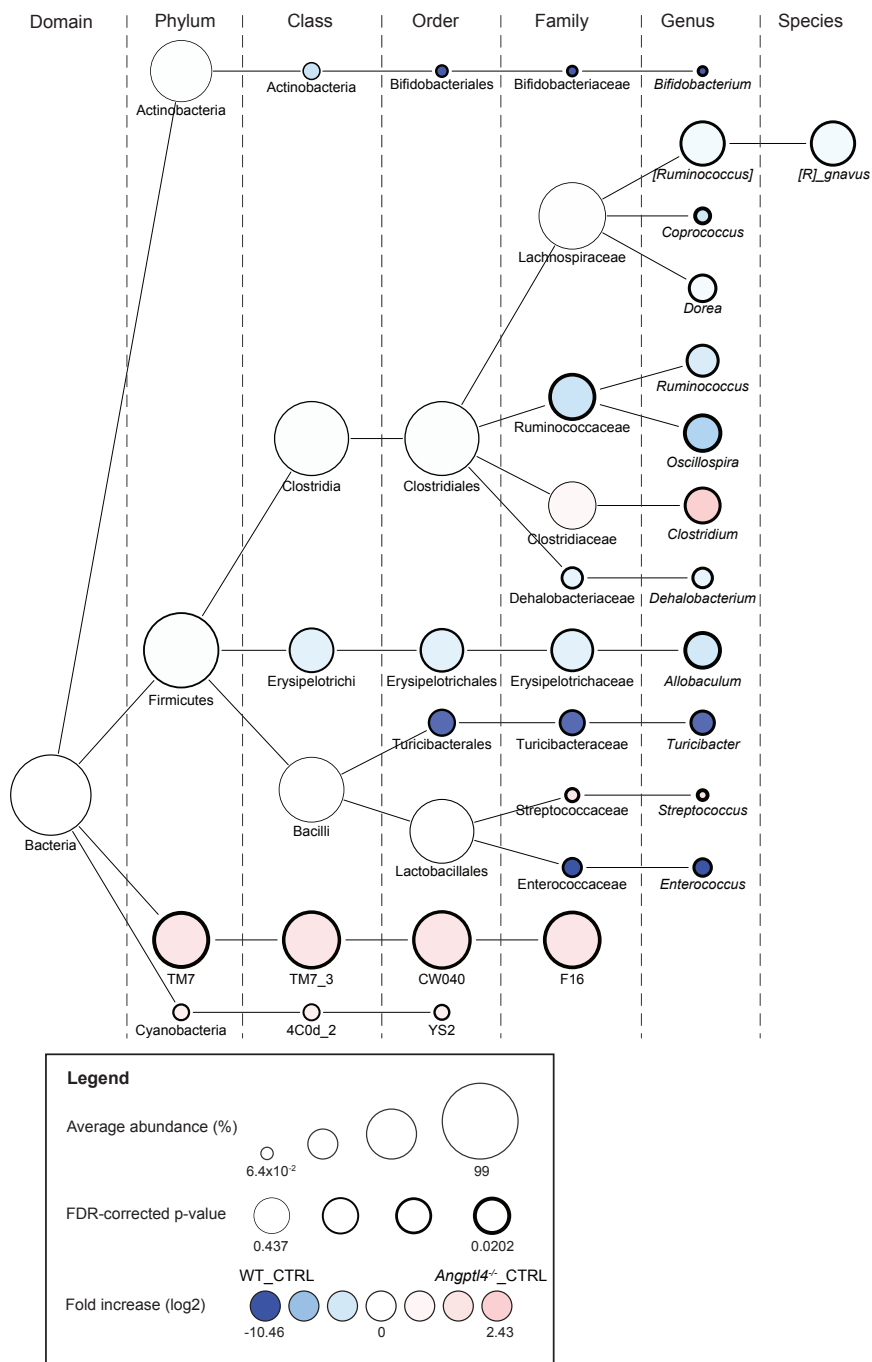
Supplemental figures and tables



Supplemental figure 1. Bodyweight and food intake in wild-type and *Angptl4*^{-/-} mice fed chow or chow supplemented with TCA. (A) Final body weight of wild-type and *Angptl4*^{-/-} mice fed chow (CTRL) or chow supplemented with TCA for 7 days. (B) Mean food intake per day during dietary intervention. Data are presented as mean ± SEM. Asterisks indicate significant differences between groups as indicated by bars according to two-way ANOVA followed by a Bonferroni post-hoc test. **p*<0.05, ***p*<0.001



Supplemental figure 2. Ileal and hepatic gene expression in wild-type and *Angptl4*^{-/-} mice fed chow or chow supplemented with TCA. (A) Relative gene expression of ileal *Abcc2* and *Fabp6* in wild-type and *Angptl4*^{-/-} mice fed chow (CTRL) or chow supplemented with TCA for 7 days. Relative hepatic expression portal BA transporters (B) and genes involved in canalicular bile acid, cholesterol, and phosphatidylcholine export (C). Gene expression levels in wild-type mice fed CTRL diet were set at 1. Data are presented as mean ± SEM. Asterisks indicate significant differences compared with wild-type mice or between groups as indicated by bars according to two-way ANOVA followed by a Bonferroni post-hoc test. **p*<0.05, ***p*<0.001



Supplemental figure 3. Differences in microbial composition between wild-type and *Angptl4*^{-/-} mice fed the control diet. Nodes represent taxa and the edges link the different taxonomic levels. The fold increase is calculated as the ²log of the ratio of the relative abundance in *Angptl4*^{-/-} and wild-type mice fed the control (CTRL) diet. Significance is expressed as the FDR-corrected p-value.

Supplemental table 1. Primer sequences used for qPCR

Name	Primer Sequence	
	Forward	Reverse
<u>General</u>		
<i>mAngptl4</i>	GTTTGCAGACTCAGCTCAAGG	CCAAGAGGTCTATCTGGCTCTG
<u>Liver</u>		
<i>mβ-Actin</i>	GATCTGGCACCACACCTTCT	GGGGTGTGAAGGTCTCAAA
<i>mAngptl3</i>	ACTGTGATACCCAATCAGGCA	CCTCCCAAAGCCCTTTTCGTA
<i>mAngptl8</i>	CACTGTACGGAGACTACAAGTGC	GTGGCTCTGCTTATCAGCTCG
<i>mCyp7a1</i>	CAGGGAGATGCTCTGTGTTCA	AGGCATACATCCCTTCCGTGA
<i>mCyp27a1</i>	CCAGGCACAGGAGAGTACG	GGGCAAGTGACACACATAG
<i>mCyp8b1</i>	CCTCTGGACAAGGGTTTGTG	GCACCGTGAAGACATCCCC
<i>mFgfr4</i>	CGTGGTCGCTACTGGTACAAA	CCTCTCCAACCCCGTACTC
<i>mShp</i>	CCTAGCCAAGACAGTAGCCTTC	CCAACCCAAGCAGGAAGAGAG
<i>mNtcp</i>	ATGACCACCTGCTCCAGCTT	GCCTTGTAGGGCACCTTGT
<i>mOatp1a1</i>	GTGCATACCTAGCCAAATCACT	CCAGGCCCATACCACACATC
<i>mBsep</i>	CTGCCAAGGATGCTAATGCA	CGATGGCTACCCCTTGTCTTCT
<i>mMrp2</i>	GTGTGGATTCCCTTGGGCTTT	CACAACGAACACCTGCTTGG
<i>mAbcg5</i>	TCAGGACCCCAAGGTCATGAT	AGGCTGGTGGATGGTGACAAT
<i>mAbcg8</i>	GACAGCTTCACAGCCCACAA	GCCTGAAGATGTCAGAGCGA
<i>mMdr2</i>	TATCCGCTATGGCCGTGGGAA	ATCGGTGAGCTATCACAATGG
<i>mApoC1</i>	TCCTGTCTGATTGTGGTCGT	CCAAAGTGTTCCCAAACCTCTT
<i>mApoC2</i>	AGCTGCCTGATATGGAAGGA	GCTGTCTGGGACCTGAATGT
<i>mApoC3</i>	TACAGGGCTACATGGAACAAGC	CAGGGATCTGAAGTGATTGTCC
<i>mApoA5</i>	TCCTCGCAGTGTTTCAAG	CGAAGCTGCCTTTCAGTTCT
<u>Intestine</u>		
<i>m36b4</i>	ATGGGTACAAGCGCGTCCTG	GCCTTGACCTTTTCAGTAAG
<i>mAsbt</i>	ATGGCGACATGGACCTCAGT	CCCGAGTCAACCCACATCTTG
<i>mIbabp</i>	CTTCCAGGAGACGTGATTGAAA	CCTCCGAAGTCTGGTGATAGTTG
<i>mMrp2</i>	GGATGGTGACTGTGGGCTGAT	GGCTGTTCTCCCTTCTCATGG
<i>mFgf15</i>	GCTCTGAAGACGATTGCCATC	TTCTCCCTGAAGGTACAGTC
<i>mFxr</i>	GACCTCCACAACCAAGTTTTGC	TGATTTCTGAGGCATTCTGTGT
<i>mOsta</i>	GTTCCAGGTGCTTGTATCC	CCACTGTTAGCCAAGATGGAGAA
<i>mOstβ</i>	GATGCGGCTCCTTGAATTA	GGAGGAACATGCTTGTATGAC

Supplemental table 2. Relative abundance of microbiota in colonic luminal of wild-type and *Angptl4*^{-/-} mice fed chow supplemented with TCA

Phylum	Class	Order	Family	Genus	Species	Wild-type (%)	<i>Angptl4</i> ^{-/-} (%)	FC	FDR-corrected P-value*
Actinobacteria						3.05	6.03	2.0	0.16
	Coriobacteriia					2.57	5.99	2.3	0.12
		Coriobacteriales				2.57	5.99	2.3	0.12
			Coriobacteriaceae			2.57	5.99	2.3	0.19
				<i>Adlercreutzia</i>		1.51	4.77	3.2	0.11
Firmicutes						70.13	72.28	1.0	ns
	Clostridia					48.04	59.24	1.2	0.12
		Clostridiales				48.04	59.24	1.2	0.12
			Lachnospiraceae			16.68	24.23	1.5	0.19
				<i>[Ruminococcus]</i>		6.32	8.28	1.3	0.11
				<i>[Ruminococcus] gnavus</i>		6.32	8.28	1.3	0.06
				<i>Dorea</i>		0.41	1.13	2.7	0.11
			Ruminococcaceae			13.53	11.36	-1.2	ns
				<i>Ruminococcus</i>		2.98	4.46	1.5	0.11
			Mogibacteriaceae			0.14	0.46	3.4	0.19
	Erysipelotrichi					7.89	3.46	-2.3	ns
		Erysipelotrichales				7.89	3.46	-2.3	ns
			Erysipelotrichaceae			7.89	3.46	-2.3	ns
				<i>Allobaculum</i>		7.30	1.69	-4.3	0.11
	Bacilli					14.19	9.57	-1.5	ns
		Lactobacillales				14.03	9.54	-1.5	ns
			Lactobacillaceae			13.96	9.37	-1.5	ns
				<i>Lactobacillus</i>		13.96	9.37	-1.5	ns
				<i>Lactobacillus reuteri</i>		0.12	0.00	-205.1	0.06
Bacteroidetes						8.13	3.57	-2.3	0.16
	Bacteroidia					8.13	3.57	-2.3	0.12
		Bacteroidales				8.13	3.57	-2.3	0.12
			[Paraprevotellaceae]			1.10	0.13	-8.2	0.19
				<i>[Prevotella]</i>		1.10	0.13	-8.2	0.11
			Prevotellaceae			0.26	0.07	-3.7	0.19
				<i>Prevotella</i>		0.25	0.07	-3.6	0.11
Proteobacteria						11.99	13.27	1.1	ns
	Gammaproteobacteria					0.03	3.65	119.4	0.12
		Enterobacteriales				0.02	3.63	158.7	0.12
			Enterobacteriaceae			0.02	3.63	158.7	0.19
	Deltaproteobacteria					8.65	7.16	-1.2	ns
		Desulfobivionales				8.65	7.15	-1.2	ns
			Desulfobivibrionaceae			8.65	7.15	-1.2	ns
				<i>Bilophila</i>		1.44	0.38	-3.8	0.11
Cyanobacteria						0.31	0.07	-4.8	0.10
	4C0d_2					0.31	0.05	-5.9	0.12
		YS2				0.31	0.05	-6.0	0.12

Threshold for presentation: an abundance of >0.1% in one of the two genotypes, a relative foldchange of >0.25 and a p-value <0.1 in the lowest identifiable taxon

* significance according to unpaired Wilcoxon rank-sum test followed by a Benjamini-Hochberg correction.

A FDR-corrected P-value <0.20 was considered statistically significant

Supplemental table 3. Relative abundance of microbiota in colonic luminal of wild-type and *Angptl4*^{-/-} mice fed chow

Phylum	Class	Order	Family	Genus	Species	Wild-type (%)	<i>Angptl4</i> ^{-/-} (%)	FC	FDR-corrected P-value*
Actinobacteria						9.80	8.95	-1.1	ns
	Actinobacteria					0.14	0.02	-7.6	ns
		Bifidobacteriales				0.13	0.00	-548.7	0.09
			Bifidobacteriaceae			0.13	0.00	-548.7	0.06
				<i>Bifidobacterium</i>		0.13	0.00	-548.7	0.05
Firmicutes						72.51	60.86	-1.2	0.15
	Clostridia					54.33	45.36	-1.2	ns
		Clostridiales				54.33	45.36	-1.2	ns
			Lachnospiraceae			17.29	18.13	1.0	ns
				[<i>Ruminococcus</i>]		3.87	2.29	-1.7	0.05
				[<i>Ruminococcus</i>] <i>gnavus</i>		3.87	2.29	-1.7	0.05
				<i>Coprococcus</i>		0.31	0.06	-5.7	0.02
				<i>Dorea</i>		0.58	0.37	-1.6	0.05
			Ruminococcaceae			8.30	1.22	-6.8	0.03
				<i>Ruminococcus</i>		1.28	0.31	-4.2	0.05
				<i>Oscillospira</i>		3.63	0.17	-21.1	0.02
			Clostridiaceae			1.73	2.44	1.4	ns
				<i>Clostridium</i>		0.39	2.08	5.4	0.05
			Dehalobacteriaceae			0.31	0.12	-2.7	0.06
				<i>Dehalobacterium</i>		0.31	0.12	-2.7	0.05
	Erysipelotrichi					3.28	1.06	-3.1	0.13
		Erysipelotrichales				3.28	1.06	-3.1	0.09
			Erysipelotrichaceae			3.28	1.06	-3.1	0.06
				<i>Allobaculum</i>		2.90	0.56	-5.2	0.02
	Bacilli					14.89	14.44	1.0	ns
		Turicibacterales				0.66	0.00	-252.5	0.09
			Turicibacteraceae			0.66	0.00	-252.5	0.06
				<i>Turicibacter</i>		0.66	0.00	-252.5	0.05
		Lactobacillales				14.23	14.44	1.0	ns
			Streptococcaceae			0.06	0.15	2.5	0.04
				<i>Streptococcus</i>		0.05	0.15	2.8	0.02
			Enterococcaceae			0.34	0.00	-1408.6	0.06
				<i>Enterococcus</i>		0.34	0.00	-1398.8	0.05
TM7						8.91	22.83	2.6	0.02
	TM7_3					8.91	22.83	2.6	0.03
		CW040				8.91	22.83	2.6	0.04
			F16			8.91	22.83	2.6	0.03
Cyanobacteria						0.07	0.13	1.8	0.10
	4C0d_2					0.07	0.12	1.8	0.13
		YS2				0.07	0.12	1.8	0.09

Threshold for presentation: an abundance of >0.1% in one of the two genotypes, a relative foldchange of >0.25 and a p-value <0.1 in the lowest identifiable taxon

* significance according to unpaired Wilcoxon rank-sum test followed by a Benjamini-Hochberg correction.

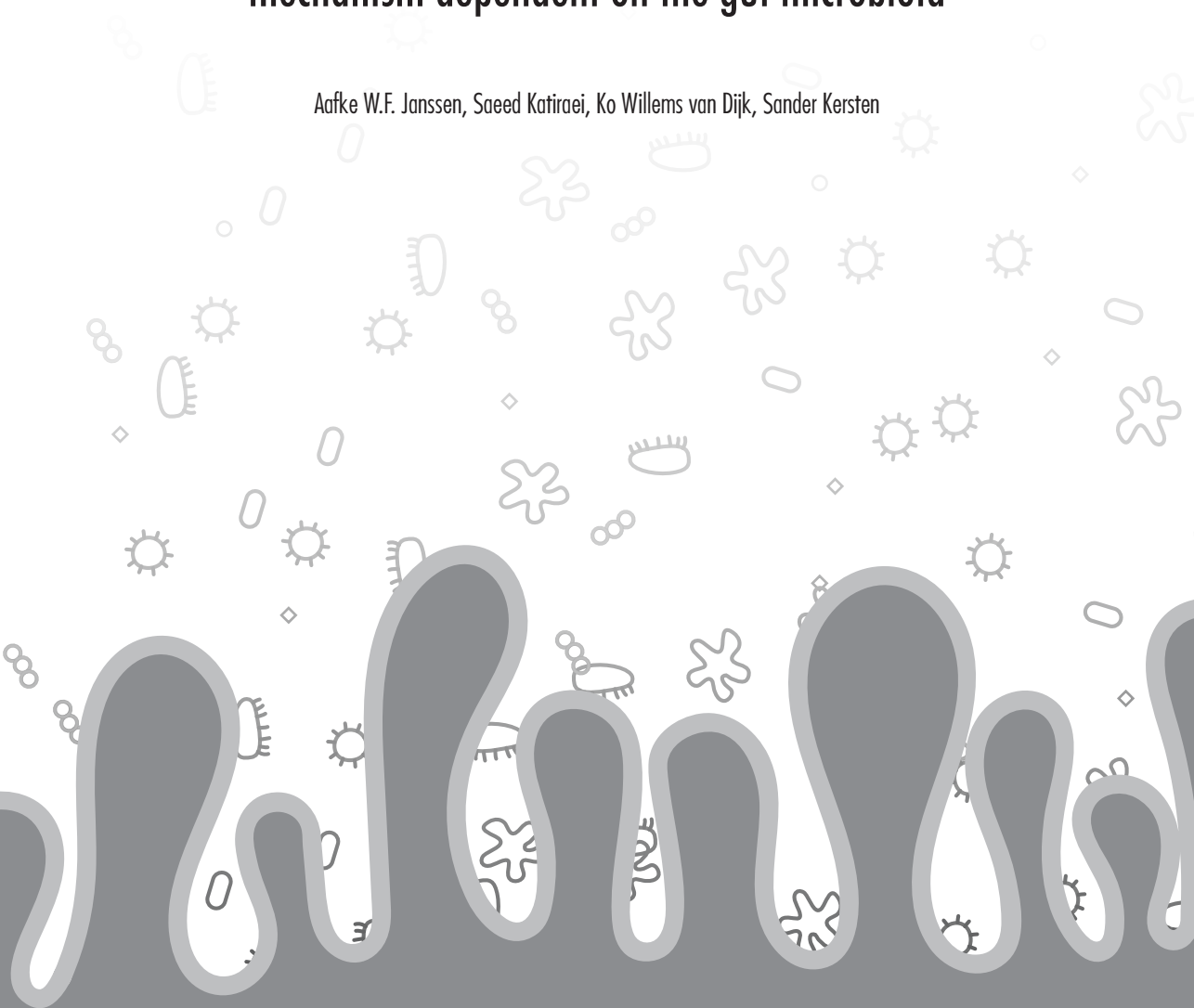
A FDR-corrected P-value <0.20 was considered statistically significant

9



Loss of ANGPTL4 in diet-induced obese mice uncouples visceral obesity from glucose intolerance partly via a mechanism dependent on the gut microbiota

Aafke W.F. Janssen, Saeed Katiraei, Ko Willems van Dijk, Sander Kersten



Submitted for publication

Abstract

ANGPTL4 is an important regulator of triglyceride metabolism by inhibiting the enzymes lipoprotein lipase and pancreatic lipase. Although ANGPTL4 has been implicated in obesity, study of the direct role of ANGPTL4 in diet-induced obesity and related metabolic dysfunction is hampered by the massive acute phase response and lethal chylous ascites and peritonitis in *Angptl4*^{-/-} mice fed the standard high fat diet. To overcome that obstacle and to investigate the influence of ANGPTL4 on diet-induced obesity and metabolic dysfunction, we fed wild-type and *Angptl4*^{-/-} mice a high fat diet rich in unsaturated fat, combined with fructose and cholesterol.

Mice lacking *Angptl4* displayed increased bodyweight gain, adipose tissue LPL activity, adipose tissue mass, and adipose tissue inflammation, but unexpectedly had markedly improved glucose tolerance. The improved glucose tolerance was accompanied by elevated insulin levels, whereas insulin sensitivity was not affected. Inasmuch as the gut microbiota have been suggested to influence insulin secretion and as ANGPTL4 has been proposed to link the gut microbiota to host metabolism, we hypothesized a potential role for the gut microbiota. Gut microbiota composition was significantly different between *Angptl4*^{-/-} mice and wild-type mice. Interestingly, suppression of the gut microbiota using antibiotics largely abolished the differences in glucose tolerance and insulin levels between wild-type and *Angptl4*^{-/-} mice.

In conclusion, despite increasing fat mass, loss of ANGPTL4 improves glucose tolerance, at least partly via a mechanism dependent on the gut microbiota.

Introduction

In the last few decades, obesity has become an immense global health problem. Obesity is often accompanied by a state of insulin resistance, which greatly increases the risk of cardiometabolic complications such as type 2 diabetes, non-alcoholic fatty liver disease, and coronary artery disease (1, 2). Part of the effect of insulin resistance on cardiometabolic risk is mediated by changes in plasma lipoproteins. The concentrations of plasma lipoproteins are regulated at the level of production and/or degradation via a complex interplay of enzymes, receptors and transporters active in a variety of tissues.

A particular class of lipoproteins are the triglyceride-rich lipoproteins consisting of chylomicrons produced in the intestine and very low density lipoproteins (VLDL) produced by the liver (3). Once in the blood, the triglyceride-rich lipoproteins are quickly captured by lipoprotein lipase (LPL) in the capillaries of fat and muscle tissue (4–6). Apart from binding the triglyceride-rich lipoproteins, LPL also catalyzes the hydrolysis of the triglyceride cargo into fatty acids. These fatty acids are subsequently taken up by the underlying fat and muscle cells and either stored or used as fuel (4, 7). To ensure that the rate of uptake of fatty acids matches the physiological conditions and local energy demands, the activity of LPL is subject to numerous regulatory mechanisms. An important group of physiological regulators of LPL activity are the Angiopoietin-like proteins, consisting of ANGPTL3, ANGPTL4, and ANGPTL8. These three secreted proteins share the ability to inhibit LPL, thereby raising plasma levels of triglyceride-rich lipoproteins. Whereas ANGPTL3 and ANGPTL8 are mainly produced in the liver, ANGPTL4 is synthesized by a variety of tissues including liver, intestine, skeletal muscle, heart, and adipose tissue (8). We and others have shown that ANGPTL4 post-translationally inhibits LPL activity under various physiological conditions, including fasting, exercise and cold exposure, thereby raising plasma triglyceride levels (9–13). Biochemical studies have shown that ANGPTL4 inhibits LPL by promoting the unfolding of LPL, resulting in the dissociation of the catalytically active LPL dimers into inactive LPL monomers. In adipocytes, these events likely serve as the trigger leading to the intracellular breakdown of LPL (14–16).

Besides inhibiting LPL, ANGPTL4 has also been shown to inhibit pancreatic lipase, the main enzyme responsible for the hydrolysis of dietary triglycerides in the gastro-intestinal tract and a structural homolog of LPL. Consequently, mice lacking ANGPTL4 have enhanced dietary lipid absorption as compared with wild-type mice, resulting in higher fat mass and bodyweight (17).

In addition to a role in lipid metabolism, a number of studies have also implicated ANGPTL4 in the regulation of glucose metabolism. Whereas plasma glucose levels do not appear to be changed in *Angptl4*^{-/-} mice, overexpression of *Angptl4* by adenovirus was shown

to lower circulating glucose levels and improve glucose tolerance, which was suggested to be mediated by decreased hepatic glucose production (18). By contrast, glucose tolerance was lower in whole-body *Angptl4*-transgenic mice after prolonged high-fat feeding (19). According to clamp studies, transgenic *Angptl4* overexpression leads to impaired glucose utilization and insulin resistance in the periphery, but higher insulin-mediated suppression of glucose production in the liver (15). Hence, published data do not present a uniform picture on the influence of ANGPTL4 on glucose metabolism and insulin sensitivity.

Considering the involvement of ANGPTL4 in fat uptake and storage and its potential role in glucose metabolism, it is of interest to investigate the role of ANGPTL4 in metabolic dysfunction and insulin sensitivity during obesity. Unfortunately, the study of ANGPTL4 in diet-induced obesity and associated metabolic dysfunction is hampered by the massive acute phase response and lethal chylous ascites and peritonitis in *Angptl4*^{-/-} mice fed a high fat diet. This severe inflammatory response is specifically provoked by a diet high in saturated fatty acids. By contrast, feeding *Angptl4*^{-/-} mice a diet rich in *cis*- or *trans*-unsaturated fatty acids does not trigger an inflammatory response (20). Accordingly, in the present paper we investigated the influence of ANGPTL4 on diet-induced obesity and metabolic dysfunction by feeding wild-type and *Angptl4*^{-/-} mice a high fat diet rich in unsaturated fatty acids, followed by detailed investigation of the metabolic phenotype.

Materials and methods

Animals and diet

Animal studies were performed using pure-bred wild-type and *Angptl4*^{-/-} mice on a C57Bl/6 background that were bred and maintained in the same facility for more than 20 generations (21). Mice were individually housed in temperature- and humidity-controlled specific pathogen-free conditions. Mice had *ad libitum* access to food and water.

In study 1, 10-week-old wild-type (n=12) and *Angptl4*^{-/-} mice (n=12) were fed a high fat/high cholesterol/high fructose diet, providing 45% energy as triglycerides (formula D12451 Research Diets, Inc., manufactured by Research Diet Services, Wijk bij Duurstede, Netherlands, sterilized with γ -irradiation at 9kGy) for 18 weeks. The fat source of this diet was replaced by safflower oil and supplemented with 1% cholesterol (Dishman, Veenendaal, Netherlands). Fructose was administered by adding 20% fructose (wt/vol) to the drinking water. In study 2, 21-week-old wild-type (n=18) and *Angptl4*^{-/-} mice (n=22) received the same diet (formula 58V8 manufactured by TestDiet, St. Louis, USA, sterilized with γ -irradiation at 18-50kGy) as in study 1 for 18 weeks. The fat source of this diet was also replaced by safflower oil. A mixture of broad-spectrum antibiotics was provided in the drinking water (1g/l Ampicillin, 1g/l Neomycin sulphate and 0.5g/l Metronidazole). Bodyweight and food intake were assessed weekly in both studies.

At the end of each study, mice were anesthetized using isoflurane and blood was collected by orbital puncture. Mice were sacrificed via cervical dislocation after which tissues were excised and weighed and intestinal content was sampled. Animal experiments were approved by the local animal ethics committee of Wageningen University.

Plasma measurements

Plasma was collected in EDTA-coated tubes and spun down for 15 minutes at 3000 rpm to obtain plasma. Plasma concentration of serum amyloid A was measured with a kit from Life technologies (Bleiswijk, Netherlands). Plasma triglyceride concentrations were determined according to the manufacturer's instructions using a commercially available kit (HUMAN Diagnostics, Wiesbaden, Germany). The commercially available Limulus Amebocyte Lysate assay (Lonza, Walkerville, USA) was used to quantify plasma endotoxin levels.

Intraperitoneal glucose tolerance test

A glucose tolerance test was performed one week before the mice were euthanized. Mice were placed in clean cages without food and fructose water was replaced by tap water with or without the antibiotic mixture at 8.00h. After 5 hours of fasting, mice were weighed and a blood sample was drawn. Mice were injected intraperitoneally with glucose (0.8 g/kg

bodyweight) and blood was drawn at specific time points for measurement of glucose using Accu-chek Compact (study 1) or Glucofix Tech (study 2).

In study 1, plasma concentrations of insulin were measured after 5 hours of fasting and in study 2 after 5 hours of fasting and 20 and 60 minutes after glucose injection. The insulin measurement was done according to manufacturer's instructions (Crystal Chem, Downers Grove, USA).

Insulin tolerance test

In study 2, an insulin tolerance test was performed 2 weeks before the mice were euthanized. Mice were fasted for 5 hours prior to the insulin tolerance test. During this period fructose water was replaced by tap water with or without the antibiotic mixture. Blood samples were collected from the tail vein immediately before ($t=0$ min) and at selected time points after insulin injection (0.75U/kg bodyweight). Glucose was measured using Glucofix Tech.

RNA isolation and qPCR

Total RNA was extracted using TRIzol reagent (Life technologies, Bleiswijk, Netherlands). RNA from mesenteric fat depots and pancreatic islets was purified using the RNeasy minikit (Qiagen, Venlo, The Netherlands). RNA was reverse transcribed to cDNA using the iScript cDNA synthesis kit (Bio-Rad Laboratories, Veenendaal, the Netherlands). Changes in gene expression were determined by real-time PCR on a CFX384 Real-Time PCR detection system (Bio-Rad) by using SensiMix (Bioline, GC biotech, Alphen aan den Rijn, the Netherlands). The data were analyzed using the Bio-Rad CFX Manager 3.0. The housekeeping genes *36b4* was used for normalization. Sequences of the used primers are listed in Supplemental Table 1.

Intestinal permeability assay

In study 2, an intestinal permeability assay was performed 3 weeks before the mice were euthanized. To correct for autofluorescence, blood was drawn from the tail vein prior to administration of fluorescein isothiocyanate (FITC)-dextran (4 kilodaltons) by oral gavage (600mg/kg bodyweight, 40mg/ml). After 1 hour blood was drawn, stored on ice in the dark and centrifuged for 15 minutes at 3000 rpm to obtain plasma. Plasma was diluted in PBS and fluorescent intensity was measured using a Fluorescence Spectrophotometer (Fluoroskan Ascent, Thermo Fisher Scientific, λ^{ex} 485nm and λ^{em} 538nm). FITC-dextran concentrations were determined from a standard curve generated by diluting FITC-dextran in PBS.

Cell culture

Mouse β -TC6 cell were grown in Dulbecco's modified Eagle's medium (DMEM)

supplemented with 15% heat-inactivated FCS and 1% penicillin/streptomycin (Lonza, Verviers, Belgium) under 5% CO₂ at 37°C. RNA isolation was performed from cells that were seeded in a 24-wells plate.

Mouse pancreatic islet isolation

Pancreatic islets were isolated from C57Bl/6 mice using Liberase TL Research Grade (Roche) as previously described (22). Briefly, Liberase TL was dissolved in low glucose DMEM (Gibco) and 2-3ml was injected into the bile duct. After incubation of the perfused pancreas at 37°C, the digestion was stopped by adding DMEM containing FCS. The islet suspension was subsequently filtered (420 µm mesh) and centrifuged using Histopaque 1077 (Sigma-Aldrich). Islets were collected from the interphase between Histopaque 1077 and DMEM, and washed twice with CMRL medium (Gibco) containing 15% heat-inactivated FCS, 11mM glucose, 0.15% NaHCO₃, 50 µM β-mercaptoethanol and 1% penicillin/streptomycin. Subsequently, pancreatic islets were collected for RNA isolation.

LPL activity measurements

LPL activity in mesenteric white adipose tissue was quantified using a ³H-oleic acid-labelled triolein substrate as previously described (23).

¹H NMR spectroscopy

Short-chain fatty acids levels in the content of the cecum were measured in an Avance III NMR spectrometer, as previously described (24).

Western blot

Mesenteric fat pads were lysed in ice-cold Pierce IP lysis buffer (ThermoScientific) containing protease and phosphatase inhibitors (Roche). Lysates were centrifuged 4 times for 10min at 13000g to remove fat droplets. 15µg of protein were loaded on a Criterion TGX gel, 8-16% and subsequently transferred onto a PVDF membrane using a Transblot Turbo system (Bio-Rad). After blocking in TBS, 0.1% Tween-20 and 5% nonfat dry milk, the membranes were incubated overnight with a goat anti-mouse LPL antibody (25) or a rabbit anti-goat HSP90 (Cell Signalling, #4874) antibody, both at 1:2000 dilutions. Finally, the blots were exposed to Enhanced Chemiluminescent substrate (Bio-Rad) for the visualization of the protein bands by using the ChemiDoc MP Imaging System (Bio-Rad).

DNA extraction

In study 1, fecal samples derived from the second part of the colon were suspended in 10 mM Tris, 1mM EDTA, 0.5% SDS and 0.2mg/ml Proteinase K (ThermoScientific, Rockford,

USA). After addition of 0.1-0.25mm and 4mm glass beads, buffered phenol (Invitrogen, Carlsbad, USA) was added and cells were lysed by mechanical disruption using a bead beater (MP biomedical, Santa Ana, USA) for 3 minutes. DNA was subsequently extracted using phenol:chloroform:isoamylalcohol [25:24:1] (Invitrogen, Carlsbad, USA), precipitated with isopropanol and washed with 70% ethanol.

In study 2, fecal samples (~15-60mg) derived from the second part of the colon were suspended in 500µL S.T.A.R. buffer (Roche). After addition of 0.1mm zirconia and 2.5mm glass beads (BioSpec, Bartlesville, USA), cells were lysed by mechanical disruption using a bead beater (MP biomedical, Santa Ana, USA) for 3x1 minute. DNA was subsequently extracted and purified using Maxwell 16 System (Promega). In brief, homogenates (250 µL) were transferred to a prefilled reagent cartridge (Maxwell® 16 Tissue LEV Total RNA Purification Kit, Custom-made, Promega). Sixteen samples were processed at the same time. After 30 minutes the purification process was completed and DNA was eluted in 50 µL of water (Nuclease free)(Promega).

16S rRNA gene sequencing

For 16S rRNA gene sequencing DNA samples were sent to the Broad Institute of MIT and Harvard (Cambridge, USA). Microbial 16S rRNA gene was amplified targeting the hyper-variable region V4 using forward primer 515F (5'-GTGCCAGCMGCCGCGGTAA-3') and the reverse primer 806R (5'- GGACTACHVGGGTWTCTAAT-3'). The cycling conditions consisted of an initial denaturation of 94°C for 3 min, followed by 25 cycles of denaturation at 94°C for 45 sec, annealing at 50 °C for 60 sec, extension at 72°C for 5 min, and a final extension at 72°C for 10 min. Sequencing was performed using the Illumina MiSeq platform generating paired-end reads of 175 bp in length in each direction. Overlapping paired-end reads were subsequently aligned. Detailed of this protocol are as previously described (26).

Raw sequence data quality was assessed using FastQC, version: 0.11.2 (<http://www.bioinformatics.babraham.ac.uk/projects/fastqc/>). Reads quality was checked with Sickel, version: 1.33 (<https://github.com/najoshi/sickle>) and low quality reads were removed. For visualising the taxonomic composition of the fecal microbiota and further beta diversity analysis, QIIME, version: 1.9.0 was used(27). In brief, closed reference OTU picking with 97% sequence similarity against GreenGenes 13.8 reference database was done. Jackknifed beta-diversity of unweighted UniFrac distances with 10 jackknife replicates was measured at rarefaction depth of 22000 reads/sample. For statistical significance, biological relevance and visualisation we used linear discriminant analysis (LDA) effect size (LEfSe) method (<https://bitbucket.org/biobakery/biobakery/wiki/lefse>) (28).

Bacterial 16S rRNA gene quantification

Standard curves were constructed by amplifying 16S rRNA gene using fecal DNA of the control group using the universal 16S primers 27F (5'-GTTTGATCCTGGCTCAG-3') and 1492R (5'-CGGCTACCTTGTTACGAC-3'). The cycling conditions consisted of an initial denaturation of 95°C for 5 min, followed by 35 cycles of denaturation at 95°C for 30 sec, annealing at 52°C for 40 sec and extension at 72°C for 90 sec and a final extension at 72°C for 7 min. Amplicon size was verified by agarose gel electrophoresis and amplicon was purified using a commercial available PCR purification kit (ThermoScientific). After the DNA concentration was quantitated and copy number was calculated, a serial dilution ranging from 10⁸ to 10¹ 16S rRNA gene copies/μl was generated.

Real-time PCR for the 16S rRNA gene was performed using fecal DNA samples from study 2 and standards on a CFX384 Real-Time PCR detection system (Bio-Rad Laboratories, Veenendaal, Netherlands) with SensiMix (Bioline, GC biotech, Alphen aan den Rijn, Netherlands). 16S rRNA gene was amplified using the forward primer 1369F (5'-CGGTGAATACGTTTCYCGG-3')(29) and the reverse primer 1492R (5'-GGWTACCTTGTTACGACTT-3')(30). The cycling conditions consisted of an initial denaturation of 95°C for 5 min, followed by 40 cycles of denaturation at 95°C for 15 sec, annealing at 60 °C for 30 sec and extension at 72°C for 30 sec. The data were analyzed using the Bio-Rad CFX Manager 3.0.

Statistics

Data are presented as mean ± SEM, unless otherwise indicated. Statistical analysis were performed using an unpaired Student's t-test or two-way analysis of variance followed by a Bonferroni test for post-hoc analysis. (GraphPad Software, Inc., La Jolla, USA). P<0.05 was considered as statistically significant.

Results

To elicit a phenotype that includes (visceral) obesity, insulin resistance and NAFLD/NASH, wild-type and *Angptl4*^{-/-} mice were fed a high fat diet rich in unsaturated fatty acids complemented with fructose and cholesterol (24, 31, 32). In contrast to feeding *Angptl4*^{-/-} mice a diet rich in saturated fatty acids, feeding a diet rich in unsaturated fatty acids did not significantly raise plasma serum amyloid A concentrations (**Figure 1A**). *Angptl4*^{-/-} mice gained more weight and had a higher visceral (mesenteric) fat mass compared to wild-type mice, despite having a similar level of food intake (**Figure 1B-C**). In accordance with the function of ANGPTL4 as LPL inhibitor, LPL activity and the amount of LPL was significantly higher in the mesenteric white adipose tissue of *Angptl4*^{-/-} mice as compared to wild-type mice (**Figure 1E, F**). In addition, plasma triglyceride levels were significantly lower in the *Angptl4*^{-/-} mice than in the wild-type mice (**Figure 1G**). Consistent with the increased bodyweight and elevated mesenteric fat pad weight, *Angptl4*^{-/-} mice displayed increased inflammation in mesenteric adipose tissue as compared to wildtype mice, as revealed by the higher expression of several inflammatory genes (**Figure 1H**).

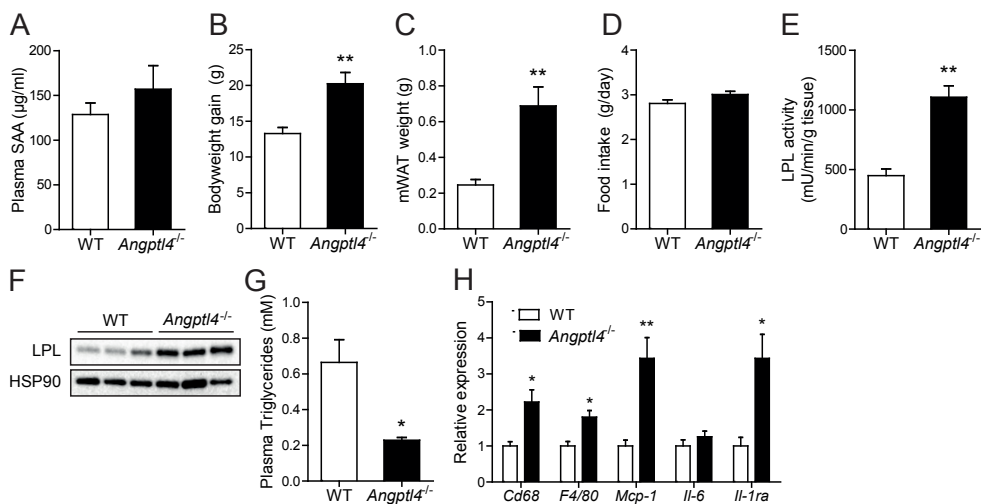


Figure 1. ANGPTL4 protects against diet-induced obesity and reduces adipose tissue inflammation

(A) Plasma serum amyloid A concentration. (B) Bodyweight gain of wild-type (WT) and *Angptl4*^{-/-} mice at the end of the dietary intervention. (C) Mesenteric white adipose tissue (mWAT) weight. (D) Average food intake per mouse per day during dietary intervention. (E) LPL activity and (F) LPL protein levels in mWAT homogenates. (G) Plasma triglyceride levels. (H) Relative expression of inflammatory genes in mWAT. Gene expression levels of WT mice were set at 1. Data are presented as mean ± SEM. Asterisks indicate significant differences according to a Student's t-test. **p*<0.05 ***p*<0.001.

Loss of ANGPTL4 leads to improved glucose tolerance

Strikingly, despite the higher visceral adipose tissue mass and inflammation, blood glucose levels during a glucose tolerance test were markedly lower in the *Angptl4*^{-/-} mice than in wild-type mice (**Figure 2A**). The lower glucose levels in the *Angptl4*^{-/-} mice were accompanied by elevated fasting plasma insulin levels (**Figure 2B**). These data suggest *Angptl4*^{-/-} mice are more glucose tolerant than wild-type mice, possibly due to higher plasma insulin levels.

When exploring the potential origin of the elevated plasma insulin levels in the *Angptl4*^{-/-} mice, we considered the possibility that ANGPTL4 may be expressed in pancreatic islets, together with LPL, and thereby influence insulin secretion. LPL has been proposed as a mediator of the effect of dietary lipids on insulin secretion (33). However, whereas the expression of *Lpl* was relatively high in primary pancreatic islets and in the β -cell line beta-TC6, with Ct values of ~21-22, *Angptl4* expression was very low, showing Ct values of ~30.5-32 (**Figure 2C**). Hence, the effect of ANGPTL4 on glucose tolerance is unlikely to be mediated via ANGPTL4 produced in β -cells. BIOGPS supports the minimal expression of *Angptl4* in the mouse pancreas (<http://biogps.org/>). Furthermore, analysis of a number of microarray datasets of mouse pancreatic islets (GSE43620), the β -cell line bTC3 (GSE31102), β -cells from adult mice (GSE54374), and human islets (Dr. Eelco de Koning, personal communication)

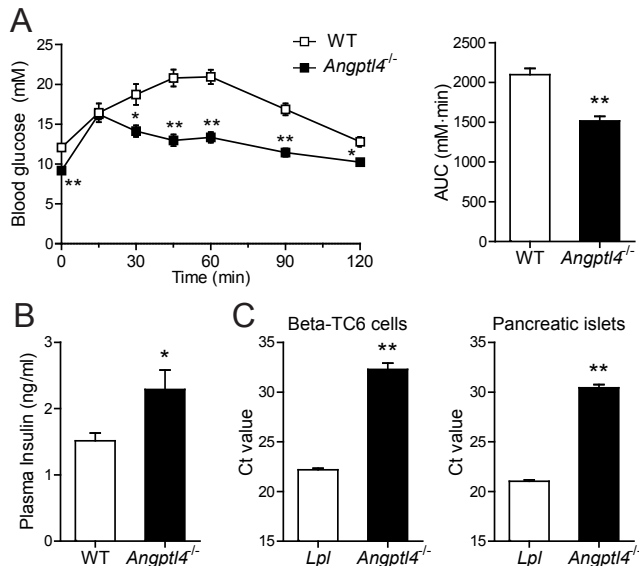


Figure 2. ANGPTL4 deteriorates glucose tolerance

(A) Intraperitoneal glucose tolerance and areas under the curve (AUC) of wild-type (WT) and *Angptl4*^{-/-} mice one week before sacrifice. (B) Fasting plasma insulin levels. (C) Ct values of *Lpl* and *Angptl4* in mouse Beta-TC6 cell and pancreatic islets isolated from C57Bl/6 mice. Data are presented as mean \pm SEM except for the data from Beta-TC6 cells and pancreatic islets. Asterisks indicate significant differences according to a Student's t-test. * $p < 0.05$ ** $p < 0.001$.

verified the minimal expression of ANGPTL4 in pancreatic islets and β -cells.

The above data do not exclude a role of circulating ANGPTL4 in the regulation of islet LPL. However, upregulation of LPL activity in β -cells has been shown to lead to hyperglycemia during a glucose tolerance test (34). Accordingly, it is unlikely that the observed hypoglycaemia and hyperinsulinemia in *Angptl4*^{-/-} mice are linked to loss of inhibition of LPL activity in islet cells, whether via ANGPTL4 produced in the pancreas or elsewhere. Together, these findings suggest that ANGPTL4 probably does not influence plasma insulin levels via a direct effect on insulin secretion in pancreatic islets.

Loss of ANGPTL4 alters levels of gut-derived metabolites and changes gut microbial composition

Considering that the gut microbiota have been suggested to influence insulin secretion (35–37), and since ANGPTL4 has been suggested to link changes in gut microbial composition to host metabolism (38, 39), we hypothesized a potential role of the gut microbiota. To explore the possibility that *Angptl4*^{-/-} mice may carry a different gut microbiota, we first measured the levels of several gut-derived metabolites, including luminal short-chain fatty acids and succinate and plasma LPS. In the cecum, the concentration of the short-chain fatty acid butyrate was significantly lower in the *Angptl4*^{-/-} mice as compared to the wild-type mice (**Figure 3A**). Moreover, in the colon, levels of both propionate and butyrate were significantly lower and levels of succinate were significantly higher in the *Angptl4*^{-/-} mice (**Figure 3A**). Also, plasma LPS levels were higher in the *Angptl4*^{-/-} mice than in the wild-type mice, even though intestinal permeability measured using FITC-dextran was similar (**Figure 3B–C**). Together, these alterations in gut-derived metabolites suggest a potential difference in gut microbiota composition between the *Angptl4*^{-/-} and wild-type mice.

To further examine the gut microbiota in the wild-type and *Angptl4*^{-/-} mice, we performed 16S rRNA sequencing. Principle coordinate analysis of unweighted UniFrac distance demonstrated a significant clustering of microbiome sequences of *Angptl4*^{-/-} and wild-type mice (**Figure 3D**). The majority of the difference in bacterial community between *Angptl4*^{-/-} and wild-type mice can be explained by the phyla Actinobacteria and Firmicutes. Indeed, only small non-significant differences were observed within the phyla Bacteroidetes, Deferribacteres and Proteobacteria. The phylum Actinobacteria was 2.5-fold more abundant in the *Angptl4*^{-/-} mice, which was mainly accounted for by a significant increase in the genus *Adlercreutzia*. Although the relative abundance of the phylum Firmicutes was comparable between the genotypes, the genera *Lactobacillus* and *SMB53* were overrepresented in the *Angptl4*^{-/-} mice, whereas the genus *Allobaculum* was more abundant in the wild-type mice (**Figure 3E–G**, **Supplemental Table 2**). Overall, these data indicate that the gut bacterial composition is significantly different between *Angptl4*^{-/-} and wild-type mice.

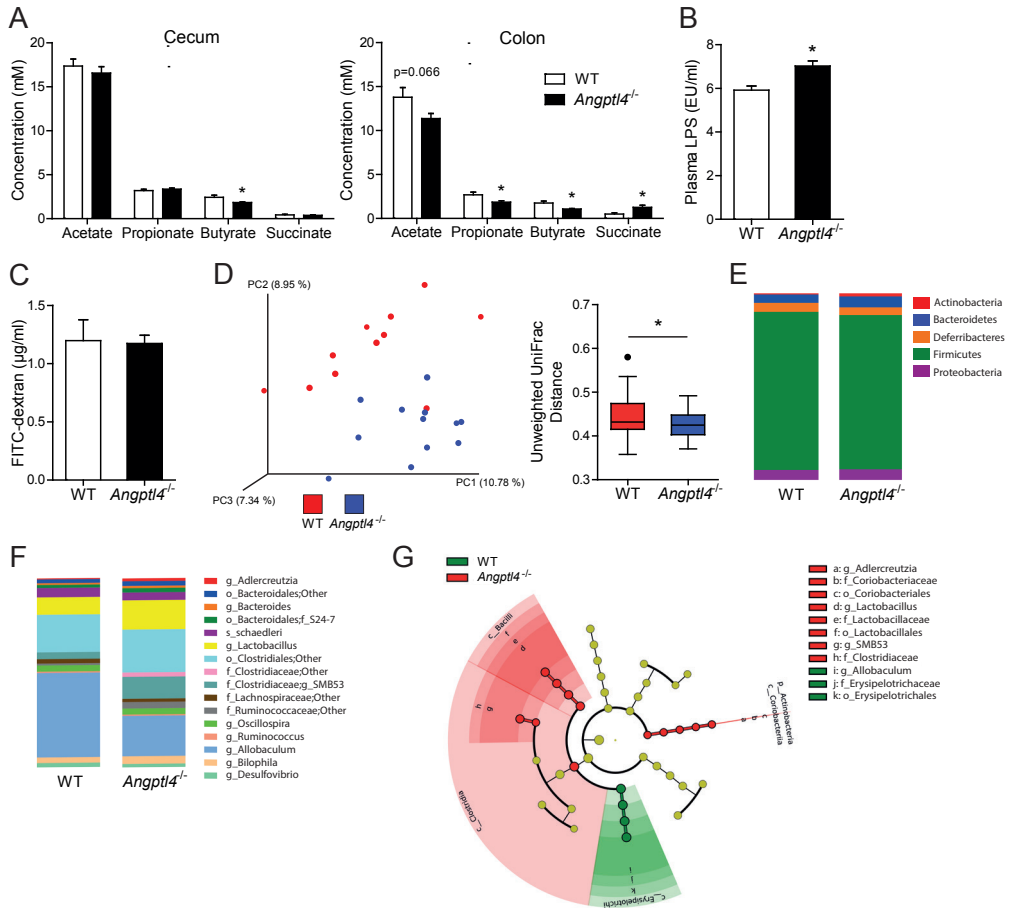


Figure 3. ANGPTL4 alters levels of gut-derived metabolites and changes gut microbial composition

(A) Concentration of acetate, propionate, butyrate and succinate in the cecum and colon of wild-type (WT) and *Angptl4*^{-/-} mice. (B) LPS levels in plasma of WT and *Angptl4*^{-/-} mice. (C) Intestinal permeability as assessed by plasma FITC-dextran concentration 1 hour after oral administration. (D) Principle coordinates analysis plot and boxplots of unweighted UniFrac distances of the intestinal microbiota. Mean relative abundance of the colonic bacteria (E) at phylum level and (F) to the lowest identifiable level. The letter preceding the underscore indicates the taxonomic level: o, order; f, family; g, genus; s, species. (G) Cladogram generated from LEfSe analysis displaying bacterial taxa significantly enriched in WT (green) or *Angptl4*^{-/-} (red) mice. The domain bacteria is depicted by the central point and each ring represents the next lower taxonomic level (phylum to genus). Data are presented as mean \pm SEM. Asterisks indicate significant differences according to a Student's t-test. * $p < 0.05$ ** $p < 0.001$.

Suppression of the gut bacteria abolishes the increase in glucose tolerance in *Angptl4*^{-/-} mice

To further study the role of the gut microbiota in mediating the effect of loss of ANGPTL4 on glucose tolerance, we repeated the diet-induced obesity study in wild-type and *Angptl4*^{-/-} mice with or without the addition of antibiotics in their drinking water. As shown previously (24), antibiotic supplementation significantly reduced the number of 16S rRNA gene copies in the feces (**Figure 4A**) and caused a marked increase in cecum weight (**Figure 4B**), indicating an effective suppression of the gut bacteria.

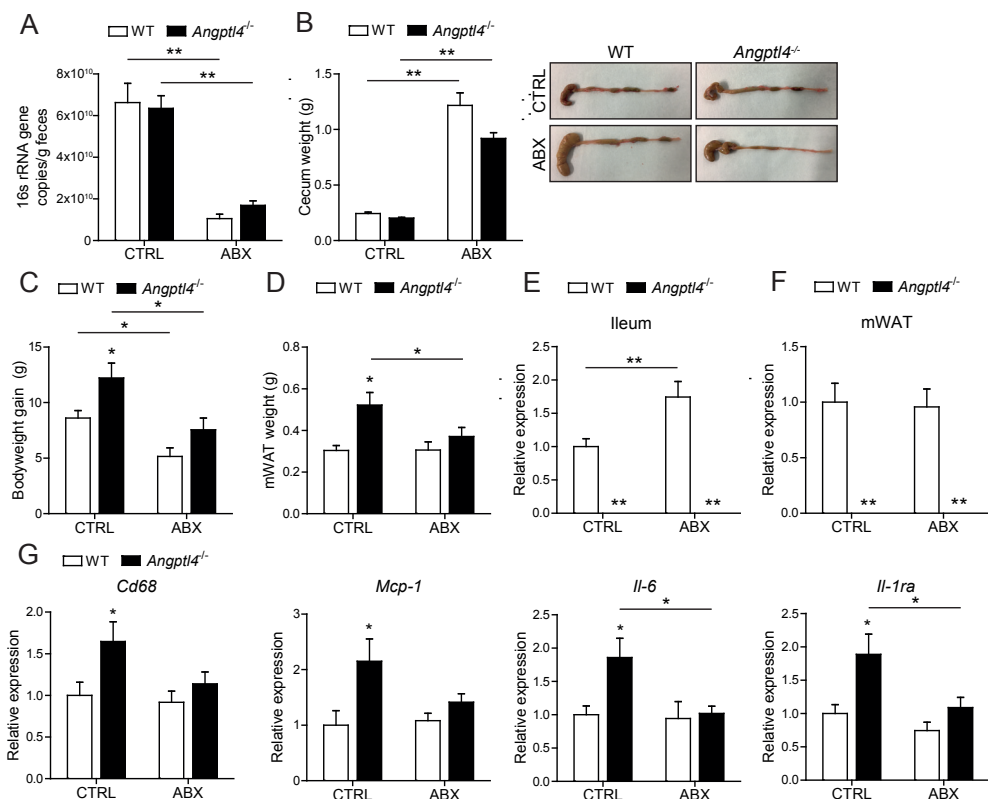


Figure 4. Antibiotics largely abolish the difference in adipose tissue inflammation between wild-type and *Angptl4*^{-/-} mice

(A) 16S rRNA gene copies per gram feces of wild-type (WT) and *Angptl4*^{-/-} mice fed the high fat/high cholesterol/high fructose diet with or without antibiotics supplementation. (B) Weight of the cecum and representative pictures of the cecum. (C) Bodyweight gain of wild-type (WT) and *Angptl4*^{-/-} mice at the end of the dietary intervention. (D) Mesenteric white adipose tissue (mWAT) weight. Relative mRNA levels of *Angptl4* in the (E) ileum or (F) mWAT. (G) Relative expression of inflammatory genes in mWAT. Gene expression levels of WT mice fed the CTRL diet were set at 1. Data are presented as mean ± SEM. Asterisks indicate significant differences compared to WT or between groups as indicated by bars according to two-way ANOVA with Bonferroni post-hoc test. **p* < 0.05 ***p* < 0.001.

Although antibiotic supplementation reduced overall bodyweight gain, *Angptl4*^{-/-} mice still gained more bodyweight as compared to wild-type mice (**Figure 4C**). In agreement with the first study, in the absence of antibiotics, *Angptl4*^{-/-} mice had elevated mesenteric fat pad weight at the end of the dietary intervention. Surprisingly, after antibiotic treatment mesenteric fat mass was not significantly different anymore between *Angptl4*^{-/-} mice and wild-type mice (**Figure 4D**). Interestingly, in the wild-type mice, antibiotics treatment increased *Angptl4* mRNA levels in the ileum but not the mesenteric adipose tissue, suggesting a suppressive effect of the gut bacteria on intestinal *Angptl4* expression (**Figure 4E-F**).

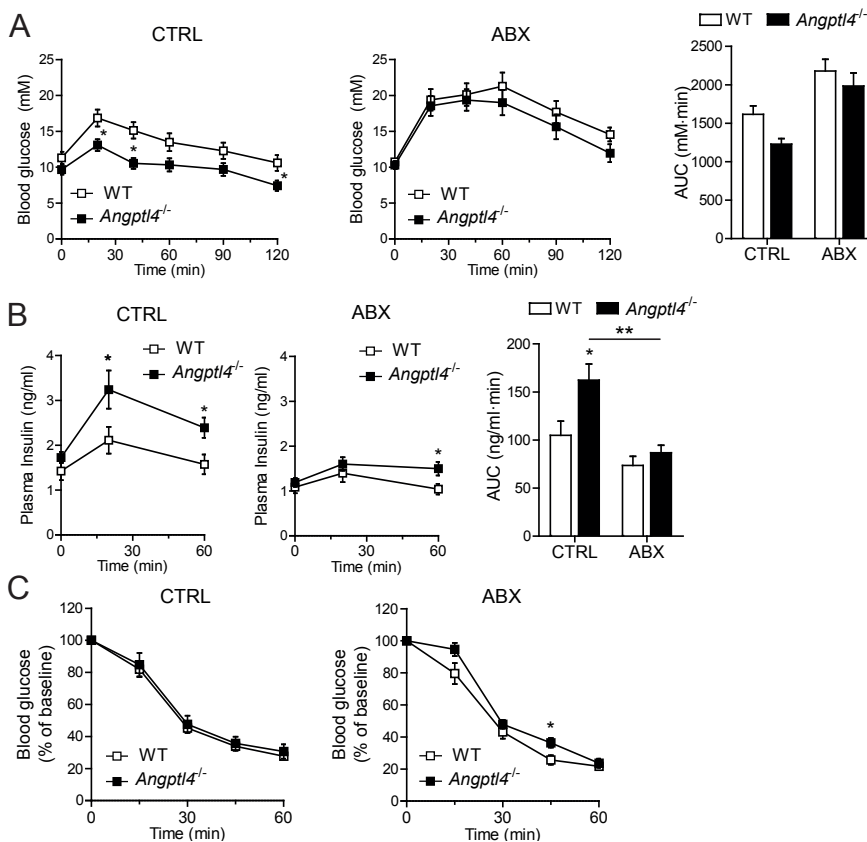


Figure 5. Antibiotics largely abolish the difference in glucose tolerance between wild-type and *Angptl4*^{-/-} mice

(A) Intraperitoneal glucose tolerance and areas under the curve (AUC) of wild-type (WT) and *Angptl4*^{-/-} mice fed the high fat/high cholesterol/high fructose diet with or without antibiotics supplementation. (B) Plasma insulin levels and corresponding AUC during the glucose tolerance test. (C) Blood glucose levels as percentage of baseline during an insulin tolerance test. Data are presented as mean \pm SEM. Asterisks indicate significant differences compared to WT or between groups as indicated by bars according to a Student's t-test or two-way ANOVA with Bonferroni post-hoc test. * $p < 0.05$ ** $p < 0.001$.

Concurrent with the elevated fat mass, the expression of several inflammatory genes, including *Cd68*, *Mcp-1*, *Il-6* and *Il-1ra*, was elevated in *Angptl4*^{-/-} mice as compared to wild-type mice in the absence of antibiotics. However, in the presence of antibiotics these differences in adipose tissue inflammation between the genotypes were largely abolished (**Figure 4G**), suggesting that the elevated fat mass and subsequent increase in adipose tissue inflammation in *Angptl4*^{-/-} mice is partly dependent on the gut bacteria.

Consistent with the data presented in **Figure 2A**, blood glucose levels during a glucose tolerance test were significantly lower in *Angptl4*^{-/-} mice than in wild-type mice (**Figure 5A**). Suppression of the gut bacteria using antibiotics in part abolished the differences in blood glucose levels between the two sets of mice, suggesting a role for the gut microbiota in mediating the effect of loss of ANGPTL4 on glucose tolerance. The lower glucose levels in the *Angptl4*^{-/-} mice were accompanied by higher plasma insulin levels (**Figure 5B**). However, an insulin tolerance test did not reveal any difference between *Angptl4*^{-/-} and wild-type mice (**Figure 5C**), irrespective of the antibiotics treatment (**Figure 5C**). Overall, our findings suggest that loss of ANGPTL4 promotes (visceral) obesity but, by raising insulin levels, improves glucose intolerance, which is partly mediated via a mechanism dependent on the gut bacteria.

Discussion

In the present study we investigated the role of ANGPTL4 in metabolic dysfunction in diet-induced obese mice. Consistent with the known biological functions of ANGPTL4 (13, 14, 17, 20), *Angptl4*^{-/-} mice gained more weight, had elevated fat mass, displayed increased adipose LPL activity and LPL protein abundance, and had lower plasma triglyceride levels compared to wild-type mice. Unexpectedly, despite these changes, mice lacking ANGPTL4 had improved glucose tolerance. Interestingly, suppression of the gut bacteria using antibiotics largely abolished the increased glucose tolerance in *Angptl4*^{-/-} mice as compared to wild-type mice. Together, our results indicate that loss of ANGPTL4 uncouples visceral obesity from glucose intolerance partly via a mechanism dependent on the gut microbiota.

In contrast to the well-established role of ANGPTL4 in lipid metabolism, much less is known about the impact of ANGPTL4 on glucose metabolism. Previously, we found that mice overexpressing *Angptl4* have impaired glucose tolerance and reduced peripheral insulin sensitivity (15). Conversely, *Angptl4*^{-/-} mice fed a high (saturated) fat diet were reported to have improved glucose tolerance (40), although these data were likely confounded by the development of an acute phase response and chylous ascites and peritonitis (20). Our present data indicate that, despite being heavier, mice lacking ANGPTL4 also have improved glucose tolerance when fed a high fat diet rich in unsaturated fatty acids, which does not trigger a pro-inflammatory response, as shown by the lack of elevation of plasma serum amyloid A in the *Angptl4*^{-/-} mice. Interestingly, recently it was reported that *Angptl4*^{-/-} mice fed chow have impaired glucose tolerance (41). Similarly, in a previous study, we found that *Angptl4*^{-/-} mice fed a low fat diet have impaired glucose tolerance ((20), unpublished data). However, in the latter study, the impaired glucose tolerance was probably due to the more rapid weight gain in the *Angptl4*^{-/-} mice. In human subjects, plasma ANGPTL4 levels appear to be positively correlated with fasting blood glucose levels (42), which may hint at a detrimental effect of ANGPTL4 on glucose tolerance in humans.

We found that the improvement in glucose tolerance in the *Angptl4*^{-/-} mice was accompanied by elevated insulin levels and not by increased insulin sensitivity, suggesting that the lower plasma glucose levels are probably caused by increased insulin secretion. Since lipids can potentiate insulin secretion of pancreatic β -cells (33, 43, 44), we hypothesized that the increased insulin levels in the *Angptl4*^{-/-} mice may be due to increased lipid uptake in β -cells as a result of loss of LPL inhibition. Interestingly, LPL does not appear to be localized on the cell surface but primarily within the pancreatic β -cells (45), implying that β -cell LPL may not be involved in lipid uptake. Furthermore, mice with β -cell-specific overexpression of LPL and a concomitant increase in LPL activity were hyperglycemic during a glucose tolerance test (34). Paradoxically, a similar phenotype was observed in β -cell-specific LPL

knock-out mice (34). Accordingly, it is difficult to assess the potential role of β -cell LPL in conferring the effect of loss of ANGPTL4 on glucose tolerance and insulin secretion. In any case, the effects of loss of ANGPTL4 on glucose tolerance are unlikely to be mediated by ANGPTL4 produced in β -cells, as we and others found that *Angptl4* is minimally expressed in pancreatic islets and β -cells (41).

Intriguingly, human genetic studies do suggest a link between LPL and glucose metabolism. Specifically, a gain-of-function variant in LPL in humans was found to be associated with higher insulin sensitivity, lower fasting glucose, and lower risk of type 2 diabetes (46). Conversely, a loss-of-function variant in LPL was found to be associated with a higher risk of type 2 diabetes (46). Whether these effects are specifically connected to LPL in β -cells, the hypothalamus, or elsewhere, remains unclear.

Our data suggest that the effects of loss of ANGPTL4 on glucose tolerance are at least partly dependent on the gut microbiota. There is growing evidence that alterations in the gut microbiota composition can modulate insulin sensitivity (38, 47–49) and insulin secretion (35–37). For example, it has been shown that germ-free mice and mice treated with antibiotics have an improved insulin sensitivity as compared to conventionally-raised or untreated mice (47–49). Furthermore, it has been demonstrated that the difference in insulin secretion between different mouse strains could largely be recapitulated via microbial transfer (35). In human subjects, transfer of the fecal microbiota from lean donors to recipients with the metabolic syndrome was found to increase insulin sensitivity (50).

One microbial family that has been shown to have a strong positive correlation with plasma insulin levels is Clostridiaceae (35). Interestingly, we found a higher relative abundance of Clostridiaceae in the colon of *Angptl4*^{-/-} mice, concurrent with elevated plasma insulin levels. However, because certain Clostridiaceae family members also positively correlate with obesity and other metabolic perturbations (51, 52), it is difficult to link Clostridiaceae specifically to insulin secretion in our study. Interestingly, in human subjects ingestion of a specific *Lactobacillus* strain, *L. reuteri*, for four weeks improved glucose-induced insulin secretion (37). In our study, *Lactobacillus* was—with a relative abundance of 15.82%—almost 2-fold more abundant in the colon of the *Angptl4*^{-/-} mice as compared with the wild-type mice. It can thus be speculated that the increase in *Lactobacillus* might contribute to the elevated insulin levels in *Angptl4*^{-/-} mice.

Several mechanisms have been suggested by which the gut microbiota may affect glucose metabolism, including via altered production of short-chain fatty acids and LPS. Short-chain fatty acids have been suggested to promote insulin secretion via several mechanisms, including the intestinal GPCR43 receptor, either dependent (53) or independent of GLP-1 secretion (54). In addition, evidence was provided that acetate produced by the gut microbiota may increase glucose-stimulated insulin secretion via activation of the parasympathetic

nervous system (55). We observed that the improved glucose tolerance in *Angptl4*^{-/-} mice was associated with lower short-chain fatty acids levels, suggesting that the improved glucose-stimulated insulin secretion can probably not be attributed to short-chain fatty acids. Of note, short-chain fatty acid fluxes, rather than concentrations, have been found to correlate with several metabolic markers. For this reason, measurement of short-chain fatty acid fluxes is more valuable to understand the role of short-chain fatty acids in host metabolism (56).

Another potential candidate that may link the gut microbiota to glucose tolerance is LPS. In our study, elevated plasma insulin levels in the *Angptl4*^{-/-} mice were associated with higher levels of circulating LPS. However, conflicting results have been reported regarding the role of LPS in insulin secretion. Whereas Amyot *et al.* reported that LPS attenuates insulin secretion (57), Nguyen *et al.* found that LPS stimulates insulin secretion (58). Another study reported that LPS does not affect plasma insulin levels (47), rendering it difficult to link the higher LPS levels in the *Angptl4*^{-/-} mice to the elevated plasma insulin levels. Hence, short-chain fatty acids and LPS are probably not involved in conferring the effect of the gut bacteria on insulin levels in *Angptl4*^{-/-} mice.

Interestingly, in our study we found an increased abundance of equol-producing bacteria, including *Adlercreutzia*, *Lactobacillus* and *Coriobacteriaceae* (59). As equol improves glucose tolerance (60), it may be hypothesized that the improved glucose tolerance in the *Angptl4*^{-/-} mice may be related to altered production of equol. However, future studies should investigate the role of equol and other potential candidates that may mediated the effects of the gut microbiota on insulin levels and glucose tolerance.

In our study, we suppressed the gut bacteria by adding broad-spectrum antibiotics to the drinking water. Although treating mice with antibiotics is a commonly used strategy to investigate whether the gut bacteria influence host metabolism, it is important to note that antibiotics also possess direct immunomodulatory properties and may influence mitochondrial function (61, 62).

Bäckhed and colleagues suggested that intestinal ANGPTL4 mediates the stimulatory effects of the gut microbiota on fat storage (38, 39). Although our results are consistent with their studies showing that the gut bacteria suppress *Angptl4* expression in the intestine but not in the adipose tissue (38, 39), we did not observe that the effect of the microbiota on mesenteric fat storage is mediated by ANGPTL4. Specifically, we only observed a stimulatory effect of the gut microbes on mesenteric fat mass in mice lacking ANGPTL4. Future studies using intestinal-specific *Angptl4*^{-/-} mice should shed more light on the link between intestinal ANGPTL4 and fat storage.

In conclusion, we show that loss of ANGPTL4 in diet-induced obese mice promotes visceral obesity, while improving glucose tolerance. Suppression of the gut bacteria by

antibiotics largely abolished the difference in glucose tolerance between the wild-type and *Angptl4*^{-/-} mice, suggesting that ANGPTL4 influences glucose tolerance partly via a mechanism dependent on the gut bacteria.

Acknowledgements

We thank Gunilla Olivecrona for the LPL activity measurements. This research was supported by The Netherlands Cardiovascular Research Committee IN-CONTROL grant (CVON 2012-03).

References

1. Redinger, R. N. (2007) The pathophysiology of obesity and its clinical manifestations. *Gastroenterol. Hepatol.* **3**, 856–863
2. Yamato, M., Shiba, T., Yoshida, M., Ide, T., Seri, N., Kudou, W., Kinugawa, S., and Tsutsui, H. (2007) Fatty acids increase the circulating levels of oxidative stress factors in mice with diet-induced obesity via redox changes of albumin. *FEBS J.* **274**, 3855–3863
3. Voshol, P. J., Rensen, P. C. N., van Dijk, K. W., Romijn, J. A., and Havekes, L. M. (2009) Effect of plasma triglyceride metabolism on lipid storage in adipose tissue: studies using genetically engineered mouse models. *Biochim. Biophys. Acta.* **1791**, 479–485
4. Kersten, S. (2014) Physiological regulation of lipoprotein lipase. *Biochim. Biophys. Acta.* **1841**, 919–933
5. Davies, B. S. J., Beigneux, A. P., Barnes, R. H., Tu, Y., Gin, P., Weinstein, M. M., Nobumori, C., Nyrén, R., Goldberg, I., Olivecrona, G., Bensadoun, A., Young, S. G., and Fong, L. G. (2010) GPIHBP1 is responsible for the entry of lipoprotein lipase into capillaries. *Cell Metab.* **12**, 42–52
6. Beigneux, A. P., Davies, B. S. J., Gin, P., Weinstein, M. M., Farber, E., Qiao, X., Peale, F., Bunting, S., Walzem, R. L., Wong, J. S., Blamer, W. S., Ding, Z. M., Melford, K., Wongsiriroj, N., Shu, X., de Sauvage, F., Ryan, R. O., Fong, L. G., Bensadoun, A., and Young, S. G. (2007) Glycosylphosphatidylinositol-Anchored High-Density Lipoprotein-Binding Protein 1 Plays a Critical Role in the Lipolytic Processing of Chylomicrons. *Cell Metab.* **5**, 279–291
7. Wang, H., and Eckel, R. H. (2009) Lipoprotein lipase : from gene to obesity. *Am. J. Physiol. – Endocrinol. Metab.* **297**, E271–E288
8. Dijk, W., and Kersten, S. (2016) Regulation of lipid metabolism by angiopoietin- like proteins. *Curr. Opin. Lipidol.* **27**, 249–256
9. Dijk, W., Heine, M., Vergnes, L., Boon, M. R., Schaart, G., Hesselink, M. K., Reue, K., van Marken Lichtenbelt, W. D., Olivecrona, G., Rensen, P. C., Heeren, J., and Kersten, S. (2015) ANGPTL4 mediates shuttling of lipid fuel to brown adipose tissue during sustained cold exposure. *Elife.* **4**, e08428
10. Catoire, M., Alex, S., Paraskevopoulos, N., Mattijssen, F., Evers-van Gogh, I., Schaart, G., Jeppesen, J., Kneppers, A., Mensink, M., Voshol, P. J., Olivecrona, G., Tan, N. S., Hesselink, M. K. C., Berbée, J. F., Rensen, P. C. N., Kalkhoven, E., Schrauwen, P., and Kersten, S. (2014) Fatty acid-inducible ANGPTL4 governs lipid metabolic response to exercise. *Proc. Natl. Acad. Sci. U. S. A.* **111**, E1043–52
11. Dijk, W., and Kersten, S. (2014) Regulation of lipoprotein lipase by Angptl4. *Trends Endocrinol. Metab.* **25**, 146–55
12. Bergö, M., Olivecrona, G., and Olivecrona, T. (1996) Forms of lipoprotein lipase in rat tissues: in adipose tissue the proportion of inactive lipase increases on fasting. *Biochem. J.* **313**, 893–898
13. Kroupa, O., Vorrjö, E., Stienstra, R., Mattijssen, F., Nilsson, S. K., Sukonina, V., Kersten, S., Olivecrona, G., and Olivecrona, T. (2012) Linking nutritional regulation of Angptl4, Gpihbp1, and Lmfl to lipoprotein lipase activity in rodent adipose tissue. *BMC Physiol.* **12**, 13
14. Sukonina, V., Lookene, A., Olivecrona, T., and Olivecrona, G. (2006) Angiopoietin-like protein 4 converts lipoprotein lipase to inactive monomers and modulates lipase activity in adipose tissue. *Proc. Natl. Acad. Sci. U. S. A.* **103**, 17450–5
15. Lichtenstein, L., Berbée, J. F. P., van Dijk, S. J., van Dijk, K. W., Bensadoun, A., Kema, I. P., Voshol, P. J., Müller, M., Rensen, P. C. N., and Kersten, S. (2007) Angptl4 upregulates cholesterol synthesis in liver via inhibition of LPL- and HL-dependent hepatic cholesterol uptake. *Arterioscler. Thromb. Vasc. Biol.* **27**, 2420–7
16. Dijk, W., Beigneux, A. P., Larsson, M., Bensadoun, A., Young, S. G., and Kersten, S. (2016) Angiopoietin-like 4 (ANGPTL4) promotes intracellular degradation of lipoprotein lipase in adipocytes. *J. Lipid Res.* **58**, 7250–7
17. Mattijssen, F., Alex, S., Swarts, H. J., Groen, A. K., van Schothorst, E. M., and Kersten, S. (2014) Angptl4 serves as an endogenous inhibitor of intestinal lipid digestion. *Mol. Metab.* **3**, 135–144
18. Xu, A., Lam, M. C., Chan, K. W., Wang, Y., Zhang, J., Hoo, R. L. C., Xu, J. Y., Chen, B., Chow, W., Tso, A. W. K., and Lam, K. S. L. (2005) Angiopoietin-like protein 4 decreases blood glucose and improves glucose tolerance but induces hyperlipidemia and hepatic steatosis in mice. *Proc. Natl. Acad. Sci. U. S. A.* **102**, 6086–6091
19. Mandard, S., Zandbergen, F., van Straten, E., Wahli, W., Kuipers, F., Müller, M., and Kersten, S. (2006) The fasting-induced adipose factor/angiopoietin-like protein 4 is physically associated with lipoproteins and governs plasma lipid levels and adiposity. *J. Biol. Chem.* **281**, 934–44
20. Lichtenstein, L., Mattijssen, F., de Wit, N. J., Georgiadi, A., Hooiveld, G. J., van der Meer, R., He, Y., Qi, L., Köster, A., Tamsma, J. T., Tan, N. S., Müller, M., and Kersten, S. (2010) Angptl4 protects against severe proinflammatory effects of saturated fat by inhibiting fatty acid uptake into mesenteric lymph node macrophages. *Cell Metab.* **12**, 580–92
21. Köster, A., Chao, Y. B., Mosior, M., Ford, A., Gonzalez-DeWhitt, P. a, Hale, J. E., Li, D., Qiu, Y., Fraser, C.

- C., Yang, D. D., Heuer, J. G., Jaskunas, S. R., and Eacho, P. (2005) Transgenic angiotensin-like (angptl4) overexpression and targeted disruption of angptl4 and angptl3: regulation of triglyceride metabolism. *Endocrinology*. **146**, 4943–50
22. Yesil, P., Michel, M., Chwalek, K., Pedack, S., Jany, C., Ludwig, B., Bornstein, S. R., and Lammert, E. (2009) A new collagenase blend increases the number of islets isolated from mouse pancreas. *Islets*. **1**, 185–190
 23. Ruge, T., Wu, G., Olivecrona, T., and Olivecrona, G. (2004) Nutritional regulation of lipoprotein lipase in mice. *Int. J. Biochem. Cell Biol.* **36**, 320–329
 24. Janssen, A. W. F., Houben, T., Katiraei, S., Dijk, W., Boutens, L., van der Bolt, N., Wang, Z., Brown, M. J., Hazen, S. L., Mandard, S., Shiri-Sverdlov, R., Kuipers, F., Dijk, K. W. van, Vervoort, J., and Rinke Stienstra, Guido JEJ Hooiveld, S. K. (2017) Modulation of the gut microbiota impacts non-alcoholic fatty liver disease: a potential role for bile acids. *J. Lipid Res.* **58**, 1399–1416.
 25. Weinstein, M. M., Yin, L., Beigneux, A. P., Davies, B. S. J., Gin, P., Estrada, K., Melford, K., Bishop, J. R., Esko, J. D., Dallinga-Thie, G. M., Fong, L. G., Bensadoun, A., and Young, S. G. (2008) Abnormal patterns of lipoprotein lipase release into the plasma in GPIHBP1-deficient mice. *J. Biol. Chem.* **283**, 34511–34518
 26. Gevers, D., Kugathasan, S., Denson, L. A., Vázquez-Baeza, Y., Van Treuren, W., Ren, B., Schwager, E., Knights, D., Song, S. J., Yassour, M., Morgan, X. C., Kostic, A. D., Luo, C., González, A., McDonald, D., Haberman, A., Walters, T., Baker, S., Rosh, J., Stephens, M., Heyman, M., Markowitz, J., Baldassano, R., Griffiths, A., Sylvester, F., Mack, D., Kim, S., Crandall, W., Hyams, J., Huttenhower, C., Knight, R., and Xavier, R. J. (2014) The treatment-naïve microbiome in new-onset Crohn's disease. *Cell Host Microbe*. **15**, 382–392
 27. Caporaso, J. G., Kuczynski, J., Stombaugh, J., Bittinger, K., Bushman, F. D., Costello, E. K., Fierer, N., Peña, A. G., Goodrich, J. K., Gordon, J. I., Huttley, G. a, Kelley, S. T., Knights, D., Koenig, J. E., Ley, R. E., Lozupone, C. a, McDonald, D., Muegge, B. D., Pirrung, M., Reeder, J., Sevinsky, J. R., Turnbaugh, P. J., Walters, W. a, Widmann, J., Yatsunenko, T., Zaneveld, J., and Knight, R. (2010) QIIME allows analysis of high-throughput community sequencing data. *Nat. Methods*. **7**, 335–336
 28. Segata, N., Izard, J., Waldron, L., Gevers, D., Miropolsky, L., Garrett, W. S., and Huttenhower, C. (2011) Metagenomic biomarker discovery and explanation. *Genome Biol.* **12**, R60
 29. Suzuki, M. T., Taylor, L. T., and DeLong, E. F. (2000) Quantitative analysis of small-subunit rRNA genes in mixed microbial populations via 5'-nuclease assays. *Appl. Environ. Microbiol.* **66**, 4605–4614
 30. Weisburg, W. G., Barns, S. M., Pelletier, D. A., and Lane, D. J. (1991) 16S ribosomal DNA amplification for phylogenetic study. *J. Bacteriol.* **173**, 697–703
 31. Basciano, H., Federico, L., and Adeli, K. (2005) Fructose, insulin resistance, and metabolic dyslipidemia. *Nutr Metab.* **2**, 5
 32. Chung, S., and Parks, J. S. (2015) Dietary cholesterol effects on adipose tissue inflammation. *Curr. Opin. Lipidol.* **27**, 19–25
 33. Cruz, W. S., Kwon, G., Marshall, C. a, McDaniel, M. L., and Semenkovich, C. F. (2001) Glucose and insulin stimulate heparin-releasable lipoprotein lipase activity in mouse islets and INS-1 cells. A potential link between insulin resistance and beta-cell dysfunction. *J. Biol. Chem.* **276**, 12162–8
 34. Pappan, K. L., Pan, Z., Kwon, G., Marshall, C. a., Coleman, T., Goldberg, I. J., McDaniel, M. L., and Semenkovich, C. F. (2005) Pancreatic β -cell lipoprotein lipase independently regulates islet glucose metabolism and normal insulin secretion. *J. Biol. Chem.* **280**, 9023–9029
 35. Kreznar, J. H., Keller, M. P., Traeger, L. L., Rabaglia, M. E., Schueler, K. L., Stapleton, D. S., Zhao, W., Vivas, E. I., Yandell, B. S., Broman, A. T., Hagenbuch, B., Attie, A. D., and Rey, F. E. (2017) Host Genotype and Gut Microbiome Modulate Insulin Secretion and Diet-Induced Metabolic Phenotypes. *Cell Rep.* **18**, 1739–1750
 36. Cani, P. D., Neyrinck, A. M., Fava, F., Knauf, C., Burcelin, R. G., Tuohy, K. M., Gibson, G. R., and Delzenne, N. M. (2007) Selective increases of bifidobacteria in gut microflora improve high-fat-diet-induced diabetes in mice through a mechanism associated with endotoxaemia. *Diabetologia*. **50**, 2374–2383
 37. Simon, M. C., Strassburger, K., Nowotny, B., Kolb, H., Nowotny, P., Burkart, V., Zivehe, F., Hwang, J. H., Stehle, P., Pacini, G., Hartmann, B., Holst, J. J., Mackenzie, C., Bindels, L. B., Martinez, I., Walter, J., Heinrich, B., Schloot, N. C., and Roden, M. (2015) Intake of lactobacillus reuteri improves incretin and insulin secretion in Glucose-Tolerant humans: A proof of concept. *Diabetes Care*. **38**, 1827–1834
 38. Bäckhed, F., Ding, H., Wang, T., Hooper, L. V., Koh, G. Y., Nagy, A., Semenkovich, C. F., and Gordon, J. I. (2004) The gut microbiota as an environmental factor that regulates fat storage. *Proc. Natl. Acad. Sci. U. S. A.* **101**, 15718–15723
 39. Bäckhed, F., Manchester, J. K., Semenkovich, C. F., and Gordon, J. I. (2007) Mechanisms underlying the resistance to diet-induced obesity in germ-free mice. *Proc. Natl. Acad. Sci. U. S. A.* **104**, 979–84
 40. Lee, E.-C., Landes, G. M., Chung, K., Chen, L., Desai, U., Powell, D. R., and Hong, S. (2006) Monoclonal

- antibodies against Angptl4
41. Kim, H.-K., Kwon, O., Park, K.-H., Lee, K. J., Youn, B.-S., Kim, S.-W., and Kim, M.-S. (2017) Angiopoietin-like peptide 4 regulates insulin secretion and islet morphology. *Biochem. Biophys. Res. Commun.* **485**, 113–118
42. Mehta, N., Qamar, A., Qu, L., Qasim, A. N., Mehta, N. N., Reilly, M. P., and Rader, D. J. (2014) Differential association of plasma angiopoietin-like proteins 3 and 4 with lipid and metabolic traits. *Arterioscler. Thromb. Vasc. Biol.* **34**, 1057–1063
43. Mulder, H., Yang, S., So, M., Holm, C., and Ahre, B. (2004) Inhibition of Lipase Activity and Lipolysis in Rat Islets Reduces Insulin Secretion. *Diabetes*. **53**, 122–128
44. Koyama, K., Chen, G., Wang, M. Y., Lee, Y., Shimabukuro, M., Newgard, C. B., and Unger, R. H. (1997) Beta-Cell Function in Normal Rats Made Chronically Hyperleptinemic By Adenovirus-Leptin Gene Therapy. *Diabetes*. **46**, 1276–1280
45. Nyrén, R., Chang, C. L., Lindström, P., Barmina, A., Vorrjö, E., Ali, Y., Juntti-Berggren, L., Bensadoun, A., Young, S. G., Olivecrona, T., and Olivecrona, G. (2012) Localization of lipoprotein lipase and GPIHBP1 in mouse pancreas: effects of diet and leptin deficiency. *BMC Physiol.* **12**, 14
46. Lotta, L. A., Gulati, P., Day, F. R., Payne, F., Ongen, H., van de Bunt, M., Gaulton, K. J., Eicher, J. D., Sharp, S. J., Luan, J., De Lucia Rolfe, E., Stewart, I. D., Wheeler, E., Willems, S. M., Adams, C., Yaghootkar, H., EPIC-InterAct Consortium, Cambridge FPLD1 Consortium, Forouhi, N. G., Khaw, K.-T., Johnson, A. D., Semple, R. K., Frayling, T., Perry, J. R. B., Dermitzakis, E., McCarthy, M. I., Barroso, I., Wareham, N. J., Savage, D. B., Langenberg, C., O'Rahilly, S., and Scott, R. A. (2017) Integrative genomic analysis implicates limited peripheral adipose storage capacity in the pathogenesis of human insulin resistance. *Nat. Genet.* **49**, 17–26
47. Caesar, R., Reigstad, C. S., Bäckhed, H. K., Reinhardt, C., Ketonen, M., Lundén, G. Ö., Cani, P. D., and Bäckhed, F. (2012) Gut-derived lipopolysaccharide augments adipose macrophage accumulation but is not essential for impaired glucose or insulin tolerance in mice. *Gut*. **61**, 1701–7
48. Rabot, S., Membrez, M., Bruneau, A., Gérard, P., Harach, T., Moser, M., Raymond, F., Mansourian, R., and Chou, C. J. (2010) Germ-free C57BL/6J mice are resistant to high-fat-diet-induced insulin resistance and have altered cholesterol metabolism. *FASEB J.* **24**, 4948–59
49. Hwang, I., Park, Y. J., Kim, Y. R., Kim, Y. N., Ka, S., Lee, H. Y., Seong, J. K., Seok, Y. J., and Kim, J. B. (2015) Alteration of gut microbiota by vancomycin and bacitracin improves insulin resistance via glucagon-like peptide 1 in diet-induced obesity. *FASEB J.* **29**, 2397–2411
50. Vrieze, A., Van Nood, E., Holleman, F., Salojärvi, J., Kootte, R. S., Bartelsman, J. F. W. M., Dallinga-Thie, G. M., Ackermans, M. T., Serlie, M. J., Oozeer, R., Derrien, M., Druesne, A., Van Hylckama Vlieg, J. E. T., Bloks, V. W., Groen, A. K., Heilig, H. G. H. J., Zoetendal, E. G., Stroes, E. S., de Vos, W. M., Hoekstra, J. B. L., and Nieuwdorp, M. (2012) Transfer of intestinal microbiota from lean donors increases insulin sensitivity in individuals with metabolic syndrome. *Gastroenterology*. **143**, 913–6
51. Ussar, S., Griffin, N. W., Bezy, O., Bry, L., Gordon, J. I., Kahn, C. R., Ussar, S., Griffin, N. W., Bezy, O., Fujisaka, S., Vienberg, S., Softic, S., and Deng, L. (2015) Interactions between Gut Microbiota , Host Genetics and Diet Modulate the Predisposition to Obesity and Metabolic Syndrome. *Cell Metab.* **22**, 1–15
52. Karlsson, F. H., Tremaroli, V., Nookaew, I., Bergstrom, G., Behre, C. J., Fagerberg, B., Nielsen, J., and Backhed, F. (2013) Gut metagenome in European women with normal, impaired and diabetic glucose control. *Nature*. **498**, 99–103
53. Priyadarshini, M., Wicksteed, B., Schiltz, G. E., Gilchrist, A., and Layden, B. T. (2016) SCFA Receptors in Pancreatic β Cells: Novel Diabetes Targets? *Trends Endocrinol. Metab.* **27**, 653–664
54. Priyadarshini, M., Villa, S. R., Fuller, M., Wicksteed, B., Mackay, C. R., Alquier, T., Poitout, V., Mancebo, H., Mirmira, R. G., Gilchrist, A., and Layden, B. T. (2015) An Acetate-Specific GPCR, FFAR2, Regulates Insulin Secretion. *Mol. Endocrinol.* **29**, 1055–66
55. Perry, R. J., Peng, L., Barry, N. A., Cline, G. W., Zhang, D., Cardone, R. L., Petersen, K. F., Kibbey, R. G., Goodman, A. L., and Shulman, G. I. (2016) Acetate mediates a microbiome-brain- β -cell axis to promote metabolic syndrome. *Nature*. **534**, 213–217
56. den Besten, G., Havinga, R., Bleeker, A., Rao, S., Gerding, A., van Eunen, K., Groen, A. K., Reijngoud, D.-J., and Bakker, B. M. (2014) The short-chain Fatty Acid uptake fluxes by mice on a guar gum supplemented diet associate with amelioration of major biomarkers of the metabolic syndrome. *PLoS One*. **9**, e107392
57. Amyot, J., Semache, M., Ferdaoussi, M., Fontés, G., and Poitout, V. (2012) Lipopolysaccharides impair insulin gene expression in isolated islets of langerhans via toll-like receptor-4 and NF- κ B signalling. *PLoS One*. **7**, e36200
58. Nguyen, A. T., Mandard, S., Dray, C., Deckert, V., Valet, P., Besnard, P., Drucker, D. J., Lagrost, L., and Grober, J. (2014) Lipopolysaccharides-mediated increase in glucose-stimulated insulin secretion: Involvement of the GLP-1 pathway. *Diabetes*. **63**, 471–482

59. Setchell, K. D. R., and Clerici, C. (2010) Equol : History, Chemistry, and Formation. *J. Nutr.* **3**, 1355–1362
60. Cheong, S. H., Furuhashi, K., Ito, K., Nagaoka, M., Yonezawa, T., Miura, Y., and Yagasaki, K. (2014) Antihyperglycemic effect of equol, a daidzein derivative, in cultured L6 myocytes and ob/ob mice. *Mol. Nutr. Food Res.* **58**, 267–277
61. Tauber, S. C., and Nau, R. (2008) Immunomodulatory properties of antibiotics. *Curr. Mol. Pharmacol.* **1**, 68–79
62. Wang, X., Ryu, D., Houtkooper, R. H., and Auwerx, J. (2015) Antibiotic use and abuse: A threat to mitochondria and chloroplasts with impact on research, health, and environment. *BioEssays.* **37**, 1045–1053

Supplemental tables

Supplemental table 1. Primer sequences used for qPCR

Name	Primer Sequence	
	Forward	Reverse
<i>m36b4</i>	ATGGGTACAAGCGCGTCCTG	GCCTTGACCTTTTCAGTAAG
<i>mCd68</i>	CCAATTCAGGGTGGAAGAAA	CTCGGGCTCTGATGTAGGTC
<i>mF4/80</i>	CTTTGGCTATGGGCTTCCAGTC	GCAAGGAGGACAGAGTTTATCGTG
<i>mMcp-1</i>	CCCAATGAGTAGGCTGGAGA	TCTGGACCCATTCTTCTTG
<i>mIl-6</i>	CTTCCATCCAGTTGCCTTCTTG	AATTAAGCCTCCGACTTGTGAAG
<i>mIl-1ra</i>	AAATCTGCTGGGGACCCTAC	TGAGCTGGTTGTTTCTCAGG
<i>mLPL</i>	CAGCTGGGCCTAACTTTGAG	GACCCCCTGGTAAATGTGTG
<i>mAngptl4</i>	GTTTGCAGACTCAGCTCAAGG	CCAAGAGGTCTATCTGGCTCTG

Supplemental table 2. Relative abundance of microbiota in colonic luminal content

Phylum	Class	Order	Family	Genus	Species	Wild-type (%)	<i>Angptl4^{-/-}</i> (%)	FC	P-value*
Actinobacteria						0.67	1.68	2.5	0.004
	Coriobacteriia					0.67	1.68	2.5	0.004
		Coriobacteriales				0.67	1.68	2.5	0.004
			Coriobacteriaceae			0.67	1.68	2.5	0.004
				<i>Adlercreutzia</i>		0.67	1.68	2.5	0.004
Bacteroidetes						4.61	5.86	1.3	ns
	Bacteroidia					4.61	5.86	1.3	ns
		Bacteroidales				4.61	5.86	1.3	ns
			Unidentified			2.04	2.46	1.2	ns
			Bacteroidaceae			0.95	1.14	1.2	ns
				<i>Bacteroides</i>		0.95	1.14	1.2	ns
			S24-7			1.61	2.26	1.4	ns
				<i>Unidentified</i>		1.61	2.26	1.4	ns
Deferribacteres						4.67	4.26	-1.1	ns
	Deferribacteres					4.67	4.26	-1.1	ns
		Deferribacterales				4.67	4.26	-1.1	ns
			Deferribacteraceae			4.67	4.26	-1.1	ns
				<i>Mucispirillum</i>		4.67	4.26	-1.1	ns
				<i>Mucispirillum schaedleri</i>		4.67	4.26	-1.1	ns
Firmicutes						84.95	82.24	-1.0	ns
	Bacilli					8.82	15.82	1.8	0.023
		Lactobacillales				8.82	15.82	1.8	0.023
			Lactobacillaceae			8.82	15.82	1.8	0.023
				<i>Lactobacillus</i>		8.82	15.82	1.8	0.023
	Clostridia					29.88	46.49	1.6	0.011
		Clostridiales				29.88	46.49	1.6	0.011
			Unidentified			19.04	23.21	1.2	ns
			Clostridiaceae			3.84	14.19	3.7	0.001
				<i>Unidentified</i>		0.00	1.97	>2000	<0.001
				<i>SMB53</i>		3.84	12.22	3.2	0.001
			Lachnospiraceae			2.22	1.61	-1.4	ns
				<i>Unidentified</i>		2.22	1.61	-1.4	ns
			Ruminococcaceae			4.78	7.49	1.6	ns
				<i>Unidentified</i>		0.90	3.67	4.1	ns
				<i>Oscillospira</i>		3.23	3.15	1.0	ns
				<i>Ruminococcus</i>		0.64	0.66	1.0	ns
	Erysipelotrichi					46.25	19.93	-2.3	0.016
		Erysipelotrichales				46.25	19.93	-2.3	0.016
			Erysipelotrichaceae			46.25	19.93	-2.3	0.016
				<i>Allobaculum</i>		46.25	19.93	-2.3	0.016
Proteobacteria						5.09	5.96	1.2	ns
	Deltaproteobacteria					5.09	5.96	1.2	ns
		Desulfovibrionales				5.09	5.96	1.2	ns
			Desulfovibrionaceae			5.09	5.96	1.2	ns
				<i>Bilophila</i>		2.84	4.09	1.4	ns
				<i>Desulfovibrio</i>		2.26	1.87	-1.2	ns

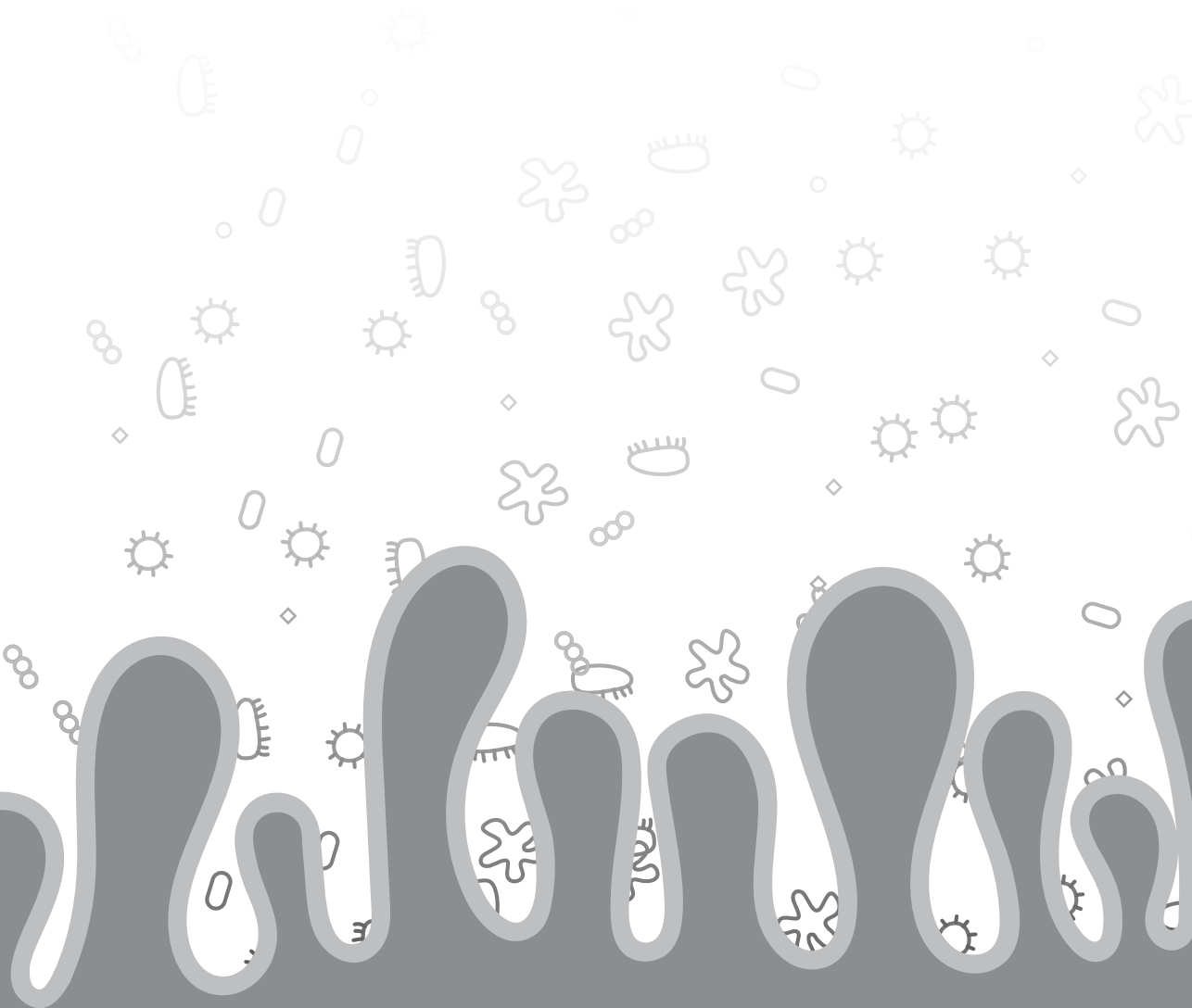
Abundance threshold for presentation in the table >0.5% in at least one of the two genotypes

* significance according to unpaired Wilcoxon rank-sum test

10



General discussion



Everyday researchers are looking for potential mechanisms to reduce or at least stop the increasing prevalence of obesity and related metabolic diseases. To be able to develop effective treatment and prevention strategies, better understanding the underlying mechanisms and factors contributing to these metabolic diseases is of utmost importance.

Therefore, the aim of this thesis was to increase our understanding regarding the role of various mediators in metabolic health, with a special focus on the gut microbiota, bile acids, and ANGPTL4. To comprehensively elucidate the role of these mediators, we pursued a number of approaches, including the use of mice with an altered gut microbial composition, mice lacking *Angptl4*, and an *ex vivo* model to study the liver. In the previous chapters we demonstrated that the gut microbiota, bile acids, and ANGPTL4 influence various aspects of metabolic health.

The main outcomes of this thesis were:

- In **Chapter 4**, we showed that the gut microbiota are causally involved in the pathogenesis of non-alcoholic fatty liver disease (NAFLD), likely mediated by alterations in portal delivery of bile acids.
- In **Chapter 5**, we demonstrated that the mucin-degrading bacteria *A. muciniphila* and *B. thetaiotaomicron* do not influence features of NAFLD in an obese model of NAFLD.
- In **Chapter 6** and **Chapter 7**, we demonstrated the suitability of precision-cut liver slices to study the human liver by using agonists of the nuclear receptors PPAR α and FXR.
- In **Chapter 8**, we switched to ANGPTL4 and investigated whether ANGPTL4 may be responsible for the triglyceride-lowering effect of bile acids. Although we find that the triglyceride-lowering effect of bile acids is not mediated by ANGPTL4, we uncover a novel function of ANGPTL4 in regulating bile acid reabsorption.
- In **Chapter 9** we studied the effects of ANGPTL4 in diet-induced obesity, where we reveal a new role for ANGPTL4 in regulating glucose metabolism.

The role of intestinal microbiota in metabolic disorders

In the last two decades, the intestinal microbiota have been increasingly linked to obesity and metabolic diseases, such as type 2 diabetes, NAFLD, and cardiovascular disease (1–5). However, as discussed in **Chapter 2** and **Chapter 3**, many of these studies are associative and do not discriminate whether changes in gut microbiota causally contribute to metabolic disease or are merely a consequence of the metabolic disturbances.

Intestinal microbiota and NAFLD

The liver receives about 70% of its blood supply from the gut via the portal vein and is therefore the first organ that is exposed to potential harmful gut-derived factors. Alterations

in gut microbial composition and function may therefore also influence liver physiology. Indeed, many studies hint at the possibility that disturbances in the gut microbiota are linked to NAFLD (6–9). However, the number of studies providing direct causal evidence is limited and use methods to induce liver injury that do not encompass all features of NAFLD in humans, including obesity, insulin resistance, steatohepatitis and fibrosis (10–16). In **Chapter 4**, we show that feeding mice a diet rich in fat, cholesterol and fructose induces all features of NAFLD and therefore represents a suitable model to study NAFLD. Accordingly, we show that stimulation of the gut microbiota promotes the progression of NAFLD, while suppression of the gut microbiota using antibiotics attenuates hepatic inflammation and fibrosis. The effects of the gut microbiota on NAFLD were found to be mediated by changes in the portal delivery of bile acids (**Figure 1**). Although these data clearly point to a causal role of the gut microbiota in NAFLD, several aspects require further investigation.

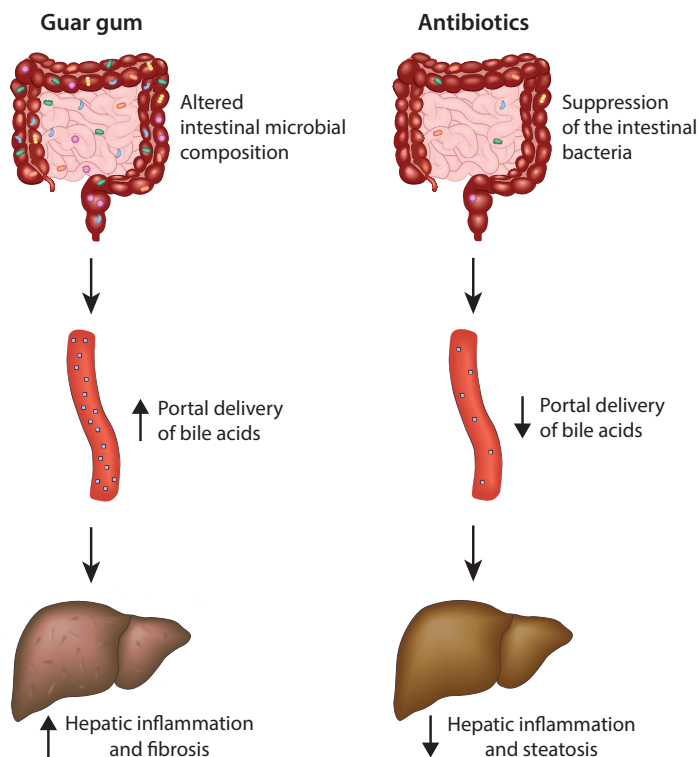


Figure 1. The intestinal microbiota impacts hepatic inflammation and fibrosis via changes in the portal delivery of bile acids

Stimulation of the gut microbiota using the highly fermentable dietary fiber guar gum enhanced hepatic inflammation and fibrosis, concurrent with elevated portal delivery of bile acids. By contrast, suppression of the gut bacteria using antibiotics reduced portal delivery of bile acids and attenuated hepatic inflammation and fibrosis. Suppression of the intestinal bacteria did not influence hepatic steatosis.

First, the lack of an effect of the antibiotics treatment on hepatic steatosis is highly intriguing (**Chapter 4**). Although we did find that the stimulation of the gut microbiota using guar gum reduced hepatic steatosis, this effect is likely a consequence of the lower bodyweight and is not due to changes in the gut microbiota. These data therefore imply that the gut microbiota are only involved in the more advanced stages of NAFLD, including hepatic inflammation and fibrosis, but not in hepatic steatosis *per se*. However, several studies do report an effect of the gut microbiota in hepatic steatosis (12, 15, 17). One possibility for this discrepancy may be the difference in intestinal microbial composition and/or function between the different studies. Indeed, the composition of the gut microbiota is influenced by many factors, including diet, age, gender, and genome (18–20), and can also vary substantially between different animal facilities (21). Consequently, the metabolites produced and released by the microbiota may be different, resulting in different effect on the liver. For example, Bergheim *et al.* found that hepatic steatosis was associated with an increased translocation of lipopolysaccharide (LPS) to the portal vein (12), whereas in our study plasma LPS levels were not different upon antibiotic treatment or guar gum feeding. Additionally, a difference in intestinal microbial composition may also indirectly influence hepatic steatosis, as the gut microbiota have also been reported to influence hepatic steatosis via intestinal FXR-mediated induction of ceramides (14). Despite the difference in microbial composition, it would be of great interest to identify the bacterial species responsible for the effects on NAFLD, which would allow for a better comparison of studies with different outcomes. Moreover, apart from the colonic microbiota, the study of the bacteria located in the small intestine in NAFLD also warrants further investigation, as small intestinal bacterial overgrowth is increasingly linked to the pathogenesis of NAFLD (22, 23).

Secondly, of particular importance is the mechanism by which the microbiota-mediated changes in bile acids induce NAFLD. In three independent studies we have demonstrated that bile acids influence the pathogenesis of NAFLD, but the mechanism underlying this effect is not exactly clear (**Chapter 4**). While we hypothesize that the increased portal delivery of bile acids promotes liver injury and subsequently hepatic inflammation and fibrosis, we cannot exclude a role for the nuclear receptor FXR. FXR is abundantly expressed in the liver and intestine and is thought to be the master regulator of bile acid metabolism. Indeed, mice lacking FXR have impaired bile acid synthesis, biliary bile acid secretion, and intestinal and hepatic uptake of bile acids (24, 25). Interestingly, FXR knockout mice also display hepatic inflammation and spontaneously develop hepatocellular carcinomas (26–28). Consistent with a suppressive effect of FXR on inflammation, activation of the FXR receptor using synthetic FXR ligands, including bile acid derivatives, was demonstrated to attenuate hepatic inflammation and fibrosis in animal models of NASH (29, 30). In fact, FXR agonists are currently under investigation in several clinical trials for the treatment

of patients with NAFLD (31). In our study, based on the expression of FXR-target genes in the liver and ileum, the increase hepatic inflammation and fibrosis upon guar gum feeding, was associated with increased FXR activation in the liver but reduced FXR activation in the ileum (**Chapter 4**). It could therefore be hypothesized that hepatic inflammation and fibrosis in mice fed guar gum is linked to the reduced activation of FXR specifically in the ileum. Indeed, inhibition of intestinal FXR by T β -MCA has been suggested to promote NAFLD (14). If the stimulation of NAFLD by bile acids is independent of FXR, then the question remains whether one bile acid in particular induces liver injury or whether the liver injury may be caused by the hepatic accumulation of the bile acids as a group. However, it is possible that the mechanism underlying the bile-acid induced NAFLD involves both FXR and intrahepatic accumulation of cytotoxic bile acids. To gain further insight, ideally an elaborate experiment should be performed using targeted deletion of enzymes involved in the production of the different bile acids species in the liver and the gut. In addition, studies using FXR knockout mice may also be helpful to understand underlying mechanisms.

Administration of specific bacterial species to treat NAFLD

The observation that the gut microbiota are causally involved in the development of NAFLD led us to hypothesize that targeting the gut microbiota may provide therapeutic tools to treat NAFLD (**Chapter 4**). In addition to bile acids, impairment of the intestinal barrier is also suggested to mediate the effects of the gut microbiota on NAFLD (9, 32). Recently, Rahman *et al.* demonstrated that mice with an impaired intestinal barrier develop more severe non-alcoholic steatohepatitis. Importantly, depletion of the gut bacteria using antibiotics abolished the difference in hepatic inflammation and fibrosis (33), further confirming an important role for the gut microbiota and their metabolites in NAFLD.

Therefore, in **Chapter 5**, we aimed to attenuate NAFLD in an obese mouse model of NAFLD by administrating bacterial species that have been suggested to improve the intestinal barrier, namely *Akkermansia muciniphila* and *Bacteroides thetaiotaomicron*. *A. muciniphila* and *B. thetaiotaomicron* are both gram-negative anaerobic bacteria that are able to degrade mucins in the mucus layer. As a result, mucin synthesis is stimulated and thinning of the mucus layer may be prevented (34–36). We found that daily administration of *A. muciniphila* and *B. thetaiotaomicron* for 5 weeks to mice with NAFLD did not alter intestinal permeability or features of NAFLD (**Chapter 5**). Although these data imply that *A. muciniphila* and *B. thetaiotaomicron* are not promising therapeutics to treat NAFLD, several aspects of this study merit consideration.

First of all, *B. thetaiotaomicron* was not able to colonize the colon after five weeks daily *B. thetaiotaomicron* administration (**Chapter 5**). Since *B. thetaiotaomicron* has been shown to very efficiently colonize the gastrointestinal tract of germ-free mice (37), it may

be hypothesized that *B. thetaiotaomicron* is rejected by the commensal microbiota, thereby limiting the effect of *B. thetaiotaomicron* on intestinal permeability. Developing strategies to improve the establishment of *B. thetaiotaomicron* in the recipients' gastrointestinal tract, should clarify whether *B. thetaiotaomicron* indeed has no effect on at least intestinal permeability or whether the results are explained by lack of effective colonization.

Secondly, in contrast to the standard high fat diet, the diet that we used also contains cholesterol and fructose, leading to a more advanced form of NAFLD (**Chapter 4**). Although *A. muciniphila* effectively colonized the colon, it is conceivable that the effect of diet on NAFLD overrules the potential effect of *A. muciniphila* on NAFLD. Alternatively, as the abundance of *A. muciniphila* increases upon bodyweight loss (38, 39), the decrease in bodyweight of all groups upon the start of the oral gavages (**Chapter 5**) might already have caused an increase in the abundance of *A. muciniphila*. Consequently, it may be possible that the relatively small increase in *A. muciniphila* abundance in the control group during the first week of oral gavages already influenced metabolic health of the host and that a further increase in *A. muciniphila* abundance did not have an additional effect. To avoid the potential interference caused by the frequent oral gavages, future studies should investigate how often *A. muciniphila* needs to be administered to effectively colonize the colon. Additionally, one could start with weekly oral gavages containing PBS at the start of the dietary intervention, in order to avoid a stress response at the start of the *A. muciniphila* administration.

Limitations and future perspectives of studying the gut microbiota

As already briefly mentioned, there is considerable controversy with respect to whether and how the gut microbiota influence metabolic health. For example, several studies have provided evidence that the gut microbiota are causally involved in the development of obesity (40–42), but there are also studies reporting no effect (43–45). Although it was not our initial research question, in **Chapter 4** and **Chapter 9** we also investigated the effect of the gut bacteria on the development of obesity. Interestingly, it was observed that suppression of the gut microbiota using antibiotics resulted in a lower final bodyweight than mice that were not treated with antibiotics. However, this effect was mainly accounted for by a reduction in food intake during the first two weeks of the dietary intervention, when the mice have to get used to the antibiotics. Subsequently, after these two weeks, the rate of bodyweight gain was not different between the mice that received or did not receive antibiotics, indicating that in our study the absence of bacteria does not protect against diet-induced obesity. With regard to glucose metabolism, many studies also suggest that gut microbiota influence glucose metabolism (40, 46, 47). For example, compared to conventionally-raised mice, germ-free mice were found to have an improved glucose tolerance, likely due to an improvement in insulin sensitivity (48). However, since many of these studies also report an effect on

bodyweight, it is unclear whether the effects on glucose metabolism are directly mediated by the gut microbiota, or indirectly via the difference in bodyweight. To circumvent effects of bodyweight on glucose metabolism, Carvalho *et al.* (49) and Membrez *et al.* (50) pair-fed mice and treated them with and without antibiotics. They found that suppression of the gut bacteria improved glucose tolerance. In **Chapter 9**, we also investigated the effect of gut bacteria on glucose tolerance. In our study we found that depletion of the gut bacteria using antibiotics reduced bodyweight gain, but surprisingly worsened glucose tolerance (**Chapter 9**).

A reasonable explanation for the apparent discrepancies between the various studies is the variation in gut bacterial composition and function between different mouse strains (51) and between different animal facilities (21, 52). Although differences in genotype explain some bacterial variation, it turns out that diet has a dominant role in shaping the gut microbial composition (53, 54). Yet even within the same facility, the bacterial community of the same mouse strains consuming identical diets may differ over subsequent generations (55). It can be hypothesized that these differences in bacterial communities may translate into different experimental outcomes. Indeed, two mice strains with the same genetic background from two different breeders were shown to either protect or to promote obesity, depending on their gut microbial composition (56). Furthermore, even with a similar gut microbial composition, the function of the microbiota may be different.

While animal studies point to a causal role for the gut microbiota in obesity-related metabolic disturbances, current causal evidence from human studies is limited. The advantage of animal studies is that multiple factors that may influence the gut microbiota can be controlled for. In humans, the bacterial community is influenced by a plethora of environmental factors. Indeed, recently 126 intrinsic and extrinsic factors were found to be associated with inter-individual variation of the gut microbiome (57). Interestingly, in four independent cross-sectional studies, an association between metabolic syndrome and the gut microbiota was found (2, 41, 58, 59). Strikingly, however, when these four studies were pooled and examined, no associations between BMI and bacterial composition could be observed. A possible explanation for the lack of an association may be the large difference in research design and methodology between the different studies, including the study populations, as well as the methodology used, including the DNA extraction method, the 16S region that is sequenced, and the sequencing platform used (60). In fact, it is estimated that to adequately assess a relationship between metabolic disease and the intestinal microbiota while correcting for confounding factors, a study should contain at least 1700 subjects (61).

A powerful method to study the potential causal relationship between microbiota and metabolic health in humans is fecal microbiota transplantation. To date, only one human study has performed fecal microbial transplantations to assess the relationship between

microbiota and metabolic syndrome. It was found that infusion of gut microbiota from lean subjects into individuals with metabolic syndrome significantly improved peripheral insulin sensitivity (62). Careful examination of the individual responses indicates that some individuals benefit from the treatment while others do not (62). These so-called responders and non-responders have also been observed in probiotic interventions (63). Because it has been suggested that the success of colonization increases if the bacterial species already exists in the recipient (64), one possible explanation might be that the individuals who do not respond to the treatment do not harbour some of the infused bacterial species and therefore have limited colonization. However, it should be realized that without proper replication studies in the same individuals, the concept of responders and non-responders is methodologically questionable.

To overcome the above mentioned limitations, it is critical that existing studies are repeated. This will help to determine whether the overall effects, such as induced by human fecal microbial transplantations, are consistent. As with the animals studies, repeating the human studies may help to identify bacterial species that are causally involved in or are beneficial to metabolic diseases. Subsequent targeted approaches involving modification of only one strain might give useful insight into the role of specific gut bacteria in obesity and related disturbances. Identification of these important bacterial strains might benefit from the quantification of the absolute abundance of bacterial species, instead of the relative abundance.

In addition to the bacteria, the gastrointestinal tract also harbours fungi, protozoa, viruses and archaea. In **Chapter 4** we observed an outgrowth of fungi upon antibiotic treatment. Accordingly, the observation that antibiotic treatment protects against features of NAFLD might not only be related to the gut bacteria but also to changes in the mycobiome. Moreover, the intestinal mycobiome has been found to be different between lean and obese individuals, which implies that at least the fungi may also have a modulating role in metabolic health (65). Therefore, future studies should also focus on these less prevalent inhabitants of the gastrointestinal tract.

Nevertheless, an important step in further elucidating the role of the gut microbiota in metabolic health would be to not solely look at the presence or absence of microbiota but also to determine their function. One approach would be to identify and isolate intestine-derived metabolites from portal blood of patients and rodents with various metabolic diseases and determine which metabolites have detrimental effects on host health, for example by adding these metabolites to *in vitro* cell culture systems and *ex vivo* models. Accordingly, targeted inhibition of the bacterial enzymes responsible for the production of these harmful metabolites might reveal novel targets for the treatment of metabolic diseases.

Liver slices as a model to study human liver

As mentioned in the previous sections, intestine-derived metabolites represent an important link between disturbances in the gut microbiota and NAFLD. Hence, the identification of these harmful metabolites might reveal novel therapeutic targets for NAFLD. To investigate if certain metabolites are harmful to the liver, an *in vivo* or *ex vivo* system that reflects the human liver is essential. In **Chapter 6**, we demonstrate the suitability and superiority of human liver slices over primary hepatocytes to study the human liver. By comparing whole genome expression profiles of human liver slices with the expression profiles of primary hepatocytes in response to activation of the nuclear receptor PPAR α , we reveal that the induction of gene expression by PPAR α is in general well captured by the two model system. On the contrary, downregulation of gene expression was almost exclusively observed in human PCLS, which was largely connected to cells of the immune system. These cells are present in PCLS, but absent in primary human hepatocytes (**Chapter 6**). Because the multicellular and structural organization is very well reflected in liver slices, this *ex vivo* model may provide a suitable *ex vivo* model for the screening of harmful and beneficial intestine-derived metabolites, but also to test pharmacological agents in liver diseases.

One disadvantage of liver slices, however, is that hepatic functionality declines quite rapidly once they are taken into culture. Hence, liver slices can be cultured for only a maximum of five days (66), which precludes the use of liver slices for long-term functional and toxicological studies. Alternatively, a novel technique that is increasingly used over the past few years are hepatic 3D spheroids, in which primary human hepatocytes are cultured as 3D microtissues (67). Based on whole proteome analysis, these primary human hepatocyte spheroids were shown to more closely resemble the donors' *in vivo* liver than primary human hepatocytes spheroids obtained from another donor, indicating that inter-individual variability is maintained (68). Importantly, as compared to liver slices, primary human hepatocytes spheroids have been shown to remain functional and viable for at least five weeks in culture (68, 69). Accordingly, co-culturing these primary human hepatocyte spheroids with non-parenchymal cells, including Kupffer cells, stellate cells and biliary cells allows for the study of complex diseases such as hepatic steatosis (68). However, the limited availability of primary human hepatocytes and non-parenchymal cells remains a problem. Therefore, current approaches attempt to generate hepatocytes from induced pluripotent stem cells (iPSC) (70, 71). The advantage of iPSC over primary human hepatocytes is that iPSC can be obtained from nearly any somatic cell including renal tubular cells from urine (72), keratinocytes (73) and hair follicle cell (74), all sources that are easily accessible and available. However, currently the differentiation of iPSC into hepatocytes is not optimal as the generated hepatocytes more closely resemble fetal-like hepatocytes than mature adult

hepatocytes (75, 76) and also have features of colon and fibroblast lineages (76). Despite current advances made in the development of 3D liver model systems, co-culturing hepatocytes with non-parenchymal cells in 3D spheroids probably does not very well resemble the architecture and ratio of hepatocytes to non-parenchymal cells of human liver *in vivo*. It is expected that the architecture and cell ratio will be better captured in liver slices. Accordingly, also disease states such as NAFLD are probably better reflected in liver slices obtained from patients with NAFLD than co-cultured primary cells obtained from NAFLD patients in 3D spheroids. Overall, human liver slices provide the closest representation of the *in vivo* human liver with all relevant cell types in the appropriate structural organization.

PPAR α and FXR as therapeutic targets for NAFLD

Approximately 25% of the patients with NAFLD have non-alcoholic steatohepatitis, of which approximately 20% will progress to cirrhosis (77). Weight loss and exercise are the most effective treatments for NAFLD. A large prospective study with biopsy-proven NASH showed that already a bodyweight loss of more than 5% significantly improved NAFLD activity score, whereas of the patients who lost more than 10% of their bodyweight 90% had NASH resolution and 45% had regression of fibrosis (78). However, lifestyle modifications are often very challenging and maintaining weight loss is difficult, which increases the need for pharmacological interventions. Although there are currently no approved drugs for NAFLD, several therapeutic targets, including PPAR α and FXR appear to be very promising.

In **Chapter 6**, we treated precision cut liver slices with the PPAR α agonist Wyl4643 to gain insight into the molecular function of PPAR α in human liver. We provide evidence that the response of the liver to activation of the nuclear receptor PPAR α is highly dependent on the interaction between hepatocytes and non-parenchymal cells. Since PPAR α is very weakly expressed in non-parenchymal cells (79, 80), and activation of PPAR α hepatocytes reduces the expression of immune-related genes in liver slices but not in primary hepatocytes, we hypothesized that the interaction between hepatocytes and non-parenchymal cells is essential for regulation of the immune response (**Chapter 6**). It remains, however, questionable how PPAR α activation in hepatocytes regulates gene expression in non-parenchymal cells. As PPAR α is a potent inducer of fatty acid oxidation (81, 82) and multiple genes involved in lipid metabolism were upregulated upon PPAR α activation (**Chapter 6**), one possible scenario is that PPAR α -induced fatty acid oxidation in hepatocytes reduced lipotoxicity which, together with induction of the unfolded protein response, reduces ER stress and consequently suppresses the immune response in non-parenchymal cells (83). Indeed, deletion of PPAR α in mice was shown to induce hepatic ER stress and promote fat storage in the liver upon high-fat feeding (84–86). Conversely, PPAR α activation in wild-type mice prevented ER stress and reduced hepatic steatosis and inflammation (86, 87).

Irrespective of the underlying mechanism, the marked immunosuppressive effect of PPAR α in human liver indicates that PPAR α may be a therapeutic target for NAFLD. To date, several clinical pilot studies have been conducted to assess the impact of PPAR α activation on NAFLD. Unfortunately, the activation of PPAR α using fibrates showed only mild effects on hepatic steatosis, inflammation and fibrosis (88, 89), which may likely be explained by reduced expression of PPAR α upon the progression of NAFLD in humans (90). Therefore current efforts attempt to develop novel synthetic PPAR α agonists with greater potency (91). In spite of solely activating PPAR α , activation of multiple PPAR isotypes may also be promising in the treatment of NAFLD. For example, the dual PPAR α / δ agonist GFT505 (Elafibranor), which is currently in phase II clinical trials, has been demonstrated to inhibit hepatic steatosis, inflammation and fibrosis in animal models and to lower dyslipidemia, liver function tests, and hepatic and peripheral insulin sensitivity in human subjects (92, 93).

In addition to PPAR agonists, activation of FXR also holds promise as novel therapeutic target for NAFLD. One FXR ligand that is especially promising is obeticholic acid (OCA). OCA is a semisynthetic derivative of the primary bile acid chenodeoxycholic acid (CDCA) that is 100-fold more potent in activating FXR than CDCA, the most potent natural FXR agonist (94). In animals models of diabetes and NAFLD, activation of FXR by OCA was shown to reverse insulin resistance and to improve liver dysfunction markers, hepatic steatosis and inflammation (95–98). In 2013, Mudaliar *et al.* performed the first proof of concept study in patients with NAFLD and type 2 diabetes and showed that OCA treatment improved insulin sensitivity and reduced markers of liver inflammation and fibrosis (99). More recently in the FLINT trial, administration of OCA to patients with NASH improved all histological features of NASH, including hepatic fibrosis, whereas improvement in NAFLD activity score occurred in only 21% of the patients treated with placebo, with no effect on fibrosis (100). OCA is currently being tested in phase III clinical trials, which hopefully will provide more evidence on the efficacy of OCA (NCT02548351, clinicaltrials.gov). In **Chapter 7**, we have for the first time investigated the effect of OCA on whole genome gene expression in human liver. It was found that human liver slices do maintain their ability to respond to FXR activation. More recently, OCA was shown to induce FXR-target genes in an *in vitro* model system of the human liver as well, but also activated anti-inflammatory and anti-fibrotic pathways (101). Although all these results are very promising, OCA treatment was also found to cause a striking increase in LDL cholesterol levels and a decrease in HDL cholesterol in both healthy subjects and patients with NASH (100, 102). It has been hypothesized that the increase in LDL cholesterol is related to downregulation of the LDL receptor and that the lower HDL cholesterol levels are mediated by the upregulation of the HDL scavenger receptor SR-B1 or a decrease in ApoA1 (102). However, in our study no difference in the expression of *SR-B1* or *APOA1* was found upon OCA treatment, while

expression of *LDLR* was induced (**Chapter 7**). Conversely, it may be possible that the lower *LDLR* mRNA levels are related to the elevated HDL cholesterol levels, as mice lacking *Ldlr* have elevated HDL levels (103). Irrespective of the underlying mechanism by which OCA influences plasma lipoprotein levels, long term studies are needed to investigate whether this dyslipidemia results in an increased cardiovascular disease risk, but also whether OCA treatment can reverse NASH-related cirrhosis.

Angptl4 and metabolic health

Angptl4 as regulator of bile acid metabolism

Disturbed lipid metabolism is an important risk factor for several metabolic diseases, including NAFLD and cardiovascular diseases (104). Hence, lipid metabolism is tightly regulated by a number of proteins, including ANGPTL4 (105, 106). ANGPTL4 regulates plasma triglyceride levels by inhibiting the activity of the enzyme lipoprotein lipase (107–111). Interestingly, bile acids and bile acid resins also have been shown to influence plasma triglyceride levels (112–116). Because we have observed that bile acids lower ANGPTL4 secretion by intestinal cells, in **Chapter 8**, we propose that the triglyceride-lowering effect of bile acids may be mediated by ANGPTL4. Although we found that ANGPTL4 is not required for the plasma triglyceride lowering action of bile acids, we unexpectedly observed that ANGPTL4 promotes bile acid uptake during taurocholic acid feeding concomitant with changes in the gut microbial composition (**Chapter 8**). In fact, we found that suppression of the gut microbiota using antibiotics abolished the difference in bile acid absorption between wild-type and *Angptl4*^{-/-} mice, indicating that ANGPTL4 reduces bile acid absorption via a mechanism that is dependent on the gut microbiota (**Chapter 8**).

Although it can be hypothesized that changes in the gut microbial composition caused by loss of ANGPTL4 directly impacts bile acid metabolism, it cannot be excluded that ANGPTL4 directly influences bile acid absorption via a mechanism that is dependent on the gut microbiota. Similarly, it is currently also unknown whether *Angptl4* locally produced in the intestine is responsible for the altered bile acid metabolism or whether the effect on bile acid uptake is related to ANGPTL4 produced elsewhere. Indeed, it has been suggested that intestinal- and liver-derived ANGPTL4 may have an endocrine function (40, 111, 117, 118). Downregulation of intestinal *Angptl4* expression by the gut microbiota has been proposed to promote peripheral fat storage by increasing adipose tissue lipoprotein lipase activity (40, 117). However, although we and others have observed that gut bacteria decreased intestinal *Angptl4* expression, this finding did not translate into an increased fat mass (43) (**Chapter 9**). Currently it is still unclear to what extent ANGPTL4 has an endocrine function, which is also hampered by the absence of proper functioning antibodies for murine ANGPTL4. Nonetheless, there is growing evidence that ANGPTL4 acts more locally than systemically

(119). In fact, it has been suggested that intestinal ANGPTL4 primarily targets pancreatic lipase to reduce fat absorption (120). Whether intestinal ANGPTL4 also locally targets the bile acid transporter SLC10A2 (ASBT) would merit further investigation using intestinal-specific *Angptl4*^{-/-} mice.

Additionally, it would be interesting to investigate whether ANGPTL4 also regulates bile acid absorption under other physiological conditions or during feeding of other primary bile acids. The majority of the difference in bile acid absorption between wild-type and *Angptl4*^{-/-} mice could be related to differences in the classical bile acid synthesis pathway, as the bile acids cholic acid and deoxycholic acid, and the expression of the bile acid synthesis enzymes *Cyp7a1* and *Cyp8b1*, were specifically altered between wild-type and *Angptl4*^{-/-} mice upon taurocholic acid feeding (**Chapter 8**). Accordingly, to gain further insight into the regulation of bile acid absorption by ANGPTL4 it would be interesting to know if feeding wild-type and *Angptl4*^{-/-} mice a bile acid synthesized by the alternative pathway, such as chenodeoxycholic acid, also leads to differences in bile acid absorption.

An intriguing question concerns the differences in bile acid levels in the presence and absence of the gut microbiota. In **Chapter 4** and **Chapter 8** we observed that antibiotic treatment reduced total level of plasma bile acids upon high fat feeding and during taurocholic acid supplementation, respectively. As expected, this decrease was mainly related to a decrease in deconjugated primary bile acids and secondary bile acids, as a consequence of the absence of intestinal microbes to metabolize primary bile acids. By contrast, there are also studies reporting an increase in plasma bile acids upon antibiotic treatment (121, 122). These differences may be explained by the different types of antibiotics used, which in turn differentially impact gut microbiota and bile acid metabolism, resulting in altered expression of the ileal bile acid transporter *Slc10a2* (*Asbt*) or hepatic bile acid transporter *Slc10a1* (*Ntcp*) (121–123). To gain further insight into underlying mechanism, it will be important to elucidate how the intestinal microbes affect ileal and hepatic bile acids transporters, as also differences in microbial composition in mice not treated with antibiotics could be responsible for the apparent differences in plasma bile acid levels.

Angptl4 as regulator of glucose metabolism

In **Chapter 9** we investigated the influence of ANGPTL4 on diet-induced obesity and metabolic dysfunction and reveal another novel function of ANGPTL4 in regulating glucose metabolism. Although we convincingly demonstrated that ANGPTL4 improved glucose metabolism by elevating plasma insulin levels via a mechanism that is partly dependent on the gut microbiota, our data did not shed light on the mechanism by which alterations in the gut microbiota composition elevated plasma insulin levels. Although glucose is the primary stimuli for pancreatic β -cells to secrete insulin (124), there are various factors that can

influence insulin secretion, including amino acids (125), fatty acids (126), gastrointestinal hormones (127), but also microbial-derived factors such as LPS (128, 129), short chain fatty acids (130, 131) and bile acids (132, 133). In **Chapter 9**, we propose that short chain fatty acids and LPS are probably not involved in conferring the effect of the gut microbiota on insulin levels in *Angptl4*^{-/-} mice. As bile acids are influenced by ANGPTL4 (**Chapter 8**), but also by the intestinal microbes (**Chapter 4**), it might be possible that bile acids link changes in gut microbiota to the elevated insulin secretion. In addition, many other bacterial-derived metabolites that were not quantified in our study or that are still unknown could play a role in mediating the effect of the gut microbiota on glucose metabolism. To study how changes in the gut microbiota composition and/or function may relate to an improved insulin secretion, it would be worthwhile to assess the functional profile of the intestinal microbes in wild-type and *Angptl4*^{-/-} mice. This can be achieved by predicting the bacterial function from 16s rRNA gene sequences using PICRUSt or by performing bacterial transcriptomics using RNA-seq. Combining one of these approaches with portal blood metabolomics of wild-type and *Angptl4*^{-/-} mice may reveal novel metabolites that are potentially involved in insulin secretion.

Angptl4 as modulator of gut microbial composition

An interesting question based on the data in **Chapter 8** and **Chapter 9** concerns the mechanism by which ANGPTL4 modifies the gut bacterial composition. One possibility is that the difference in host genotype shapes the gut microbial composition (134). Indeed, in our studies we found that mice lacking *Angptl4* had a lower relative abundance of the genus *Allobaculum* than wild-type mice, irrespective of whether the mice were fed a high fat diet, chow, or chow supplemented with taurocholic acid (**Chapter 8** and **Chapter 9**). However, the majority of the bacterial taxa that were different between wild-type and *Angptl4*^{-/-} mice was not consistently changed in the two studies (**Chapter 8** and **Chapter 9**), indicating that the effect of loss of ANGPTL4 on the gut microbiota is dependent on the diet. Given the established role of ANGPTL4 in intestinal lipid digestion (120) and the observation that elevated levels of lipids can markedly influence gut microbial composition (135, 136), it can be hypothesized that the origin of the difference in gut microbial composition between wild-type and *Angptl4*^{-/-} mice may be during suckling when the pups receive high amounts of lipid-containing milk. Alternatively, since we showed that ANGPTL4 impacts bile acid metabolism (**Chapter 8**), the difference in fecal bile acids may also have impacted the gut microbiota composition. Indeed, recently Watanabe *et al.* demonstrated that each free bile acid has a different bactericidal activity (137), indicating that different fecal bile acid levels result in a different bacterial composition. Alternatively, bile acids may also impact the gut microbiota indirectly through the intestinal immune system via the induction of ileal FXR-

mediated antimicrobial genes (138). Although we did not quantify fecal bile acid levels in **Chapter 9**, high fat diets are known to elevate bile secretion. It is thus possible that ANGPTL4 also regulates bile acid metabolism during high fat feeding and subsequently alters gut bacterial composition. Interestingly, not only bile acids, but also ANGPTL4 may influence microbial composition via differences in intestinal immunity. Recently, it was shown that *Angptl4*^{-/-} mice have increased leukocyte infiltration and inflammation in the colon upon DSS treatment, concurrent with differences in gut microbial composition (139). Future studies should clarify how ANGPTL4 influences the gut microbiota composition, for example by using intestine-specific *Angptl4*^{-/-} mice.

Gut microbiota, bile acids and Angptl4: a complex interplay

In this thesis, we have investigated the role of various mediators of metabolic health, including the gut microbiota, bile acids and ANGPTL4. We demonstrated that the gut microbiota likely plays an important role in the pathogenesis of NAFLD. Modulation of the gut microbiota was found to worsen features of NAFLD, whereas suppression of the gut bacteria protected against NAFLD, which was likely mediated via changes in the portal delivery of bile acids. Accordingly, we investigated whether it would be possible to treat

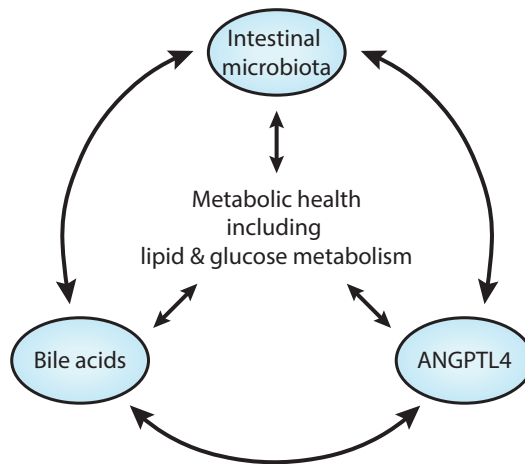


Figure 2. Model of the interaction between the intestinal microbiota, bile acids and ANGPTL4 and their influence on metabolic health

An intricate relationship exists between the intestinal microbiota, bile acids and ANGPTL4. Data presented in this thesis demonstrated that the intestinal microbiota influence bile acid metabolism but also vice versa as bile acids were also shown to alter the intestinal microbiota composition. In addition, we showed that the gut microbiota and bile acids alter intestinal *Angptl4* expression, but also that ANGPTL4 influences bile acid metabolism and intestinal microbial composition. Furthermore, previous studies and data presented in this manuscript have shown that all these three factors also influence metabolic health, including lipid and glucose metabolism and vice versa.

NAFLD by administrating specific bacteria to obese mice with NAFLD. It was found that, in our experimental setup, the bacteria *A. muciniphila* and *B. thetaiotaomicron* did not affect features of non-alcoholic fatty liver disease. Subsequently, we demonstrate the suitability of precision-cut liver slices to study the human liver. These studies highlight the possibility to study the response of the human liver to various gut-derived metabolites. Furthermore, we show that the triglyceride-lowering effects of bile acids is not mediated by ANGPTL4. Finally, we uncover two novel functions of ANGPTL4 in mediating bile acids absorption and glucose metabolism. Taken together, our studies have clarified and strengthened the role of the intestinal microbiota, bile acids and ANGPTL4 in metabolic health.

Moreover, we provide evidence for an intricate relationship between the intestinal microbiota, bile acids and ANGPTL4 (**Figure 2**). While intestinal *Angptl4* expression was found to be influenced by bile acids and the gut microbiota, we showed that ANGPTL4 also influences bile acid metabolism and the intestinal microbial composition (**Chapter 8** and **Chapter 9**). In addition, we showed that the gut microbiota influence bile acid metabolism (**Chapter 4** and **Chapter 8**), while vice versa bile acids are able to alter the gut microbial composition (**Chapter 8**). Although our studies have expanded our knowledge of the role of these mediators in metabolic diseases, there are still questions that need to be addressed. Since the intestinal microbiota, bile acids and ANGPTL4 are all interconnected and all have a role in lipid and glucose metabolism, it is important to realize that modulation of one of the three mediators likely also affects the other two mediators, including their metabolic responses (**Figure 2**).

References

- Karlsson, F. H., F. Fåk, I. Nookaew, V. Tremaroli, B. Fagerberg, D. Petranovic, F. Bäckhed, and J. Nielsen. 2012. Symptomatic atherosclerosis is associated with an altered gut metagenome. *Nat. Commun.* **3**: 1245.
- Qin, J., Y. Li, Z. Cai, S. Li, J. Zhu, F. Zhang, S. Liang, W. Zhang, Y. Guan, D. Shen, Y. Peng, D. Zhang, Z. Jie, W. Wu, Y. Qin, W. Xue, J. Li, L. Han, D. Lu, P. Wu, Y. Dai, X. Sun, Z. Li, A. Tang, S. Zhong, X. Li, W. Chen, R. Xu, M. Wang, Q. Feng, M. Gong, J. Yu, Y. Zhang, M. Zhang, T. Hansen, G. Sanchez, J. Raes, G. Falony, S. Okuda, M. Almeida, E. LeChatelier, P. Renault, N. Pons, J.-M. Batto, Z. Zhang, H. Chen, R. Yang, W. Zheng, S. Li, H. Yang, et al. 2012. A metagenome-wide association study of gut microbiota in type 2 diabetes. *Nature*. **490**: 55–60.
- Schwartz, A., D. Taras, K. Schäfer, S. Beijer, N. a Bos, C. Donus, and P. D. Hardt. 2010. Microbiota and SCFA in lean and overweight healthy subjects. *Obesity (Silver Spring)*. **18**: 190–195.
- Duncan, S. H., G. E. Lobley, G. Holtrop, J. Ince, A. M. Johnstone, P. Louis, and H. J. Flint. 2008. Human colonic microbiota associated with diet, obesity and weight loss. *Int. J. Obes.* **32**: 1720–1724.
- Lee, H., and G. Ko. 2014. Effect of Metformin on Metabolic Improvement and Gut Microbiota. *Appl. Environ. Microbiol.* **80**: 5935–5943.
- Mouzaki, M., E. M. Comelli, B. M. Arendt, J. Bonengel, S. K. Fung, S. E. Fischer, I. D. McGilvray, and J. P. Allard. 2013. Intestinal microbiota in patients with nonalcoholic fatty liver disease. *Hepatology*. **58**: 120–127.
- Leung, C., L. Rivera, J. B. Furness, and P. W. Angus. 2016. The role of the gut microbiota in NAFLD. *Nat. Rev. Gastroenterol. Hepatol.* **13**: 412–425.
- Fouts, D. E., M. Torralba, K. E. Nelson, D. A. Brenner, and B. Schnabl. 2012. Bacterial translocation and changes in the intestinal microbiome in mouse models of liver disease. *J. Hepatol.* **56**: 1283–1292.
- Jiang, W., N. Wu, X. Wang, Y. Chi, Y. Zhang, X. Qiu, Y. Hu, J. Li, and Y. Liu. 2015. Dysbiosis gut microbiota associated with inflammation and impaired mucosal immune function in intestine of humans with non-alcoholic fatty liver disease. *Sci. Rep.* **5**: 8096.
- De Minicis, S., C. Rychlicki, L. Agostinelli, S. Saccomanno, C. Candelaresi, L. Trozzi, E. Mingarelli, B. Facinelli, G. Magi, C. Palmieri, M. Marziani, A. Benedetti, and G. Svegliati-Baroni. 2014. Dysbiosis contributes to fibrogenesis in the course of chronic liver injury in mice. *Hepatology*. **59**: 1738–1749.
- Henao-Mejia, J., E. Elinav, C. Jin, L. Hao, W. Z. Mehal, T. Strowig, C. a Thaiss, A. L. Kau, S. C. Eisenbarth, M. J. Jurczak, J.-P. Camporez, G. I. Shulman, J. I. Gordon, H. M. Hoffman, and R. a Flavell. 2012. Inflammation-mediated dysbiosis regulates progression of NAFLD and obesity. *Nature*. **482**: 179–85.
- Bergheim, I., S. Weber, M. Vos, S. Krämer, V. Volynets, S. Kaserouni, C. J. McClain, and S. C. Bischoff. 2008. Antibiotics protect against fructose-induced hepatic lipid accumulation in mice: Role of endotoxin. *J. Hepatol.* **48**: 983–992.
- Lin, Y., L.-X. Yu, H.-X. Yan, W. Yang, L. Tang, H.-L. Zhang, Q. Liu, S.-S. Zou, Y.-Q. He, C. Wang, M.-C. Wu, and H.-Y. Wang. 2012. Gut-derived lipopolysaccharide promotes T-cell-mediated hepatitis in mice through Toll-like receptor 4. *Cancer Prev. Res. (Phila)*. **5**: 1090–102.
- Jiang, C., C. Xie, F. Li, L. Zhang, R. G. Nichols, K. W. Krausz, J. Cai, Y. Qi, Z. Fang, S. Takahashi, N. Tanaka, D. Desai, S. G. Amin, I. Albert, A. D. Patterson, and F. J. Gonzalez. 2015. Intestinal farnesoid X receptor signaling promotes nonalcoholic fatty liver disease. *J. Clin. Invest.* **125**: 386–402.
- Le Roy, T., M. Llopis, P. Lepage, A. Bruneau, S. Rabot, C. Bevilacqua, P. Martin, C. Philippe, F. Walker, A. Bado, G. Perlemuter, A.-M. Cassard-Doulcier, and P. Gérard. 2013. Intestinal microbiota determines development of non-alcoholic fatty liver disease in mice. *Gut*. **62**: 1787–94.
- Zhou, D., Q. Pan, F. Shen, H. Cao, W. Ding, Y. Chen, and J. Fan. 2017. Total fecal microbiota transplantation alleviates high-fat diet-induced steatohepatitis in mice via beneficial regulation of gut microbiota. *Sci. Rep.* **7**: 1529.
- Pappo, I., H. Becovier, E. M. Berry, and H. R. Freund. 1991. Polymyxin B reduces cecal flora, TNF production and hepatic steatosis during total parenteral nutrition in the rat. *J. Surg. Res.* **51**: 106–112.
- Sommer, F., and F. Bäckhed. 2013. The gut microbiota--masters of host development and physiology. *Nat. Rev. Microbiol.* **11**: 227–38.
- Wen, L., and A. Duffy. 2017. Factors Influencing the Gut Microbiota, Inflammation, and Type 2 Diabetes. *J. Nutr.* **147**: 1468S–1475S.
- David, L. a, C. F. Maurice, R. N. Carmody, D. B. Gootenberg, J. E. Button, B. E. Wolfe, A. V. Ling, a S. Devlin, Y. Varma, M. a Fischbach, S. B. Biddinger, R. J. Dutton, and P. J. Turnbaugh. 2014. Diet rapidly and reproducibly alters the human gut microbiome. *Nature*. **505**: 559–63.
- Rausch, P., M. Basic, A. Batra, S. C. Bischoff, M. Blaut, T. Clavel, J. Gläsner, S. Gopalakrishnan, G. A. Grassl, C. Günther, D. Haller, M. Hirose, S. Ibrahim, G. Loh, J. Mattner, S. Nagel, O. Pabst, F. Schmidt, B. Siegmund, T. Strowig, V. Volynets, S. Wirtz, S. Zeissig, Y. Zeissig, A. Bleich, and J. F. Baines. 2016.

- Analysis of factors contributing to variation in the C57BL/6J fecal microbiota across German animal facilities. *Int. J. Med. Microbiol.* **306**: 343–355.
22. Miele, L., V. Valenza, G. La Torre, M. Montalto, G. Cammarota, R. Ricci, R. Mascianà, A. Forgione, M. L. Gabrieli, G. Perotti, F. M. Vecchio, G. Rapaccini, G. Gasbarrini, C. P. Day, and A. Grieco. 2009. Increased intestinal permeability and tight junction alterations in nonalcoholic fatty liver disease. *Hepatology*. **49**: 1877–1887.
 23. Kapil, S., A. Duseja, B. K. Sharma, B. Singla, A. Chakraborti, A. Das, P. Ray, R. K. Dhiman, and Y. Chawla. 2016. Small intestinal bacterial overgrowth and toll like receptor signaling in patients with nonalcoholic fatty liver disease. *J. Gastroenterol. Hepatol.* **31**: 213–221.
 24. Eloranta, J. J., and G. A. Kullak-Ublick. 2008. The Role of FXR in Disorders of Bile Acid Homeostasis. *Physiology*. **23**: 286–295.
 25. Sinal, C. J., M. Tohkin, M. Miyata, J. M. Ward, G. Lambert, and F. J. Gonzalez. 2000. Targeted Disruption of the Nuclear Receptor FXR/BAR Impairs Bile Acid and Lipid Homeostasis. *Cell*. **102**: 731–744.
 26. Yang, F., X. Huang, T. Yi, Y. Yen, D. D. Moore, and W. Huang. 2007. Spontaneous development of liver tumors in the absence of the bile acid receptor farnesoid X receptor. *Cancer Res.* **67**: 863–867.
 27. Kim, I., K. Morimura, Y. Shah, Q. Yang, J. M. Ward, and F. J. Gonzalez. 2007. Spontaneous hepatocarcinogenesis in farnesoid X receptor-null mice. *Carcinogenesis*. **28**: 940–946.
 28. Wang, Y.-D., W.-D. Chen, M. Wang, D. Yu, B. M. Forman, and W. Huang. 2008. Farnesoid X receptor antagonizes nuclear factor κ B in hepatic inflammatory response. *Hepatology*. **48**: 1632–1643.
 29. Fiorucci, S., E. Antonelli, G. Rizzo, B. Renga, A. Mencarelli, L. Riccardi, S. Orlandi, R. Pellicciari, and A. Morelli. 2004. The nuclear receptor SHP mediates inhibition of hepatic stellate cells by FXR and protects against liver fibrosis. *Gastroenterology*. **127**: 1497–1512.
 30. Zhang, S., J. Wang, Q. Liu, and D. C. Harnish. 2009. Farnesoid X receptor agonist WAY-362450 attenuates liver inflammation and fibrosis in murine model of non-alcoholic steatohepatitis. *J. Hepatol.* **51**: 380–388.
 31. Arab, J. P., S. J. Karpen, P. A. Dawson, M. Arrese, and M. Trauner. 2017. Bile acids and nonalcoholic fatty liver disease: Molecular insights and therapeutic perspectives. *Hepatology*. **65**: 350–362.
 32. Bashiardes, S., H. Shapiro, S. Rozin, O. Shibolet, and E. Elinav. 2016. Non-alcoholic fatty liver and the gut microbiota. *Mol. Metab.* **5**: 782–794.
 33. Rahman, K., C. Desai, S. S. Iyer, N. E. Thorn, P. Kumar, Y. Liu, T. Smith, A. S. Neish, H. Li, S. Tan, P. Wu, X. Liu, Y. Yu, A. B. Farris, A. Nusrat, C. A. Parkos, and F. A. Anania. 2016. Loss of Junctional Adhesion Molecule A Promotes Severe Steatohepatitis in Mice on a Diet High in Saturated Fat, Fructose, and Cholesterol. *Gastroenterology*. **151**: 733–746.e12.
 34. Derrien, M., E. E. Vaughan, C. M. Plugge, and W. M. de Vos. 2004. *Akkermansia muciniphila* gen. nov., sp. nov., a human intestinal mucin-degrading bacterium. *Int. J. Syst. Evol. Microbiol.* **54**: 1469–1476.
 35. Everard, A., C. Belzer, L. Geurts, J. P. Ouwerkerk, C. Druart, L. B. Bindels, Y. Guiot, M. Derrien, G. G. Muccioli, N. M. Delzenne, W. M. de Vos, and P. D. Cani. 2013. Cross-talk between *Akkermansia muciniphila* and intestinal epithelium controls diet-induced obesity. *Proc. Natl. Acad. Sci. U. S. A.* **110**: 9066–71.
 36. Wrzosek, L., S. Miquel, M.-L. Noordine, S. Bouet, M. Joncquel Chevalier-Curt, V. Robert, C. Philippe, C. Bridonneau, C. Cherbuy, C. Robbe-Masselot, P. Langella, and M. Thomas. 2013. *Bacteroides thetaiotaomicron* and *Faecalibacterium prausnitzii* influence the production of mucus glycans and the development of goblet cells in the colonic epithelium of a gnotobiotic model rodent. *BMC Biol.* **11**: 61.
 37. Samuel, B. S., and J. I. Gordon. 2006. A humanized gnotobiotic mouse model of host-archaeal-bacterial mutualism. *Proc. Natl. Acad. Sci. U. S. A.* **103**: 10011–6.
 38. Zhang, H., J. K. DiBaise, a Zuccolo, D. Kudrna, M. Braidotti, Y. Yu, P. Parameswaran, M. D. Crowell, R. Wing, B. E. Rittmann, and R. Krajmalnik-Brown. 2009. Human gut microbiota in obesity and after gastric bypass. *Proc Natl Acad Sci U S A.* **106**: 2365–2370.
 39. Remely, M., I. Tesar, B. Hippe, S. Gnauer, P. Rust, and A. G. Haslberger. 2015. Gut microbiota composition correlates with changes in body fat content due to weight loss. *Benef. Microbes*. **6**: 431–439.
 40. Bäckhed, F., H. Ding, T. Wang, L. V Hooper, G. Y. Koh, A. Nagy, C. F. Semenkovich, and J. I. Gordon. 2004. The gut microbiota as an environmental factor that regulates fat storage. *Proc. Natl. Acad. Sci. U. S. A.* **101**: 15718–15723.
 41. Ridaura, V. K., J. J. Faith, F. E. Rey, J. Cheng, A. E. Duncan, A. L. Kau, N. W. Griffin, V. Lombard, B. Henrissat, J. R. Bain, M. J. Muehlbauer, O. Ilkayeva, C. F. Semenkovich, K. Funai, D. K. Hayashi, B. J. Lyle, M. C. Martini, L. K. Ursell, J. C. Clemente, W. Van Treuren, W. a Walters, R. Knight, C. B. Newgard, A. C. Heath, and J. I. Gordon. 2013. Gut microbiota from twins discordant for obesity modulate metabolism in mice. *Science*. **341**: 1241214.
 42. Murphy, E. F., P. D. Cotter, A. Hogan, O. O'Sullivan, A. Joyce, F. Fouhy, S. F. Clarke, T. M. Marques, P. W. O'Toole, C. Stanton, E. M. M. Quigley, C. Daly, P. R. Ross, R. M. O'Doherty, and F. Shanahan. 2013. Divergent metabolic outcomes arising from targeted manipulation of the gut microbiota in diet-induced

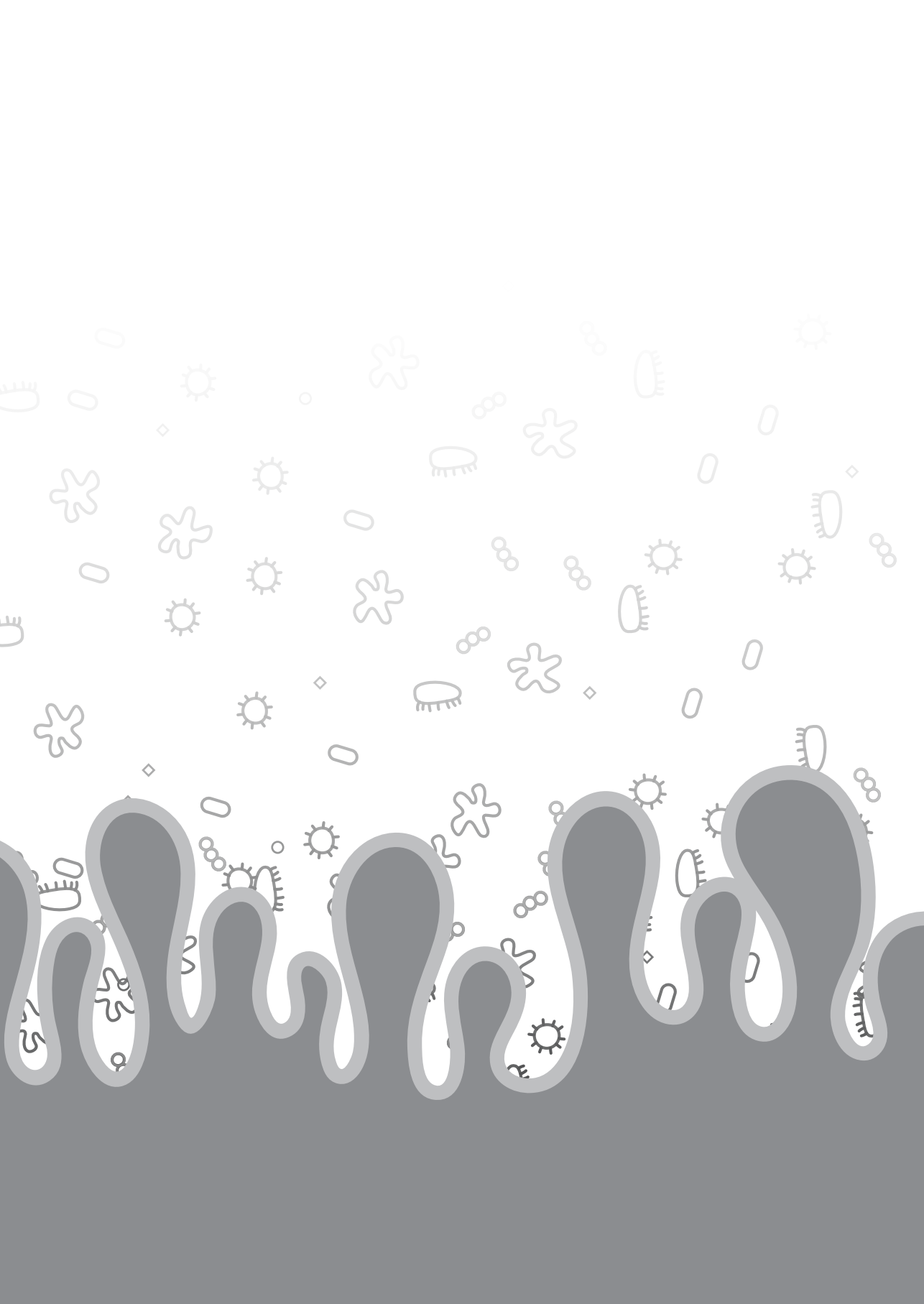
- obesity. *Gut*. **62**: 220–6.
43. Fleissner, C. K., N. Huebel, M. M. Abd El-Bary, G. Loh, S. Klaus, and M. Blaut. 2010. Absence of intestinal microbiota does not protect mice from diet-induced obesity. *Br J Nutr*. **104**: 919–929.
 44. Rabot, S., M. Membrez, F. Blancher, B. Berger, D. Moine, L. Krause, R. Bibiloni, A. Bruneau, P. Gérard, J. Siddharth, C. L. Lauber, and C. J. Chou. 2016. High fat diet drives obesity regardless the composition of gut microbiota in mice. *Sci. Rep.* **6**: 32484.
 45. Reijnders, D., G. H. Goossens, G. D. A. Hermes, E. P. J. G. Neis, C. M. van der Beek, J. Most, J. J. Holst, K. Lenaerts, R. S. Kootte, M. Nieuwdorp, A. K. Groen, S. W. M. Olde Damink, M. V. Boekschoten, H. Smidt, E. G. Zoetendal, C. H. C. Dejong, E. E. Blaak, F. Bäckhed, H. Ding, T. Wang, L. V. Hooper, G. Y. Koh, A. Nagy, C. F. Semenkovich, J. I. Gordon, D. Bates, M. Mächler, B. Bolker, S. Walker, G. V. Bech-Nielsen, C. H. Hansen, M. R. Hufeldt, D. S. Nielsen, B. Aasted, F. K. Vogensen, T. Midtvedt, A. K. Hansen, A. Brehm, M. Krssak, A. I. Schmid, P. Nowotny, W. Waldhäusl, M. Roden, J. R. Brestoff, D. Artis, C. A. Brighton, J. Rievaj, R. E. Kuhre, L. L. Glass, K. Schoonjans, et al. 2016. Effects of Gut Microbiota Manipulation by Antibiotics on Host Metabolism in Obese Humans: A Randomized Double-Blind Placebo-Controlled Trial. *Cell Metab.* **24**: 63–74.
 46. Caesar, R., C. S. Reigstad, H. K. Bäckhed, C. Reinhardt, M. Ketonen, G. Ö. Lundén, P. D. Cani, and F. Bäckhed. 2012. Gut-derived lipopolysaccharide augments adipose macrophage accumulation but is not essential for impaired glucose or insulin tolerance in mice. *Gut*. **61**: 1701–7.
 47. Cani, P. D., R. Bibiloni, C. Knauf, A. M. Neyrinck, and N. M. Delzenne. 2008. Changes in Gut Microbiota Control Metabolic Endotoxemia-Induced Inflammation in High-Fat Diet – Induced Obesity and Diabetes in Mice. *Diabetes*. **57**: 1470–1481.
 48. Rabot, S., M. Membrez, A. Bruneau, P. Gérard, T. Harach, M. Moser, F. Raymond, R. Mansourian, and C. J. Chou. 2010. Germ-free C57BL/6J mice are resistant to high-fat-diet-induced insulin resistance and have altered cholesterol metabolism. *FASEB J*. **24**: 4948–59.
 49. Carvalho, B. M., D. Guadagnini, D. M. L. Tsukumo, a a Schenka, P. Latuf-Filho, J. Vassallo, J. C. Dias, L. T. Kubota, J. B. C. Carvalheira, and M. J. a Saad. 2012. Modulation of gut microbiota by antibiotics improves insulin signalling in high-fat fed mice. *Diabetologia*. **55**: 2823–34.
 50. Membrez, M., F. Blancher, M. Jaquet, R. Bibiloni, P. D. Cani, R. G. Burcelin, I. Corthesy, K. Macé, and C. J. Chou. 2008. Gut microbiota modulation with norfloxacin and ampicillin enhances glucose tolerance in mice. *FASEB J*. **22**: 2416–26.
 51. Kreznar, J. H., M. P. Keller, L. L. Traeger, M. E. Rabaglia, K. L. Schueler, D. S. Stapleton, W. Zhao, E. I. Vivas, B. S. Yandell, A. T. Broman, B. Hagenbuch, A. D. Attie, and F. E. Rey. 2017. Host Genotype and Gut Microbiome Modulate Insulin Secretion and Diet-Induced Metabolic Phenotypes. *Cell Rep.* **18**: 1739–1750.
 52. Friswell, M. K., H. Gika, I. J. Stratford, G. Theodoridis, B. Telfer, I. D. Wilson, and A. J. McBain. 2010. Site and strain-specific variation in gut microbiota profiles and metabolism in experimental mice. *PLoS One*. **5**: 1–9.
 53. Carmody, R. N., G. K. Gerber, J. M. Luevano, D. M. Gatti, L. Somes, K. L. Svenson, and P. J. Turnbaugh. 2015. Diet Dominates Host Genotype in Shaping the Murine Gut Microbiota. *Cell Host Microbe*. **17**: 72–84.
 54. Zhang, C., M. Zhang, S. Wang, R. Han, Y. Cao, W. Hua, Y. Mao, X. Zhang, X. Pang, C. Wei, G. Zhao, Y. Chen, and L. Zhao. 2010. Interactions between gut microbiota, host genetics and diet relevant to development of metabolic syndromes in mice. *ISME J*. **4**: 232–41.
 55. Choo, J. M., P. J. Trim, L. E. X. Leong, G. C. J. Abell, C. Brune, N. Jeffries, S. Wesselingh, T. N. Dear, M. F. Snel, and G. B. Rogers. 2017. Inbred Mouse Populations Exhibit Intergenerational Changes in Intestinal Microbiota Composition and Function Following Introduction to a Facility. *Front. Microbiol.* **8**: 1–14.
 56. Ussar, S., N. W. Griffin, O. Bezy, L. Bry, J. I. Gordon, C. R. Kahn, S. Ussar, N. W. Griffin, O. Bezy, S. Fujisaka, S. Vienberg, S. Softic, and L. Deng. 2015. Interactions between Gut Microbiota , Host Genetics and Diet Modulate the Predisposition to Obesity and Metabolic Syndrome. *Cell Metab.* **22**: 1–15.
 57. Zhernakova, A., A. Kurilshikov, M. J. Bonder, E. F. Tigchelaar, M. Schirmer, T. Vatanen, Z. Mujagic, A. V. Vila, G. Falony, S. Vieira-Silva, J. Wang, F. Imhann, E. Brandsma, S. A. Jankipersadsing, M. Joossens, M. C. Enit, P. Deelen, M. A. Swertz, R. K. Weersma, E. J. M. Feskens, M. G. Netea, D. Gevers, D. Jonkers, L. Franke, Y. S. Aulchenko, C. Huttenhower, J. Raes, M. H. Hofker, R. J. Xavier, C. Wijmenga, and J. Fu. 2016. Population-based metagenomics analysis reveals markers for gut microbiome composition and diversity. *Science (80-.)*. **352**: 565–569.
 58. Karlsson, F. H., V. Tremaroli, I. Nookaew, G. Bergstrom, C. J. Behre, B. Fagerberg, J. Nielsen, and F. Bäckhed. 2013. Gut metagenome in European women with normal, impaired and diabetic glucose control. *Nature*. **498**: 99–103.
 59. Le Chatelier, E., T. Nielsen, J. Qin, E. Prifti, F. Hildebrand, G. Falony, M. Almeida, M. Arumugam, J.-M. Batto, S. Kennedy, P. Leonard, J. Li, K. Burgdorf, N. Grarup, T. Jørgensen, I. Brandlund, H. B. Nielsen, A.

- S. Juncker, M. Bertalan, F. Levenez, N. Pons, S. Rasmussen, S. Sunagawa, J. Tap, S. Tims, E. G. Zoetendal, S. Brunak, K. Clément, J. Doré, M. Kleerebezem, K. Kristiansen, P. Renault, T. Sicheritz-Ponten, W. M. de Vos, J.-D. Zucker, J. Raes, T. Hansen, P. Bork, J. Wang, S. D. Ehrlich, and O. Pedersen. 2013. Richness of human gut microbiome correlates with metabolic markers. *Nature*. **500**: 541–6.
60. Finucane, M. M., T. J. Sharpton, T. J. Laurent, and K. S. Pollard. 2014. A taxonomic signature of obesity in the microbiome? Getting to the guts of the matter. *PLoS One*. **9**: e84689.
61. Falony, G., M. Joossens, S. Vieira-Silva, J. Wang, Y. Darzi, K. Faust, A. Kurilshikov, M. J. Bonder, M. Valles-Colomer, D. Vandeputte, R. Y. Tito, S. Chaffron, L. Rymenans, C. Verspecht, L. De Sutter, G. Lima-Mendez, K. Dhoe, K. Jonckheere, D. Homola, R. Garcia, E. F. Tigchelaar, L. Eeckhaut, J. Fu, L. Henckaerts, A. Zhernakova, C. Wijmenga, and J. Raes. 2016. Population-level analysis of gut microbiome variation. *Science* (80-.). **352**: 560–564.
62. Vrieze, A., E. Van Nood, F. Holleman, J. Salojärvi, R. S. Kootte, J. F. W. M. Bartelsman, G. M. Dallinga-Thie, M. T. Ackermans, M. J. Serlie, R. Oozeer, M. Derrien, A. Druesne, J. E. T. Van Hylckama Vlieg, V. W. Bloks, A. K. Groen, H. G. H. J. Heilig, E. G. Zoetendal, E. S. Stroses, W. M. de Vos, J. B. L. Hoekstra, and M. Nieuwdorp. 2012. Transfer of intestinal microbiota from lean donors increases insulin sensitivity in individuals with metabolic syndrome. *Gastroenterology*. **143**: 913–6.
63. Reid, G., E. Gaudier, F. Guarner, G. B. Huffnagle, J. M. Macklaim, A. M. Munoz, M. Martini, T. Ringel-Kulka, B. Sartor, R. Unal, K. Verbeke, J. Walter, and International Scientific Association for Probiotics. 2010. Responders and non-responders to probiotic interventions: how can we improve the odds? *Gut Microbes*. **1**: 200–204.
64. Li, S. S., A. Zhu, V. Benes, P. I. Costea, R. Hercog, F. Hildebrand, J. Huerta-cepas, M. Nieuwdorp, J. Salojärvi, and A. Y. Voigt. 2016. Durable coexistence of donor and recipient strains after fecal microbiota transplantation. *Science* (80-.). **352**: 586–590.
65. Mar Rodríguez, M., D. Pérez, F. Javier Chaves, E. Esteve, P. Marin-Garcia, G. Xifra, J. Vendrell, M. Jové, R. Pamplona, W. Ricart, M. Portero-Otin, M. R. Chacón, and J. M. Fernández Real. 2015. Obesity changes the human gut mycobiome. *Sci. Rep.* **5**: 14600.
66. Starokozhko, V., S. Vatakuti, and B. Schievink. 2017. Maintenance of drug metabolism and transport functions in human precision-cut liver slices during prolonged incubation for 5 days. *Arch. Toxicol.* **91**: 2079–2092.
67. Lauschke, V. M., D. F. G. Hendriks, C. C. Bell, T. B. Andersson, and M. Ingelman-Sundberg. 2016. Novel 3D Culture Systems for Studies of Human Liver Function and Assessments of the Hepatotoxicity of Drugs and Drug Candidates. *Chem. Res. Toxicol.* **29**: 1936–1955.
68. Bell, C. C., D. F. Hendriks, S. M. Moro, E. Ellis, J. Walsh, A. Renblom, L. Fredriksson Puigvert, A. C. Dankers, F. Jacobs, J. Snoeys, R. L. Sison-Young, R. E. Jenkins, A. Nordling, S. Mkrtchian, B. K. Park, N. R. Kitteringham, C. E. Goldring, V. M. Lauschke, and M. Ingelman-Sundberg. 2016. Characterization of primary human hepatocyte spheroids as a model system for drug-induced liver injury, liver function and disease. *Sci. Rep.* **6**: 25187.
69. Messner, S., I. Agarkova, W. Moritz, and J. M. Kelm. 2013. Multi-cell type human liver microtissues for hepatotoxicity testing. *Arch. Toxicol.* **87**: 209–213.
70. Sauer, V., N. Roy-Chowdhury, C. Guha, and J. Roy-Chowdhury. 2014. Induced pluripotent stem cells as a source of hepatocytes. *Curr. Pathobiol. Rep.* **2**: 11–20.
71. Palakkan, A. A., J. Nanda, and J. A. Ross. 2017. Pluripotent stem cells to hepatocytes, the journey so far. *Biomed. reports*. **6**: 367–373.
72. Zhou, T., C. Benda, S. Duzinger, Y. Huang, X. Li, Y. Li, X. Guo, G. Cao, S. Chen, L. Hao, Y.-C. Chan, K.-M. Ng, J. C. Ho, M. Wieser, J. Wu, H. Redl, H.-F. Tse, J. Grillari, R. Grillari-Voglauer, D. Pei, and M. A. Esteban. 2011. Generation of induced pluripotent stem cells from urine. *J. Am. Soc. Nephrol.* **22**: 1221–8.
73. Piao, Y., S. S.-C. Hung, S. Y. Lim, R. C.-B. Wong, and M. S. . Ko. 2014. Efficient Generation of Integration-Free Human Induced Pluripotent Stem Cells From Keratinocytes by Simple Transfection of Episomal Vectors. *Stem Cells Transl. Med.* **3**: 787–791.
74. Lim, S. J., S. C. Ho, P. L. Mok, K. L. Tan, A. H. K. Ong, and S. C. Gan. 2016. Induced pluripotent stem cells from human hair follicle keratinocytes as a potential source for *in vitro* hair follicle cloning. *PeerJ*. **4**: e2695.
75. Baxter, M., S. Withey, S. Harrison, C. P. Segeritz, F. Zhang, R. Atkinson-Dell, C. Rowe, D. T. Gerrard, R. Sison-Young, R. Jenkins, J. Henry, A. A. Berry, L. Mohamet, M. Best, S. W. Fenwick, H. Malik, N. R. Kitteringham, C. E. Goldring, K. Piper Hanley, L. Vallier, and N. A. Hanley. 2015. Phenotypic and functional analyses show stem cell-derived hepatocyte-like cells better mimic fetal rather than adult hepatocytes. *J. Hepatol.* **62**: 581–589.
76. Godoy, P., W. Schmidt-Heck, K. Natarajan, B. Lucendo-Villarin, D. Szkolnicka, A. Asplund, P. Björquist, A. Widera, R. Stöber, G. Campos, S. Hammad, A. Sachinidis, U. Chaudhari, G. Damm, T. S. Weiss, A. Nüssler, J. Synnergren, K. Edlund, B. Küppers-Munther, D. C. Hay, and J. G. Hengstler. 2015. Gene

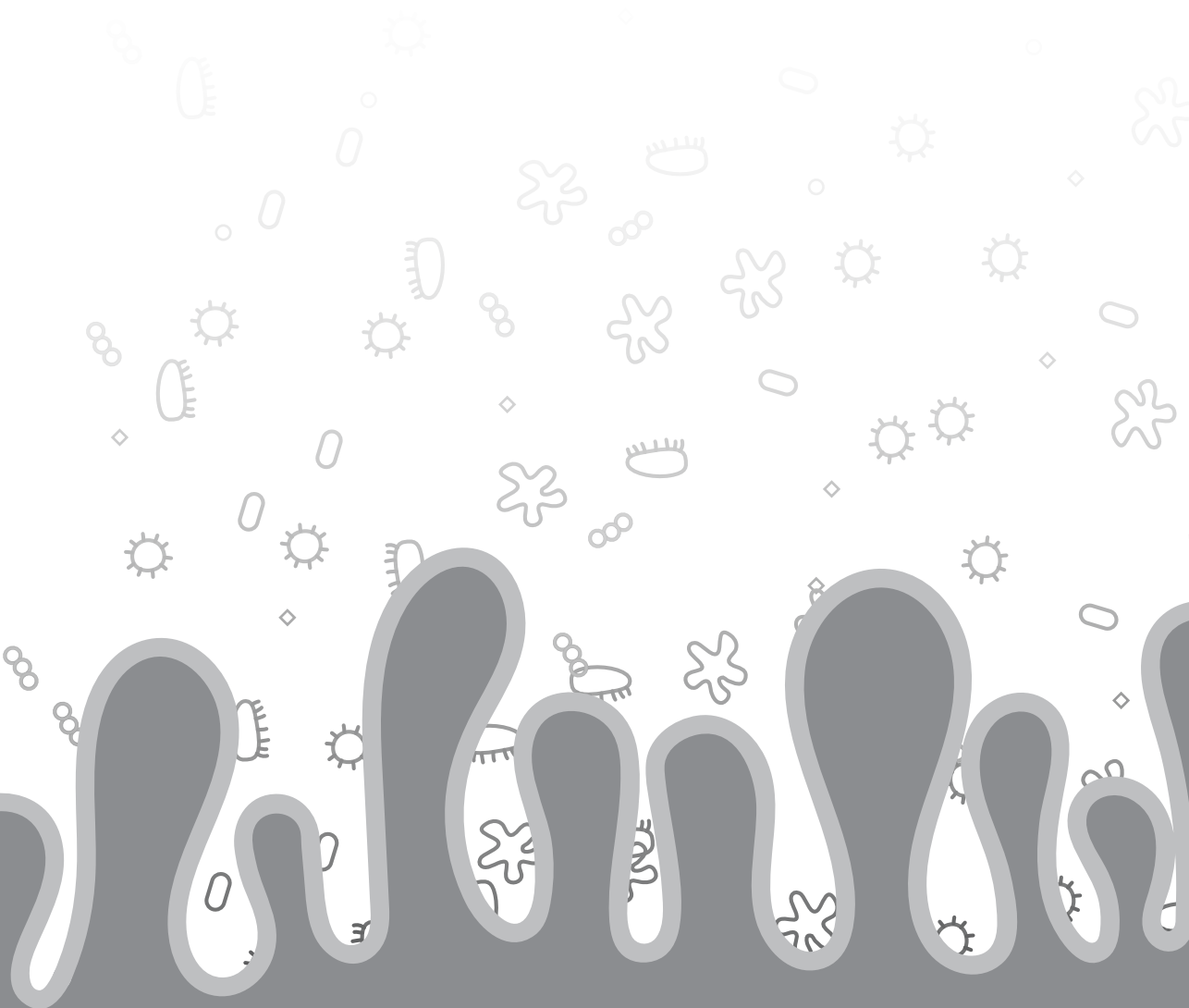
- networks and transcription factor motifs defining the differentiation of stem cells into hepatocyte-like cells. *J. Hepatol.* **63**: 934–942.
77. Rinella, M. E. 2015. Nonalcoholic Fatty Liver Disease: a systematic review. *Jama.* **313**: 2263–2273.
 78. Vilar-Gomez, E., Y. Martinez-Perez, L. Calzadilla-Bertot, A. Torres-Gonzalez, B. Gra-Oramas, L. Gonzalez-Fabian, S. L. Friedman, M. Diago, and M. Romero-Gomez. 2015. Weight loss through lifestyle modification significantly reduces features of nonalcoholic steatohepatitis. *Gastroenterology.* **149**: 367–378.e5.
 79. Peters, J. M., I. Rusyn, M. L. Rose, F. J. Gonzalez, and R. G. Thurman. 2000. Peroxisome proliferator-activated receptor alpha is restricted to hepatic parenchymal cells, not Kupffer cells: implications for the mechanism of action of peroxisome proliferators in hepatocarcinogenesis. *Carcinogenesis.* **21**: 823–826.
 80. Szalowska, E., H. a Tesfay, S. a F. T. van Hijum, and S. Kersten. 2014. Transcriptomic signatures of peroxisome proliferator-activated receptor α (PPAR α) in different mouse liver models identify novel aspects of its biology. *BMC Genomics.* **15**: 1106.
 81. Kersten, S., J. Seydoux, J. M. Peters, F. J. Gonzalez, B. Desvergne, and W. Wahli. 1999. Peroxisome proliferator – activated receptor α mediates the adaptive response to fasting. **103**: 1489–1498.
 82. Hashimoto, T., W. S. Cook, C. Qi, A. V. Yeldandi, J. K. Reddy, and M. S. Rao. 2000. Defect in peroxisome proliferator-activated receptor α -inducible fatty acid oxidation determines the severity of hepatic steatosis in response to fasting. *J. Biol. Chem.* **275**: 28918–28928.
 83. Zhang, J., K. Zhang, Z. Li, and B. Guo. 2016. ER Stress-induced Inflammasome Activation Contributes to Hepatic Inflammation and Steatosis. *J. Clin. Cell. Immunol.* **7**: 457.
 84. Ip, E., G. C. Farrell, G. Robertson, P. Hall, R. Kirsch, and I. Leclercq. 2003. Central role of PPAR α -dependent hepatic lipid turnover in dietary steatohepatitis in mice. *Hepatology.* **38**: 123–132.
 85. Stienstra, R., S. Mandard, D. Patouris, C. Maass, S. Kersten, and M. Müller. 2007. Peroxisome proliferator-activated receptor alpha protects against obesity-induced hepatic inflammation. *Endocrinology.* **148**: 2753–63.
 86. Su, Q., C. Baker, P. Christian, M. Naples, X. Tong, K. Zhang, M. Santha, and K. Adeli. 2014. Hepatic mitochondrial and ER stress induced by defective PPAR α signaling in the pathogenesis of hepatic steatosis. *Am. J. Physiol. - Endocrinol. Metab.* **306**: E1264–73.
 87. Ip, E., G. Farrell, P. Hall, G. Robertson, and I. Leclercq. 2004. Administration of the Potent PPAR α Agonist, Wy-14,643, Reverses Nutritional Fibrosis and Steatohepatitis in Mice. *Hepatology.* **39**: 1286–1296.
 88. Laurin, J., K. D. Lindor, J. S. Crippin, A. Gossard, G. J. Gores, J. Ludwig, J. Rakela, and D. B. McGill. 1996. Ursodeoxycholic Acid or Clofibrate in the Treatment of Non – Alcohol-Induced Steatohepatitis : A Pilot Study. *Hepatology.* 1464–1467.
 89. Fernández-Miranda, C., M. Pérez-Carreras, F. Colina, G. López-Alonso, C. Vargas, and J. A. Solís-Herruzo. 2008. A pilot trial of fenofibrate for the treatment of non-alcoholic fatty liver disease. *Dig. Liver Dis.* **40**: 200–205.
 90. Francque, S., A. Verrijken, S. Caron, J. Prawitt, R. Paumelle, B. Derudas, P. Lefebvre, M. R. Taskinen, W. Van Hul, I. Mertens, G. Hubens, E. Van Marck, P. Michielsens, L. Van Gaal, and B. Staels. 2015. PPAR α gene expression correlates with severity and histological treatment response in patients with non-alcoholic steatohepatitis. *J. Hepatol.* **63**: 164–173.
 91. Fruchart, J. 2013. Selective peroxisome proliferator-activated receptor α modulators (SPPARM α): the next generation of peroxisome proliferator-activated receptor α -agonists. *Cardiovasc. Diabetol.* **12**: 82.
 92. Staels, B., A. Rubenstrunk, B. Noel, G. Rigou, P. Delataille, L. J. Millatt, M. Baron, A. Lucas, A. Tailleux, D. W. Hum, V. Ratzin, B. Cariou, and R. Hanf. 2013. Hepatoprotective effects of the dual peroxisome proliferator-activated receptor alpha/delta agonist, GFT505, in rodent models of nonalcoholic fatty liver disease/nonalcoholic steatohepatitis. *Hepatology.* **58**: 1941–1952.
 93. Cariou, B., Y. Zaïr, B. Staels, and E. Bruckert. 2011. Effects of the new dual PPAR α / δ agonist GFT505 on lipid and glucose homeostasis in abdominally obese patients with combined dyslipidemia or impaired glucose metabolism. *Diabetes Care.* **34**: 2008–2014.
 94. Pellicciari, R., S. Fiorucci, E. Camaioni, C. Clerici, G. Costantino, P. R. Maloney, A. Morelli, D. J. Parks, and T. M. Willson. 2002. 6 α -Ethyl-Chenodeoxycholic Acid (6-ECDCA), a Potent and Selective FXR Agonist Endowed with Anticholestatic Activity. *J. Med. Chem.* **45**: 3569–3572.
 95. Wang, Y., W. Chen, M. Wang, D. Yu, and B. M. Forman. 2008. Farnesoid X receptor antagonizes NF-kB in hepatic inflammatory response. *Hepatology.* **48**: 1632–1643.
 96. Mencarelli, A., B. Renga, M. Migliorati, S. Cipriani, E. Distrutti, L. Santucci, and S. Fiorucci. 2009. The bile acid sensor farnesoid X receptor is a modulator of liver immunity in a rodent model of acute hepatitis. *J. Immunol.* **183**: 6657–6666.
 97. Cipriani, S., A. Mencarelli, G. Palladino, and S. Fiorucci. 2010. FXR activation reverses insulin resistance and lipid abnormalities and protects against liver steatosis in Zucker (fa/fa) obese rats. *J. Lipid Res.* **51**: 771–784.

- 286

- F. Veenman, W. Wahli, M. Müller, and S. Kersten. 2004. The direct peroxisome proliferator-activated receptor target fasting-induced adipose factor (FIAF/PGAR/ANGPTL4) is present in blood plasma as a truncated protein that is increased by fenofibrate treatment. *J. Biol. Chem.* **279**: 34411–34420.
119. Dijk, W., and S. Kersten. 2014. Regulation of lipoprotein lipase by Angptl4. *Trends Endocrinol. Metab.* **25**: 146–55.
 120. Mattijssen, F., S. Alex, H. J. Swarts, A. K. Groen, E. M. van Schothorst, and S. Kersten. 2014. Angptl4 serves as an endogenous inhibitor of intestinal lipid digestion. *Mol. Metab.* **3**: 135–144.
 121. Out, C., J. V. Patankar, M. Doktorova, M. Boesjes, T. Bos, S. de Boer, R. Havinga, H. Wolters, R. Boverhof, T. H. van Dijk, A. Smoczek, A. Bleich, V. Sachdev, D. Kratky, F. Kuipers, H. J. Verkade, and A. K. Groen. 2015. Gut microbiota inhibit Asbt-dependent intestinal bile acid reabsorption via Gata4. *J. Hepatol.* **63**: 697–704.
 122. Li, Y., M. J. Hafey, H. Duong, R. Evers, K. Cheon, D. J. Holder, A. Galijatovic-Idrizbegovic, F. D. Sistare, and W. E. Glaab. 2017. Antibiotic-induced Elevations of Plasma Bile Acids in Rats Independent of Bsep Inhibition. *Toxicol. Sci.* **157**: kfx015.
 123. Zhang, Y., P. B. Limaye, H. J. Renaud, and C. D. Klaassen. 2014. Effect of various antibiotics on modulation of intestinal microbiota and bile acid profile in mice. *Toxicol. Appl. Pharmacol.* **277**: 138–145.
 124. Komatsu, M., M. Takei, H. Ishii, and Y. Sato. 2013. Glucose-stimulated insulin secretion: A newer perspective. *J. Diabetes Investig.* **4**: 511–516.
 125. Newsholme, P., L. Brennan, B. Rubi, and P. Maechler. 2005. New insights into amino acid metabolism, β -cell function and diabetes. *Clin. Sci.* **108**: 185–194.
 126. Nolan, C. J., M. S. R. Madiraju, V. Delghingaro-Augusto, M.-L. Peyot, and M. Prentki. 2006. Fatty Acid Signaling in the β -Cell and Insulin Secretion. *Diabetes*. **55**: S16–S23.
 127. Drucker, D. J. 2007. The role of gut hormones in glucose homeostasis. *J. Clin. Invest.* **117**: 24–32.
 128. Nguyen, A. T., S. Mandard, C. Dray, V. Deckert, P. Valet, P. Besnard, D. J. Drucker, L. Lagrost, and J. Grober. 2014. Lipopolysaccharides-mediated increase in glucose-stimulated insulin secretion: Involvement of the GLP-1 pathway. *Diabetes*. **63**: 471–482.
 129. Amyot, J., M. Semache, M. Ferdaoussi, G. Fontés, and V. Poitout. 2012. Lipopolysaccharides impair insulin gene expression in isolated islets of langerhans via toll-like receptor-4 and NF- κ B signalling. *PLoS One*. **7**: e36200.
 130. Priyadarshini, M., S. R. Villa, M. Fuller, B. Wicksteed, C. R. Mackay, T. Alquier, V. Poitout, H. Mancebo, R. G. Mirmira, A. Gilchrist, and B. T. Layden. 2015. An Acetate-Specific GPCR, FFAR2, Regulates Insulin Secretion. *Mol. Endocrinol.* **29**: 1055–66.
 131. Perry, R. J., L. Peng, N. A. Barry, G. W. Cline, D. Zhang, R. L. Cardone, K. F. Petersen, R. G. Kibbey, A. L. Goodman, and G. I. Shulman. 2016. Acetate mediates a microbiome–brain– β -cell axis to promote metabolic syndrome. *Nature*. **534**: 213–217.
 132. Kumar, D. P., S. Rajagopal, S. Mahavadi, F. Mirshahi, J. R. Grider, K. S. Murthy, and A. J. Sanyal. 2012. Activation of transmembrane bile acid receptor TGR5 stimulates insulin secretion in pancreatic β cells. *Biochem. Biophys. Res. Commun.* **427**: 600–605.
 133. Renga, B., A. Mencarelli, P. Vavassori, V. Brancialeone, and S. Fiorucci. 2010. The bile acid sensor FXR regulates insulin transcription and secretion. *Biochim. Biophys. Acta - Mol. Basis Dis.* **1802**: 363–372.
 134. Goodrich, J., J. Waters, A. Poole, J. Sutter, O. Koren, R. Blekman, M. Beaumont, W. Van Treuren, R. Knight, J. Bell, T. Spector, A. Clark, and R. E. Ley. 2014. Human genetics shape the gut microbiome. *Cell*. **159**: 789–799.
 135. Robinson, D. T., and M. S. Caplan. 2015. Linking fat intake, the intestinal microbiome, and necrotizing enterocolitis in premature infants. *Pediatr. Res.* **77**: 121–6.
 136. Huang, E. Y., V. A. Leone, S. Devkota, Y. Wang, M. J. Brady, and E. B. Chang. 2013. Composition of dietary fat source shapes gut microbiota architecture and alters host inflammatory mediators in mouse adipose tissue. *JPEN. J. Parenter. Enteral Nutr.* **37**: 746–54.
 137. Watanabe, M., S. Fukiya, and A. Yokota. 2017. Comprehensive evaluation of the bactericidal activities of free bile acids in the large intestine of humans and rodents. *J. Lipid Res.* **58**: 1143–1152.
 138. Inagaki, T., A. Moschetta, Y. K. Lee, L. Peng, G. Zhao, M. Downes, R. T. Yu, J. M. Shelton, J. A. Richardson, J. J. Repa, D. J. Mangelsdorf, and S. A. Kliewer. 2006. Regulation of antibacterial defense in the small intestine by the nuclear bile acid receptor. *Proc Natl Acad Sci U S A.* **103**: 3920–3925.
 139. Phua, T., M. K. Sng, E. H. P. Tan, D. S. L. Chee, Y. Li, J. W. K. Wee, Z. Teo, J. S. K. Chan, M. M. K. Lim, C. K. Tan, P. Zhu, V. Arulampalam, and N. S. Tan. 2017. Angiotensin-like 4 Mediates Colonic Inflammation by Regulating Chemokine Transcript Stability via Tristetraprolin. *Sci. Rep.* **7**: 44351.



Summary



The global prevalence of obesity has increased substantially over the past decades. As a consequence, there has been a rise in obesity-related comorbidities, such as diabetes mellitus, non-alcoholic fatty liver disease (NAFLD), and dyslipidemia, each of which serves as an independent risk factor for cardiovascular diseases. While the increase in obesity rates and related metabolic diseases are believed to be primarily the result of an increased consumption of calorie-dense foods in combination with reduced levels of physical activity, various factors have been suggested to influence the progression of these metabolic diseases, including the gut microbiota, bile acids and angiopoietin-like protein 4 (ANGPTL4).

The gut microbiota live in a close relationship with the host and have an essential role in several aspects of host physiology, such as conferring protection against invading pathogens and facilitating the digestion of complex carbohydrates. The composition of the gut microbiota varies greatly between individuals, which is caused by differences in host genome and environmental factors, and may also be affected by specific disease states. Emerging evidence suggests that changes in intestinal microbiota are not merely a consequence of metabolic health, but may in fact contribute to certain diseases. To link changes in gut microbiota to metabolic health, several mechanisms have been proposed, including lipopolysaccharides, short-chain fatty acids, bile acids and ANGPTL4, which are extensively described in **Chapter 2** and **Chapter 3**. Bile acids are primarily known for their role in lipid absorption. By emulsifying triglycerides and stimulating pancreatic lipase activity, bile acids facilitate the digestion of dietary lipids and promote their absorption, although it is becoming increasingly apparent that bile acids also have major regulatory roles in the control of lipid, glucose and energy metabolism. Another important mediator of metabolic health is ANGPTL4. ANGPTL4 is a potent inhibitor of lipoprotein lipase (LPL), and is active under various physiological conditions, including fasting, exercise and cold exposure, thereby ensuring the proper distribution of plasma triglycerides over different tissues. In addition to inhibiting LPL, ANGPTL4 is also able to inhibit intestinal pancreatic lipase, thereby limiting dietary lipid absorption. Next to its role in lipid metabolism, ANGPTL4 has also been suggested to influence glucose metabolism. Although it is well-established that the gut microbiota, bile acids and ANGPTL4 influence metabolic health, the exact mechanisms are far from being completely understood. Therefore, the main of this thesis is to increase our understanding regarding the role of these mediators in metabolic health.

The first part of this thesis focuses on the role of the gut microbiota in NAFLD. NAFLD describes a spectrum of liver diseases ranging from simple steatosis to non-alcoholic steatohepatitis, liver fibrosis and cirrhosis. In **Chapter 4** we studied the influence of modulation of the gut microbiota in the development of NAFLD. To that end, in a mouse

model of NAFLD, we stimulated the gut bacteria by feeding mice the highly fermentable fiber guar gum (GG) and suppressed the gut bacteria via oral administration of antibiotics. We found that stimulation of the gut microbiota using GG enhanced hepatic inflammation and fibrosis, concurrent with elevated plasma and hepatic bile acid levels. In contrast, suppression of the gut bacteria using antibiotics decreased portal secondary bile acid levels and attenuated hepatic inflammation and fibrosis. Together, these data suggest a causal link between disturbances in gut microbial community and NAFLD. To investigate if bile acids are causally involved in the progression of NAFLD upon GG feeding, we fed mice chow supplemented with the primary bile acid taurocholic acid. Provision of taurocholic acid raised plasma bile acid levels and stimulated hepatic inflammation and fibrosis. Taken together, our data indicate that the gut microbiota have a marked impact on NAFLD, possibly via changes in the portal delivery of bile acids. Accordingly, in **Chapter 5**, we hypothesized that targeting the gut microbiota may provide therapeutic tools to treat NAFLD. As impairments of the intestinal barrier are also suggested to mediate the effect of the gut microbiota on NAFLD, we administered *Akkermansia muciniphila* and *Bacteroides thetaiotaomicron* to obese mice with NAFLD, which have both been suggested to improve the intestinal barrier. It was found that daily administration of *A. muciniphila* or *B. thetaiotaomicron* for 5 weeks to obese mice with NAFLD did not influence hepatic steatosis, inflammation or fibrosis. Importantly, we also found no difference in intestinal permeability as well as portal lipopolysaccharide levels. In conclusion, although we demonstrate that the gut microbiota have a marked impact on NAFLD, in our experimental setup, administration of *A. muciniphila* or *B. thetaiotaomicron* to obese mice with NAFLD did not improve features of NAFLD.

The liver receives about 70% of its blood supply from the intestine via the portal vein and is therefore the first organ that may be exposed to potentially harmful metabolites released by the intestinal microbiota. Identification of these harmful metabolites are very important as it might reveal novel therapeutic targets for NAFLD. To investigate if certain metabolites are harmful to the liver, it is important to utilize *in vivo* or *ex vivo* systems that reflect the human liver. In the second part of this thesis, we investigated whether precision-cut liver slices (PCLS) may be a suitable *ex vivo* model to study the human liver. Accordingly, in **Chapter 6**, we used whole genome gene expression profiling to compare the effect of activation of the nuclear receptor PPAR α between human PCLS and primary human hepatocytes. We show that the induction of gene expression by PPAR α is in general well captured by both the human primary hepatocytes and human PCLS, as activation of PPAR α consistently upregulates genes involved in lipid and xenobiotic metabolism in both models. By contrast, downregulation of gene expression by PPAR α activation was almost exclusively observed in human PCLS, which was largely connected to cells of the immune system, which are

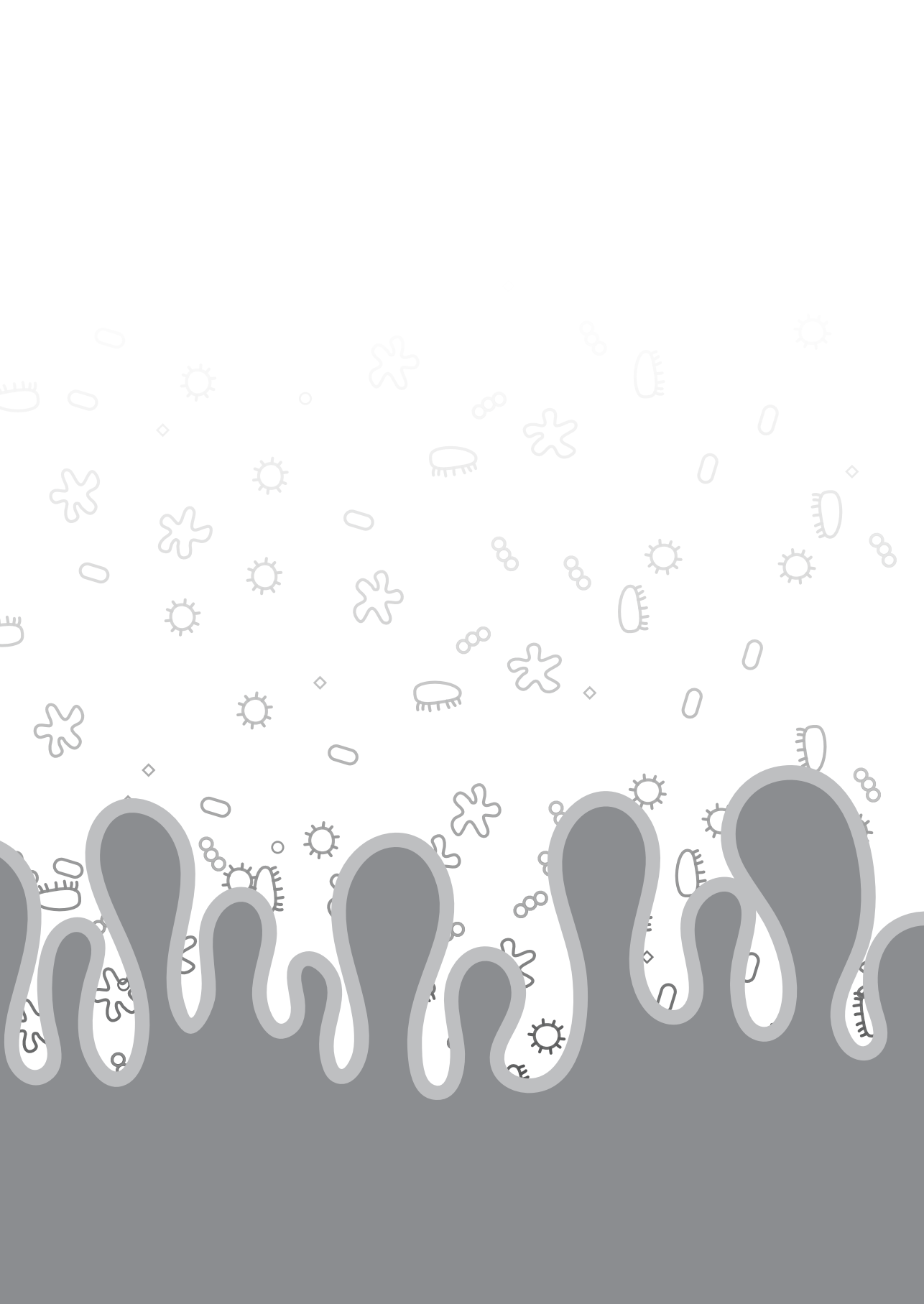
present in PCLS but absent in the primary hepatocytes. Taken together, we show that human PCLS are a suitable and superior model over primary hepatocytes to study PPAR α activation in human liver. Subsequently, in **Chapter 7**, we show, for the first time, the response of the human liver to FXR activation by obeticholic acid (OCA), a promising drug for the treatment of non-alcoholic steatohepatitis that is now in phase 3 clinical trials. It was found that human PCLS are highly and consistently responsive to FXR activation. In addition, by comparing the response of human PCLS to wild-type and *FXR*^{-/-} mice receiving obeticholic acid, we were also able to identify putative novel FXR target genes. Taken together, these results indicate that human PCLS are a suitable model to study human liver and represent a very useful tool for testing the response of human liver to intestinal-derived metabolites.

In the third part of this thesis, we focused on the metabolic effects of ANGPTL4. ANGPTL4 raises plasma triglyceride levels by inhibiting the enzyme lipoprotein lipase. Interestingly, bile acids and bile acids resins also have been shown to influence plasma triglyceride levels. Because we previously observed that bile acids lower ANGPTL4 secretion by intestinal cells, in **Chapter 8**, we hypothesized that the triglyceride-lowering effect of bile acids is mediated by ANGPTL4. To test this hypothesis, wild-type and *Angptl4*^{-/-} mice were fed chow supplemented with the primary bile acid taurocholic acid. It was found that the triglyceride-lowering effect of bile acids was not mediated by ANGPTL4, but may be mediated by downregulation of the LPL inhibitors ANGPTL3 and APOC3. Intriguingly, plasma and hepatic BA concentrations were significantly lower in TCA-supplemented *Angptl4*^{-/-} mice than in TCA-supplemented wild-type mice, suggesting that loss of ANGPTL4 impairs intestinal bile acid absorption. Since the gut microbiota converts primary bile acids into secondary bile acids, we hypothesized that the elevated excretion of primary bile acids and decreased bile acid absorption in *Angptl4*^{-/-} mice may be dependent on the gut microbiota. Indeed, suppression of the gut bacteria using antibiotics abolished the differences in bile acid absorption. In conclusion, our data indicate that ANGPTL4 is not involved in the triglyceride-lowering effect of bile acids but promotes bile acid absorption during taurocholic acid supplementation via a mechanism dependent on the gut microbiota.

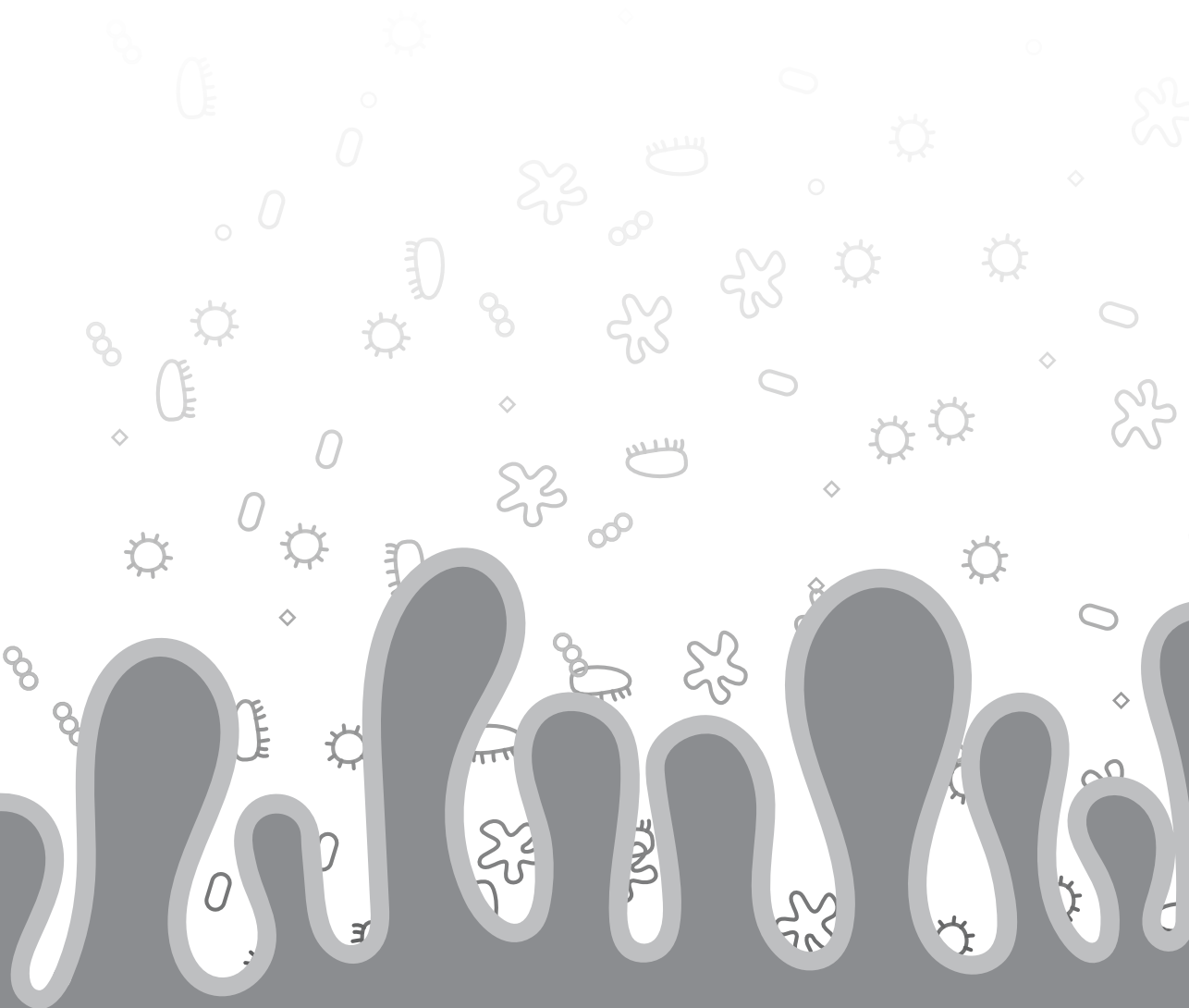
The observation that *Angptl4*^{-/-} mice develop a massive acute phase response, lethal chylous ascites and peritonitis when fed a high fat diet rich in saturated fat, has hampered the study of ANGPTL4 in diet-induced obesity and related metabolic dysfunction. To overcome that obstacle, in **Chapter 9**, we investigated the influence of ANGPTL4 on diet-induced obesity and metabolic dysfunction by feeding wild-type and *Angptl4*^{-/-} mice a high fat diet rich in unsaturated fat, combined with fructose and cholesterol. It was found that *Angptl4*^{-/-} mice displayed increased bodyweight gain, adipose tissue mass and adipose tissue inflammation, but unexpectedly had markedly improved glucose tolerance, which was

accompanied by elevated plasma insulin levels. Inasmuch as the gut microbiota has been suggested to influence insulin secretion and as ANGPTL4 has been proposed to link the gut microbiota to host metabolism, we hypothesized a potential role for the gut bacteria. Indeed, the gut bacterial composition was profoundly different between wild-type and *Angptl4*^{-/-} mice. Furthermore, suppression of the gut bacteria using antibiotics largely abolished the differences in glucose tolerance and insulin levels between wild-type and *Angptl4*^{-/-} mice. Taken together, loss of ANGPTL4 improves glucose tolerance at least partly via changes in the gut microbiota. Nevertheless, future studies are warranted to investigate how ANGPTL4 alters the gut bacterial composition and how this may influence insulin levels and glucose tolerance.

In summary, the studies presented in this thesis have clarified and strengthened our understanding regarding the role of the gut microbiota, bile acids and ANGPTL4 in metabolic health. We showed that the gut microbiota have an important role in the pathogenesis of NAFLD, which is likely mediated via changes in portal delivery of bile acids. Subsequently, we demonstrated that human PCLS provide a suitable model to study the human liver and provide a pivotal tool for testing the effect of intestinal metabolites on human liver. Finally, we show that the triglyceride-lowering effects of bile acids is not mediated by ANGPTL4 and reveal two novel functions of ANGPTL4 in mediating bile acids absorption and glucose metabolism. Although our studies extended our knowledge of the role of these mediators in metabolic diseases, several questions remain. Since the intestinal microbiota, bile acids and ANGPTL4 are all interconnected and are all involved in lipid and glucose metabolism, it is important to realize that modulation of one of these three mediators likely also affects the other two mediators, including their metabolic responses, reflecting a strong interdependence.



Acknowledgements



Zo, en dan (ineens) schrijf ik de eerste woorden van mijn dankwoord op papier. Hiermee komt de afsluiting van een belangrijke periode in mijn leven toch opeens heel dichtbij. Ik kan terugkijken op vier zeer plezierige jaren waarin ik enorm veel heb geleerd met als resultaat mijn naam pronkend op de voorkant van dit proefschrift. Echter, zonder hulp van velen zou dit boekje er niet zijn. Daarom wil ik graag alle mensen bedanken die, elk op hun eigen manier aan mijn promotie hebben bijgedragen en deze periode zo onvergetelijk voor mij hebben gemaakt.

Allereerst zou ik graag mijn promotor **Prof. Kersten** willen bedanken. Sander, bedankt voor het vertrouwen om samen met mij het avontuur aan te gaan om onderzoek te doen naar de microbiota. Gedurende de afgelopen vier jaar hebben wij ervaren dat dit zeker geen gemakkelijk onderzoeksveld is, maar dankzij jouw kennis, hulp en ervaring hebben wij een aantal zeer interessante nieuwe bevindingen kunnen doen en publiceren. Ik ben je erg dankbaar voor alles wat je me hebt geleerd. Zowel je optimisme als je kritische blik gaven mij de kans om mezelf te verbeteren en daar waar nodig trapte je op de rem als ik weer eens te snel wilde gaan. Ik bewonder je toewijding voor de wetenschap, je gedrevenheid en je taalkundig perfectionisme. Enorm bedankt voor al je hulp en vertrouwen. Ik had me geen betere promotor kunnen wensen!

I also thank the committee, **Jerry Wells, Erwin Zoetendal, Max Nieuwdorp and Hans Jonker** for the critical review and judgement of my thesis.

Lily, al vanaf dag één zijn we kamergenootjes en hebben we alle ups en downs van het leven als PhD student met elkaar gedeeld. Zonder jou zou dit promotietraject een stuk minder gezellig zijn geweest. Ik bewonder je creativiteit, je doorzettingsvermogen en je brede interesse. Heel erg bedankt voor je gezelligheid, je deskundig advies, je luisterend oor en je (sarcastische) humor de afgelopen vier jaar. Met jou is het nooit saai :-). Ik wens je heel veel succes met het afronden van je PhD. Ik zal je missen!

Wieneke, het was wel even wennen toen je ons had verlaten voor het zonnige Frankrijk. Door je enorm goede geheugen en kennis kon ik altijd bij je terecht voor hulp of advies, maar ook gewoon voor een gezellig praatje. Gelukkig hebben we dit na je vertrek in stand kunnen houden door regelmatig met elkaar te bellen. Ik wil je bedanken voor al je hulp tijdens mijn promotietraject, ik kon altijd op je rekenen. Als ik weer eens zo nodig op vakantie moest en ik had een muisexperiment lopen, nam jij het van mij over. Als ik secties had en ik had hulp nodig, kwam jij mij helpen. Bedankt daarvoor. Ik wens je heel veel succes met je toekomstige onderzoek!

Lily en Wieneke, bedankt dat jullie naast mij willen staan tijdens mijn verdediging!

Uiteraard wil ik ook mijn kamergenoten in Helix bedanken voor de gezellige tijd. **Lily**, hoewel het voor ons wennen was om na drie jaar met z'n tweetjes, ineens in een kamer met zes personen te belanden, hebben we het er denk ik wel goed vanaf gebracht ;-). **Benthe**, in september 2016 was er ineens een PhD student die ook aan het microbioom ging werken. Ik vond het altijd ontzettend fijn om hiervoor met jou te kunnen sparren en vooral de input van Siri was dan altijd erg welkom :-). Je bent een harde werker en hebt veel goede ideeën. Ik wens je veel succes met je promotietraject! **Karin**, bedankt voor de gezellige gesprekken, je bereidbaarheid om last minute samples uit het vriesveem te halen en het toestoppen van groenten uit eigen tuin. **Marlies** en **Pieter**, bedankt voor jullie interesse in mijn project. Ik wens jullie heel veel succes in de toekomst!

Rinke en **Guido**, na het doorstaan van alle flauwe grappen en geouwehoer van jullie kant, stond bij jullie de deur altijd open voor vragen. Rinke, onder jouw begeleiding ben ik in 2012 begonnen met mijn master stage. Tijdens deze periode, maar ook tijdens mijn promotietraject, heb ik erg veel van je kunnen leren. Je hebt veel kennis over diverse onderwerpen, bent vol ideeën en bent goed op de hoogte van de laatste literatuur, inclusief die van de microbiota. Bedankt voor je suggesties voor mijn onderzoek en alle analyses die je voor mij in Nijmegen hebt uitgevoerd. Guido, ik wil je bedanken voor alle keren dat ik bij je terecht kon met lastige maar ook met simpelere vragen over de microbiota, statistiek en de droplet PCR. Tevens bedankt voor je deskundig commentaar op mijn manuscripten.

Naast mijn tijd op het lab heb ik ook flink wat tijd doorgebracht in het CKP. **Rene**, **Bert** en **Wilma** maar ook **Lisette** en **Judith**, heel erg bedankt voor al jullie hulp en kunde de afgelopen jaren. Ik kon altijd op jullie rekenen en ook last minute veranderingen in de planning waren geen probleem. Er was altijd een oplossing. Zonder jullie hulp waren veel van mijn studies niet mogelijk geweest, hartelijk bedankt!

Tijdens mijn promotie had ik het voorrecht om met humane leverschijfjes te mogen werken. **Geert**, heel erg bedankt voor het leren van deze interessante techniek en je hulp tijdens alle experimenten. **Noortje**, bedankt voor de prettige samenwerking tijdens het OCA-project. **Jacques**, ik wil je bedanken voor alle interessante gesprekken, maar vooral voor je hulp bij alle NMR-metingen en het identificeren van onbekende pieken. **Steven** en **Clara**, het was erg prettig om met jullie samen te werken tijdens de bacterie studie. Bedankt dat ik altijd allerlei vragen op jullie af mocht vuren over microbiota analyses.

Uiteraard wil ik ook alle andere (ex)-collega's van de NMG en Pharma groep bedanken. **Wilma**, bij jou kon ik altijd terecht om mijn frustraties over het publiceren van papers te uiten. Dank daarvoor! Ik heb respect voor je dat je iedere dag zo vroeg op het lab bent. Mij is

het niet gelukt :-). **Lydia**, je enthousiasme werkt erg aanstekelijk. Bedankt voor je interesse en gezellige gesprekken. **Mark**, bedankt voor al je hulp bij de array analyses. **Jocelijnn, Klaske, Marco en Michiel**, bedankt voor jullie interesse in mijn onderzoek! **Shohreh**, despite your busy schedule you were always willing to help me. Thank you for all the help with histology and mouse experiments, it is much appreciated. **Jenny, Mechteld, Mieke, Carolien en Karin**, jullie werk is onmisbaar op het lab. Bedankt voor de gezelligheid, de leuke gesprekken en het plaatsen van mijn (soms last minute) bestellingen! **Merel**, bedankt voor je vrolijkheid, betrokkenheid en grappige Belgische uitspraken :-). Je bent ook al weer over de helft van je promotietraject en ik weet zeker dat je het geweldig gaat afronden. **Sophie**, heel veel succes met de laatste loodjes, er gaat ongetwijfeld een mooi eindresultaat uitkomen! **Frits**, ik ben je flauwe grappen wel gaan missen na je vertrek! Bedankt dat ik ook via de mail altijd bij je terecht kon voor vragen over de eilandjes of beta cellen! **Diederik**, als jij er bent, gaan er deuren voor mij open ;-). Bedankt voor je grappen en interesse in mijn project. **Nikkie**, bedankt voor het dienen als vraagbaak bij het afronden van mijn promotie. Heel veel succes met je verdere carrière. **Inge, Katja en Juri** bedankt voor alle gezellige praatjes in het lab of zomaar even op de gang. **Roland and Neeraj**, you're almost there. I wish you all the best! **Charlotte, Rogier, Montse, Anwi and Philip**, thanks for all the fun times and good luck with your PhD projects. **Xanthe, Mara en Miranda**, jullie zijn nog maar relatief kort geleden aan jullie PhD avontuur begonnen. Heel veel succes de komende jaren!

I would also like to thank the students that helped with the experiments. **Nieke, Philip, Yuan, Alivia and Philippe**, thank you for your willingness to help with my study. I very much appreciate all your contributions and wish you all the best for your future careers.

Also many thanks to all the members of the **CVON IN-CONTROL** project, for the pleasant collaborations, the support and all the good science I learned from you. In het bijzonder wil ik **Tom en Saeed** bedanken voor alle hulp bij de analyses van de microbiota en de hulp bij de kleuringen van de levers. **Lisa, Saeed, Vanessa, Tom en Inge** bedankt voor jullie gezelschap tijdens de Papendal cursussen en bij de verschillende congressen!

Familie en vrienden zijn van essentieel belang tijdens een promotie. Niet omdat zij je kunnen helpen met het schrijven van artikelen of het uitvoeren van experimenten, hoewel sommigen dat graag hadden willen doen, maar vooral om ervoor te zorgen dat je met beide benen op de grond blijft staan, je verhalen aan te horen en te zorgen voor de nodige afleiding.

Christa, Tom, Ilse en Nick, door ofwel de afstand of het drukke gezinsleven zien we elkaar helaas niet meer wekelijks. Toch ben ik jullie erg dankbaar voor alle gezellige avonden en etentjes, dat er nog velen mogen volgen :-). **Michaela en Nalia**, hoewel ik jullie 4 jaar geleden als collega bij Burgers' Zoo moest verlaten, is onze vriendschap gelukkig niet verloren gegaan.

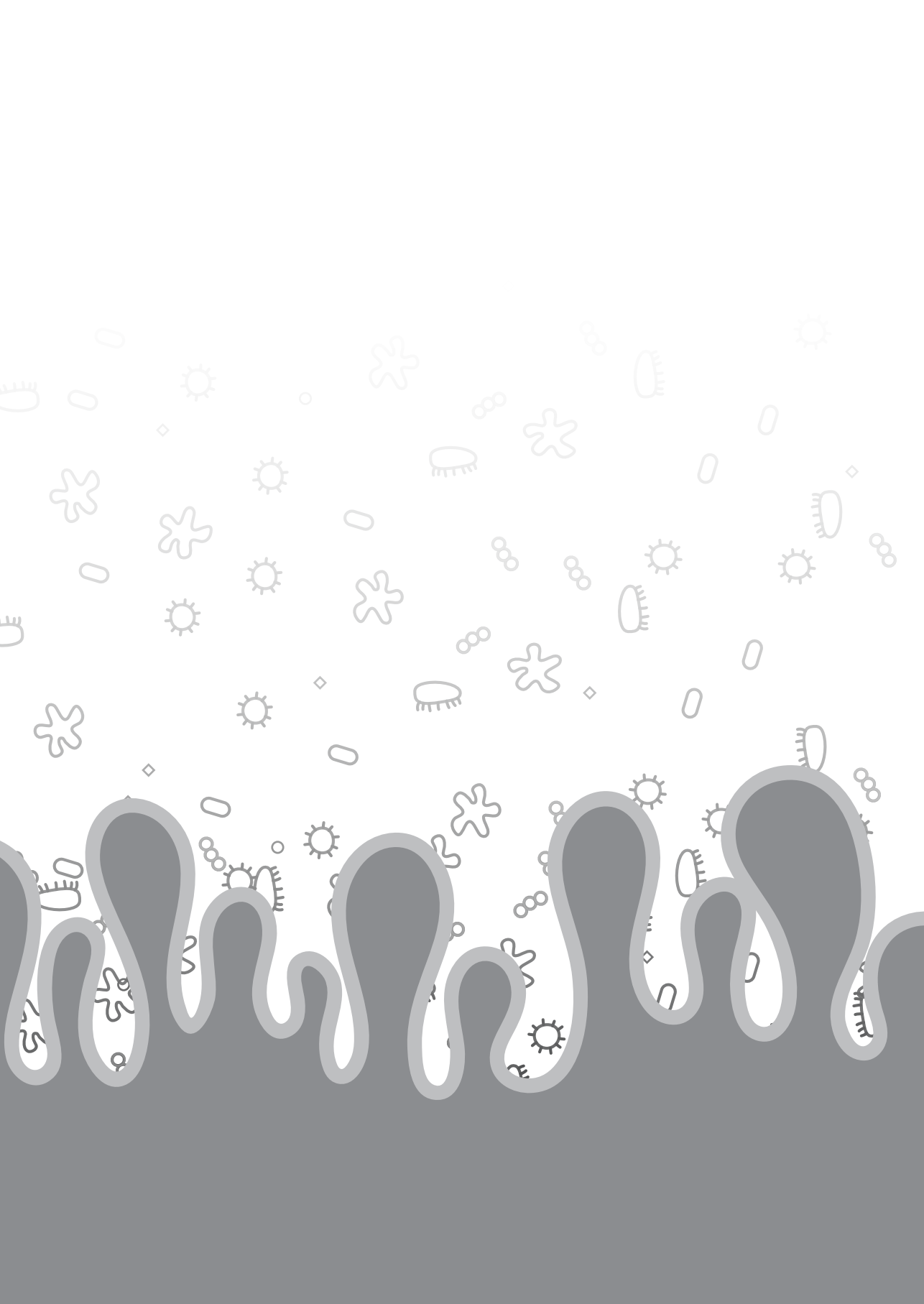
Regelmatig kreeg ik van jullie een appje of een belletje dat er weer een nieuw restaurant was geopend die we zeker moesten gaan proberen. Bedankt! **Frederike** en **Mike**, via de Engineers groep van Ruben heb ik jullie zo'n vier jaar geleden leren kennen en er was direct een klik. Heel erg bedankt voor jullie interesse, jullie humor, de gezellige (spelletjes)avonden en de jaarlijkse weekendjes weg. Ik weet zeker dat dit voor de broodnodige afleiding tijdens mijn promotie heeft gezorgd! **Lotte**, we hebben samen enorm veel meegemaakt en hoewel we elkaar een tijdje uit het oog verloren zijn, ben ik erg dankbaar dat onze vriendschap beter is dan ooit tevoren. Bedankt voor je interesse, de gezellige avonden, uitjes en je vriendschap!

Arend, Anja, Hugo en Melissa, bedankt voor de gezelligheid en jullie interesse de afgelopen jaren.

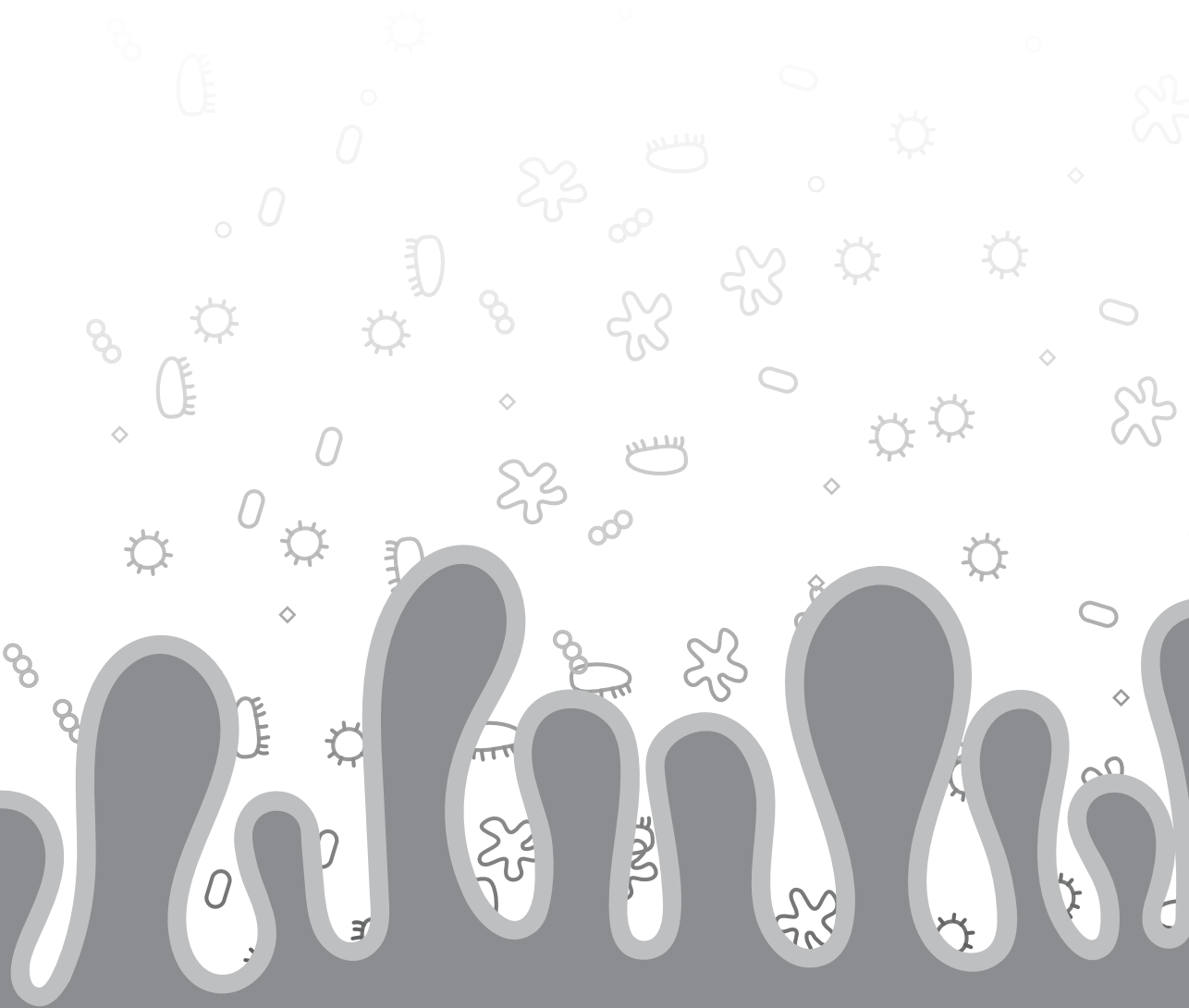
Lieve **papa** en **mama**, we hebben het niet altijd even makkelijk gehad, maar ik ben enorm trots hoe jullie je er doorheen geslagen hebben! Jullie zijn de beste en liefste ouders die iemand zich maar kan wensen. Ik kan altijd op jullie terugvallen! Bedankt voor jullie onvoorwaardelijke steun, liefde en geloof in mij. Ik hou van jullie.

Als laatste in de rij, maar met stip op nummer 1: **Ruben**. Lieverd, wat moet ik zonder jou! Je bent mijn maatje, grootste steun en allerliefste man. Er zijn enorm veel dingen waar ik je voor zou moeten bedanken, maar vooral bedankt voor alle goede zorgen, je begrip, geduld en liefde de afgelopen 4 jaar. Ik kijk uit naar onze toekomst, samen met de kleine!

A handwritten signature in black ink that reads "Aafke". The signature is written in a cursive, flowing style.



About the author



Curriculum vitae

Aafke Janssen was born on January 4, 1988 in Gendringen, the Netherlands. She started her academic career at the Utrecht University where she received her bachelor's degree (*cum laude*) in Biomedical Sciences in 2011. She continued with the master program in Biology of Disease at Utrecht University and received her master's degree in 2013. During her master she performed two internships. She did her first internship at the department of Cardiology at Utrecht University which was about the validation of Necrostatin-1 in reducing myocardial reperfusion injury in a preclinical porcine model. She then performed her second internship at the Nutrition, Metabolism & Genomics group at Wageningen University, where she investigated the role of Angiopoietin-like protein 4 in atherosclerosis development in mice.

In October 2013, Aafke started her PhD project within a consortium funded by the Netherlands Cardiovascular Research Committee entitled 'the role of the gut microbiota and chronic inflammation as drivers of cardiovascular disease'. She performed her research at the Nutrition, Metabolism & Genomics group of the Division of Human Nutrition at Wageningen University and focussed on the role of the gut microbiota, bile acids and Angiopoietin-like protein 4 in metabolic health. She was supervised by Prof. Sander Kersten. During her PhD she presented her work at different symposia, conferences and meetings. In 2015, she was awarded with the first poster price. She finished her PhD in 2017. The results of the PhD project 'Investigation into mediators of metabolic health. A role for the gut microbiota, bile acids and ANGPTL4' are described in this thesis.

List of publications

This thesis

Janssen AWF, Aalvink S, Cani PD, Belzer C, de Vos WM, Kersten S. The mucin-degrading bacteria *A. muciniphila* and *B. thetaiotaomicron* have no effect in an obese mouse model of non-alcoholic fatty liver disease. *In preparation*.

Janssen AWF, Katiraei S, Willems van Dijk K, Kersten S. Loss of ANGPTL4 in diet-induced obese mice uncouples visceral obesity from glucose intolerance partly via a mechanism dependent on the gut microbiota. *Submitted*.

Janssen AWF*, Dijk W*, Boekhorst J, Kuipers F, Groen AK, Lukovac S, Hooiveld GJEJ, Kersten S. ANGPTL4 promotes bile acid absorption during taurocholic acid supplementation via a mechanism dependent on the gut microbiota. *Biochim Biophys Acta*. 2017;1862(10Pt A):1056-1067.

Janssen AWF, Houben T, Katiraei S, Dijk W, Boutens L, van der Bolt N, Wang Z, Brown JM, Hazen SL, Mandard S, Shiri-Sverdlov R, Kuipers F, Willems van Dijk K, Vervoort J, Stienstra R, Hooiveld GJEJ, Kersten S. Modulation of the gut microbiota impacts nonalcoholic fatty liver disease: a potential role for bile acids. *J Lipid Res*. 2017;58(7):1399-1416.

Janssen AWF, Kersten S. Potential mediators linking gut bacteria to metabolic health: a critical view. *J Physiol*. 2017;595(2):477-487.

Ijssennagger N, **Janssen AWF**, Milona A, Ramos Pittol JM, Hollman DAA, Mokry M, Betzel B, Berends FJ, Janssen IM, van Mil SWC*, Kersten S*. Gene expression profiling in human precision cut liver slices in response to the FXR agonist obeticholic acid. *J. Hepatol*. 2016;64(5):1158-1166.

Janssen AWF, Betzel B, Stooopen G, Berends FJ, Janssen IM, Peijnenburg AA, Kersten S. The impact of PPAR α activation on whole genome gene expression in human precision cut liver slices. *BMC Genomics*. 2015;16:760.

Janssen AWF, Kersten S. The role of the gut microbiota in metabolic health. *FASEB J*. 2015;29(8):3111-3123.

Others

Koudstaal S, Oerlemans MI, Van der Spoel TI, **Janssen AWF**, Hoefer IE, Doevendans PA, Sluijter JP, Chamuleau SA. Necrostatin-1 alleviates reperfusion injury following acute myocardial infarction in pigs. *Eur J Clin Invest*. 2015;45(2):150-159.

Georgiadi A, Wang Y, Stienstra R, Tjeerdema N, **Janssen AWF**, Stalenhoef A, van der Vliet JA, de Roos A, Tamsma JT, Smit JW, Tan NS, Müller M, Rensen PC, Kersten S. Overexpression of angiopoietin-like protein 4 protects against atherosclerosis development. *Arterioscler Thromb Vasc Biol.* 2013;33(7):1529-37.

*equal contribution

Overview of completed training activities

Discipline specific activities

Courses

PhD training course

Atherosclerosis and Thrombosis	DHF	Arnhem	2014
Vascular Biology	DHF	Arnhem	2015
The Intestinal Microbiome and Diet in Human and Animal Health	VLAG	Wageningen	2014

Conferences

NVDO meeting	NVDO	Oosterbeek	2013-2016
1 st European Fatty Liver Conference	MUMC	Maastricht	2015
Monothematic Conference	EASL	Innsbruck, Austria	2015
Microbiota, Metabolism and NAFLD			
Nutritional Science Days	NWO	Heeze	2015
Gut microbiota, Metabolic Disorders and beyond	Keystone symposia	Rhode Island, USA	2016
Bile acid Receptors as Signal Integrators in Liver and Metabolism	Keystone symposia	Monterey, USA	2017

General courses

VLAG PhD week	VLAG	Baarlo	2014
Advanced visualisation, integration and biological interpretation of -omics data	VLAG	Wageningen	2014
Presenting with impact	WGS	Wageningen	2015
Techniques for Writing and Presenting a Scientific Paper	WGS	Wageningen	2016
Career Perspectives	WGS	Wageningen	2017

Optionals

Preparation research proposal	WUR	Wageningen	2013
NMG/Pharma scientific meetings	WUR	Wageningen	2013-2017
Scientific meetings/journal clubs TSK	WUR	Wageningen	2013-2017
Six-monthly projects meetings	CVON	various locations	2014-2017

The research described in this thesis was supported by a grant of the Dutch Heart Foundation (CVON 2012-03 IN-CONTROL).

Financial support by Wageningen University and the Dutch Heart Foundation for the publication of this thesis is gratefully acknowledged.

Cover design James Jardine || designyourthesis.com

Lay-out Aafke W.F. Janssen

Printed by Digiforce || proefschriftmaken.nl

